NUREG/CP-0091
Vol. 5

Proceedings of the U.S. Nuclear Regulatory Commission

Fifteenth Water Reactor Safety Information Meeting

Volume 5
- Industry Safety Research
- International Code Assessment Program

Held at
National Bureau of Standards
Gaithersburg, Maryland
October 26-29, 1987

U.S. Nuclear Regulatory Commission

Office of Nuclear Regulatory Research

Proceedings prepared by
Brookhaven National Laboratory

NOTICE

These proceedings have been authored by a contractor of the United States Government. Neither the United States Government nor any agency thereof, or any of their employees, makes any warranty, expressed or implied, or assumes any legal liability or responsibility for any third party's use, or the results of such use, of any information, apparatus, product or process disclosed in these proceedings, or represents that its use by such third party would not infringe privately owned rights. The views expressed in these proceedings are not necessarily those of the U.S. Nuclear Regulatory Commission.

Available from

Superintendent of Documents
U.S. Government Printing Office
P.O. Box 37082
Washington D.C. 20013-7082

and

National Technical Information Service
Springfield , VA 22161

NUREG/CP-0091
Vol. 5
R2, R4

Proceedings of the U.S. Nuclear Regulatory Commission

Fifteenth Water Reactor Safety Information Meeting

Volume 5
- Industry Safety Research
- International Code Assessment Program

Held at
National Bureau of Standards
Gaithersburg, Maryland
October 26-29, 1987

Date Published: February 1988

Compiled by: Allen J. Weiss

Office of Nuclear Regulatory Research
U.S. Nuclear Regulatory Commission
Washington, DC 20555

Proceedings prepared by
Brookhaven National Laboratory

ABSTRACT

This six-volume report contains 140 papers out of the 164 that were presented at the Fifteenth Water Reactor Safety Information Meeting held at the National Bureau of Standards, Gaithersburg, Maryland, during the week of October 26-29, 1987. The papers are printed in the order of their presentation in each session and describe progress and results of programs in nuclear safety research conducted in this country and abroad. Foreign participation in the meeting included twenty-two different papers presented by researchers from Belgium, Czechoslovakia, Germany, Italy, Japan, Russia, Spain, Sweden, The Netherlands and the United Kingdom. The titles of the papers and the names of the authors have been updated and may differ from those that appeared in the final program of the meeting.

PROCEEDINGS OF THE
15th WATER REACTOR SAFETY INFORMATION MEETING

October 26-29, 1987

Published in Six Volumes

GENERAL INDEX

REGISTERED ATTENDEES (NON-NRC)
15th WATeR REACTOR SAFETY INFORMATION MEETING

D. ACKER
CEA FRENCH ATOMIC ENERGY COMMISSION
DEMT/SMTS/RDMS
GIF S/YVETTE 91191
FRANCE

H. ADACHI
JAPAN ATOMIC ENERGY RES. INSTITUTE
TOKAI-MURA
IBARAKI 319-11
JAPAN

L. J. AGEE
ELECTRIC POWER RESEARCH INSTITUTE
3412 HILLVIEW AVENUE
PALO ALTO CA 94303
USA

H. AKIMOTO
JAPAN ATOMIC ENERGY RES. INSTITUTE
TOKAI-MURA
IBARAKI 319-11
JAPAN

P. ALBRECHT
UNIVERSITY OF MARYLAND
DEPT. OF CIVIL ENGINEERING
COLLEGE PARK MD 20742
USA

D. J. ALEXANDER
OAK RIDGE NATIONAL LAB.
P.O. BOX X, BLDG 4500-S
OAK RIDGE TN 37831
USA

R. P. ALLEN
BATTELLE PACIFIC NORTHWEST LAB.
P.O. BOX 999
RICHLAND WA 99352
USA

K. K. ALMENAS
UNIVERSITY OF MARYLAND
COLLEGE PARK MD 20742
USA

A. ALONSO
MADRID POLYTECHNICAL UNIVERSITY
JOSE GUTIERREZ ABASCAL, 2
MADRID 28006
SPAIN

M. AMIN
SARGENT & LUNDY
55 E. MONROE
CHICAGO IL 60603
USA

P. S. ANDERSEN
DYNATREK, INC.
2115 E. JEFFERSON STREET
ROCKVILLE MD 20852
USA

J. M. ANDERSON
BECHTEL
15740 SHADY GROVE RD.
GAITHERSBURG MD 20850
USA

F. ARAYA
JAPAN ATOMIC ENERGY RES. INSTITUTE
3000 TRINITY DR.
LOS ALAMOS NM 87544
USA

W. C. ARCIERI
ENSA, INCORPORATED
15825 SHADY GROVE ROAD
ROCKVILLE MD 20850
USA

K. H. ARDRON
CENTRAL ELECTRICITY GENERATING BOARD
BDCD
GLOUCESTER
UK

J. G. ARENDTS
EG&G IDAHO, INC.
P.O. BOX 1625
IDAHO FALLS ID 83415
USA

D. A. ARMSTRONG
WASHINGTON PUBLIC POWER SUPPLY SYS.
3000 G. WASH. WAY-P.O. BOX 968
RICHLAND WA 99352
USA

A. ARNAUD
CEA FRENCH ATOMIC ENERGY COMMISSION
CEN CADARACHE
ST. PAUL LEZ DURANCE 13115
FRANCE

W. W. ASCROFT-HUTTON
HM NUCLEAR INSTALLATIONS INSPECTORATE
BAYNARDS HOUSE, CHEPSTOW PLACE
LONDON W2 4TF
UK

V. G. ASMOLOV
I. V. KURCHATOV INST. OF ATOMIC ENERGY
KURCHATOV SQUARE
MOSCOW 123182
USSR

D. ASFORD
ATOMIC ENERGY OF CANADA, LTD.
15 ISABEL STREET
PETAWAWA ONTARIO K8H1Z1
CANADA

W. J. BABYAK
WESTINGHOUSE BETTIS ATOMIC PWR LAB.
P.O. BOX 79
WEST MIFFLIN PA 15122
USA

A. J. BAKER
HM NUCLEAR ISTALLATIONS INSPECTORATE
ST. PETERS HOUSE, BALLIOL ROAD
BOOTLE MERSEYSIDE L203LZ
UK

J. L. BALLIF
SCIENTECH
P.O. BOX 1406
IDAHO FALLS ID 83403-1406
USA

W. H. BAMFORD
WESTINGHOUSE
P. O. BOX 2728
PITTSBURGH PA 15230
USA

M. C. BAMPTON
BATTELLE PACIFIC NORTHWEST LAB
P.O. BOX 999
RICHMOND WA 99352
USA

K. K. BANDYOPADHYAY
BROOKHAVEN NATIONAL LAB.
BLDG 129
UPTON NY 11973
USA

R. A. BARI
BROOKHAVEN NATIONAL LAB.
BLDG 130
UPTON NY 11973
USA

B. R. BASS
OAK RIDGE NATIONAL LAB.
P.O. BOX Y
OAK RIDGE TN 37831
USA

J. A. BAST
GENERAL ELECTRIC COMPANY
P.O. BOX 1072
SCHENECTADY NY 12301
USA

R. C. BAUER
WESTINGHOUSE BETTIS ATOMIC PWR LAB.
P.O. BOX 79
WEST MIFFLIN PA 15122
USA

K. R. BAUMGARTEL
GESELLSCHAFT FUR REAKTORSICHERHEIT
SCHWERTNERGASSE 1
KOELN 8046
FRG

S. L. BAXTER
UNIVERSITY OF MARYLAND
4100 CONNECTICUT AVENUE
BALTIMORE MD 21045
USA

P. D. BAYLESS
EG&G IDAHO, INC.
P.O. BOX 1625
IDAHO FALLS ID 83415
USA

A. BECERRA
INSURGENTES SUR 1776
MEXICO CITY
MEXICO 01030
MEXICO

R. J. BEELMAN
EG&G IDAHO, INC.
P.O. BOX 1625
IDAHO FALLS ID 83415
USA

J. O. BENNETT
LOS ALAMOS NATIONAL LAB.
P.O. BOX 1663, MS-J570
LOS ALAMOS NM 87544
USA

E. D. BERGERON
SANDIA NATIONAL LABORATORIES
P.O. BOX 5800, DIV 6412
ALBUQUERQUE NM 87185
USA

K. D. BERGERON
SANDIA NATIONAL LABORATORIES
P.O. BOX 5800
ALBUQUERQUE NM 87185
USA

E. BESWICK
CENTRAL ELECTRICITY GENERATING BOARD
BOOTHS HALL, CHELFORD ROAD
KNUTSFORD CHESHIRE WA16 8QG
UK

P. BEZLER
BROOKHAVEN NATIONAL LABORATORY
BLDG 129
UPTON NY 11973
USA

M. J. BIRD
UKAEA/AEE WINFRITH
DORCHESTER
DORSET DT2 8DH
UK

D. P. BIRMINGHAM
BABCOCK & WILCOX
1562 BEESON STREET
ALLIANCE OH 44601
USA

M. M. BLEAKLEY
UKAEA/SRD
WIGSHAW LANE, CULCHETH
WARRINGTON WA3 4NE
UK

J. L. BOCCIO
BROOKHAVEN NATIONAL LABORATORY
BUILDING 130
UPTON NY 11973
USA

B. R. BOHER
FRAMATOME
25 4 RAINPRINT SQUARE
MURRYSVILLE PA 15668
USA

J. M. BOONE
DUKE POWER
422 SOUTH CHURCH ST.
CHARLOTTE NC 28242
USA

R. B. BORSUM
BABCOCK & WILCOX CO.
7910 WOODMONT AVE., SUITE 220
BETHESDA MD 20814
USA

W. M. BOWEN
BATTELLE PACIFIC NORTHWEST LAB.
P.O. BOX 999
RICHLAND WA 99352
USA

D. R. BRADLEY
SANDIA NATIONAL LABORATORIES
P.O. BOX 5800
ALBUQUERQUE NM 87185
USA

M. BRANDANI
ANSALDO
VIA D'ANNUNZIO 113
GENOVA 16129
ITALY

R. J. BREEDING
SANDIA NATIONAL LABORATORIES
P.O. BOX 5800, DIV 6413
ALBUQUERQUE NM 87185
USA

D. BREWER
DUKE POWER
422 SOUTH CHURCH ST.
CHARLOTTE NC 28242
USA

I. BRITTAIN
UKAEA/AEE WINFRITH
DORCHESTER
DORSET DT2 8DH
UK

J. M. BROUGHT.
EG&G IDAHO, INC.
P.O. BOX 1625
IDAHO FALLS ID 83415
USA

R. H. BRYAN
OAK RIDGE NATIONAL LAB.
P.O. BOX Y
OAK RIDGE TN 37831
USA

B. J. BUESCHER
EG&G IDAHO, INC.
P.O. BOX 1625
IDAHO FALLS ID 83415
USA

N. E. BUTTERY
CENTRAL ELECTRICITY GENERATING BOARD
BERKELEY NUCLEAR LABORATORIES
BERKELEY GLOUCESTERSHIRE GL13 9PB
UK

A. L. CAMP
SANDIA NATIONAL LABORATORIES
P.O. BOX 5800, DIV 6412
ALBUQUERQUE NM 87185
USA

N. G. CATHEY
EG&G IDAHO, INC.
P.O. BOX 1625
IDAHO FALLS ID 83415
USA

S. CHAKRABORTY
EIR-EDV, INST. FUR REAKTORFORSCHUNG
WURENLINGEN CH5303
SWITZERLAND

K. CHEN
INSTITUTE OF NUCLEAR ENERGY RESEARCH
P.O. BOX 3-3
LUNG-TAN, TAIWAN 32500
ROC

J. C. CHEN
LEHIGH UNIVERSITY
WHITAKER LAB #5
BETHLEHEM, PA
USA

T. CHEN
ADVANCED NUCLEAR FUELS CORP.
2101 HORN RAPIDS RD., P.O. BOX 130
RICHLAND, WA 99352
USA

H. S. CHENG
BROOKHAVEN NATIONAL LAB.
BLDG 475B
UPTON, NY 11973
USA

J. CHENG
UNIVERSITY OF MARYLAND
DEPT. OF CIVIL ENGINEERING
COLLEGE PARK, MD 20742
USA

A. CHEUNG
WESTINGHOUSE
P.O. BOX 355
PITTSBURGH, PA 15230
USA

U. K. CHOPRA
ARGONNE NATIONAL LAB.
9700 S. CASS AVE.-BLDG 208
ARGONNE, IL 60439
USA

J. CHRISTENSEN
BATTELLE PACIFIC NORTHWEST LAB.
P.O. BOX 999
RICHLAND, WA 99352
USA

R. CLASPER
UKAEA/SRD
WIGSHAW LANE, CULCHETH
WARRINGTON, WA34NE
UK

J. W. CLEVELAND
SEA CONSULTANTS, INC.
2001 GATEWAY PLACE, SUITE 610-W
SAN JOSE, CA 95110
USA

M. COLAGROSSI
ENEA/DISP
VIA VITALIANO BRANGATI 48
ROME, 00144
ITALY

R. K. COLE
SANDIA NATIONAL LABORATORY
P.O. BOX 5800, DIVISION 6418
ALBUQUERQUE, NM 87185
USA

M. W. CONEY
CENTRAL ELECTRICITY GENERATING BOARD
BERL-KELVIN AVE.
LEATHERHEAD, KT227SE
UK

I. COOK
UKAEA
CULHAM LABORATORY
ABINGDON, OXFORDSHIRE OX14 3DB
UK

K. Y. COOK
OAK RIDGE NATIONAL LAB.
P.O. BOX X, 45005
OAK RIDGE, TN 37831
USA

B. A. COOK
EG&G IDAHO, INC.
P.O. BOX 1625
IDAHO FALLS, ID 83415
USA

W. R. CORWIN
OAK RIDGE NATIONAL LAB.
P.O. BOX Y, BLDG. 9204-1
OAK RIDGE, TN 37831
USA

R. COWARD
MPR ASSOCIATES, INC.
1050 CONNECTICUT AVE, N.W.
WASHINGTON, DC 20036
USA

S. R. COWNE
BALTIMORE GAS & ELECTRIC
CALVERT CLIFFS - P.O. BOX 1535
LUSBY, MD 20657
USA

W. R. CRAMOND
SANDIA NATIONAL LABORATORY
P.O. BOX 5800
ALBUQUERQUE, NM 87185
USA

M. W. CRUMP
COMBUSTION ENGINEERING
1001 PROSPECT HILL ROAD
WINDSOR, CT 06095
USA

W. H. CULLEN
MATERIALS ENGINEERING ASSOCIATES, INC.
9700-B MARTIN LUTHER KING HWY.
LANHAM, MD 20706
USA

G. E. CUMMINGS
LAWRENCE LIVERMORE NATIONAL LAB.
P.O. BOX 808, L-198
LIVERMORE, CA 94550
USA

R. A. CUSHMAN
NIAGARA MOHAWK POWER CO.
301 PLAINFIELD ROAD
SYRACUSE, NY 13212
USA

D. A. DAHLGREN
SANDIA NATIONAL LABORATORY
P.O. BOX 5800
ALBUQUERQUE, NM 87185
USA

P. M. DALING
BATTELLE PACIFIC NORTHWEST LAB.
P.O. BOX 999
RICHLAND, WA 99352
USA

P. S. DAMERELL
MPR ASSOCIATES, INC.
1050 CONNECTICUT AVE N.W.
WASHINGTON, DC 20036
USA

J. DARLASTON
BERKELEY NUCLEAR LABS
C.E.G.B.
BERKELEY GLOS GL139PB
UK

G. DAVIS
COMBUSTION ENGINEERING
1000 PROSPECT HILL ROAD
WINDSOR, CT 06095
USA

G. DeGRASSI
BROOKHAVEN NATIONAL LAB.
BLDG. 129
UPTON, NY 11973
USA

R. S. DENNING
BATTELLE COLUMBUS
505 KING AVENUE
COLUMBUS, OH 43201
USA

V. DEVITA
ROCKETDYNE (ETEC)
DESOTO AND NORDHOFF
CANOGA PARK, CA 91304
USA

R. DEWIT
NATIONAL BUREAU OF STANDARDS
RM A113, MATERIALS BLDG
GAITHERSBURG, MD 20854
USA

D. R. DIEROKS
ARGONNE NATIONAL LAB.
9700 S. CASS AVE.
ARGONNE, IL 60439
USA

M. diMARZO
UNIVERSITY OF MD.
MECH. ENG. DEPT.
COLLEGE PARK, MD 20742
USA

S. R. DOCTOR
BATTELLE PACIFIC NORTHWEST LAB.
P.O. BOX 999
RICHLAND, WA 99352
USA

C. Y. DODD
OAK RIDGE NATIONAL LAB.
P.O. BOX X, 45005, MS-151
OAK RIDGE, TN 37831
USA

P. K. DOHERTY
COMBUSTION ENGINEERING
WINDSOR
CT, 1000 PROSPECT HILL ROAD, 06095
USA

B. J. DOLAN
DUKE POWER
422 SOUTH CHURCH ST.
CHARLOTTE, NC 28242
USA

J. DROEC
NUCLEAR POWER PLANT KRSKO
VRBINA 12, 68270 KRSKO
KRSKO, 68270
YUGOSLAVIA

S. S. DUA
GENERAL ELECTRIC COMPANY
175 CURTNER AVE.
SAN JOSE, CA 925125
USA

S. W. DUCE
EG&G IDAHO, INC.
P.O. BOX 1625
IDAHO FALLS, ID 83415
USA

J. J. DUCO
CEA FRENCH ATOMIC ENERGY COMMISSION
DAS/SASC,DEN/FAR,BP NO 6
FONTENAY-AUX-ROSES CEDEX, CEDEX 92260
FRANCE

R. DUFFEY
EG&G IDAHO, INC.
P.O. BOX 1625
IDAHO FALLS, ID 83415
USA

S. R. DUGAN
UNIVERSITY OF MARYLAND
RT. 1
COLLEGE PARK, MD 21093
USA

K. DWIVEDY
VIRGINIA POWER
5000 DOMINION BLVD.
GLEN ALLEN, VA 23060
USA

D. B. EBELING-KONING
WESTINGHOUSE
P.O. BOX 355, M/S E 4-12A
PITTSBURGH, PA 15230
USA

J. L. EDSON
EG&G IDAHO, INC.
P.O. BOX 1625
IDAHO FALLS, ID 83415
USA

G. R. EIDAM
BECHTEL
P.O. BOX 72
MIDDLETOWN, PA 17057
USA

D. M. EISSENBERG
OAK RIDGE NATIONAL LAB.
P.O. BOX Y, BLDG 9104-1 MS-1
OAK RIDGE, TN 37831
USA

J. EKMAN
ROLLS-ROYCE & ASSOCIATES LTD.
P.O. BOX 31
DERBY, DE2 8BJ
UK

Z. J. ELAWAR
ARIZONA NUCLEAR POWER PROJECT
11226 NORTH 23RD AVE.
PHOENIX, AZ 85029
USA

T. W. ELLISON
GENERAL ELECTRIC COMPANY
P.O. BOX 1072
SCHENECTADY, NY 12301
USA

G. T. EMBLEY
KNOLLS ATOMIC POWER LABORATORY
BOX 1072
SCHENECTADY, NY 12301
USA

D. ERB
DEPARTMENT OF ENERGY
WASHINGTON, DC 20545
USA

H. A. ERNST
GEORGIA INSTUTUTE OF TECHNOLOGY
ATLANTA, GA 30332
USA

M. ERVE
SIEMENS/KWU
HAMMERBACHERSTRASSE 12 + 14
ERLANGEN, D-8520
FRG

H. FABIAN
SIEMENS/KWU
HAMMERBACHERSTRASSE 12 + 14
ERLANGEN, D-8520
FRG

A. M. FABRY
SCK-CEN
200 BOERETANG
2400 MOL
BELGIUM

C. R. FARRAR
LOS ALAMOS NATIONAL LAB.
MS 5576
LOS ALAMOS, NM 87545
USA

J. FELL
UKAEA/AEE WINFRITH
DORCHESTER
DORSET, DT2 8DH
UK

D. FIGLHUBER
UTL
1000 ABERNATHY RD.
ATLANTA, GA 30328
USA

H. E. FLORA
UNITED ENGINEERS
305 17TH STREET
PHILADELPHIA, PA 19101
USA

E. FOTOPOULOS
BECHTEL
15740 SHADY GROVE ROAD
GAITHERSBURG MD 20877
USA

E. C. FOX
OAK RIDGE NATIONAL LAB
P. O. BOX X
OAK RIDGE TN 37831
USA

M. D. FRESHLEY
BATTELLE PACIFIC NORTHWEST LAB.
P.O. BOX 999
RICHLAND WA 99352
USA

B. C. FRYER
ADVANCED NUCLEAR FUELS CORP.
2101 HORN RAPIDS RD., P.O. BOX 130
RICHLAND WA 99352
USA

E. L. FULLER
ELECTRIC POWER RESEARCH INSTITUTE
3412 HILLVIEW AVE., P.O. BOX 10412
PALO ALTO CA 94303
USA

S. FURUKAWA
TOSHIBA
8 SHINSUGITA-ISOGO-KU
YOKOHAMA KANAGAWA-KEN 235
JAPAN

J. L. GANDRILLE
FRAMATOME
TOUR FIAT CEDEX 16
PARIS FR 92084
FRANCE

F. J. GARDNER
BECHTEL POWER COMPANY
GAITHERSBURG
MD 15740 SHADY GROVE RD. 20878
USA

P. T. GEORGE
CENTRAL ELECTRICITY GENERATING BOARD
BOOTHS HALL
KNUTSFORD CHESHIRE
UK

J. A. GIESEKE
BATTELLE COLUMBUS
505 KING AVENUE
COLUMBUS OH 43201
USA

P. A. GILLES
FRAMATOME
505 KING AVENUE
COLUMBUS OH 43201
USA

T. GINSBERG
BROOKHAVEN NATIONAL LAB
BLDG 820M
UPTON NY 11973
USA

B. GITNICK
ENSA, INC.
P.O. BOX 5537
ROCKVILLE MD 20855
USA

M. W. GOLAY
MASS. INSTITUTE OF TECHNOLOGY
77 MASS. AVE.
CAMBRIDGE MA 02139
USA

M. GOMOLINSKI
CEA FRENCH ATOMIC ENERGY COMMISSION
CEN-FAR, IPSN
FONTENAY-AUX-ROSES CEDEX 92265
FRANCE

R. L. GOODMAN
BATTELLE PACIFIC NORTHWEST LAB
P.O. BOX 999
RICHLAND WA 99352
USA

N. GOTOH
HITACHI, LTD
3-1-1, SAIWAI-CHO
HIYACHI IBARAKI 317
JAPAN

S. R. GREENE
OAK RIDGE NATIONAL LAB
P.O. BOX Y, BLDG 9104-1
OAK RIDGE TN 37831
USA

G. A. GREENE
BROOKHAVEN NATIONAL LAB
BLDG 820M
UPTON NY 11973
USA

W. L. GREENSTREET
OAK RIDGE NATIONAL LAB
P.O. BOX Y, BLDG 9201-3, MS 2
OAK RIDGE TN 37831
USA

M. V. GREGORY
SAVANNAH RIVER LABORATORY
773-41A
AIKEN SC 29808
USA

E. F. GRIER
LAUREL INDUSTRIES
SUITE 1001, 1611 N. KENT ST.
ARLINGTON VA 22209
USA

P. GRIFFITH
MASSACHUSETTS INST. OF TECH.
ROOM 7-044
CAMBRIDGE MA 02139
USA

P. GRUBER
KRAFTWERK UNION AG
HAMMERBACHERSTRASSE 12 + 14
ERLANGEN D-8520
FRG

P. GRUNER
GESELLSCHAFT FUR REAKTORSICHERHEIT
SWERTNERGASSE 1
COLOGNE 5000
FRG

W. E. GUNTHER
BROOKHAVEN NATIONAL LAB
BLDG 130
UPTON NY 11973
USA

J. G. GUPPY
BROOKHAVEN NATIONAL LAB
BLDG 475B
UPTON NY 11973
USA

D. E. GUYON
WESTINGHOUSE BETTIS ATOMIC PWR LAB
P.O. 79
WEST MIFFLIN PA
USA

G. L. GYOREY
GENERAL ELECTRIC
19941 WINTER LN.
SARATOGA CA 015070
USA

F. M. HAGGAG
OAK RIDGE NATIONAL LAB
P.O. BOX X, BLDG 4500-S
OAK RIDGE TN 37831
USA

A. E. HALL
BROOKHAVEN NATIONAL LABORATORY
BLDG. 130
UPTON NY 11973
USA

R. G. HANSON
EG&G IDAHO, INC.
P.O. BOX 1625
IDAHO FALLS ID 83415
USA

D. J. HANSON
EG&G IDAHO, INC.
P.O. BOS 1625
IDAHO FALLS IL 83415
USA

Y. A. HASSAN
TEXAS A & M, DEPT. OF NUCLEAR ENGR.
COLLEGE STATION TX 77843
USA

J. R. HAWTHORNE
MATERIALS ENGINEERING ASSOCIATES, INC.
9700-B MARTIN LUTHER KING HWY.
LANHAM MD 20706
USA

M. HAYASHI
JAPAN NUS
875 FUTOCHO KOUHOKUKU
YOKOHAMA
JAPAN

Y. HAYASHI
KANSAI ELECTRIC POWER CO., INC.
1100 17TH STREET N.W. SUITE 500
WASHINGTON DC 20036
USA

M. R. HAYNS
UKAEA/SRD
WIGSHAW LANE, CULCHETH
WARRINGTON WA3 7NB
UK

T. J. HEAMES
SAIC
2109 AIR PARK RD. SE
ALBUQUERQUE NM 87106
USA

R. A. HEDRICK
TECHNOLOGY FOR ENERGY CORP.
P.O. BOX 22996
KNOXVILLE TN 37933
USA

J. A. HEIL
NETHERLANDS ENERGY RES. FOUNDATION
POSTBOX 1
PETTEN NH 175520
NETHERLANDS

J. C. HELTON
ARIZONA STATE UNIVERSITY
TEMPE AZ 85287
USA

F. P. HENNESSY
E.I. DUPONT
117 COUNTRY PLACE DR.
N. AUGUSTA SC 29841
USA

H. K. HERKENRATH
COMMISSION OF EUROPEAN COMMUNITIES
J.R.C. ISPRA
ISPRA VA 21020
ITALY

R. J. HERTLEIN
KRAFTWERK UNION AG
HAMMERBACHERSTRASSE 12 + 14
ERLANGEN D-8520
FRG

R. T. HESSIAN
STONE & WEBSTER
3 EXECUTIVE CAMPUS
CHERRY HILL NJ 08053
USA

G. F. HEWITT
UKAEA/WRPD
B 392, HARWELL LABORATORY
OXFORDSHIRE OX10 0DY
UK

E. F. HICKEN
GESELLSCHAFT FUR REAKTORSICHERHEIT
FORSCHUNGSGELAENDE
GARCHING 8046
FRG

D. HICKS
UKAEA/WRPD
B 329, HARWELL LABORATORY
OXFORDSHIRE OX11 0RA
UK

L. J. HIGGINBOTHAM
UNIVERSITY OF MARYLAND
1200 FALLS ROAD
BALTIMORE MD 21011
USA

J. C. HIGGINS
BROOKHAVEN NATIONAL LABORATORY
BLDG. 130, 32 LEWIS
UPTON NY 11973
USA

P. R. HILL
PENNSYLVANIA PWR & LIGHT CO.
2 NORTH NINTH STREET
ALLENTOWN PA 18101
USA

J. H. HINTON
SAVANNAH RIVER LABORATORY
707-C RM. 329
AIKEN SC 29808
USA

T. J. HIRONS
LOS ALAMOS NATIONAL LAB
P.O. BOX 1663, MS E561
LOS ALAMOS NM 87545
USA

A. L. HISER
MATERIALS ENGINEERING ASSOCIATES, INC.
9700-B MARTIN LUTHER KING HWY.
LANHAM MD 20706
USA

N. HOBSON
NATIONAL NUCLEAR CORP.
BOOTHS HALL, CHELFORD ROAD
KNUTSFORD CHESHIRE
UK

S. A. HODGE
OAK RIDGE NATIONAL LAB
P.O. BOX Y, BLDG 9104-1
OAK RIDGE TN 37831
USA

L. G. HOEGBERG
SWEDISH NUCLEAR POWER INSPECTORATE
SEHLSTEDTSGATAN 11, BOX 27106
STOCKHOLM S10252
SWEDEN

P. HOFMANN
KERNFORSCHUNGSZENTRUM (KFK)
P.O. BOX 3640
D-7500 KARLSRUHE 1
FRG

C. HOFMAYER
BROOKHAVEN NATIONAL LAB
BLDG. 129
UPTON NY 11973
USA

G. S. HOLMAN
LAWRENCE LIVERMORE NATIONAL LAB
P.O. BOX 808, L-197
LIVERMORE CA 94550
USA

H. L. O. HOLMSTROM
TECHNICAL RESEARCH CENTRE OF FINLAND
P.O. BOX 169
HELSINKI SF 00181
FINLAND

K. W. HOLTZCLAW
GENERAL ELECTRIC COMPANY
175 CURTNER AVENUE, M/C 754
SAN JOSE CA 95125
USA

R. G. HOPPE
WESTINGHOUSE BETTIS ATOMIC PWR LAB
P.O. BOX 79
WEST MIFFLIN PA 15122
USA

J. HORTAL
BROOKHAVEN NATIONAL LAB
BLDG 475B
UPTON, NY 11973
USA

P. Y. HOSEMANN
EIR-EIGG. INST. FUR REAKTORFORSCHUNG
WURENLINGEN OH5303
SWITZERLAND

T. W. HSU
VIRGINIA POWER
5000 DOMINION BLVD.
GLEN ALLEN, VA 23060
USA

Y. Y. HSU
UNIVERSITY OF MARYLAND
RT. 1
COLLEGE PARK, MD 20742
USA

J. M. HU
UNIVERSITY OF MARYLAND
DEPT. OF CIVIL ENGINEERING
COLLEGE PARK, MD 20742
USA

E. W. HUNT, JR.
SAVANNAH RIVER LABORATORY
773-41A, 182
AIKEN, SC 29808
USA

P. H. HUTTON
BATTELLE PACIFIC NORTHWEST LAB
P.O. BOX 999
RICHLAND, WA 99352
USA

J. G. HWANG
ENSA, INC.
P.O. BOX 20130
SAN JOSE, CA 95160
USA

M. L. HYDER
SAVANNAH RIVER LABORATORY
773-41A
AIKEN, SC 29808
USA

T. IGUCHI
JAPAN ATOMIC ENERGY RES. INSTITUTE
TOKAI-MURA
IBARAKI 319-11
JAPAN

H. INHABER
NUS CORPORATION
910 CLOPPER ROAD
GAITHERSBURG, MD 20878
USA

G. R. IRWIN
UNIVERSITY OF MD., DEPT. OF MECH. ENG.
COLLEGE PARK, MD 20742
USA

T. ISHIDA
JAPAN INSTITUTE OF NUCLEAR SAFETY
MITA KOKUSAI BLDG. 1-4-28, MITA
MINATO-KU, TOKYO 108
JAPAN

M. ISHII
ARGONNE NATIONAL LABORATORY
9700 S. CASS AVENUE
ARGONNE, IL 60439
USA

S. K. ISKANDER
OAK RIDGE NATIONAL LAB
P.O. BOX X
OAK RIDGE, TN 37831
USA

K. ITOH
JAPAN NUS COMPANY
2864-3 NAGACHO MIDORI-KU
YOKOHAMA, JAPAN
JAPAN

R. IVANY
COMBUSTION ENGINEERING
1000 PROSPECT HILL ROAD
WINDSOR, CT 06095-500
USA

T. IWAMURA
JAPAN ATOMIC ENERGY RES. INSTITUTE
TOKAI-MURA
IBARAKI 319-11
JAPAN

J. L. JACOBSON
EG&G IDAHO, INC.
P.O. BOX 1625
IDAHO FALLS, ID 83415
USA

P. JAMET
CEA FRENCH ATOMIC ENERGY COMMISSION
DEMT/SMTS/EMSI
GIF S/YVETTE 91191
FRANCE

J. F. JANSKY
BTB-LEONBERG
TONWEG-3
LEONBERG
FRG

D. B. JARRELL
BATTELLE PACIFIC NORTHWEST LAB
510 SIGMA 3 3160 G. W. WAY
RICHLAND, WA 99352
USA

L. JARRIEL
INTERNATIONAL TECHNOLOGY, INC.
575 OAK RIDGE TURNPIKE
OAK RIDGE, TN 37830
USA

R. P. JENKS
LOS ALAMOS NATIONAL LAB
P.O. BOX 1663, MS K555
LOS ALAMOS, NM 87545
USA

G. W. JOHNSEN
EG&G IDAHO, INC.
P.O. BOX 1625
IDAHO FALLS, ID 83415
USA

E. R. JOHNSON
WESTINGHOUSE ELECTRIC CORP.
P.O. BOX 2728
PITTSBURGH, PA 15230
USA

W. R. JOHNSON
U. OF VIRGINIA
NUCLEAR ENERGY DEPT-REACTOR BLDG
CHARLOTTESVILLE, VA 22903
USA

A. B. JOHNSON
BATTELLE PACIFIC NORTHWEST LAB
P.O. BOX 999
RICHLAND, WA 99352
USA

E. R. JOHNSON
WESTINGHOUSE
P.O. 355
PITTSBURGH, PA 15230
USA

R. JOO
CNSNS
INSURGENTES SUR 1776
MEXICO CITY, D.F. 01030
MEXICO

J. A. JOYCE
U.S. NAVAL ACADEMY
MS 11C
ANNAPOLIS, MD 21402
USA

S. P. KALRA
ELECTRIC POWER RESEARCH INSTITUTE
P.O. BOX 10412
PALO ALTO, CA 94303
USA

F. B. K. KAM
OAK RIDGE NATIONAL LAB
P.O. BOX X, 3001
OAK RIDGE, TN 37831
USA

L. D. KANNBERG
BATTELLE PACIFIC NORTHWEST LAB
P.O. BOX 999
RICHLAND, WA 99352
USA

M. F. KANNINEN
SOUTHWEST RESEARCH INSTITUTE
6220 CULEBRA RD.
SAN ANTONIO, TX 78284
USA

H. KANTEE
IMATRON VOIMA OY (IVO)
P.O. BOX 138
HELSINKI SF00101
FINLAND

H. KARWAT
TECHNIGAL UNIVERSITAT MUNCHEN
8046 GARSHING FORSCHUNGSGELANDE
GARCHING 08046
FRG

W. Y. KATO
BROOKHAVEN NATIONAL LABORATORY
BLDG. 197C
UPTON, NY 11973
USA

K. R. KATSMA
EG&G IDAHO, INC.
P.O. BOX 1625
IDAHO FALLS, ID 83415
USA

R. KAWABE
ENERGY RESEARCH LAB., HITACHI, LTD.
1168 MORIYAMA-CHO
HITACHI-SHI IBARAKI-KEN 316
JAPAN

W. KAWAKAMI
JAPAN ATOMIC ENERGY RES. INSTITUTE
1233 WATANUKI-MACHI
TAKASAKI GUNMA KEN 370-12
JAPAN

J. M. KELLY
BATTELLE PACIFIC NORTHWEST LAB
P.O. BOX 999
RICHLAND, WA 99352
USA

R. M. KEMPER
WESTINGHOUSE
4043 W. BENDEN DRIVE
MURRYSVILLE, PA 15668
USA

M. F. KENNEDY
ENSA, INC.
4550 N. BAILEY
BUFFALO, NY 14226
USA

R. C. KERN
UAI/CDC
6003 EXECUTIVE BLVD.
ROCKVILLE, MD 20852
USA

J. G. KEUSENHOFF
BESELLSCHAFT FUR REAKTORSICHERHEIT
SCHWERTNERGASSE 1
COLOGNE 5000
FRG

S. KIM
KOREAN ATOMIC ENERGY RESEARCH INST.
DAEDUK-DANJI, P.O. BOX 7
CHOONG-NAM
KOREA

F. D. KING
SAVANNAH RIVER LABORATORY
773-41A, ROOM 252
AIKEN, SC 29808
USA

W. L. KIRK
LOS ALAMOS NATIONAL LAB
P.O. BOX 1663
LOS ALAMOS, NM 87545
USA

M. KODA
MITSUBISHI ATOMIC POWER INDUSTRIES
SHIBAKOUEN
MINATO-KU, TOKYO 105
JAPAN

S. J. KOSKI
TVO POWER COMPANY LTD.
SF-27160 OLKILUOTO
SUOMI
FINLAND

C. A. KOT
ARGONNE NATIONAL LAB.
9700 S. CASS AVE.-BLDG 335
ARGONNE, IL 60439
USA

J. J. KOZIOL
COMBUSTION ENGINEERING, INC.
1000 PROSPECT HILL ROAD
WINDSOR, CT 06095-0500
USA

B. KUCZERA
KERNFORSCHUNGSZENTRUM (K.F.K.)
P.O. BOX 3640
D-7500 KARLSRUHE 1
FRG

Y. KUKITA
JAPAN ATOMIC ENERGY RES. INSTITUTE
TOKAI-MURA
IBARAKI 319-11
JAPAN

Z. R. KULJIS
COMBUSTION ENGINEERING
1000 PROSPECT HILL ROAD
WINDSOR, CT 06095
USA

D. KUPPERMAN
ARGONNE NATIONAL LABORATORY
9700 S. CASS AVENUE
ARGONNE, IL 60302
USA

R. J. KURTZ
BATTELLE PACIFIC NORTHWEST LAB
P.O. BOX 999
RICHLAND, WA 99352
USA

K. P. KUSSMAUL
UNIVERSITY OF STUTTGART
PFAFFENWALDRING 32
SUTTGART 80 7000
FRG

T. E. LAATS
EG&G IDAHO, INC.
P.O. BOX 1625
IDAHO FALLS, ID 83415
USA

F. LAM
ONTARIO HYDRO
700 UNIVERSITY AVE., H-11
TORONTO M5G1X6
CANADA

R. T. LANDET
ROCKWELL INTERNATIONAL
6716 DARYN DR.
WESTHILLS, CA 91307
USA

P. M. LAND
U.S. DEPARTMENT OF ENERGY
NE-42
WASHINGTON, DC 20545
USA

R. E. LAND
DEPARTMENT OF ENERGY
9800 S. CASS AVE
ARGONNE, IL 60439
USA

B. P. LALIZAU
AMERICAN ELECTRIC POWER SERVICE CORP.
1 RIVERSIDE PLAZA
COLUMBUS OH 43215
USA

S. Y. LEE
ARGONNE NATIONAL LABORATORY
9700 S. CASS AVENUE
ARGONNE, IL 60439
USA

M. LEE
BROOKHAVEN NATIONAL LABORATORY
BUILDING 130
UPTON, NY 11973
USA

J. R. LEHNER
BROOKHAVEN NATIONAL LABORATORY
BUILDING 130
UPTON, NR. 11973
USA

I. S. LEVY
BATTELLE PACIFIC NORTHWEST LAB
P.O. BOX 999
RICHLAND, WA 99352
USA

C. K. LEWE
NUS CORPORATION
910 CLOPPER ROAD
GAITHERSBURG MD 20878
USA

K. J. LIESCH
GESELLSCHAFT FUR REAKTORSICHERHEIT
FORSCHUNGSGELAENDE
GARCHING 8046
FRG

T.-K. LIN
INSTITUTE OF NUCLEAR ENERGY RESEARCH
P.O. BOX 3
LUNG-TAN, TAIWAN
ROC

C. W. LIN
ROBERT L. CLOUD ASSOCIATES
125 UNIVERSITY AVENUE
BERKLEY, CA 94710
USA

F. W. LINCOLN
WESTINGHOUSE
W. MIFFLIN, PA
USA

W. B. LOEWENSTEIN
ELECTRIC POWER RESEARCH INSTITUTE
3412 HILLVIEW AVE., P.O. BOX 10412
PALO ALTO, CA 94303
USA

R. J. LOFARO
BROOKHAVEN NATIONAL LAB.
BLDG 130
UPTON, NY 11973
USA

J. Y. LOPEZ
ETSII CATEDRA DE TECHNOLOGIA NUCLEAR
JOSE GUTIERREZ ABASCAL, 2
MADRID 28006
SPAIN

F. J. LOSS
MATERIALS ENGINEERING ASSOCIATES, INC.
9700-B MARTIN LUTHER KING HWY.
LANHAM, MD 20706
USA

A. L. LOWE
BABCOCK & WILCOX
P.O. BOX 10935
LYNCHBURG, VA 24506
USA

R. J. LUTZ, JR.
WESTINGHOUSE ELECTRIC
P. O. BOX 355
PITTSBURGH, PA 15230
USA

P. E. MacDONALD
EG&G IDAHO, INC.
P.O. BOX 1625
IDAHO FALLS, ID 83415
USA

L. L. MADNI
BROOKHAVEN NATIONAL LAB.
BLDG 130
UPTON, NY 11973
USA

J. MALHERBE
CEA FRENCH ATOMIC ENERGY COMMISSION
DEMT/SMTS/RDMS
GIF S/YVETTE 91191
FRANCE

A. P. MALINAUSKAS
OAK RIDGE NATIONAL LAB.
P.O. BOX X, BLDG 45005 MS-135
OAK RIDGE, TN 37831
USA

A. N. MALLEN
BROOKHAVEN NATIONAL LAB.
BLDG 475B
UPTON, NY 11973
USA

P. MARSILI
ENEA/DISP
VIA VITALIANO BRANDATI 48
ROME 00144
ITALY

J. MARTIN
MASS. INST. OF TECHNOLOGY
77 MASSACHUSETTS AVE., RM 24-210
CAMBRIDGE, MA 02139
USA

A. MARYRAY
TEXAS UTILITIES ELECTRIC
400 NORTH OLIVE STREET, L. B. 81
DALLAS, TX 75201
USA

F. MASUDA
TOSHIBA CORP.
9-3-104, 5-CHOME 15000
YOKOHAMA
JAPAN

M. J. MATSUBARA
CEN. RES. INST. OF ELEC. POWER INDUSTRY
11-1 IWATO-KITA, 2-CHOME
KOMAE, TOKYO 157
JAPAN

B. MAVKO
J. STEFAN INSTITUTE
JAMOVA 39
LJUBLJANA 6111
YUGOSLAVIA

R. K. McCARDELL
EG&G IDAHO, INC.
P.O. BOX 1625
IDAHO FALLS, ID 83415
USA

D. J. McCLOSKEY
SANDIA NATIONAL LABORATORY
P.O. BOX 5800
ALBUQUERQUE, NM 87185
USA

D. E. McCREERY
EG&G IDAHO, INC.
P.O. BOX 1625
IDAHO FALLS, ID 83415
USA

W. N. McELROY
BATTELLE PACIFIC NORTHWEST LAB.
P.O. BOX 999
RICHLAND, WA 99352
USA

M. McGURK
BABCOCK & WILCOX
P.O. BOX 10935, 3315 OLD FOREST RD.
LYNCHBURG, VA 24506-0935
USA

R. N. H. McMILLAN
UKAEA/SRD
WIGSHAW LANE, CULCHETH
WARRINGTON WA34NE
UK

D. M. MEARS
BABCOCK & WILCOX
P.O. BOX 10935, 3315 OLD FOREST RD.
LYNCHBURG, VA. 24506-0935
USA

C. MEDICH
VIA NINO BIXIO
PIACENZA
ITALY

J. A. MEINKE
CONSUMER POWER CO.
1945 W. PARNALL RD.
JACKSON, MI
USA

D. M. MELIN
CEA FRENCH ATOMIC ENERGY COMMISSION
SETH/LES - C.E.N.G. - BSX
GRENOBLE CEDEX 38041
FRANCE

B. MERCER
UNIVERSITY OF MARYLAND
COLLEGE PARK, MD 20742
USA

O. M. MERCIER
EIR-EIDG. INST. FUR REAKTORFORSCHUNG
WURENLINGEN OH5303
SWITZERLAND

Y. MEYZAUD
FRAMATOME
TOUR FIAT CEDEX 16
PARIS, FR 92084
FRANCE

J. S. MILLER
GULF STATES UTILITIES CO.
P. O. BOX 220
ST. FRANCISVILLE, LA 70775
USA

C. S. MILLER
EG&G IDAHO, INC.
P.O. BOX 1625
IDAHO FALLS, ID 83415
USA

R. L. MILLER
WESTINGHOUSE HANFORD COMPANY
P.O. BOX 1970
RICHLAND, WA 99352
USA

H. A. MITCHELL
INTERNATIONAL TECHNOLOGY CORP.
575 OAK RIDGE TURNPIKE
OAK RIDGE, TN 37830
USA

S. M. MODRO
EG&G IDAHO, INC.
P.O. BOX 1625
IDAHO FALLS, ID 83415
USA

C. L. MOHR
MOHR & ASSOCIATES
1440 AGNES
RICHLAND, WA 99352
USA

R. O. MONTGOMERY
TEXAS A&M UNIVERSITY
NUCLEAR ENGINEERING DEPT.
COLLEGE STATE, TX 77843
USA

B. S. MONTY
WESTINGHOUSE ELECTRIC
P.O. BOX 355
PITTSBURGH, PA 15235
USA

J. MORIN
SAVANNAH RIVER LABORATORY
773-41A
AIKEN, SC 29808
USA

J. A. MORTENSEN
EG&G IDAHO, INC.
P.O. BOX 1625
IDAHO FALLS, ID 83415
USA

F. E. MOTLEY
LOS ALAMOS NATIONAL LAB.
P.O. BOX 1663
LOS ALAMOS, NM 87545
USA

L. D. MUHLSTEIN
WESTINGHOUSE HANFORD COMPANY
P.O. BOX 1970
RICHLAND, WA 99352
USA

Y. MURAO
JAPAN ATOMIC ENERGY RESEARCH INST.
TOKAI-MURA
IBARAKI 319-11
JAPAN

R. C. MURRAY
LAWRENCE LIVERMORE NATIONAL LAB.
P. O. BOX 808, L-197
LIVERMORE, CA 94550
USA

S. A. NAFF
KRAFTWERK UNION AG
HAMMERBACHERSTRASSE 12 + 14
ERLANGEN D-8520
FRG

R. K. NANSTAD
OAK RIDGE NATIONAL LAB.
P.O. BOX X, BLDG 4500-S
OAK RIDGE, TN 37831
USA

D. J. NAUS
OAK RIDGE NATIONAL LAB.
P.O. BOX Y, BLDG. 9204-1
OAK RIDGE, TN 37831
USA

H. H. NEELY
ROCKWELL INTERNATIONAL
6633 CANOGA AVENUE
CANOGA PARK, CA 91304
USA

L. A. NEIMARK
ARGONNE NATIONAL LABORATORY
9700 S. CASS AVENUE
ARGONNE, IL 60302
USA

L. Y. NEYMOTIN
BROOKHAVEN NATIONAL LAB.
BLDG 475B
UPTON, NY 11973
USA

S. J. NIEMCZYK
GULL ASSOCIATES
1545 18TH ST. NW #112
WASHINGTON, DC 20036
USA

M. V. NIKITIN
SCIAE, INTERNATIONAL RELATIONS DEPT.
STAROMONETNYI, 26
MOSCOW 109180
USSR

S. NISHINO
ELECTRIC POWER RESEARCH INSTITUTE
3412 HILLVIEW AVE., P.O. BOX 10412
PALO ALTO, CA 94303
USA

C. K. NITHIANANDAN
BABCOCK & WILCOX
LYNCHBURG, VA 24503
USA

K. K. NIYOGI
UNITED ENGINEERS & CONST. INC.
30 S. 17TH STREET
PHILADELPHIA PA 19101
USA

Y. NOGUCHI
CHUBU ELECTRIC POWER CO. INC.
900 17TH ST. N.W., SUITE 714
WASHINGTON DC 20006
USA

P. NORTH
EG&G IDAHO, INC.
P. O. BOX 1625
IDAHO FALLS ID 83415
USA

J. G. O'BRIEN
UNIVERSITY OF MARYLAND
RT. 1
COLLEGE PARK MD 21093
USA

C. F. OBENCHAIN
EG&G IDAHO, INC.
P.O. BOX 1625
IDAHO FALLS ID 83415
USA

K. OKABE
MITSUBISHI ATOMIC POWER INDUSTRIES
4-1, SHIBAKOUEN 2-CHOME
MINATO-KU TOKYO
JAPAN

R. C. OLSON
BALTIMORE GAS & ELECTRIC
CALVERT CLIFFS - P.O. BOX 1535
LUSBY MD 20657
USA

H. P. OLSON
SAVANNAH RIVER LABORATORY
AIKEN SC 29808
USA

A. M. OMAR
ATOMIC ENERGY CONTROL BOARD
270 ALBERT STREET
OTTAWA KIPS59
CANADA

A. OMOTO
TOKYO ELECTRIC POWER
POTOMAC
MD. 8605 TIMBER HILL LANE 20854
USA

A. T. ONESTO
ETEC
P.O. BOX 1449
CANOGA PARK CA 91304
USA

D. J. OSETEK
EG&G IDAHO, INC.
P.O. BOX 1625
IDAHO FALLS ID 83415
USA

L. J. OTT
OAK RIDGE NATIONAL LAB
P.O. BOX Y, BLDG 9104-1
OAK RIDGE TN 37831
USA

J. PAN
UNIVERSITY OF MICHIGAN
2250 G. G. BROWN
ANN ARBOR MI 48109
USA

B. PANELLA
POLITECNICO DI TORINO
CORSO DUCA DEGLI ABRUZZI, 24
TORINO 10100
ITALY

M. V. PARECE
BABCOCK & WILCOX
P.O. BOX 10935, 3315 OLD FOREST RD.
LYNCHBURG VA 24506-0935
USA

A. C. PAYNE, JR.
SANDIA NATIONAL LABORATORY
P.O. BOX 5800
ALBUQUERQUE NM 87185
USA

G. PETRANGELI
ENEA/DISP
VIA VITALIANO BRANCATI 48
ROME 00144
ITALY

L. PETRUSHA
BABCOCK & WILCOX
P.O. BOX 10935, 3315 OLD FOREST ROD.
LYNCHBURG VA 24506-0935
USA

D. A. PETTI
EG&G IDAHO, INC.
P.O. BOX 1625
IDAHO FALLS ID 83415
USA

L. K. PIPLIES
COMMISSION OF EUROPEAN COMMUNITIES
I-21020
ISPRA I-21020 ISPRA
ITALY

M. P. PLESSINGER
EG&G IDAHO, INC.
P.O. BOX 1625
IDAHO FALLS ID 83415
USA

M. G. PLYS
FAUSKE & ASSOCIATES, INC.
16W070 W. 83RD STREET
BURR RIDGE IL 60521
USA

M. Z. PODOWSKI
RENSSELAER POLYTECHNIC INST.
TROY NY 12180
USA

D. J. POSAKONY
BATTELLE PACIFIC NORTHWEST LAB.
P.O. BOX 999
RICHLAND WA 99352
USA

T. PRATT
BROOKHAVEN NATIONAL LABORATORY
BUILDING 130
UPTON NY 11973
USA

D. A. PRELEWICZ
ENSA, INC.
P.O. BOX 5537
ROCKVILLE MD 20855
USA

J. G. PRUETT
OAK RIDGE NATIONAL LAB.
P.O. BOX X, BLDG 4500S MS-135
OAK RIDGE TN 37831
USA

C. E. PUGH
OAK RIDGE NATIONAL LAB.
P.O. BOX Y
OAK RIDGE TN 37831
USA

W. R. QUEALY
HM NUCLEAR ISTALLATIONS INSPECTORATE
ST. PETERS HOUSE, BALLIOL ROAD
BOOTLE MERSEYSIDE L203LZ
UK

K. RAES
BATTELLE FRANKFURT
AM ROMERHOF 35
FRANKFORT
FRG

F. RAHN
ELECTRIC POWER RESEARCH INSTITUTE
3412 HILLVIEW AVE.
PALO ALTO CA 94303
USA

N. C. RASMUSSEN
MSASS INSTITUTE OF TECHNOLOGY
ROOM 24-205
CAMBRIDGE MA 02139
USA

M. REICH
BROOKHAVEN NATIONAL LAB.
BLDG 129
UPTON NY 11973
USA

H. RENNER
NUS CORPORATION
910 CLOPPER ROAD
GAITHERSBURG MD 20878
USA

L. N. RIB
LNR ASSOCIATES
8605 GRIMSBY COURT
POTOMAS MD 20854
USA

D. R. RILEY
ELECTRIC POWER RESEARCH INST.
501 FOREST AVE # 501
PALO ALTO CA 94301
USA

C. L. RITCHEY
BABCOCK & WILCOX
P.O. BOX 10935, 3315 OLD FOREST RD.
LYNCHBURG VA 24506-0935
USA

C. M. ROBERTS
UNIVERSITY OF MARYLAND
COLLEGE PARK MD 20742
USA

D. E. ROBERTSON
BATTELLE PACIFIC NORTHWEST LAB
P.O. BOX 999
RICHLAND WA 99352
USA

G. E. ROBINSON
PENN STATE UNIVERSITY
231 SACKETT BLDG
UNIVERSITY PARK PA 16902
USA

U. S. ROHATGI
BROOKHAVEN NATIONAL LAB.
BLDG 475B
UPTON NY 11973
USA

J. Y. ROTZ
BECHTEL
15740 SHADY GROVE RD.
AITHERSBURG MD 20877
USA

J. C. ROUSSEAU
CEA FRENCH ATOMIC ENERGY COMMISSION
CENTRE D'ETUDES NUCLEAIRES
GRENOBLE 38041
FRANCE

D. RUBIO
ELECTRIC POWER RESEARCH INSTITUTE
3412 HILLVIEW AVE.
PALO ALTO CA 94303
USA

K. D. RUSSEL
EG&G IDAHO, INC.
P.U. BOX 1625
IDAHO FALLS ID 83415
USA

B. SAFFELL
BATTELLE COLUMBUS DIVISION
505 KING AVENUE
COLUMBUS OH 43201
USA

H. SAKAMOTO
NUCLEAR POWER ENGINEERING TEST CENTER
3-13, 4-CHOME, TORANOMON
MINATO-KU, TOKYO 105
JAPAN

H. SAKURAGI
JAPAN INSTITUTE OF NUCLEAR SAFETY
MITA KOKUSAI BLDG., 1-4-28, MITA
MINATO-KU, TOKYO 108
JAPAN

J. SALUJA
VIKING SYSTEMS INTERNATIONAL
12; 1; HIGHLAND AVE.
PITTSBURG PA 15206
USA

J. E. SALYARDS
BALTIMORE GAS & ELECTRIC
CALVERT CLIFFS - P.O. BOX 1535
LUSBY MD 20657
USA

M. SARRAM
UNITED ENGINEERS & CONST. INC.
30 S. 17TH ST., P.O. BOX 8223
PHILADELPHIA PA 19101
USA

I. SATO
JAPAN STEEL WORKS
4 CHATSU-MACHI
MURORAN HOKKAIDO
JAPAN

D. G. SATTERWHITE
EG&G IDAHO, INC.
P.O. BOX 1625
IDAHO FALLS ID 83415
USA

M. B. SATTISON
EG&G IDAHO, INC.
P.O. BOX 1625
IDAHO FALLS ID 83415
USA

J. C. SCARBOROUGH
JCS LIMITED
6936 RACE NORSE LANE
ROCKVILLE MD 20852
USA

P. J. SCHALLY
GESELLSCHAFT FUR REAKTORSICHERHEIT
SCHWERTNERGASSE 1
KOELN 5060
FRG

A. P. SCHMITT
CEA FRENCH ATOMIC ENERGY COMMISSION
CEN-FAR IPSN
FONTENAY-AUX-ROSES CEDEX 92265
FRANCE

R. R. SCHULTZ
EG&G IDAHO, INC.
P.O. BOX 1625
IDAHO FALLS ID 83415
USA

C. W. SCHWARTZ
UNIVERSITY OF MD., DEPT. OF CIVIL ENG.
COLLEGE PARK MD 20742
USA

J. H. SCOBEL
WESTINGHOUSE
MEC E. 3-21
PITTSBURGH PA 15230
USA

F. SEARS
NORTHEAST UTILITIES
P. O. BOX 270
HARTFORD CT 06141-0270
USA

S. S. SETH
THE MITRE CORPORATION
7525 COLSHIRE DRIVE, MAIL - W721
McLEAN VA 22102
USA

R. T. SEWELL
RISK ENGINEERING INC.
5255 PINE RIDGE ROAD
GOLDEN CO 80403
USA

W. J. SHACK
ARGONNE NATIONAL LABORATORY
BUILDING 212
ARGONNE IL 60302
USA

V.K. SHAH
EG&G IDAHO, INC.
11428 ROCKVILLE PIKE, SUITE 410
ROCKVILLE MD 20852
USA

R. H. SHANNON
CONSULTANT
P.O.BOX 2264
ROCKVILLE MD 20852
USA

R. SHARMA
AMER. *N ELECTRIC POWER SERVICE CORP
1 RIVERSIDE PLAZA
COLUMBUS OH 43216
USA

R. A. SHAW
EG&G IDAHO, INC.
P.O. BOX 1625
IDAHO FALLS ID 83415
USA

J. M. SHEA
NORTHEAST UTILITIES
107 SELDEN ST., W-15
BERLIN CT 06037
USA

L. SHEN
ATOMIC ENERGY COUNCIL,EXECUTIVE YUAN
67, LANE144, KEELUNG RD., SEC.4
TAIPEI TAIWAN 107
ROC

D. L. SHERWOOD, JR.
U.S. DEPARTMENT OF ENERGY
GERMANTOWN MD 20767
USA

P. SHEWMON
ADVISORY COMM. ON REACTOR SAFEGUARDS
2477 LYTHAM ROAD
COLUMBUS OH 43220
USA

D. J. SHIMEOK
WESTINGHOUSE
RD2, BOX 194
EXPORT PA 15632
USA

M. SHIMIZU
JAPAN ATOMIC ENERGY RES. INSTITUTE
TOKAI-MURA IBARAKI-KEN 319-11
JAPAN

M. S. SHINKO
EMERGENCY RESPONSE TEAM
P.O. BOX 129
WASHINGTON GROVE MD 20880
USA

E. G. SILVER
OAK RIDGE NATIONAL LAB.
P.O. BOX Y, BLDG 9201-3, MS 5
OAK RIDGE TN 37831
USA

F. A. SIMONEN
BATTELLE PACIFIC NORTHWEST LAB
P.O. BOX 999
RICHLAND WA 99352
USA

O. M. SLAUGHTER
OAK RIDGE NATIONAL LAB.
P.O. BOX X, BLDG 4500-S
OAK RIDGE TN 37831
USA

M. K. SMITH
BABCOCK & WILCOX
P.O. BOX 10935, 3315 OLD FOREST RD.
LYNCHBURG VA 24506-0935
USA

A. W. SNYDER
SANDIA NATIONAL LABORATORY
P.O. BOX 5800, DIVISION 6500
ALBUQUERQUE NM 87185
USA

K. SODA
JAPAN ATOMIC ENERGY RES. INSTITUTE
TOKAI-MURA IBARAKI-KEN 319-11
JAPAN

H. G. SONNENBURG
GESELLSCHAFT FUR REAKTORSICHERHEIT
FORSCHUNGSGELAENDE
GARCHING 8046
FRG

P. SOO
BROOKHAVEN NATIONAL LAB.
BLDG 830
UPTON NY 11973
USA

J. L. SPRUNG
SANDIA NATIONAL LABORATORY
P.O. BOX 5800
ALBUQUERQUE NM 87185
USA

D. SQUARER
WESTINGHOUSE R&D
1310 BEULAH RD.
PITTSBURGH PA 15235
USA

M. G. SRINIVASAN
ARGONNE NATIONAL LAB.
9700 S. CASS AVE-BLDG 335
ARGONNE IL 60439
USA

K. E. ST. JOHN
YANKEE ATOMIC ELECTRIC COMPANY
1671 WORCESTER RD.
FRAMINGHAM MA 01701
USA

H. STADTKE
COMMISSION OF EUROPEAN COMMUNITIES
121020, ISPRA
ISPRA
ITALY

R. STEELE
EG&G IDAHO, INC.
P.O. BOX 1625
IDAHO FALLS ID 83415
USA

J. P. STEELMAN
BALTIMORE GAS & ELECTRIC
LUSBY POST OFFICE
LUSBY MD 20657
USA

N. PONOMAREV- STEPNOI
I. V. KURCHATOV INST. OF ATOMIC ENERGY
KURCHATOV SQUARE
MOSCOW 123182
USSR

P. M. STOOP
NETHERLANDS ENERGY RES.FOUNDATION ECN
3 WESTERDUINWEG, P.O. BOX 1
PETTEN (NH) 1755 ZG
NETHERLANDS

E. STUBBE
TRACTEBEL
31 RUE DE LA SCIENCE
BRUSSELS 1040
BELGIUM

M. SUBUDHI
BROOKHAVEN NATIONAL LAB.
BLDG 130
UPTON NY 11973
USA

W. SUBNET
ELECTRIC POWER RESEARCH INSTITUTE
3412 HILLVIEW AVE.
PALO ALTO CA 94303
USA

R. M. SUMMERS
SANDIA NATIONAL LABORATORY
P.O. BOX 5800, DIVISION 6418
ALBUQUERQUE NM 87185
USA

B. SUN
ELECTRIC POWER RESEARCH INSTITUTE
3412 HILLVIEW AVE.
PALO ALTO CA 94303
USA

R. K. SUNDARAM
YANKEE ATOMIC ELECTRIC COMPANY
1671 WORCESTER ROAD
FRAMINGHAM MA 01519
USA

D. G. SWANSON
PDI TECHNOLOGY
246 VIKING AVE.
BREA CA 92621
USA

H. TAKAHASHI
MITSUBISHI ATOMIC POWER INDUSTRIES
4-1, SHIBAKOUEN 2-CHOME
MINATO-KU TOKYO
JAPAN

Y. K. TANG
ELECTRIC POWER RESEARCH INSTITUTE
3412 HILLVIEW AVE.
PALO ALTO CA 94303
USA

H. T. TANG
ELECTRIC POWER RESEARCH INST.
3412 HILLVIEW AVE.
PALO ALTO CA 94303
USA

K. TASAKA
JAPAN ATOMIC ENERGY RES. INSTITUTE
TOKAI-MURA IBARAKI-KEN 319-11
JAPAN

J. H. TAYLOR
BROOKHAVEN NATIONAL LAB.
BLDG 130
UPTON NY 11973
USA

T. A. THEOFANOUS
UNIV. OF CALIF., SANTA BARBARA
817 SEA RANCH DRIVE
SANTA BARBARA CA 93109
USA

E. W. THOMAS
BECHTEL EASTERN POWER
SHADY GROVE ROAD
GAITHERSBURG MD
USA

B. J. TOLLEY
COMMISSION OF THE EUROPEAN COMM.
200, RUE DE LA LOI
BRUSSELS 1049
BELGIUM

B. TOLMAN
EG&G IDAHO, INC.
2355 TASMAN
IDAHO FALLS ID 83401
USA

K. TOMOMURA
CENTURY RESEARCH CENTER CORPORATION
3-6-2 NIHONBASHI- HONCHO 3-CHOME
CHUO-KU, TOKYO 103
JAPAN

L. S. TONG
TAI
9733 LOOKOUT PLACE
GAITHERSBURG MD 20879
USA

F. TOTSUKA
ENERGY RESEARCH LAB., HITACHI, LTD
1-29-4 HANAYAMA-CHO
HITACHI-SHI IBARAKI-KEN 316
JAPAN

H. E. TRAMMELL
OAK RIDGE NATIONAL LAB.
P.O. BOX Y, BLDG 9201-3
OAK RIDGE TN 37831
USA

T. M. TRAN
TENNESSEE VALLEY AUTHORITY
400 SUMMIT HILL
KNOXVILLE TN 37902
USA

J. R. TRAVIS
LOS ALAMOS NATIONAL LAB.
GROUP T-3, M/S B216
LOS ALAMOS NM 87545
USA

D. E. TRUE
ERIN ENGINEERING
1650 MT. DIABLO BLVD., SUITE 600
WALNUT CREEK CA 94596
USA

A. A. TUDOR
SAVANNAH RIVER LABORATORY
773-41A
AIKEN SC 29808
USA

N. K. TUTU
BROOKHAVEN NATIONAL LABORATORY
BUILDING 820M
UPTON NY 11973
USA

T. UESHIMA
ELECTRIC POWER RESEARCH INSTITUTE
3412 HILLVIEW AVE., P.O. BOX 10412
PALO ALTO CA 94303
USA

T. UMEMOTO
ISHIKAWAJIMA-HARIMA HEAVY INDUSTRIES
1-SHIN-NAKARA JSOOO-KU
YOKAHAMA 235
JAPAN

K. D. UNDERWOOD
UNIVERSITY OF MARYLAND
COLLEGE PARK MD 20742
USA

S. UNWIN
BROOKHAVEN NATIONAL LABORATORY
BLDG 130
UPTON NY 11973
USA

R. A. VALENTIN
ARGONNE NATIONAL LAB.
9700 S. CASS AVE-BLDG 208
ARGONNE IL 60439
USA

R. M. VAN KUIJK
N. V. KEMA
POSTBUS 9035, UTRECHTSEWEG 310
6800 ET ARNHEM
NETHERLANDS

N. VASUDEVAN
BABCOCK & WILCOX
P.O. BOX 10935, 3315 OLD FOREST ROAD
LYNCHBURG VA 24506-0935
USA

C. M. VERTES
WESTINGHOUSE
NORTHERN PIKE RD.
MONROEVILLE PA 15146
USA

O. VESCOVI
SIET
NINO BIXIO 27
PIACENZA
ITALY

W. E. VESELY
SAIC
SUITE 245, 2929 KENNY ROAD
COLUMBUS OH 43221
USA

J. L. VON HERRMANN
IT-DELIAN
2011 EYE STREET
WASHINGTON DC 20006
USA

W. A. VON RIESEMANN
SANDIA NATIONAL LABORATORY
P.O. BOX 5800, DIVISION 6442
ALBUQUERQUE NM 87185
USA

M. WALTER
UNIVERSITY OF MARYLAND
663 W. FAYETTE STREET
BALTIMORE MD 21201
USA

S. F. WANG
INSTITUTE OF NUCLEAR ENERGY RESEARCH
P.O. BOX 3-13
LUNG-TAN TAIWAN 32500
ROC

M. E. WATERMAN
EG&G IDAHO, INC.
11428 ROCKVILLE PIKE, #410
ROCKVILLE MD
USA

W. L. WEAVER
EG&G IDAHO, INC.
P.O. BOX 1625
IDAHO FALLS ID 83415
USA

E. T. WEBER
WESTINGHOUSE HANFORD COMPANY
P.O. BOX 1970
RICHLAND WA 99352
USA

J. R. WEEKS
BROOKHAVEN NATIONAL LAB
BLDG 130
UPTON NY 11973
USA

P. A. WEISS
SIEMENS-KWU
HAMMERBACHERSTRASSE 12 + 14
ERLANGEN D-8520
FRG

A. J. WEISS
BROOKHAVEN NATIONAL LAB
BLDG 197C
UPTON NY 11973
USA

E. WENZINGER
MPR ASSOCIATES, INC.
1050 CONNECTICUT AVE N.W.
WASHINGTON DC 20036
USA

E. T. WESSEL
EDWARD T. WESSEL, CONSULTING ENG.
316 WOLVERINE STREET
HAINES CITY FL 33844
USA

R. A. WESTON
COMBUSTION ENGINEERING
1000 PROSPECT HILL RD.
WINDSOR CT 06095
USA

H. WESTPHAL
GESELLSCHAFT FUR REAKTORSICHERHEIT
SCHWERTNERGASSE 1
COLOGNE 5000
FRG

D. L. WHITCOMB
WASHINGTON PUBLIC POWER SUPPLY SYS.
3000 G. WASH. WAY-P.O. BOX 968
RICHLAND WA 99352
USA

T. J. WHITEHEAD
SAIC
101 S. PARK AVE
IDAHO FALLS ID 83402
USA

P. G. WHITCOP
SAVANNAH RIVER LABORATORY
773-41A
AIKEN SC 29808
USA

G. M. WILKOWSKI
BATTELLE-COLUMBUS DIVISION
505 KING AVENUE
COLUMBUS OH 43201
USA

K. A. WILLIAMS
SAIC
2109 AIR PARK RD. SE
ALBUQUERQUE NM 87106
USA

K. WINEGARDNER
BATTELLE PACIFIC NORTHWEST LAB
P.O. BOX 999
RICHLAND WA 99352
USA

F. WINKLER
KRAFTWERK UNION AG
HAMMERBACHERSTRASSE 12 + 14
ERLANGEN D-8520
FRG

L. WOLF
PROJECT HDR/KERNFORSCHUNGSZENTRUM
HOSTFACH 3640
7500 KARLSRUHE 1
FRG

K. WOLFERT
GESELLSCHAFT FUR REAKTORSICHERHEIT
FORSCHUNGSGELAENDE
GARCHING 8046
FRG

Y. C. WONG
CEGB GENERATION DEV. & CONST. DIV.
BARNETT WAY
BARNWOOD GLOUCESTER GL4 7RS
UK

D. WONG
GENERAL PUBLIC UTILITIES
1 UPPER POND ROAD
PARSIPPANY NJ 07054
USA

L. R. WOOD
GENERAL ELECTRIC COMPANY
P.O. BOX 1072, BUILDING P-1, ROOM 111
SCHENECTADY NY 12301
USA

W. WULFF
BROOKHAVEN NATIONAL LAB
BLDG 475B
UPTON NY 11973
USA

O. YAGAWA
UNIVERSITY OF TOKYO
HONGO, BUNKYOKU
TOKYO 113
JAPAN

K. K. YOON
BABCOCK & WILCOX
P.O. BOX 10935, 3315 OLD FOREST ROAD
LYNCHBURG VA 24506-0935
USA

E. YOSHIKOWA
NUCLEAR POWER ENGINEERING TEST CENTER
NO. 2 AKIYAMA BLDG., 6-2, 3-CHOME, MIN.
TOKYO 105
JAPAN

R. YOUNG
UKAEA/SRD
WIGSHAW LANE
CULCHETH WARRINGTON WA3 4NE
UK

J. ZDAREK
CZECHOSLOVAK EMBASSY
3900 LINNEAN AVE. N.W.
WASHINGTON DC 20008
CZECHESLOVAKIA

K. ZIEGLOWSKI
KWU-OFFENBACH
6050 OFFENBACH BERLINER STR.
FRG

R. ZIPPER
GESELLSCHAFT FUR REAKTORSICHERHEIT
SCHWERTNERGASSE 1
COLOGNE
FRG

R. ZOGRAN
MPR ASSOCIATES, INC.
1050 CONNECTICUT AVE N.W.
WASHINGTON DC 20036
USA

PROCEEDINGS OF THE
FIFTEENTH WATER REACTOR SAFETY INFORMATION MEETING

October 26-29, 1987

TABLE OF CONTENTS - VOLUME 5

INTERNATIONAL CODE ASSESSMENT PROGRAM
(Cont'd)

NUCLEAR SAFETY RESEARCH
RESPONSIVE INDUSTRY RESULTS

Prepared by

Abdon Rubio
Walter B. Loewenstein
Richard Oehlberg
Nuclear Power Division
Electric Power Research Institute

ABSTRACT

Nuclear power is completing another momentous year.

The U.S. has 108 licensed reactors which should supply ~18% of all U.S. electric power. New initiatives were undertaken in the U.S. nuclear industry with the formation of the Nuclear Management and Resources Council (NUMARC), the reorganization of nuclear industry associations, the American Nuclear Energy Council (ANEC) and the U.S. Committee for Energy Awareness (USCEA) and the disappearance of the Atomic Industrial Forum (AIF). The intention was to take actions to be "more effective in meeting the challenges of tomorrow". EPRI technical support of NUMARC is and will be a challenge to focus technical results to address technical and policy issues which the nuclear industry faces.

EPRI's nuclear safety research program made a number of technical advances this past year. EPRI has completed a study of common cause failure, developed software for plant reliability and safety, studied reliability-centered maintenance, studied the consequences of steam generator tube rupture, completed the study of eastern seismic activity, looked at piping design improvements, qualified RETRAN for simulator applications, conducted intermediate-scale molten corium-concrete interaction tests and completed a mechanistic code to calculate core melt.

A major owner's group experimental effort on hydrogen combustion has been completed, characterizing hydrogen combustion behavior in BWR6 Mark III containments.

Within the United States, EPRI is involved in many national and international collaborative efforts such as the TREAT STEP and the MIST B&W tests, the OECD LOFT program and the LACE, ACE, and Marviken aerosol-behavior experimental programs. Also, EPRI is participating the NRC's important Severe Fuel Damage Program.

This paper reviews EPRI's nuclear safety research program in the context of this new transitional phase and how it is meeting the everyday challenges of commercial nuclear power.

A. INTRODUCTION

Nuclear power is completing another momentous year.

The United States has 108 licensed reactors which should supply ~18% of all U.S. electric power. New initiatives were undertaken in the U.S. nuclear industry with the formation of the Nuclear Management and Resources Council (NUMARC), the reorganizations of nuclear industry associations, the American Nuclear Energy Council (ANEC) and the U.S. Committee for Energy Awareness (USCEA), and the disappearance of the Atomic Industrial Forum (AIF). The intention was to take actions to be "more effective in meeting the challenges of tomorrow". EPRI technical support of NUMARC is and will be a challenge to focus technical results to address technical and policy issues which the nuclear industry faces.

EPRI's nuclear safety research program made a number of technical advances this past year. EPRI has completed a study of common cause failure, developed software for plant reliability and safety, studied reliability-centered maintenance, studied the consequences of steam generator tube rupture, completed the study of eastern United States seismic activity, looked at piping design improvements, qualified RETRAN for simulator applications, conducted intermediate scale molten corium-concrete interaction (MCCI) tests, and completed a mechanistic code to calculate core melt.

A major owner's group experimental effort on hydrogen combustion has been completed, characterizing hydrogen combustion behavior in BWR6 Mark III containments.

Within the United States, EPRI is involved in many national and international collaborative efforts, such as the TREAT STEP and MIST B&W tests, the OECD LOFT program, and the LACE, ACE, and Marviken aerosol behavior experimental programs. The LACE program successfully completed its experiments and is well on its way to completing all associated work shedding important light on aerosol behavior in containment and release from containment. Also, EPRI is participating in NRC's important Severe Fuel Damage Program.

A.1 Nuclear Management and Resources Council (NUMARC)

Late last year, leaders of the nuclear electric power industry endorsed a reorganization of U.S. nuclear industry associations. The goal was to improve the coordination of the activities of these associations and concentrate their efforts on efficiently assuring the continued contribution of nuclear power. The challenges of the future--operating excellence of nuclear plants and the use of nuclear power as one way to meet the growing demand for electricity--will be taken up by NUMARC.

The changes were officially brought into being on July 1, 1987.

The realignment eliminated the old Atomic Industrial Forum (AIF), assigning its duties to NUMARC and to a reorganizated U.S. Committee for Energy Awareness (USCEA). The Utility Nuclear Power Oversight Committee (UNPOC) was

constituted in 1979 following the TMI-2 accident to guide the utility efforts necessary following that event. UNPOC will become NPOC (Nuclear Power Oversight Committee) with the addition of nonutility organizations and will serve as a formally constituted coordianting and oversight organization for all nuclear industry association activities.

NUMARC will concentrate its efforts on regulation and technical support. It is made up of senior utility executives (one from each of the U.S. utilities with nuclear power plants in operation or under construction) and nonvoting members consisting of selected supplier industry executives. It will work within the industry and with the U.S. Nuclear Regulatory Commission (NRC) to develop nonregulatory solutions to nuclear operational issues--management, philosophy, policies, responsibiliies, organization, and training. It will coordinate the work of all nuclear utilities in solving problems in these areas and helps assure corrective actions are taken. EPRI and INPO will provide important direct support to NUMARC in their areas of expertise.

The USCEA will provide the communications and education aimed at a broader public understanding that a strong and expanding American economy requiring an adequate supply of electric energy from a diversity of energy sources. The American Nuclear Energy Council (ANEC) will be involved with governmental affairs.

The new initiatives in our industry bring vitality and excitement for the future, as James O'Conner of Commonwealth Edison stated: "By focusing our attention more precisely on the key issues facing us in the future, we should be all the more effective in maintaining nuclear power as a major source of our electric power supply."

B. LWR SYSTEMS ANALYSIS AND APPLICATION

B.1 Introduction

The Reactor Safety Study (RSS) (B-1) showed that judgment alone is not an adequate guide to those design and operational features of a plant that are most important to safety. The licensing process before RSS focused on large loss-of-coolant accidents (LOCAs) and single failures. In contrast, the RSS showed that small LOCAs, transients, maintenance, operator error, and dependent failures dominated risk (B-2). Such an analysis, a "Level 1" Probability Risk Assessment [PRA; (B-3)], is the most comprehesnive type of analysis in the nuclear power industry. Its usual objectives are to: (1) delineate accident sequences that contribute most to the probability of causing severely damaged cores; (2) assess this probability; and, (3) deduce the key components, equipment, systems and procedures that are most significant in initiating and/or mitigating these sequences. The bulk of the effort in a Level 1 PRA involves Probabilistic Systems Analysis (PSAs).

Recent NRC plans for seeking individual plant evaluations for operating plants and full-scale PRAs for new plant applications constitute increasing adoption of PSA techniques. PSA is also becoming increasingly important in day-to-day running of plants. Attention to day-to-day activities is essential to ensure that a currently safe and economical operation is retained over the long term.

EPRI's objective in this area are to both assure the availability of adequate PSA tools and, once available, help to assure the tools are applied usefully to response to industry strategic needs. These needs are:

1. Identification and resolution of safety issues.

2. Plant investment risk estimation considering individual plants having selectively higher accident risk potential.

3. Operational safety and enhanced plant operating availability.

The specific working objective of the PSA effort at EPRI is to make its use an effective process that can be employed by utilities to address their strategic needs. To do this, the program develops:

1. Credible methodology.

2. Procedures, computer codes, and technology transfer to ensure efficient and cost-effective implementation.

3. Appropriate applications addressing the strategic industry needs and within the capabilities of the methodology.

Highlights of the progress in these areas are described below.

B.2 Progress in PRA Methodology

A credible PRA study requires scientifically defensible methods and data that are sufficiently comprehensive in scope and amenable to peer review. PRA methodology is currently undergoing the early stages of standardization that is necessary for it to become a mature discipline using "proven" methods and data. This effort has been hampered by the lag in the development of the key technical area of common cause failure analysis (CCFA).

B.2.1 The Issue of Common Cause Failures. Those responsible for the safe design and operation of nuclear power plants have for a long time recognized the vulnerability of engineered systems, and the credibility of their reliability analysis, to dependent events. The vulnerability of systems to single failures was addressed in the United States by the inclusion of the single failure criterion in the General Design Criteria (B-4). However, redundant systems can be defeated by a special class of events that affect many similar components at the same time. The theoretical high reliability of very redundant systems was always open to question. Further, historical experience has shown a high incidence of common cause failures (CCFs) in events which challenge reactor safety systems. Finally, many probabilistic risk assessments (PRAs) have found CCFs to contribute significantly to risk (B-5). This has led to our current awareness of CCFs as significant contributors to the residual risk from nuclear plant operation.

Notwithstanding the importance of these events, our attempts to treat them in safety analysis have in the past been incomplete and of variable quality. EPRI's reviews of PRAs (B-6, B-7) have shown a repeated lack of consistent CCF treatment for important systems and a wide variation in parameter values used to quantify such events. The worldwide nuclear industry has lacked a database that could be used with confidence despite pioneering efforts by Edwards and Watson (B-8) and Atwood (B-9, B-10) among many others. Much of the difficulty with data came from incompleteness of failure event reports, the relative complexity of multiple failure events and the ways in which they can occur, and the number of assumptions, usually unstated, that underlie their analysis.

In 1981, EPRI initiated a research project to address these issues. The original objective was to provide guidance on data interpretation to bring some uniformity to how failure event reports were analyzed and used for parameter estimation. During the process of evaluating and refining a proposed data classification system (B-11), a preliminary CCF database was prepared (B-12). The work was subsequently widened to include improvements to modeling methods (B-13) with a much greater emphasis on qualitative engineering evaluation of plant-specific features and vastly improved parameter estimation procedures. A further objective was to find information from both data analysis and industry experience on the tactics available in design and operation, to make redundancy not only a defense against the impact of single failures but also effective against multiple failures from a shared cause.

These objectives have all been achieved. The data classification system and modeling guidelines have been extremely successful, thanks to the contribution of many organizations and individuals within the United States and abroad. The database is useful but is only a beginning. The preparation of a large definitive database was never a part of EPRI research project but should be a target for future development. The technical basis for a defensive strategy and tactical guidelines has also been successful, but is arguably still at an early stage. It was always recognized that the work on defenses was the more speculative part of the project requiring the most infusion of analysts' and industry judgments. The remarkable thing is that it appears to be possible to do it at all. Nevertheless, practical applications of the defenses conclusions are yet to be implemented and also form a target for the future. Some issues remain to be resolved in the modeling areas and are listed later as subjects for research. It is now possible to see fairly clearly the requirements for future data reporting so that quality CCF information will be available on a continuing basis. The process of changing existing data recording and collection systems, e.g., NPRDS (B-14), has not yet begun.

B.2.2 Approach. This section will briefly describe the procedure followed to achieve the above objectives, including the roles of the principal collaborating organizations.

EPRI's research project was initially oriented by a peer input group, including Westinghouse, Pickard, Lowe and Garrick (PLG), UKAEA Systems Reliability Service, USNRC, Battelle Columbus Laboratories, and Los Alamos Technical Associates. The general conclusion was that work on data interpretation should be followed by efforts on modeling methods. The data

classification system that was subsequently proposed (B-11) by Los Alamos Technical Associates carefully distinguished between component failure requiring repair and component unavailability due to other causes. This distinction broadly separates events likely to need implicit CCF modeling from those likely to be already modeled in system logic models, e.g., fault trees. Secondly, it distinguished between component faults having other component faults as causes and those with other "root" causes, e.g., human error. This distinguished between sequential or cascading events that do not, in fact, share a common cause and those where a shared root cause produces multiple components faults, in a sense, "in parallel." This scheme was tested in a benchmark comparison experiment in which Duke Power, General Electric, JBF Associates, NUS, TVA, and the UKAEA analyzed a set of LER reports to identify and categorize common cause failures. The results were very encouraging and a larger-scale evaluation was conducted by PLG (B-12) that resulted in a preliminary database using nuclear power experience reports of LERs. This database, although limited in size, is probably the most self-consistent CCF database that exists for the use of PRA specialists at the present time. Unfortunately, because it was produced while evaluating an interim version of the classification sysems, there are some minor differences between the way data is classified in this database and the final scheme subsequently published by EPRI (B-14, B-15) after appropriate refinements. To further ensure its coherence and the clarity of the instructions, the refined classification scheme was benchmarked by a second multinational peer evaluation process, including the Central Electricity Generating Board of the United Kingdom, the CEC Joint Research Center of Italy, Electricité de France, INPO, RISO National Laboratory of Denmark; the Swedish Nuclear Power Inspectorate, and the Technical Research Center of Finland, before being finalized. Further review comments were sought from the CEGB, USNRC, EG&G Idaho Falls, and Yankee Atomic Electric Company.

Improvements to modeling approaches followed two major directions. One emphasized the importance of interpreting each event in the database in order to prepare a "pseudo database" relevant to the plant being modeled. The idea was to use as many events in the database as possible (plant-specific data being too scarce to be useful on its own) but to "customize" the events in relation to system and operational characteristics of the plant being modeled. The second approach was to integrate (i) the data interpretation process, (ii) plant modeling, (iii) the definition of groups of components to be analyzed for common cause impacts, (iv) model selection and definition, and (b) parameter estimation, into a systematic multistep procedure that can be followed by systems analysts with a moderate level of experience. This approach neither advances a particular method or technique, nor does it rigidly constrain the analyst to a prescribed recipe for common cause analysis. The purpose of the procedural framework is to allow the analyst to make intelligent choices along the way, while obliging him to consider the issues involved, the consequences of his decisions, and the need to document the process very carefully.

Preliminary ideas used by PLG in the Seabrook Risk Assessment (B-5, B-12) were used in the U.S. team's participation under the auspices of EPRI and USNRC in the Reliability Benchmark Exercise on Common Cause Failures (CCF-RBE)

organized by the Joint Research Center of the CEC at Ispra, Italy. The CCF-RBE had a major impact on the methodology development in the EPRI project. First, it exposed the proposed methods and the preliminary database to the critical evaluation of 10 teams representing 8 countries: Belgium, Denmark, Frnace, Federal Republic of West Germany (FRG), Italy, Sweden, United Kingdom, and the United States. Second, the findings of the CCF-RBE, reported in the CEC report (B-16), represent significant advances and became central to the development program, although some of these were issues raised originally in the U.S. methodology. Details of these findings can be found in a paper by Poucet et al. (B-17). Third, there were important specific issues raised by various participants: for example, (i) the need for adjustment of the number of independent events appearing in the pseudo database as a result of extrapolating redundancy levels between historic events and the plant being modeled (FRG) and (ii) the need for thorough, systematic qualitative analysis that addresses plant design and operational defenses against CCF, when formulating the pseudo database (UK).

EPRI has collaborated closely with the Office of Research at the USNRC in integrating the above findings into the systematic procedural framework that is the main product (B-13) of this phase of our research project. USNRC has supported NUS, JBF Associates, and Sandia Laboratories in this collaboration, and a joint EPRI/NUREG report will be published in 1987 containing the results. The EPRI contractor, PLG, is reporting the work in a paper by Fleming et al. (B-18). A list of some of the issues dealth with in the procedure gives an idea of its scope and depth: qualitative analysis of component groups; quantitative screening of component groups; definition of common cause basic events; inclusion of basic events in system logic models; screening of common cause cut sets; selection of probability models; database selection for independent events and common cause events; data classification and screening; definition of impact vectors for historic events and plant being modeled; redundancy extrapolation up and down; normalization of independent events to account for redundancy extrapolation; normalization of independent events and exposures to account for historic events rejected from database; parameter estimation; system quantification; uncertainty analysis; sensitivity analysis and reporting.

The work on defenses by Saratoga Engineering Consultants (formerly Los Alamos Technical Associateas) has also produce a database. This database (B-19) contains over 2000 events classified as before but with additional information concerning applied defensive tactics, methods of discovery and corrective actions. The events contain about 250 common cause events and were obtained from LERs on Auxiliary Feedwater, Reactor Protection and Emergency Electric Power Systems. These data has been interpreted in several ways, (i) event-by-event evaluation of effectiveness of various defensive tactics, (ii) evaluation of the spectrum of causes, subsequently used with judgments of the effectiveness of the tactics for each cause, (iii) formulation of a survey of industry judgments on defenses with participation from nine U.S. utilities, PLG, and the UKAEA. These judgments have been applied to operating power plants and to new plant designs. The former application implies greater use of tactics involving maintenance, design review, surveillance testing and training, than the application to new designs where there is more

cost-effective scope for hardware changes involving barriers, separation, redundancy, and diversity. It is generally agreed that redundancy alone is a poor defense against CCF and that many other ingredients can and must be added to the range of defenses. Although this conclusion confirms our prior beliefs, it is satisfying to see this message emerging very clearly from the analysis of data. Details of the work on defenses can be found in a paper by Crellin et al. (B-20) and in an EPRI report (B-19).

B.2.3 Conclusion. The most importance advance in the last five years has been realization of a universal consensus that common cause failures can be a significant contributor to risk, that they represent complex phenomena requiring considerable resources and attention in a safety system reliability or risk analysis. Their credible treatment requires consideration of plant-specific design, operational characteristics, and defenses in a systematic framework. The means to do this are available and the remaining large uncertainties do not invalidate the analysis.

The second most important advance has been the drawing together, at an international level, of many disparate but valid views and approaches to modeling CCF into a coherent conceptual and practical framework for systematic analysis. That this consensus should integrate qualitative and quantitative aspects of generic industry and plant-specific operating history, and design and operating characteristics, is both remarkable but inevitable if real progress is being made. We believe that EPRI and JRC Ispra have played leading roles in obtaining this consensus.

Clearly, data reporting deficiencies need to be addressed at utilities and within national data systems such as NPRDS. Judgments on the effectiveness of specific defenses must be incorporated in an increasingly quantitative way, perhaps by use of techniques such as the partial-β factor (B-13, B-21). Several issues relating to parameter estimation need further illumination from additional applications.

However, the structured approach developed in EPRI research project will undoubtedly help to make future CCF contributions to risk and reliability studies, (i) more tractable from the point of view of the analyst, (ii) more consistent and scrutable to peer and industry reviewers, (iii) more realisticfrom the point of view of plant operators, and (iv) more defensible by study sponsors. Implementation of design and operation movements as a result of more credible risk analysis and the application of the most effective defenses will ultimately lead to safer and more reliable plants.

B.3 Development and Use of Control Room Tools for Improving Nuclear Power Plant Safety and Operations

EPRI conducts research related to the development of nuclear plant control and information systems. This effort focuses on mission-oriented development of computerized hardware and software systems and their implementation in operating power plants (usually with specific utility involvement). The 1987 effort has seen notable deployment and use of such systems in existing plants.

The primary goals of this EPRI effort are to develop systems to:

1. Meet the need of sponsoring utility companies to safety and economically upgrade the reliability and performance of plant systems, i.e., to operate at maximum allowable optimum conditions, while making systems simpler and easier to operate.

2. Prevent and control nuclear power plant accidents.

B.3.1 The RAPID Software Environment for Plant Reliability and Safety Analysis

EPRI has developed a software tool whose primary functions are: (1) to maintain a living PRA, (2) to improve efficiency in execution of reliability and risk calculations, (3) to provide a permanent audit trail for such activities, and (4) to facilitate the exchange and update of data derived from station information management computer systems and destined for use in PRA or reliability trending or monitoring projects. The name of the computer code is Reliability Analysis Program with In-Plant Data (RAPID). RAPID also has on-line functions that are not the subject of this report.

Many nuclear utility companies have now performed plant-specific system reliability assessments (SRAs) for a variety of applications, such as determination of alternative system design modifications, assessment of testing and maintenance strategies, examination of procedural changes, responding to regulatory inquiries, etc. Manually updating the SRA logic models and component reliability data to keep them up-to-date is a tedious, time-consuming, manpower-intenstive and, sometimes, impractical task. The amount of information as well as the lack of adequate computer software for automated updating makes it difficult to keep the SRAs current. RAPID's RAM and UM software, which are part of EPRI's RAPID (B-22) software development effort under the Risk Assessment Program of the Nuclear Power Division, are designed to overcome many of these difficulties and to provide a productive environment for performing various system reliability engineering activities. The following summarizes the development and demonstration of the RAPID/RAM-UM software at ANPP's (Arizona Nuclear Power Project) Palo Verde Nuclear Generation Station.

The RAPID/RAM software procides a computer environment to perform reliability tasks. The major functions of RAPID/RAM include:

- Conduct topical system modeling and data analyses;
- Maintain and upkeep system models and data; and,
- Ensure traceability and quality control.

The software is menu-driven and transparent to the user. Figure B-1 is a brief description of the RAM's major functions. As an example of RAPID/RAM operation, a user may wish to update, quantify, and review the results of the system model.

The user would first invoke the elements 1, 2, 3, 4, 7, 10, 11, 12, 13, 11, 10, 2, 3, and 5 in figure B-1 to retrieve an existing system model to the user's workstation for model editing. Following model editing, the user could employ elements 2, 3, 4, 7, 10, 11, 12, 14, 13, 17, and 16 to send the model back to the mainframe for execution, storage, and documentation. Finally, the user could use elements 2, 3, 4, 7, 10, 11, 12, 17, 11, 10, and 6 to view the results on the workstation. RAM software automates these operations. A user is only required to interactively select and respond to the prompts and menus on the workstation, with assistance from the help-menus, if needed.

The RAPID/UM software interfaces and extracts plant-specific data from the plant information management system. The data are then aggregated, periodically updated, and documented in support of RAPID/RAM and other application modules. The UM software has automated the data handling. Figure B-2 outlines the data tables available to the RAPID/UM users for accumulating plant-specific information. The combined use of RAPID/RAM and RAPID/UM has created an automated environment for maintaining and modifying logic models and associated reliability data with the support of documentation.

The RAM and UM software have been developed under a cooperative agreement between ANPP and EPRI. The software is developed in a generic fashion to operate in a wide variety of computer environments. Currently, it is installed on an IBM 3084 mainframe computer using the MVS/XA operating system; IBM AT microcomputers are used as the engineering workstations. Both RAM and UM software are operational at ANPP's computer service center.

The ANPP's Palo Verde plant-specific information has been used in this demonstration. The PRA engineering staff at ANPP are using RAM and UM software for developing systems fault tree models and event tree sequences to describe a small LOCA scenario, constructing several GO (B-23) system models for the plant availability study, and compiling plant-specific data from Palo Verde's station information management system. The functions of RAPID/RAM and RAPID/UM are being tested as these activities progress.

RAPID/RAM-UM activities are now focused on refining its application. The plant component failure rate data compiled by the UM can be used with INPO and other industry failure data information to identify adverse failure data trends. Actual plant failure rates can be compared to industry average failure rates to automatically initiate root cause analysis where necessary. Failure data are being applied to improve preventative maintenance activities and spart parts programs. ANPP is also evaluating the addition of new data tables to facilitate INPO's safety system unavailability performance indicator program (B-24). In this program, safety system models are updated with component unavailability information from the plant to track system unavailability with service life.

In summary, RAPID/RAM-UM provides an integrated environment for performing systems reliability analysis activities using logic models, generic and plant data and evaluation codes. It couples these required resources by providing automaticity, consistency, auditability, continuity, and accessibility.

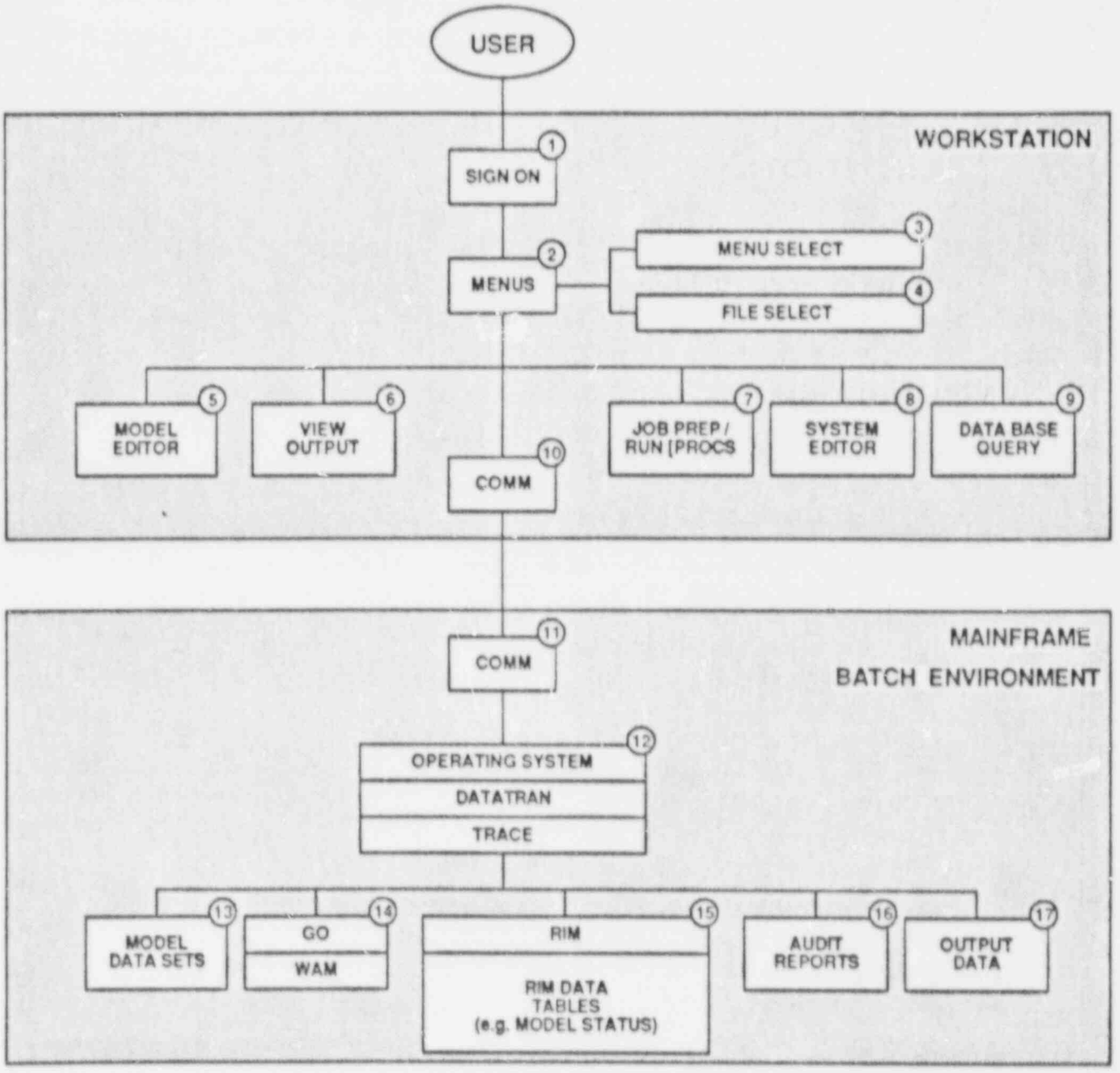

Figure B-1 Major Functional Elements of the Reliability Assessment Module (RAM)

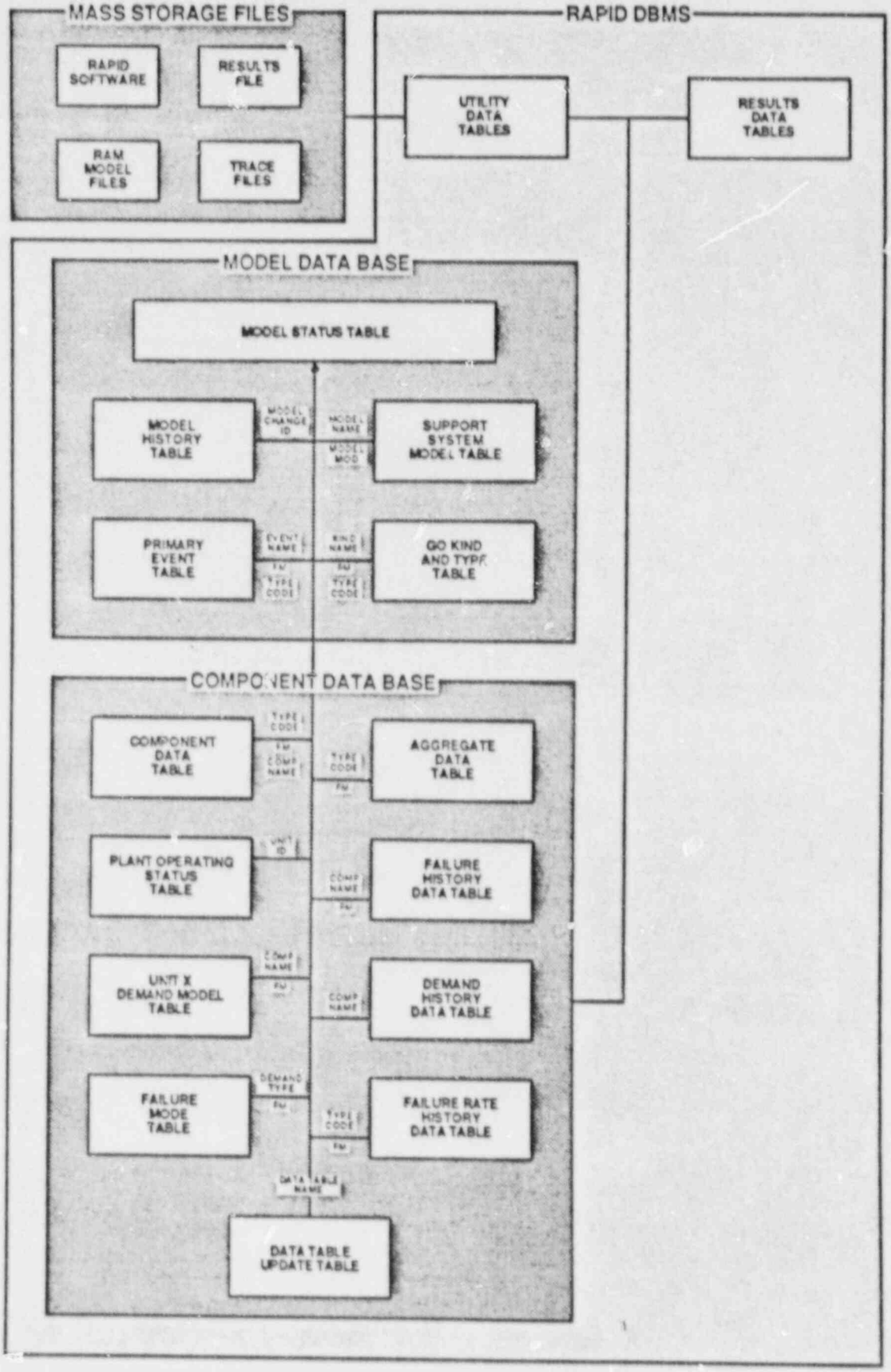

Figure B-2 Rapid DBM Structure for Off-Line Functions

Thus, costs to develop and dynamically maintain PSA reliability models and PRAs are reduced, the ability of utility engineers to assess proposed changes is improved, and a capability to apply reliability techniques to O&M issues is provided where it was difficult or impossible to apply them before.

B.4 Reliability-Centered Maintenance Studies

Reliability-centered maintenance (RCM) is a systematic methodology for identifying applicable and effective preventive maintenance tasks. With the application of RCM at Turkey Point (B-25) and McGuire (B-26), EPRI demonstrated the validity and usefulness of the traditional RCM methodology in nuclear plants. EPRI initiated a third RCM pilot application on the San Onofre auxiliary feedwater system, which would serve to customize the RCM progress to better reflect the unique aspects of the commercial nuclear power industry. In particular, two objectives were defined for this study:

- To apply RCM to a standby safety system.
- To utilize within the RCM process several of the quantitative reliability analysis techniques that are in widespread use in the nuclear industry.

Standby safety systems pose several unique challenges for an RCM application. These systems stress safety rather than process functions and, in general, are governed by more stringent design and operating criteria. These systems are only infrequently run and are typically deenergized and depressurized during standby periods. Therefore, limited operating experience is available and system failures are often not obvious to the plant staff until a demand for the system occurs.

In this course of performing this study, several modifications were made to the traditional RCM methodology. The modifications were made to incorporate quantitative reliability analysis techniques as an alternative to a failure modes and effects analysis (FMEA) and to redefine the logic tree analysis (LTA) process to reflect the results of the quantitative analyses and to better address hidden failures.

The auxiliary feedwater (AFW) system at San Onofre unit 2 was selected for this study because it is an important system needed for the mitigation of routine and nonroutine transients and because it was believed that a reevaluation of the existing PM program, using the RCM methodology, could result in a reduction in the preventive maintenance requirements currently imposed upon this system. In addition, both fault tree and GO logic models had been previously prepared for the system; hence, several analytical techniques could be simultaneously applied as part of the RCM evaluation.

System boundaries were defined and five major subsystems were identified: condensate supply, pump motive power, pumps, flow control, and containment isolation. A review of the operating experience of the system was then performed to identify significant operating and maintenance characteristics. A quick review of the current PM program was also performed in order to

identify all the AFW components currently subjected to PM and surveillance requirements.

A functional failure analysis (FFA) was then performed for the entire system and for each of the subsystems. The objective of the FFA is to identify each function which the system (or subsystem) is expected to perform, as well as the top-level failures that could prevent this function from being adequately fulfilled.

Following the completion of the FFA, an appropriate evaluation method was selected to determine the most signficant failures that could cause loss of each specified function. A number of functions were evaluated using quantitative reliability analysis techniques instead of functional FMEA's utilized in the traditional RCM process.

In order to determine an optimal PM program for the "high" and "medium" criticality component failures, a series of detailed interviews were conducted with plant maintenance personnel. Emphasis during the intorvew process was placed upon known equipment problems, why those problems exists, and what might be done to eliminate them.

The RCM-based PM and surveillance program recommendations were then compared to the current programs, and a basis for differences from the current programs was identified. A key difference of the RCM surveillance program recommendations is the expanded use of data collection and trending of the currently performed monthly pump operability test results. The RCM PM program recommendations supported the deletion of a number of PM tasks or the replacement of routine overhaul tasks with specific condition-directed maintenance actions. The results of the comparisons are summarized in table B-1.

Table B-1

RCM IMPACTS UPON CURRENT SURVEILLANCE AND PM PROGRAMS

Surveillance Programs (26 Current Tasks)

- Retain 21 tasks "as-is"
- Add 3 tasks
- Reduce scope or frequency of 2 tasks
- Expand 6 tasks
- Delete 1 task

PM Program (21 Current Tasks)

- Retain 3 tasks "as-is"
- Add 7 condition-directed tasks
- Reduce scope of 4 tasks
- Condition-direct 6 existing time-directed tasks
- Delete 8 tasks
- Consider elimination of one existing time-directed task through design change.

This study has demonstrated the usefulness of the RCM methodology for standby systems. The study also developed a number of refinements to the RCM process that better tailor the process to these standby systems and take advantage of the quantitative analysis tools that many utilities already have. This streamlining of the process makes it more cost-effective to apply RCM to a wide variety of plant systems, thereby permitting greater use of this valuable methodology.

B.5 Evaluation of Utility Experiences and NRC Perceptions in the Application of PRA

There has been increasing interest in the use of probabilistic methods, including probabilistic risk analysis (PRA), reliability models, and related techniques to address nuclear plant design, operation, and regulatory issues and decisions. This interest has come from both utilities and NRC. Motivated by the apparent benefits gained by some utilities from the performance of PRAs and other applications of probabilistic techniques, other utilities are planning programs of their own to employ such techniques and resulting models. However, at the same time, still other utilities have been reluctant to initiate programs on their own because of perceptions that the NRC would not accept arguments supported by risk analysis or, for other reasons, the benefits of PRA would not justify the costs. Some of these perceptions are based on knowledge of utility experiences with risk techniques in which either the desired regulatory acceptance was not received or results inconsistent with the realities of plant design and operation were generated by nonutility personnel.

A pending EPRI report (B-27) objectively documents and analyzes (i) the U.S. utilities' track record in the development and application of PRA and (ii) the perceptions of NRC managers towards utilities' use of PRA in support of regulatory interactions. The database was derived from personal interviews with dozens of personnel on the staff of ten utilities which have been involved with significant PRA programs and with fifteen NRC personnel with similar experience.

At each utility, three fundamental questions were addressed: what was done, what benefits were received, what program characteristics enhanced or inhibited success? The utilities concerned had performed some level of PRA for 26 plants, ranging from individual systems to Level 3 PRAs. All reported that the accrued benefits were worth the development cost. However, the extent of benefits varied widely. Some utilities, which had performed their PRAs primarily to satisfy some NRC need, had received few benefits beyond achieving their original objective. Others, which had continuously applied their PRAs in a variety of ways, continued to accrue benefits. The general benefits can be categorized as follows:

- Specific direct beneficial impacts on design and operation.
- Improved design control process.
- Improved staff capabilities.
- Improved ability to interact with NRC.

A few utilities cited some detrimental impacts as follows:

- Erroneous identification of a safety problem.
- Providing to NRC new issues with little safety importance.

All utilities, citing the above concerns, also stated that their PRA also provided the means of effective resolution.

Information gathered from over 50 experienced PRA managers and engineers indicates that utilities can best ensure success by:

- Viewing the PRA as a legitimate engineering investigation expected to provide new and valuable information about design and operation of the plant.

- Assigning experience and respected utility engineers to contribute to the assessment. Personnel with experience in operations and having good communication skills and credibility within their companies are especially important.

- Having senior management advocacy and commitment to appropriate cost-beneficial changes to design or operation indicated by PRA.

- Identifying specific objectives that are visibly important within the utility for safe and economic operation of the plant.

The perceptions of the NRC staff were gauged by posing to each of 15 interviewees a set of hypotheses about the value of RPA to the NRC and utilities. These hypotheses were statements, beliefs, or opinions that are often heard in utility discussions concerning the use of PRA. Interviewees were asked to express their (dis)agreement or lack of opinion, and to comment with examples, if possible. The primary conclusions from the NRC interviews are:

1. A trend has been developing for several years in which the insights from and safety perspective associated with PRA are becoming increasingly important in NRC decision making.

2. While nearly all NRC interviewees identified several areas in which PRA methodology could be improved, there was virtually unanimous agreement that PRA methodology, as it stands today, can be used as an effective decision support tool at NRC.

3. The more frequent concerns expressed by NRC staff about PRA methodology and applications were:

   --Treatment of operator performance.

   --The inability (or difficulty) in characterizing the effect of management environment and corporate culture on both the operator's effectiveness and the readiness state of the plant at any point in time.

   --Erosion of safety margins. Utilities only use their PRAs to justify some relaxation of requirements and not to enhance safety.

4. The factors identified by the NRC staff as contributing to a successful PRA program were almost identical to those identified by utility personnel and listed above.

C. CONTROL AND DIAGNOSTICS

C.1 Boiling Water Reactor (BWR) Digital Feedwater Control System

Feedwater control system (FCS) problems are the largest contributor to control-related plant outages in light water reactors. Current FCSs consist of analog control loops using 20-year old technology. Electrical component and sensor failures typically cause FCS failures, and utilities have difficulty obtaining analog controller spare parts. Northern States Power Company (NSP) engineers determined that analog controller component failures were a major cause of FCS-related outages at Monticello Nuclear Power Station. Given recent developments in microprocessors and applications of fault-tolerant computer systems in other industries, NSP realized that digital technology could improve FCS reliability and operation.

Under RP2126-2 and 2448-3 and 5, EPRI, NPS, and Science Applications International Corp. jointly funded the design, implementation, and testing of a prototype high-reliability digital FCS. This system replaces and upgrades the main and statup analog controllers at Monticello. It features automatic control, on-line signal validation, controller self-diagnostics, and fault tolerance. The dual-redundant hardware configuration minimizes spare parts availability problems. At a control room panel, operators select each feedwater valve's operating mode (three element control, manual, and so on) or set bias inputs for individual feedwater-valve demand. These and other features permit more exact FCS tuning, improving feedwater control in all modes of plant operation. During a recent recirculation pump trip at Monticello, the system precisely controlled the vessel water level. Parity-space and (analytic) redundancy techniques isolate failed sensors and permit system switching to accurate sensors, thus avoiding outages. The digital design also facilitates operator training. This microprocessor-based desgin will improve the reliability of the old FCS by at least a factor of three.

Benefits:

- NSP estimates that the dual-redundant digital system will reduce FSC-related outages.
- The new system increases plant reliability and safety by reducing challenges to safety systems.
- The system enables more precise control of BWR feedwater.

C.2 Signal Validation for Safety Parameter Display System (SPDS)

Since the Three Mile Island accident, nuclear plant owners have conducted an accelerated effort to improve instrumentation. One of the most significant systems required is SPDS, which helps operating staff determine the safety status of the reactor and plant critical systems. Sensors that measure and transmit process variables are subject to instrument calibration drift, sensing line problems, and sensor failures. Engineers at Northeast Utilities Service Company (NUSCO) knew that these deviations can cause inaccurate sensor information, and as operating experience shows, they contribute to nuclear unit unavailability. NUSCO also recognized that a computer implementation such as SPDS can present useful daily information under nonemergency conditions. The challenge for NUSCO was to develop and implement an improved SPDS that provides accurate and unambiguous on-line information to operators and meets regulatory requirements--all at a reasonable cost to the utility.

In an EPRI project (RP2292-1) on sensor signal validation, researchers developed the basic technology to solve the on-line information problem. Software methods developed in this project improve the accuracy and reliability of SPDS information. The software uses parity-space algorithms to validate signals, and analytic redundancy techniques further enhance this process when an inadequate number of sensors are present. NUSCO extended this EPRI approach to include off-line, daily analyses by developing the Off-site Facility Information System (OFIS). An integral part of the Emergency Response Facility for NUSCO's Millstone 3 unit, OFIS runs on existing corporate mainframe computers. OFIS stores and retrieves plant operational data in preselected formats, such as custom-scaled trend plots of up to four points or parameter-versus-parameter plots, which yield sensor correlation information. Sensor-to-sensor comparisons are also possible, potentially reducing unnecessary sensor calibrations. OFIS helps NUSCO engineers analyze plant normal and off-normal conditions and aids in-depth plant engineer training.

Benefits:

- By using the enhanced SPDS, including OFIS, NUSCO expects to increase plant availability and reduce manpower requirements and exposure.
- Ready access to accurate plant operation data will benefit NUSCO by improving plant operation.

C.3 Expert Systems

Expert systems, a major essence of the artificial intelligence (AI) technology, are referred to as computer software and hardware systems, which are designed to capture and emulate the knowledge, reasoning, judgment, and to store the expertise of humans. EPRI has launched a broad-based exploration of potential applications intended to augment the diagnostic and decision-making capabilities of utility personnel for the goal of enhancing utility productivity and performance.

Two parallel efforts are being performed at the Electric Power Research Institute (EPRI) to help the electric utility industry take advantage of the expert system technology. The first effort is the development of expert system building tools which are tailored to electric utility industry applications. The second effort is the development of expert system application prototypes. These two efforts complement each other. The application development tests the tools and identifies additional tool capabilities which are required. The tool development helps define the applications which can be successfully developed. The AI technology, as demonstrated by the applications to operations and maintenance, is being established as a credible technological tool for the electric utility industry.

A challenge to transferring the expert systems technology to the utility industry is to gain utility users' acceptance of this modern information technology. To achieve successful technology transfer, the technology developers need to (1) understand the problems which can be addressed successfully using AI technology, (2) involve with users throughout the development and testing phases, and (3) demonstrate the benefits of the technology by the users.

D. SAFETY MARGINS AND TESTING

D.1 Water Hammer

Although not perceived as a serious safety risk, water hammer incurs damage in plant systems and components, resulting in large financial losses. Water hammer keeps recurring, and a comprehensive, coherent effort to tackle the problem fundamentally is beginning at EPRI. A utility workshop on water hammer was attended by approximately 90 participants, representing 25 utilities, universities, U.S. NRC, INPO, consulting companies, vendors and architect engineers. Recent water hammer events brought a renewed interest and attention. Summary of the workshop (D-1) recommendations are given below:

D.1.1 Prevention.

- Plant operation should be reviewed (and improved) periodically from the standpoint of water hammer relative to operating experiences, especially in view of recent increased number and severity of events;

- Maintenance procedures need additional attention. Training of maintenance engineers/technicians should be intensified;

- Improvement of valve operability testing methods (use of acoustic monitoring) should be more aggressively pursued;

- Individual plant design reviews and improvements to prevent hydrodynamic event recurrence should be encouraged (at Hanford, 7 out of 8 water hammer events resulted in design changes);

- Plant operating personnel should be trained to understand water hammer phenomena, to be sensitive to the various system manipulations that cause it, and to evaluate and review unusual plant configurations that may result in water hammer.

D.1.2 Mitigation

Water hammer events evolve very quickly. Therefore, it is difficult to mitigate all events. However, the following additional aids should be considered:

- Train operators to assure that mitigation systems are reliable and available (e.g., operable keep-fill systems);

- Design improvements to system configurations (drip legs, dump valves, surge tanks, sloping lines);

- Plant valve closure time relaxation to preclude flow-induced hammering;

- Installation of system void detectors.

D.1.3 Accommodation.

The classic plant water hammer events probably can be accommodated (first-line defense) without a significant impact on plant safety. However, they will result in plant damage, damage that is certainly costly. There are some things that may be done to "soften" these events. These include:

- Thoroughly understanding water hammer potential ramifications in degraded equipment (e.g., aged components, IGSCG piping systems, etc.);

- Developing methodology/analysis techniques to evaluate, power plant configurations, so as to avoid agitated failure modes;

- Understanding proposed nonrestraint piping system performance relative to water hammer;

- Investigating potential impacts of large-scale condensation waterhammer events.

D.1.4 R&D Recommendations.

The following recommendations were developed:

- Develop a water hammer "handbook" which would include simple methods for evaluating design configurations, component performance and reliability, testing guidelines, maintenance and operation guidelines, training guidelines, available data base of water hammer events, post-mortem evaluations, etc. It would improve water hammer prevention, mitigation and accommodation for operators and engineers by providing tools and methodology necessary to perform self-evaluation of events and pre-event situations;

- Perform testing to investigate physical processes under various water hammer initiating events. Compare expected to measured loadings;

- Develop a method to analyze sensitive system configuration from the viewpoint of their ability to generate and withstand waterhammer events;

- Further improve the science, methods and applications of fluid-structure interaction analyses;

- Perform economic evaluation of water hammer impact (e.g., equipment repair, engineering time, interfacing with federal agencies, local and state agencies, press and public; modifying design, procedures; lost credibility, etc.).

D.1.5 Additional Considerations. Water hammer events are a frequent nuisance for the plant operators. Fifty-eight events have been reported between 1981 and 1985 (over 11 events/years) but these are only the so-called "macro-events". That is, events of consequence large enough to be written up in plant License Event Reports (LERs). Scores of other minor "micro-events", unreported, occur frequently in the nonsafety BOP systems and are thus not subject to Tech. Spec. violation reporting or control. However, these events many times cause significant unscheduled shutdowns, sometimes involve costly repairs and always results in some degree of economic loss. Everytime, the "wheel must be reinvented" to fix the problem in order to quickly get back on-line. Thus, the concept of a handbook (and the R&D work required to support it) is so appealing to virtually everyone who participated in the workshop. It is an operation self-help aid to water hammer avoidance, evaluation, and treatment.

D.1.6 Summary. The conclusions of the workshop (D-1) identified needed specific R&D areas to prevent, mitigate, and accommodate water hammer.

EPRI is currently making headway in meeting this important challenge. We have formed a Water Hammer Advisory Committee consisting of utility representatives and EPRI staff, which will interact with utilities, review progress of the project, and provide advice and guidelines to complete the project successfully.

The ultimate product of this project will be a handbook of water hammer that can be conveniently used by engineers and plant operators on routine basis.

D.2 Two-Phase Pump Model Development

D.2.1 Introduction. Head and torque degradation of the pump operating under two-phase flow conditions is well-known and experienced in many applications such as the recirculating coolant pump of pressurized water reactor (PWR) (see the review paper by Kim (D-2) on this subject). Many experiments were conducted to date for both air/water and steam/water two-phase flow media with various types of pumps. These include the papers and reports of Aerojet(D-3), Babcock & Wilcox (D-4), Combustion Engineering (D-5), and Creare (D-6). However, the characteristics of the head and torque degradation obtained there varied so widely, depending upon the pump geometry, physical and mechanical conditions of experiments. Thus, even empirical correlations could not be used reliably. Furthermore, the thermohydraulic phenomena causing the drastic head and torque degradation were not identified despite the effort of various researchers.

An analytical tool was developed for predicting the performance of pumps operating under noncondensable two-phase flow media with the assumption of incompressibility [see the report and paper by Furuya (D-7) and (D-8)]. The method seemed to predict the head and torque degradation well over an entire range of the inlet void fraction. Furthermore, it has been discovered that the head degradation of the two-phase flow pump is attributable to the slip between two phases. The liquid is accelerated much faster than the single-phase flow case whereas the gas phase is decelerated. It is obvious, from the formula of Euler's head or the velocity triangle at the pump outlet [figure D-1 from the paper of Furuya (D-8)], that if the flow relative velocity increases at the outlet, the head should degrade. This is analogous to the head degradation of the cavity-choking pump. It has also been found that a drastic head degradation for larger inlet void fractions stems from the transition of two-phase flow condition, i.e., from bubbly flow to churn turbulent flow. In the latter condition, the interfacial drag force between two phases becomes so small that the extent of slip becomes much larger, thus resulting in a larger head degradation.

From the viewpoint of primary coolant pump in the pressurized water reactor, the condensable one-component, two-phase flow through pump is of prime interest rather than the noncondensable/incompressible two-phase flow. The basic theory developed is now extended for such cases by incorporating the energy equation into the basic mathematical formulation.

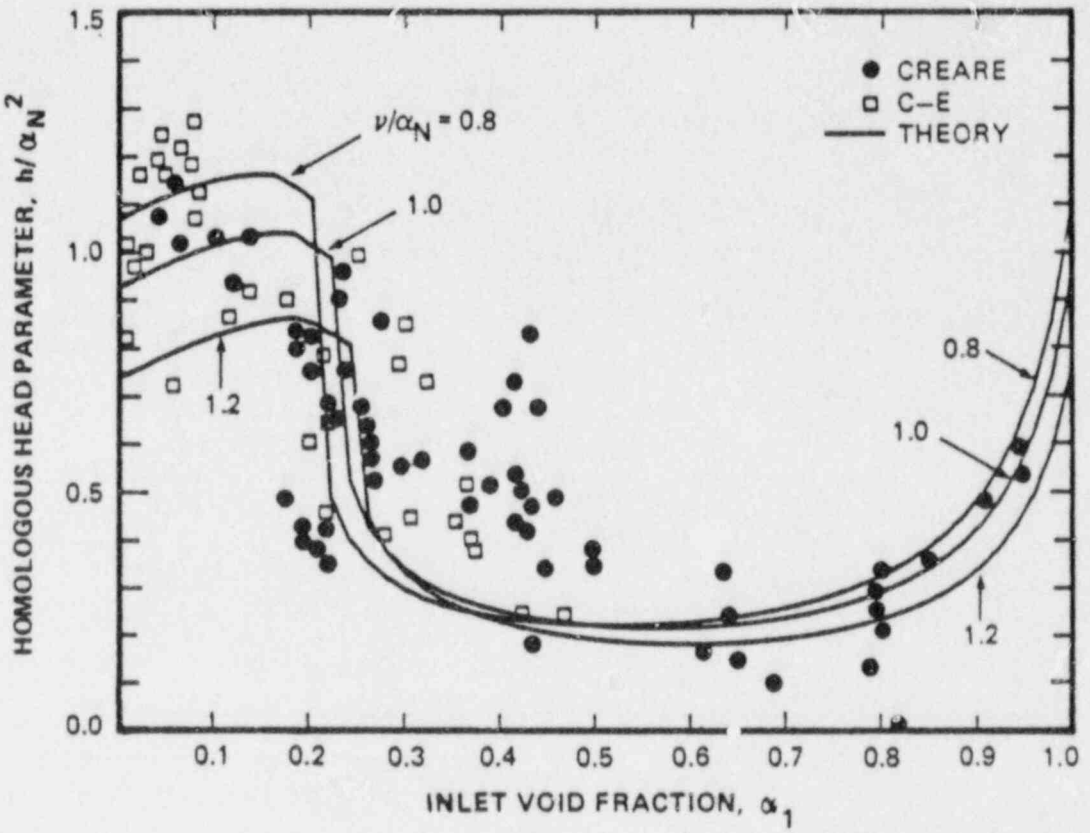

Figure D-1 Comparison of the head between the theory and experimental data for a mixed-flow pump for ν/α_N between 0.8 and 1.2 (steam/water case)

Figure D-1 shows a typical comparison between prediction based on the present analytical model and test data.

D.2.2 Conclusions. Based on the findings made above, the following conclusions can be drawn.

1. The mathematical model developed for prediction of the performance of condensable, compressible, one-component, two-phase flow compares well with experimental data.

2. The effects of condensation and compressibility work favorably in reducing the head degradation, even increasing the head higher than that of single-phase flow for small inlet void fraction cases.

3. For some small inlet void fraction cases, the gas bubbles were found completely condensed before reaching the pump exit.

4. For large inlet void fraction cases, however, the head degradation is drastic since the slip between the two phases and thus the void fraction increase is very large (i.e., the condensation effect can have little impact on the overall head degradation).

5. The head degradation for the radial-flow pump is much more severe than that the mixed-flow pump since the two-phase slip effect for the former is much larger. This fact was reported in the first phase of the pump project for the noncondensable and incompressible cases [see the report of Furuya (D-7)] and remains the same even for the condensable and incompressible pump flow cases.

6. It has been found that a mixed-flow pump provides a much better head characteristic, i.e., less head degradation than a radial pump under two-phase flow conditions.

7. For flow conditions at which the effects of centrifugal force are dominant (i.e., for the case of radial-flow pump or for the case of mixed-flow pump at low v/a_N values), there existed gas-phase stagnation phenomena where the gas bubble lost its momentum completely against the static pressure gradient built up in the pump.

8. For the off-design conditions where v/a_N is substantially different from unity, the present results did not compare well with experiments. However, the present theory provides a powerful tool for the performance prediction of the primary coolant pump for the practical purposes since the most important area of performance of interest is still $v/a_N \approx 1$.

D.3 Core Barrel Heating and Coolant Recirculation During Severe Accidents

Two models and corresponding computer codes were developed, which are intended to codefy our understanding of the complex processes taking place in a PWR core under simulated, severe accident conditions (D-11). The knowledge should lead to more realistic computer system models for simulating loss of coolant accidents which result in severe undercooling transient and degraded cores. The primary attention is on the thermal hydraulics of the uncovered core rather than on the primary cooling system. This focus greatly simplifies the modeling and computational needs through elimination, as either irrelevgant or unresolvable, of specific models for the balance of the primary and of the secondary reactor loop.

The first model is intended to predict the transient temperature distribution in the core barrel. Failure of the core barrel can greatly alter the postulated accident scenarios. To this end, the temperature distributions in the uncovered reactor core, core barrel, thermal shield, and reactor pressure vessel are also predicted during an undercooling transient. In the model, the reactor is considered to be a porous medium, and the core is cooled by once-through, one-dimensional coolant flow in the axial direction. The fuel rods are assumed to be in "thermal equilibrium" with the coolant. The core baffle, core barrel, thermal shield, and reactor pressure vessel are coupled through a boundary condition at the core baffle. The steaming rate from the covered portion of the core is calculated on the basis of axial and radial radioactive heat decay. The instantaneous two-phase mixture (froth) level and the temperature distributions in the core as well as the four structural components are predicted.

A number of numerical simulations of the core uncovery of the TMI-2 reactor and the subsequent heat-up of the core have been performed. The results of the calculations show that the exothermic heat release due to Zircaloy oxidation contributes to the sharp rise in its temperature. However, the core barrel temperature rise which is driven by the temperature increase of the edge of the core (i.e., the core baffle) is much more modest (see figure D-2). The maximum temperature of the core barrel never exceed 610 K (at a system pressure of 68 bar) after 75 min. simulation following the start of core uncovering. The results of simulations also show that water makeup flow rate into the core and porosity of the core are important model parameters and need to be known accurately for realistic predictions. Neglect of steam dissociation results in conservative maximum core temperatures.

The second model is inteded to assess the importance of the coolant recirculation on the thermal hydraulics in the uncovered part of a PWR core. The attention is focused only on the core. The core is treated as a heterogeneous porous medium with different permeabilities and effective thermal conductivities in the radial and axial directions. The flow in the core is modeled as a porous medium by the Brinkman-Forchheimer extended Darcy equation. Buoyancy effects due to both temperature and concentration (hydrogen) gradients are accounted for in the Darcy equation.

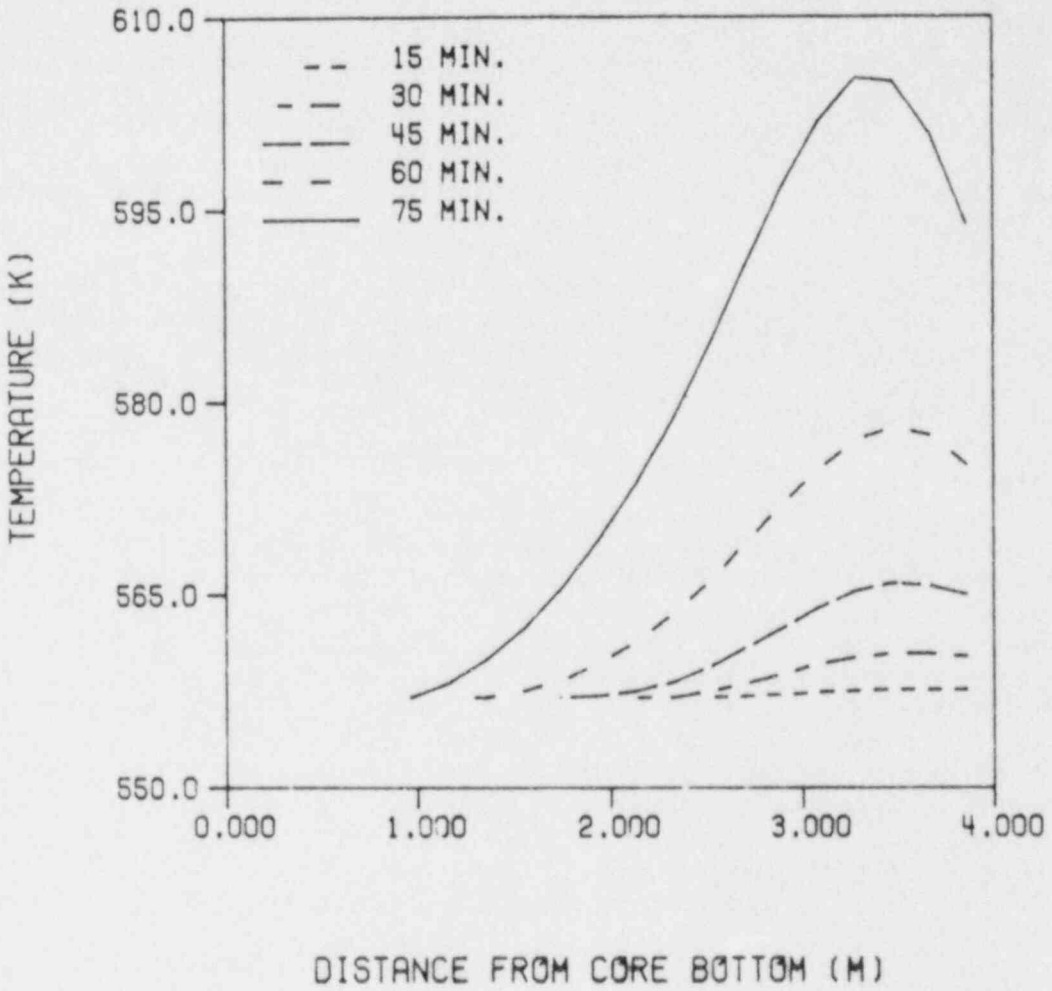

Figure D-2: Temperature Variation Along the Core Barrel at Various Times

The dependence of the thermophysical properties of the coolant (steam-hydrogen mixture) and of the fuel rods on the temperature is accounted for. Oxidation of Zircaloy is also modeled, and transport of hydrogen in the uncovered portion of the core is considered in the analysis.

Numerical simulations are reported for typical TMI-2 reactor conditions by assuming that the water level in the core remains constant during a simulation. The results of the calculations show that strong recirculating flow is established between the upper plenum and the uncovered core (see figure D-3). Colder coolant from the upper plenum is entrained into the core. The entrainment greatly reduces the core heat-up and the course of the accident. This mitigates the the core heat-up, slows down Zircaloy oxidation, and is expected to reduce the core damage as well as release of radioactive nuclides into the coolant.

D.4 BWR Dynamic Stability Model

D.4.1 Introduction. The analyses of dynamic instability and frequency response characteristics of boiling flow systems based on an unequal velocity, unequal temperature two-fluid model of such flow (D-12) were incorporated into a sequence of three computer codes, viz., DI-01 (steady state, or equilibrium point analysis), DI-02 (linear stability analysis), and DI-03 (nonlinear analysis). The frequency response analysis is incorporated into the computer code FREQ-1.

Dynamic instability experiments were carried out in a Refrigerant-113 boiling flow rig.

Descriptions of the model, the computational techniques, the computer codes and the experiments are divided into a four-volume report (D-13):

- Volume 1: Theoretical Model, Computational Formulation, and Results
- Volume 2: Coding Description
- Volume 3: User's Manual
- Volume 4: Experiments and Model Comparison

The governing conservation equations and constitutive equations of the model are described in volume 1 of this report. Also described are the computational techniques used. The Stability Analysis Method for Two-Fluid Dynamic Application (SATYA) code has both time domain and frequency domain options.

- Option 1: Full-time domain (nonlinear) analysis
- Option 2: Frequency domain (dervied from time domain linear port) analysis.

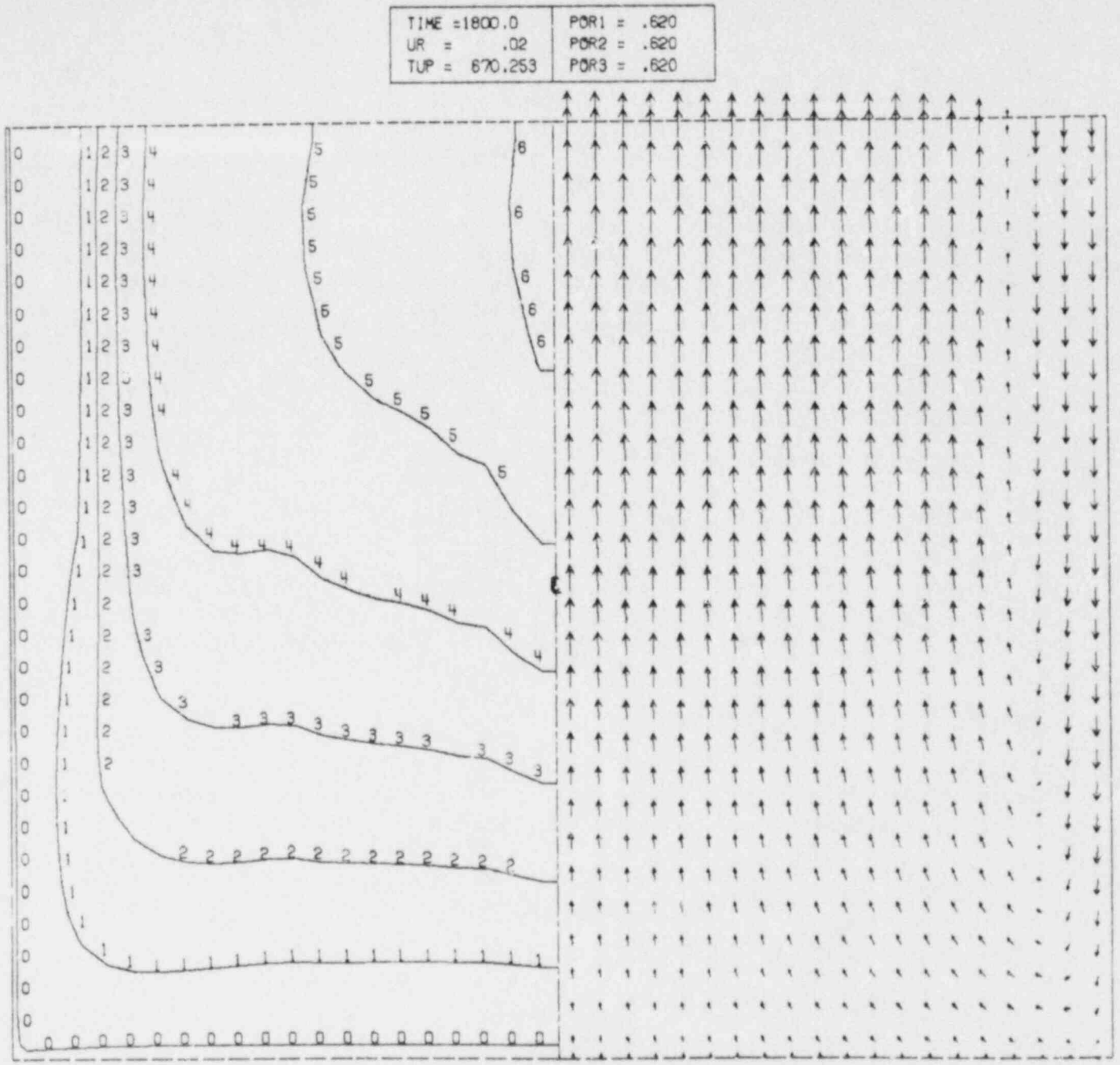

MIN VALUE = 557.00

LABEL	VALUE
0	596.48
1	714.90
2	833.33
3	951.75

MAX VALUE = 1346.50

LABEL	VALUE
4	1070.18
5	1188.60
6	1307.03

Figure D-3 Isotherms and Streamlines showing a Strong Recirculation Pattern

D.4.2 Summary. The two-fluid model of boiling flow and the numerical solution schemes was adopted for analysis of the dynamic instability and frequency response characteristics of systems in which such flow occurs. The particular instability of interest is a low-frequency oscillatory flow instability of the limit cycle type termed "density-wave oscillations (DWO)." The two-fluid model phase conservation equations are time-dependent and quasi-one-dimensional (in the sense that the local questions have been averaged over the flow cross section). In our dynamic instability model, the central feature is that both a linear stability analysis and a direct nonlinear simulation of the instability are carried out. This approach is facilitated by the fact that the linear analysis is performed in the time domain also (rather than in the frequency domain as has been the usual approach). Furthermore, obtaining frequency responses of a system to various input perturbations becomes a simple procedure via the state vector method.

Computational results from each of the four solution steps, viz., steady-state analysis, linear stability analysis, nonlinear analysis, and frequency response analysis, have been compared to experimental data from various sources (see table D-1). All the experiment systems feature joule-heated test channels and either water or Refrigerant-113 as the test fluid (see figure D-4).

A simple linear reactivity feedback description has been incorporated into the time domain portion of the model to enable a simplified analysis of boiling water reactor (BWR) core channel dynamic instability. The feedback model features a single delayed neutron group which is considered to be infinitely delayed and linear reactivity feedback for coolant density and fuel temperature.

D.5 TRAC-BWR Model Development

The boiling water reactor (BWR) version of TRAC was first developed in cooperation with the Idaho National Engineering Laboratory (INEL) under the Refill/Reflood (R/R) Program. Under that program, the main emphasis was on the development of models for the controlling basic phenomena in a loss-of-coolant accident (LOCA) in the BWR and for specific BWR components (D-16, D-17). TRAC-BWR was developed to be a best-estimate computer code for the thermal-hydraulic conditions in a BWR LOCA. At the end of the R/R program, TRAC-BWR was extensively assessed. It was found that TRAC-BWR predicted the BWR phenomena very well, but that the computation costs were high.

One purpose of the FIST program (D-18) has been to reduce the cost of executing TRAC and to extend its applicability to other transients. The first task was addressed by developing more implicit numerics for TRAC, whereby the Courant limitation on the time step size was removed, and by significantly improving the reliability of the code (D-19). This task is described in volume 1 of this document and has led to a significant reduction in the cost of executing TRAC both in terms of computer time as well as engineering time.

Table D-1

COMPARISON OF DYNAM CODE (D-15) PREDICTED DWO THRESHOLD INPUT POWERS AND OSCILLATION PERIODS WITH EXPERIMENTAL DATA (D-14) AND THE PRESENT MODEL

Expt. No.	p (Pa)	G ($kg/m^2/s$)	$T_{L_{in}}$ (K)	K_{inlet}*	Expt. Q_{in} (kW)	Expt. τ_{osc} (s)	Present Model Q_{in} (kW)	Present Model τ_{osc} (s)	DYNAM Q_{in} (kW)	DYNAM τ_{osc} (s)
128-07	4.255×10^6	318.	425.1	250	92.5	6.0	88.5	6.5	77.2	6.3
1008-06	4.255×10^6	298.	417.1	250	86.1	6.5	86.1	7.1	78.8	6.7
1125-22	4.083×10^6	220.	419.1	250	63.6	9.0	62.3	9.2	59.4	8.0
122-05	4.053×10^6	220.	422.1	260	61.9	9.0	62.3	9.0	53.6	8.6

* $K_{inlet} \triangleq \frac{\Delta P_{inlet\ valve}}{\rho u^2}$

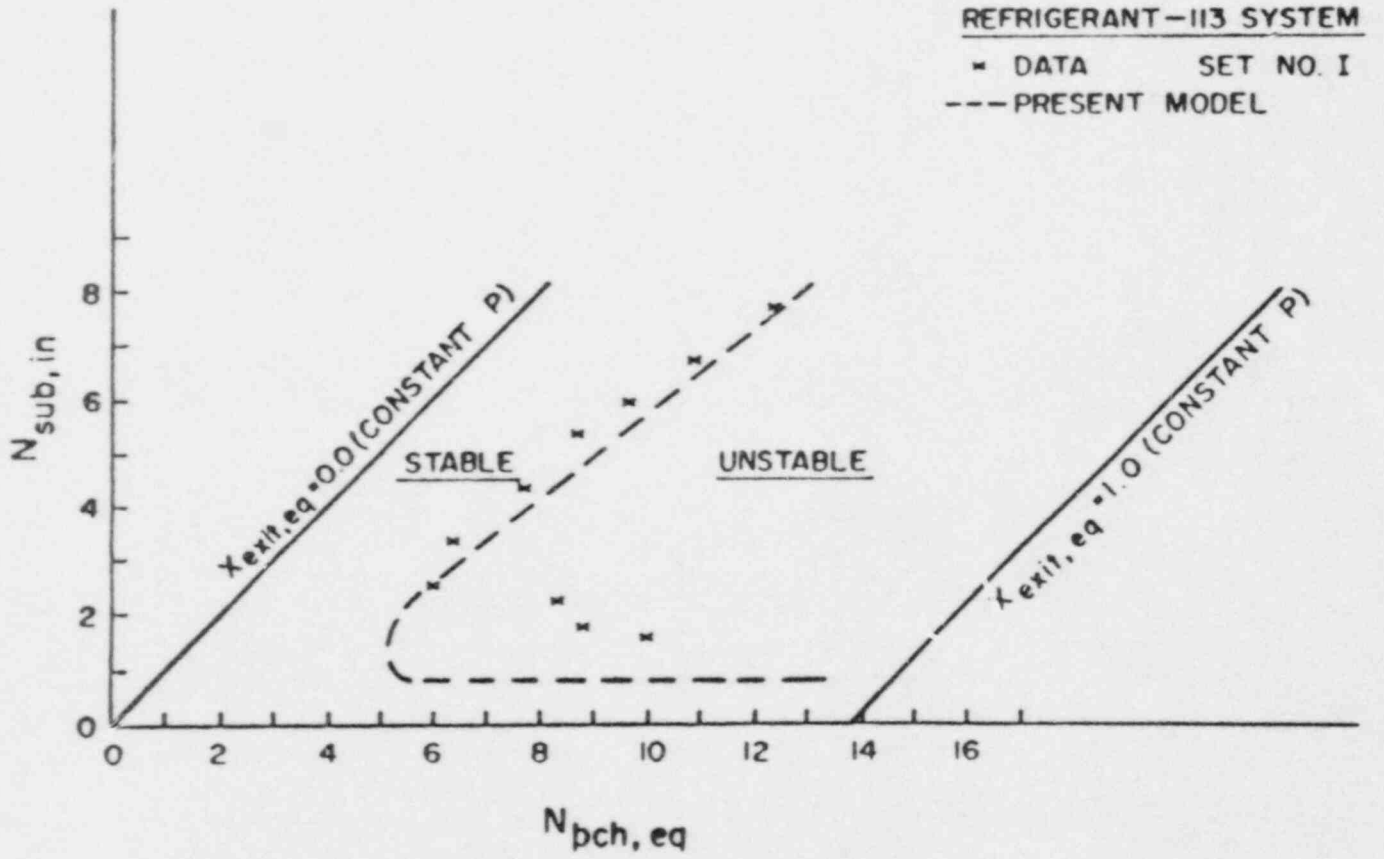

Figure D-4 Comparison of model thresholds with data of Saha ( )

The second task of extending the applicability of TRAC involved implementation of a noncondensible gas (air) field, a boron transport model accounting for stratification and mixing, a model for the two-phase level, generalized heat transfer between the components and component models for the containment, turbine, and heat exchanger. These models are described in volume 2 of this document. Figure D-5 shows the evolution of various versions of TRAC, the GE and INEL developments, and the interactions between various versions of TRAC.

During the development of the improved numerical methods and new models for TRAC, the models were individually tested. This developmental assessment is reported together with the respective models in volumes 1 and 2 of ref. (D-17). The purpose was to describe the assessment of TRAC for BWR plant cases. This not only tests the phenomena and component interactions in TRAC but also provides valuable information on the performance of the BWR (D-20). For this purpose, calculations have been performed for a BWR/2 and a BWR/4 plant.

The assessment calculation for the BWR/2 plant is a large break (DBA) LOCA with containment response. In this case, both the reactor assembly and the containment are modeled. The main objectives of this calculation are to test new models such as the air field and containment, to assess the effects of containment feedback, and to provide best-estimate BWR/2 DBA calculational results.

The assessment calculation for the BWR/4 plant is also a large break (DBA) LOCA. In this case, the low-pressure coolant injection (LPCI) water is injected in to the lower plenum through the recirculation drive line and the core is reflooded from the refilling of the lower plenum. The objectives of this calculation was to test the code numerics and reliability, and to provide best-estimate BWR/4 DBA calculational results.

D.6 Retention of Radionuclides in a U-Tube Steam Generator During Steam Generator Tube Rupture Events

Steam generator tube rupture events may occur in pressurized water reactors and can lead to the release of radioactive species to the environment. During this event, the primary coolant flows into the secondary side through the ruptured tubes, thus contaminating the secondary side of the steam generator. A fraction of the released material will be retained on the secondary side, and the rest will be released in the form of vapor and entrained aerosols.

In order to determine the system response and quantify the amount of releases during an SGTR, it is essential that a validated predictive tool be developed which simulates the key physical phenomena involved. It is, therefore, the objective of this work to (a) develop a thermal-hydraulic model simulating the primary and secondary sides of a U-tube steam generator, (b) develop a radio activity transport and retention model for the secondary side of a U-tube steam generator, (3) validate the developed models using available experimental data, and (4) perform sensitivity and parametric calculations for a PWR plant to determine the system response and identify the key parameters involved.

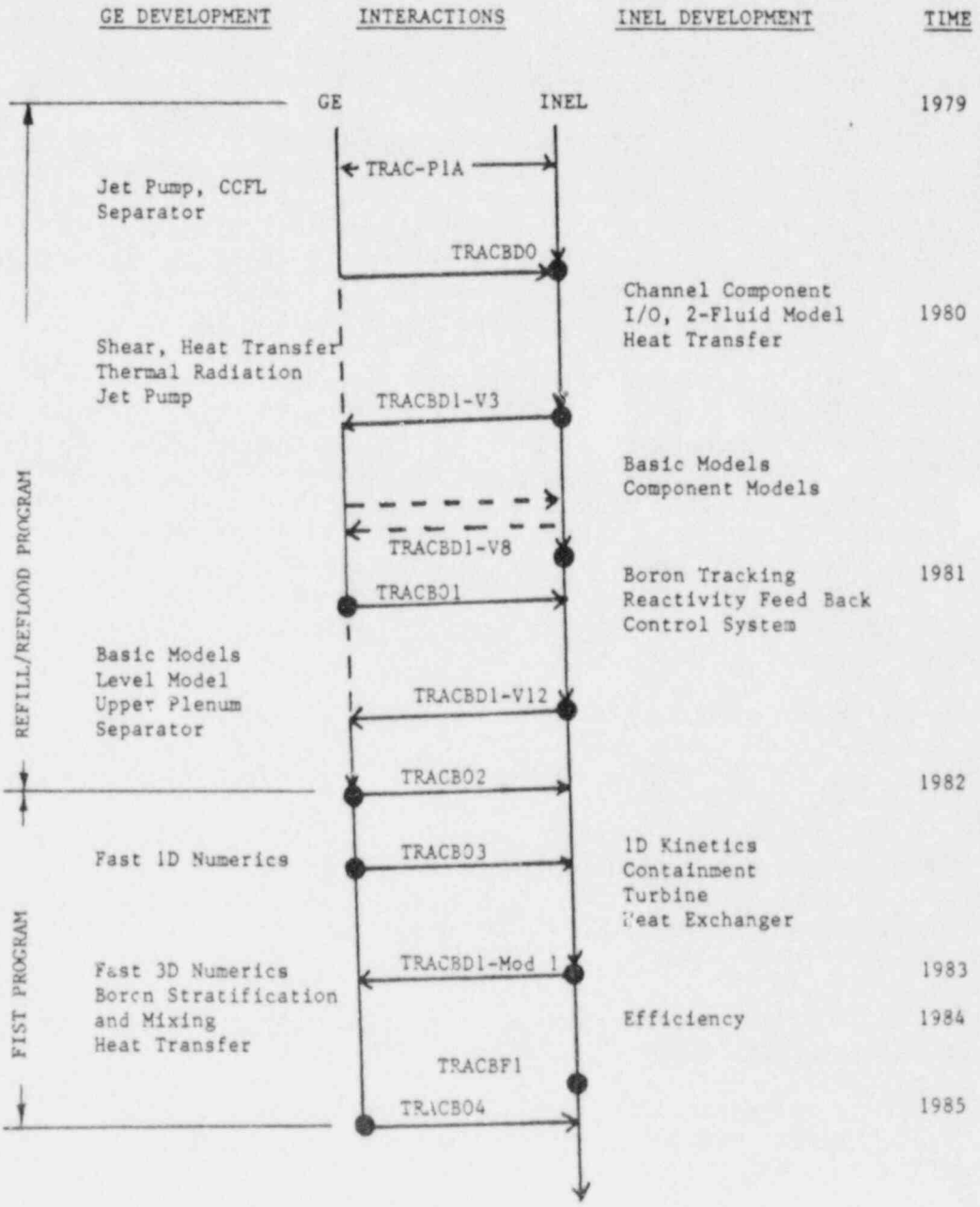

Figure D-5 Major Milestone in TRAC-BWR Development

D.6.1 Solution. Under EPRI research project RP2453, the computer code STARRS (Secondary-Side Transport And Retention of Radioactive Species) was developed. The STARRS computer code simulates the U-tube steam generator during an STGR event. It contains a stand-alone reactivity transport and release module (D-21) and a thermal-hydraulic module which utilizes the modular modeling system (MMS) routines (D-22). Stand-alone thermal-hydraulic or transport calculations (D-23), or coupled thermal-hydraulic and transport calculations can be performed.

The thermal-hydraulic module simulates the dynamic response of both the primary and secondary sides. The secondary side can be full, partially full, or completely dry. The reactivity transport and release module simulates the coupled heat and mass transfer processes, and aerosol scrubbing on the secondary side. The transport module simulates (1) flashing and atomization of the break flow, (2) rise of a swarm of bubbles, (3) entrainment at the two-phase swell level, and (4) removal in separator, dryer and vapor space.

D.6.2 Validation and Sensitivity Calculations. The developed modules have been validated using available experimental data. The thermal-hydraulic model was validated using data generated at the MB-2 and Semiscale MOD-2B facilities (10 cases) (D-24). The transport and retention module was validated using the MB-2 radioactivity and dry secondary side experiments (14 cases). Sensitivity calculations were also performed assessing the effects of break location, iodine partition coefficient, primary and secondary side iodine mass fractions, and aerosol droplet size distribution on the decontamination factors. Coupled transient thermal-hydraulic and transport calculations were also performed for a Westinghouse plant.

Good agreement with the experimental data has been achieved.

D.6.3 Benefits.

- The model provides a powerful tool for evaluating the SG transient response during tube rupture events.
- The model can be readily modified to simulate any U-tube steam generator.
- Coupled transient thermal-hydraulic and transport calculations can be performed.
- The transport and retention module can be coupled to general purpose thermal-hydraulic computer codes such as RELAP and TRAC.

D.7 Steam Generator Tube Rupture Consequence, Prototypical Simulation in MB-2

The steam generator tubes in PWRs can be damaged by a variety of reasons (e.g., corrosion, mechanical wear) during the life of its normal operation. The tube degradation can cause leak or rupture which can result in the direct

release of radioactive fission products due to venting of steam to atmosphere. Therefore, full double-ended guillotine break of a single steam generator tube is considered a design basis fault by the Nuclear Regulatory Commission (NRC) and the activity release limites are specified in 10CFR100.

In any SGTR fault, the amount of activity released will depend on the degree of active species retention in the steam generator, as well as on the activity levels in the primary coolant. For primary coolant that has mixed fully with the bulk steam generator, the retention is assumed to be similar to that which exists under normal operating conditions. Thus, it is assumed that there is no retention of noble gases, 1% carry-over by mass of iodine with the steam, and 0.1% carry-over by mass of cesium (and similar nonvolatile fission products).

In addition to the release of fission products from the bulk steam generator water, there exists the possibility that some primary coolant may be released without having first mixed with the bulk water. Here, it is postulated that the primary coolant will flash as it leaves the tube break and in so doing it will form very fine droplets which may be carried in steam bubbles through the bulk water to the separators. A fraction of these droplets may be small enough to pass through the separators to be released to the atmosphere. Such uncertainties cannot be quantified because of lack of experimental data, and as a consequence no retention may occur in SGTR faults. NRC is evaluating status of SGTR issue (NUREG-0844) for assessing the current regulation.

D.7.1 EPRI Response. EPRI project on steam generator transient response (RP1845) focused efforts in assessing the retention mechanism by experimental data under prototypical conditions and by developing mechanistic model for predicting the SGTR consequences. Based on significant industry interest, EPRI initiated a joint cooperation and cofunded program with Westinghouse (W) and NRC, and later Central Electricity Generating Board (CEGB), UK, joined this major testing program (D-25, D-26, D-27).

The first-phase efforts were focused on the thermal-hydraulic system response characteristics due to a range of SGTR transients (D-28). The follow-on phase II testing was performed simulating activity transport phenomena under the prototypical pressure and temperature (e.g., primary ≈2250 psia, ≈620°F, secondary ≈1000 psia, ≈545°F) conditions in a large-scale (≈full height) model boiler facility. The strategy was to quantify retention of nonvolatile activity during the various phases of the transient (i.e., high pressure to low pressure) of both the design bases and beyond design base accident conditions. The approach also included assessing the sensitivity on operating conditions, such as downcomer levels. The moisture carry-over is the major factor which will carry nonvolatile radioactive fission products (e.g., cesium and iodine). Therefore, carry-over from the primary and secondary sides was separately monitored, including the associated phenomenon of bypassing without mixing in the secondary side.

In addition, small-scale support testing at full pressure and temperature was also performed as cooperative, cofunded projects with NRC in order to confirm some of the assumptions (e.g., partition coefficient) in assessing the activity transport during SGTR (D-28, D-29).

D.7.2 Research Results. The key research results include:

- The release of radioactive fission products by moisture carry-over or entrainment of liquid droplets is not a significant factor for both a design base or beyond design base (i.e., stuck open relief valves following SGTR) accident conditions.

- A significant mixing and scrubbing of primary activity takes place and therefore very little evidence of primary coolant bypassing under steady-state levels is present.

- The data supports the existence of greater safety margins than those used in current prescription for licensing calculations and safety analysis reports.

The principal observation made during the test program was that very little or no primary coolant bypassing was detected under steady-state SGTR/SORV fault conditions, either at normal water level or when the break location was exposed. Under all test conditions, both at low power or at 100% power, moisture carry-over was very low, and under steady-state SGTR/SORV fault conditions, no significant increase in moisture carry-over was detected. However, following short-term perturbations, various types of transient releases were identified which could be the equivalent of steady-state releases over many hours.

It is anticipated that the data provided by these programs will have a significant impact on the design and on the operational and inspection requirements needed to meet regulatory requirements for activity release. In particular, they may determine the importance placed on maintaining very low primary coolant activity levels, the economic consequences for fuel integrity, the assumed frequencies of SGTR and SORV events, and, finally, the costs and operational exposure incurred in maintenance and inspection if iether the SGTR frequency (unresolved issues A-3, A-4, and A-5) or SORV frequency needs to be reduced.

D.7.3 Using the Research Results. This research has provided the database which industry can use not only to meet the requirements for activity release but also to identify enhanced safety margins for relieving other operational and inspection requirements.

Westinghouse, Inc. (W), for example, is using the result to validate their best-estimate method for industry application. EPRI has initiated a parallel effort to develop predictive tool for calculating retention of activity in the secondary side following SGTR. The EPRI method called STARRS (Secondary Side Transport And Retention of Radioactive Species) has been validated using the selected database from this test program. The NRC, as a result of this database, reevaluated their regulatory requirements and closed the unresolved safety issues (A-3, A-4, and A-5).

The primary use of these results is to demonstrate the degree of conservatism in the current requirements, to form a basis for best-estimate analysis tool for the industry, and to enhance operational flexibility by utilizing margins.

In addition, the test results extend its application to beyond current design base requirements. A specific use of these results (beyond U.S. design base requirement) was made by CEGB in UK in showing the assumption of no retention in the Sizewell B safety case for SGTR with SORV is conservative. This is the unique large-scale database and it should provide significant economic payoff for operating reactors in specific applications by utilizing the large margins indicated.

D.8 Small-Break Critical Flow Model (Dartsmouth)

It is expected that in the course of a loss-of-coolant accident, the reactor coolant pumps will be shut off and natural circulation will be established between the reactor vessel and the steam generator. Thus, low-fluid flow rates will prevail and stratified flow will probably be present in the horizontal piping of the primary loop.

In the considerations, here, a small break is of particular concern, since stratification of water and vapor, and therefore, break orientation with respect to the fluid interface will determine the amount of water and vapor escaping through the break. If computer safety codes like TRAC or RELAP could predict fluid inventory loss in the system during such a small-break loss-of-coolant accident (SBLOCA), the control room personnel could plan for timely action. But according to D-30, both TRAC and RELAP currently overestimate the fluid loss by an order of magnitude in the initial phase of such an accident.

Therefore, the flow regime and break orientation has to be considered when calculating discharge rates. If the small break is at the bottom of a horizontal pipe and stratified flow is present, the fluid loss will be initially similar to the draining of a bath tub. If the liquid level is high enough, only liquid will enter the break. With decreasing liquid level, the liqud vapor interface will dip down toward the break and eventually a water-vapor mixture will escape through the break. This phenomenon is called "vapor pull-through." If the break is located above the fluid interface, high vapor velocities in the vicinity of the break (close to the break), might create roll waves, and droplets might be entrained from the crest into the steam flow.

Another important phenomenon to be considered is that the two-phase flow through the break is choked. This means that, like in single-phase compressible flow, there is a maximum or critical flow out of a valve or break of a vessel during depressurization, which cannot be exceeded when the downstream pressure is lower than a certain critical fraction of the pressure vessel. In the EPRI report (D-31), several critical two-phase models are discussed in detail.

A third phenomenon to be considered in all modeling efforts is the size and physical property scale. Experiments of large-break diameters were performed in the Marviken test facility (D-31) with break diameters up to 0.5 mm at pressures up to 5 MPa. A guillotine break of a main pipe in a 100-MW reactor would represent a break diameter of about 0.1 m (D-32). The initial pressure in a reactor system is about 15 MPa. However, there are no small break

experiments in a similar size test facility and pressure range as the Marviken experiments. To fill this gap, the Idaho National Engineering Laboratory performed in 1984 the "TPFL Tee/Critical Flow Experiments" (D-30), which are the basis for the model developed in ref. (D-33).

It is always desirable to base the analytical effort of developing a model on the physical processes at hand. This will give more credibility to use the developed correlation scheme for other geometries, pressures, or other fluids. For example, the phenomenon of vapor pull-through is such a case and was studied extensively by several authors (D-34), (D-35), and (D-36). From dimensional analysis, the onset of vapor pull-through, as described above, can be modeled with a very simple correlation of the type

$$Fr \left(\frac{\rho_f}{\Delta\rho}\right)^{0.5} = A \left(\frac{h_b}{d}\right)^n ,$$

where h_b is the liquid height above the break at onset of entrainment, d is the break diameter, A and n are constants, and Fr is the Froude number based on the break dimater and the fluid velocity in the break. Schrock et al. (D-37) found that the published data for A vary in the range from 0.2 to 3.2, and n from 1.5 to 2.5. This indicates that multidimensional effects might be of important as well as fluid properties like surface tension (D- 37). It is feasible to develop a three-dimensional solution for the vapor pull-through phenomenon using potential theory.

The above vapor pull-through correlation and critical flow models are used to predict the experimental results of the studies performed by the Idaho National Engineering Laboratory (D-30). Typical comparisons of the model against experimental data are shown in figures D-6 and D-7 for bottom and side breaks, respectively.

E. EARTHQUAKE HAZARD AND DESIGN RESEARCH AT EPRI

E.1 Introduction

Nuclear power plants are required by regulation to be designed and built to withstand earthquakes. Seismic design is a major factor in the cost of constructing and licensing the plants; some authorities (E-1) have estimated that seismic costs are now 9% to 15% or more of the total for a typical plant in either the Eastern United States (EUS--east of the Rockies) or the West Coast plants, respectively. These cost percentages assume that the engineering and installation is done only once. More typically in recent years, the instability of the licensing process has caused changes to occur during design, construction, and preoperation periods. Earthquake protection costs for these units are probably more than doubled. Finally, for operating plants, there are recurrent concerns (E-2, E-3) about their seismic adequacy and expensive evaluations, and retrofits are being done.

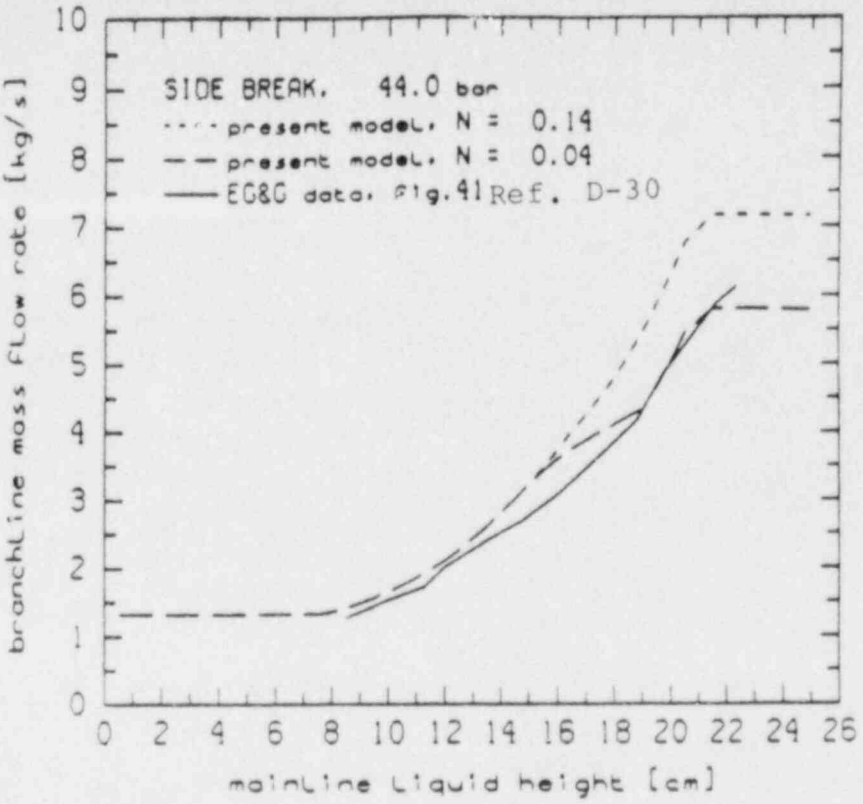

Figure D-7a (Branchline Mass Flow Rate as a Function of Mainline Liquid Height. Comparison of Model and Experiment

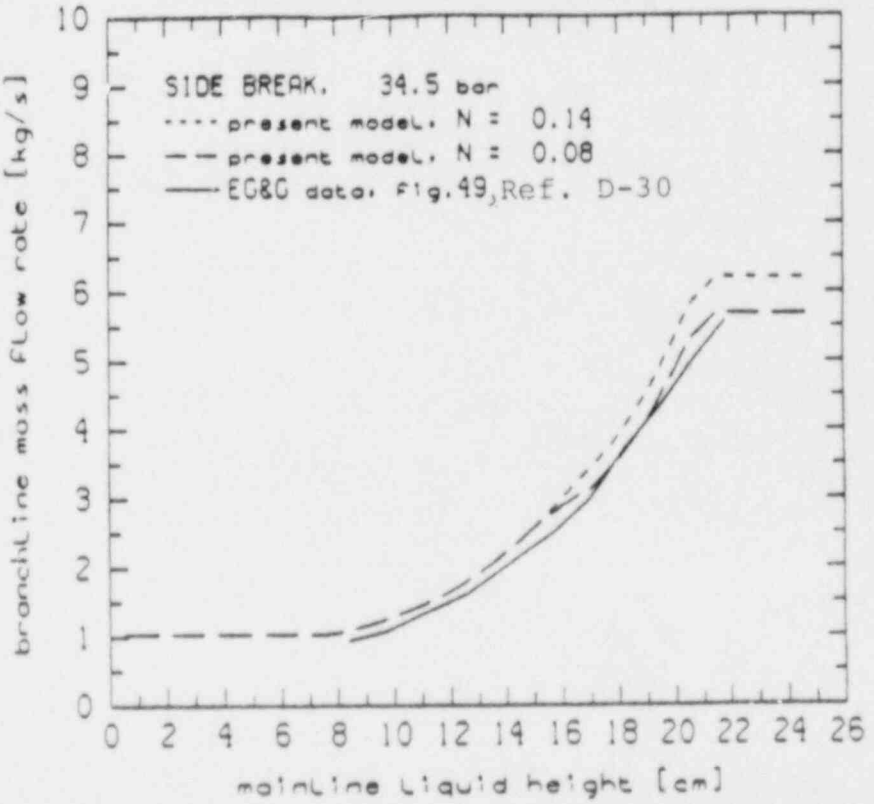

Figure D-7b (Branchline Mass Flow Rate as a Function of Mainline Liquid Height. Comparison of Model and Experiment

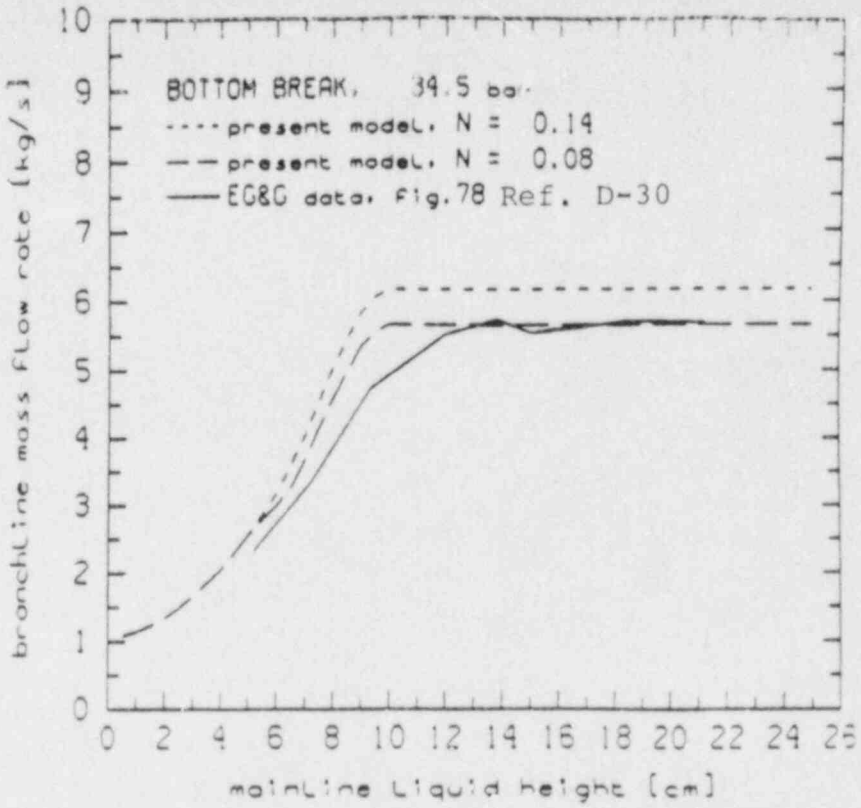

Figure D-6a (Branchline Mass Flow Rate as a Function of Mainline Liquid Height. Comparison of Model and Experiment

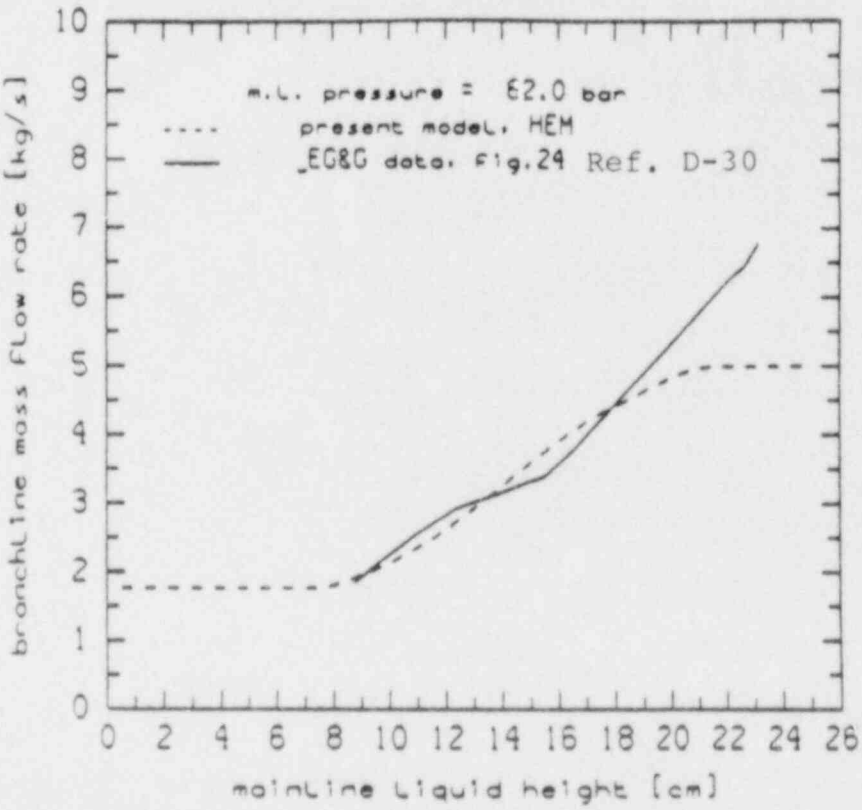

Figure D-6b (Branchline Mass Flow Rate as a Function of Mainline Liquid Height. Comparison of Model and Experiment

Recognizing the importance of the seismic issue, EPRI formed a Seismic Center in 1983 as a focal point for EPRI research supporting the resolution of seismic issues and the development of advanced technology and enhanced criteria for nuclear-related facilities. The Seismic Center has both a Technical Advisory Panel of seven distinguished earthquake specialists and an Advisory Group of ten utility engineers, and the center also works closely with NUMARC working groups.

Through interactions with utility engineers and their consultants, the Seismic Center staff have identified nine seismic issues facing utilities, as shown in table E-1. Issues needing near-term (before 1988) resolution are distinguished from others with farther horizons and/or requiring long-term research. At this time, EPRI research is focused on all issues except procurement of fragility data. The ongoing seismic research work is discussed below.

Table E-1

SEISMIC ISSUES FACING UTILITIES

Through 1988	Post 1987
1. Seismic Hazard in EUS (SOG)	Ground Motion Input
2. Soil-Structure Interaction	
3. Seismic Adequacy of Equipment	
4. Seismic Margins for EUS Plants	Fragility Data
5. Startup Criteria Following an OBE	
6. Piping Design Improvement (Snubber Removal)	
7.	Design of Future LWRs

E.2 Reassessment of Seismic Hazard Within the Eastern United States

Past practice in siting most existing EUS nuclear plants has involved an assumption of geographic stationarity of large earthquakes. Since issuing the NRC siting regulation, 10 CFR 100, Appendix A, in 1974, a demonstration that such large earthquakes are associated with local tectonic structure has been required. However, the historical record of earthquake occurences continued to strongly influece regulatory decisions. If an area had experienced a large earthquake (e.g., Charleston, South Carolina, in 1886), it was assumed that some local tectonic structure was the cause, even when the structure was unknown. Increased understanding of earthquake processes has weakened the assumption of stationarity and reliance on historical record; and, in a recent letter (E-4), the USGS removed its support of the more traditional practice of assuming that large earthquakes would reoccur only in their historic locations.

As a result, NRC is reassessing the seismic hazard at every nuclear site in the eastern United States. An interim report (E-5) has examined ten sites. In 1983, NRC described their program and suggested that industry should organize a parallel assessment. EPRI prepared a program plan and the utilities organized the Seismicity Owners Group in August 1983 to jointly sponsor the EPRI research. The program has been completed and a Topical Report (E-6) was submitted to NRC in July 1986. Completion of the NRC Safety Evaluation Report is scheduled for the end of 1987.

Major products of this effort are: (1) a comprehensive interpretation structure for all necessary inputs; (2) a computational package, EQHAZARD; and (3) the maps of seismic sources, one of which is shown in figure E-1.

Verification and validation of the computational package EQHAZARD has been completed and a quality assurance audit was conducted to meet the requirements of 10 CFR 50, Appendix B. The entire computational package will be released as an EPRI production code following completion of the NRC's review.

Seismic wave attenuation and the selection of a lower bound earthquake magnitude are two key parameters for seismic hazard computation. EPRI held state-of-the-art workshops on these two topics early in 1987. The workshops resulted in compilation and evaluation of the results of relevant EPRI, government, and university research. The proceedings of these workshops are scheduled for publication during the last quarter of 1987. From these state-of-the-art results, EPRI is forming technical bases to support industry technical positions on seismic wave attenuation in the eastern United States and the proper lower bound magnitude for seismic hazard and computation for nuclear plants. These positions are scheduled for completion in the last quarter of 1987.

E.3 Ground Motion Input for Seismic Design

The response spectrum specified by NRC Regulatory Guide 1.60 is designed to envelope spectral shapes corresponding to a range of different soil conditions and thus, for a given site condition, is unnecessarily conservative over some frequency band. Notwithstanding the excessive conservatism in the Reg. Guide spectrum, small but very close earthquakes can generate high-frequency, short-duration ground motions which have little or no damage potential but may exceed the spectrum at high frequencies. In order to reduce excessive conservatism and to stabilize the licensing process, actual time histories must be obtained during strong ground shaking, under various source site conditions.

EPRI has implemented a ground motion experiment near the Parkfield segment of the San Andreas fault in central California. During the past 150 years, the Parkfield segment has ruptured on the average of every 22 years causing an earthquake of Richter magnitude 5 or greater. The last earthquake was in 1966, so one is estimated in January 1988. EPRI has designed a dense array of 13 surface and 8 downhole accelerometers which is located about 7 km from the San Andreas fault, as shown in figure E-2. The array is designed to measure the coherency (i.e., spatial variability) of ground motion over distances

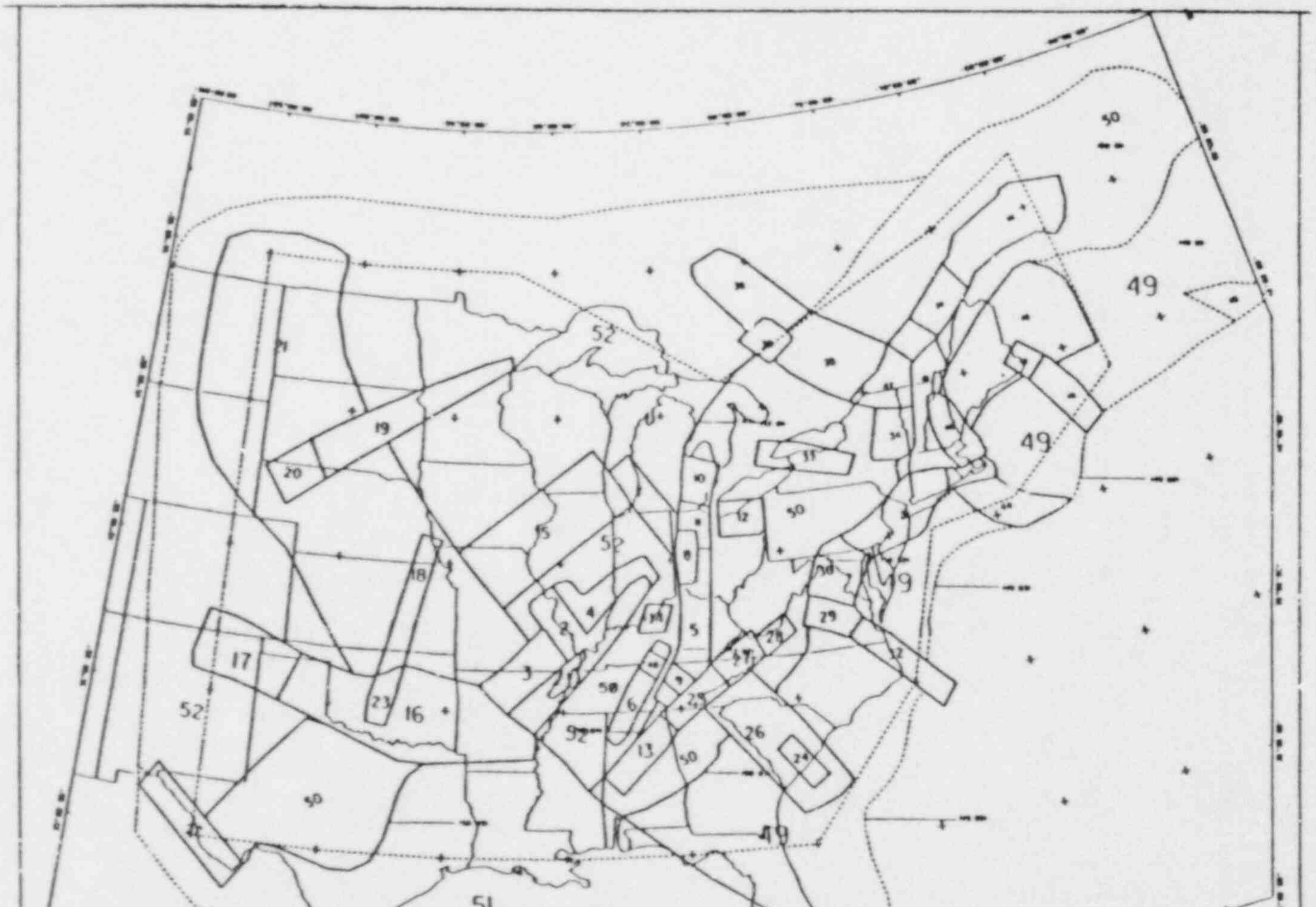

Figure E-1 Map of seismic source zones in EUSAC. The numbers refer to the table in Appendix C which gives the 'a' and 'b' values as well as an identifying name for each of the seismic source zones.

Figure E-2 EPRI/USGS Experiments at Parkfield

Parkfield Strong-Motion Array: Waiting for the Next One

An area of the San Andreas Fault near Parkfield in central California has regularly experienced earthquakes of Richter magnitude 5–6 about every 22 years; the last one, in June 1966, was a magnitude of 5.5. Regression analysis indicates the next one is due around 1988. Researchers from USGS, EPRI, and several universities are planning two major experiments to study soil liquefaction and the spatial variability of seismic waves along the expected break between Parkfield and Cholame.

In the dense seismic array experiment, surface and downhole accelerometers will measure the coherency of earthquake ground motion over short distances and, acting like a directional antenna, will permit accurate mapping of the location of seismic energy sources. A second array will measure (for the first time) seismic motion in a saturated soil to assess the dynamics of liquefaction during an actual earthquake.

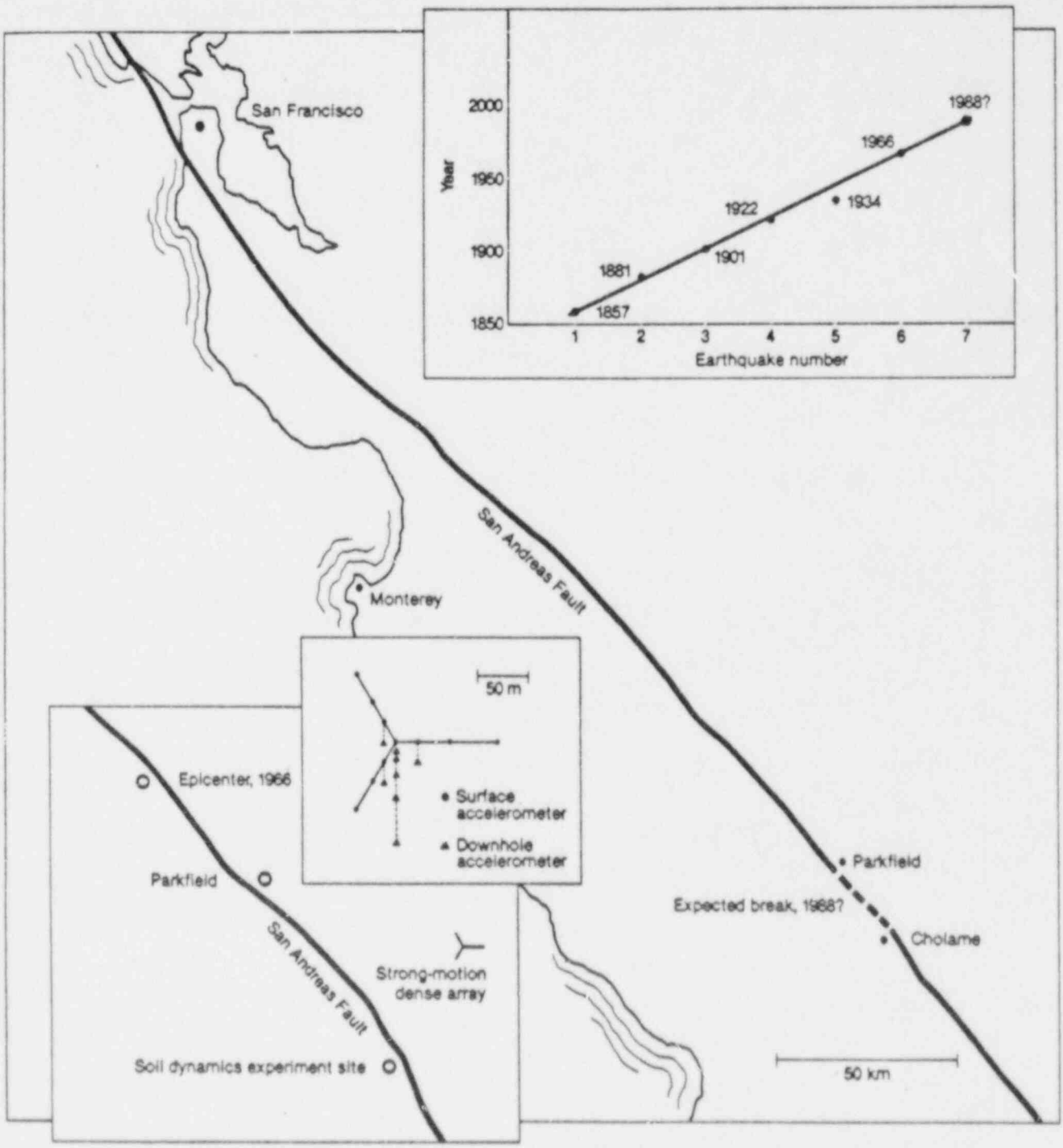

comparable to the dimensions of a nuclear power plant. Reduction in structural response due to incoherency of input motion has been postulated in past licensing applications, but a high-quality data set to test the phenomenon has been lacking. Free-field measurements of incoherency on firm ground have never been made over the distances of interest here.

Data from this array will serve the important additional function of permitting a detailed analysis of the fault rupture during the earthquake. To strengthen the value of the data for this analysis, the California Strong Motion Instrumentation Program (SMIP) is installing instruments to extend the EPRI array about 1 km in each direction. Recordings from this extended array will permit detailed analysis of the earthquake rupture process and the testing of source motion modeling procedures.

In cooperation with the USGS, EPRI is conducting a soil dynamics experiments at a site 0.5 km from the San Andreas fault (figure E-2), where water-saturated cohesionless soil layers are near the surface. The objective is to measure simultaneously, at various depths, the buildup of pore-water pressure and the time history of ground acceleration--data critical for validating predictive models of soil response to strong ground shaking. The data from this experiment will be used to conduct testing of site response computational models and the nonlinear behavior of soils under strong earthquake loading.

E.4 Soil-Structure Interaction Research

During a strong-motion earthquake, the dynamic coupling between massive plant buildings and their underlying soil significantly influences the responses of structures and hence components such as piping. In design analyses, free-field ground accelerations determine motions of building foundations through soil-structure interaction (SSI) models. NRC's Standard Review Plan (SRP) 3.7.2 specifies a conservative enveloping of existing models since there is a lack of data to support a more realistic approach. The objective of EPRI's SSI research is to be able to support a revision of SRP 3.7.3 through the generation of an experimental database to validate SSI models encompassing nonlinear behavior under strong ground motion.

EPRI has sponsored two series of strong-motion SSI experiments using buried explosives. The first series of tests (E-7, E-8), also called SIMQUAKE I and SIMQUAKE II tests, was conducted on a soft soil site near Albuquerque, New Mexico; the second series of tests, cosponsored by Niagara Mohawk Power Corporation, was performed on a rock site near the Nine Mile Point (NMP) nuclear power station.

These experiments used 1/48- to 1/8-scale cylindrical containment models with various foundation and embedment conditions. The models were initially subjected to low-level vibratory tests in order to measure their natural rocking frequency. During the actual experiments, the waves induced by the detonation of explosives propagate through the soil to the model structures. The motions of the surrounding soil and of the structures were recorded. Although the explosive-generated wave characteristics are different from those under actual earthquakes, the SSI observed during the ringdown phase of the

excitation should qualitatively represent the actual earthquake-induced responses.

In the SIMQUAKE experiments with soft soil, the models experienced peak accelerations in the range of 1 to 4 g. Under a strong-motion environment, the structure rocking frequency significantly downshifted from that induced by low-amplitude vibration, e.g., 16 Hz to about 4 Hz. But the NMP experiments on rock, the shift in the rocking frequency was minor. These qualitative results suggest that, for soft soil sites, the current practice of extrapolating linear SSI response into the nonlinear range may be overly conservative. The SIMQUAKE data have been used to validate EPRI's nonlinear finite-difference code STEALTH-SEISMIC (E-9, E-10).

In order to supplement these simulatee earthquakes with small models in real earthquakes, EPRI, with the support of Taiwan Power Company, has constructed 1/4-scale and 1/12-scale models of a PWR containment building in Lotung, Taiwan. The location is a seismically active one, containing a large array of strong-motion accelerometers (figure E-3). Both the containment and internal components have been heavily instrumented. Free-field ground and downhole motions are also monitored. NRC has sponsored low-amplitude forced vibration tests on the scaled containment models. Since the experiment was inaugurated in October 1985, the model has experienced four strong-motion earthquakes giving free-field ground motions in the neighborhood of 0.2 G. EPRI and NRC have contracted with several A/Es, consulstants, and universities to make blind predictions of the model's response motions. By comparing these calculations to the measurements, conservatisms can be quantified and a more technically justified analytical approach can be derived. The Lotung site has soft soil, which is of particular importance in view of the strong soil-structure interaction in this environment.

E.5 Seismic Qualification of Equipment

The Seismic Qualification Utility Group (SQUG) has taken the lead, with EPRI support, on seismic qualification and has been most effective in working with NRC to resolve USI A-46.

EPRI's Seismic Center has initiated three new projects in support of SQUG: (a) a relay functionality project; (2) a survey of the literature for field experience on seismic demand; and (3) a post-earthquake investigation project. The latter has been initiated to document experience of industrial facilities, especially power plants, which have been exposed to strong ground motion.

Methods are being developed and tested to determine those critical electrical relays which must chatter or change state during earthquake shaking. This work will form the technical basis for addressing seismic relay chatter in assessments of equipment qualification. Qualification of equipment relies on seismic demand spectra. Ground spectra are used for equipment below 40 ft above grade, and floor spectra are used for equipment higher in the plant. the seismic demand project is compiling and analyzing both free-field and within structure motions to develop realistic experienced base floor spectra

Large-Scale Soil-Structure Interaction Experiment

EPRI and Taiwan Power Co. have constructed and instrumented two scale-model PWR concrete containment buildings within an existing U.S. National Science Foundation dense seismographic array at Lotung, Taiwan, to study the interaction of soil and structures during actual earthquakes. The models, 1/4 and 1/12 actual size, are on a soft-soil site on the island, which experiences frequent, strong seismic activity.

Data from two recent temblors of Richter magnitude >6.0 were recorded by instruments buried in the ground and mounted on the structures, as well as by instruments on a mockup steam generator and pipe run inside the 1/4-scale model. Expert interpretation of the data, now under way, will help substantiate predictive models of soil-structure interaction and contribute to assessment of the dynamic response of reactor containments and components to actual earthquake-induced motion.

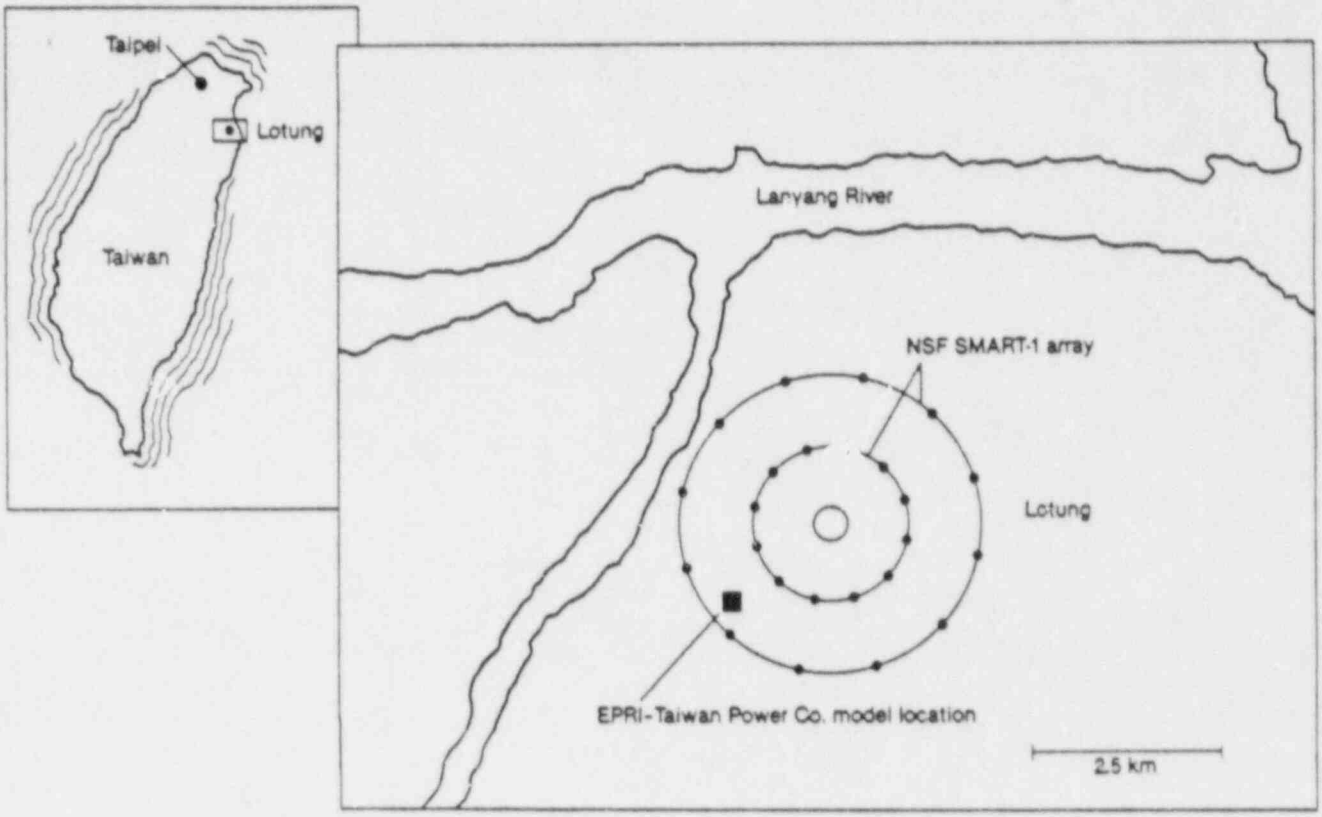

Figure E-3

for equipment qualification. The post-earthquake investigation program is an ongoing activity designed to augment the experience database on equipmet performance in earthquakes.

E.6 Seismic Margins for EUS Plants

The interim LLNL report (E-5) reassessed the seismic hazard for ten sites. For a representative site, the new NRC methodology suggests that their existing design bases (Safe Shutdown Earthquake--SSE) have an exceedance probability of about 10^{-3} per year. Past NRC staff positions for an SSE have been 10^{-3} to 10^{-4}, and the Advisory Committee on Reactor Safeguards (ACRS) has beep suggesting that earthquakes with a probability in the range of 10^{-4} to 10^{-5} per year should be considered (E-3).

The ACRS (E-2, E-3) has been concerned with the degree of margin that exists in nuclear power plant seismic design, and, for the past five years, has requested that such a methdodology be developed. To quantify the feeling of confidence widely held in the industry about the conservatism of nuclear plant seismic design, EPRI initiated a seismic margins project in 1985.

By the strictest meaning of the term margin, the objective would be to ascertain the level of earthquake motion leading to unacceptable consequences and to compare that level to the design basis. EPRI proposes to quantify the seismic margin by: (1) defining a ground motion level based on the results of the EUS seismic hazard assessment; and (2) establishing the capability of the plant to achieve a stable shutdown configuration for that earthquake. This evaluation is intended to use state-of-the-art methods for inspection, evaluation, and analysis. Preferred functional paths to reach shutdown are defined; and those systems and components in that path are evaluated for the larger earthquake. This path is conceptually determined and ultimately chosen based on walkdowns of important components and systems in the plant.

The EPRI Seismic Margins project has interacted with the NRC Margins program for information exchange and has coordinated heavily with SQUG for use of ruggedness data, for consistency in criteria and procedures, and for a measure of utility peer review.

Both the EPRI and NRC programs were organized in three phases: methods development, a trial evaluation of a PWR plant, and finally a second trial evaluations of a BWR plant. The EPRI methodology and trial PWR evaluation were both completed in the first half of 1987. The evaluation was performed on the Duke Power Catawba unit 2 plant. A similar evaluation by NRC was done for the Maine Yankee plant and resulted in an SER closing the remaining outstanding seismic issues for the plant. The EPRI and NRC programs have recently been merged. Under this arrangement, NRC has sponsored a Peer Review Panel to evaluate the EPRI methodology, and EPRI will perform the trial BWR evaluation on Georgia Power's Hatch unit 1 plant. NRC will also sponsor a parallel Peer Group to interact with and review the Hatch evaluation. This phase of the program will be completed in the fall of 1988 after which EPRI will modify the methodology based on the trial evaluation results and submit a Topical Report for formal NRC approval through NUMARC. Margin review are

expected to be used to resolve issues raised by the Eastern Seismicity Reevaluation and the NRC Severe Accident Policy.

E.7 Piping Design Improvement

A typical LWR contains 45 miles of piping and 550 miles of cable, all of which are supported by about 6000 hangers, snubbers, and trays. Each of these supports is seismically engineered at least once and often several times due to changes and retrofits. The resulting congested configuration and the requirement for frequent maintenance of this support hardware have impacted piping system reliability during normal operating thermal cycles. Plant shutdowns for in-service inspection, maintenance, and repair of seismic hardware have also contributed to both loss of availability and increasing occupational radiation exposure.

It is widely believed within the technical community that the resulting piping systems are overly stiff and that more flexible systems would be more conducive to safety. Surveys of field experience (referred to earlier) have never found a piping failure due to inertial loads in flexible systems.

EPRI has been conducting piping research since 1977. The objectives are: (1) generation of an experimental database; (2) development of a sophisticated nonlinear finite-element computer code, ABAQUS (E-11) [which adequately represents piping behavior beyond the elastic regime]; (3) development of a simplified method for designers to account for nonlinear piping behavior; (4) improvement of piping design rules; and (5) the development and qualification of alternative piping support systems. These products will help support modification of ASME code and NRC requirements resulting in more realistic dynamic behavior of piping systems. This should facilitate removal or deactivation of a substantial number of snubbers from existing plants and use of fewer snubbers in new construction.

As part of this effort, EPRI, in collaboration with Consolidated Edison Company, sponsored a series of dynamic tests on a 110-ft long, 8-in. diameter feedwater line at the Indian Point 1 plant. Over 200 forced vibration and transient snapback tests were conducted (E-12). The damping data obtained from the experiment was provided to the Pressure Vessel Research Committee as part of a database in formulating the ASME code case N411 (E-13) on improved damping values. On the basis of the ASME code case, several utilities are assessing the potential for removing many existing snubbers. EPRI is continuing its research support in the areas of snubber reduction and damping improvement.

The existing ASME code bases its stress limits on plastic collapse under statically applied loads without recognizing the margin is often much greater for a dynamic load than for a static load of equal magnitude. Also, the ASME code assumes that seismic loads are primary and requires them to be combined with dead weight, thermal loads, and others. It is now recognized that the likely or primary failure mode induced by seismic loads will be fatigue ratcheting. In order to more thoroughly support modification of the ASME code and to allow larger and more realistic stress limits, additional experimental data are being obtained.

EPRI has sponsored large amplitude dynamic tests on a series of piping systems. The first system (E-14) was a simple 22-ft, 4-in. diameter Z-shaped pipe which was internally pressurized to 1000 psig and supported at three locations. The second and third systems (E-15) were complex three-dimensional systems of 3-in. and 6-in. piping which were fabricated in compliance with ASME Class 2 specifications and were internally pressurized to about 1150 psig. All piping systems were dynamically loaded to three to five times their level D stress allowances without failure or even leakage. Concurrent tests of mechanical snubbers showed that their capcity was about two to four times larger than their level D loads.

To provide further technical basis in developing realistic and improved piping design rules for seismic and dynamic loads, in 1985 EPRI initiated with NRC's participation a three-year effort (E-16) to systematically demonstrate and evaluate the piping dynamic capacity and fatigue-ratcheting failure behavior. The test matrix consists of 40 component tests, 3 system tests, and 110 material specimen tests. To fail the pipe, the dynamic energy input to this test series is much higher than that used in the earlier high-amplitude testing. Component testing is under way on a specially designed high-power shake table. The test matrix includes nominal 6-in. fittings (elbows, tees, reducers, etc.) with parametric variations in pipe schedule, material, internal pressure, and loading type. Results from elbow tests have shown that fatigue ratcheting (viz., swelling and through-wall cracking) occurred, instead of plastic collapse, after two to three applications of a 20-sec seismic loading with peak input accelration of about 20 g (10 to 24 times level D stresses). The measured peak dynamic moment at the elbow reached twice the static collapse moment and the apparent damping was as high as 34%. The component tests will be completed in early 1988. System tests to demonstrate fatigue ratcheting failure mode and quantify seismic margin are also under way and will be completed in 1988. Using the test results, improved experimentally based piping design rules will be recommended for inclusion in the ASME code. A code case considering removal of operating basis earthquake (OBE) stress from the primary stress category for class 1 piping systems for interim application has been submitted to and accepted by ASME.

EPRI's research effort in the area of alternative piping support systems includes: (1) the development of a passive support system using seismic stoppers, and (2) further qualification of a ductile energy-absorbing device. EPRI is participating in the HDR test program in West Germany to demonstrate both system's effectiveness in replacing snubbers.

F. Analysis Development and Validation

F.1 Qualification of RETRAN for Simulator Applications

The use of full-scope control room replica simulators has increased substantially in the years following the accident at Three Mile Island unit 2 (TMI-2). In most simulators purchased since the TMI-2 accident, the technical capability required to represent severe events has been included in varying degrees. Also, the ability of the instructor to create a large

variety of combinations of malfunctions has also greatly expanded in recent years.

The nuclear industry has developed a standard which establishes the minimum functional requirements for full-scope nuclear control room simulators used for operator training. This standard, ANSI/ANS-3.5, was first issued in 1981 and has been revised and reissued in 1985 (F-1, F-2). Section 3.1.2 and 4.2.1 of the ANSI/ANS-3.5 calls for the simulator to be compared to actual plant response or best-estimate plant response.

EPRI has been working with the nuclear utility industry to develop improved methods for the qualification of nuclear power control room simulators. The EPRI report, NP-4243, "Analytical Simulator Qualification Methodology," (F-3) presents approaches for developing qualification criteria based on training requirements, and documents the development and testing of the use of an engineering code to provide the required reference "best-estimate response" information for the qualification process. This EPRI work also presents an approach for developing a matrix of simulator test transients that may be used to qualify a simulator.

The use of actual plant data is always the best way to qualify the capability of a power plant training simulator. However, plant data for the entire spectrum of plant transients which must be covered in training exercises is not available. The use of an analytical model to establish reference information for simulator qualification is a logical and necessary step in order to cover all possible modes and accident scenarios. ANSI/ANS-3.5 allows for the use of analytical models to provide "best-estimate" information to be used in the qualification process.

The extent to which RETRAN has been qualified with actual data is generally important in establishing the capabilities of the code for all applications in the design, licensing, and analysis of nuclear power plants (F-4). The extent of qualification to actual data is a particularly significant element in establishing its capabilities for use in the qualification of power plant training simulators. Realistic responses to complex and severe scenarios are necessary for training reactor operators to experience and handle events that normally will never occur. Some of the situations they must be completely capable of handling will occur only once, if ever, in their professional lives. It is difficult, if not impossible, to evaluate the performance of the simulator models without developing reference (comparative) best-estimate information with a computer code.

The question is, how is the capability of that computer code established. The capability of the reference code can be assessed by examining the physical models on which the code is based, by comparing it to other codes that may have established capabilities, and by comparing the code to actual plant or system test data. The best method to qualify the computer code is by examining the performance of the code as compared to actual data from power plant tests, events that may have been recorded at power plants, or tests at a wide variety of facilities that have been designed to test power plant design features. Although the documentation of the qualification of RETRAN occurs in

a wide variety of papers, documents, and reports, a large number of the analyses are included in ref. (F-1) and refs. (F-5) - F-8).

In order to evaluate the extent to which RETRAN has been exposed to the complete spectrum of possible thermal-hydraulic conditions that may be required for training during expected and severe events, the Electric Power Research Institute is funding the preparation of a report that summarizes the analyses that have been performed since 1977, when the prerelease activities on RETRAN-01 began (F-9). In addition to the plant and system tests that are summarized in ref. (F-9), a substantial amount of RETRAN analysis work has been performed where RETRAN was compared to other codes, small separate effects tests and analytical solutions. This work is documented through EPRI publications, professional society transactions, topical reports, etc.

Ref. (F-9) focuses on the RETRAN analyses that have been performed where the results are compared to plant or test facility data. The report summarizes each model, the event, and evaluates the results of the analysis that was performed. The analysis are summarized with respect to the variety of different thermal-hydraulic conditions that have been experienced by the code and a rating scheme provides a measure of the quality of the results.

F.2 Licensing Application of RETRAN-02 and VIPRE-01

F.2.1 RETRAN-02. Since the beginning of its development in 1976, the RETRAN system transient thermal-hydraulic analysis computer code (F-10, F-11) has been used both domestically and internationally to analyze a broad spectrum of operating plant events. For the last several years, domestic utilities have used RETRAN analyses of their nuclear power plants to further their understanding of plant behavior during anticipated operational occurrences, to support technical staff training, to provide benchmarks for simulator qualification, and to evaluate specific plant safety considerations independent from their NSSS or fuel vendors (F-5) - (F-8). The flexible structure of RETRAN allows its application to BWR and PWR nuclear power plants and also to test facilities and separate plant components.

One of the primary objectives of the RETRAN development effort is to provide a tool that can be used to perform plant safety analysis in support of core reload licensing. To pave the way for utility licensing applications of RETRAN, EPRI has performed rigorous verification and validation of the code and conducted a design review to demonstrate RETRAN applicability. The NRC issued a safety evaluation report (SER) for the RETRAN-02 code in 1984 (F-12) and approved its sue for licensing applications subject to certain conditions. The NRC SER concludes that RETRAN".... is an acceptable computer code for calculating the transients described in chapter 15 of NUREG-0880, and other transients and events as appropriate and necessary for nuclear power plant operation." Technical evaluation reports (TER) for reviewed versions of RETRAN summarize the review findings and indicate areas where model limitations have been identified and where user-specific models and topical reports will be examined in detail.

Several domestic utilities have applied RETRAN to licensing analysis or are developing RETRAN models and topical reports, based upon the NRC RETRAN SER and TER, for application to reload fuel licensing. The experiences of some of these utilities is summarized below.

Tennessee Valley Authority (TVA), Virginia Electric Power Company (VEPCO), and Yankee Atomic Electric Company (YAEC) have all used RETRAN for licensing applications (F-13). TVA began formal submittals of topical reports describing their RETRAN models for the Browns Ferry plant (BWR) in 1981 and began performing reload licensing analyses with RETRAN in 1984. VEPCO began submittals of topical reports of their RETRAN models for the North Anna plants (PWR) in 1981 and has received an SER for limited RETRAN licensing application. YAEC has prepared a topical report for RETRAN analysis of the PWR main steamline break accident and received an SER from the NRC.

Baltimore Gas and Electric and Florida Power and Light have prepared topical reports of their RETRAN plant models and submitted them for NRC review. Duke Power Company and Pennsylvania Power and Light are preparing RETRAN topical reports for application to their plants.

GPU Nuclear Corporation (GPUNC) is using the methodology and guidelines of the EPRI Reactor Analysis Support Package (F-14) to develop a licensing analysis capability. GPUNC is in the process of preparing topical reports for their reload licensing analysis including a topical report on RETRAN application.

These and other utilities have long-term plans to perform much or all of their reload fuel licensing analysis in-house. Plant-specific RETRAN models are planned for the transient thermal-hydraulic analyses.

F.2.2 VIPRE-01. EPRI developed the VIPRE computer code (F-15) for the utility industry use in the area of thermal-hydraulic analysis of LWR cores for safety analyses and licensing applications. The VIPRE-01, MOD-01 code received a safety evaluation report (SER) form to NRC in May 1986 accepting it for PWR licensing calculations. The utility industry is using VIPRE for licensing applications, CHF correlation development, reload safety analyses, Tech. Spec. limit improvement, etc. (F-16).

Northern States Power Co. (NSP) used VIPRE-01 analyses of their Prairie Island nuclear plant in preparating a topical report on reload safety evaluation methodology which received NRC approval in May 1986 (F-17). NSP used VIPRE-01 for thermal margin analysis after Prairie Island reactor along with the WRB-1 CHF correlation (F-18).

Work is in progress with VIPRE-01 application at other utilities (e.g., Commonwealth Edison Co., Duke Power Co., TVA, GPU, TU Electric Co., MSU, System Services, Houston Light & Power Co., Wisconsin Public Service Co., and WPPSS) in the area of CHF correlation development, statistical analysis, sensitivity studies, Tech. Spec. improvement analyses, thermal limit calculations, etc. Some of these utilities are preparing topical reports on their work for submittals to NRC approval.

F.3 Verification and Validation of FREY for Application to CILC

In a few BWRs, unexpected fuel failures have been encountered. They were found to be associated with the crud-induced localized corrosion (CILC) mechanism. The failure of the CILC-affected rods may be attributed to the pellet-clad-interaction (PCI) phenomenon.

A diagnostic analysis of this problem requires a fuel rod behavior code capable of correct simulation of the PCI failure mechanism. Although PCI has been known for some 15 years, it is perceived differently by different people. Thus, the simulation of PCI in fuel rod codes varies widely, and in many codes such as COMETH, this simulation is "hardwired" in the code to provide agreement with observed clad ridging. This simplistic treatment of a very complex phenomenon is incapable of diagnosing PCI failure phenomena not considered in the "hardwiring."

The protagonists of the PCI phenomenon, namely, the fuel pellets and the cladding, respond to the heat load as a system of master and slave. Upon initial contact at low power, the pellet acts as the master and drives the cladding with a strong force. At higher power, however, this driving force begins to unload the cladding through its own relaxation. At very high power, the pellet virtually loses all of its driving force and can be contained by the cladding with little or no effort.

For PCI to lead to premature cladding failure, two conditions must be satisfied: (1) fuel-clad contact must be established at low power levels (<3KW/ft); and (2) this contact must be "hard", i.e, the cracked configuration of the pellet must be non-compliant under compression. Cracking in CILC failures have been observed at burnup levels in excess of 10 GWD/T. This burnup level happens to be near the saturation limit for fuel relocation, and thus a rate of 0.11 kW/ft/hr as recommended by some fuel vendors would not be adequate to counteract the stress rise rate in the thinned regions of the cladding. It appears that the CILC problem involves the following parameters: clad thinning, ramp rate, and power threshold to begin power ramp rate restrictions. Unlike ridging which is an r-z deformation mode, simulation of this mechanism requires an r-θ modeling capability. GE's SAFE-2D (F-19) code and EPRI's FREY (F-20) code are the only codes known to treat both modes of deformation and to have the necessary physical and material models needed for PCI analysis.

The geometric modeling that is appropriate for this PCI simulation is based on an r-θ model as shown in figure F-1. The physical and material models needed are the following:

(a) Thermal properties of the fuel and cladding

(b) Mechanical properties of the fuel and cladding

(c) Fission gas

(d) Power generation

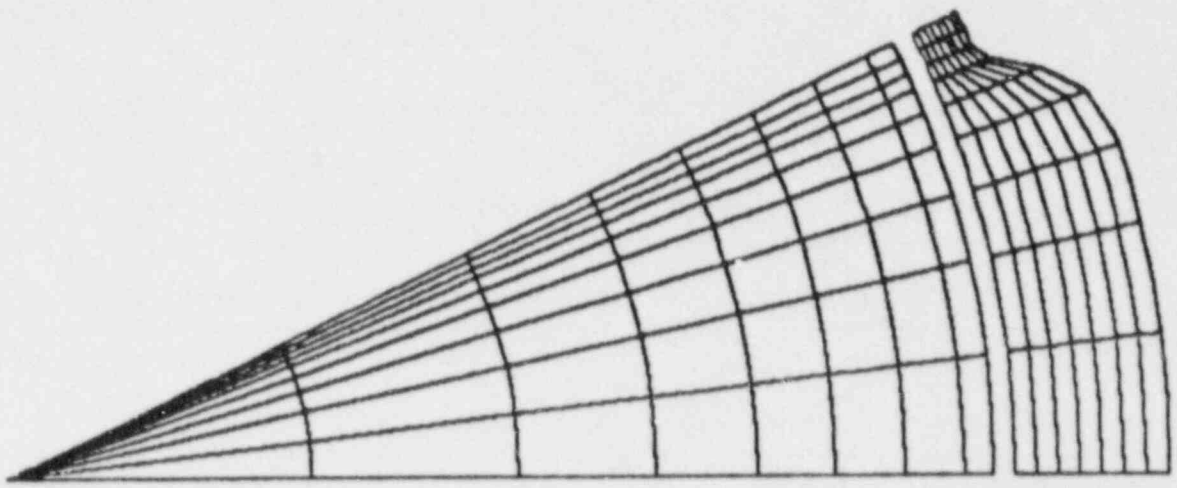

(IN)

Figure F-1 r-θ Model for CILC/PCI Analysis

(e) Gap conductance

(f) Pellet-clad mechanical interaction model

(g) Cladding failure criterion

(h) Gadolinia fuel properties and power generation

(i) Barrier properties

In FREY, the MATPRO material properties package (F-21) is fully utilized. The fission-gas release model is that specified by ANS5.4 The gap conductance model is the Russ-Stout model, and the power generation makes use of the RADAR flux depression mode. The parameters of the ISCC failure criterion came originally from Bettis.

Gadolinia fuel properties and the barrier properties are not present in FREY. These, however, are not important issues for the case at hand since

1. Gadolinium will have already been burned at the burnup level when PCI becomes an issue, and

2. We are using a failure criterion for barrier rods based on strain limit in the Zircaloy cladding, which is little affected by the presence of the barrier.

EPRI's initial charter for the FREY code was to develop a state-of-the-art code for the analysis of the transient behavior of fuel rods. The code's capabilities for analyzing PCI problems under steady state conditions evolved as a natural consequence of developing the r-θ modeling capability. Several steady-state problems were included in FREY's verification report (F-22). These analyses exercise all the physical and material models that are needed for the PCI/CILC problems. Table F-1 summarizes the results of these early verifications. The FREY steady-state initialization capability has also been benchmarked by comparison with data from 47 plant irradiated rods. More recent analyses include comparing FREY calculated gas pressure and centerline temperature with those of Halden rods (F-22). These comparisons show that FREY results match well with the test data. (figure F-2).

The real test of FREY's capabilities for PCI analysis is shown in figure F-3, which presents results of an R2 ramp failure experiment. This analysis has been done recently to support FREY's application to the CILC problem. As can be seen from figure F-3, failure power is accurately predicted by FREY.

A similar analysis was conducted for a typical BWR rod using a power history of the type used by GE in their GETR test reactor in the 1970s to establish the failure threshold for BWR fuel. The results are depicted in figure F-4. As can be seen from the figure, FREY analysis confirms what is already accepted in the industry and what has been established experimentally.

Table F-1

FREY VERIFICATION AND QUALIFICATION

PROBLEM	MODELS OR EFFECTS	COMPARISONS	PARAMETERS COMPARED	QUALITY
Vertical Upflow in a Round Tube	• Saturated Nucleate Boiling • Stable Film Boiling	AERE-R Experiment and RETRAN Code	• Wall Surface Temp. • Dryout Prediction	Good Good
Vertical Upflow in an Annulus	• Forced Convection Vaporization	AERE-R Experiment and RETRAN Code	• Wall Surface Temp. • Flow Pressure	Good
Steady State Power Ramp for Helium-Filled Relocated Fuel	• Gap Conductance Model • Relocated Fuel • Gas Thermal Conductivity	Halden Experiment (HPR-80)	• Fuel Centerline Temp. • Gap Conductance • Gap Closure Prediction	Good Good Good
Steady State Power Ramp for Xenon-Filled Relocated Fuel	Same as Above	Halden Experiment (IFA-431)	• Fuel Centerline Temp. • Fuel-Clad Gap • Fuel-Clad Lockup	Good Fair Fair
Transient Power Drop for Helium-Xenon Mixture Relocated Fuel	Same as Above	Halden Experiment (IFA-513)	• Fuel Centerline Temp. • Gap Conductance	Good Fair
Zircaloy High Temp. Inelastic Behavior	• Material Creep under Thermal & Mechanical Loading	MATPRO-11 and Hardy's Experiments	• Diametral Strain	Good
Zircaloy Failure	• Material Creep under Thermal & Mechanical Loading • Failure Model	MATPRO-11 and Tube Rupture Measurements	• Circumferential Strain at Failure • Damage Index	Good Good
Fission Gas Release	• ANS-5.4 Model • MATPRO FGASRL Model	B&W Data and MATPRO Calculations	• Fractional Release • Fractional Release	Good Good
LOCA for PWR	• Overall Effects	FRAP-T4 Code	• Fuel Centerline Temp. • Cladding Surface Temp. • Cladding Hoop Strain	Fair Good Disagree
Fuel Rod Failure in TREAT - Transient Reactor Test Facility	• Overall Effects	TREAT Experiment	• Cladding Surface Temp. • Rod Internal Pressure • Clad Swelling • Clad Rupture	Good Fair Fair Good

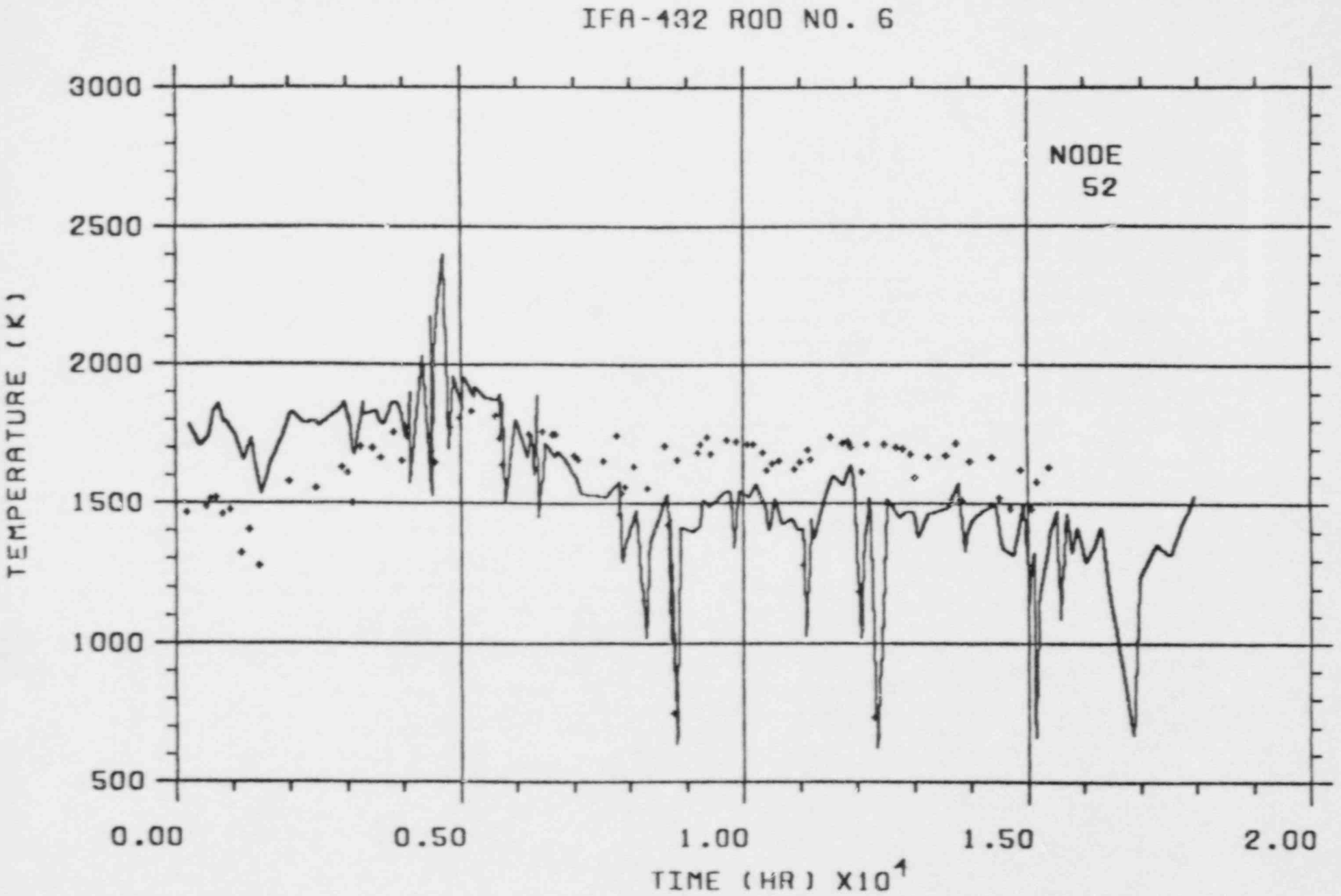

Figure F-2 Lower Fuel Centerline Temperature

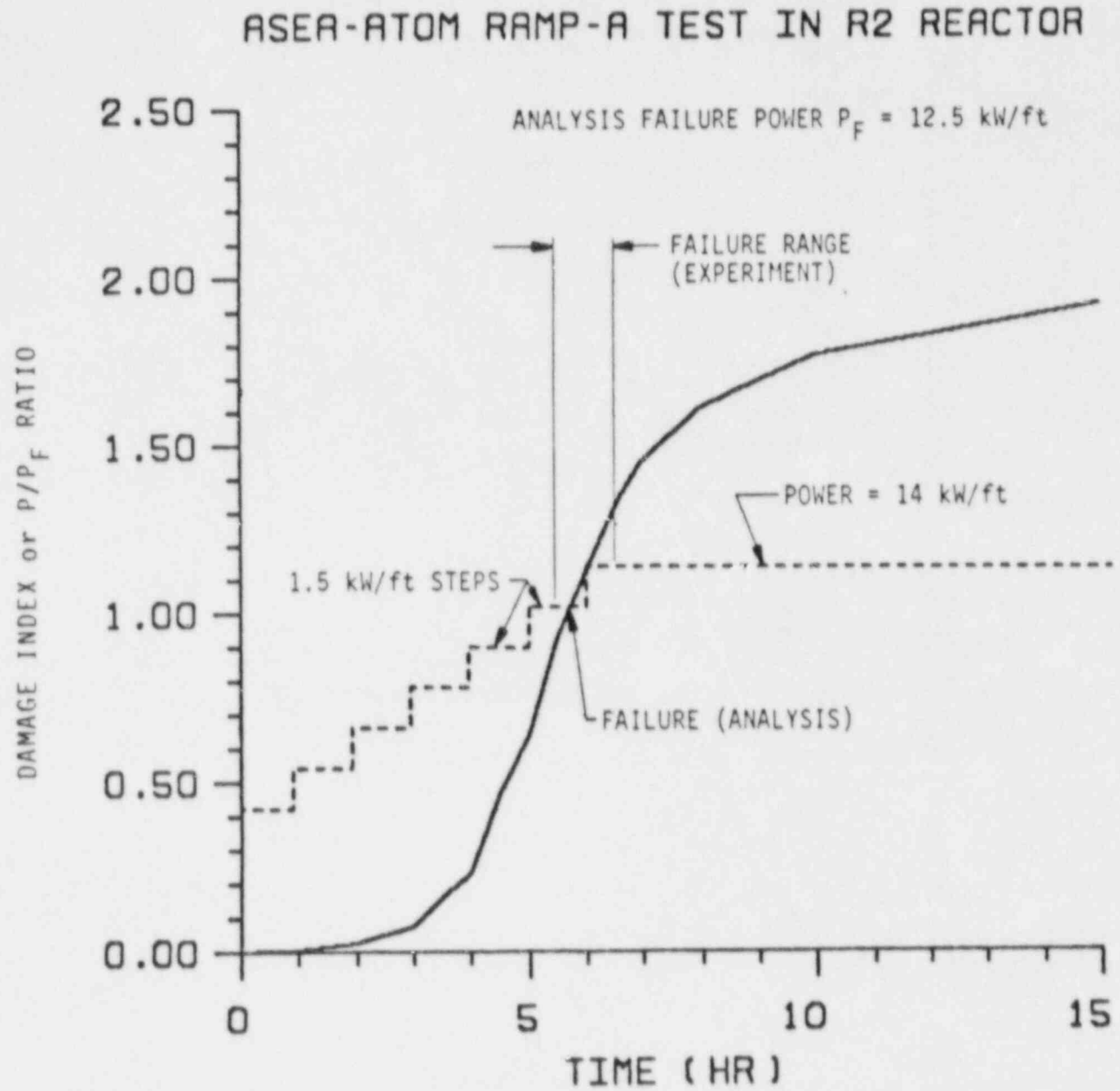

Figure F-3 Comparison with FREY Predictions of Failure Power for the ASEA-ATOM Ramp-A Test

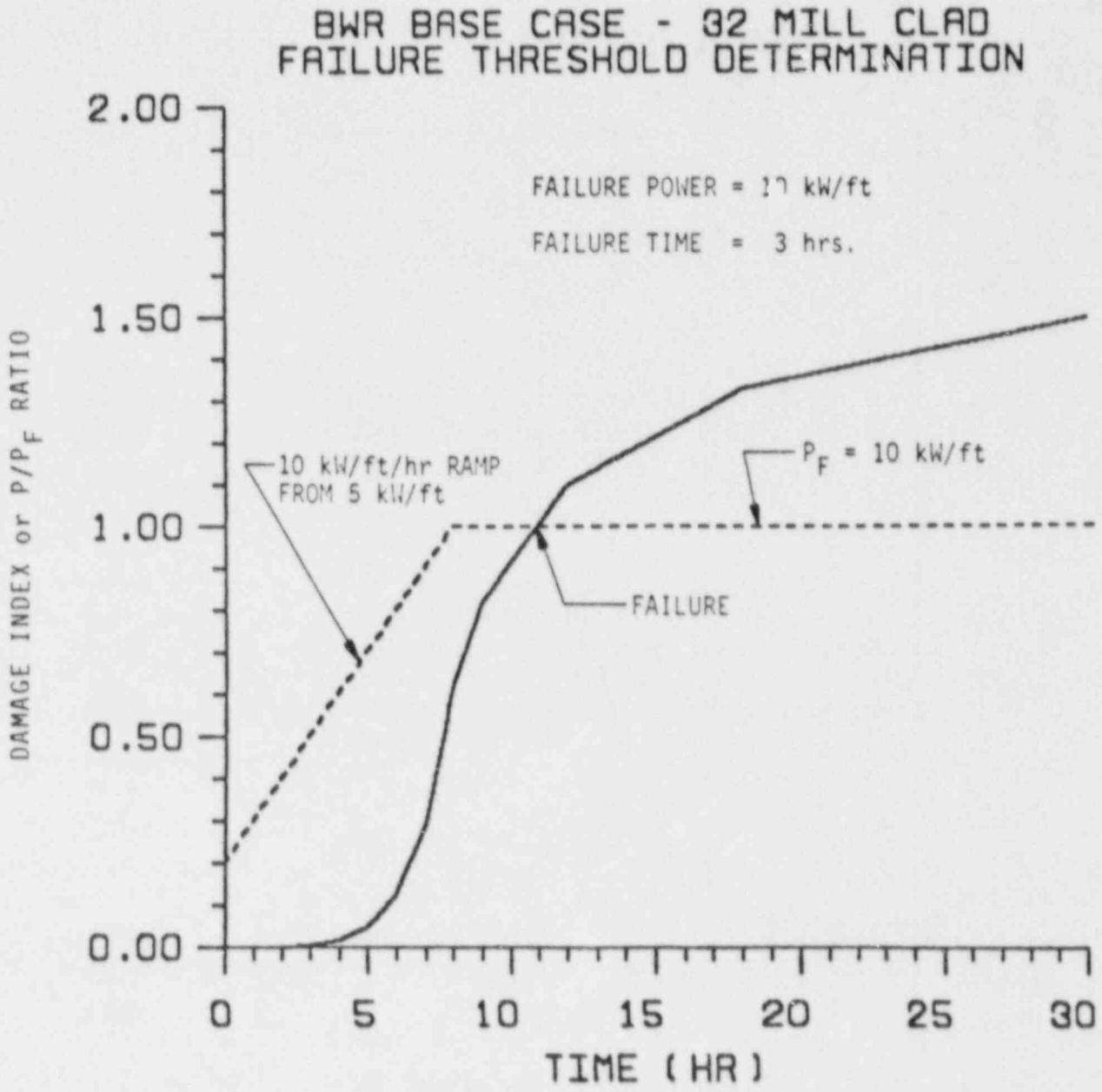

Figure F-4 FREY Prediction of Failure Power for 8x8 BWR Rod at 20,000 MWD/T Burnup

Three analyses were carried out for two remaining cladding thickness and power ramp rates to demonstrate FREY's applicability to the evaluation of the CILC problem. Although no-barrier rods were analyzed, the results can be applied to barrier fuel provided a ductility-limit criterion is used as the failure measure instead of the stress corrosion cracking criterion. The results and conclusions from these analyses are summarized below. We should caution that these results and conclusions must be applied statistically, namely, within the same failure probability limits as already exists for BWR fuel.

F.3.1 Standard Fuel. Heavily corroded (remaining thickness <10 mils) is susceptible to failure at power level below 9 kW/ft. This is illustrated in figure F-5. As shown in this figure, the failure criterion value of unity is exhausted almost immediately upon starting ramp. This implies that the 8.4 kW/ft unrestricted threshold is already too high. Reducing the ramp rate by 50% offers no advantage for the 6-mil case nor for the 10-mil case.

F.3.2 Barrier Fuel. Using the 2% ductility limit, the analysis shows that very heavily corroded rods (remaining thickness <6 mils) will fail mechanically during both ramps, 0.11 kW/ft/hr and 0.055 kW/ft/hr, at 35 hours and 65 hours, respectively, when the local strain, averaged through the thickness, exceeds 2% which corresponds to about 12 kW/ft power level for both ramps (see figures F-6 and F-7).

Under the same conditions, rods corroded down to 10-mils thick are borderline cases. This is illustrated in figure F-8, which shows that cladding strain has just begun to exceed the 2% ductility limit at the end of the ramp (element 128). However, the average strain across the thickness remains below the 2% limit (element 73).

F.3.3 Summary. In conclusion, FREY's capability of analyzing CILC-related PCI phenomena has been established through validation with test results. Its (r-θ) modeling capability makes FREY an effective and appropriate tool for analyzing both transient fuel behavior and PCI problems under steady-state conditions.

G. HYDROGEN CONTROL RESEARCH

The hydrogen burn that occurred during the TMI-2 accident led to a requirement for U.S. nuclear power plants to control the potential impact of hydrogen produced during an in-vessel recoverable degraded core accident. Specifically, it was necessary to show that the plants could accommodate an amount of hydrogen equivalent to that which would be produced from the oxidation of 75% of the fuel rod Zircaloy cladding in the active core region--known as the 75% metal-water reaction (75% MWR), a condition representing very severe core degradation. Accommodating the effects of 75% MWR hydrogen refers to: (1) the ability to maintain adequate accident response safety system capabilities during and after such an event, and (2) assurance that containment integrity during any in-vessel recoverable degraded core accident will not be threatened should a hydrogen deflagration occur.

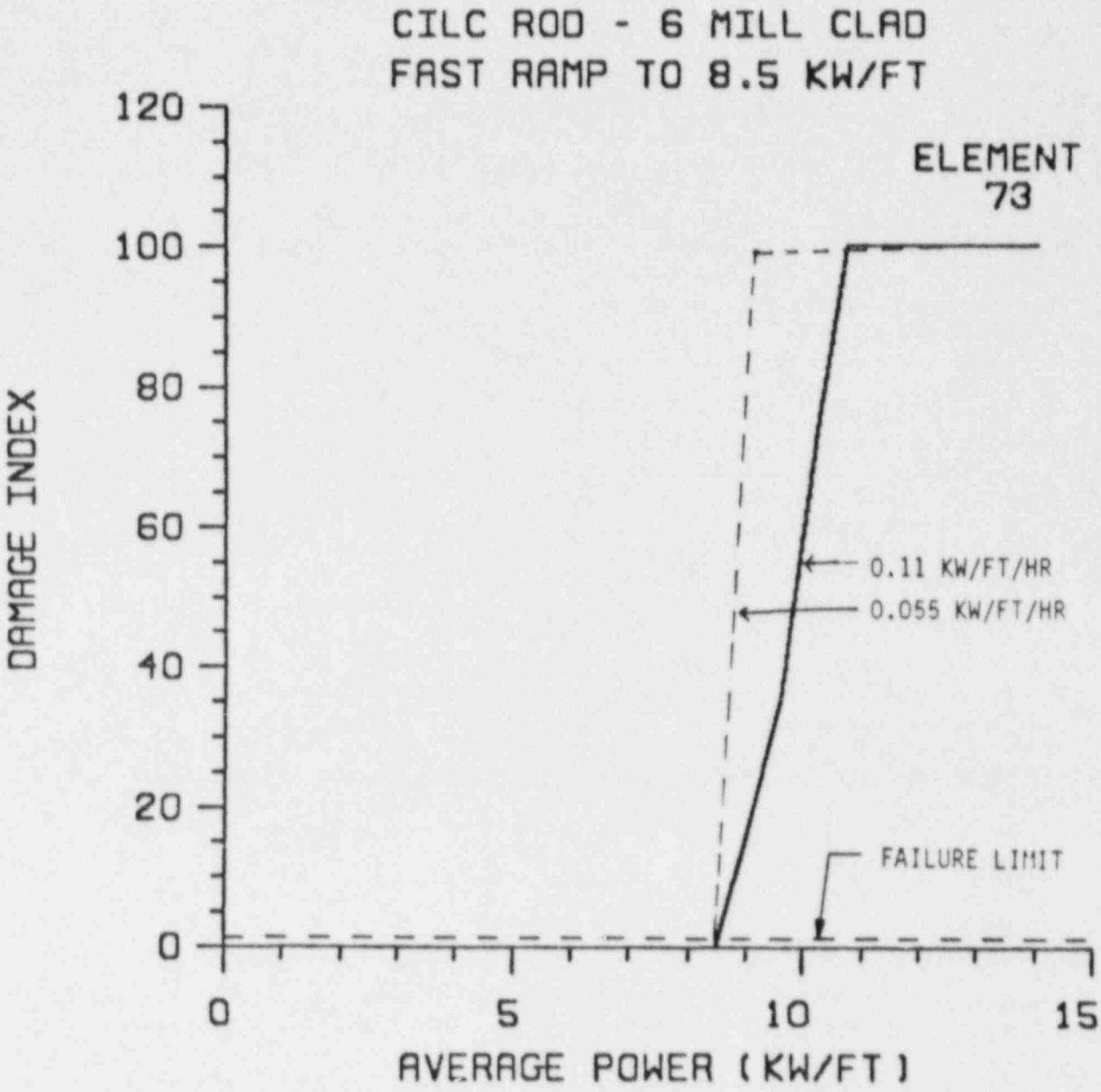

Figure F-5 Cladding Damage Index at Pellet Crack

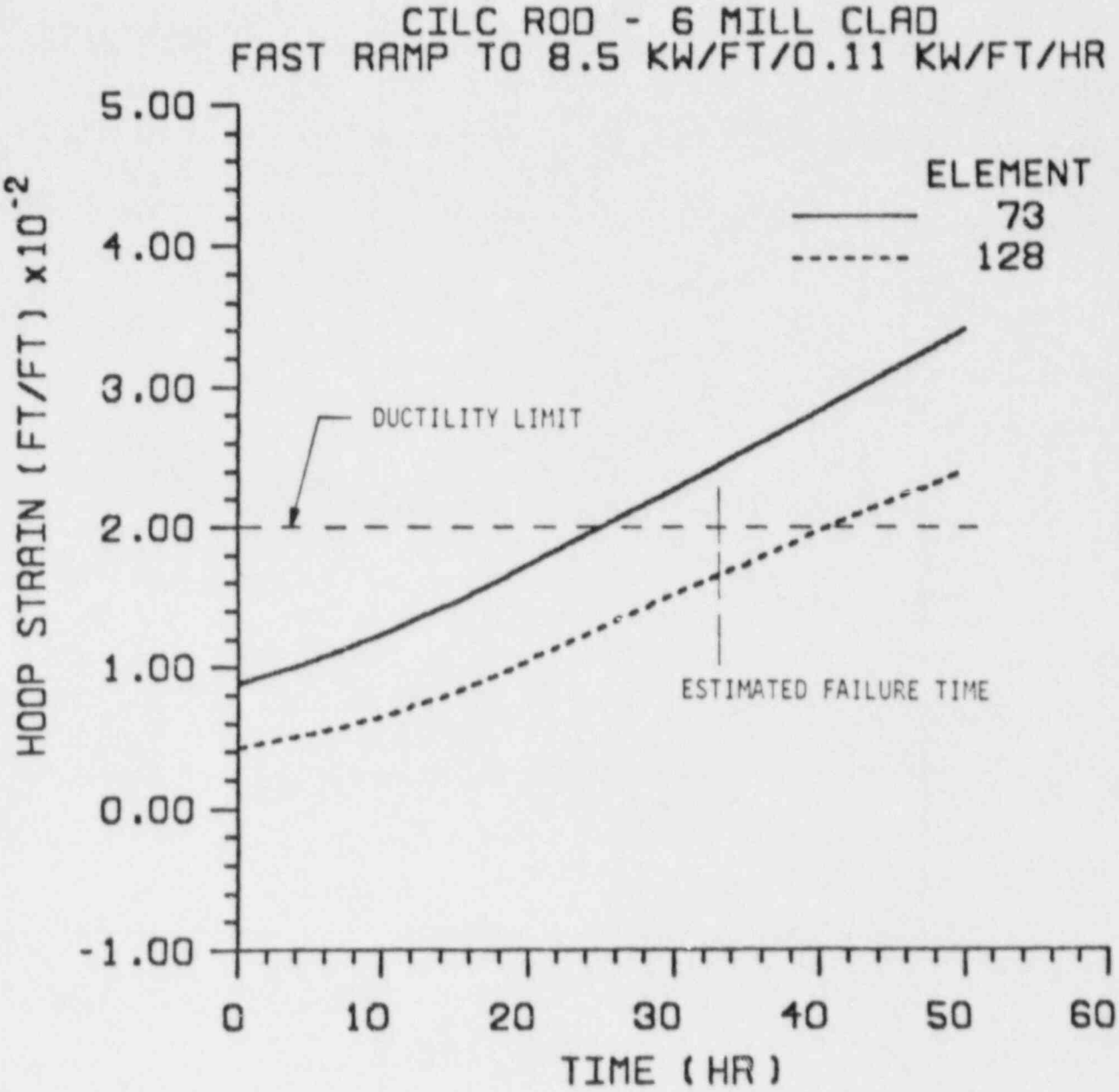

Figure F-6 Cladding Hoop Strain at Pellet Crack

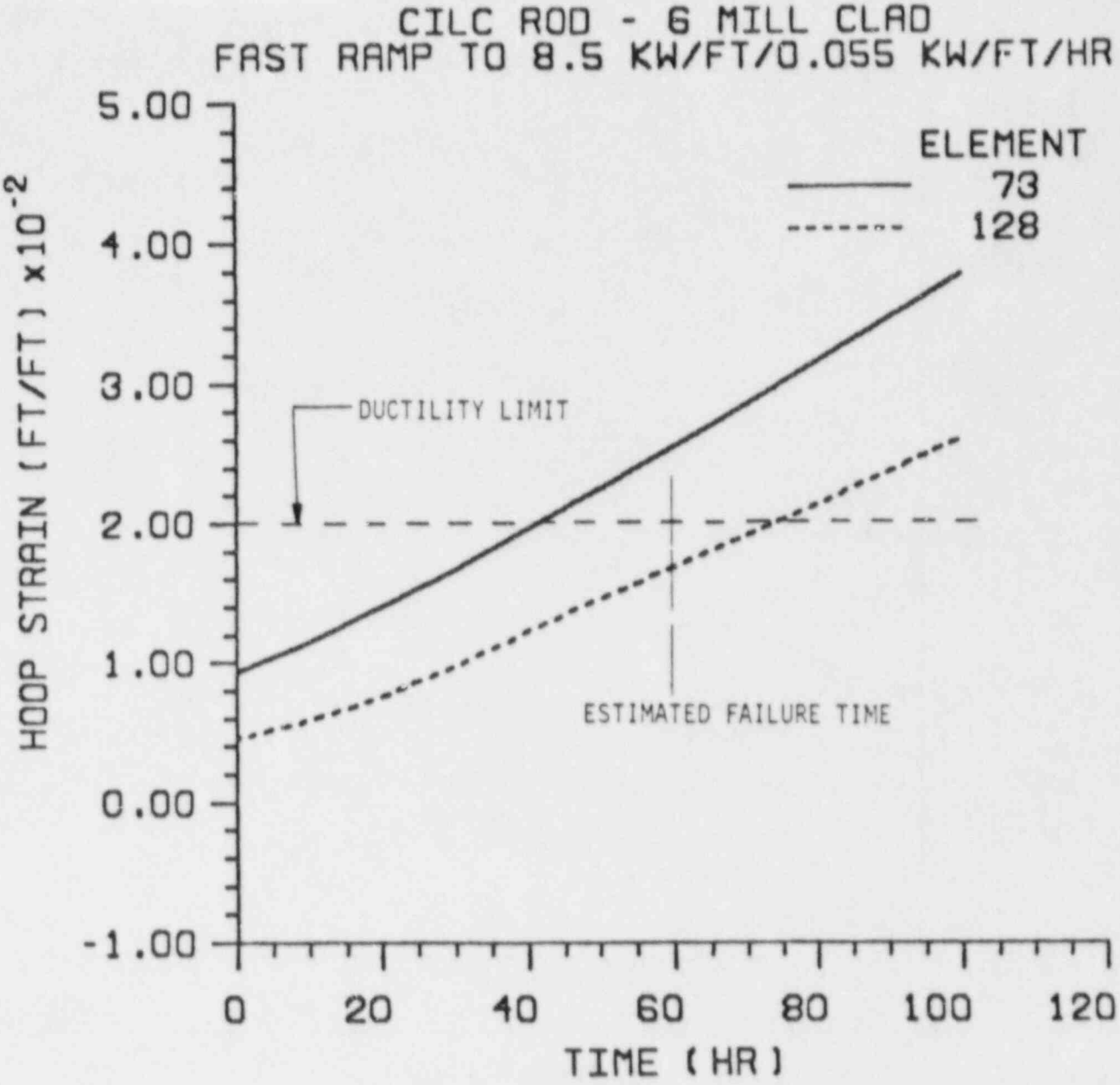

Figure F-7 Cladding Hoop Strain at Pellet Crack

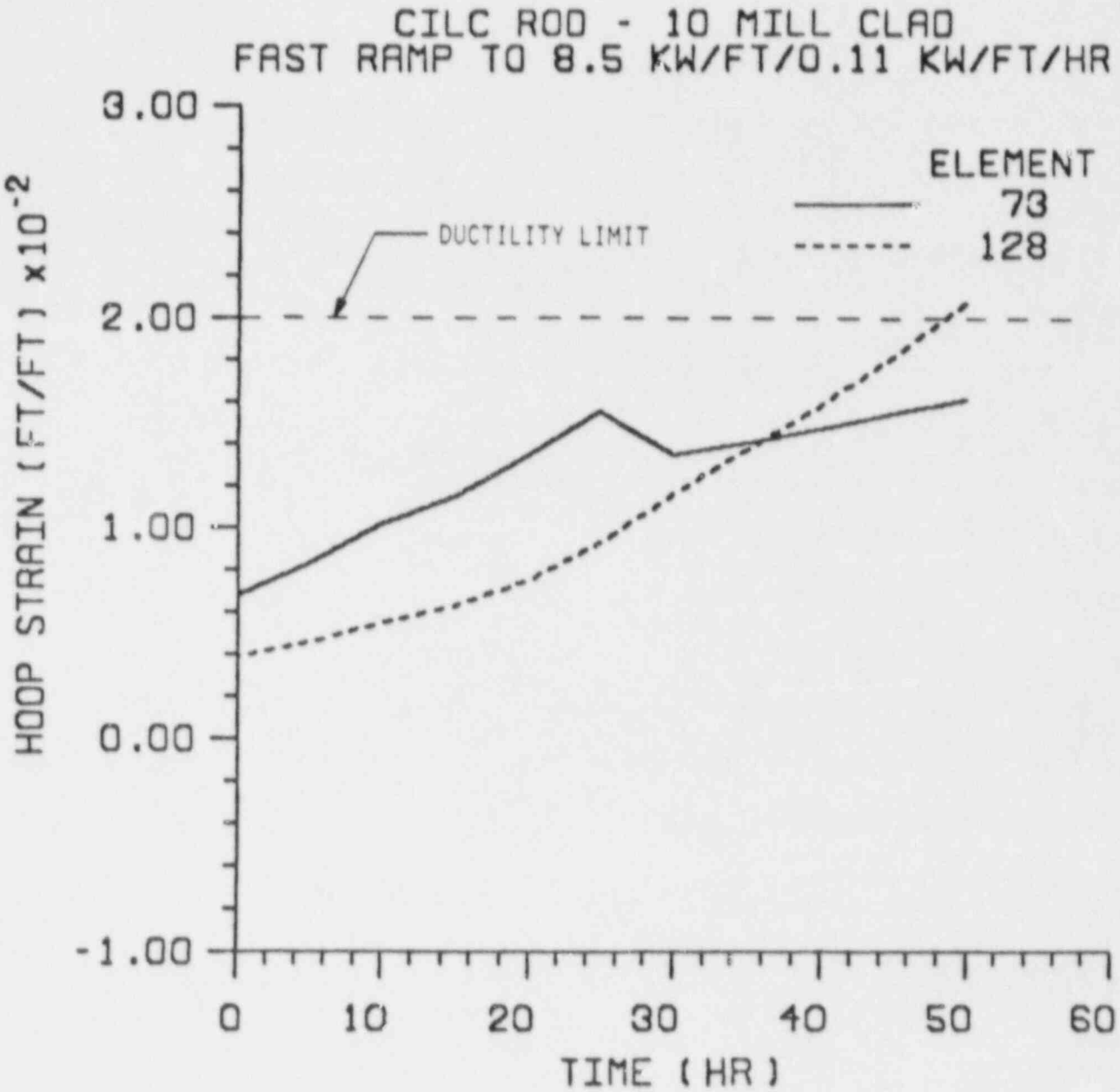

Figure 8 Cladding Hoop Strain at Pellet Crack

G.1 EPRI's Hydrogen Control Program

Over the past four years, EPRI has managed several major research programs directed at improving the state of knowledge both in the areas of hydrogen mixing and combustion and the capabilities of specific safety-related equipment to withstand such combustion. A generic hydrogen research program has been completed at EPRI (G-1) to G-4), which includes:

1. Hydrogen ignition limit testing over a wide range of hydrogen, air, and steam mixtures;

2. Intermediate-scale hydrogen mixing experiments in a scale model of the PWR ice condenser lower compartment; and

3. Large-scale hydrogen mixing/combustion and equipment survivability testing in a 15.9-m diameter sphere.

Portions of this program were cosponsored by EPRI, NRC, Ontario Hydro, Electricité de France, Taiwan Power Company, and the West German Federal Ministry for Research and Technology.

In addition, the BWR¢/Mark III Containment Hydrogen Control Owner's Group (HCOG) has been the primary sponsor (in conjunction with EPRI) of a research program directed at defining both the unique hydrogen mixing and combustion phenomena in a Mark III containment during a recoverable degraded core accident and the resulting heat loading to required safety-related equipment. This test program, which is focused on experiments performed in a 1/4-scale model of a Mark III containment building was completed in early 1987. A final report (nonproprietary version) will be completed by December 1987.

G.2 U.S. LWR Containment Design Features

Commercial nuclear units in the United States employ containment designs of two basic types: "large dry" and "pressure suppression."

The large dry containments are characterized by large volumes (~2 x 10^6 ft^3 or ~60,000M^3) and high design features (~60 psia or ~0.4 MPa). These units were designed to have large size and strength to contain the effects of steam and hydrogen release during a LOCA.

The pressure suppression containments use either a large pool of water (BWR Mark I, II, and III) or ice (PWR ice condenser) to condense the steam released during a LOCA to limit containment pressurization. Some of these units are designed with relatively smaller containment volumes (~1 x 10^6 ft^3 or ~30,000 M^3). Various design pressures were realized, with some as low as ~30 psia or ~0.2 MPa.

The ultimate failure pressure of all these units is much higher than their design pressure by a factor of 2-3.

G.3 Hydrogen Control Methods Currently in Use

Since the TMI-2 accident, actions have been taken to provide improved hydrogen control for the smaller or lower design pressure units. BWR Mark I's and II's were inerted with nitrogen. BWR Mark III's and PWR ice condensers installed hydrogen control systems. The chosen systems employ glow plug igniters distributed throughout the containment building. These systems are designed to deliberately burn hydrogen as it is released to limit the accumulation of hydrogen to concentrations well below levels at which rapid combustion could threaten containment integrity.

G.4 Research Supporting Hydrogen Control Methods

G.4.1 **PWR Large Dry Units**. Typical large dry containment buildings for U.S. PWRs have ultimate pressure capabilities of the order of two to 3 times the nominal ~60 psia (~0.4 MPa) design pressure. A release of hydrogen into such containments without any combustion resulting from a 75% metal-water reaction would bring the hydrogen concentration to ~13% by volume.

Tests performed in the large 15.0-m diameter sphere located in Nevada at hydrogen concentrations consistent with large dry containments (~13% volume fractions) resulted in pressure increases of less than 45 psi or 0.31 MPa (G-3). Therefore, large dry containments do not feature special hydrogen control systems to control overpressure.

These tests also demonstrated that critical safety-related equipment will withstand the thermal environment imposed by 13% hydrogen burns (G-4). Therefore, large dry units also are adequately protected with respect to functioning of needed equipment.

G.4.2 **PWR Ice Condenser Units**. Testing performed in a scale model of the lower compartment of an icde condenser containment demonstrated excellent mixing (G-2). Subsequent analyses of combustion phenomena in these units indicates that with the distributed ignition system operational, containment integrity will not be challenged by hydrogen combustion (G-5). Similarly, analyses of equipment thermal response to such burns indicates that critical equipment will function (G-6).

G.4.3 **BWR Mark I and II Units**. These units are currently inerted with nitrogen which precludes combustion resulting from hydrogen release.

G.4.4 **BWR Mark III Units**. The 1/4-scale testing performed in the HCOG-sponsored program indicates that the distributed ignition system is extremely efficient in limiting the accumulation of hydrogen in the containment. Therefore, with an operational distributed ignition system, hydrogen combustion does not pose a significant challenge to containment integrity. Analyses of the thermal response of critical equipment to hydrogen combustion for Mark III units is currently in progress.

H. SEVERE ACCIDENT SAFETY

The EPRI Source Term Program has a number of active projects. This year the LACE (LWR Aerosol Containment Experiments), and the in-reactor Source Term Experimental Program (STEP) tests have been completed and these programs are reaching a conclusion. The EPRI Molten Corium-Concrete Interaction (MCCI) work is expected to be focused in another emerging international consortium ACE (Aerosol Containment Experiments). The EPRI analytical work in ATWS-TC sequence in BWRs has resulted in a scenario of oscillating power and temperature with a partially uncovered core and no cladding oxidation during the oscillation phase. Finally, a report on integration of an RCS code, an aerosol code, and a core response code provides first principles insight.

H.1 LACE Objectives

The LWR aerosol containment experiments (LACE) program is investigating aerosol behavior for postulated high consequence accident situations where data is needed and which are not being studied by other test programs. These accident situations are where either the containment is bypassed altogether, the containment function in impaired early in the accident, or delayed containment failure occurs simultaneously with a large fission-product release. Significant aerosol retention would reduce the consequences presently calculated for these postulated accident situations. Therefore, the results of the LACE program are of special interest to LWR risk assessment and emergency planning. The LACE program is sponsored by an international consortium, organized by EPRI, consisting of fourteen sponsors. The lead organizations of the LACE consortium are: Commission of the European Communities (CEC); Va'tion Teknillen Tutkimuskeskus (VTT), Finland; Ontario-Hydro (OH), Canada; Centre d'Etudes Nucleaires de Fontenay-aux-Roses (CEA), France; Bundesministerium für Forschung und Technology (BMFT), Germany; Comitato Nazionale per la Ricerca e per lo Sviluppo dell'Energia Nucleare e delle Energie Alternative (ENEA), Italy; Japan Atomic Energy Research Institute (JAERI), Japan; N.V. Tot Keuring Van Electrotechische Materialen (KEMA), The Netherlands; Unidad Electrica, S.A. (UNESA), Spain; Kärnkraft-inspektion (SKI), Sweden; Eidgenössisches Institut für Reaktorforschung (EIR), Switzerland; Atomic Energy Establishment Winfrith (AEA), United Kingdom; and Electric Power Research Institute (EPRI), Department of Energy (DOE), and Nuclear Regulatory Commission (NRC), United States.

The LACE program consists of three main tasks.

- Large-Scale Tests: These tests experimentally investigate inherent aerosol retention behavior for conditions which simulate selected high-consequence accident conditions. They provide a database for validation of containment aerosol and related thermal-hydraulic computer codes.

- Computer Code Validation: Both pretest and blind posttest calculations using aerosol behavior and thermal-hydraulic computer codes are being compared to experimental data.

- Support Program: The support program provide direct support needed to perform or interpret the large-scale experiments. The support program also included separate effects tests needed to clarify individual phenomena.

The computer code validation efforts and support program are being conducted by many groups within the sponsoring organizations.

H.1.1 LACE Test Matrix. The LACE Program consists of six large-scale tests in the Containment Systems Test Facility (CSTF) located at the Hanford Engineering Development Laboratory (HEDL). The six tests focused on three postulated accident situations: the containment bypass or so-called V-sequence, failure to isolate containment, and delayed containment failure. The LACE test matrix is summarized in table H-1.

Table H-1

LACE PROGRAM TEST MATRIX

Test Number	Title and Simulated Accident Situation
LA1	Containment Bypass, focuses on the pipe and downstream building
LA2	Failure to Isolate Containment
LA3	Containment Bypass, focuses on pipe flow only
LA4	Late Containment Failure With Overlapping Aerosol Injection Periods
LA5	Rapid Depressurization With Spiked Pool
LA6	Rapid Depressurization With Aerosol Injection

H.1.2 Results of Tests LA2 and LA4. The experimental results from test LA1 and LA3 are presented in a previous paper (H-1) dealing with aerosol behavior in LWR primary systems. The results from test LA2, "Failure to Isolate Containment," and test LA4, "Late Containment Failure," are presented below. Although tests LA5 and LA6, the rapid depressurization experiments, have been successfully performed in early 1987, the data have not been analyzed completely enough to allow presentation at this time.

H.1.2.1 Failure to isolate containment - test LA2. The objective of test LA2 was to simulate a postulated accident situation where a failure to isolate containment occurs. In addition to measuring the quantity and particle size spectrum of the leaked fission products, a major test goal was to determine the effect of leak path location. If the aerosol in the containment is well mixed, the aerosol release would be independent of leak location. On the other hand, if stratification of the containment atmosphere occurs due to a temperature inversion or other phenomena,

aerosols would not necessarily be well mixed and leak location might be important. Since evidence existed from the DEMONA experiments that stratification could occur under some particular conditions, test LA2 attempted to clarify the conditions under which stratification might exist.

A short 200-mm diameter pipe ran between the aerosol generator and containment vessel, and aerosols were fed through this pipe at low velocities. Little aerosol deposition in this pipe was expected or observed. While most of the steam/N_2 aerosol carrier gas entered at roughly mid-height of the containment, a smaller quantity of steam (only) was injected near the containment bottom directed upward along the center line. This was done to simulate the steam which would rise upward into the containment during accidents of practical interest. The major facility modification was the installation of a second leakage path near the containment bottom to evaluate stratification effects. Figure H-1 illustrates the setup and shows some of the instrumentation used in test LA2. The LA2 mass balance was excellent, with 98% of the aerosol material recovered.

No significant difference was found in the mass of aerosol leaked through the upper and lower leak paths. This is a result of the similar geometry of the two paths and the good mixing in the containment atmosphere between the leak path locations.

It was observed that it is possible to stratify the containment under special circumstances. For instance, it appears that the small region in the containment below the lower steam injection point was not well mixed. This is not surprising since a similar effect was observed in some of the Marviken tests. It is of interest to note that about half of the leaked material was found in the short duct between the leak opening and the final scrubber. However, there was considerably less CsOH in the lower leak path duct than the upper one (table H-2). It is believed that water was condensed in both ducts. In the lower duct, because of its downward slope, the highly soluble CsOH was carried with the water into the scrubber, where it was found, while MnO remained in the duct.

H.1.2.2 Late containment failure - test LA4. The test LA4 objective was to perform an integral experiment to determine aerosol behavior with multiple species, overlapping aerosol injection periods and a late containment failure. The experimental configuration was similar to test LA2, except for additional instrumentation and the removal of the lower leak path.

Significant differences in this test from LA2 include the overlapping injection of aerosols and late venting. In test LA4, CsOH injection lasted 50 minutes, 30 minutes alone and 20 minutes with MnO. Then the CsOH injection stopped and MnO injection continued alone another 30 minutes. During this time, pressure in the containment increased to ~3 bar and was maintained constant for 200 minutes after which the containment was vented.

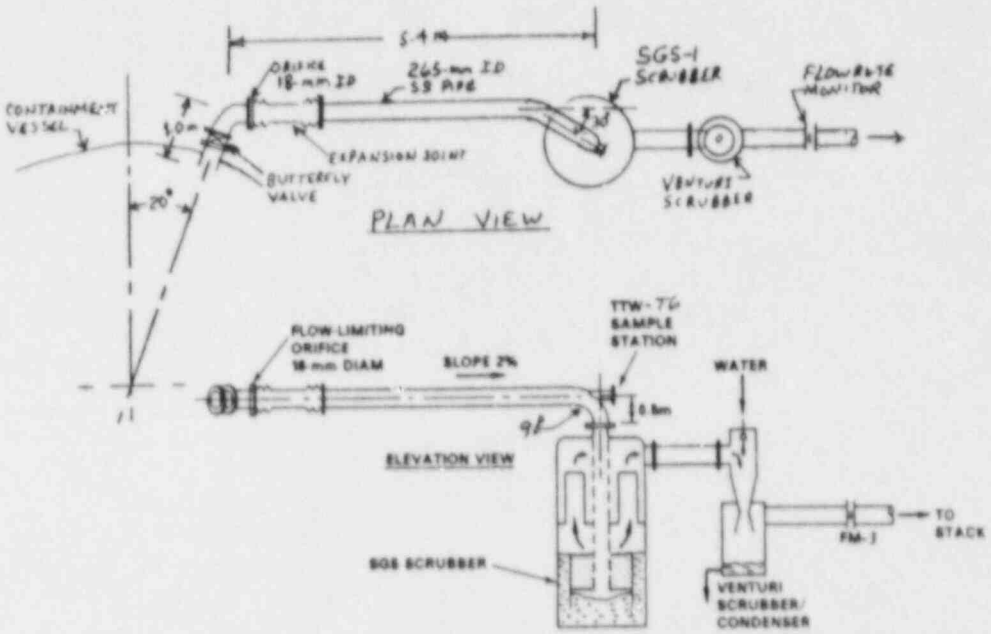

Figure H-1 Details of the upper leak path in test LA2. The lower leak path was slightly different, principally in slope of the pipe leading to the scrubber unit.

Table H-2

AEROSOL DEPOSITION IN LEAK PATH DUCTS - LA2

	Fraction of Mass Entering Found in Duct		
	CsOH	MnO	CsOH + MnO
Upper Path Duct	0.66	0.48	0.56
Lower Path Duct	0.06*	0.63	0.39*

*Missing CsOH was found in scrubber.

Posttest examination of the aerosols by SEM/EDXA techniques revealed that agglomerates were approximately spherical, made up of primary particles with mostly hexagonal, but some cubic shapes. The agglomerates ranged in size from 0.5 to 4.0 μm, and contained from 3 to over 100 primary particles. The hexagonal particles were most Mn, with approximately 2% Cs, while the cubic particles contained only Mn, probably in the chemical form MnO.

Data was also obtained on the amount of liquid water suspended in the containment vessel, as well as the gas velocities at six locations. Optical spectrometer and turbidity/photometer data were also obtained. The atmosphere of the containment vessel was not as well mixed as in test LA2. Over 90% of the injected CsOH was recovered as was 84% of the MnO. Small but measurable quantities of aerosol vented from the containment vessel were observed.

H.2 STEP Results

The four STEP in-reactor tests, designed to provide characterization data on materials that would be released during severe core damage accidents, were successfully performed in 1984 and 1985. Since then, extensive posttest examination and analysis work has been done to establish the thermal-hydraulic performance of each test, to identify the chemical elements that were released and transported away from the fuel rods, and to determine the properties of the aerosol populations and vapor deposits that were formed. This work is now complete and the principal observations and conclusions arising from the analyses of these experiments may be summarized as follows.

- The thermal hydraulic response was quite different between the low-pressure tests (STEP-1, -2) and the high-pressure tests (STEP-3, -4). The former were characterized by much faster fuel heatup rates, higher peak temperatures, and different temperature profiles in the capsules than the latter. It was determined that forced convection (once-through) gas flow was

dominant in the low-pressure tests, and the gas phase did not serve as a major sink for the heat generated in the fuel rods. On the other hand, natural circulation flows (between the fuel rod and plenum regions of the capsules) were dominant in the high-pressure tests, and the reservoir of relatively dense steam became a significant heat sink in these tests. Conventional heat transfer models (with or without a natural circulation driving force) were able to produce good estimates of the recorded temperatures and the measured hydrogen generation (cladding oxidation) rates in each of the tests.

- Instrumental analysis of deposition samples recovered from the four tests exhibited the presence of a variety of chemical elements. Those from STEP-1, -2 were abundant in certain fission products (cesium, molybdenum, rubidium) and cladding material (tin) elements. Those recovered from STEP-3, -4 were much less heavy and consisted primarily of structural components (iron, silicon, aluminum) with some fission product (cesium). The deposits from all tests included small fragments of cladding and fuel material. Some fission product iodine along with silver from sample coupons were identified in deposits from the higher heatup rate tests (STEP-1, -2). Fission product tellurium was detected only in samples from STEP-1 which is the only test in which nearly complete cladding oxidation occurred. Additional analyses suggested compound formation took place between fission product cesium (and presumably rubidium) and each of the other fission products (molybdenum, iodine and tellurium). The principal species were likely cesium molybdate, cesium iodide, and cesium telluride.

- Particle size distribution measurements showed that somewhat larger aerosol particles were formed and transported in the high-pressure tests than in the low-pressure tests. The mass concentrations of the aerosol suspended in the flowing gas were found to vary both during each test and between the four tests. An example of a mass distribution function (MDF) and a corresponding cumulative mass plot (with approximate lognormal function fit) obtained from analysis of scanning electron microscope images of aerosols deposited on impactor wires and a settling plate taken from the STEP-1 test are shown in figure H-2. The lognormal parameters derived for this particular distribution indicate an aerosol mass median diameter of 1.05 micrometers and a geometric standard deviation of 1.84. Additional data for STEP-1 and the other tests and a more complete discussion of results and conclusions are presented in a project summary report that should be published by the end of the year.

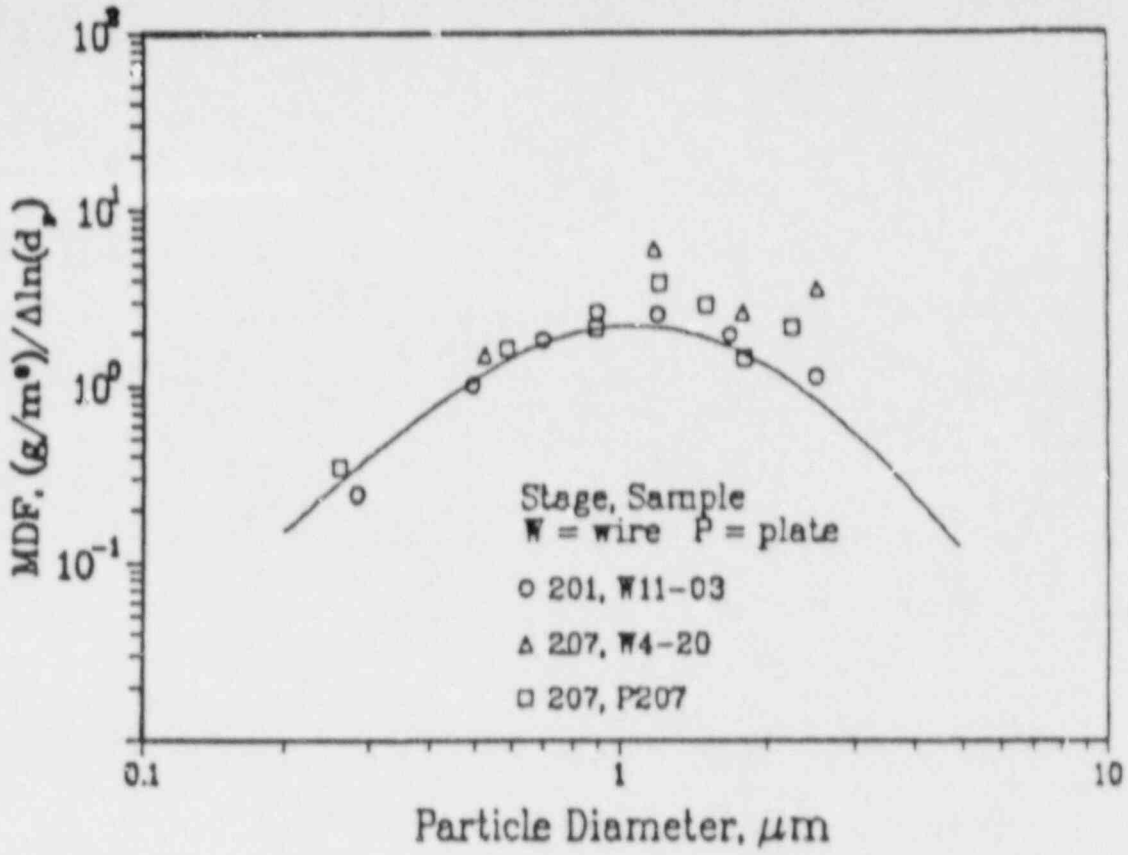

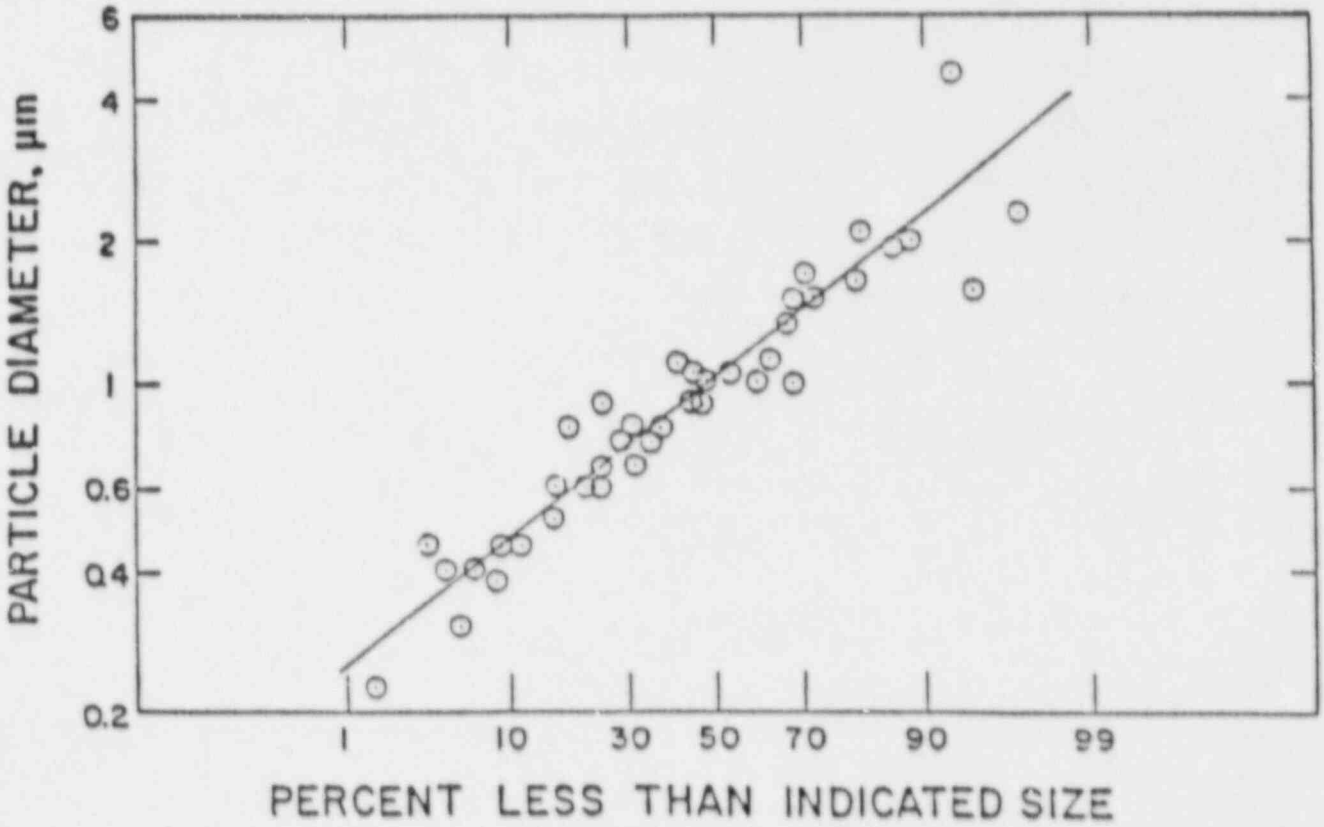

Figure H-2 Example of STEP Aerosol Particle Size Distribution Determination Results.

H.3 Molten Corium-Concrete Interactions (MCCI)

The magnitude, the content, and the physical and chemical character of the MCCI aerosol source are important in estimating the source term from postulated accidents. In addition to these parameters, the timing of the MCCI aerosol release, relative to that of the fission-product aerosol release from the primary system, and to that of the containment failure, is of importance. If the timing is opportunine, the relatively copious MCCI aerosol will help scrub the relatively dilute aerosol that may be discharged from the vessel on revolatization of the fission products deposited on the primary system surfaces. Similarly, if containment failure does not follow soon after the start of the MCCI, there is little danger of having a large airborne source in the containment at the time containment failure, since natural processes of aerosol removal from the containment atmosphere would have been active for a sufficiently long time.

The EPRI program on MCCI has been focused on accurate modeling of the release of fission products during MCCI. To this end, the analysis development work was the first to be put in place at Massachusetts Institute of Technology (MIT) and University of Wisconsin and has produced important results. The MIT work has investigated the heat transfer from corium to the concrete and to the containment and proposed models for these. A semiempirical correlation was developed to describe the heat transfer at the horizontal core/concrete interface. The model assumes periodic contact between corium and concrete at low gas evoluation rates, and separation of a stable film at high gas generation rates. The model was incorporated in the CORCON-2 code, with the revised code named as CORCON/MIT. This code has been applied to the analysis of the Sandia tests and, more significantly, the series of tests performed at the German BETA facility. The proposed model is capable of predicting erosion results of the BERA experiments with a mean error of 5% and a standard deviation of 27%. Sensitivity studies performed with CORCON/MIT indicated that the initial debris temperature was the most significant parameter affecting release of the refractory fission products, e.g., Ba, La during MCCI.

Work at Wisconsin University has extended the CORCON code to represent a much larger set of chemical reactions than originally incorporated in CORCON-2. This work is being completed presently. Its feature of fully coupled chemical and thermal-hydraulic treatment will be useful in checking the results of sequential CORCON-2 and VANESA calculations for the MCCI source term.

The Wisconsin work has also developed a model for mixing of different density immiscible layers with gas injection from bottom surface. The model is based on experiments performed with simulant fluids. The important effects of density differences, density ratio, surface tension, and viscosity have been delineated. A set of correlations has been obtained for mixing of layers and implemented in the CORCON code. The current calculations indicate that mixing between the oxidic and metallic phases will occur during the early part of MCCI. The effect of layer mixing on the fission-product vaporization estimates is currently being evaluated. It appears that zirconium metal may react with the iron oxides and UO_2 contained in the oxide layer, before reacting with the steam generated on concrete dissolution.

Experimental work on MCCI was started two years ago at Argonne National Laboratory (ANL).

Real reactor materials are utilized in a long-term interaction with an underlying slab of concrete. Sustained internal heat generation is provided by the method of direct electrical heating (DEH) to simulate decay heat or to control the corium temperature at a prescribed quasi-static level. The tests are evolving from small scale (5 kg corium mass) to larger scale (30 kg and 300 kg) as the experiment technique and diagnostic tools are progressively improved. Presently, 5 kg and 30 kg size gas sparging tests have been completed and 30 kg integral MCCI tests are under way. The corium mixtures are either fully oxidized for tests applicable to the long-term erosion stage or contain metallic constituents for tests applicable to the early, aggressive interaction stage. The corium mixtures consist of UO_2, ZrO_2, stainless steel oxides, plus nonradioactive fission-product mock-ups La_2O_3, BaO, and SrO; Zr and metallic stainless steel are added for tests involving a metallic constituent. Current tests utilize a limestone/common sand concrete of specific composition matching that used at the Zion station; future tests are also planned to examine limestone/limestone and basaltic concrete. The tests are presently one-dimensional, designed to minimize (but measure) lateral heat losses such that the predominant heat transport processes are vertically upward and downward.

The experimental approach is to provide instrumentation to enable evaluations of concrete erosion rate, melt layer temperature and heat balance measurements, time variation of gas release rate and composition, and time variation of aerosol release rate and characteristics.

The apparatus for the 30 kg size MCCI tests is illustrated in figure H-3. It consists of a series of U-shaped brass segments, electrically insulated from each other, that are stacked side by side to form the base and sides of the electrical melt generator. Tungsten electrodes, supported in machined electrical insulators, form the ends of the apparatus. The sides and ends of the apparatus are water-cooled. Heat losses are individually monitored through each wall. A thick layer of thermal insulation rests on the top of the apparatus and supports the top cover, which is the base of the aerosol collection and gas sampling system.

A carrier gas injector introduces an annular stream of inert gas around the off-gas leaving the test cavity. This measured flow of inert gas reduces the temperature of the off-gas and dilutes the aerosol concentration. The sampling system contains bottles for collecting gas samples and stainless steel coupons in the main gas stream to collect aerosol samples. The system consists of the carrier gas injection, main flow piping and filters, a bank of five filter and gas sample lines, an aerosol sample canister similar to that used in the Source Term Experimental Program (STEP) in-reactor tests, plus CO, CO_2, and H_2O monitors. An on-line gas mass spectrometer is presently being added. Borosilicate glass filters located in the main gas line and the sample gas lines had a minimum retention efficiency of 93% for 0.1 μm particles and collected aerosols principally by impaction.

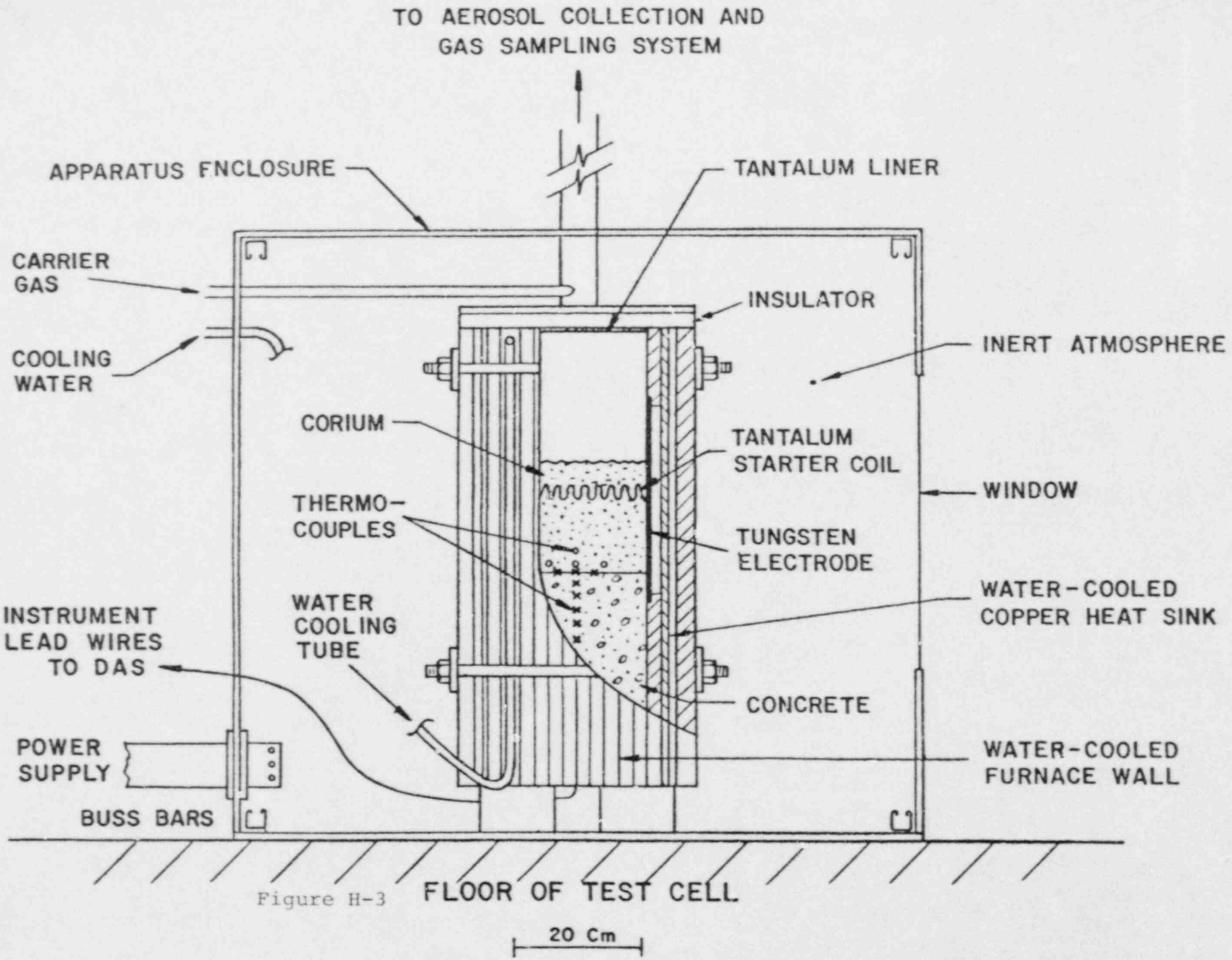
TO AEROSOL COLLECTION AND
GAS SAMPLING SYSTEM
APPARATUS FNCLOSURE
TANTALUM LINER
CARRIER
GAS
INSULATOR
COOLING
WATER
INERT ATMOSPHERE
CORIUM
TANTALUM
STARTER COIL
WINDOW
THERMO-
COUPLES
TUNGSTEN
ELECTRODE
WATER-COOLED
COPPER HEAT SINK
INSTRUMENT
LEAD WIRES
TO DAS
WATER
COOLING
TUBE
CONCRETE
POWER
SUPPLY
WATER-COOLED
FURNACE WALL
BUSS BARS
FLOOR OF TEST CELL
20 Cm

Figure H-3

The apparatus for an MCCI test is assembled around the concrete basemat. Blended corium powder is loaded into the test cavity atop the basemat and tamped to a density of about 3.5 g/cm^3. Thermowells and tantalum starter coils are installed at the selected elevations during the corium loading process.

H.3.1 **MCCI Test Results.** Interactions of a fully oxidized core melt with a limestone/common sand basemat has been simulated in three MCCI tests to date. The tests differed in the power input sequence and the capabilities of the aerosol collection and gas sampling system.

Parameters for MCCI tests I-5, I-6, and I-7 are summarized in table H-3. The MCCI tests were limited by electrode size to a maximum concrete ablation depth of 7.6 cm. The interface between the concrete and the melt, shown in figure H-4 for MCCI test I-5, was smooth and flat. This was typical of the interface in all the MCCI tests. The density of the melt layer in MCCI tests was only 60% of that in the earlier gas sparge tests, indicating that concrete constituents were incorporated into the melt as confirmed by subsequent chemical analyses. Small-diameter gas passages penetrated the melt layer to the concrete surface.

Table H-3

CORIUM INVENTORY AND MELT LAYER CHARACTERISTICS
IN INTERMEDIATE-SCALE MCCI TESTS

	Test		
	I-5	I-6	I-7
Corium inventory, kg	21	27	28.8
Fission products, g	8 La_2O_3	42 BaO	45 BaO
42 La_2O_3	45 La_2O_3		
24 SrO	25 SrO		
Preheat, min.	955	54	41
High power, min.	82	60	90
Depth of concrete ablation, cm	7.6	~7	~7.5
Melt layer thickness, cm	4,6	~2.5	~5.5
Density of melt layer, g/cm^3	4.1	4.2	~4.2

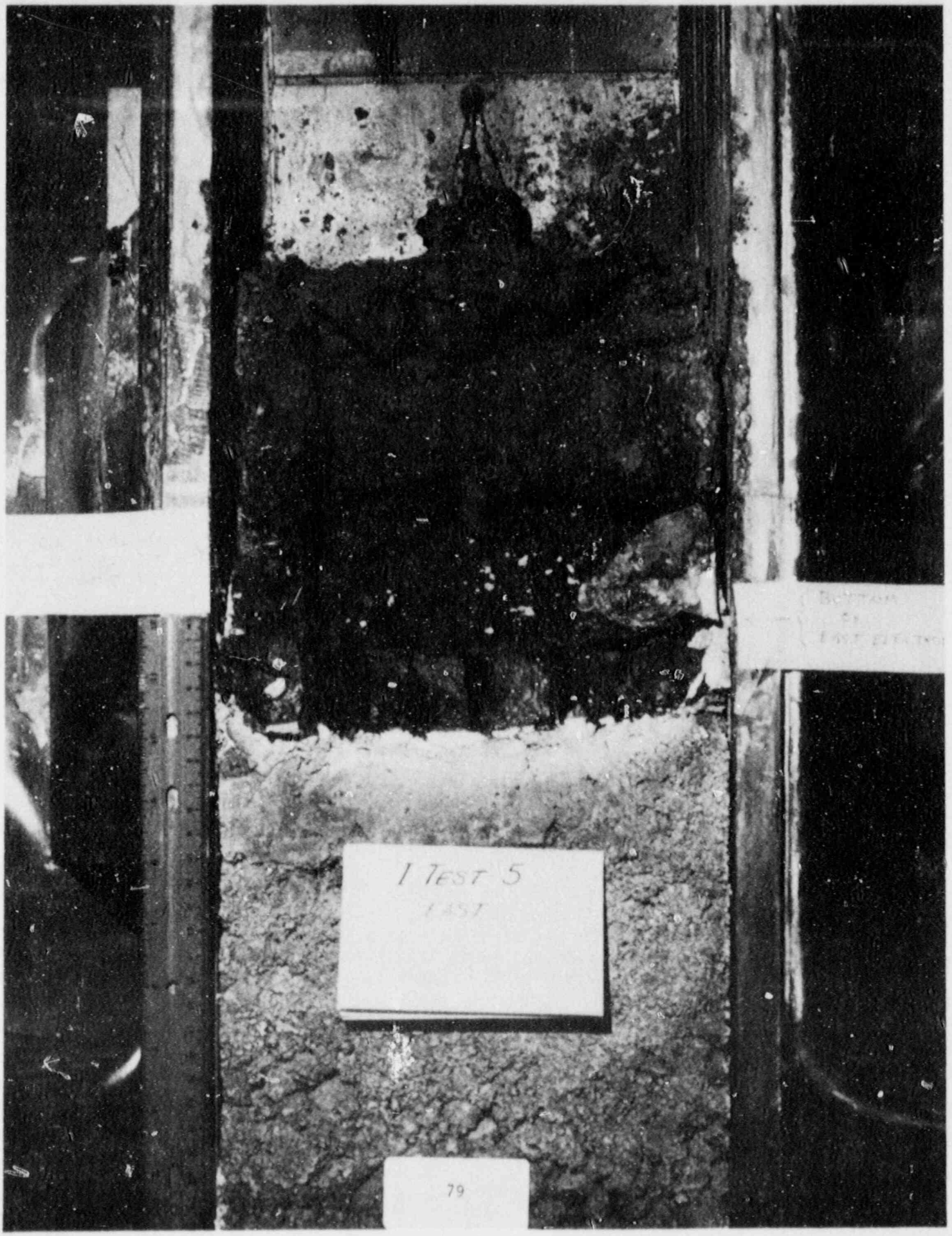

Figure H-4: Interface Between Concrete & Melt for Test I-5

The rate of concrete ablation was sensitive to test power input. Ablation rates determined from the in-concrete thermocouple responses are shown in figure H-5. They vary from a maximum of 3.9 mm/min in tests I-6 and I-7 to a minimum of about 0.9 mm/min. The ablation distance as a function of time for test I-7 as calculated by the code CORCON is also shown in figure H-6.

A total of 400 mg of aerosol was collected during test I-7. The average aerosol transport during I-7 power operation was 4.5 mg/min. This rate did not remain fixed. Data from the sample-line filters indicate that during the initial interaction of molten corium with the concrete the rate (10 min average) was three times higher than during subsequent sample intervals. The concentration of aerosol in the isokinetic sample during the 10-minute interval bounding the initial corium concrete interaction was 0.37 mg/liter.

Peaks in the concentration of CO_2, CO, and moisture in the off-gas stream were also observed coincident with the initial contact of molten corium and concrete. The peak CO_2 concentration was 8%; corresponding peak concentration for moisture and CO were 1.5 and 0.09%, respectively.

Aerosols released during the MCCI tests were collected by gravitational settling, impaction, interception, and diffusion. In test I-5, sets of four stainless steel coupons were positioned at two elevations in the gas system and exposed to the off-gas flow stream for the entire test. In tests I-6 and I-7, the STEP canister was the principal aerosol sampling device and was open to sample gas flow for part of the power operation. Settling plates in the step canister collected particles by gravitational settling and diffusion; the fine wires collected particles by impaction, interception, and diffusion. The coupons, settling plates, and wires were examined by SEM to determine particle size, shape, extent of agglomeration, and elemental composition for atomic numbers > 13.

In MCCI test I-5, particles collected on the downward facing coupons consisted of submicron spherical particles and irregular, stringy agglomerates composed of submicron particles. The particles ranged from 0.1 to 1 μm in diameter with 0.4 μm as the average. The deposits on gravitational settling coupons (facing upward) consisted of large particles and large rounded agglomerates 2 to 3 μm in diameter. These agglomerates frequently contained a large particfle upon which submicron particles had nucleated.

The wire impactors in MCCI test I-7 had three particle populations: 2-6 μm spheres, submicron particles, and irregular agglomerates. Figure H-7 shows a platinum wire from the last stage of the STEP canister with these three particle populations; 2-6 μm spheres were also detected on the settling plates but not in as great a concentration as that on the wires. In addition, the deposits on the settling plates contained significant numbers of submicron particles and some larger particles and agglomerates. Submicron particle nucleation on larger particles and spheres was observed, as in test I-5. The average diameter of the larger particles and agglomerates varied from 3 to 12 μm with an averate of 8 μm.

MCCI Test I-7: CORCON-Calculated Ablation Rate and Corium Temperatures

Time (min)	Ablation Rate (mm/min)	Corium Temperatures (K) Average	Interface	Solidus	Liquidus
66.7	0.13	1649	1460	1870	2572
70.8	0.22	1778	1598	1858	2564
75.0	1.12	1822	1825	1823	2541
79.2	1.21	1766	1766	1765	2497
83.3	1.01	1727	1728	1727	2463
87.5	1.45	1727	1728	1727	2463

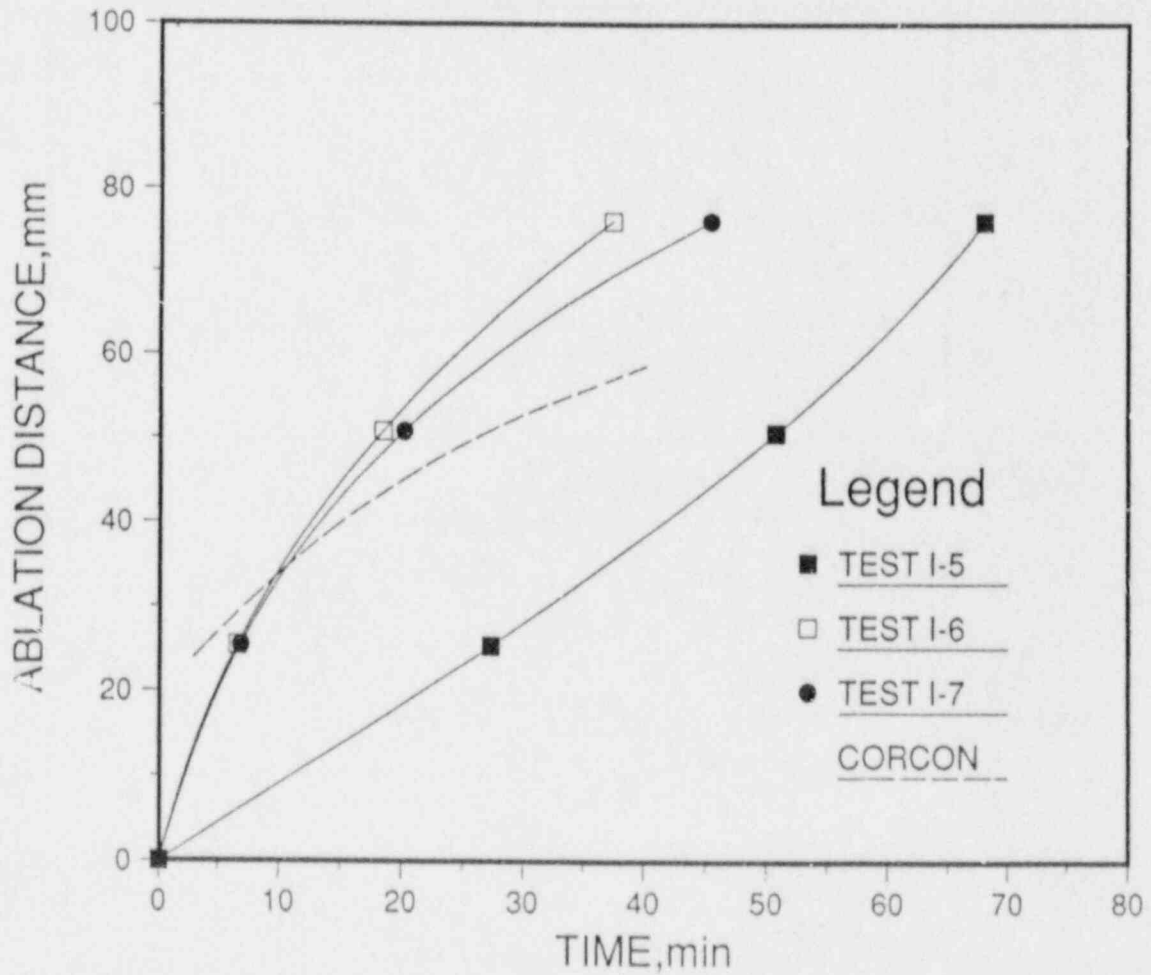

Figure H-5 Ablation Distance vs. Time during MCCI Tests

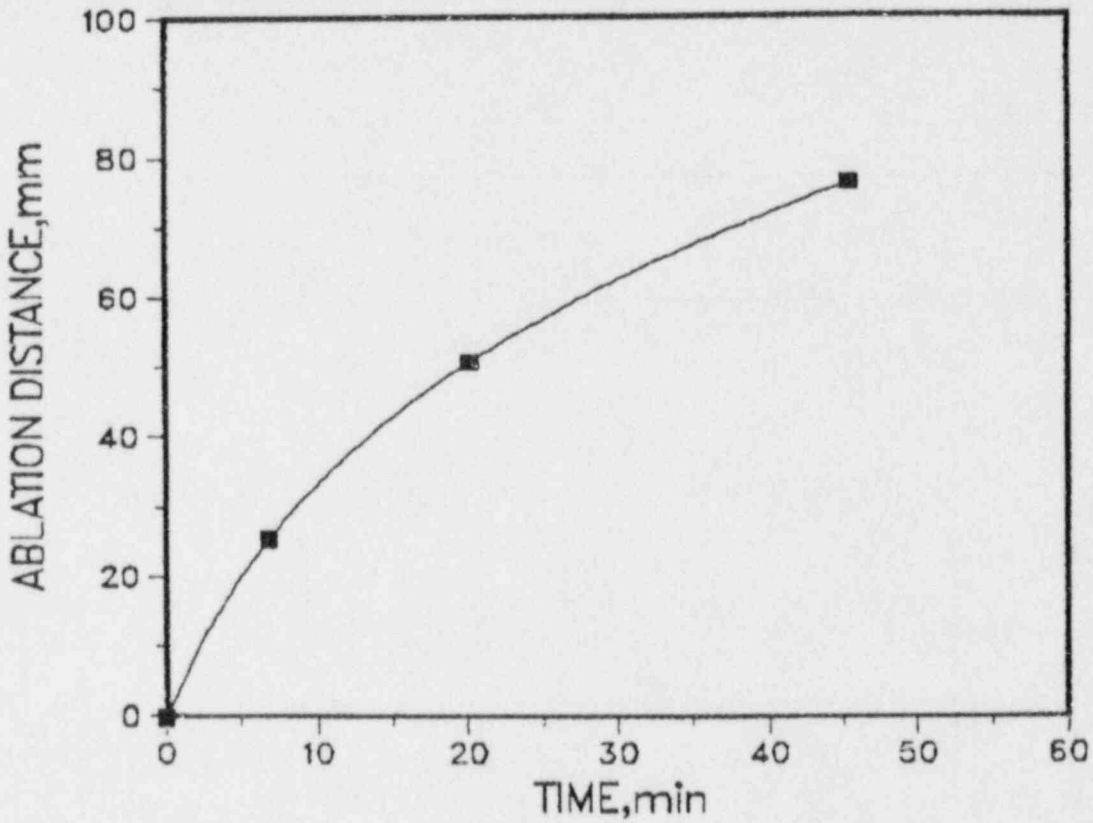

Figure H-6 Ablation Distance vs. Time during MCCI Test I-7

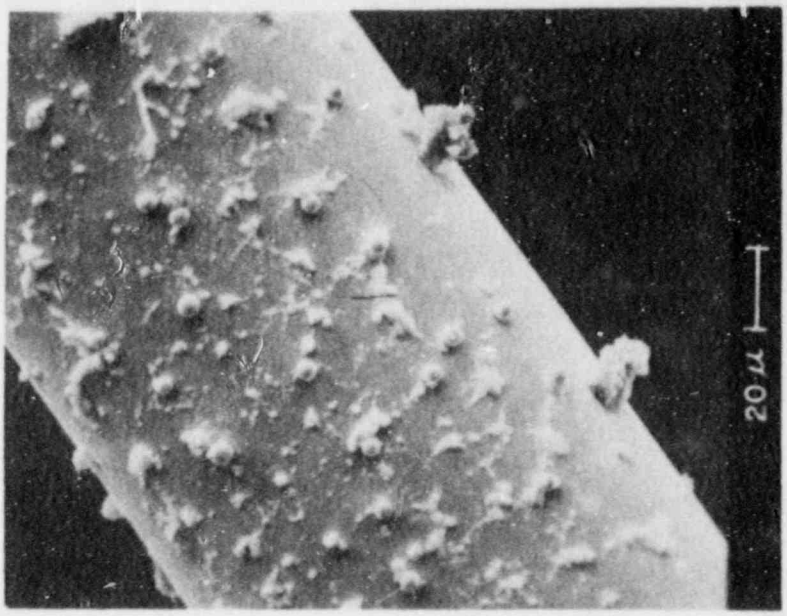

Figure H-7: Platinum Wire From Last Stage of STEP Canister With Three Particle Populations: 2-6 m Spheres Submicron Particles and Irregular Agglomerates

Application of Newton's law of resistance to the size and shape of aerosol particles collected gave settling velocities of the order of 1-4 cm/s. The gas velocity in MCCI test I-7 through the eructation is estimated to be 61 cm/s. Thus, these particles could easily be carried from the melt through this opening by the escaping gas. Gas velocities through the injector region and the main gas line are about 40 cm/s and 65 cm/s, respectively, well above the settling velocities of these large particles and spheres.

Aerosol deposits were examined by SEM for elemental composition. Deposits on test I-5 coupon B-1 (lower sample elevation, upward facing coupon) consist predominantly of zirconium with smaller amounts of chlorine and a trace of potassium. The deposits on the impaction coupon B-2 (lower sample elevation, downward facing coupon), also from test I-5, contained chlorine, potassium, silicon, and possibly some zirconium.

A number of deposits from the MCCI test I-7 were also examined by SEM. The dominant elements detected include uranium, iron, silicon, calcium, potassium, and chlorine with smaller amounts of chromium, aluminum, magnesium, and nickel. Barium was detected in one particle. Uranium was found only in spheres; almost all the 2-6 μm spheres contained uranium. Spheres on settling plates and wires were composed of uranium, silicon, and calcium, sometimes with smaller amounts of iron.

Spheres composed of uranium and iron, sometimes with small amounts of calcium and chromium, were found only on wires. The spherical shape indicates that the material comprising the spheres was molten. A number of crystalline deposits was detected on wires and settling plates. Cubic crystals composed of potassium and chlorine, which are most likely potassium chloride, were frequently observed. Often these crystals comprised part of a larger agglomerate. A number of large particles contained silicon, and/or calcium, and magnesium. These may have been particulates from the concrete that was transported by mechanical entrainment. No lanthanum or strontium was detected in any aerosols from MCCI tests. In test I-7, no zirconium was detected but uranium was dominant in the spheres; whereas, in test I-5, zirconium was frequently found in gravitational settling deposits but no uranium was detected. In both tests, silicon, potassium, and chlorine were found. An SEM examination of the main filter revealed a heavy surface loading of aerosol.

Analysis of the measured data in the intermediate scale tests I-5, I-6, and I-7 is currently being pursued. Further intermediate scale tests are planned and a proposal has been made for joint sponsorship of large-scale (300 kg) tests by an international consortium.

H.4 Detailed Analysis of BWR ATWS Severe Accidents

The BWR anticipated transient without scram (ATWS) scenario TC as analyzed by IDCOR (MAAP code) and NRC (STCP code) shows core melt occurring in about one hour with containment failure relatively close in time to core melt time. The calculated results show substantial releases of volatile and refractory fission products.

In 1986, EPRI initiated work on TC sequence to establish technical feasibility of a procedure for coping with TC type ATWS events by limiting the power generalted to a level so low that the residual heat removal system is capable of removing the reactor heat. The reactor power is controlled by limiting the rate at which cooling water is supplied to the reactor vessel using existing equipment. The intent is to maintain containment integrity while keeping the fuel cool and precluding any damage to fuel or the safety relief valves. Thus, the objective of the work was to perform detailed analysis of the phase of the ATWS accident when the core may be partially uncovered.

The base plant selected for analysis is the Peach Bottom unit 2, a BWR/4 reactor with Mark I containment. Nuclear parameters used in neutron kinetics calculations are specific to the end of cycle 6 core. Two significant deviations from the base plant parameters are (a) the RHR capacity employed is not that of Peach Bottom but of Fitzpatrick plant, which is considerably smaller and (b) two-stage Target Rock safety/relief valves are employed, rather than the three-stage Target Rock valves installed on Peach Bottom.

The scenario employed for analysis is shown in table H-4. The accident begins with main steam isolation valve (MSIV) closing and failure to scram; later, alternate rod injection (ARI) and standby liquid control system (SLCS) are assumed to fail. The operator then follows the EPGs and lowers the water level in the downcomer to top of active fuel (TAF). When the heat capacity temperature limit is reached, the operator depressurizes the vessel as per the requirements of the EPGs. Thereafter, no explicit operator actions are assumed and the response of the plant will be as inherent to the plant and system design.

The results of the calculations performed with the TRACG code (2 fluid model, 3-D core, 1-D neutron kinetics) are shown in figures H-8 through H-10 for the reactor power, reactor pressure, and downcomer level. Some parts of the scenario are explained in the following paragraphs.

At 1100 seconds into the event, the reactor pressure has fallen to about 2.3 MPa (330 psi) above the drywell pressure, the LPCS shutoff head. As the vessel continues to depressurize, the LPCS pumps will generate higher flow rates and the vessel will begin to refill when the incoming ECCS mass flow exceeds the total S/RV mass flow. This point of minimum vessel fluid inventory occurs at about 1200 seconds and marks the beginning of the ECCS reflood phase. Because the vessel is being refilled primarily by LPCS flow which enters the vessel above the core, this period is marked by an overall low-frequency cycle of variation of reactor pressure, ECCS flow, and reactor power, wherein downcomer liquid level is very steady. LPCS flow fills the upper plenum, replacing core voids with liquid and increasing the reactor pwoer. This causes void generation and an increase in pressure, reducing the incoming LPCS flow. When the pressure again exceeds the LPCS shutoff pressure, flow stops, the upper plenum drains, and voids shut down the core. Power then falls to the decay heat level until pressure drops and LPCS flow can again fill the upper plenum. The long period (about 170 seconds) power cycling is therefore directly related to the LPCS flow and reactor pressure cycling.

Table H-4

SEQUENCE OF EVENTS FOR TRACG SIMULATION

	Event/Action	Approximate Time (sec)
1.	MSIV closure, scram fails	0
2.	RPT and S/RVs lift	5
3.	ARI fails	30
4.	Feedwater flow stops as feedwater turbines coast down	90
5.	HPCI and RCIC start	120
6.	SLCS fails	120
7.	Operator reduces water level to TAF and inhibits ADS	300
8.	Operator places two loops of RHR in pool cooling	600
9.	Pool temperature reaches HCTL and operator blows down using ADS valves (operator turns off HPCI)	900
10.	Pressure in RPV is less than LPCS shutoff head and LPCS flow starts	1100
11.	Drywell pressure rises, causing relief valves to close; pressure and valves cycle	5700

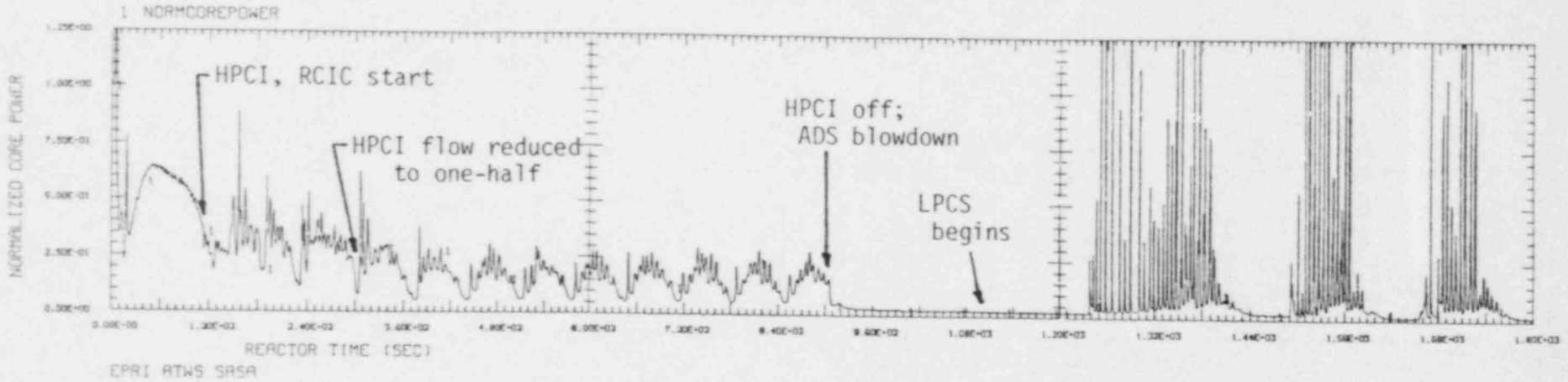

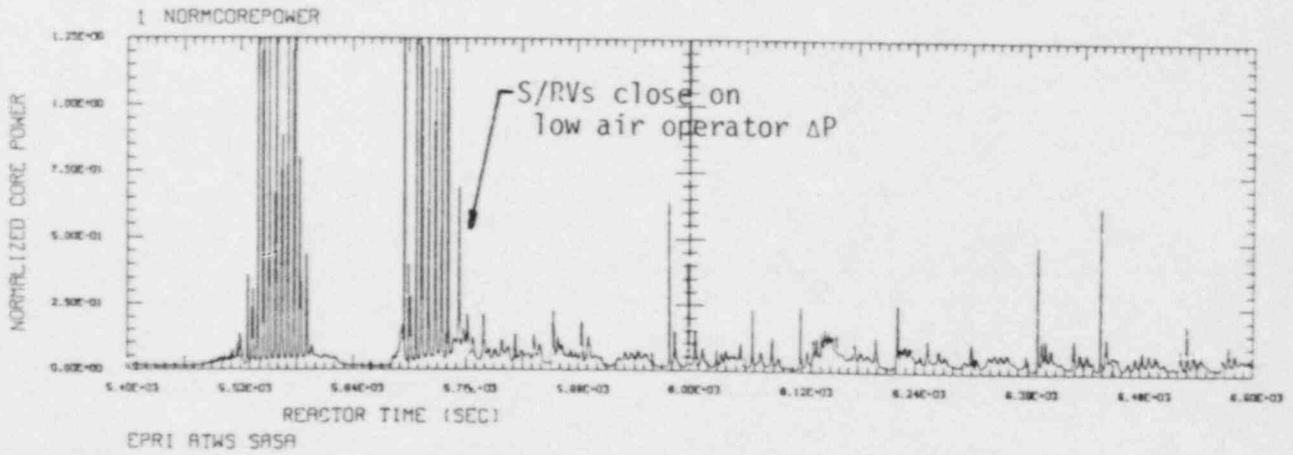

Figure H-8 Core Thermal Power for ATWS Severe Accident Scenario

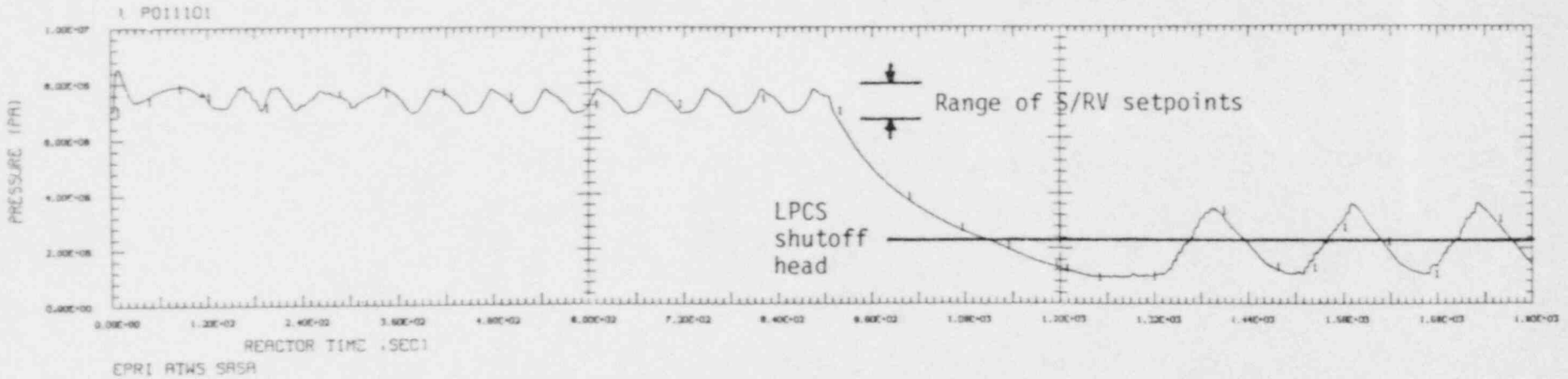

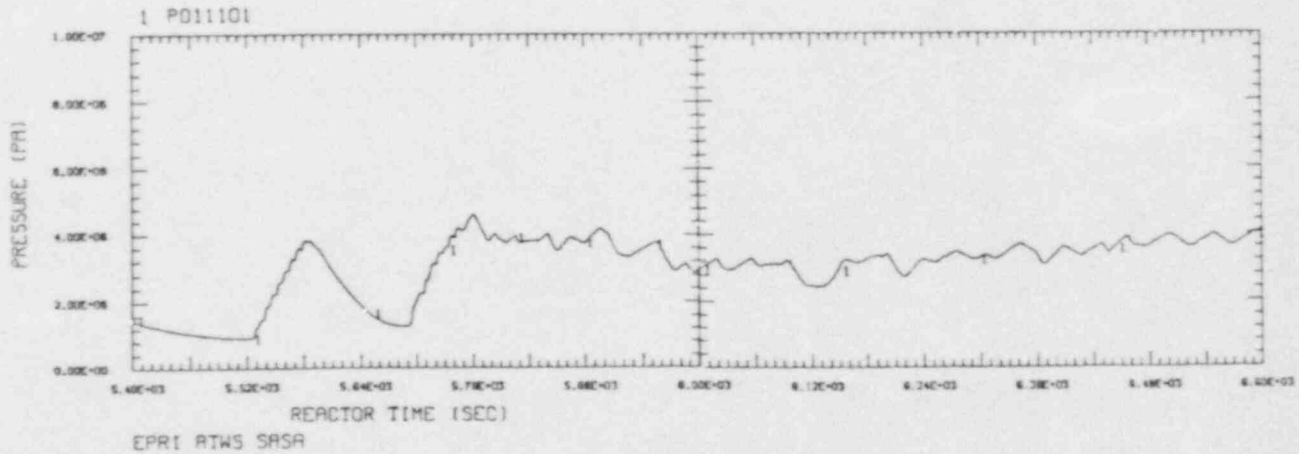

Figure H-9 **Reactor Vessel Dome Pressure for ATWS Severe Accident Scenario**

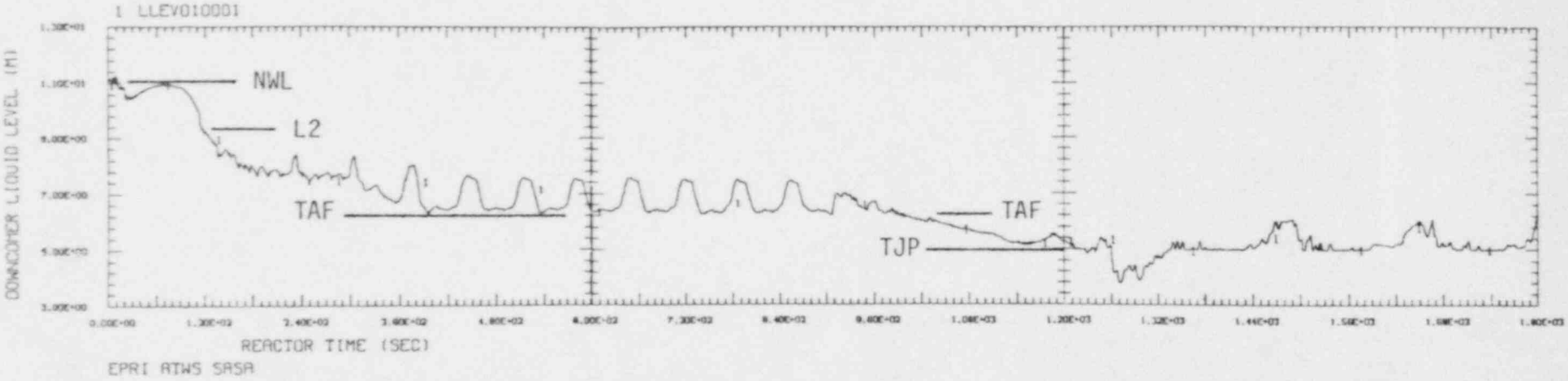

NWL - Normal Water Level

L2 - Level 2

TAF - Top of Active Fuel

TJP - Top of Jet Pump

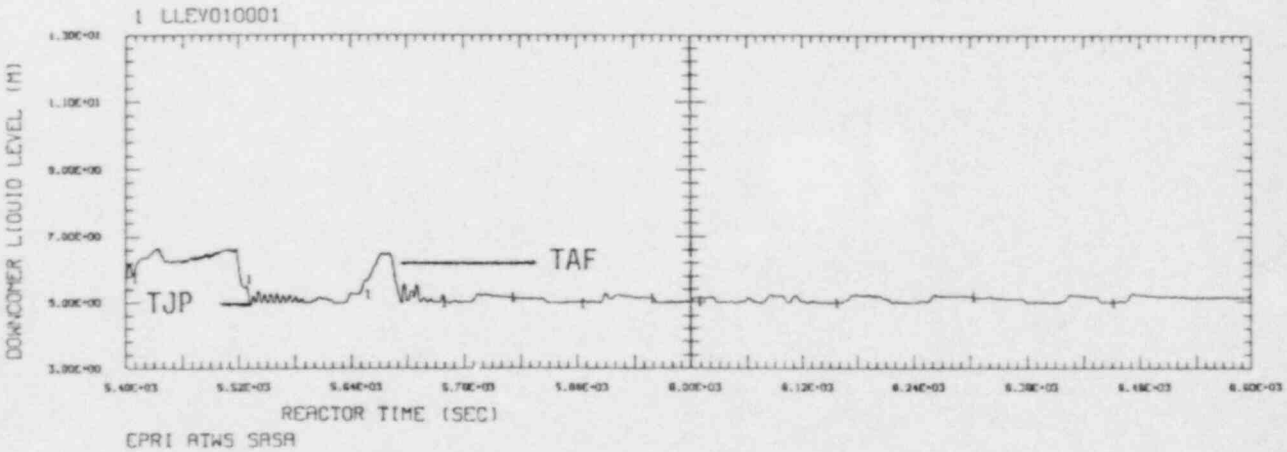

Figure H-10 **RPV Downcomer Collapsed Liquid Level for ATWS Severe Accident Scenario**

The narrow high frequency (5- to 6-second period) power excursions are due primarily to countercurrent flow limiting (CCFL) breakdown at the fuel assembly upper tie plate. This CCFL breakdown phenomenon allows flow to enter the top of the core immediately from the upper plenum rather than from the bypass region or lower plenum. The reactivity addition generates the power spike, which is turned around by the Doppler feedback.

The cycling which is typical of the ECCS reflood phase could continue indefinitely in the absence of additional equipment failures or operator actions or containment influences. This is not the case, however, because of the combination of suppression pool volume, reactor power, and RHR capacity used in this analysis. The RHR is not large enough to reject the heat being generated in the reactor core, and the suppression pool temperature and drywell pressure continue to rise during the ECCS reflood period. Because of this drywell pressure rise, the two-stage Target Rock S/RVs will close and the longperiod pressure/flow cycling will be stopped. Pneumatic pressure in the air actuator will be insufficient to hold open the two-stage valve at high drywell pressures and low system pressures. For this case, the elapsed time between the start of ECCS reflood and first valve closure is estimated to be 4500 seconds (75 minutes). The transient analysis itself, therefore, breaks off at 1800 seconds (after 600 seconds of LPCS cycling) and picks up again at 5400 seconds. The ECCS reflood cycling behavior is observed to still follow the same pattern as earlier, but the drywell pressure is sufficiently high that the S/RVs being help open pneumatically begin to close at about 5700 seconds.

The portion of the accident occurring from valve closure at 5700 seconds to the end of the simulation at 600 seconds is best described as self-regulation. As drywell pressure continues to rise, the S/RVs cycle open and close in response to continued steam generation in the core and the system behavior more closely resembles the level control phase (300 to 900 seconds) than any other mode. The core thermal power is now at an average of about 3.5% of rated, slightly more than can be removed by the RHR used in this evaluation. This mode of operation could continue with increasing drywell pressure. It is estimated that a pressure of 930 kPa (135 psia) would be reached at about 3.7 hours. For a plant with a larger RHR heat exchanger than that used in this analysis, a 930-kPa drywell pressure might never be reached, and the containment integrity never threatened. In any case, several hours would be available to the operator to either vent the containment, or insert rods or get the SLCS operational before containment integrity could be threatened.

The RPV downcomer level shown in figure H-10 is the collapsed level and remains close to the top of the jet pumps. The swell level in the core is high enough to cover the core. Thus, at no time, the temperature of clad on the fuel rods exceeds 1000 K, precluding any oxidation of Zircaloy during the phase of the accident when the core is partially uncovered.

The results detailed above do show that in this particular scenario, suitably low reactor power can be achieved without unacceptably high clad temperatures. However, because this scenario involved intermittent dump of

water on top of the core via the spray system, power and reactvity spikes would occur with unknown but probably undesirable effects. It is believed that suitable quantity of water additions from underneath (i.e., from lower downcomer) will limit the power spikes and reduce the number of times the valves have to be recycled.

H.5 Severe-Accident Integrated Analysis Methodology (SIAM)

The SIAM code provides a methodology with which thermal-hydraulic and fission-product transport and deposition calculations can be carried out simultaneously to predict fission-product behavior within reactor cooling systems (RCS) during postulated degraded core accidents. The methodology involves the coupling of the EPRI-sponsored codes CORMLT (H-17), which models the meltdown progression of a nuclear reactor; PSAAC (H-18), which models the thermal-hydraulic behavior within the RCS; and, RAFT (H-19), which performs the aerosol transport and deposition computations.

This coupling of codes is required because based on the available reactor core fission-product inventories and decay heating rates, the suspended and deposited fission-product materials are capable of substantially increasing gas and structure temperatures along the RCS. These increased gas and structure temperatures can potentially alter RCS flow patterns, induce local failure of thin structural elements, redistribute previously deposited aerosol material via revaporization and transport, and actually affect the release of fission products from the core and from the RCS. Thus, the actual fission product and thermal-hydraulic behavior during a degraded core accident may be substantially different than that predicted by an uncoupled process.

Simulations of the TMLB' (PWR) and TW (BWR) sequences have been carried out with SIAM (H-20). The results indicate that, for both sequences, coupling aerosol and thermal-hydraulic calculations affects the aerosol behavior within the RCS very minimally. The coupled thermal-hydraulic conditions for the TMLB' case, principally the gas and structure temperatures, were, however, significantly different from the uncoupled thermal hydraulics. For example, the upper plenum gas phase temperature is up to 300 K higher if fission-product heating effects are included in the calculation.

In contrast, the coupled thermal-hydraulic conditions for the TW scenario were essentially unchanged from the uncoupled values. Coupling of the code package has been completed and it is in the early stages of being validated against experimental data obtained from the TMI-2 examination, LOFT FP-2 test, and TREAT STEP tests. Sensitivity and scenario calculations will be performed to assess the adequacy of the coupling between the thermal-hydraulic and the radionuclide transport processes.

I. NATIONAL AND INTERNATIONAL COLLABORATIVE SAFETY RESEARCH

In recent years, the research focus on high burden-low probability events has placed requirements for the verification of analytical methods which predict highly complex phenomena. Generally, their veracity is established through the conduct of relatively large-scale experiments and tests. The conduct of

such tests is generally rather expensive. To this end, major research programs have recently taken on a highly collaborative and cooperative manner and spirit both within the United States and with foreign research organizations. While most of these efforts are experimenta, collaborative analytical efforts a' ' growing.

In addition to expanding the available funding base resulting in enlarged scope to enhance the databases for validating predictions, the collaborative efforts provide a basis for mutual interchange of ideas and information. As a result, these programs become more critically planned and evaluated, and often produce the highest quality technical results.

The approaches to such collaborative efforts have evolved involving foreign and domestic government agencies, EPRI, utilities, and reactor manufacturers. Only relatively current ones with EPRI involvement are cited below (some have already been referred to but current participant restrictions on use and dissemination of results precludes additional detailed reference at this time). The Organization for Economic Cooperation and Development (OECD) has recently been instrumental in facilitating nuclear safety research testing. One extreme is the multinational-multimillion dollar thermal-hydraulic and fission-product release and transport program in the LOFT reactor in Idaho organized by DOE. A more modest sample is the OECD TMI-2 standard problem analysis.

The LACE (Large Aerosol Containment Experiment) aerosol transport investigation organized by EPRI is focusing on aerosol behavior in containment and ancillary structures. The newer (just organized) ACE (Advanced Containment Experiments) will include aerosol removal experiments and corium-concrete expeirments. The Marviken project, organized in Sweden, focused on aerosol and volatile fission-product behavior within the primary system.

EPRI's participation in NRC's severe fuel damage consortium reflects EPRI's and NRC's recognition of the importance of collaborative efforts for the national good.

All projects noted above were sponsored by more than ten international partners with U.S. sponsorship from DOE, NRC, and EPRI in most cases.

Some hydrogen mixing and combustion investigations, the TREAT-STEP program and some fission-product behavior studies at ANL were organized by EPRI and had less extensive sponsorship.

A cooperative effort involving principally domestic sponsors is the Multiple Integral System Test (MIST) for thermal-hydraulic studies of systems with once-through steam generators. A prior related study called OTIS was sponsored by a foreign industrial organization.

Specific cooperative and collaborative efforts are emerging relative to the maintenance, use, and development of major or large computer codes. Costs here are also growing and various collaborative approaches are evolving. The EPRI-sponsored RETRAN and MMS (Modular Modeling System) codes are currently in the most advanced stages of such software development.

To summarize, most of the OECD and CEC countries with nuclear programs have been or are involved with one or more of such collaborative efforts.

J. CONCLUSION

In recent years, changes in the direction of nuclear safety research have occurred, particularly with emphasis on work related to power plant applications. Many research and development results are now being beneficially used in the industry.

With the recent reorganization in the nuclear industry, a promise of more effective operation of nuclear plants to contribute to the advancement of the American way of life is offered. We all will need to do our part to fulfill this promise, and EPRI is committed to making a contribution.

EPRI's research is one small part of that promise for the future. The results from EPRI research in the safety area reported here, and outside the safety area in maintenance, operations, materials, etc., will also have an important role to play. The key to the application of EPRI research is the adoption of technology by the utilities. The utilities, with EPRI support, have been showing leadership in accepting new technology to help them do things better.

K. REFERENCES

K.1 LWR Systems Analysis and Application

B-1. "Reactor Safety Study - An Assessment of Accident Risks in U.S. Commercial Nuclear Power Plants." WASH-1400 (NUREG/75-014), October 1975.

B-2. I. B. Wall. "The Reactor Safety Study - Its Influence Upon Reactor Safety." Nuclear Power Experience, vol. 4, 1983.

B-3. "PRA Procedures Guide." NUREG/CR-2300, January 1983.

B-4. "General Design Criteria for Nuclear Power Plants." Appendix A of Title 10 Code of Federal Regulations Part 50.

B-5. Pickard, Lowe & Garrick, Inc. "Seabrook Station Probabilistic Safety Assessment." Prepared for Public Service Company of New Hampshire and Yankee Atomic Electric Company, December 1983. PLG-0300.

B-6. V. Joksimovich et al. "A Review of Some Early Large-Scale PRA Studies." Palo Alto, Calif.: Electric Power Research Institute, October 1983. NP-3265.

B-7. V. Joksimovich et al. "A Review of Selected Topics From PRA Studies." Palo Alto, Calif.: Electric Power Research Institute, May 1985. NP-3838.

B-8. G. Edwards and I. Watson. "A Study of Common Mode Failures." UKAEA, July 1979. SRD R146.

B-9. C. L. Atwood and J. Stevenson. "Common Cause Fault Rates for Diesel Generators." NUREG/CR-2099, June 1982.

B-10. C. L. Atwood. "Common Cause Fault Rates for Pumps." NUREG/CR-2098, February 1983; For Valves, NUREG/CR-2770, February 1983; For Instrumentation and Control Assemblies, NUREG/CR-2771, February 1983.

B-11. G. Crellin, I. Jacobs, and A. Smith. "Common Cause Failures - Phase I: A Classification System." Palo Alto, Calif.: Electric Power Research Institute, January 1984. NP-3383.

B-12. K. Fleming et al. "Classification and Analysis of Reactor Operating Experience Involving Dependent Events." Palo Alto, Calif.: Electric Power Research Institute, June 1985. NP-3867.

B-13. K. Fleming, A. Mosleh, G. Parry, H. Paula, M. Bohn, D. Rasmusson, and D. Worledge. "Procedures for Treating Common Cause Failures in Safety and Reliability Studies: Vol. 1, Procedural Framework and Practical Guidelines; Vol. 2, Analytical Background and Techniques." Joint EPRI NP/NUREG report to be published in 1987.

B-14. R. L. Simard. "Nuclear Plant Reliability Data System: Program Description." INPO 86-010, February 1986.

B-15. G. Crellin et al. "Common Cause Failures Final Classification System." Palo Alto, Calif.: Electric Power Research Institute, June 1985. NP-3837.

B-16. A. Poucet, A. Amendola, and P. Cacciabue. "CCF-RBE Common Cause Failure Benchmark Exercise." CEC Technical Note 1.05.C1.86.114, PER 1240, November 1986.

B-17. A. Poucet, A. Amendola, and P. Cacciabue. "European Benchmark Exercise on Common Cause Failure Analysis." International Topical Conference on Probabilistic Safety Assessment and Risk Managmeent, Zurich, Switzerland, August 1987.

B-18. K. Fleming, A. Mosleh, and D. Worledge. "Development of a Systematic Approach for the Analysis of System-Level Dependent Failures." International Topical Conference on Probabilistic Safety Assessment and Risk Management, Zurich, August 1987.

B-19. G. Crellin, A. Smith, and I. Jacobs. "Data-based Defensive Strategies for Reducing Susceptibility to Common Cause Failures: Vol. 1, Defensive Strategies; Vol. 2, Data Analysis and Database." EPRI report to be published in 1987.

B-20. G. Crellin, J. Mott, A. Smith, and D. Worledge. "Defensive Measures for Common Cause Failures." International Topical Conference on Probabilistic Safety Assessment and Risk Management, Zurich, August 1987.

B-21. G. Edwards and I. Watson. Private Communication. SRD UKAEA.

B-22. B. B. Chu, D. H. Worledge, and I. B. Wall. "Overview - Use of PSA for Enhancing Plant Operational Safety and Productivity." Submitted to International Meeting on Nuclear Power Plant Operation, Chicago, Illinois, August 30-September 3, 1987.

B-23. GO Methodology. Palo Alto, Calif.: Electric Power Research Institute, November 1983. NP-3123.

B-24. Safety System Unavailability Monitoring. INPO 86-021, August 1986.

B-25. R. Vasuvedan, A. M. Smith, T. D. Matteson, and B. R. Hao. Application of Reliability-Centered Maintenance to Component Cooling Water System at Turkey Point Units 3 and 4. Palo Alto, Calif.: Electric Power Research Institute, October 1985. NP-4271.

B-26. G. L. Crellin, T. D. Matteson, and A. M. Smith. Use of Reliability-Centered Maintenance for the McGuire Nuclear Station Feedwater System. Palo Alto, Calif.: Electric Power Research Institute, September 1986. NP-4795.

B-27. P. Wood et al. Utility Experiences and NRC Perceptions in the Application of PRA. Palo Alto, Calif.: Electric Power Research Institute, to be published.

K.2 Control and Diagnostics

C-1. M. Divakaruni. "EPRI-Sponsored Demonstration of Signal Validation at BWR and PWR Nuclear Stations." IEEE Nuclear Power Symposium, Orland, Florida, November 1984.

C-2. M. Divakaruni. "Industry Practices for Plant Signal Validation and EPRI Projects." EPRI Safety Control Seminar, February 4-6, 1985.

C-3. M. Divakaruni and B. K.-H. Sun. "Signal Validation: A New Industry Tool." Presented at the NRC-RSR Information Meeting, Gaithersburg, Madison, October 22-25, 1985.

C-4. Validation and Integration of Critical PWR Signals for SPDS. Palo Alto, Calif.: Electric Power Research Institute, May 1986. NP-4566.

C-5. S. M. Divakaruni, B. Lutz, D. Firth, and O. Deutsch. "Signal Validation of SPDS Variables for Westinghouse & CE Plants - An EPRI Project." Presented at the EPRI SPDS/Emergency Response Facility Seminar, May 1986.

C-6. Validation of Critical Signals for the Safety Parameter Display System. Vols. 1, 2, & 3. Palo Alto, Calif.: Electric Power Research Institute, April 1987. NP-5066M, NP-5066-SL.

C-7. User's Guide for Signal Validation Software. Palo Alto, Calif.: Electric Power Research Institute, September 1987. NP-5389.

C-8. Digital Feedwater Controller for a BWR: A Conceptual Design Study. Palo Alto, Calif.: Electric Power Research Institute, 1984. NP-3323.

C-9. M. Divakaruni, B. K.-H. Sun, and A. C. Rogers. "Power Plant Digital Control and Fault-Tolerant Microcomputers." EPRI Digital Control Seminar Notebook, Scottsdale, Arizona, April 9-12, 1985. NP-4769-SR.

C-10. M. Divakaruni. "Role of Microprocessor Systems in Power Plant Control, Monitoring and Safety." EPRI Digital Control Seminar, Scottsdale, Arizona, April 9-12, 1985.

C-11. M. Hammer, M. Divakaruni, J. Penland, L. Carmichael, and B. Pierce. "BWR Feedwater Control System Replacement in Monticello Plant." EPRI Digital Control Seminar, Scottsdale, Arizona, April 9-12, 1985.

C-12. K. F. Graham and M. Divakaruni. "EPRI Digital Feedwater Control Projects: System Verification Plans in an Operating Plant." EPRI Digital Control Seminar, Scottsdale, Arizona, April 9-12, 1985.

C-13. S. M. Divakaruni, R. Gopal, and M. Couchman. "Digital Control Technology Development." Presented at the EPRI Safety Control Seminar, Palo Alto, California, February 1985.

C-14. R. D. Fournier, M. F. Hammer, and B. K.-H. Sun. "Digital Control and Protection Retrofits in a Nuclear Power Plants." Presented at the International Meeting on Nuclear Power Plant Operation, Chicago, Illinois, August 30, 1987.

C-15. Digital Feedwater Control System - System Final Requirements and Design Specification." Palo Alto, Calif.: Electric Power Research Institute, October 1987. NP-5502.

C-16. Testing and Installation of a BWR Digital Feedwater Control System. Palo Alto, Calif.: Electric Power Research Institute. To be published.

C-17. Functional Specifications for AI Software Tools for Electric Power Applications. Palo Alto, Calif.: Electric Power Research Institute, August 1985. NP-4141.

C-18. D. G. Cain, B. K.-H. Sun, and W. S. Faught. "Artificial Intelligence Research at the Electric Power Research Institute for Nuclear Power Applications." Presented at the 9th International Conference on Modern Power Stations, Leige, Belgium, October 7-11, 1985.

C-19. B. K.-H. Sun. "Expert System Applications in the Electric Utility Industry." Presented at the International Instrumentation Society of America Conference, Houston, Texas, October 12-16, 1986.

C-20. J. A. Naser, B. K.-H. Sun, D. G. Cain, and R. W. Colley. "Artificial Intelligence Research at EPRI for Nuclear Power Plant Applications." Presented at the WATTEC 1987, Knoxville, Tennessee, February 18, 1987.

C-21. J. A. Naser and D. G. Cain. "Tools for Utility Use to Enhance Productivity and Decision Making." Proceedings of the American Power Conference, Chicago, Illinois, April 27-29, 1987.

C-22. D. G. Cain and F. Schmidt. "Expert Systesm - Basic Principles and Possible Applications in Nuclear Energy." International Topical Meeting on Advances in Reactor Physics, Mathematics and Computation, Paris, April 27-30, 1987.

C-23. D. G. Cain, J. A. Naser, and B. K.-H. Sun. "EPRI Projects: Technical Progress Update." EPRI Seminar: Expert Systems Applications in Power Plants, Boston, Massachusetts, May 27-29, 1987.

C-24. D. G. Cain. "Selecting Expert Systems Applications." EPRI Seminar: Expert Systems Applications in Power Plants, Boston, Massachusetts, May 27-29, 1987.

C-25. J. Naser, R. Colley, J. Gaiser, T. Brookmire, and S. Engle. "A Fuel Insert Shuffler Planner Expert System." EPRI Seminar: Expert Systems Applications in Power Plants, Boston, Massachusetts, May 27-29, 1987

C-26. R. Touchton, A. Gunter, and D. G. Cain. "Reactor Emergency Action Monitor (REALM): An Expert System for Classifying Emergencies." EPRI Seminar: Expert Systems Applications in Power Plants, Boston, Massachusetts, May 27-29, 1987

C-27. Assessment of Verificaiton and Validation of Expert Systems Developed for Nuclear Power Applications. Palo Alto, Calif.: Electric Power Research Institute, August 1987. NP-5236.

C-28. J. Naser, R. Colley, J. Gaiser, and T. Brookmire. "Fuel Insert Shuffler: A Case Study of Expert System Development." Submitted for ANS Topical Meeting on Artificial Intelligence and Other Innovative Computer Applications in the Nuclear Industry, Snowbird, Utah, August 31-September 2, 1987.

C-29. Emergency Operating Procedures Tracking System. Palo Alto, Calif.: Electric Power Research Institute, June 1987. NP-5250M.

C-30. W. Petrick, K. Ng, C. Stuart, D. Shen, D. G. Cain, and B. K.-H. Sun. "Emergency Procedures Tracking System for Nuclear Power Plants." Presented at the ANS Topical Meeting on Artificial Intelligence and Other Innovative Computer Applications in the Nuclear Industry, Snowbird, Utah, August 31-September 2, 1987

K.3 Safety Margins and Testing

D-1. Jong H. Kim, Boyd Brooks, John Power, and Jean-Pierre Sursock. EPRI Workshop on Water Hammer in Nuclear Power Plants. Private Communication, June 1987.

D-2. J. H. Kim. "Perspectives on Two-Phase Flow Pump Modeling for Nuclear Reactor Safety Analysis." Cavitation and Multiphase Flow Forum 1983, J. W. Hoyt, ed., ASME, Houston, Texas, June 1983, pp. 29-33.

D-3. D. J. Olson. Single- and Two-Phase Performance Characteristics of the MOD-1 Semiscale Pump Under Steady State and Transient Fluid Condition. Aeroject Nuclear Company Report, October 1974. ANC-1165.

D-4. One-Third Scale Air-Water Pump Program, Test Program, and Pump Performance. Palo Alto, Calif.: Electric Power Research Institute, July 1977. NP-135.

D-5. Pump Two-Phase Performance Program. NP-1556, 7 vols. Palo Alto, Calif.: Electric Power Research Institute, September 1980.

D-6. Two-Phase Performance of Scale Models of a Primary Coolant Pump. Palo Alto, Calif.: Electric Power Research Institute, September 1982. NP-2578.

D-7. Development of an Analytical Model to Determine Pump Performance Under Two-Phase Flow Conditions. Palo Alto, Calif.: Electric Power Research Institute, May 1984. NP-3519.

D-8. O. Furuya. "An Analytical Model for Prediction of Two (Noncondensable) Flow Pump Performance." Journal of Fluids Engineering, ASME Transactions, vol. 107, no. 1.

D-9. W. Kastner and G. J. Seeberger. "Pump Behavior and Its Impact on a Loss-of-Coolant Accident in a Pressurized Water Reactor." Nuclear Technology, vol. 60, February 1983.

D-10. G. G. Loomis. Intact Loop Pump Performance During the Semiscale MOD-1 Isothermal Test Series. Aerojet Nuclear Company Report, October 1975. ANCR-1240.

D-11. Thermal Analysis of Core Barrel Heating and Cooling Recirculation During Uncovering Core Conditions Simulating Severe PWR Accidents. Palo Alto, Calif.: Electric Power Research Institute (Report to be published).

D-12. SATYA Computer Code Manual. EPRI Report, 4 vols. Palo Alto, Calif.: Electric Power Research Institute (to be published).

D-13. Stability Analysis for Two-Fluid Systems Application Code. EPRI Report, 4 vols. Palo Alto, Calif.: Electric Power Research Institute (to be published).

D-14. P. Saha. "Thermally Induced Two-Phase Flow Instabilities Including the Effect of thermal NEQ Between Phases, Ph. D. Thesis, Georgia Institute of Technology, 1974.

D-15. L. Efferding. "DYNAM - A Digital Computer Program for Study of the Dynamic Stability of Once-Through Boiling Flow With Steam Superheat." GAMD-8656, 1968.

D-16. BWR 64 Rod Bundle Blowdown Heat Transfer. Palo Alto, Calif.: Electric Power Research Institute, February 1981. NP-1720.

D-17. BWR Large Break Simulation Tests. NP-1783, 2 vols. Palo Alto, Calif.: Electric Power Research Institute, April 1982.

D-18. BWR Full Integral Simulation Test (FIST) Program Plan. Palo Alto, Calif.: Electric Power Research Institute, September 1983. NP-2313.

D-19. BWR Full Integral Simulation Test Program: TRAC BWR Model Development. NP-3897, 3 vols. Palo Alto, Calif.: Electric Power Research Institute, March 1986.

D-20. BWR Full Integral Simulation Test Results (Phase 2) and TRAC BWR Qualification. Palo Alto, Calif.: Electric Power Research Institute, March 1986. NP-3988.

D-21. C. C. Lin, T. Wassel, S. P. Kalra, and A. Singh. "The ThermalHydraulics of a Simulated PWR Facility During Steam Generator Tube Rupture Transients." Nuclear Engineering & Design, vol. 98, 1986, pp. 15-38.

D-22. "Simulation of Steam Generator Tube Rupture Experiments." MMS Workshop. New Orleans, Louisiana, September 26-28, 1984.

D-23. "Thermal Hydraulics During Steam Generator Tube Rupture Transients." Proceedings of the 5th ANS National Heat Transfer Conference, Denver, Colorado, August 1985, pp. 456-474.

D-24. Modular Modeling System Analysis of the Semi-Scale Steam Generator Tube Rupture Experiment. Palo Alto, Calif.: Electric Power Research Institute, September 1986. NP-4783.

D-25. Loss of Feedwater, SGTR and Steam Line Break Experiments. NP-4786, 3 vols. Palo Alto, Calif.: Electric Power Research Institute,, January 1987.

D-26. Steam Generator Tube Rupture and Stuck-Open Safety Relief Valve Carryover Tests. NP-4787, 2 vols. Palo Alto, Calif.: Electric Power Research Institute, July 1987.

D-27. Prototypical Steam Generator Transient Testing Program: Test Plan/ Scaling Analysis. Palo Alto, Calif.: Electric Power Research Institute, September 1984. NP-3494.

D-28. Heat Transfer, Carryover and Fallback in PWR Steam Generator During Transients. Palo Alto, Calif.: Electric Power Research Institute, Febuary 1986. NP-4298.

D-29. Modeling PWR Steam Separators During Transients. Palo Alto, Calif.: Electric Power Research Institute, August 1987. NP-5272.

D-30. J. M. Anderson and W. A. Owia. Data Report for the TPFL Tee/Critical Flow Experiments. NUREG/CR-4164, 1985.

D-31. The Marviken Full-Scale Critical Flow Tests. NP-2370, vol. 1. Summary Report. Palo Alto, Calif.: Electric Power Research Institute, May 1982.

D-32. Critical Flow Data Review and Analysis. Palo Alto, Calif.: Electric Power Research Institute, January 1982. NP-2192.

D-33. Critical Flow Through Small Pipe Breaks. Palo Alto, Calif.: Electric Power Research Institute, May 1986. NP-4532.

D-34. C. J. Crowley and P. M. Rothe. "Flow Visualization and Break Mass Flow Measurements in Small Break Separate Effects Experiments." Small Break Loss-of-Coolant Accident Analysis in LWRs. Palo Alto, Calif.: Electric Power Research Institute, August 1981. WS-81-201.

D-35. J. Reimann and M. Khan. Flow Through a Small Break at the Bottom of a Large Pipe With Stratified Flow. Presented at the 2nd International Topical Meeting on Nuclear Reactor Thermal Hydraulics, Santa Barbara, California, January 11-14, 1983.

D-36. J. Reimann and C. Smoglie. Flow Through a Small Pipe at the Top of a Large Pipe With Stratified Flow. Presented at the Annual Meeting of the European Two-Phase Flow Group, Zurich, Switzerland, June 14-16, 1983.

D-37. V. E. Schrock, S. T. Revanker, R. Mannheimer, C. H. Wang. "Small Break Critical Discharge - The Roles of Vapor and Liquid Entrainment in a Stratified Two-Phase Region Upstream of the Break." NUREG/CR-4761, LBL-22024, 1986.

K.4 Seismic Center Research

E-1. J. D. Stevension. "Designing for Extreme Loads--The Impact on Cost and Schedule." Nuclear Engineering International, vol. 29, no. 357, July 1984.

E-2. J. J. Ray, Chairman, ACRS. "Quantification of Seismic Design Margins." Letter to N. J. Palladino, Chairman, Nuclear Regulatory Commission, January 11, 1983.

E-3. J. C. Ebersole, Chairman, ACRS. "Quantification of Seismic Design Margins." Letter to N. J. Palladino, Chairman, Nuclear Regulatory Commission, January 18, 1984.

E-4. J. Devine (USGS). Letter to R. Jackson (NRC), November 18, 1982.

E-5. D. L. Bernreuter et al. "Seismic Hazard Characterization of the Eastern U.S.: Methodology and Results at Ten Sites." UCID-20421, April 1985.

E-6. Seismic Hazard Methodology for the Central and Eastern United States. Volumes I through 10. Palo Alto, Calif.: Electric Power Research Institute, July 1986. NP-4726.

E-7. "SIMQUAKE-I--An Explosive Test Series Designed to Simulate the Effects of Earthquake-Like Ground Motions on Nuclear Power Plants Models. Palo Alto, Calif.: Electric Power Research Institute, February 1981. NP-1728.

E-8. SIMQUAKE-II--A Multiple Detonation Explosive Test to Simulate the Effects of Earthquake-Like Ground Motions of Nuclear Power Plant Models. Palo Alto, Calif.: Electric Power Research Institute, August 1983. NP-2916.

E-9. STEALTH--A Lagrange Explicit Finite-Difference Code for Solids, Structural, and Thermohydraulic Analysis. NP-2080-CCM, vol. 5. STEALTH-SEISMIC Code User's Manual. Palo Alto, Calif.: Electric Power Research Institute, December 1984.

E-10. STEALTH--A Lagrange Explicit Finite-Difference Code for Solids, Structural, and Thermohydraulic Analysis. NP-2080-CCM, vol. 9. SEISMIC Code Procedures Manual. Palo Alto, Calif.: Electric Power Research Institute, December 1984.

E-11. ABAQUS-EPGEN: A General Purpose Finite-Element Code. Palo Alto, Calif.: Electric Power Research Institute, October 1982. NP-2709-CCM.

E-12. Testing and Analysis of Feedwater Piping at Indian Point Unit 1. Palo Alto, Calif.: Electric Power Research Institute, July 1983. NP-3108.

E-13. "Technical Position on Damping Values for Piping--Interim Summary Report." Welding Research Council Bulletin 300, December 1984.

E-14. Dynamic Response of Presurized Z-Bend Piping Systems Tested Beyond Elastic Limits and With Support Failures. Palo Alto, Calif.: Electric Power Research Institute, December 1984. NP-3746.

E-15. High-Amplitude Dynamic Tests of Prototypical Nuclear Piping Systems. Palo Alto, Calif.: Electric Power Research Institute, February 1985. NP-3916.

E-16. Piping and Fitting Dynamic Reliability Program: First Semi-Annual Progress Report, May-October 1985. General Electric Report, November 1985. NEDC-31272.

K.5 Analysis Development and Validation

F-1. Nuclear Power Plant Simulators for Use in Operator Training. ANSI/ANS-3.5-1981, April 13, 1981.

F-2. Nuclear Power Plant Simulators for Use in Operator Training. ANSI/ANS-3.5-1985, October 25, 1985.

F-3. B. Kraje et al. Analytical Simulator Qualification Methodology. Palo Alto, Calif.: Electric Power Research Institute, September 1985. NP-4243.

F-4. K. V. Moore et al. RETRAN-02 - A Program for Transient Thermal-Hydraulic Analysis of Complex Fluid Flow Systems. Palo Alto, Calif.: Electric Power Research Institute, vols. 1-5, May 1981. NP-1850-CCM.

F-5. Conference Proceedings: First International RETRAN Conference. WS-80-150. L. J. Agee, ed. Palo Alto, Calif.: Electric Power Research Institute, April 1981.

F-6. Conference Proceedings: Second International RETRAN Conference. NP-2494-SR. L. J. Agee, ed. Palo Alto, Calif.: Electric Power Research Institute, July 1982.

F-7. Conference Proceedings: Third International RETRAN Conference. NP-3803-SR. L. J. Agee, ed. Palo Alto, Calif.: Electric Power Research Institute, February 1985.

F-8. Conference Proceedings: Fourth International RETRAN Conference. NP-4558-SR. L. J. Agee and J. Naser, eds. Palo Alto, Calif.: Electric Power Research Institute, May 1986.

F-9. J. F. Harrison and J. Loomis. Qualification of RETRAN for Simulator Applications. Palo Alto, Calif.: Electric Power Research Institute, to be published.

F-10. K. V. Moore et al. RETRAN--A Program for One-Dimensional Transient Thermal-Hydraulic Analysis of Complex Fluid Flow Systems. EPRI Computer Code Manual, CCM-5, vols. 1-3. Palo Alto, Calif.: Electric Power Research Institute, December 1978.

F-11. J. H. McFadden et al. RETRAN-02--A Program for Transient Thermal-Hydraulic Analysis of Complex Fluid Flow Systems. NP-1850-CCM, vols. 1-3. Palo Alto, Calif.: Electric Power Research Institute, May 1981.

F-12. Letter from Cecil O. Thomas (NRC) to Dr. Thomas W. Schnatz (Chairman of Utility Group for Regulatory Application), Acceptance for Referencing of Licensing Topical Reports, EPRI CCM-5, "RETRAN--A Program for One-Dimensional Transient Thermal-Hydraulic Analysis of Complex Fluid Flow Systems," and EPRI NP-1850-CCM, "RETRAN-02--A Program for Transient Thermal-Hydraulic Analysis of Complex Fluid Flow Systems," September 2, 1984.

F-13. Minutes of the RETRAN Working Group Meeting, May 6, 1987.

F-14. VIPRE-01: A Thermal-Hydraulic Analysis Code for Reactor Cores. NP-2511-CCM (Rev. 2). Vol. 1: Mathematical Modeling. Vol. 2: User's Manual. Vol. 3: Programmer's Manual. Palo Alto, Calif.: Electric Power Research Institute, July 1985.

F-15. The Reactor Analysis Support Package (RASP). NP-4498, vol. 1. Introduction and Overview. Palo Alto, Calif.: Electric Power Research Institute, April 1986.

F-16. Nuclear Plant Safety, September-October 1986, p. 45.

F-17. U.S. NRC Docket Nos. 50-282/306, May 1986.

F-18. Reload Safety Evaluation Methods. Topical Report, NSP NAD-8102, rev. 3, April 1985.

F-19. Y. R. Raschid and H. Nerman. "Application of SAFE-2D Program to the Analysis of Fuel Rod Ramp Tests." Trans. ANS International Conference on World Nuclear Energy, vol. 24, TANSAO 21 1-510, 1976.

F-20. Y. M. Lu, R. S. Dunham, and Y. R. Raschid. FREY-01: Fuel Rod Evaluation System. NP-3277-CCM. Vol. 1: Theoretical and Numerical Bases. Vol. 3: Verification and Qualification.

Palo Alto, Calif.: Electric Power Research Institute, October 1983.

F-21. MATPRO - Version 11 (Rev. 2): A Handbook of Material Properties for Use in the Analysis of Light Water Reactor Fuel Rod Behavior. NUREG/CR-0497, August 1981.

F-22. D. D. Lanning and E. R. Bradley. "Irradiation History and Interim Postirradiation Data for IFA-432." NUREG/CR-3071, PNL-4543, March 1984.

K.6 Hydrogen Control

G-1. Effectiveness of Thermal Ignition Devices in Lean Hydrogen-Air-Steam Mixtures. Palo Alto, Calif.: Electric Power Research Institute, March 1985. NP-2956.

G-2. Hydrogen Mixing and Distribution in Containment Atmospheres. Palo Alto, Calif.: Electric Power Research Institute, March 1983. NP-2669.

G-3. Large-Scale Hydrogen Combustion Experiments. Palo Alto, Calif.: Electric Power Research Institute, to be pubished. NP-3878.

G-4. Large-Scale Hydrogen Burn Equipment Experiments. Palo Alto, Calif.: Electric Power Research Institute, December 1985. NP-4354.

G-5. "IDCOR Technical Summary Report: Nuclear Power Plant Response to Severe Accidents." The Industry Degraded Core Rulemaking Program, November 1984.

G-6. "IDCOR Technical Report 17: Equipment Survivability in a Degraded Core Environment." The Industry Degraded Core Rulemaking Program, July 198.3

K.7 Severe Accident Safety

H-1. W. B. Loewenstein and G. R. Thomas. "Nuclear Safety, Forward on Technology and Backward on Perception." 14th Water Reactor Safety Research Meeting, October 1986. NUREG/LP-0082, vol. 5, pp. 445-522.

H-2. D. Cubicciotti and B. R. Sehgal. "Fission Products and Material Vapor Transport During Molten Corium-Concrete Interactions." Proceedings of the Fifth International Meeting on Thermal Nuclear Reactor Safety, Karlsruhe, September 9-13, 1984.

H-3. M. Silberberg et al. "Reassessment of the Technical Bases for Estimating Source Term." NUREG-0956 (draft), July 1985. Also, " Reactor Risk Reference Document." NUREG-1150, USNRC, 1987.

H-4. M. Lee, M. S. Kazimi, and G. Brown. "A Heat Transfer Model for the Corium/Concrete Interface." Proc. ANS/ENS Int. Mtg. on Light Water Reactor Severe Accident Evaluation, Cambridge, Massachusetts, August 28-September 1, 1983.

H-5. M. Lee and M. S. Kazimi. "Modeling of Corium-Concrete Interactions." MITNE-267, M.I.T., Dept. of Nucl. Engg., June 1985. Also, EPRI NP-5403, 1987).

H-6. L. S. Kao, M. Lee, and M. S. Kazimi. "Assessment of Heat Transfer Models for Corium-Concrete Interaction." Proceedings of Third International Meeting on Reactor Thermal Hydraulics, Newport, Rhode Island, October 1985.

H-7. L. S. Kao and M. S. Kazimi. "Impact of Heat Transfer Models on Core/Concrete Interaction." OECD, CSNI Specialist Meeting on Core Debris/Concrete Interactions, Palo Alto, California, September 1986. NP-5054-SR.

H-8. L. S. Kao and M. S. Kazimi. "A Heat Transfer Model for Core/Concrete Interactions." AIChE Symposium Series, 83, p. 383. National Heat Transfer Conference, Pittsburgh, Pennsylvania, August 1987.

H-9. M. L. Corradini. "Current Modelling of Molten Core Concrete Interactions." National Heat Transfer Conference, Denver, Colorado, 1985.

H-10. F. Gonzalez and M. Corradini. "Experimental Study of Pool Entrainment and Mixing Between Two Immiscible Liquids With Gas Injection." OECD, CSNI Specialist Meeting on Core Debris/Concrete Interactions, Palo Alto, California, September 1987. NP-5054-SR.

H-11. M. L. Corradini, F. Gonzalez, and T. K. Norlens. "CORCON-MOD2 Modifications: Immiscible Fluid Mixing and Fission Product Vaporization." AIChE Symposium Series, 83, p. 397, 1987. National Heat Transfer Conference, Pittsburgh, Pennsylvania, August 1987.

H-12. B. W. Spencer, W. H. Gunther, D. R. Armstrong, D. H. Thompson, M. G. Chasanov, and B. R. Sehgal. "EPRI/ANL Investigations of MCCI Phenomena and Aerosol Release." OECD, CSNI Specialist Meeting on Core Debris/Concrete Interactions, Palo Alto, California, EPRI NP-5054-SR, September 1986.

H-13. B. W. Spencer, D. H. Thompson, D. R. Armstrong, J. K. Fink, W. H. Gunther, D. J. Kilsdonk, and B. R. Sehgal. "Investigation of Molten Corium-Concrete Interaction Phenomena and Aerosol Release." AIChE Symposium Series, 83, p. 375, 1987. National Heat Transfer Conference, Pittsburgh, Pennsylvania, August 1987.

H-14. B. J. Schlenger, P. F. Dunn, and E. L. Horton. "Versatile Aerosol Sampling System Developed for Nuclear Reactor Safety Experiments." Accepted for publication in Particulate Science and Technology.

H-15. T. B/ Schlenger, P. F. Dunn, J. E. Herceg, R. Simons, E. L. Horton, L. Baber, Jr., and R. L. Ritzman. "Chemical Characteristics of Material Released During Source Term Experiments Project (STEP). In-Pile Tests, Part I.

J. K. Fink, M. F. Rocha, C. A. Seils, D. V. Steidl, C. E. Johnson, and R. L. Ritzman. "Chemical Characteristics of Material Released during Source Term Experiments Project (STEP). In-Pile Tests, Part II. Proceedings of the Symposium on Chemical Phenomena Associated With Radioactivity Release During Severe Nuclear Power Plant Accidents. American Chemical Society, Anaheim, California, September 1986.

H-16. Gunnar Erickson. Chemica Scripta, 8, pp. 100-103, 1985.

H-17. V. E. Denny. The CORMLT Code for the Analysis of the Degraded Core Accidents. Palo Alto, Calif.: Electric Power Research Institute, December 1984. NP-3767-CCM.

H-18. A. T. Wassel, M. S. Hoseyni, J. L. Farr, Jr., and S. M. Ghiaasiaan. Thermal-Hydraulic Modeling of the Primary Coolant System of the Light Water Reactors During Severely Degraded Core Accidents. Palo Alto, Calif.: Electric Power Research Institute, July 1984. NP-3563.

H-19. K. H. Im, R. K. Ahluwalia, and C. F. Chuang. "RAFT: A Computer Model for Formation and Transport of Fission Product Aerosols in LWR Primary Systems." Proceedings: American Nuclear Society Meeting on Fission Product Behavior and Source Term Research, Palo Alto, Calif.: Electric Power Research Institute, July 1985. NP-4113-SR.

H-20. D. C. Bugby, J. L. Farr, Jr., A. T. Wassel, and B. R. Sehgal. "Coupled Thermal-Hydraulic and Fission-Product Transport Analysis of Reactor Coolant Systems During Degraded Core Accidents." ASME/AIChE/ANS National Heat Transfer Conference, Pittsburgh, Pennsylvania, August 1987.

ACKNOWLEDGMENTS

The breadth of scope of this paper required written input and critical review from many--and the authors wish to pass on their appreciation to the staff of the Safety Technology Department (STD) for this help. Also, without the cheerful, creative and accurate typing (and retyping) of this paper by Conchita Ace, there would be no coherent text to read.

Recent MAAP Developments

E.L. Fuller and R.L. Ritzman, EPRI

Z.T. Mendoza, SAIC

R.R. Sherry, JAYCOR

R.E. Henry, FAI

ABSTRACT

In this paper, recent MAAP developments are described. In particular, the most recent enhancements made both by EPRI and IDCOR are discussed. The status of the independent verification and validation project is presented. Finally, the results of a comparison between MAAP 3.0 and the Source Term Code Package (STCP) on the Peach Bottom plant are given and discussed.

I. Introduction

The Modular Accident Analysis Program (MAAP)[1] was originally developed by the Industry Degraded Core Rulemaking (IDCOR) Program to analyze severe accident behavior in an integrated manner. Models were developed for various phenomena, plant systems, geometries, and for simulating various events for four light water reactor (LWR) designs in the United States. Each was characterized by a reference plant, including Peach Bottom (Mark I BWR), Grand Gulf (Mark III BWR), Zion (large dry PWR) and Sequoyah (ice condenser PWR). Subsequently, EPRI enhanced MAAP's capabilities by developing the capability to analyze three additional plant types, namely, Mark II BWR (Susquehanna), Babcock & Wilcox large dry PWR (Oconee), and Combustion Engineering large dry PWR (Calvert Cliffs). Improved phenomenological modeling was also added and a model for treating auxiliary buildings and secondary containment buildings was added. The result is a new archived version, MAAP 3.0. A formal line-by-line verification of this code is in progress. Additionally, sensitivity studies are being carried out with it, in order to address key phenomenological uncertainties and the effects of differences in sequence description.

In the remainder of this paper, the following will be discussed:

1. A brief description of the new MAAP enhancements.

2. Status of the verification and validation effort.

3. Results of a sensitivity study for Peach Bottom, where sequences analyzed by Battelle-Columbus with the Source Term Code Package (STCP)[2] in NUREG/CR-4624[3] (a supporting document for NUREG-1150[4]) were run with

MAAP 3.0. Comparisons between MAAP 3.0 and the STCP will be made, and the differences discussed.

II. MAAP 3.0 Enhancements

As part of still ongoing industry-NRC interactions, an issue resolution phase was initiated to identify and resolve differences between the NRC and IDCOR models[5]. This resulted in further improvements in the MAAP code, including phenomenological models covering in-vessel core meltdown progression, core-concrete attack, and debris coolability within the containment. With active interest by the industry to continue with the MAAP advancement program, EPRI sponsored additional modeling development for the BWR and PWR codes which, along with the Issue Resolution modeling changes, provided the full enhancement package to produce MAAP 3.0. Tables 1 and 2 summarize the modeling changes made to MAAP as a result of the IDCOR issue resolution effort and EPRI MAAP advancement programs, respectively.

Detailed descriptions of the models in MAAP 3.0 may be found in the MAAP User's Manual [1]. These models represent the various stages of severe accident progression from the initial core uncovery to fission product release to the environment. There are key models, however, which have significant influence in the overall accident progression and calculation of environmental source terms. These models are briefly described below.

A. Core Melt Progression Model

The physical and chemical processes which occur as core materials begin to melt and relocate are very complicated, and detailed modeling of these complex phenomena is difficult to implement. In the earlier version of MAAP (version 2.0), the core meltdown and relocation process was not modeled and molten core material was simply allowed to heat up adiabatically until a user-specified mass had collected. At that point, the molten material was assumed to slump into the vessel bottom head where it could thermally attack and fail the vessel. This simple procedure predicted unreasonably high debris temperatures under certain conditions; therefore, a model was added to MAAP by IDCOR during the issue resolution process, to track the global progression of core melting and movement of molten material to the bottom head[5].

The meltdown process model assumes that the core components (UO_2, Zr and ZRO_2) formed a eutectic which melts at a user-specified temperature and latent heat of fusion (melting of undissolved Zr is not explicitly modeled). As the materials melt, they flow downward until they reach a frozen node or a node which is completely full. (The code calculates that once an individual node begins to melt, the molten mass can flow downward provided that the flooding criterion has been exceeded. This criterion states that molten core material can be held up in the core provided that an adequate pressure exists below the molten mass). The molten material and the previously molten but frozen (or unmelted) nodes are homogeneously mixed, which usually freezes the molten material. The model assumes that the convective motion within the homogeneous pool is sufficient to prevent significant temperature differences. The calculations of core melt progression indicate a rapid increase in molten mass once the first node begins melting. This model is similar to the NRC STCP core

meltdown model (model "A") in the MARCH code module. In that model, core slumping is triggered by a user-supplied parameter defining the amount of core mass that must be molten for core support failure.

B. Ex-Vessel Heat Transfer and Fission Product Release

The physical processes of a core meltdown progression within the vessel set the stage for the ex-vessel physical and chemical interactions which occur following vessel failure. Molten core material will relocate to the floor directly underneath the vessel or be dispersed to other parts of the containment as a consequence of vessel failure. MAAP models couple the upward convection and radiation heat transferred from the core debris with natural circulation flows in the containment. The upward heat losses control the corium upper crust thickness and debris bulk temperature. Downward heat transfer models determine concrete erosion rates. Because of the coupling employed in the integrated analysis of containment response, MAAP predicts more upward energy loss and less erosion than the NRC STCP decoupled approach. This is in part related to the inherently more distributed core debris configuration (lesser amounts, greater surface area, and smaller depth than the STCP predictions). The lower core debris temperatures and lower concrete erosion rates would also tend to predict smaller ex-vessel fission product releases. The fission product species present in the molten corium and concrete mixture are released by three physical processes, the most important of which is vapor stripping by concrete decomposition gaseous products. Off-gas generation from concrete decomposition is determined by the rate of concrete thermal attack. Therefore, ex-vessel fission product releases are expected to be sensitive to models which influence the debris temperature and chemical equilibria.

The release of fission products and other materials from the mixture of core materials as the gases are evolved assumes that they are in equilibrium with the melt. Thus, the concrete decomposition gases bubbling through the melt contain the partial pressure of each constituent of the pool.

C. Fission Product Aerosol Transport Behavior

The MAAP models for fission product aerosol deposition in the RCS and containment use a correlation to describe the time evolution and deposition process as fission product material is released from the core and transported within the RCS and containment. The sedimentation correlation was developed using airborne aerosol concentrations similar to those occurring in various accident sequences in BWR and PWR reactor designs. These models are different from the NRC-developed models, which use basic representations of aerosol agglomeration and deposition processes. Calculations using both models show that substantial RCS retention could occur. Given such deposition, the influence of containment parameters, sequence timing, or containment failure (its size and location) may not play significant roles in the prediction of environmental source terms. Note, however, that the decay energy associated with these deposited aerosols within the RCS structure surfaces could have a significant influence in the ultimate release since revaporization of these materials could occur later in time. The MAAP 3.0 aerosol numerical model provides a significant calculational improvement upon the simplified aerosol

correlation contained in the MAAP 2.0 models. Correlations of aerosol behavior for a number of deposition mechanisms have been developed to evaluate the spectrum of conditions during the course of a severe accident. Correlations have been developed[5] for sedimentation, inertial impaction, and turbulent deposition under steady-state or decaying conditions. Combination laws for more than one removal mechanism, as well as moisture accumulation for hygroscopic aerosols, envelope the spectrum of possible conditions during a degraded core accident. The changes in the sedimentation correlation and addition of deposition models could alter the distribution of various aerosol species, but the overall impact on previously calculated environmental releases is not expected to be significant.

III. Status of MAAP Verification and Validaton

In order to assure that MAAP can credibly be used confidently by the nuclear industry, EPRI instituted an independent verification and validation project. The elements of this process are listed in Table 3. The prioritization was necessary in order to identify those models which are most important in determining the principal code outputs, for example, time of containment failure and source terms. This enabled the early work to be concentrated on the most important models. The priorities that resulted are shown on Table 4. Since the original prioritization was done, several new models have been added, such as corium/concrete interactions chemistry (METOXA), a generalized auxiliary/reactor building treatment, and improvements in steam generator modeling. These are also being verified and validated.

The line-by-line verification methodology can be illustrated by Figures 1 and 2. The entire code is verified in this manner. Potential errors and other questions are highlighted by numbered comments (e.g., comments 3 and 4 on the right side of Figure 2). Resolution of the comments either leads to correcting the code, educating the independent verifier, or both. To date, priority items 1-5 (see Table 4) have been verified, and most of the questions raised have been resolved.

To date, model validation has been carried out on the corium/concrete interaction module and on the hydrogen combustion module. The methodology used is to first develop stand-alone "submodels" for experiment analysis by identifying all major routines which are involved in a particular process or phenomenological calculation, determine all support routines required for the calculation, and combine these routines with an executive "driver" routine which controls the calculation. Then, these stand-alone models are used to analyze experiments and for comparison with detailed models. Table 5 lists the routines incorporated into the stand-alone model for corium/concrete interaction. In addition to the main driver, several routines had to be added to treat the experiments analyzed, since they are not completely prototypic of actual plant situations. As can be seen from Table 5, many MAAP subroutines were tested.

The experiments analyzed with the "DECOMP stand-alone model" included CC1, CC2, SWISS 1 and SWISS 2 from Sandia, and several of the Beta tests. In general, the agreement was very good. Total concrete erosion compared very well but the split between radial and axial erosion could not be predicted,

because DECOMP has only a one-dimensional treatment of heat transfer from corium to walls and floors, and for resultant erosion. However, when a two-dimensional treatment of these effects was added, excellent agreement resulted. One final point should be made about this validation. When comparing against the SWISS tests, excellent agreement resulted. MAAP also calculates that debris would not be coolable by the overlying water under these non-prototypic experimental conditions.

Validation of the hydrogen combustion module was done in the same fashion as described for the corium/concrete interaction module. Results of the FITS tests and Nevada tests were used for the comparison. Agreement with the FITS data was excellent. Very good agreement also resulted for the Nevada tests where the hydrogen concentration was 8% or greater. Some manipulation of parameters in the incomplete combustion models was necessary to achieve good agreement for those tests where the hydrogen concentration was low.

IV. MAAP Peach Bottom Analyses and Comparison With STCP Results

In support of NUREG-1150, Battelle-Columbus Laboratories (BCL) has carried out calculations with the STCP for five plants, including Peach Bottom. In this section, results of MAAP 3.0 analyses of the sequences analyzed will be compared with the STCP results. The sequences considered include ATWS (TC1, TC2, TC3), and station blackout (TB1 and TB2). The sequence definitions appear in Tables 6 and 7. Great care was taken to assure that the assumptions made in the STCP analyses were also made in the MAAP analyses, even if they made little sense. Most noteworthy in this regard is the assumption of a 7 ft^2 containment failure size, occurring from overpressurization in the drywell. Analysis by Chicago Bridge and Iron indicates that the failure would either be:

1. Overpressure failure in the wetwell airspace, or

2. Leakage from the drywell head, and/or

3. Overtemperature failure in the drywell.

The event summaries obtained from the MAAP analyses are shown in Tables 8 and 9. They agree relatively well with the BCL analyses. Agreement is not good, however, on the source term results, as evidenced in Tables 10 and 11. Major differences are as follows:

For the TC1 and TC2 sequences, significant differences are apparent between the two calculations from the wide range of values shown for: 1) RCS retention of the volatile CsI fission product species; 2) the suppression pool retention of CsI; and 3) the reactor building versus drywell/pedestal retention for the Sr group. The high degree of CsI retention in the RCS predicted by the STCP code models is due to the assumption of no revolatilization after vessel breach. In MAAP, initially high deposition rates may be calculated, but upon vessel breach, revolatilization would subsequently release the initially deposited aerosols into the drywell. Because of the relatively high drywell temperatures, most of the secondary releases (revolatilized materials) are not permanently captured by the containment drywell surfaces but find

their way into the reactor building. The relatively high retention of aerosols* in the reactor building ultimately reduces the airborne fission products available for release to the environment; hence, the CsI environmental source terms are comparable in the STCP code and MAAP calculations.

A secondary impact of the initial high deposition of CsI in the RCS is noted in TC2. In this scenario, the ADS valves are closed (or the SRVs cycle). Consequently, the fraction of CsI deposited in the wetwell is observed to be less than for the corresponding STCP code scenario. In the STCP code calculations, extremely high flow rate of high temperature steam and hydrogen gases occurs (particularly at core slump) causing the SRVs to open, sweeping substantial amounts of CsI into the suppression pool.

The calculation of Sr releases varies in both models as illustrated by the high mass fraction of Sr retained in the fuel/debris for MAAP (a factor of at least 2 higher than STCP predictions). Most of the released SR is deposited in the drywell for MAAP, whereas the STCP predictions show negligible amounts retained in the drywell. Most of the Sr aerosols are released from the containment in the latter analysis, where they are deposited on the relatively cold surfaces in the reactor building or released to the environment. Although the retention in the reactor building is significant in the STCP calculations, the volume leaked into the environment nearly equals it for TC2 and far exceeds it for TC1. In the MAAP calculations most of the Sr fission product species are retained in the fuel debris. The Sr fission products release which occurs during core-concrete attack is mostly deposited in the drywell/pedestal regions.

The pedestal cavity is modeled as a separate compartment volume within the containment system in MAAP. This region, like all regions, can exchange mass and energy (including fission product aerosols) with the reactor coolant system and the drywell region. Density driven flows between the pedestal and the drywell occur through the pedestal openings. Hot gases will rise and move into the drywell and cooler drywell gases will enter the pedestal. Fission product transport and deposition within the two regions would occur along with the mass exchange. Therefore, a significant fraction of Sr aerosols released from the corium debris is calculated to be deposited equally between these two regions. In the STCP code calculations, a very significant fraction of the Sr inventory is released from the fuel debris ex-vessel into the single drywell volume and swept out of the containment through the reactor building to the environment. Therefore, a very large difference in the predicted Sr environmental releases is noted between the two calculational models.

For TB1 and TB2, conclusions similar to those reached for TC apply with regard to the predictions of in-vessel and ex-vessel fission product distributions

---

* The CsI released early (shortly after containment failure) is predominantly transported as aerosols. Late secondary fission product sources are released from the containment in vapor form. These condense and form aerosols on transport within the reactor building.

and releases to the environment. The differences noted for the TC scenarios (relative to CsI and Sr deposition and leakage to the environment) are also observed for the TB scenarios. As illustrated by the retention fractions in the RCS, the suppression pool, and the reactor building (in Table 11), the transport behavior of fission product aerosols as modeled between the MAAP and STCP codes differs in many respects. Although the releases to the environment for CsI may be comparable (see TB2), the distributions within the containment system vary significantly such that general conclusions regarding congruence in the source term predictions cannot be made.

For sequence TB1, the time of containment failure is significantly different between the two codes (MAAP predicts a failure time of 33 hours based on overpressure conditions, whereas STCP calculations indicate that the containment will fail at 15 hours into the accident); therefore, predictions of environmental releases and aerosol distribution within the containment system would be expected to vary. This variation in results is predominant in the calculations for the CsI fission product group. The trend noted in the CsI release fraction to the environment between MAAP (longer containment failure time) versus STCP (shorter containment failure time) is related to the difference in the assumptions relative to revolatilization. This is contrary to general conclusions [6] regarding mitigation of fission product releases for sequences for which the containment integrity is maintained long after vessel breach. In MAAP, the initially deposited CsI materials in the RCS and the drywell are re-emitted as the temperature of the internal surfaces increase. Therefore, when the containment fails, there is a significant inventory of airborne volatile materials which can then be swept out as the containment is depressurized. (This revolatilization is not modeled in the STCP calculations after vessel breach).

For TB2, the environmental release fraction of CsI is comparable in both codes. However, as noted above, the distribution in the plant is very different. In the MAAP calculations, CsI retained within the containment system is mostly deposited within the reactor building (75% of the core inventory), a factor of 10 higher than the STCP predictions. On the other hand, the amount scrubbed in the suppression pool is a factor of 4 less than that of the STCP code calculations (6 versus 22% CsI). This difference in the reactor building and pool retention fractions is consistent with the modeling of revolatilization following vessel breach for MAAP, which is not considered in STCP. The initially deposited volatile material in the RCS is eventually remitted for deposition in the reactor building.

In this scenario, the suppression pool is available only intermittently for scrubbing prior to vessel breach since the ADS valves were not actuated during core melt, and flow to the pool is bypassed following vessel failure (and containment failure). Additionally, the leakage rate from containment during the extended time involved in the revolatilization from the RCS allows a significant deposition to occur as the fission product material is transported through the reactor building. The time to containment failure is predicated upon the assumed drywell shell failure at vessel breach; thus the relative times are the same in both models.

A. <u>TC Sensitivity Variations</u>

Variations in the TC sequences were defined relative to systems or model parameters which could affect the thermal-hydraulic response of the reference cases, the sequence timing, and/or release characteristics. For example, for TC1, RHR systems availability and ADS valves temporary reclosure as the containment is pressurized were examined. Since the focus of the evaluation was also a comparative examination of the NUREG-1150 basis, the sequence variations were directed towards parameters found in the NRC STCP models which could impact the release characteristics, within the constraints of the MAAP best-estimate modeling assumptions. Results of the variations are shown in Table 12.

1. TC Sensitivity Case 1

This scenario is basically a TC1 event where core coolant makeup was provided by the low pressure systems upon ADS actuation. The RHR systems were assumed not available and the ADS valves were assumed to reclose upon containment pressurization. Since the impact of these changes was more related to the RCS response and fission product deposition in the suppression pool prior to vessel breach, the accident simulation was conducted up to 4 hours only. Since the ADS valves reclosed, the RCS pressure increased, and the low pressure systems capability to inject coolant makeup was lost. Core melting occurred prior to containment failure, which occurred at vessel failure. This variation in essence substantially changed the unique characteristic of TC1, that of containment failure before core melt. Fission product released from the RCS during core heatup and melting is transported to an intact containment. Fission product releases to the environment may be slightly delayed, but since gross containment failure occurs at vessel failure (when the airborne fission products concentration in containment is still relatively high), these are expelled to the environment at such a rate that precludes substantial mitigation.

2. TC Sensitivity Case 2

This case is a variation of the TC1 scenario where the RHR was lost, but gross containment overpressure failure was precluded by venting the containment at 75 psia. With the pressure in containment relieved prior to exceeding the differential pressure requirement to keep the ADS valves open, the flow from the pressure vessel to the suppression pool was maintained. Most of the fission products not retained in the RPV are removed by the suppression pool via discharge through the ADS valves.

The containment integrity was lost early (48 minutes) by operator venting, which results in coolant injection systems failure. The core melts but fission products released from the containment are scrubbed by the suppression pool through the vent path. In this scenario, the suppression pool plays a significant role in mitigating the releases by maintaining the ADS valves open during core melt and venting the containment in the wetwell airspace. Both allow the flow of radioactive materials to be directed to the suppression pool. Therefore, as seen in Table 12, removable fission product species released to the environment are calculated to be quite small.

3. TC Sensitivity Case 3

One of the key observations in the TC1 scenario was the relatively high removal afforded by the reactor building surfaces, particularly due to impaction. Recirculating flow velocity in the reactor building supports significant removal of aerosols by impaction. This scenario evaluated the effect of not considering impaction as a removal mechanism for the potentially high flow conditions induced by the ATWS event. A variation of TC1 which neglected impaction (by setting the surface area for impaction to zero) was evaluated. In the reference case, the total aerosol deposited in the reactor building was 2125 kg, principally made up of removal by impaction (74%). Gravitational settling accounted for 21%. By neglecting reactor building impaction, the total aerosol mass retained was essentially unchanged, i.e., 2050 kg was removed. Retention by impaction was zero, but the other mechanisms for removal compensated for this reduction. Almost all (93%) was due to gravitational settling. The amount of material removed by condensation and thermophoresis increased slightly (approximately 50%) over that of the reference case TC1. This interesting result indicated the dependence of the removal efficiency on the overall thermal-hydraulics. It appeared that thermal-hydraulics controlled the effective residence time of the fission products in the reactor building. As long as the leakage rate could not compete with the removal rates, the integrated removal became significant regardless of mechanism. The time constants for leakage in either case remained the same; thus, the total removal did not change significantly, although the already small environmental source term (.038 CsI release fraction) was observed to increase slightly over the reference case (a factor of 1.5).

4. TC Sensitivity Case 4

One of the major assumptions made in defining the reference case TC2 is containment failure induced by the pressure and temperature loads on the primary containment at vessel breach. It was noted earlier that the ultimate pressure capacity was actually not exceeded. Therefore, if the containment integrity is not assumed arbitrarily to be lost at vessel failure, the containment could be challenged much later in time. The impact of later containment failure on TC2 was examined in this sensitivity case. Note that containment failure was predicted at 22 hours into the accident. The mass of fission product aerosols released from containment was reduced due to the extended time to containment failure. A reduction of at least a factor of 4 for the volatile vapor species and more than a factor of 10 to 20 was observed for Ba, Sr group and Mo, respectively, relative to reference case TC2.

5. TC Sensitivity Case 5

This scenario is basically TC2. The intent in defining this sequence was to investigate the sensitivity of hydrogen production in-vessel by preventing core blockage. In the previous version of MAAP, this was modeled by assuming that core blockage and cessation of clad oxidation would occur as the temperature in a core node exceeded a user-defined value. In MAAP 3.0, this flexibility no longer exists.

Core blockage was modeled in MAAP 3.0 as a function of clad ballooning and melting. Since the fuel melting point was defined at the lower eutectic temperature of UO_2, Zr, and ZrO_2, the amount of clad oxidation predicted was lower than estimated in NRC evaluations. To investigate the effect of increased hydrogen production, instead of making the usual assumption that clad oxidation is terminated and blockage ensues once core melting at the eutectic temperature of 4040°F occurs, the equivalent melting point of the fuel was defined to be that of UO_2 (5150°F) in this sensitivity case. The assumption of a higher fuel melting temperature was made to simulate the NRC modeling of continued clad oxidation during core melting. The event timing was not substantially changed, but the amount of clad and can-wall oxidation increased to 14.5% versus the nominal 4.7% obtained in the reference scenario. NRC calculations give 60% for the reference case. This includes the enhanced oxidation in the vessel (relative to the NRC TC1 reference scenario) due to continued CRD injection and the core-coolant interaction in the lower plenum following core slump. Without CRD injection for TC1 in NUREG-1150, the clad oxidation calculated by MARCH is approximately 25%, substantially lower than that calculated for TC2.

The increased liquefaction fuel temperature resulted in higher RCS surface temperatures. The debris temperature was notably higher as well; thus, retention in the RCS was reduced. The increased debris temperature resulted in increased releases from the fuel during core-concrete interactions.

6. TC Sensitivity Case 6

One of the key differences observed between the MAAP calculations for Peach Bottom versus NRC STCP calculations is the mass of ex-vessel fission products released through core-concrete interaction. In examining the BMI data set, it was noted that a much larger area for interaction was defined in STCP. Case 6 examined the impact of using the area from STCP for concrete attack in the MAAP analysis. In addition to the larger interaction area, the fuel liquefaction temperature of 5150°F (defined in the previous case) was used in this sensitivity variation. The result indicated a significantly higher concrete aerosol production; 24200 kg was produced versus 7480 kg for the reference case. (This used the Peach Bottom IDCOR data defined in the parameter file for a BWR Mark I).

As a result of this change, the fission product aerosols released to the environment increased by a factor of 40 for Mo (fission product group 5) representing the fission product species likely to be released during concrete attack. A slight increase was noted for CsI (a factor of 2), due to the increased driving force brought about by the increased non-condensible gas generation.

2. TB Sequences Sensitivity to Variation in Failure Size

The two principal station blackout scenarios analyzed variations in the fission product transport behavior for early (TB2) and late (TB1) containment failures for otherwise the same sequence of events. The trends in the release were noted to be consistent with previous source term assessments, i.e., early containment failures tend to generate higher releases from the containment,

although the difference noted was not as significant as anticipated*. The environmental source terms (release from the reactor building) did not show a corresponding relationship. This illustrates the importance of the reactor building as a mitigating feature of the Mark I containment designs. Further variations of the reference cases examined are discussed below. The sensitivity of source terms to containment failure size was studied for the station blackout cases.

Figures 3 and 4 correlate the variation of fission product source terms to the failure size (area) assumed for the TB scenarios. The CsI release to the environment demonstrates the impact of the competing mechanisms of removal by leakage versus deposition. The airborne concentration of CsI within the containment system is reduced by natural removal mechanisms at the same time that it is transported by gas flow between the containment volumes as well as the environment. If the leakage rates for transport from the containment to the reactor building and the atmosphere are small (as compared to the deposition rates) the natural removal processes are able to deplete the airborne fission product available for leakage. Hence, smaller integrated releases are possible.

The noble gas release fraction illustrates the direct relationship of the leakage rate on the release. The curves indicate an increasing trend in the integrated releases as the failure area is increased, indicative of the higher leakage rates obtained with the larger break area. For the TB1 scenario, as the containment rapidly depressurizes with failure areas approaching 7 ft^2, the driving force for leakage is not maintained; hence,the integrated release approached an asymptote after reaching a failure of approximately 4 or 5 ft^2.

The variation of the noble gases and CsI release fractions to failure size is illustrated in Figure 4 for sequence TB2. Due to the extended time following containment failure during which leakage from the containment could occur (for the early containment failure cases, TB2), the integrated releases do not show as much sensitivity between the scenarios**. On the other hand, the

---

* The late containment failure scenario (TB1) involved a significant revaporization of the volatile fission products in a closed system, thus forming a secondary source of release later in time. When the containment eventually failed (although it occurred late relative to core melt), the amount of airborne fission products in containment was still significant.

** The noble gas release fraction became asymptotic at a break area of less than 1 ft^2 for TB2, smaller than the 4-5 ft^2 break area observed for TB1. For the nonremovable species, the integrated release is principally determined by the total leakage from the containment and reactor building (no competing mechanisms for removal exist. Therefore, as the time from containment failure

environmental releases of the removable species are relatively more sensitive to failure size in both TB1 and TB2 scenarios. This is demonstrated by the lower release fraction of CsI as compared with noble gases. Furthermore, as the driving force is reduced (as demonstrated by the TB2 scenario variations) the integrated release from the reactor building becomes even lower. Figures 5 and 6 show the sensitivity of the CsI releases from the containment to the reactor building (RCB) and to the environment. These demonstrate the variation in the effectiveness of the reactor building retention for the failure area sensitivity cases. Note that as the failure area is increased, the relative amount of reactor building retention decreased. Figure 5 indicates some sensitivity of the reactor building DF on failure area for the range of failure sizes of 0.08 to 7 ft^2 for TB1. For TB2, there is a slight sensitivity for failure sizes up to 1-2 ft^2.

V. References

1. MAAP (3.0) Modular Accident Analysis Program User's Manual, Technical Report 16-2-3, Fauske & Associates, Inc., February 1987.

2. Source Term Code Package, A User's Guide (Mod. 1), NUREG/CR-4587, BMI-2138.

3. R.S. Denning, et al. "Radionuclide Release Calculations for Selected Severe Accident Scenarios, BWR, Mark I Design." NUREG/CR-4624, Vol. 1, July 1986.

4. U.S. Nuclear Regulatory Commission, "Reactor Risk Reference Document," NUREG-1150, draft for comment, February 1987.

5. Technical Support for Issue Resolution, IDCOR 85-2, Fauske & Associates, Inc., July 1985.

6. M. Silberberg, et al. "Reassessment of the Technical Bases for Estimating Source Terms, Final Report." NUREG-0956, July 1986.

extends, the total release fraction approaches unity. For TB1, the time interval is only 8 hours, but for TB2, the time interval is more than a day.

Table 1

Summary of Modeling Improvements in MAAP 3.0 For Issue Resolution *

Issue	Agreed Upon Path To Resolution	Modeling Change
Fission product release prior to vessel failure	Incorporate release models from NUREG-0772 and consider Te released in-vessel or ex-vessel	NUREG-0772 models incorporated into MAAP along with EPRI steam oxidation model User option. Te released in-vessel or ex-vessel - recommended uncertainty analysis
In-vessel natural circulation	Incorporate in-vessel natural circulation model into MAAP and benchmark with TMI-2	Incorporated in-vessel natural circulation model into MAAP-PWR
Fission product and aerosol deposition in the Reactor Coolant System (RCS)	Perform extensive numerical experiments with a sectionalized aerosol code to validate and/or update aerosol deposition correlations in MAAP	Extensive numerical experiments have provided more comprehensive aerosol deposition correlations for the MAAP codes
In-vessel hydrogen production	IDCOR would benchmark their calculations against TMI-2 behavior as well as the SFD tests - NRC would investigate the possibility of carrying out the same benchmarking calculations	Core debris levitation model added to MAAP
Core slump, collapse and vessel failure	A core melt progression model should be incorporated into MAAP	Core melt progression models incorporated into the MAAP-BWR and MAAP-PWR codes

* This does not represent an exhaustive list of technical issues identified in the Issue Resolution Effort. Only those issues which resulted in modeling changes have been listed here.

ELF/cb/3825ST87

Table 1

Summary of Modeling Improvements in MAAP 3.0 For Issue Resolution (Continued)

Issue	Agreed Upon Path To Resolution	Modeling Change
Ex-vessel fission product release	IDCOR will increase the number of chemical species tracked during ex-vessel core-concrete attack	IDCOR has developed a chemical thermodynamic equilibrium model for tracking more fission product species in the core debris and their release due to stripping
Fission product and aerosol deposition in the containment		Addressed in the resolution of fission product deposition in the RCS
Amount and timing of suppression pool bypass	Incorporate an aerosol plugging model into the MAAP codes	An aerosol plugging model has been incorporated into MAAP
	Carry out sequence evaluations using the plugging model and for a sequence assuming a stuck-open vacuum breaker with the plugging model overridden	Grand Gulf sequences run with the plugging model show environmental releases to be dominated by noble gases
		Release fractions for a sequence with an assumed stuck-open vacuum breaker and the plugging model overridden result in 1% of the volatile species released

Table 2

EPRI MAAP Modifications Incorporated in MAAP 3.0

Task	Modeling Enhancement	Effect of Modeling Change
Add the secondary containment and auxiliary building models to MAAP	AUX code integrated into MAAP such that the code can be run separately or as an integral part of the systems analysis	Increased user convenience and the code can now treat flow from the auxiliary building into the primary containment
Model containment strain	A simplified containment wall strain model was developed and incorporated into the MAAP codes	The influence of containment growth on the timing of key events is an integral part of the calculation. Also, the wall strain required to achieve the ultimate stress in the wall is calculated by the code and can be used to examine the effect on local penetrations
Calvert Cliffs specific models	RCS modified to represent four cold legs and two hot legs	No major changes from the IDCOR reference plant analyses
	A new recirculation line-up was added	
	Containment model was changed to allow debris to be dispersed from the reactor cavity into the upper compartment and accumulate on the refueling pool floor	
	Core-concrete attack models were added to the upper compartment	
	A model for direct heating of the upper compartment atmosphere was included for a user-specified fraction of the mass dispersed from the reactor cavity	

Table 2

EPRI MAAP Modifications Incorporated in MAAP 3.0 (Continued)

Task	Modeling Enhancement	Effect of Modeling Change
Oconee specific models	RCS modified to represent four cold legs and two hot legs	No major changes from the IDCOR reference plant analyses
	Model added to describe coolant state entering the pressurizer	
	A letdown system term was added to the A-loop water mass	
	A flapper valve model was added along with a description of downcomer condensation	
	Water level and atmosphere dump valve controls were added for each steam generator	
	Steam generator water level control was modified to model "bang-bang" operation	
	Steam generator primary-to-secondary side heat transfer was modified to represent the auxiliary feed spray at the top of the tube bundle	
	RCS gas transport was coupled to the steam generator model to represent the influence of hydrogen on the primary side heat transfer	

Table 2

EPRI MAAP Modifications Incorporated in MAAP 3.0 (Continued)

Task	Modeling Enhancement	Effect of Modeling Change
Susquehanna specific models (continued)	RCS model changed to allow high pressure core spray for Mark II designs Core debris released from the reactor vessel can spread on the drywell floor and eventually drain into the suppression pool Model added to describe the quenching of core debris in the suppression pool Model added to represent debris decay heat deposition in the suppression pool Additional containment heat sinks were added to represent the Mark II containment Separate drywell/wetwell vent or failure areas were added A model was added to allow wetwell drywell coupling (loss of pressure suppression)	Debris transport to the suppression pool provides a substantial change in the system response compared to the IDCOR Mark I and Mark III reference plant analyses. In particular, no significant core-concrete attack would occur and long term cooling of debris produces low drywell temperatures and limited revaporization
Increased RCS nodalization	BWR nodalization includes separate nodes for the separators and the upper plenum. Also, the downcomer is divided into two nodes PWR nodalization includes separate nodes for the upper plenum, the reactor dome, the horizontal portion of the hot legs, the vertical portion of the hot legs (steam generator tubes), the cold leg side of the steam generator tubes, the volume between the steam generators and the reactor coolant pumps, the horizontal cold legs and the downcomer	Generally no major changes from previous analyses, but some differences in timing of revaporization and fission product transport

ELF/cb/3825ST87

Table 2

EPRI MAAP Modifications Incorporated in MAAP 3.0 (Continued)

Task	Modeling Enhancement	Effect of Modeling Change
Improved RCS heat sink definition	Both BWR and PWR RC systems have several additional heat sinks. More importantly, the new model for the heat sink allow the node to be partially covered by a changing water level	No major differences from previous reference plant analyses, but there are some changes in the timing of revaporization and fission product transport
Improved relief/ safety valve modeling	A model was added to represent the opening/closing deadband within a valve group to more accurately characterize the fission product transport from the RCS early in the accident	No major difference from previous reference plant analyses
Decay heating of gases and structures	A model was added to allow the decay power to be absorbed by either the gases or the structures within the primary system	Due to the good heat transfer between the gases and the structures, both models give essentially the same result
Suppression pool	A model was added as part of IDCOR/85 Issue Resolution to represent aerosol plugging of leakage paths between the drywell and the wetwell A particle size dependent DF correlation was developed from the SUPRA code results and integrated into MAAP to give a mechanistic representation of the fission product scrubbing in the suppression pool A model was added to describe scrubbing of aerosols from compartment atmospheres due to water sprays	The aerosol plugging model reduced the calculated releases for the Mark I sequences with wetwall venting and the Mark III with drywell leakage to essentially noble gases. The containment spray model was also found to be very effective in removing aerosols and reduced released to essentially noble gases. With the time and particle size dependent DF, the average value over the entire accident is somewhat less than the constant value used in previous analyses
PWR hot leg natural circulation	Models were added for both U-tube and OTSG geometries	Less upper plenum and more steam generator heating in high pressure sequences in U-tube plants

ELF/cb/3825ST87

Table 2

EPRI MAAP Modifications Incorporated in MAAP 3.0 (Continued)

Task	Modeling Enhancement	Effect of Modeling Change
Quenching of a degraded core	A conduction model was developed for heat removal from solid core debris. This was implemented for each core node	Allows some recovery but no major changes from previous IDCOR analyses

Table 3

Independent IV&V Process

The IV&V process includes the following elements:

- Code Logic Evaluation and Model Sensitivity
  - Prioritization and sensitivity analysis
  - Development of line-by-line flow charts and block logic diagrams for all routines
  - Development of a master index for all major variables which describe the variable, identify its physical units and how it is used
- Line-by Line Verification
  - Detailed line-by-line review of the coding, translation of the coding into algebraic expressions and text and association of the translated text and the coding on a line-by-line basis
  - Checking of the consistency of argument lists, common blocks, etc.
  - Dimensional analysis of all variables and expressions
  - Comparison of the coding with the model description in the User's Manual and other referenced sources
- Model Validation
  - Comparison of code prediction with experimental data or analytical solutions

Table 4

MAAP Routine Prioritization

Priority	MAAP Routine(s)	Phenomenological Area
1	DECOMP	Debris/concrete interactions
2	FLAME/SUAD, BURN, PLH2	Hydrogen production and combustion
3	FPTRAN	Radionuclide and aerosol transport and deposition
4	HEATUP, BWRVSL, SOLPRP, PRISYS	In-vessel melt progression
5	CNAERO	Radionuclide and aerosol release-debris/concrete interactions
6	POOLDF	Suppression pool scrubbing
7	FPRATB/B	In-vessel radionuclide and aerosol release
8	(Many)	Heat transfer and gas flow rates -RCS and containment
9	PLSTM (UCRDR)	Steam production debris beds
10	(Many)	Steam condensation, heat transfer to ice beds and water pools
11	EXVIN, OMENCH	Steam production - explosions/spikes
12	ENTRAN, VFAIL, DCFAIL, JET	Gas generation rates and debris dispersal at primary vessel failure
13	SPRAY	Fission product spray removal
14	(Many)	Vessel failure timing

Table 5

Routines Incorporated into DECOMP Stand-Alone Model

Name	Purpose
	JAYCOR ROUTINES
DRIV2D	Main driver
INPUT2D	Input
PLOT2D	Plotting
INIT2D	Initialization
CPGAS	High temperature gas specific heats
HTMGO	A version of HTWALL for MGO slabs
HMIT	Film collapse, periodic contact and gas film heat transfer models
	MAAP SUBROUTINES (several are modified for 2-D model)
DECOMP	Debris/concrete thermal attack
CNAERO	Radionuclide and aerosol release
POWER	Decay heat curve
EMISS	Steel surface emissivities (oxidized)
HTWALL	Heat conduction into concrete slabs
PLSTM	Upward heat transfer to water pool
GASTRN	Gas transport properties
HTSHCR	Convective heat transfer upward
USOLID	Corium component thermal properties
SWATI	Super heated steam properties
STMSIU	Saturated water and steam properties
VWATR	Specific volume of subcooled water
TSATW	Saturation temperature of water
SOLPRP	Corium mixture properties
VFSPAR	Pool void fraction for bottom sporging
UCRCT	Critical velocity for churn turbulent flow
UCRDR	Critical velocity for liquid entrainment
CVSTS	Constant volume saturated steam specific heat
VISCST	Superheated steam dynamic viscosity
THCST	Superheated steam thermal conductivity
HWATR	Subcooled water enthalpy
TFWATR	Subcooled water temperatures
STWATF	Saturated water surface tension
LOOKUP	Table interpolation routine
BLOCK DATA	

ELF/cb/3825ST87

Table 6

Definition of the ATWS Scenarios Considered

- Initiated by MSIV closure, followed by failure of control rods to insert and failure to initiate standby liquid control (SLC)
- HPCI and RCIC initially work, initially drawing water from the condensate storage tank and then switching to the suppression pool
- HPCI turbine pumps become unavailable due to bearing degradation when pool water reaches 93°C (200°F). RCIC and CRD insufficient to keep core covered
- Containment pressurizes via steam flow through the safety/relief valves
- TC1: ADS valves somehow remain open. Low presure ECCS systems provide makeup which leads to pool heatup and eventual containment failure via overpressure
- TC2: ADS valves remain closed. After high pressure ECCS systems are lost, core uncovers and melts
- TC3: Same as TC2 but operator initiates venting through wetwell at 10% over design pressure

Table 7

Definition of Station Blackout Scenarios Considered

- Initiated by loss of all AC power
- DC power available for six hours. At this time, steam-powered ECCS systems are assumed lost (battery depletion)
- NUREG-1150 also considers immediate station blackout due to DC common mode failure
- NUREG-1150 considers station blackout to encompass the risk-dominant scenarios for Peach Bottom
- TB1: Containment failure is from overpressure at 9 bar. This occurs sometime after vessel breach
- TB2: Containment failure is postulated to occur from overpressurization immediately following vessel breach

Table 8

Major Event Timing for TC Sequences

Event Sequence	Event Timing (Hours) TC1	TC2
Transient event	0.00	0.00
HPCI on	0.02	0.02
RCIC on	0.03	0.03
RHR on	0.17	0.17
HPCI off	0.31	0.32
ADS on	0.19	
RCIC off	1.00	1.24
Containment failure	1.73	2.51
RHR off	1.73	2.51
ECC off	1.73	2.51
Core uncovered	1.74	0.44
ADS off		
Core radial region 1 blocked	2.47	1.57
Core radial region 2 blocked	2.60	1.58
Core radial region 3 blocked	2.62	1.60
Core radial region 4 blocked	2.62	1.63
Core plate failure	2.98	1.63
Vessel failure	3.00	2.51

Table 9

Major Event Timing for TB Sequences

Event Sequence	Event Timing (Hours) TB1	TB2
Transient event	0.00	0.00
HPCI on	0.01	0.01
RCIC on	0.01	0.01
HPCI off	7.3	7.29
Containment failure	31.8	10.52
Core uncovered	8.20	8.11
Core radial region 1 blocked	9.25	9.25
Core radial region 2 blocked	9.35	9.35
Core radial region 3 blocked	9.25	9.25
Core radial region 4 blocked	9.35	9.35
Core plate failure	10.50	10.50
Vessel failure	10.52	10.52

Table 10

Fission Product Distributions for NUREG-1150 Peach Bottom ATWS Cases (Fraction of Original Inventory) at end of Calculation[a]

	Sequence TC1				Sequence TC2			
	Cesium Iodide		Strontium		Cesium Iodide		Strontium	
Location	STCP	MAAP	STCP	MAAP	STCP	MAAP	STCP	MAAP
In fuel/debris	0.00	0.00	0.25	0.60	0.00	0.00	0.35	0.73
In primary system	0.16	0.01	2.4^{-4}	3.3^{-3}	0.17[b]	5.0^{-3}	0.00	0.00
In wetwell	0.76	0.72	0.12	1.3^{-3}	0.80[d]	0.10	1.2^{-3}	7.1^{-4}
In drywell/in pedestal	0.01	3.8^{-4}	7.0^{-3}	0.35	0.00	1.0^{-4}	$3.^{-3}$	.25
In reactor building	.03	0.23	0.13[c]	0.05	2.6^{-2}	0.80	0.34	0.02
Released to environment	.03	0.04	0.49	3.3^{-4}	1.4^{-2}	0.09	0.30	4.9^{-4}

(a) End of calculation is 12 to 14 hours for NRC and 50 hours for EPRI.

(b) High degree of deposition of CsI in the RCS is due to assuming no revaporization after vessel breach.

(c) The STCP takes little credit for strontium deposition in the drywell. MAAP calculates significant strontium deposition in the drywell.

(d) High degree of deposition of CsI into suppression pool for TC2 is due to extremely high flow rate of steam and hydrogen, causing SRVs to open.

ELF/cb/3825ST87

Table 11

Fission Product Distributions for NUREG-1150 Peach Bottom Station Blackout Cases

(Fraction of Original Inventory) at End of Calculation[a]

	Sequence TB1				Sequence TB2			
	Cesium	Iodide	Strontium		Cesium	Iodide	Strontium	
Location	STCP	MAAP	STCP	MAAP	STCP	MAAP	STCP	MAAP
In fuel/debris	0.00	0.00	0.16	0.68	0.00	0.00	0.16	0.60
In primary system	0.67[b]	0.21	0.00	0.00	0.67[b]	0.13	0.00	0.00
In wetwell	0.23	0.22	0.03	0.00	0.22	0.07	0.06	0.00
In drywell/	0.08	0.00	0.31	0.00	0.01	0.02	0.01	0.37[c]
In Pedestal	N/A[d]	0.00	N/A[d]	0.31				
In reactor building	0.00	0.35	0.13[c]	0.00	0.07	0.75	0.30	0.03
Released to environment	0.01	0.22	0.37	4.1^{-5}	0.04	0.04	0.46	2.8^{-4}

(a) End of calculation is 12 to 14 hours for NRC and 50 hours for EPRI.

(b) High degree of deposition o
f CsI in the RCS is due to assuming no revaporization after vessel breach.

(c) The STCP takes little credit for strontium deposition in the reactor building. MAAP calculates significant strontium deposition in the pedestal.

(d) The STCP does not model the pedestal region separately from the drywell.

ELF/cb/3825ST87

Table 12

Summary of Peach Bottom ATWS Sensitivity Analysis

ATWS Sequence Variation	Figures of Merit 1	2	3	4	5	6	7	8	9	10
1. TC1 ref. case (low pressure RCS)	1.74	2.47	3.00	1.73	50.00	0.72	0.23	0.04	0.05	8.0E-04
2. TC2 ref. case (high pressure RCS)	0.44	1.57	2.51	2.51	50.00	0.10	0.81	0.09	0.02	5.0E-04
3. TC3 ref. case (TC2 w/WW vent)	0.44	1.57	3.00	N/A	4.00	0.97	0.00	<1E-4	0.00	1.0E-05
4. TC1 w/ADS valves closing	0.97	1.40	2.09	2.10	40.00	0.16	0.23	0.05	1.0E-04	2.0E-05
5. TC1 w/WW vents	0.87	1.42	1.90	N/A	50.00	0.95	4.0E-04	<1E-4	1.4E-05	1.6E-06
6. TC1 W/no RCB impaction	1.74	2.47	3.00	1.73	50.00	0.72	0.20	0.06	0.05	1.0E-03
7. TC2 W/late DW failure	0.44	1.57	2.51	22.00	50.00	0.34	0.64	0.02	2.0E-03	4.0E-05
8. TC2 w/high core melt temp. (delayed core blockage)	0.44	1.61	2.78	2.78	50.00	0.15	0.71	0.14	0.03	4.0E-03
9. TC2 w/high core melt temp. & increased area for concrete attack	0.44	1.61	2.78	2.78	50.00	0.08	0.74	0.16	0.02	4.0E-03

Description of Figures of Merit:

1. Time core uncovered, HR
2. Time of start of core blockage, HR
3. Time of vessel breach, HR
4. Time drywell failed, HR
5. Time at end of calculation, HR
6. CsI fraction in pool
7. CsI fraction in reactor building
8. CsI released to environment
9. Sr in reactor building
10. Sr released to environment

EXAMPLE OF VERIFIED ROUTINE ARGUMENT LIST INFORMATION

```
 SUBROUTINE HTWALL(MUGI,MUGO,CPGI,CPGO,KGI,KGO,DIFI,DIFO,VGI,
1VGO,HTCPI,HTCPO,USTI,USTO,TD,TDMAX,INIT,IWALL,SCALH,ISUBI,CSFLAG,
1PPSTI,PPSTO,EGI,EGO,EWLI,EWLO,HTSUB,HTEXT,AW,XL,XDLI,XDLO,RGI,RGO,
2KW,XW,DW,CPW,TWI,TGI,TGO,PRI,PO,HSTI,HSTO,QCMRAD,
3XWF,INNOD,INNODF,XM,DUM,TSI,TSO,TFI,TFO,TW,FTW,FXM,FMW,
4FMLI,QLI,QWI,QWO,QGI,QGO,QSUBI,HCDI,HCDO,QCDI,QCDO,IMELT,ILMELT,
5SHLI,SHLO)
```

ROUTINE ARGUMENT SUMMARY		
ARGUMENT	DESCRIPTION (UNITS)	CODE
MUGI(μ_i)	-gas dynamic viscosity inside of wall (kg/m-s)	U
MUGO(μ_o)	-gas dynamic viscosity outside of wall (kg/m-s)	U
CPGI(Cp_i)	-gas constant pressure specific heat inside of wall (J/kg-°K)	U
CPGO(Cp_o)	-gas constant pressure specific heat outside of wall (J/kg-°K)	U
KGI(k_i)	-gas conductivity inside of wall (J/s-m-°K)	U
KGO(k_o)	-gas conductivity outside of wall (J/s-m-°K)	U
DIFI(D_i)	-gas diffusion coefficient inside of wall (m^2/s)	U
DIFO(D_o)	-gas diffusion coefficient outside of wall (m^2/s)	U
VGI(v_i)	-gas specific volume inside of wall (m^3/kg)	U
VGO(v_o)	-gas specific volume outside of wall (m^3/kg)	U
???? HTCPI	- to be determined when HWALL verified	#
HTCPO	- to be determined when HWALL verified	#
USTI(u_i)	-gas spec. internal energy inside of wall (J/kg)	U
USTO(u_o)	-gas spec. internal energy outside of wall (J/kg)	U
TD(Δt)	- timestep length (s)	U
TDMAX(Δt_{max})	maximum timestep length allowed (s)	U
INIT	- a flag indicating whether first call or subsequent call to HTWALL	U/R
IWALL	- a flag indicating the wall type (see below)	U
SCALH	- a scale factor generally set = 1.0	U
ISUBI	- a flag indicating the wall surface is submerged	U
CSFLAG	- a flag to indicate that the wall is either (steel lined) concrete or entirely steel	U
PPSTI(P_{st-i})	- steam partial pressure inside wall (Pa)	U
PPSTO(P_{st-o})	- steam partial pressure outside wall (Pa)	U
EGI(ϵ_i)	- gas emissivity inside wall	U
EGO(ϵ_o)	- gas emissivity outside wall	U
EWLI(ϵ_{l-i})	- liner emissivity inside wall	U
EWLO(ϵ_{l-o})	- liner emissivity outside wall	U
HTSUB(h_{sub})	- heat transfer coef. from submerged wall to liquid pool (J/s-m^2-°K)	U
HTEXT(h_o)	- heat transfer coef. from exterior surface (J/s-m^2-°K)	U
AW(A)	- wall area (m^2)	U
XL(L)	- wall length (m)	U
XDLI(X_{l-i})	- interior liner thickness (m)	U

Continued

EXAMPLE OF LINE-BY-LINE FORTRAN CODING VERIFICATION

```
     1TW(INNODF+2))/RW)*THINW
101  IF (INNOD-INNODF.LE.3) GO TO 100
     ILAST=INNOD-2
     IMID=INNODF+2
C COARSE INTERIOR WALL NODES
     DO 2 I=IMID,ILAST
2    FTW(I)=(TW(I-1)-2.EO*TW(I)+TW(I+1))/RW*THINW
C TWO NODES ON FAR SIDE OF WALL
100  FTW(INNOD-1)=((TW(INNOD-2)-TW(INNOD-1))/RW-(TW(INNOD-1)-
     1TW(INNOD))/R2O)*THINW
     FTW(INNOD)=((TW(INNOD-1)-TW(INNOD))/R2O+QWO/AW)*THINSO
C CALCULATE MOTION OF MELTING INTERFACE
     IF (TW(1) .GT.(TCNMP+1.E0)) IMELT=1
     IF (IMELT .EQ. 0) RETURN
     TW(1)=TCNMP
     FXM=FTW(1)/THINSI/(DW*(LHRCN+CPW*(TCNMP-TW(2))))
```

if number of coarse nodes(INNOD-INNODF) < 3 goto 100

ILAST = 15 - 2 = 13

IMID = 6 + 2 = 8

for i = 8 to 13--coarse nodes centered between coarse nodes

$$\frac{dT(i)}{dt} = \frac{1.}{\rho_w C p_w \Delta x_c}\left[\left[\frac{T(i-1) - T(i)}{R_c}\right] - \left[\frac{T(i) - T(i+1)}{R_c}\right]\right]$$

next to last node(last coarse node this example)

$$\frac{dT(14)}{dt} = \frac{1.}{\rho_w C p_w \Delta x_c}\left[\left[\frac{T(13) - T(14)}{R_c}\right] - \left[\frac{T(14) - T(15)}{R_{2\text{-}o}}\right]\right]$$

last node (outer liner node this example)

$$\frac{dT(15)}{dt} = \frac{1.}{\rho_{s\text{-}o} C p_{s\text{-}o} \Delta x_{s\text{-}o}}\left[\left[\frac{T(14) - T(15)}{R_{2\text{-}o}}\right] + \frac{Q_{w\text{-}o}}{A}\right]$$

if $T(1) > T_{cn\text{-}mp} + 1$--first node is melting--set IMELT = 1

3 **** note T(1) is the temperature of the first node, **** **** which for the case where a liner exits is steel-- **** **** why is the steel liner temperature compared to the**** **** concrete melting temperature--it would be correct **** **** in this case to compare T(2) with $T_{cn\text{-}mp}$ and/or **** **** T(1) with the steel melting point to determine **** **** whether the wall is melting **** ****

if the wall is not melting--RETURN

$T(1) = T_{cn\text{-}mp}$ (limit the first node temperature to the concrete melting temperature)

4 **** see note above ****

$$u = \frac{dX_s}{dt} = [\rho_{s\text{-}i} C p_{s\text{-}i} \Delta x_{s\text{-}i}]\left[\frac{dT(1)/dt}{\rho_w\left[\lambda + C p_w (T_{cn\text{-}mp} - T(2))\right]}\right]$$

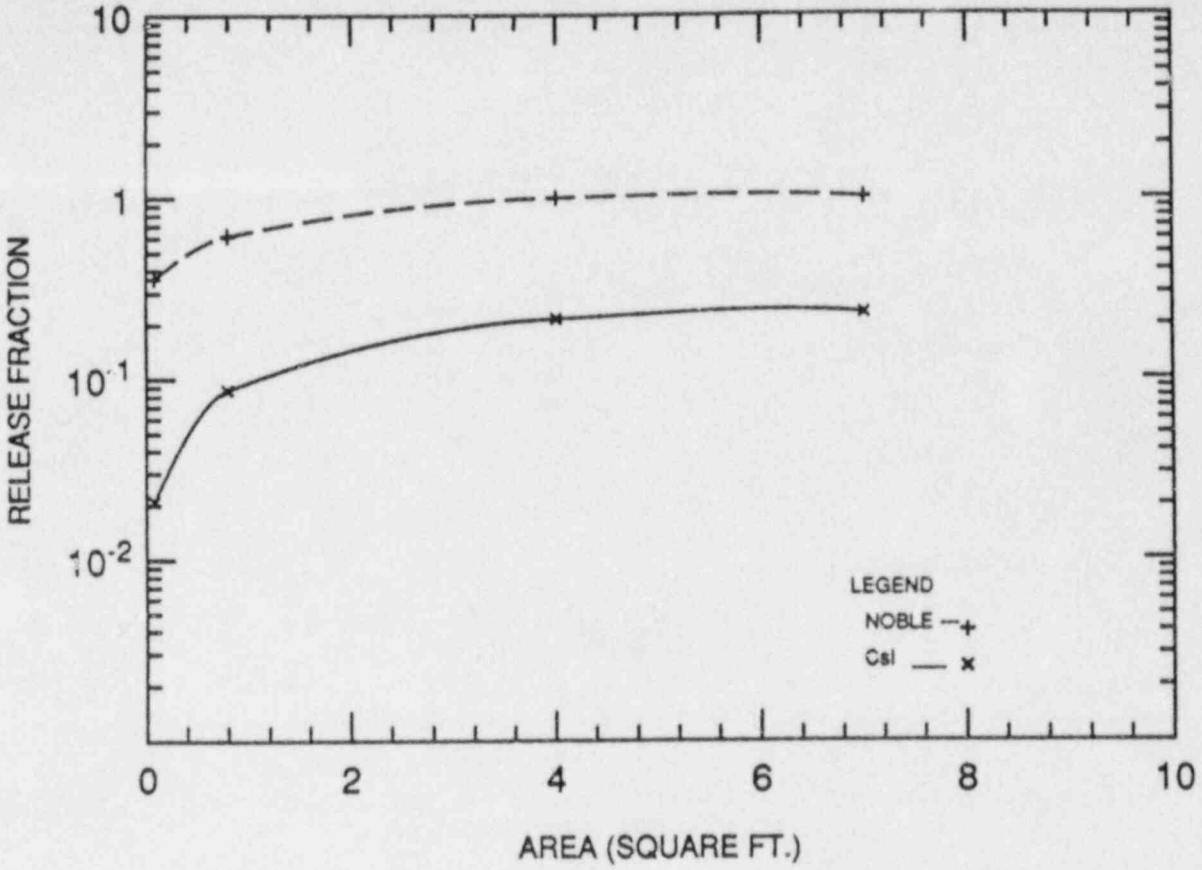

Figure 3 Sensitivity of TB1 Source Terms to Failure Size

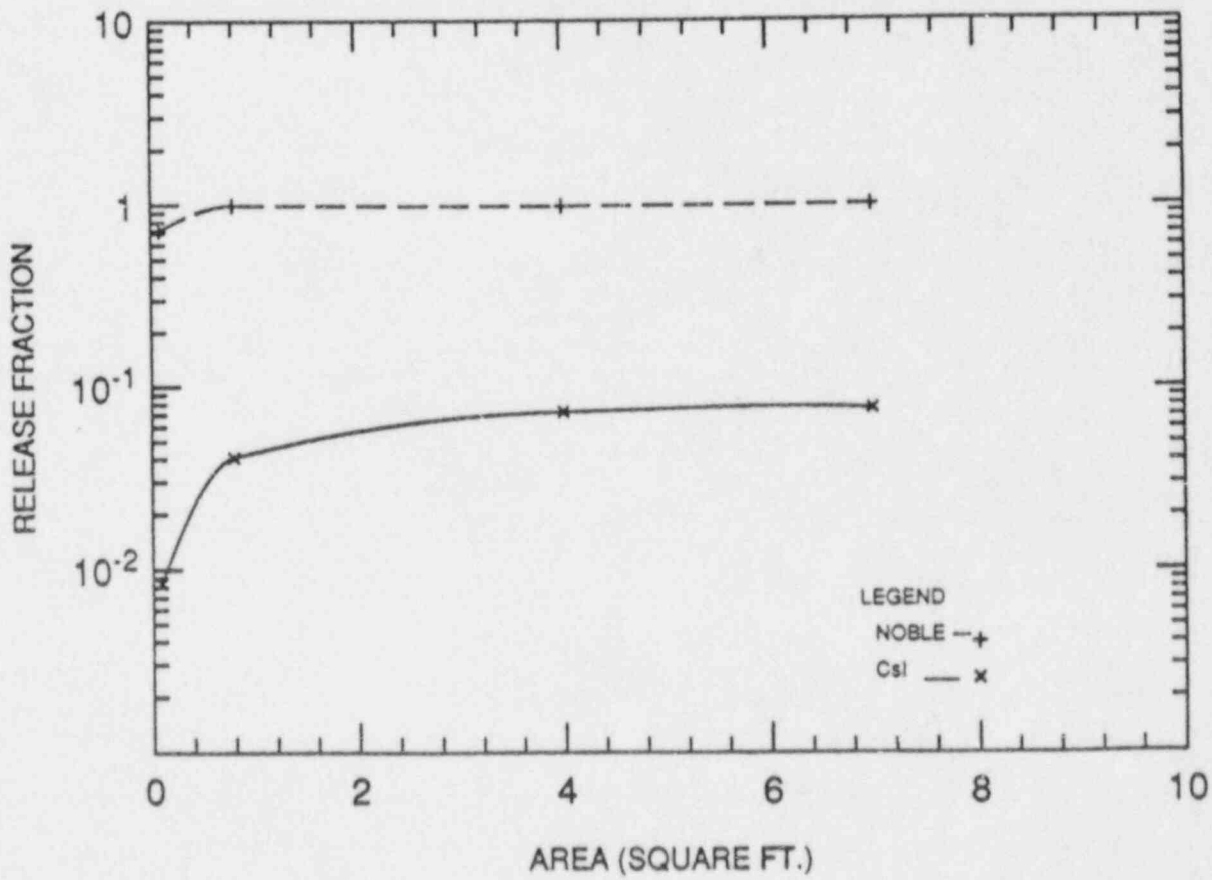

Figure 4 Sensitivity of TB2 source Terms to Failure Size

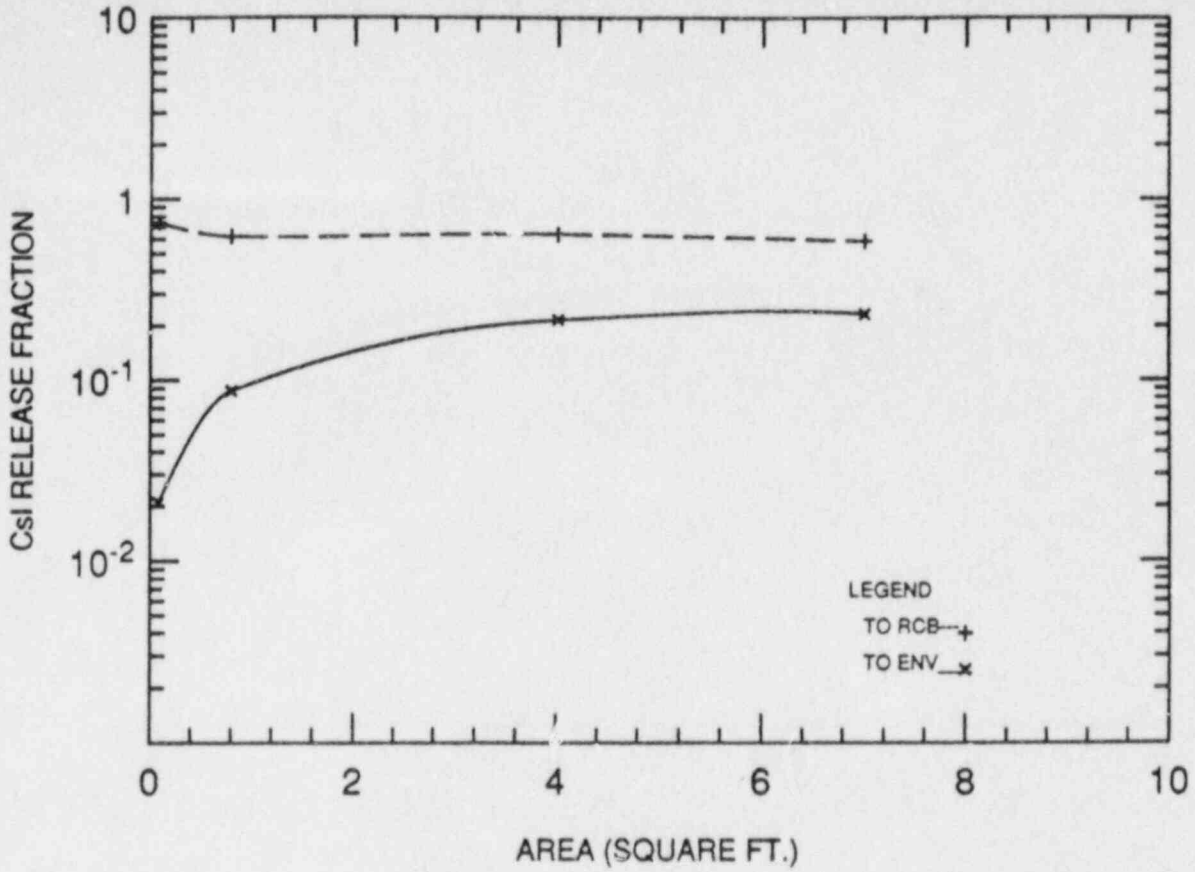

Figure 5 Sensitivity of TB1 CsI Releases to Failure Size

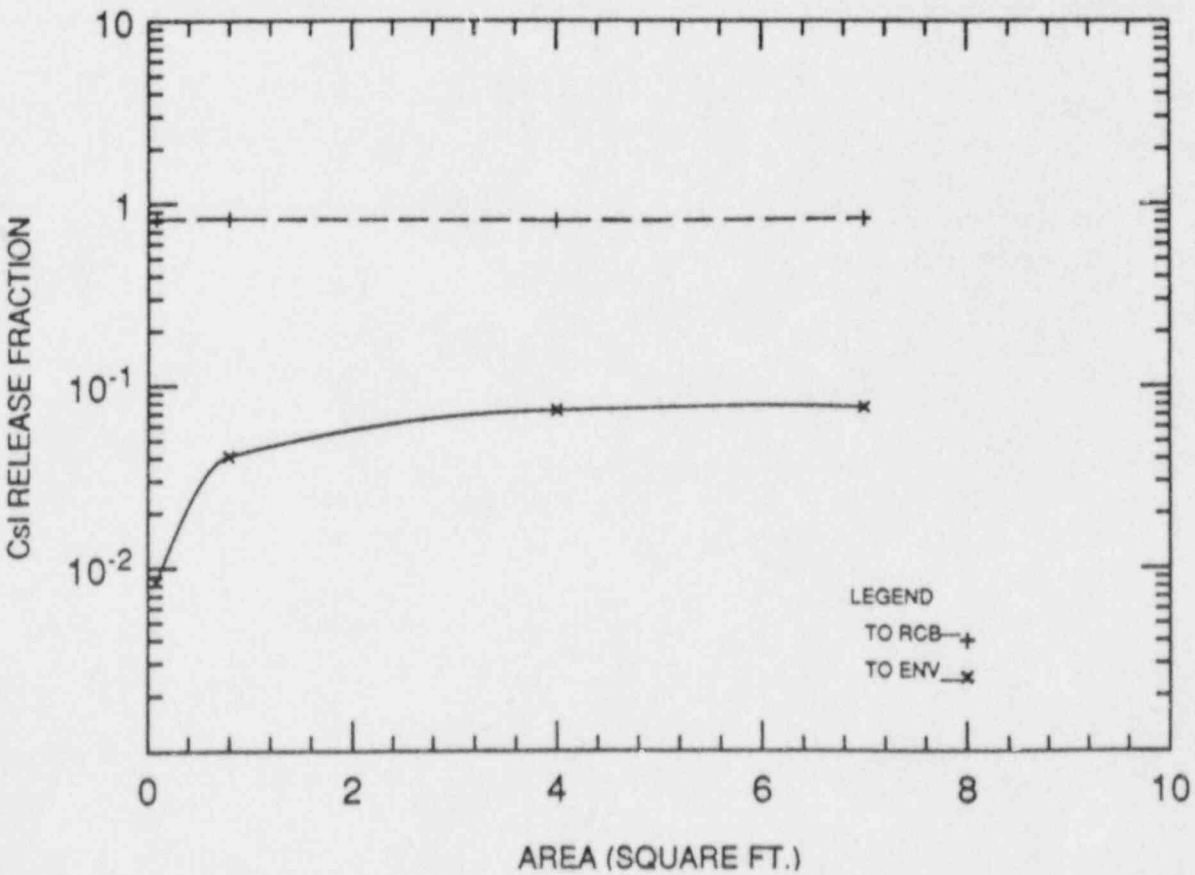

Figure 6 Sensitivity of TB2 CsI Releases to Failure Size

GROUND MOTION CHARACTERIZATION BASED ON THE LINEAR AND NON-LINEAR BEHAVIOR OF STRUCTURES AND EQUIPMENT

Robert T. Sewell *, C. Allin Cornell **
Gabriel R. Toro *, Robin K. McGuire *
Avtar Singh ***, Robert P. Kassawara ***

* Risk Engineering Inc., Golden, CO
** Dept. of Civil Engineering, Stanford University, Stanford, CA
*** Electric Power Research Institute, Palo Alto, CA

ABSTRACT: Results of recent study examining the effects of earthquake ground motion on models representative of nuclear power plant (NPP) structures and equipment is summarized. Motion characterizations based on nonlinear structure response (as opposed to linear response spectra characterizations) are first defined, and their significance is discussed. Next, equipment behavior is examined for four categories of structure-equipment response: linear-linear (i.e., linear structure, linear equipment), nonlinear-linear, linear-nonlinear, and nonlinear-nonlinear. Equipment response components for each of these cases are identified and their characteristics are examined. Relevance of this work in addressing aspects of the seismic performance of NPPs is mentioned, particularly regarding the effects of structure nonlinearity on equipment response, and the influence of small-magnitude, high-PGA, high-frequency, short-duration ground motions (typified by some recent recordings in eastern North America) on typical NPP structures and equipment. Simple understanding and analytical methods are presented that allow one to quickly assess the effects of given ground motion characteristics on structure and equipment behavior.

INTRODUCTION

This paper summarizes results of research recently performed for the Electric Power Research Institute (EPRI) through a contract with Stanford University and Risk Engineering, Inc. The purpose of this work has been to characterize ground motion (GM) based on its ability to affect (linear and nonlinear) response in structures and equipment which are representative of those found in nuclear power plants (NPPs). Simultaneously, the intent has been to identify characteristics of ground motion that have significant effects on structures and equipment, and to analytically explain the implications of these

characteristics for linear and nonlinear (NL) response conditions. This research addresses some important issues, such as the following, regarding the seismic performance of NPPs:

1. How do small-magnitude (SM), large-PGA, high-frequency (HF), short-duration records, such as those recently recorded in eastern North America (ENA)*, affect NPP-type structures (i.e., are these motions as damage-effective as large-magnitude, long-duration, design-type earthquakes of lessor or similar PGA)?

2. What are the effects of these high-frequency records on high-frequency NPP equipment for earthquakes with PGAs representative of the OBE, SSE, and beyond?

3. Do mild amounts of structure and/or equipment nonlinear behavior effectively "isolate" the equipment by reducing the dynamic forces that it experiences (i.e., vis-a-vis forces under linear response conditions) - for both the high-frequency records and design-type motions?

In the next part of this paper, structural damage effectiveness of ground motion, as analytically developed by Kennedy et al. (1984a), is reviewed and generalized from single degree-of-freedom (SDOF) models to multiple degree-of-freedom (MDOF) models. Damage effectiveness factors are defined and compared for a few structural models and ground motions. The procedure to incorporate these damage-effectiveness factors in a seismic hazard analysis based on structural damage is briefly discussed.

Emphasis is then given to examining equipment response for the following cases: linear (structure) - linear (equipment), NL-linear, linear-NL and NL-NL. The linear-linear and linear-NL cases are shown to be the most realistic for NPPs under SM HF motions, whereas all but perhaps the linear-NL cases are

* In the text that follows, these records are termed "HF ENA" motions. By this, we do not mean to imply that ENA records are always of such HF character, or that HF motions cannot be expected in the western United States. Rather, HF motion attenuates less rapidly in ENA, making the observation of these characteristic HF motions [see Fig. 1(a)] more likely in ENA. "HF ENA" motions, as applied in this paper, refers to any record with this distinct HF character, regardless of recording location.

important for NPPs under broad-band, design-basis (DB) motions. To facilitate comparisons, total equipment response for each case is divided into simpler relative components. Characteristics of each component for various situations are discussed. Analytical and conceptual "tools" useful for qualitative prediction of these relative components are presented. The procedure to properly combine these components is delineated, allowing one to readily interpret how given ground motion characteristics influence total equipment response.

STRUCTURAL DAMAGE EFFECTIVENESS OF GROUND MOTION

This section examines issues concerning the potential of earthquake ground motions to damage NPP-type structures, as predicted from theoretical concepts developed by Kennedy et al. (1984a). The inelastic spectral ordinate (for a given ductility level, say) has been shown to be a basis for comparing absolute damage effectiveness of ground motion. This ordinate can usefully be decomposed into the product of two factors: first, the (more familiar) elastic part, the elastic spectral ordinate, S_a; second, an inelastic part, $(1/F_\mu)$. As initiated by Kennedy et al., we focus here on the latter part. This decomposition implies that, given two ground motions with identical elastic spectral values (at a given frequency), their spectral deamplification factors, F_μ, are (inverse) measures of their relative inelastic damage-causing potentials. These relative inelastic damage effectiveness factors are dependent on structural characteristics, such as frequency and force-deformation behavior. There exist two alternative useful interpretations of F_μ: (1) given a structure with fixed strength, which is at incipient yield under a particular ground motion, F_μ is the GM scale factor required to just acheive a ductility μ in the fixed structure, or (2) given a fixed ground motion that produces a maximum force in a particular structure, where we specify this maximum force to be the structure's incipient yield strength, F_μ is the factor by which this incipient yield strength must be reduced to acheive a ductility μ in the structure under the fixed ground motion.

Kennedy et al. show that F_μ is governed primarily by the average "slope" of the elastic ground response spectrum (GRS) toward frequencies lower (softer) than the initial (elastic) structure natural frequency f_{st}. For instance, if

GRS amplitudes near f_{st} increase with reduced frequency, relatively small increases in scaling (beyond incipient yield) will be required to induce a given ductility μ in the structure, and vice-versa for decreases in spectral amplitudes with softening. This understanding, based simply on an informed inspection of the elastic GRS, serves as a useful tool for predicting how a structure will be affected when its yield capacity is exceeded.

Factors F_μ studied by Kennedy et al. were based on a SDOF structure model, four structure frequencies, 12 ground motions, and two levels of structure ductility (μ=1.85 and μ=4.27). The force-deformation model used had a pinched hysteresis and was derived from Banon (1980). This model [herein termed the "shear wall" (SW) model] simulates the behavior of concrete shear walls and steel braced frames which are considered representative of the structures in NPPs. Recently, Kennedy has obtained factors F_μ for an additional set of 15 (small-magnitude) ground motions (see Kennedy, 1987; Khemici, 1986).

The present research has helped to confirm the usefulness and consistency of Kennedy's damage effectiveness interpretations by obtaining F_μ results for additional ground motions and for a more complete array of structure characteristics (Sewell et al., 1986; Cornell & Sewell, 1987; Toro et al., 1987). This process has led to some important general observations that are discussed below.

In Sewell et al. (1986), a base-case structure is defined. This reference structure is a 3-Hertz (Hz) [fundamental-mode], five degree-of-freedom (DOF), shear-beam model with 5% damping specified for the first two modes and nonlinearity restricted to the bottom structural element. The reference force-deformation behavior is similar to the piecewise-linear SW element behavior described earlier, but with smooth stiffness transitions (for details, see Toro et al., 1987; Baber and Noori, 1985). This "smooth shear-wall" (SSW) element is better representative of actual structural behavior. In each instance that follows, unless noted otherwise, F_μ is based on the bottom element yield strength reduction factor necessary to acheive a ductility μ in the bottom element of the MDOF structure.

Table 1

Factors $F_{\mu=4}$ for a 3-Hz, 5-DOF Structure with Various Yield Strength Distributions and for a 3-Hz SDOF Structure (all with SSW hysteresis) - Results Based on 5 Ground Motions (see Table 2)

Ground Motion	SDOF Structure	Reference Case	Uniform Strength	Elastic Strength	Uniform Ductility
El Centro No. 5	3.80	2.26	2.67	3.40	3.51
Taft	2.96	2.23	2.33	2.54	2.99
Parkfield	1.86	1.58	1.66	1.93	1.90
Melendy Ranch	5.15	3.73	5.04	5.12	5.13
Mitchell Lake	4.23	3.58	4.25	4.78	4.28

Shown in Table 1 are factors $F_{\mu=4}$ obtained for a set of five ground motions with widely varying characteristics and for three variations on the strength distribution (with height) in the (otherwise) reference (3-Hz) structure; results for a SDOF structure are also indicated. In the uniform strength case, all elements in the structure have identical strengths, and thus, some nonlinearity is allowed in other than the bottom element. The elastic strength case is where all elements have yield strengths equal to (identical proportions of) the maximum elastic forces they experience under the given ground motion; this strength configuration generally allows significant ductilities in other than just the bottom structural element. Lastly, the uniform ductility case is where all five elements in the structure experience equal ductilities. The five ground motions considered are described in Table 2; their response spectra are shown in Figure 1. EC5 and Taft are long-duration records from large-magnitude earthquakes; Parkfield and Melendy Ranch are short-duration records from small-magnitude earthquakes; and Mitchell Lake is a very short-duration record, with mostly high-frequency content, from a small-magnitude ENA earthquake.

Examination of Table 1 reveals record-to-record differences in the value of $F_{\mu=4}$ for the reference case; $F_{\mu=4}$ is lowest for Parkfield and highest for Melendy Ranch. This can be explained by Kennedy's insight into SDOF-based damage effectiveness factors: A 3-Hz structure subjected to Parkfield, upon softening, will "climb up" the GRS and experience motion significantly more intense than initially. Melendy Ranch is an opposite case, where softening moves the structure down the GRS. Among the five records, Parkfield and Melendy

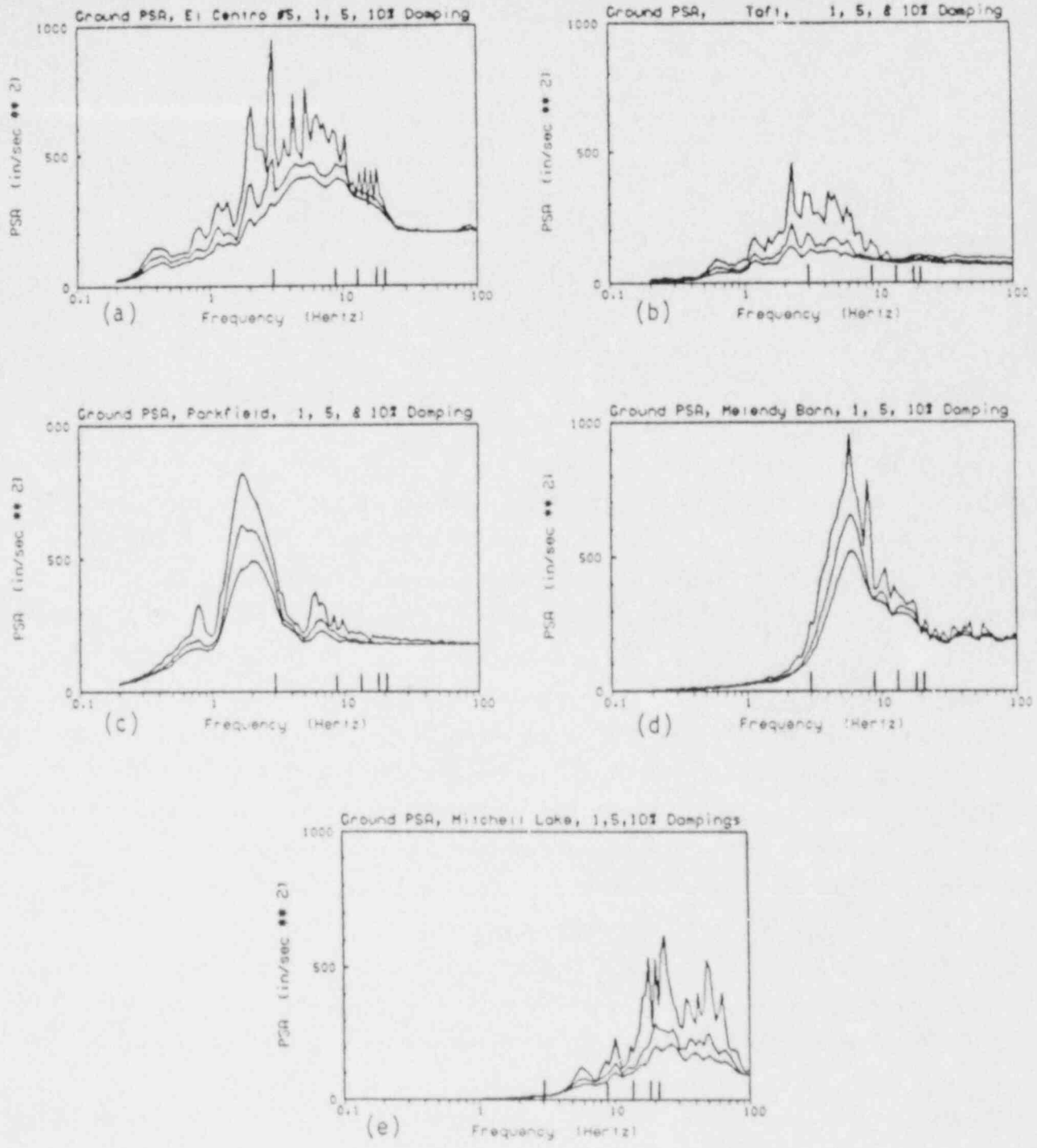

Figure 1. 1%, 5%, and 10% damped ground response spectra for the El Centro No. 5, Taft, Parkfield, Melendy Ranch, and Mitchell Lake motions (see also Table 2). (Modal frequencies of the base case structure are denoted by tick-marks at the bottom of each plot).

Table 2

Ground Motion and Earthquake Data

Earthquake	Magnitude M L	Magnitude M S	Recording Station and Component	Fault Distance (km)	PGA (in/s^2)
Imperial Valley, CA (1979)	6.6	6.9	El Centro Array 5 (140°)	1	203.6
Kern County, CA (1952)	7.2	7.7	Taft Lincoln School (S69E)	40	69.3
Parkfield, CA (1956)	5.6	6.4	Cholame-Shandon 2 (N65E)	<1	188.8
Bear Valley, CA (1972)	4.7	4.3	Melendy Ranch (N29W)	6	199.3
New Brunswick, Canada (1982)	5.0	---	Mitchell Lake Road (26°)	4	91.1

Ranch are extreme cases of these two opposite effects, and hence, they result in lowest and highest values of $F_{\mu=4}$. Study of Table 1 and Figure 1 further shows that the SDOF-based factor F_μ is a reasonably consistent measure of the different motions' relative damage effectivenesses, and that the average "slope" of the GRS is indeed the characteristic governing NL damage potential, given an elastic spectral value. (It may be noted, though, that Mitchell Lake predominantly excites the structure's second mode, and hence, a SDOF-based effectiveness factor founded on first-mode frequency response may not be as appropriate for this more complex case).

Sewell et al. present F_μ results for other parameter variations. These show, for instance, that the perception of GM damage effectiveness is only moderately sensitive to the type of structural force-deformation behavior and to the level of structural damping. Also, the absolute magnitudes of F_μ from case to case are shown to be related to the hysteretic energy absorbed. The interested reader is encouraged to consult Sewell et al. (1987) for more details.

Computation of factors F_μ for additional MDOF structures and additional motions have been performed by Cornell & Sewell (1987) and presented at the EPRI workshop on Engineering Characterization of Small-Magnitude Ground Motion (Palo Alto, January 1987). Factors F_μ for a 3-Hz, 5-DOF structure and a 9-Hz, 2-DOF structure were obtained, based on four categorizations of motions:

broad-spectrum, design-basis (DB) records and three types of small-magnitude (M<5.5) records (Types A, B, and C). The study noted that: First, the small-magnitude motions have narrower bands of frequency content, but their central frequencies can lie anywhere from 1 to 10 Hz (or higher). Second, a SM motion may have a PGA or spectral acceleration at a given frequency that is just as high as that for a DB motion, albeit with low marginal probability. Third, for structures with predominant frequencies just greater than a predominant-frequency peak in a SM GRS, factors F_μ can be lower (i.e., more severe) than for DB motions. The peakedness of the SM GRS, however, also implies that, for most structures, they lead to less severe S_a's and/or F_μ's than DB motions. Lastly, it was noted that the universal threat (i.e., to a number of structures at various frequencies) of SM motions is generally lower than that for DB motions of the same PGA.

Toro et al. (1987) also present factors F_μ (as continuous functions of μ) for six NPP-type structures subjected to the EC5 and Mitchell Lake records, and an additional ENA record (from the 1986 Northern Ohio earthquake). The structures considered were 5-DOF; 2, 3 and 6-Hz, and 2-DOF; 6, 9 and 12-Hz, shear-beam models with SSW hysteresis. Nonlinearity was restricted to occur in the bottom two elements of each structure; both bottom elements had identical yield strengths. It was found that, given a structure had reached incipient yield, the small-magnitude ENA records were equally or less effective than the large-magnitude EC5 record, as measured by F_μ. Effectiveness in terms of elastic spectral acceleration, S_a, however, was seen to be much lower for the ENA records. The implications for net or absolute effectiveness (i.e., S_a/F_μ) were that the ENA records would need to be scaled by factors varying from 2 to 10 times greater (depending on the structure) than a typical design PGA in order to produce significant nonlinear effects in a structure designed to just yield under EC5 scaled to the design PGA.

All of the above studies have confirmed the usefulness of a SDOF damage effectiveness measure and of the insights related to GRS shape as discussed by Kennedy et al. (1984a). MDOF-based F_μ's should sometimes be computed with caution, though, as there is no unique definition of F_μ in an MDOF structure, and different motion and structure configurations may result in local nonlinearities at different floors. Under such cases, one should compute F_μ

based on nonlinearity in the critical portion of the structure.

Seismic Hazard Analysis Based on Structural Damage.

Methodology to incorporate damage effectiveness factors F_μ into a seismic hazard analysis (SHA) based on limit state structural damage has been described by Cornell& Sewell (1987) and Sewell & Cornell (1987). The methodology is very similar to conventional SHA, except that attenuation laws are defined (or modified) to be in terms of inelastic spectral values (S_a/F_μ) for various frequencies f_{st}, rather than on peak ground responses (PGA or PGV) or elastic spectral values (S_a or S_v). [As an approximation, existing attenuation laws for S_a (or for S_v when multiplied by $2\pi f_{st}$) can often simply be divided by a single (frequency-dependent) average factor $F_{DM}(f_{st},\xi,fd)$, where ξ and fd denote damping ratio and force-deformation characteristics, respectively, and DM denotes any general damage measure (not necessarily ductility μ). These average factors, as well as the "exact" attenuations on (S_a/F_{DM}) themselves, for several structural frequencies, damage measures, and for the BL and SW hysteretic models (all for 5% damping), have been computed by Sewell (Ph.D. Thesis, to be published) and discussed by Cornell & Sewell (1987)]. Performing a conventional SHA with these new attenuations results in a constant-damage, uniform-hazard spectrum (CDUHS) [as opposed to the more familiar uniform hazard spectrum (UHS) based on S_v]. The CDUHS presents design yield forces (or accelerations) that result in a uniform risk of exceeding a given limit state damage threshold. Example spectra are presented in Figure 2. CDUHS for two nonlinear limit states and the linear UHS, each based on a hypothetical design probability level, are shown for a hypothetical site.

GROUND MOTION EFFECTS ON EQUIPMENT IN LINEAR AND NONLINEAR STRUCTURES

This section summarizes research work that has examined the effects of ground motion characteristics on the response of equipment in linear and nonlinear NPP-like structures. The linear-structure /linear-equipment case is considered first. Analytical formulations and intuitive understanding are presented to demonstrate why, for instance, HF motions (typified by some SM ENA records) may not generally be as severe on HF equipment as their GRS imply. The elastic floor response spectrum (FRS) is used to show results for linear

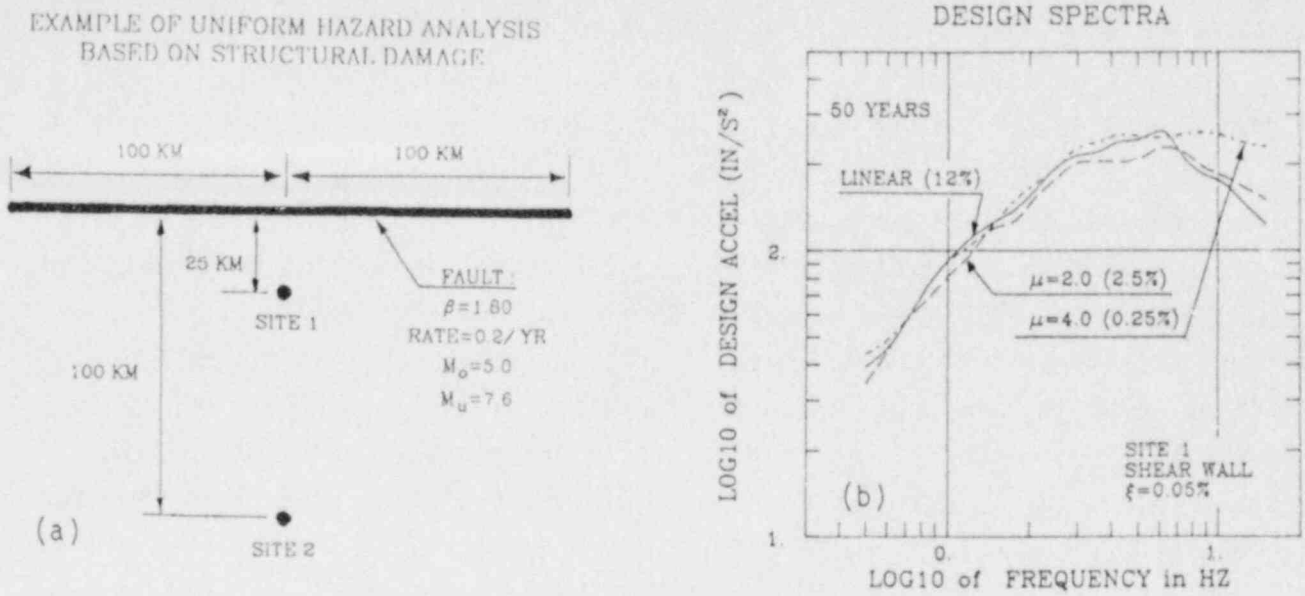

Figure 2. Example Constant-Damage, Uniform-Hazard Spectra for a hypothetical site. Values in parentheses in (b) denote 50-yr exceedance probabilities for the designated damage states.

equipment response in linear MDOF structures. The second case considered is NL-structure /linear-equipment behavior. The authors have obtained recent results that contradict the belief held by many engineers that structure nonlinearity effectively isolates HF equipment from ground motion. The floor response spectrum ratio ($FRSR_\mu$), defined as the FRS for NL MDOF structure response (at ductility level μ) normalized by the corresponding FRS for linear structural behavior, is used for comparisons. The third case considered, i.e., linear-structure /NL-equipment response is shown to generally be realistic only for NPPs subjected to HF ENA motions, whereas the (fourth) NL-structure /NL-equipment case is likely applicable only for NPPs under low-frequency (LF) California motions. A damage effectiveness factor for equipment, $F_{\mu\ eq}$, is defined, and is governed by the shape of the FRS, analogous to F_μ being dependent on the shape of the GRS. ASME code-implicit ductilities for passive equipment are discussed in comparison with computed ductilities under various cases.

The complete overall picture of how ground motion affects total equipment response is demonstrated by appropriately combining the relative response measures FRS, F_μ, $FRSR_\mu$, and $F_{\mu\ eq}$. The concepts discussed enable one to assess

qualitatively the characterisitcs of equipment response, given the input GRS along with basic structure and equipment properties.

Linear Equipment Response in Linear Structures. The authors have performed analytical studies (Toro et al., 1987; Cornell & Sewell, 1987) that examine FRS in linear MDOF structures under various ground motions. These studies have demonstrated that a simple inspection of the GRS is not adequate to predict equipment response. For instance, some engineers may hold that, because of their substantially greater HF content, SM ENA motions induce greater forces in HF equipment than LF motions of the same PGA. By the same token, one might think that a ground motion with no energy beyond 10 Hz would be incapable of inducing significant response in a, say 25-Hz, piece of equipment. Studies show, however, that in many instances, these simple reasonings do not hold. Background and insight that explain this apparent discrepancy are presented below.

Cornell & Sewell (1987) considered 3-Hz, 5-DOF and 9-Hz, 2-DOF structures subjected to DB and Type-A, -B, and -C SM ground motions. We here specifically consider results only for one DB motion (EC5), and for the two Type-C motions studied (Mitchell Lake and Northern Ohio). To facilitate comparisons in what follows, results are presented by normalizing responses for each motion by those produced for the DB-like EC5 record. [All records have been scaled to a common PGA of 0.15g (57.96 in/s^2) for analysis].

Table 3 shows 5%-damped GRS values, at 3, 9, 15 and 25 Hz, for the three ground motions, normalized by corresponding values for EC5. It is seen that GRS for the Type-C motions are much lower at 3 and 9 Hz, and much higher at 25 Hz than the corresponding GRS for EC5. Table 4 shows the ratios of (first-floor) maximum equipment acceleration (at frequencies 3, 9, 15 and 25 Hz) under each motion divided by equipment accelerations under EC5, for the two different structures (3-Hz, 5-DOF; 9-Hz, 2-DOF). It is observed that, even though GRS are about the same for all motions at 15 Hz (see Table 3), 15-Hz equipment responses to the Type-C motions are only about two-thirds (or less) those seen for EC5, regardless of the structure. For structure No. 1 (3-Hz), even the 25-Hz equipment response is less for Mitchell Lake and Northern Ohio than for EC5, despite the much greater HF GRS of these former two records. Only for very

high-frequency (25-Hz) equipment in the HF 9-Hz structure (No. 2), are relative equipment responses as severe as those implied by the GRS at 25 Hz. [This observation is confirmed by the (more comprehensive) results obtained in Toro et al. (1987).].

Table 3

GRS(f) Normalized by the Corresponding GRS(f) for the El Centro No. 5 Motion

Motion	Frequency			
	3 Hertz	9 Hertz	15 Hertz	25 Hertz
El Centro No. 5	1.00	1.00	1.00	1.00
Mitchell Lake	0.08	0.49	0.96	2.59
Northern Ohio	0.12	0.34	0.84	3.26
(Absolute) GRS(f) for the EC5 Motion Scaled to 0.15g	127. *	131. *	98.2 *	64.1 *

* Units are in/s^2

Table 4

Maximum Force in Equipment Mounted on the First Floor Normalized by that Seen for the El Centro No. 5 Motion
Structure 1: 3-Hz, 5-DOF. Structure 2: 9-Hz, 2-DOF

	Equipment Frequency							
	3 Hertz		9 Hertz		15 Hertz		25 Hertz	
Ground Motion	Structure No.1	No.2	Structure No.1	No.2	Structure No.1	No.2	Structure No.1	No.2
EC5	1.00	1.00	1.00	1.00	1.00	1.00	1.00	1.00
Mitch. Lake	0.05	0.09	0.57	0.77	0.66	0.65	0.77	2.58
Northern Ohio	0.07	0.15	0.34	0.44	0.45	0.62	0.98	3.11
(Absolute) Max. Equip. Acceleration for EC5 GM (in/s^2)	360.	136.	197.	357.	131.	140.	91.3	115.

The reasons for these observations are discussed in detail by Cornell & Sewell (1987) and Toro et al. (1987). To describe briefly, the absolute motion of equipment is comprised of both the absolute motion of the floor (structure)

and the relative response of the equipment. For HF equipment in a low frequency structure, that portion of the absolute equipment motion contributed by the (slowly varying) structure predominant-mode motion is termed "static" and that due to the (rapidly varying) higher-mode floor motion and relative motion of HF equipment is termed "dynamic." "Static" and "dynamic" components develop to degrees dependent, respectively, on GM strength at the structure's predominant frequency and at the equipment frequency (or higher-mode structure frequencies), and according to the structure's transfer function. GRS values for perhaps several frequencies may have important effects on equipment response.

Linear equipment response in linear structures has been well studied theoretically, and complex general mathematical formulations have been obtained earlier by others [e.g., see Igusa & Der Kiureghian, (1985a,b)]. Toro et al. (1987) use these formulations to confirm their agreement with analytical time-history results and to lend insight into factors that influence equipment response. By making suitable assumptions, Toro et al. present a simplified closed formulation of the Igusa & Der Kiureghian analysis, and apply it to obtain approximate FRS in MDOF structures (without performing time-history analyses) for various motions. The analysis show good agreement with time history calculations, and can be used to obtain fast and accurate estimates of linear equipment response in linear structures.

Linear Equipment Response in Nonlinear Structures. When a structure goes nonlinear, its floor motions are modified, and hence, equipment forces are also modified (vis-a-vis motions and forces under linear structural behavior). It has been thought by many engineers that such structure nonlinearity would considerably benefit equipment by "isolating" it from the ground motion. This expectation has been supported by studies that examined FRS in SDOF structures under linear and NL response conditions (e.g., Lin & Mahin, 1985). The results of these studies for SDOF structures consistently showed structure nonlinearity to dramatically reduce equipment forces for equipment frequencies at and above the fundamental structure frequency; at equipment frequencies lower than the structure's fundamental frequency, minor increases (up to about 15 %) in forces were consistently seen. Isolated studies that examined FRS for linear and NL MDOF structures, however, had not consistently demonstrated these results; although they confirmed the LF-equipment force increases and the dramatic force

decreases at the structure's predominant frequency, in some instances they showed HF-equipment forces to increase substantially with structure nonlinearity. (Newmark & Kennedy, 1979; Kennedy et al., 1981, 1984b; Wesley & Hashimoto, 1981; Bumpus, 1981). The reasons for these discrepancies in HF FRS for nonlinear MDOF vs. SDOF structures had been mostly unexplained. First, it was not clear that the isolated results for FRS in MDOF structures were correct (since these numerical-integration-based studies mainly focused on lower frequency structure response rather than on high-frequency FRS). Second, if the MDOF structure results were taken as correct, it was difficult to predict for what conditions equipment response increases with MDOF structure nonlinearity would occur.

To resolve this issue, Sewell et al. (1986) undertook a comprehensive parameter study examining all factors expected to have an influence on FRS in NL MDOF structures. The primary factors varied in the study were: numerical solution technique, structural characteristics (frequency, configuration and degree of nonlinearity, force-deformation model, damping), GM characteristics, and equipment characteristics (in-structure location and FRS damping level). The 5-DOF reference structure described earlier was used as the base case for comparison, and analyses were performed for structure bottom-element ductilities of μ=2.0 and μ=4.0. The set of five ground motions summarized in Table 2 were used. Numerous controlled variations on the above factors were studied to scrutinize their influence on results. Equipment responses were presented as (5% damped) FRS and corresponding floor response spectrum ratios $FRSR_\mu$ - i.e., the ratio of FRS for NL structure response (at ductility level μ) normalized by the corresponding FRS under linear structure response. Some of the most important results of the parameter study are summarized below; the reader is referred to Sewell et al. (1986, 1987) for a more detailed summary.

Effects of numerical solution and stiffness discontinuities on FRS. To see whether or not some numerical solution methods lead to fictitious HF FRS increases with structural nonlinearity, FRSR were computed using four numerical integration methods, each with four different integration time steps. The results demonstrated that any of the numerical procedures could possibly lead to inaccuracies in FRS, especially at high frequencies; such errors, however, could be reduced to negligible values for sufficiently small time steps, regardless of

the integration procedure. Additionally, to see if fictitious "sharp corners" in commonly used, piecewise-linear hysteretic models (of the structure) lead to artificial increases in HF FRS, floor spectra were computed for corresponding piecewise-linear and smooth-cornered force deformation models. The bilinear (BL), "smooth" bilinear (SBL) [see Wen, 1976] and SW, SSW models were employed for this purpose. Results indicated that piecewise-linear models generally led to HF FRSR only moderately greater than those for corresponding smooth (i.e., more realistic) models.

From the above results, it was concluded that HF FRS increases with structure nonlinearity were not generally attributable to numerical solution procedure or to fictitious stiffness discontinuities in force-deformation models. Rather, depending on the particular case at hand, one may or may not expect to see "legitimate" HF FRS increases with structure nonlinearity. Factors found to have the greatest influence on HF FRS in NL structures are considered below. Simple insights useful in qualitatively predicting conditions that result in large HF FRSR values are also mentioned.

Factors with significant effects on HF FRS. Factors shown to have predominate influences on HF FRS for NL structure response were: the degree and localization of structural nonlinearity, characterisitcs of the ground motion spectrum at key frequencies, and in-structure location (floor level).

Degree and localization of structural nonlinearity. HF FRSR computed at ductility level μ=2.0 were noted to be significantly greater than corresponding results for μ=4.0. Generally speaking, HF FRSR were found to increase with ductility from μ=1.0 to some higher ductility level (such as μ=1.5 to 2.0), and then decrease with increasing nonlinearity.

Localization of nonlinearity was studied by examining HF FRSR results for 3-Hz structures modeled by 1, 2, 3, 5 and 9 DOFs. Nonlinearity was restricted to occur only in the bottom structural element for each of these cases; thus, a more localized nonlinearity resulted as the number of DOFs was increased. Figures 3a and 3b plot, respectively, first-floor FRSR results for the SDOF and 9-DOF 3-Hz structures under the EC5 ground motion. Dramatic increases in HF FRSR values are seen as nonlinearity becomes more localized (i.e., as the number

of DOFs is increased). Effects of localization of structure nonlinearity were also seen by considering HF FRSR (under EC5) for structures that were identical in every respect except for their yield strength distributions. The four structure configurations considered earlier (see Table 1) were studied for their effects on FRSR. The results again indicated that structures which developed more localized nonlinearity resulted in higher HF FRSR. This is confirmed by considering Figures 4a (reference case) and 4b (uniform ductility case). For the latter case, we see HF FRSR results that begin to approach the beneficial effects seen for SDOF structures (compare Figure 3a).

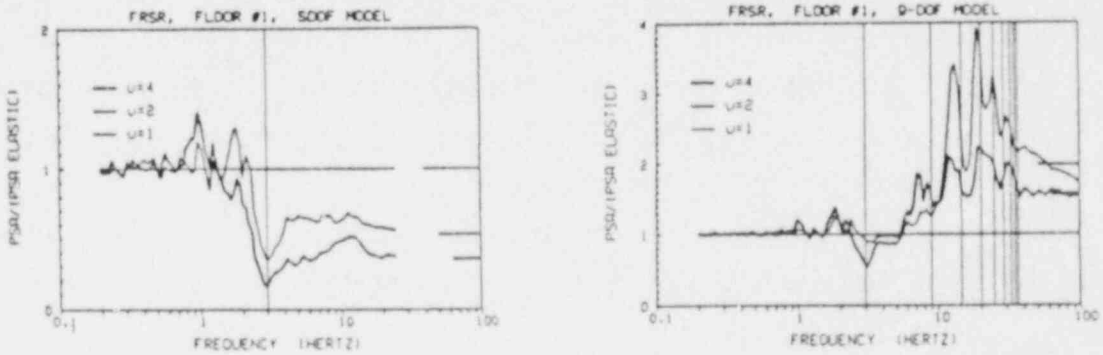

Figure 3. First-floor FRSR results for (a) SDOF and (b) 9-DOF structures.

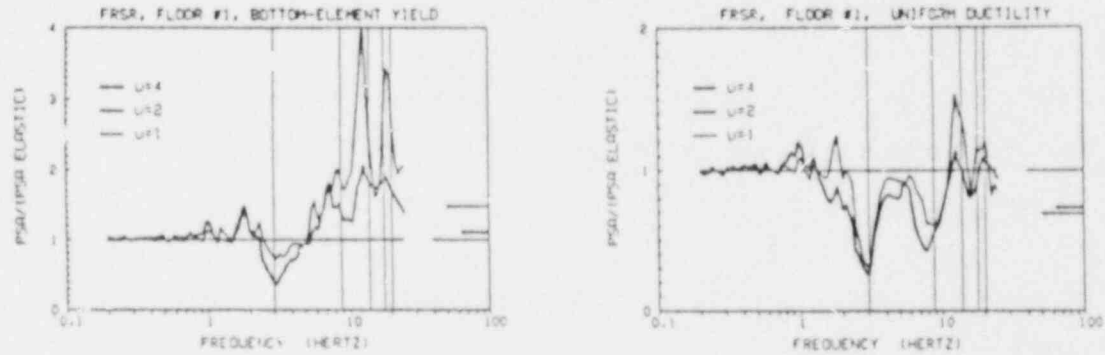

Figure 4. First-floor FRSR results for (a) Reference and (b) Uniform Strength structures.

Ground motion characteristics. HF FRSR were obtained for the five ground motions with widely varying characteristics described in Table 2. In general, it was seen that large HF FRSR values were associated with motions that contained considerable input energy at the structure's predominant frequency,

but little input energy at the higher-mode structure frequencies. (Consider, for instance, GRS for the EC5 and Mitchell Lake ground motions shown in Figure 1, and compare the base-case HF FRSR for these motions in Figure 4a versus Figure 5). This observation was further confirmed by parameter variations of structural frequency. For instance, modifying the reference (3-Hz) structure to have a 1-Hz fundamental frequency and higher-mode frequencies between 3 and 7 Hz, when subjected to EC5, resulted in (beneficially low) first-floor HF FRSR similar to those seen in Figure 5 for Mitchell Lake. For this case, relatively greater energy existed at the higher-mode frequencies than at the predominant frequency (see Figure 1), and thus, HF FRSR were much lower than those seen for the 3-Hz structure subjected to EC5.

Figure 5. First-floor FRSR results based on the Mitchell Lake ground motion and the Reference Case structure. (Note the similarity with Fig. 3a for the SDOF structure).

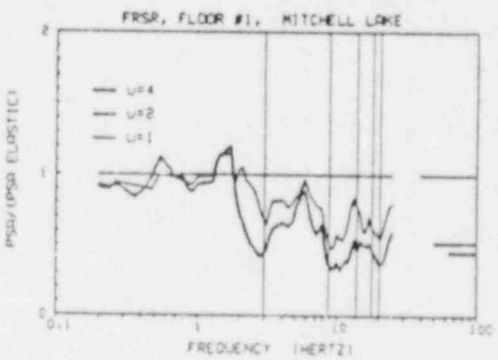

In-structure location. FRSR results presented above have always been for the first floor because this location typically yielded the most significant effects. In general, HF FRSR values were seen to diminish with height in the structure. More generally, large HF FRSR values are seen to occur in the vicinity of localized structural nonlinearity. Thus, depending on location alone, one could expect either HF FRS increases or decreases with nonlinearity, and this simple fact by itself can account for previously observed "inconsistencies" -- i.e., both decreases and increases in HF FRS for NL MDOF structures.

Insight into HF FRSR behavior. The analytical observations above help to identify conditions where large HF FRSR values can be anticipated; they do not provide direct understanding as to why these results occur. In Sewell et al. (1986) and Toro et al. (1987), the authors present such qualitative

understanding. Explanations are provided in terms of two opposing phenomena: "base-isolation" and "internally induced" effects. The "base-isolation" effect is characterized by reductions in HF equipment motion due to the increased structural damping that accompanies hysteretic behavior. The "internally induced" effect is characterized by increases in HF equipment motion (with structure nonlinearity) due to the differences in internal spring-forces that exist under nonlinear versus linear conditions; these spring-force difference "loadings" may have a configuration (e.g., for bottom-element nonlinearity only) that tends to excite higher structural modes. These concepts of "base isolation effect", "internally induced effect" and "spring-force difference loadings", and their usefulness in explaining observations of large or small HF FRSR under many different cases, are discussed at length by Sewell et al. (1986). The interested reader is encouraged to examine that reference for further details.

In the above results, it is important for one to keep in mind that the FRSR portrays response only from a relative NL versus linear structure perspective. The absolute response of equipment depends not only upon the FRSR but also upon the elastic FRS and F_{μ}. Hence, although a motion (e.g., Mitchell Lake) may result in beneficially low HF FRSR, it may produce significant HF FRS (depending on factors discussed for the linear-linear case). Such a motion may further be unlikely to induce the structural nonlinearity required to obtain HF FRS reductions. (Recall, earlier in this paper, it was seen that HF ENA motions have to be scaled to unlikely PGA levels in order to induce significant structure nonlinearity). Thus, the case of NL structure / linear equipment is, perhaps, realistic only for LF design-type motions.

Nonlinear Equipment Response in Linear Structures. As just mentioned, it is not likely that NPP-type structures will yield under HF ENA motions. Consequently, the cases of NL-structure /NL- and linear-equipment are considered to be unimportant for these motions. When considering the case of linear-structure /linear-equipment, however, it was noted that under certain HF structure - HF equipment conditions, one may see equipment forces greater than those seen correspondingly under a DB motion. Because of this, the linear-structure /NL-equipment case is thought to be of importance for HF motions. For DB motions, however, this case is not considered to be as realistic, because it is generally believed that equipment is designed such that

it remains elastic beyond or near the yield point of the structure under such motions. Thus, when we consider linear-structure /NL-equipment response, we are primarily concerned with HF ENA motions.

Nonlinear equipment response is considered in some detail in Toro et al. (1987). It is noted there that, for certain passive NPP equipment (e.g., piping), the applicable ASME code allows (elastically determined) responses to exceed component yield strengths by factors of 1.2 to 2.0 (1.2 being representative for support structures; 2.0 being representative of piping). The concern is whether or not these yield strength exceedances are accompanied by component ductilities greater than allowable ductilities and ductility capacities. To address this concern, one can define an equipment damage effectiveness factor $F_{\mu\ eq}$ that is completely analogous to F_{μ} for the structure, but where floor motions (as opposed to ground motions) are of concern. The same insights from Kennedy et al. (1984) regarding the dependency of F_{μ} on GRS shape can be used, applying them now to $F_{\mu\ eq}$ being dependent on the shape of the FRS. Thus, for a piece of equipment with frequency f_{eq} whose yield force is exceeded by a given factor $F_{\mu\ eq}$, if FRS amplitudes increase as the equipment softens (i.e., toward lower frequencies), then a significant ductility factor will be realized; vice-versa for FRS reductions with softening. FRS for the HF ENA motions may have peaks at higher-mode structure frequencies, and it thus appears equally likely to expect f_{eq} to lie either in a FRS valley or on a FRS peak. It should be noted, however, for a HF ENA motion to cause exceedance of a DB equipment capacity, often implies that it lies close to the top of a peak in the FRS. This generally suggests relatively low ductility levels, although cases can be conceived where f_{eq} may lie on the HF shoulder of a FRS peak, resulting in high equipment ductilities.

Toro et al. (1987) have compared computed ductility demands for ENA motions against allowable ductilities inferred by the ASME code. Results showed that ductility demands were generally lower or similar to the code implied allowable values, and were always lower than typical ductility capacities determined experimentally for piping and pipe supports. The allowable ductilities and ductility demands were computed for equipment frequencies that coincided with a higher-mode structure frequency (and hence, a peak in the FRS). Thus, situations that lead to more critical ductility demands can be envisioned,

but the present research suggests that they may be unlikely.

Nonlinear Equipment Response in Nonlinear Structures. The NL-structure /NL-equipment case is thought to be applicable primarily for DB motions. For this case, we are again concerned with the magnitudes of ductility that can develop in equipment. As noted above for the NL-structure /linear-equipment case, structure nonlinearity under LF DB motions causes significant higher-mode peaks in FRS (as inferrred from HF FRSR). Thus, an equipment frequency f_{eq} can be expected to lie in either a peak or valley of the FRS (just as was also noted for HF ENA motions for linear-structure /NL-equipment response). The situation is thus very similar to that discussed above; sometimes we expect mild ductility demands (because f_{eq} lies on a FRS peak), and other times we expect high demands (when f_{eq} lies in a FRS valley), with the former condition being more likely. Comparisons of computed ductility demands versus allowable equipment ductilities and ductility capacities in the present case are similar to those noted previously for nonlinear equipment in linear structures under HF ENA motions.

The above discussion speaks mainly to effects at high frequencies, well beyond the LF predominant FRS peak centered around the structure's fundamental-mode frequency. The same insight, however, also applies to LF equipment; i.e., if f_{eq} lies on the HF shoulder of the predominant-mode (LF) FRS peak and the equipment's yield capacity is exceeded, high ductility levels will result, and vice-versa if f_{eq} lies on the LF shoulder.

Re-construction of Absolute Equipment Response. So far, we have divided the complex total response of equipment into simpler relative components, and have discussed the characteristics of each component in some depth for various cases. Now, we illustrate how these components; the FRS, $FRSR_{\mu}$ and factors F_{μ}, $F_{\mu\,eq}$ can be properly "re-combined" to obtain the complete response picture.

Shown in Figure 6 are plots of (a) structure ductility factor, (b) absolute equipment response, and (c) equipment ductility factor versus ground motion scale factor. The structure and equipment are designed to just yield under the EC5 motion at unit scale factor (cases of infinite structure and/or equipment yield strengths are also shown). The structure considered is the 3-Hz, 5-DOF base-case structure described previously; the (15-Hz) equipment is located at

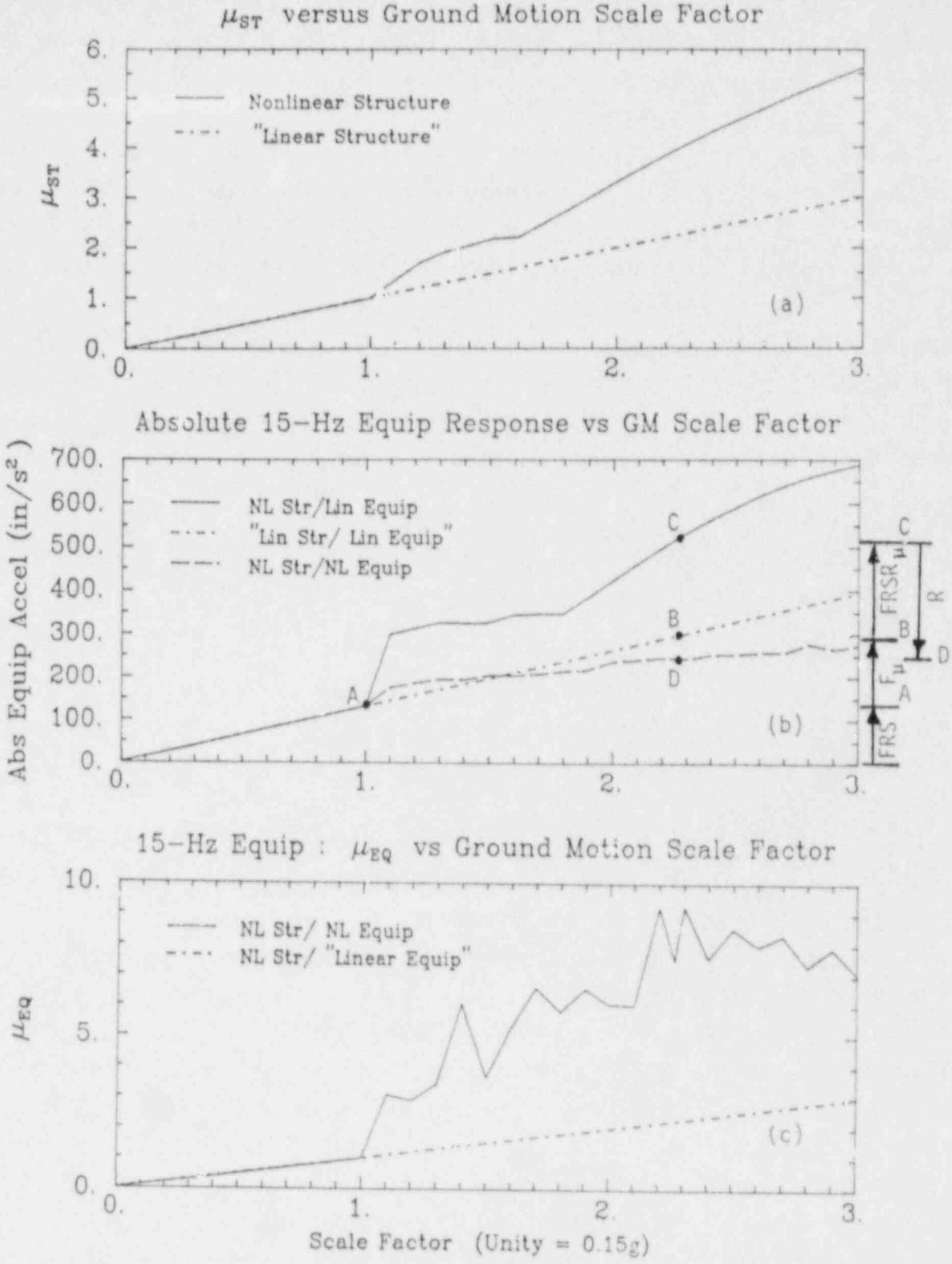

Figure 6. Structure and equipment responses as functions of ground motion scale factor: (a) structure ductility factor, (b) absolute equipment acceleration, and (c) equipment ductility factor.

the first floor; and the input motion is EC5. This example is thus representative of linear-linear, nonlinear-linear, and nonlinear-nonlinear, LF structure - HF equipment responses to a LF DB motion.

Figure 6b shows how FRS, F_μ, $FRSR_\mu$ and $F_{\mu\ eq}$ combine to obtain total equipment response. We note first that, up to unit scale factor, the response curve is linear; it leads up to the elastic (incipient yield) FRS at point A. For scale factors beyond unity, three curves are shown: NL-structure /linear-equipment, linear-structure /linear-equipment, and NL-structure /NL-equipment. The NL-linear curve is shown to be determined as $FRSR_\mu \times F_\mu \times FRS$; i.e., it is obtained simply by scaling the linear-linear trace ($F_\mu \times FRS$) by the $FRSR_\mu$. The NL-NL curve is obtained by scaling down the NL-linear curve by a factor R, approximated by:

$$R = \frac{F_{NL}}{F_L} \sim \frac{1 + \alpha_{eq}(\mu_{eq} - 1)}{F_{\mu\ eq}} \qquad (1)$$

where F_{NL}, F_L are the maximum equipment spring forces for NL-NL and NL-linear response, respectively; α is the equipment post-yield stiffness ratio (0.10 for present example); and μ_{eq} is the equipment ductility factor. Thus, the NL-NL equipment curve is obtained as $R \times FRSR_\mu \times F_\mu \times FRS$.

To exemplify, we consider the specific case where the structure experiences μ=4.0. From Fig. 6a (see also Table 1), we find $F_{\mu=4} = 2.26$. The linear FRS value of 131 in/s^2 (see Fig. 6b and Table 4), when scaled up by $F_{\mu=4} = 2.26$ moves us from point A to B on the linear-linear trace at an equipment response level of about 296 in/s^2. Because the structure actually behaves nonlinear to ductility μ=4, however, we scale this value by $FRSR_{\mu=4}$ to reach the NL-linear curve at point C. From Fig. 4a, the appropriate $FRSR_{\mu=4}$ value at 15 Hz for this case is approximately 1.75. The equipment response level at point C is therefore about 518 in/s^2. For the NL-NL case, this response at point C must be scaled down to point D; the amount we scale down by is the factor R from Eq. (1). We determine R as follows: if the equipment had remained linear, it would have experienced an acceleration of 518 in/s^2. Its yield capacity set at 131 in/s^2 would thus be exceeded by a factor $F_{\mu\ eq} = 518/131 = 3.95$. As seen from Fig. 6c, this factor corresponds to an equipment ductility of about 8.2. From

Eq. (1), we calculate in this case a reduction factor of about R=0.44, so that point D lies at an equipment response level of about (518)(0.44)= 228 in/s^2. (It should be noted, though, that the factor $F_{\mu\ eq}$ = 3.95 is much higher than allowed by the ASME code, and the present example is intended for illustration only; it may, however, be representative of GM levels considered in seismic margins studies).

These procedures to properly combine relative components of equipment and structure response, in conjuction with the insights and principles reviewed in this paper (and discussed in depth in the references cited), enable one to estimate total equipment response for any other example, given a GRS and basic properties of the structure and equipment.

SUMMARY AND CONCLUSIONS

This paper has presented results of recent research concerning the ability of ground motion to affect linear and nonlinear response in structures and equipment. These results have provided several useful insights, many of which may appear counter-intuitive at first. The results have also helped to address some important aspects related to the seismic performance of NPP-like structures and equipment.

It was demonstrated, for instance, that high-frequency (HF), small-magnitude, eastern North American (ENA) motions are generally less effective to NPP-type structures than are broad-spectrum, design-basis motions of the same PGA. This was shown to be due to the lower spectral accelerations of the HF ENA motions at NPP structure predominant frequencies and because HF ENA ground response spectra (GRS) look less severe after structural yielding (i.e., softening to lower frequencies). It was further shown that the HF ENA motions often lead to much lower HF equipment response than their GRS implied. This was seen to be a result of LF structures filtering-out much of the HF input. The case of HF equipment in HF structures that are subjected to these ENA motions, however, was noted to be worthy of close scrutiny. Additionally, it was demonstrated that HF floor response spectrum ratio (FRSR) characteristics noted from nonlinear SDOF structure studies are often not representative of HF FRSR in MDOF structures. Rather than acting to "isolate" equipment from strong

HF motions, MDOF structure nonlinearity in some instances generates high frequency motion internally, which acts to further excite HF equipment. This situation exists primarily for ground motions that possess relatively little energy at the higher-mode structure frequencies compared to their energy at the predominant structure frequency. Other important observations and insights from the research study were also noted.

Results and conclusions from this study should not be extrapolated to situations beyond the range of parameters considered, although the general principles and insights obtained apply to a wider class of structure/equipment/ground motion situations than considered here. It should also be mentioned that the cases considered in this study have some built-in conservatisms vis-a-vis actual NPP design practice and response conditions. For instance, the Reg. Guide 1.60 design spectrum would generally be more severe than the DB motions considered in this study; design FRS would be broadened around the peaks seen in the present results; and, in practice, structure-equipment interaction would reduce the FRS peaks noted in this work.

REFERENCES :

Baber T.T. and M.N. Noori (1985). "Random Vibration of Degrading, Pinching Systems," Jour. Engr. Mech. Div., ASCE, Vol. 111, No. 8, pp 1010-1026.

Banon H. (1980). Prediction of Seismic Damage in Reinforced Concrete Frames, Seismic Behavior and Design of Buildings, Rept. No. 3, Publ. No. R80-16, Dept. Civil Engr., MIT, Cambridge, MA.

Benjamin J.R. and C.A. Cornell (1970). Probability, Statistics, and Decision for Civil Engineers, McGraw-Hill, Inc., New York, NY.

Bumpus S. (1981). LLL/DOR Seismic Conservatism Program: Investigations of the Conservatism in the Seismic Design of Nuclear Power Plants - Part IX: Nonlinear Structural Response, Rept. No. UCID-18100, Lawrence Livermore Laboratories.

Cornell C.A. and R.T. Sewell (1987). "Non-Linear-Behavior Intensity Measures in Seismic Hazard Analysis," Proceedings of the International Seminar on Seismic Zonation, Guangzhou, China.

Cornell C.A. and R.T. Sewell (1987). "Equipment Response in Linear and Non-linear Nuclear Power Plant Structures: Small Magnitude versus Design-type Motions," Proceedings EPRI Workshop on Engineering Characterization of Small-Magnitude Earthquakes, Palo Alto, CA, EPRI.

Igusa T. and A. Der Kiureghian (1985a). "Dynamic Response of Multiply Supported Secondary Systems," Jour. Struc. Div., ASCE, Vol. 111, No. 1, pp 20-41.

Igusa T. and A. Der Kiureghian (1985b). "Dynamic Characterization of Two-Degree-of-Freedom Equipment-Structure Systems," Jour. Struc. Div., ASCE, Vol. 111, No. 1, pp 1-19.

Kennedy R.P. (1987). "Engineering Characterization of Small-Magnitude Earthquakes," Proceedings EPRI Workshop on Engineering Characterization of Small-Magnitude Earthquakes, Palo Alto, CA, EPRI.

Kennedy R.P., S.A. Short, K.L. Merz, F.J. Tokarz, I.M. Idriss, M.S. Power and K. Sadigh (1984a). Engineering Characterization of Ground Motion - Task I : Effects of Characteristics of Free-Field Motion on Structural Response, NUREG/CR-3805, Vol. 1, NRC.

Kennedy R.P., R.H. Kincaid and S.A. Short (1984b). Engineering Characterization of Ground Motion - Task II : Effects of Ground Motion Characteristics on Structural Response Considering a Typical PWR Reactor Building with Localized Nonlinearities, NUREG/CR-3805, Vol. 2, NRC.

Kennedy R.P., S.A. Short and N.M. Newmark (1981). "The Response of a Nuclear Power Plant to Near-Field Moderate Magnitude Earthquakes," SMiRT 6 Conference Proceedings, Paper No. K8/1.

Khemici O. (1986). "Small-Magnitude Earthquake Ground Motion Time History, Cumulative Energy and Response Spectrum Plots," Unpublished Study Prepared by Jack R. Benjamin & Assoc., Inc., Mountain View, CA.

Krawinkler H., M. Zohrei, B. Lashkari-Irvani, N.G. Cofie and H. Hadidi-Tamjed (1983). Recommendations for Experimental Studies on the Seismic Behavior of Steel Components and Materials, Tech. Rept. No. 61, John Blume Earthquake Engr. Center, Dept. Civil Engr., Stanford University, Stanford, CA.

Lin J. and S.A. Mahin (1985). "Seismic Response of Light Subsystems on Inelastic Structures," Jour Struc. Div., ASCE, Vol. 111, No. 2, pp 400-417.

McGuire R.K. (1978). FRISK - A Computer Program for Seismic Risk Analysis Using Faults as Earthquakes Sources, Open-File Rept. No. 78-1007, USGS.

McGuire R.K. (1974). Seismic Structural Response Risk Analysis, Incorporating Peak Response Regressions on Earthquake Magnitude and Distance, Research Rept. R74-51, Dept. Civil Engr., MIT, Cambridge, MA.

Newmark N.M. and R.P. Kennedy (1979). Final Report - Evaluation of a Typical PWR Reactor Building Subjected to a High-Acceleration, Short-Duration Earthquake, Prepared for Electricite de France, Contr. No. 78031.

Sewell R.T. and C.A. Cornell (1987). "Seismic Hazard Analysis Based on Limit State Structural Damage," Proceedings of ICASP-5, Vancouver, B.C., Canada.

Sewell R.T., C.A. Cornell, G.R. Toro, R.K. McGuire, R.P. Kassawara, A. Singh and J.C. Stepp (1987). "Factors Influencing Equipment Response in Linear and Nonlinear Structures," Proceedings of SMiRT-9, Vol. K2, pp. 849-856.

Sewell R.T., C.A. Cornell, G.R. Toro and R.K. McGuire (1986). A Study of Factors Influencing Floor Response Spectra in Nonlinear Multi-Degree-of-Freedom Structures, Tech. Rept. No. 82, John Blume Earthquake Engr. Center, Dept. of Civil Engr., Stanford University, Stanford, CA.

Toro G.R., R.K. McGuire, C.A. Cornell and R.T. Sewell (1987). Implications of Linear and Nonlinear Response of Structures and Equipment to California and Eastern United States Earthquakes, Final EPRI Report, Proj. No. EPRI RP2556-8.

Wen Y.K. (1976). "Method for Random Vibration of Hysteretic Systems," Jour. Engr. Mech. Div., ASCE, Vol. 102, No. 2, pp 249-263.

Wesley D.A. and P.S. Hashimoto (1981). "Nonlinear Structural Response Characteristics of Nuclear Power Plant Shear Wall Structures," Proceedings of SMiRT 6, Paper No. K8/7.

PIPING SYSTEM DAMPING STUDY

H. T. Tang
Electric Power Research Institute
3412 Hillview Avenue
Palo Alto, CA 94303

A.H. Hadjian
Bechtel Western Power Corp.
12440 East Imperial Highway
Norwalk, Ca 90650

ABSTRACT

Piping System damping research at EPRI is briefly described in this paper. The focus of the research is to derive a set of technically defensible piping system damping values which can be included in Appendix N, Section III, Division I of the ASME Boiler and Pressure Vessle Code for piping dynamic analysis. Engineering judgments and regression analyses were employed to derive damping functional relationship by first establishing a uniform experimental data base, then de-aggregating the data to sort out significant contributing parameters and finally performing regression analysis. Results to date show support density, support type, insulation, frequency, attached equipment, diameter and weight are significant parameters controlling damping. A formal recommendation to ASME and guidelines of using recommended damping in various piping analysis methods remains to be accomplished.

Background

The PVRC pipe damping recommendation (1) was accepted by ASME as Code Case N-411 and was also endorsed by NRC's piping review committee. Prior and subsequent to the adoption of Code Case N-411, the ASME special Working Group-Dynamic Analysis had raised certain basic concerns relative to these recommendations. These concerns were directed not so much to the damping values recommended, but primarily, in the context of accepting N-411 formally in the code, to the overall quality of the data reduction techniques used and the subsequent regression analysis results. The NRC staff have raised other issues relative to the use of the recommended damping values. This is reflected in the many application limitations imposed on N-411 as specified in Rev. 24 of Regulatory Guide 1.84 (2). Since damping impacts significantly the piping system dynamic response determination, it is imperative that the NRC raised issues be resolved and a formal ASME code (Appendix N) position be taken as soon as possible.

In order to achieve the above objective, EPRI sponsored a study (3) with a step by step approach of 1) establishing a uniform data base and 2) identifing the signifcant parameters that contribute to energy dissipation in piping systems, 3) quantifying the damping in piping systems for use in dynamic analyses, and 4) recommending damping values for adoption by ASME (Appendix N) code. Guidelines for the application of recommended damping criteria in various types of analysis methods is also included in the study.

The results accomplished in the EPRI project can support the NRC's plan in formally revising the conserve requirements defined in Regulatory Guide 1.61.

HTT/cn/HTT001

Results

All of the test data used in developing the PVRC damping position, excepting the Europian HDR and KFK data, were included in the evaluation in establishing a uniform data base. The quality of each set of data is merited based on the criteria and weighting agreed on by experts working in the field. Table 1 shows the summary of the rating scores and Table 2 is an example calculation for System 2, ANCO 6" xyz line with branch. By eliminating inappropriate data, such as repeats, extremely low level response, poor quality, incompleted description, etc., the total data points used in this study are considerably less than the ones compiled in the EG&G data bank as shown in Table 3. It should be noted however that, although the data bank becomes much smaller, the distribution of the data for a given parameter, viz. frequency, as shown in Figs. 1 and 2, is essentially the same. Figs. 3-7 show the damping data plotted versus the other quantitative variables adopted in the study. Trends can be discerned in all of the data plots showing that more than one variable has an important effect on the resulting damping values. The variability shown for example in Fig. 1 is due primarily to the fact that these other variables are not recognized in these type of plots. The data per se is not as variable as any one of these data plots might imply; but rather, the problem is with displaying all of the data on a two-dimensional plane.

A systematic evaluation of the data was carried out using the regression analysis method. Detailed descriptions and discussions are given in (4). Starting with a total of 21 viable variables potentially contributing to damping definition, seven variables eventually were identified as the critical ones contributing the most. These variables are diameter, weight, frequency, support density on-line equipment, insulation and support type. Table 4 summarizes various intermediate model and the final model results assuming a linear regression model of the

form $\beta = \beta_0 + \sum_{i=1}^{N} \beta_i X_i$ where X_i represent variables. It is seen in Column 6 (final model) that Insulation, in the context of liquid metal piping, adds about 2.6% of damping, all other variables being equal. A more detailed evaluation to quantify the effects of type and amount of insulation needed.

Attached equipment influences damping in a negative sense. It substracts about 2% from the total effect. This is an unexpected result that must be studied in detail both analytically and with respect to the actual test data.

As expected, relative to snubber type supports, rigidly supported systems have about 1.1% less damping, all other parameters being the same.

Of the quantitative variables, frequency, as per the PVRC results, affects damping. The difference in damping between 10 Hz and 20 Hz (the inner limits of the PVRC damping value changes) is - (10 - 20) (0.091) = 0.9%. The change from 5 Hz to 30 Hz is 2.3%.

The impact of Support Density 2 (SD2)*, rather than Support Density 1 (SD1), on damping is a very unexpected result. The lack of dependency of damping on SD1 can be attributed to the distribution of the data rather than on the physical nature of the problem. A more detailed evaluation of this phenomenon is desirable.

---

* SD2 - supports perpendicular to excitation direction.
SD1 - supports parallel to excitation direction.

Diameter and weight effects are interrelated and they affect damping in opposite directions. Since most of the data is based on pipe with 8" diameter or less, the use of these regression coefficients for data above this size of pipe needs to be carefully reviewed.

Nonlinear effects in the context of other forms of the variables, rather than regression coefficients that are dependent on the variable itself, are also considered to improve the correlation. The form of the equation selected in the study is given by

$$\beta = \beta_0 + \beta_1\sqrt{D} + \beta_2 W + \beta_3 (\ln F) + \beta_6 (SD2) + \beta_{24} X_{24} + \beta_{31} X_{31}$$

where the definitions of variables are given in Table 4. One notices that only diameter (D) and Frequency (F) exhibit nonlinear effects. Whether the additional complexity is worth the improvement is not certain at the present. Fig. 8 shows the comparison between linear and nonlinear prediction curves for a case with the following conditions:

Diameter = 8"
Weight per foot = 45
No Equipment, X_{22} = 0
No Insulation, X_{24} = 0
Rigid Strut Supports, X_{31} = 1

Discussion

Results accomplished to date show the complexity of piping damping definition in the form of linear viscous representation for linear dynamic analysis. However, the trend of damping variation associated with pertinent variables is technically tractable. Consequently, an indepth approach as the one discussed herein can be adopted to sort out the physical characteristics embedded in a seemingly uncorrelated data set

leading to a set of correlated, technically defensible damping curves for realistic piping design applications. The study is to be completed with a formal recommendation to ASME in the first quarter of 1988.

References

1. Welding Research Council, "Technical Position on Damping Values for Piping-Interim Summary Report", Bulletin 300, ISSN 0043-2326, December 1984.

2. U.S. Nuclear Regulatory Commission, "Design and Fabrication Code Case Acceptability ASME Section III Division 1", Revision 24, June 1986.

3. EPRI Research Project RP2635-2, "Piping Damping Study".

4. A.H. Hadjian, "Piping System Damping Evaluation", RP2635-2 draft report, submitted to EPRI by Bechtel Group, Inc.

Table 1
Summary of the Merit Rating Scores
in Descending Order

System ID	Title	Score
2	ANCO 6" XYZ Line w/ Branch	803
1	ANCO 6" XYZ Line w/o Branch	753
3	ANCO 4" Z Bend	741
28	Wyle SRV Discharge Line Lab Test	719
4	Caorso Main Steam Line	694
20	EG&G 3" Straight Pipe	694
21	EG&G 8" Straight Pipe	694
23	Clinch River (8" Scaled) Crossover Piping Leg	661
10	Diablo Canyon Safety Injection Pump Discharge	651
6	Diablo Canyon Containment Spray Pump Suction	633
27	Monticello T-Quencher Support	624
15	FFTF GEA 61176 1" Line	617
16	FFTF GEA 61177 1" Line	617
17	FFTF GEA 61263 3" Line	617
18	Closed Loop Module #1, 1" Line 35	617
19	Closed Loop Module #1, 3" Line 08	617
9	Diablo Canyon Pressurizer Relief Header	598
12	FFTF Secondary Crossover 16" Line	597
11	Diablo Canyon Letdown Line Loop	596
14	FFTF Prototypical 1" Line (Impulse)	564
7	Diablo Canyon CVCS Mixing Tank Outlet	540
13	FFTF Prototypical 1" Line (Snapback)	527
24	Kuosheng 3" Valve Line	527
8	Diablo Canyon Make-up Water Tank	520
25	La Salle Recirculation 24" Line	457
26	La Salle 2" Line	457
22	Indian Point Boiler Feedwater Line	Later
5	Caorso Recirculation Piping	-

Table 2
WEIGHTS AND MERIT RATING FOR DAMPING DATA
(Sheet 2 of 26)

CRITERIA			DATA ID: 02		
Criteria & Weight W_i	Subcriteria & Subweight W_i		Rating R_j	Rating $W_{ij}\ R_j$	Comments
I. Excitation Characteristics	a. Excitation type	35	9	315	
	b. Level of Excit.	45	10	450	
	c. Dimension	20	6	120	R = 1/3
	Subtotal	100		885	
20%	Weighted Subtotal	-	-	177	
II. System Characteristics	a. Prototypical	30	8	240	
	b. Dimension	30	8	240	
	c. Scale Model	20	8	160	
	d. Material	20	10	200	
	Subtotal	100		840	
15%	Weighted Subtotal	-	-	126	
III. Data Acquisition	Subtotal	100	8	800	
15%	Weighted Subtotal	-	-	120	
IV. Data Reduction	Subtotal	100	8	800	
25%	Weighted Subtotal	-	-	200	
V. Validation	Subtotal	100	6	600	
10%	Weighted Subtotal	-	-	60	
VI. Response Characteristics	Subtotal	100	8	800	
15%	Weighted Subtotal	-	-	120	
OVERALL MERIT RATING				803	

Table 3
DATA BASE COMPARISON

	Piping System	EPRI	EG&G
1.	ANCO 6" XYZ Line w/o Branch	6	6
2.	ANCO 6" XYZ Line w/ Branch	17	80
3.	ANCO 4" Z Bend	7	14
4.	Caorso Main Steam Line	-	2
5.	Caorso Recirculation Piping	-	1
6.	Diablo Canyon Containment Spray Pump Suction	2	3
7.	Diablo Canyon CVCS Mixing Tank Outlet	1	1
8.	Diablo Canyon Make-up Water Tank	1	1
9.	Diablo Canyon Pressurizer Relief Header	2	2
10.	Diablo Canyon Safety Injection Pump Discharge	8	8
11.	Diablo Canyon Letdown Line Loop	5	5
12.	FFTF Secondary Crossover 16" Line	2	22
13.	FFTF Prototypical 1" Line (Snapback)	3	29
14.	FFTF Prototypical 1" Line (Impulse)	3	24
15.	FFTF GEA 61176 1" Line	3	-
16.	FFTF GEA 61177 1" Line	2	6
17.	FFTF SEA 61263 3" Line	3	6
18.	Closed Loop Module #1, 1" Line 35	3	24
19.	Closed Loop Module #1, 3" Line 08	4	52
20.	EG&G 3" Straight Pipe	13	155
21.	EG&G 8" Straight Pipe	6	60
22.	Indian Point Boiler Feedwater Line		Later
23.	Clinch River (8" Scaled) Crossover Piping Leg	30	30
24.	Kuosheng 3" Valve Line	2	40
25.	La Salle Recirculation 24" Line	-	-
26.	La Salle 2" Line	-	-
27.	Monticello T-Quencher Support	-	5
28.	Wyle SRV Discharge Line Lab Test	2	14
	Total	125	590

Table 4
REGRESSION VARIABLES AND COEFFICIENTS
SOLUTION WITHOUT BIASES

1	2	3		4		5	6	7
				Intermediate Models			Final Model	
Variables	All Viable Variables	Best Min. Subset	Comments		B_i	B_i	B_i	Contrib. to R^2
Intercept	5.845	6.046		✓	5.489	5.506	6.067	-
Diameter	-0.737	-0.822		✓	-0.917	-0.909	-0.915	0.0271
Weight	0.100	0.116		✓	0.136	0.135	0.135	0.0222
Frequency	-0.069	-0.068		✓	-0.064	-0.063	-0.091	0.0514
Response	-0.339	-		✓	-0.379	-	-	-
SD1	0.232	-		✓	-0.160	-	-	-
SD2	1.461	1.737		✓	2.018	1.917	1.937	0.1006
X18 (2D Item)	-2.096	-2.207	Too few data	-	-	-	-	.
X19 (3D Item)	0.369	-		-	-	-	-	-
X22 (Equip. Yes)	-2.170	-2.194		✓	-1.795	-2.024	-2.040	0.0633
X23 (Equip. No)	-0.020	-		✓	0.250	-	-	-
X24 (Insul. Yes)	2.154	2.234		✓	2.482	2.459	2.592	0.0786
X26 (1st Mode)	0.922	0.895		✓	0.689	0.673	-	-
X31 (Rigid Strut)	-1.454	-1.580		✓	-1.271	-1.230	-1.082	0.0226
X33 (Guide)	-1.359	-1.299		✓	-1.021	-0.958	-	-
X34 (R-S)	0.778	-	Too few data	-	-	-	-	-
R^2	0.6652	0.6611			0.6458	0.6453	0.6357	-
No. of Variables	15	10			12	9	7	-

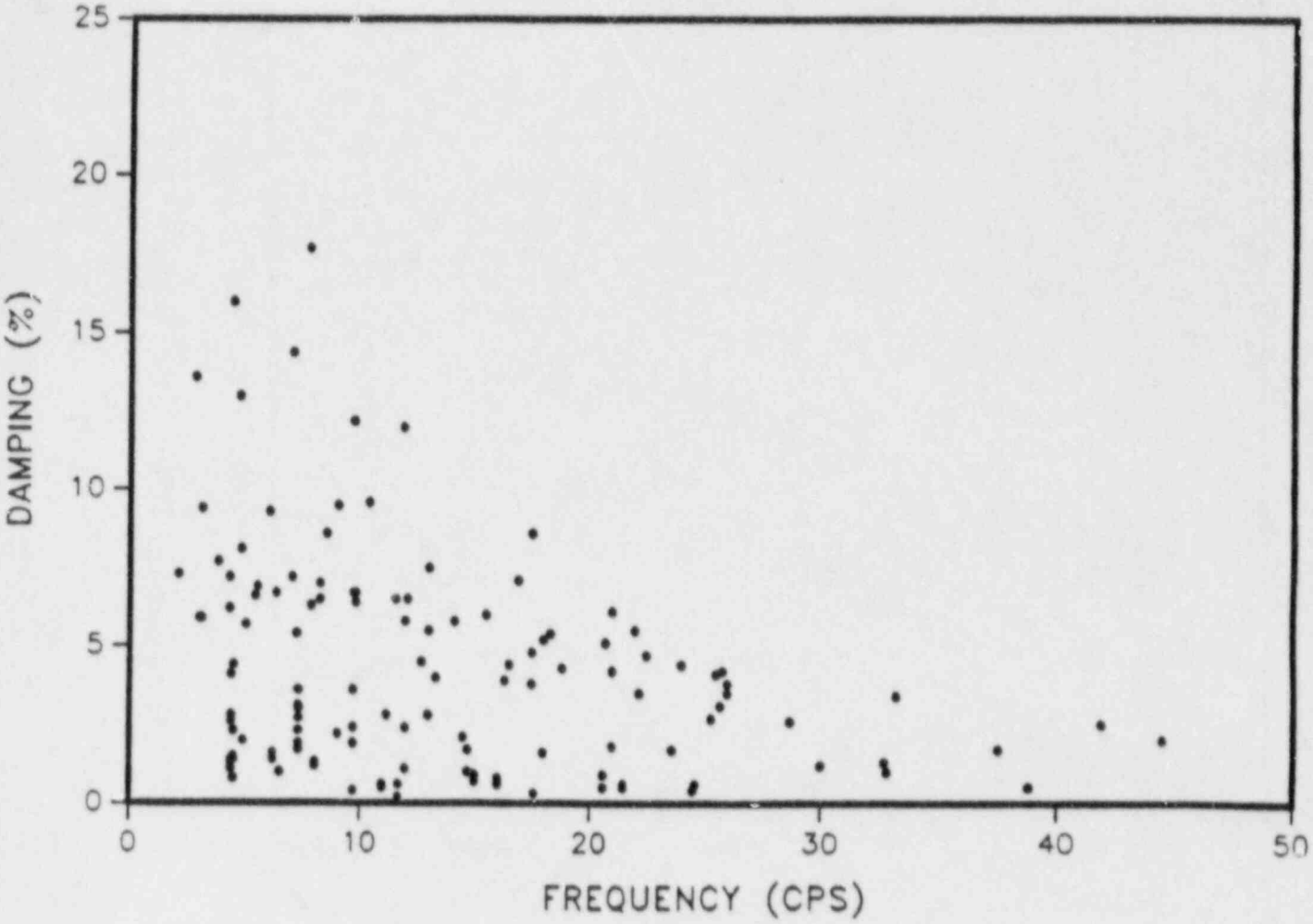

Fig. 1 All Damping Data Versus Frequency

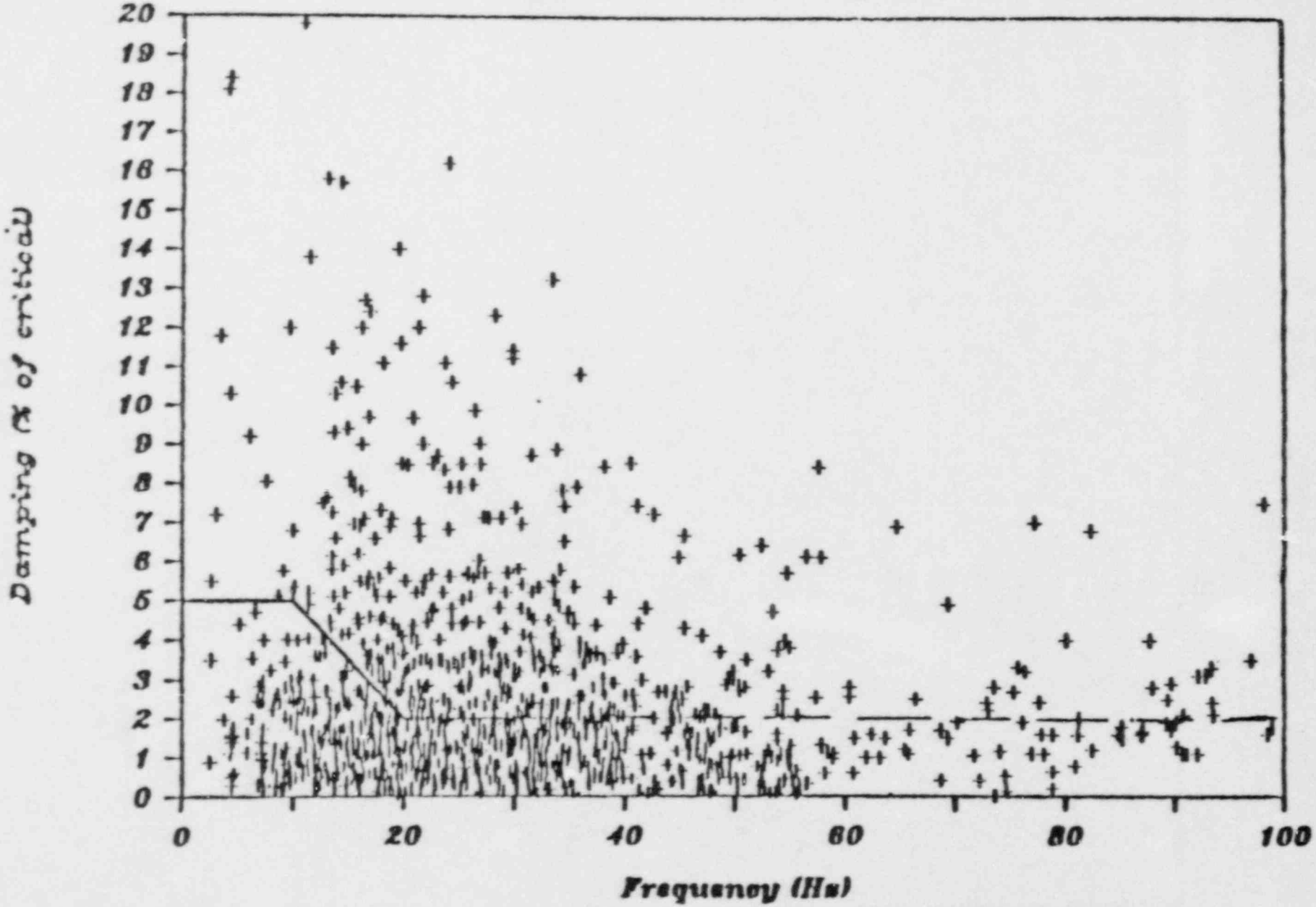

Fig. 2: Damping Database and PVRC Damping Recommendation
(Code Case N-411)

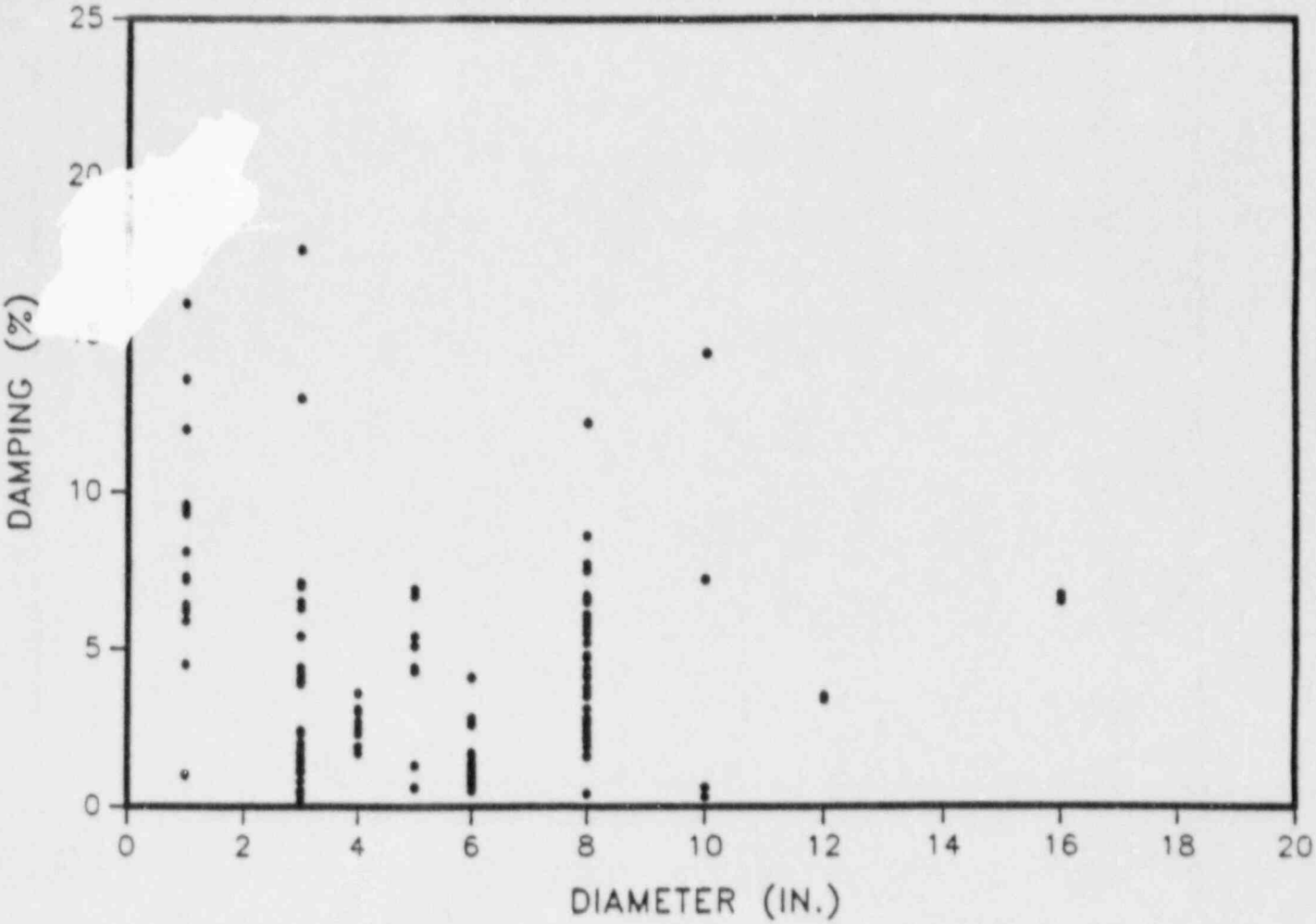

Fig. 3 All Damping Data Versus Diameter

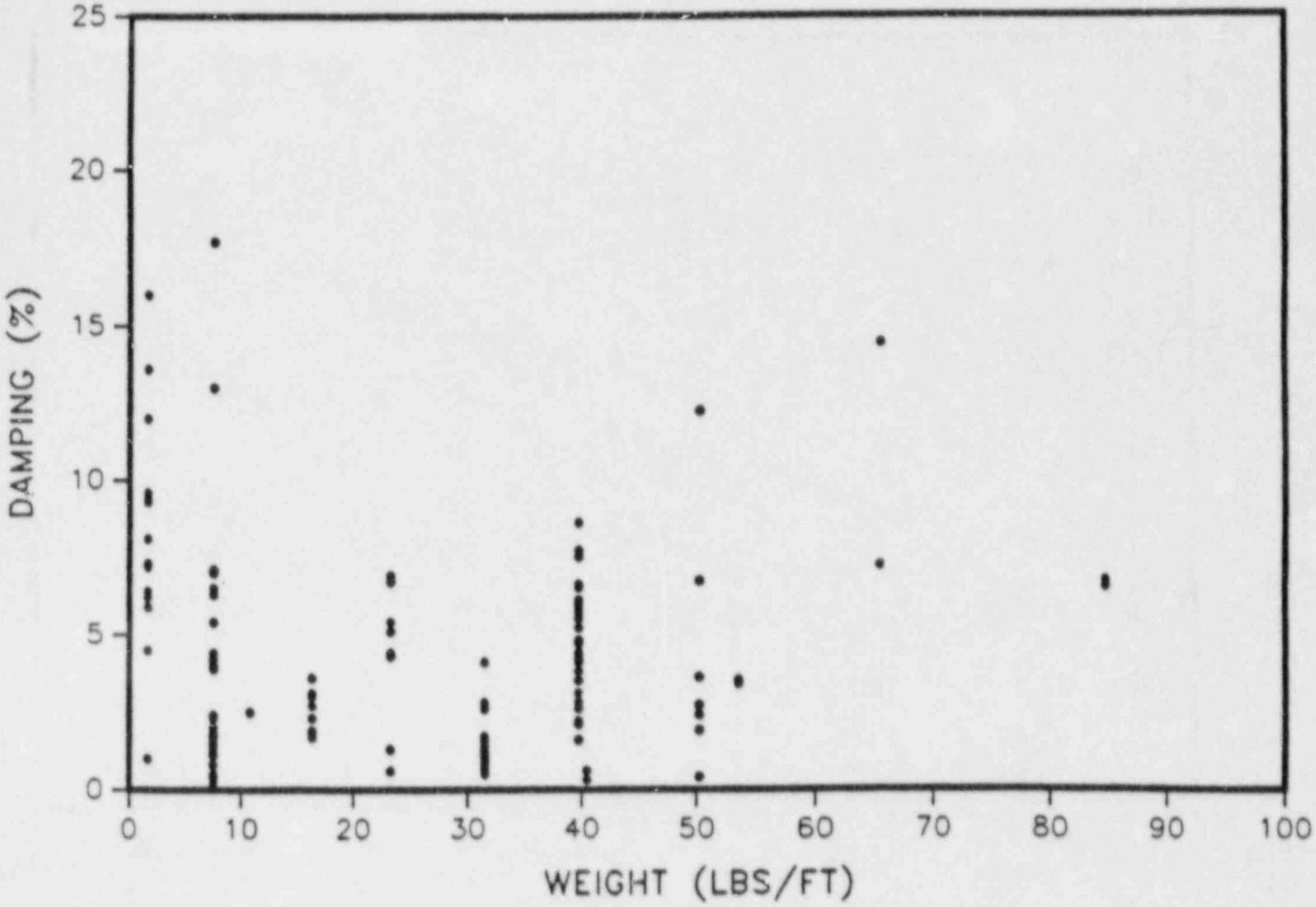

Fig. 4 All Damping Data Versus Weight

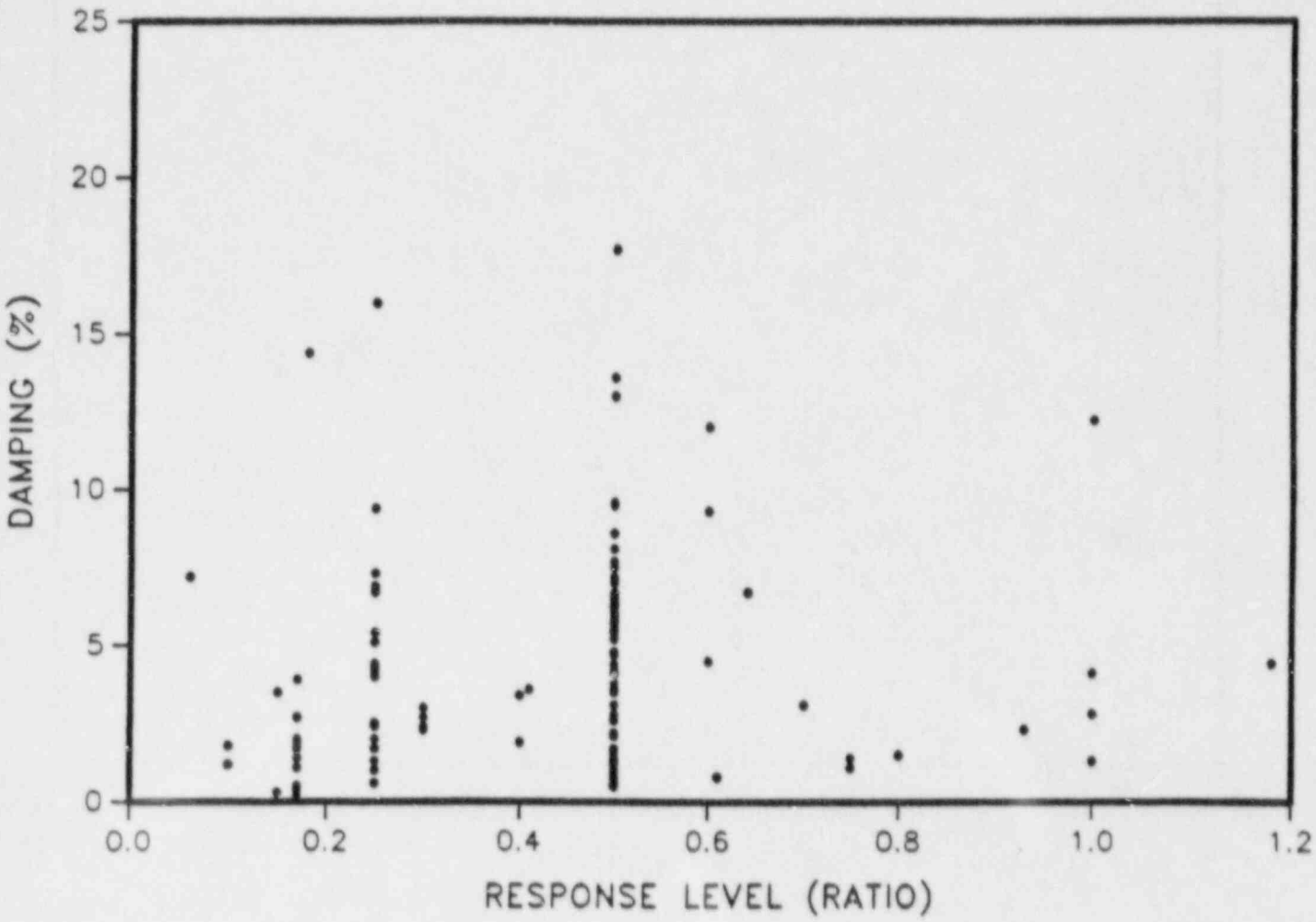

Fig. 5 All Damping Data Versus Response Level Stress Ratio

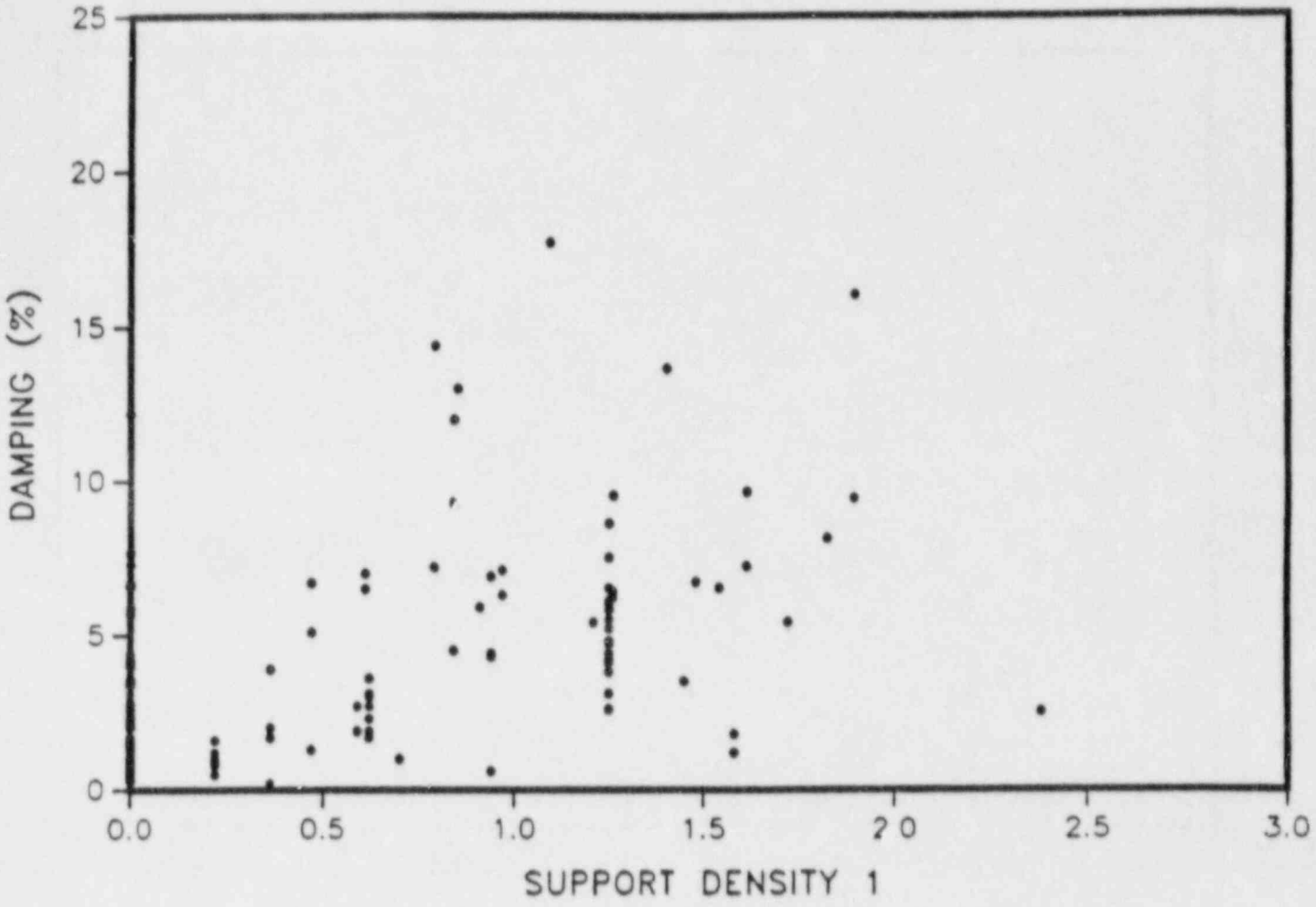

Fig. 6 All Damping Data Versus Support Density 1

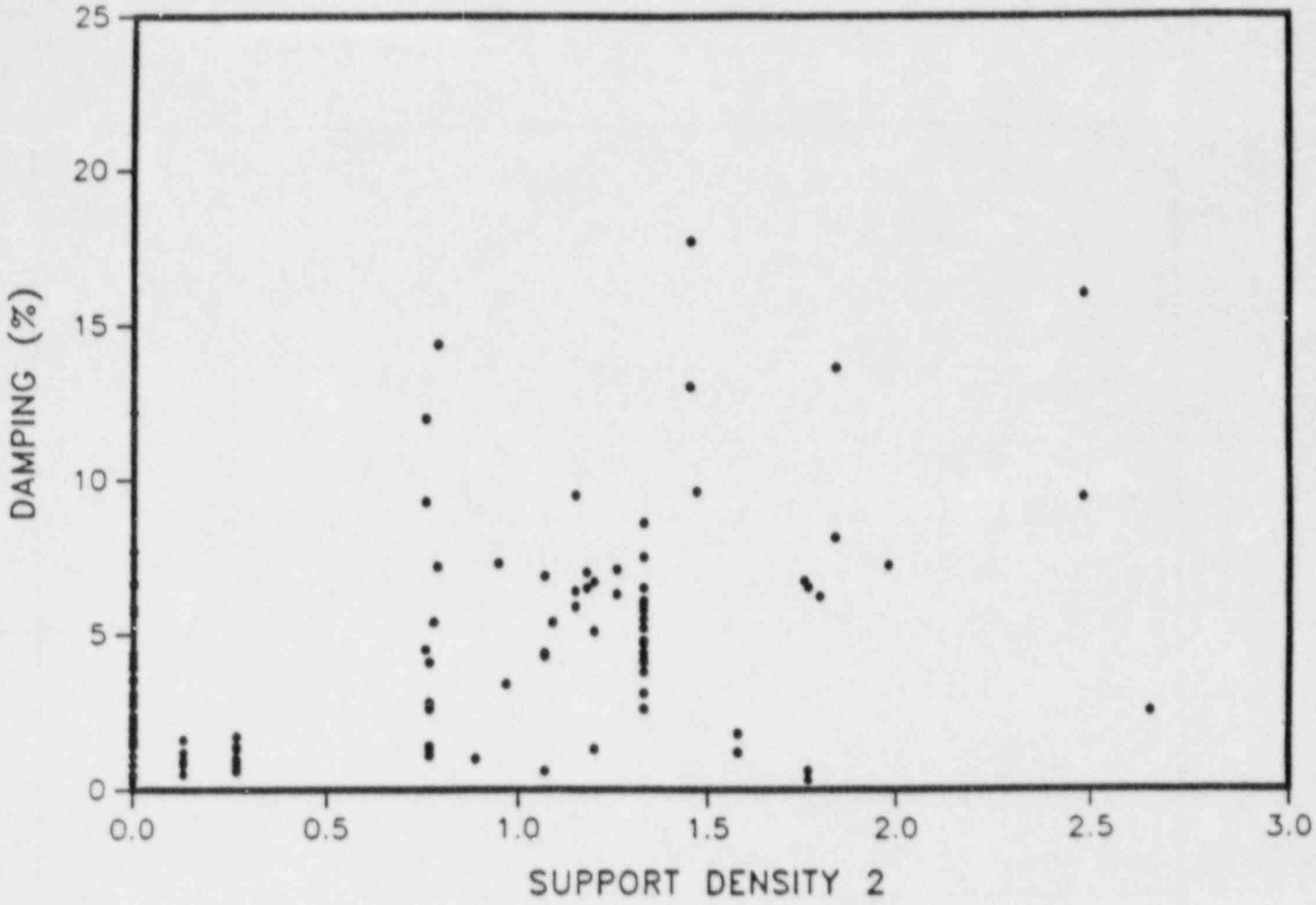

Fig. 7 All Damping Data Versus Support Density 2

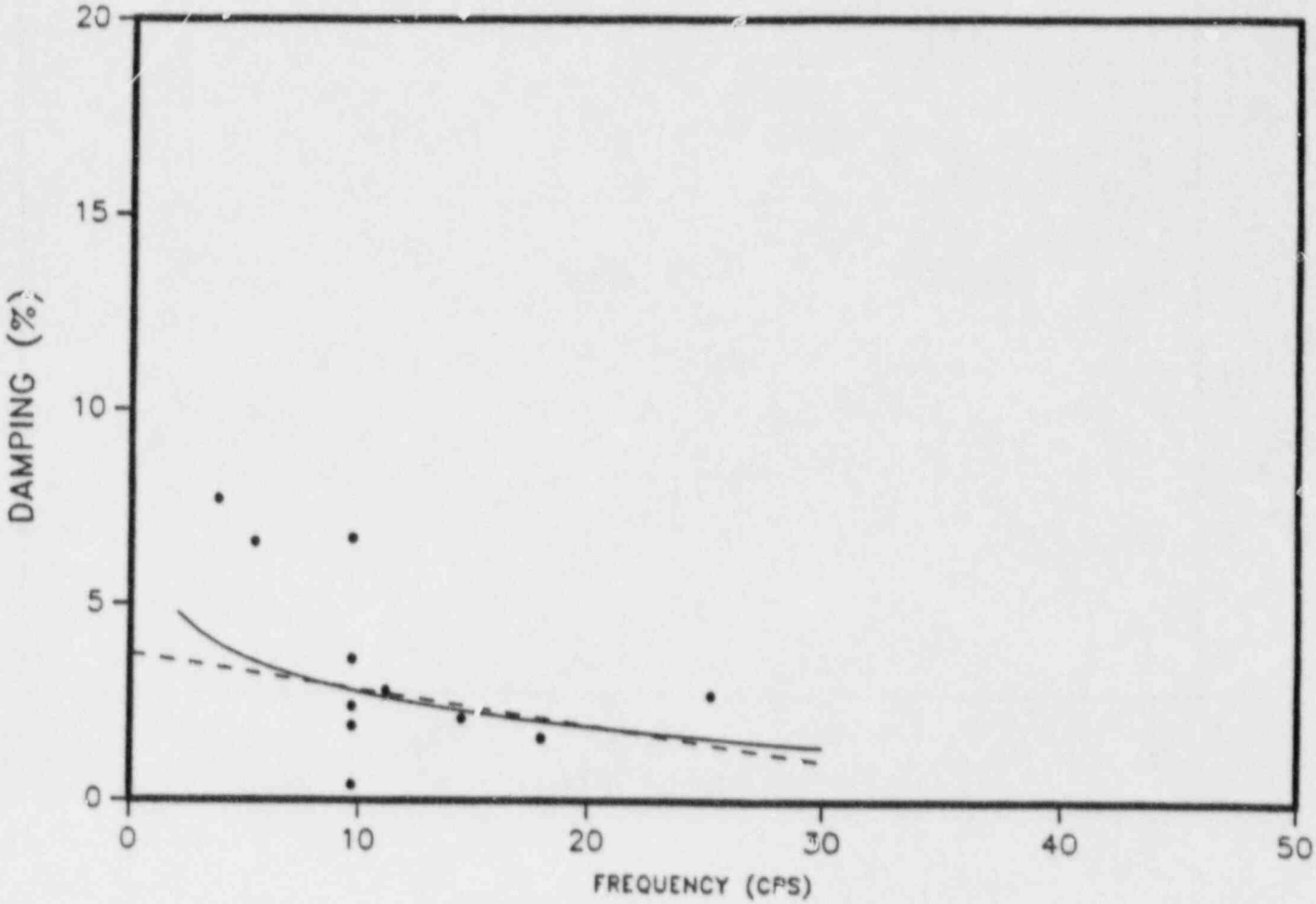

Figure 8: Comparison of Linear and Non-Linear Curves With Data

For Presentation at the 15th Water Reactor Safety Information Meeting
Gaithersburg, Maryland, October 26-29, 1987

SUMMARY

Development and Implementation of a BWR Digital Feedwater Control System

Bill Sun, Electric Power Research Institute
Mike Hammer, Northern States Power Company
Joe Penland, Science Applications International, Inc.
Jad Popovic, Atomic Energy of Canada Limited

The feedwater control systems in both BWRs and PWRs have been identified in various plant outage studies as being major contributors to plant unavailability. Outage records have shown that major causes of plant outages from failures in the feedwater control system are either attributable to component failures in the analog controllers or in a lesser degree, to erroneous level measurements.

EPRI and Northern States Power Company (NSP) realized that fault-tolerant digital technology could improve Feedwater Control System reliability and operations. The Digital Feedwater Control System (DFCS) developed and implemented at Northern States Power (NSP) Company's Monticello Boiling Water Reactor in Minnesota is the first major fault-tolerant digital control application in a nuclear power plant in the United States. The microprocessor-based controller replaced the analog controller in the feedwater control loop to improve performance and reliability of control including ease of maintenance and spare parts supply. The DFCS at Monticello plant has been operation since July 1986 without any failure of the control system.

This system replaced and upgraded the main and start-up analog controllers at Monticello BWR. It features automatic control, on-line signal validation, controller self-diagnosis, and fault tolerance. The dual-redundant hardware configuration minimizes spare parts availability problems. At a control room panel, operators select each feedwater valve's operating mode (one or three element control, manual, and so on) or set bias inputs for individual feedwater-valve demand. These and other features permit more exact feedwater control system tuning, improving feedwater control in all modes of plant operation. Signal validation using parity-space techniques isolate failed sensors and permit system switching to accurate sensors, thus avoiding outages. To ensure successful operation of the system, extensive verification and validation effort were conducted. These included design reviews, factory acceptance testing using simulation code, site acceptance testing using full-scale plant simulator, and pre-operational and operational testing at Monticello plant.

KHS:3969ST87

The successful development of a high-reliability fault-tolerant digital feedwater control system is a milestone in the U.S. nuclear industry, because it has demonstrated the process of retrofitting a high-technology product into an existing major control loop. The project also demonstrated that, with a strong utility incentive and effort, retrofit with digital technology can take advantage of the plant operation experience to achieve better integration of the primary and balance-of-plant systems.

KHS:3969ST87

For Presentation at the 15th Water Reactor Safety Information Meeting
Gaithersburg, Maryland, October 26-29, 1987

SUMMARY

Expert System Applications to Nuclear Plant for Enhancement of Productivity & Performance

Bill Sun, David Cain, Joe Naser
Robert Colley and Norris Hirota
Nuclear Power Division
Electric Power Research Institute
3412 Hillview Avenue, Palo Alto, CA 94303

Expert systems, a major essence of the artificial intelligence (AI) technology, are referred to as computer software and hardware systems which are designed to capture and emulate the knowledge, reasoning , judgment, and to store the expertise of humans. EPRI has launched a broad-based exploration of potential applications intended to augment the diagnostic and decision-making capabilities of utility personnel for the goal of enhancing utility productivity and performance.

Two parallel efforts are being performed at the Electric Power Research Institute (EPRI) to help the electric utility industry take advantage of the expert system technology. The first effort is the development of expert system building tools which are tailored to electric utility industry applications. The second effort is the development of expert system application prototypes. These two efforts complement each other. The application development tests the tools and identifies additional tool capabilities which are required. The tool development helps define the applications which can be successfully developed.

This paper summaries a number of research projects which are being performed at EPRI in both the areas of expert system building tool development and expert system applications to operations and maintenance. The AI technology as demonstrated by the development is being established as a credible technological tool for the electric utility industry.

A challenge to transferring the expert systems technology to the utility industry is to gain utility users' acceptance of this modern information technology. To achieve successful technology transfer, the technology developers need to (1) understand the problems which can be addressed successfully using AI technology, (2) involve with users throughout the development and testing phases, and (3) demonstrate the benefits of the technology by the users.

KHS:3970ST87

RELAP5/MOD2 DEVELOPMENT*

C. S. Miller
Idaho National Engineering Laboratory
EG&G Idaho, Inc.

ABSTRACT

Status of the RELAP5 code development program at the Idaho National Engineering Laboratory (INEL) is discussed. While RELAP5/MOD2 is undergoing international assessment, emphasis is on user support and code maintenance. User support is in response to user inquiries and a PC-based newsletter service is provided. The FY-1987 activities discussed include the development of a detailed model description document, a software tool for formalized tracking of the configuration of the code, the migration of the code to both larger and smaller computers, and the feedback of user experiences into a development version to become RELAP5/MOD3, which will be the next official released version of the code. Future plans discuss some of the models to be modified and added to RELAP5/MOD3.

INTRODUCTION

RELAP5/MOD2 is a pressurized water reactor (PWR) system transient analysis computer code developed for the U.S. Nuclear Regulatory Commission (USNRC) Safety Research and Regulatory Programs. MOD2 is the latest in the RELAP5 series, having been officially released in April 1984. With the completion of the basic development of RELAP5/MOD2 , emphasis has shifted toward maintenance and user support. This has been accomplished in several ways: response to user inquiries, corrections to reported code errors, provision of a RELAP5 Newsletter Service and enhancement of the code for user convenience.

ESTABLISHMENT OF FROZEN CODE

The International Code Assessment Program (ICAP), sponsored by NRC and member countries, has undertaken a rigorous plan of assessment of current light water reactor safety codes to last approximately three years. The plan calls for the use of "frozen" code versions during this period. This strategy ensures that each member utilizes the same code version. Moreover, the preclusion of code improvements during the assessment period (i.e., only error corrections or user conveniences may be added to code) provides a uniform basis for drawing conclusions on code capability. RELAP5/MOD2 Cycle 36, released in 1985, was designated as the frozen version of RELAP5. Cycles 36.02 through 36.05, reflecting error corrections and user convenience changes only, have been transmitted to all participants.

---

* Work supported by the U.S. Nuclear Regulatory Commission, Office of Nuclear Regulatory Research, under DOE Contract No. DE-AC07-76ID01570.

USER SUPPORT

There were 107 user inquiries in FY-1987. They are divided into a number of general categories as shown in Figure 1. The sector marked "physics" stands for inquiries about physical models in the code such as choked flow, critical heat flux, and condensing heat transfer models. The code is being installed on computers other than the CYBER, which it was originally developed on, and this has given rise to inquiries, as shown by the sector marked "implementation".

The sector termed "user guidance" covers such activities as finding input errors , suggesting alternate input options, and clarifying the manual. The sector marked "mechanics" represents the mechanics of running the code; i.e., restarting and plotting. The "new capabilities" sector stands for an assortment of requests for new code capabilities. The sector marked "performance" represents inquiries about code capabilities in matching experimental data about running time capabilities. The final sector marked "miscellaneous" is an assortment of inquiries not easily categorized.

The RELAP5 Newsletter Service provides a mechanism for serving the many domestic organizations using RELAP5. Membership has grown from an initial three in 1986 to eleven in 1987. This service, supported by the users themselves, utilizes a menu-based electronic newsletter stored on an IBM-PC with an auto-answer modem at the Idaho National Engineering Laboratory. By accessing the newsletter through their own local terminal, users are able to obtain code updates and up-to-date information on development and application activities. Each user may also contribute to the newsletter concerning their usage and experience. A quarterly report summarizing all reported user problems, resolution, and other code modifications is also sent to newsletter service members.

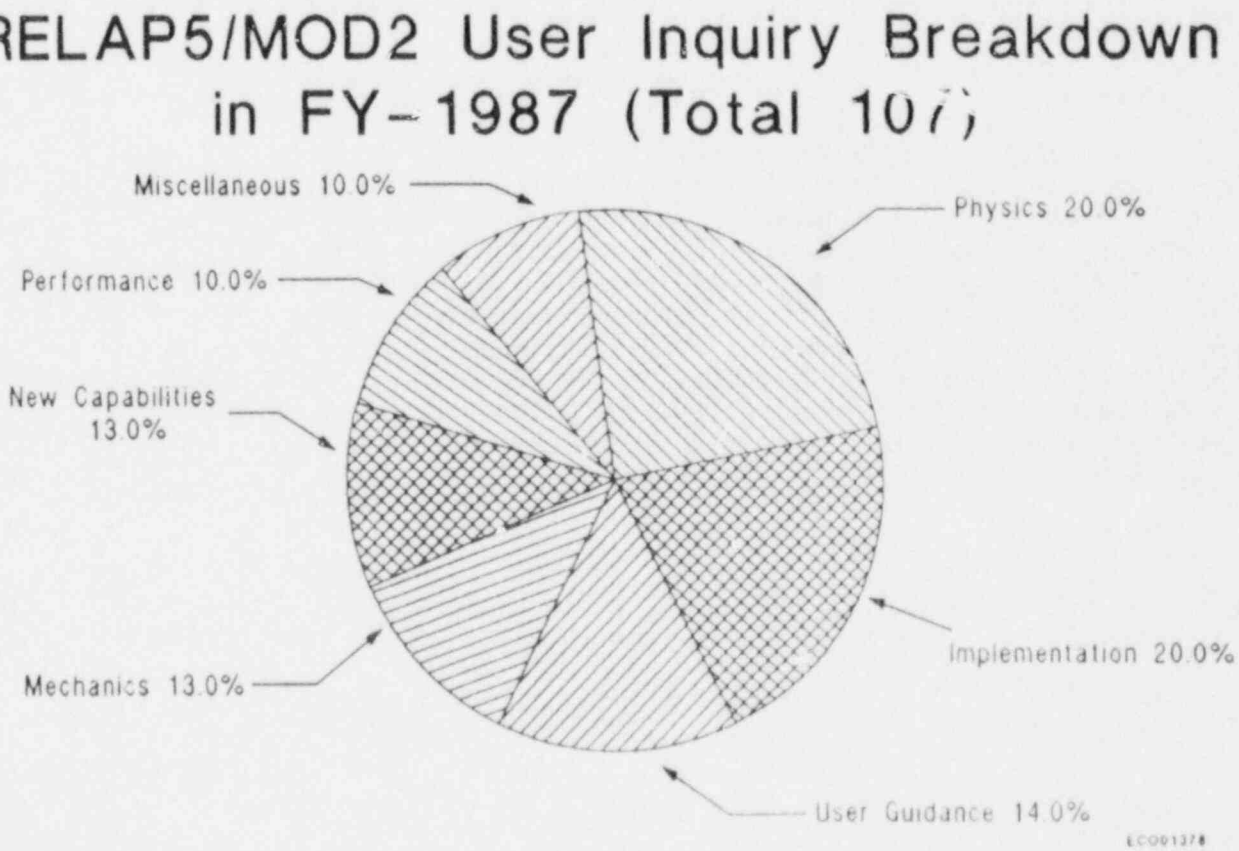

1987 ACTIVITIES

In FY-1987, development of a detailed model description document was started. In this document the constitutive models are being discussed including their original sources, the range and accuracy of the data bases that correlations or models are based upon, the implementation of the models or correlations into the code and any modifications required as a result of putting them into the code. This document will form the basis of a quality assurance check of the models in the code along with the usual developmental, internal and international assessments of the code.

A software tool that has been under development this year is a formalization and automation of the documentation procedure for changes in the code. Instead of individual sheets for user inquiries and update description listings and signoffs, one computer code keeps track of user inquiry, the cognizant engineer, the proposed change, approvals, file names, and releases. The same tool is being used by the TRAC-BWR code developers at INEL and so is unifying the configuration and tracking methods between the two codes.

One of the code improvements that arose out of a user inquiry was an improvement to the nearly implicit (two step) method. The inquiry was regarding a null transient that was running slower than expected with some unexplained oscillations. The solution was near steady state. A close look at debug output showed that a matrix in the velocity solution was being driven to an ill-conditioned form by roundoff error. The solution was changed to precondition the matrix to avoid this situation and for the reported problem showed run time improvement of 30% and a decrease in roundoff error of four orders of magnitude.

RELAP5 is migrating to both larger and smaller computers. In 1987, a CRAY X-MP/24 computer, with a four million word memory and vector as well as multi-processor capabilities, was installed at INEL. This type of machine allows larger problems to be run with the potential for significant run time reductions. Also, development work was started on a RELAP5 version to run on a co-processor board contained in a PC. Currently, the PC version run time is about 25 times that of the same problem running on a CYBER 176. An IBM version of RELAP5 is also available through the conversion work of a international participant.

Feedback from the ICAP program has provided guidance for the next version of RELAP5. During 1987, several key ICAP findings were investigated with a developmental version of the MOD2. These include findings dealing with: (a) the interphase drag; (b) CHF, and (c) CCFL.

Interphase Drag

G. Th. Analytis (EIR, Switzerland) assessed RELAP/MOD2 against rod bundle boil-off and low flood rate reflood experiments and reported that the code overpredicted liquid carryover. Users from Japan and Great Britain reported similar findings. Analytis reported better agreement with data using a modified form of the drift flux correlation developed by Bestion for bubbly/slug flow regime in rod bundles. The Bestion correlation was implemented in the INEL developmental version of MOD3 and Analytis's results were essentially duplicated. This is a candidate improvement for RELAP5/MOD3.

CHF

Users from Sweden have reported from their assessment work that the Biasi CHF correlation used in RELAP5/MOD2 overpredicts CHF. They suggested an alternate correlation, which was studied at INEL for potential use in the MOD3 version. The study pointed out a problem in that the alternate correlation did not cover the full range of reactor pressure conditions. This is still under review.

CCFL

Users have concluded that the coolant distribution is inadequately predicted for certain situations (e.g., large break LOCA flooding at the core tie plate, small break flooding at the steam generator inlet plenum and flooding at tube support plates in once through steam generators) without a counter-current flow limiting (CCFL) model. A general CCFL model, proposed by Bankoff and proposed for use in TRAC-PF1/MOD1, allows the user to select the Wallis form, the Kutateladze form, or a form somewhere between the two. A preliminary form of the Wallis-Kutateladze flooding limit expression was implemented in the developmental version of MOD2 and has been functionally verified.

FUTURE PLANS

Plans for FY-88 call for continued maintenance and user support for RELAP5. In addition, the MOD3 version of RELAP5, to supplant the frozen MOD2 version, will be released. It will embody the improvements stemming from the comments, suggestions and corrections from the combined ICAP, INEL and domestic user community. Improvements will include those models tested in the developmental version during 1987, i.e., interphase drag and CCFL. CHF models will be studied further to seek better agreement with a wider range of data. In addition, the vertical flow regime map will be modified to better account for the effects of large diameter pipes and the vapor pull through and liquid entrainment model will be modified to more accurately model break discharges from pipes with stratified flows. Also, models accounting for sprays and for metal water reactions will be added in RELAP5/MOD3. These modifications and additions will not only allow more accurate calculations with RELAP5/MOD3 but will also extend the code's range of applicability.

For RELAP5/MOD3, most of the machine dependencies have been eliminated but the goal for RELAP5 is to be independent of machine type. The ideal is to maintain one source file that can be compiled on computers from super-computers to PC's. Also, the detailed model description document for RELAP5 will be released delineating the technical basis and limitations of the physical correlations used in the code.

THE STATUS OF THE TRAC-BWR PROGRAM*

Walter L. Weaver, III
Gary W. Johnsen

Idaho National Engineering Laboratory
EG&G Idaho, Inc.

The Transient Reactor Analysis Code for Boiling Water Reactors (TRAC-BWR) is being developed and maintained at the Idaho National Engineering Laboratory (INEL) for the Division of Accident Evaluation, Office of Nuclear Regulatory Research of the United States Nuclear Regulatory Commission (USNRC).

The objective of this development is to provide the USNRC with a detailed, best estimate, efficient computer code for the analysis of postulated accidents and transients in boiling water reactor (BWR) systems. This program is unique among advanced code development projects in that it focuses on the hardware, thermal-hydraulics, and heat transfer phenomena that distinguish BWR systems and their response in transients. In addition to providing a best estimate analysis capability for BWR systems, the code can also be used to address current licensing concerns such as anticipated transients without scram (ATWS) or the small break loss-of-coolant accident (SBLOCA). It also provides analytical support to the USNRC experimental safety programs. The success of this development is attributed in part to the participation of the General Electric Company as a part of the Full Integral System Test (FIST) Experimental Program funded by General Electric, the USNRC, and the Electric Power Research Institute (EPRI).

Work on the TRAC-BWR series of codes began in 1979, starting with a developmental version of TRAC-PD2 received from the Los Alamos National Laboratory. Several versions of TRAC-BWR have been released by the INEL, the latest one being TRAC-BF1, which was released to NRC-approved recipients in June 1986. The manual for this code version was published in August 1986. Work during FY-1987 has focused on improvements to the hydrodynamic models; completion of programming changes for increased portability,

---

* Work supported by the U.S. Nuclear Regulatory Commission, Office of Nuclear Regulatory Research, under DOE Contract No. DE-AC07-76ID01570.

maintainability, and machine independence; preparation of a detailed report describing the constitutive relations and special process models such as the CCFL and critical flow models; and implementation of the hybrid Courant limit violating numerics in the three-dimensional VESSEL component.

Improvements to the hydrodynamic models include the implementation of the Bestion[1] correlation for interfacial friction in rod bundles and implementation of the Megahed[2] correlation for film condensation. The Bestion correlation was investigated as a result of the assessment of TRAC-BD1/MOD1 by EIR in Switzerland as part of the ICAP Program.[3] They assessed the code using low pressure boiloff and reflood experiments run at EIR in the NEPTUN facility and obtained poor agreement between the experiments and data. EIR postulated that the interfacial drag was too high in the bubbly-churn flow regime at the low pressures in the boiloff and reflood experiments. The Bestion correlation was developed to correct similar deficiencies observed in the simulation of low pressure boiloff experiments by the French using the Cathare code, in which the interfacial friction computed using the Zuber-Findley drift flux correlation for the bubbly-churn flow regime resulted in too much mass being ejected from the test assembly. The French had observed using optical probes in a rod bundle experiment that the void tended to migrate to the center of the subchannels while the liquid remained close to the rods. Bestion postulated that a separated flow regime analogous to the annular or inverted annular flow regime existed in rod bundles at low pressures and at low void fractions. The dimensionless number governing this assumed flow regime is the Froude number and he developed a correlation based on this dimensionless group. The constant was correlated using a number of boiloff and container blowdown experiments spanning the complete range of high to low pressures. The resulting correlation gives the same interfacial drag as the Zuber-Findley correlation at high pressure but gives a much lower drag at low pressure. This correlation was tested in the TRAC-BF1 code. Figure 1 shows the results of a simulation of a boiloff experiment in the NEPTUN facility using the Bestion and the Zuber-Findley correlations in the bubbly-churn flow regime. The figure shows a comparison of the measured and computed collapsed liquid levels. The Zuber-Findley correlation gives a higher interfacial friction at the low pressure of the test resulting in too much liquid being ejected from the test assembly, whereas the Bestion correlation

gives a lower drag resulting in a much better agreement with data. The Bestion correlation was also used in the simulation of one of the high pressure level swell experiments run by General Electric and the results are very similar to those computed using the Zuber-Findley correlation as would be expected for these high pressure experiments. The Bestion correlation has been implemented in the TRAC-BF1 code as a result of these simulations and as a result of the assessment of TRAC-BD1/MOD1 by EIR as part of the ICAP Program.

The Megahed correlation has been implemented as a result of the widespread and long standing criticism of the jet condensation correlation which has been used by both TRAC-PWR and TRAC-BWR in the annular flow regime. The jet condensation correlation gives condensation rates that are perceived to be too high. The Megahed correlation was developed recently using data taken at the University of Strathclyde and was compared to a wide data base on condensation in the annular flow regime. Figure 2 compares Stanton numbers measured by Bankoff to those computed by the correlation, and shows excellent agreement was obtained. The correlation gives lower values of the Stanton number than the constant value of 0.02 obtained from the jet condensation data, which should lower the condensation rates in the annular flow regime.

Extensive changes to the FORTRAN coding have been made to yield a code tnat is 99% ANSI Standard FORTRAN-77 for ease of portability and machine independence. The nonstandard FORTRAN has been isolated to a few subroutines and these routines have been flagged for ease of conversion. These changes include provisions for execution on 32 bit machines such as IBM mainframes, minicomputers such as the MASSCOMP 5600 and the VAX, as well as on PC compatible microcomputers with a coprocessor board. Extensive use of parameter variables has virtually eliminated the use of *IF,DEF statements in the program library leading to enhanced portability. The use of character type data has also led to increased machine independence. An IBM version of TRAC-BF1 is currently being tested at Penn State University and should be available in the near future. A CRAY version is also being developed using the CRAY-XMP/24 computer system recently installed at the INEL.

A detailed report, referred to as the "QA" report is currently being written that describes the constitutive relations and the special process models such as the CCFL model and the critical flow model used in the TRAC-BF1 code. This report will describe all of the correlations used in the code, the source of the correlation, and describe the implementation of the correlation in the code including the transitions and interpolations between correlations. The report will also describe any limits on the values obtained from the correlations as well as the rationale behind such limitations. The draft version of this report is due the the USNRC by the end of this calendar year. Similar reports are being prepared for TRAC-PWR and RELAP5.

Finally, the hybrid Courant limit violating numerics previously implemented in the one-dimensional components in TRAC-BF1 has been extended to the three-dimensional VESSEL component. The new numerics will remove the material Courant limit restriction on time step size for VESSEL component. The extension is based in part on the work at the Los Alamos National Laboratory to extend the SETS (two step) numerical procedure to the VESSEL component. The coding as developed at LANL was used as a template for the development of the needed subroutines for TRAC-BF1 but could not be used directly because LANL inverted the VESSEL component data base for ease of vectorizing the VESSEL component. Model development has been completed and several simple test cases have been executed. A completion report describing the code modifications and the results of the test cases has been written and is under review. A more extensive developmental assessment of the extension of the fast numerics to the VESSEL component is planned for FY-88 using several large BWR plant models and a variety of transients and accidents. Preliminary results obtained using the simple test cases indicate that a speedup on the order of a factor of two can be expected when using the new code version.

Work planned for FY-1988 includes improvements in the containment modeling capability of TRAC-BWR; developmental assessment of the hybrid Courant limit violating numerics in the VESSEL component; completion of the code modifications for increased portability, maintainability, and machine independence; and the initiation of the implementation of a three-dimensional neutron statics module for the generation of one-dimensional neutron cross-sections for use in the one-dimensional

neutron kinetics model in TRAC-BF1. In addition, a newsletter similar to the RELAP5 newsletter will be initiated and distributed to all members of a domestic users group. User support will be provided to all domestic and ICAP users of TRAC-BWR and model improvements will be made based on the results of the ongoing assessment of TRAC-BWR by both domestic users and ICAP members. Finally, work will continue on the ongoing task of improving the execution speed of TRAC-BWR through both vectorization and improvements to the code architecture to take advantage of the newer computer systems such as the CRAY.

REFERENCES

1. D. Bestion, "Interfacial Friction Determination for the 1D-6 Equation Two Fluid Model used in the Cathare Code", Minutes of the European Two Phase Flow Group Meeting, Southampton, U.K., June 3-7, 1985.

2. Mohamed M. Megahed, Interfacial Heat Transfer in Countercurrent Flows Of Steam and Water, EGG-RTH-2495, Idaho National Engineering Laboratory, January, 1987.

3. G. Th. Analytis, "Assessment of TRAC-BD1/MOD1 With Boiloff and Reflooding Data: Model Improvements and Numerical Problems", First Specialist Meeting of Code Users (ICAP Program), Erlangen, FRG, June 9-11, 1986.

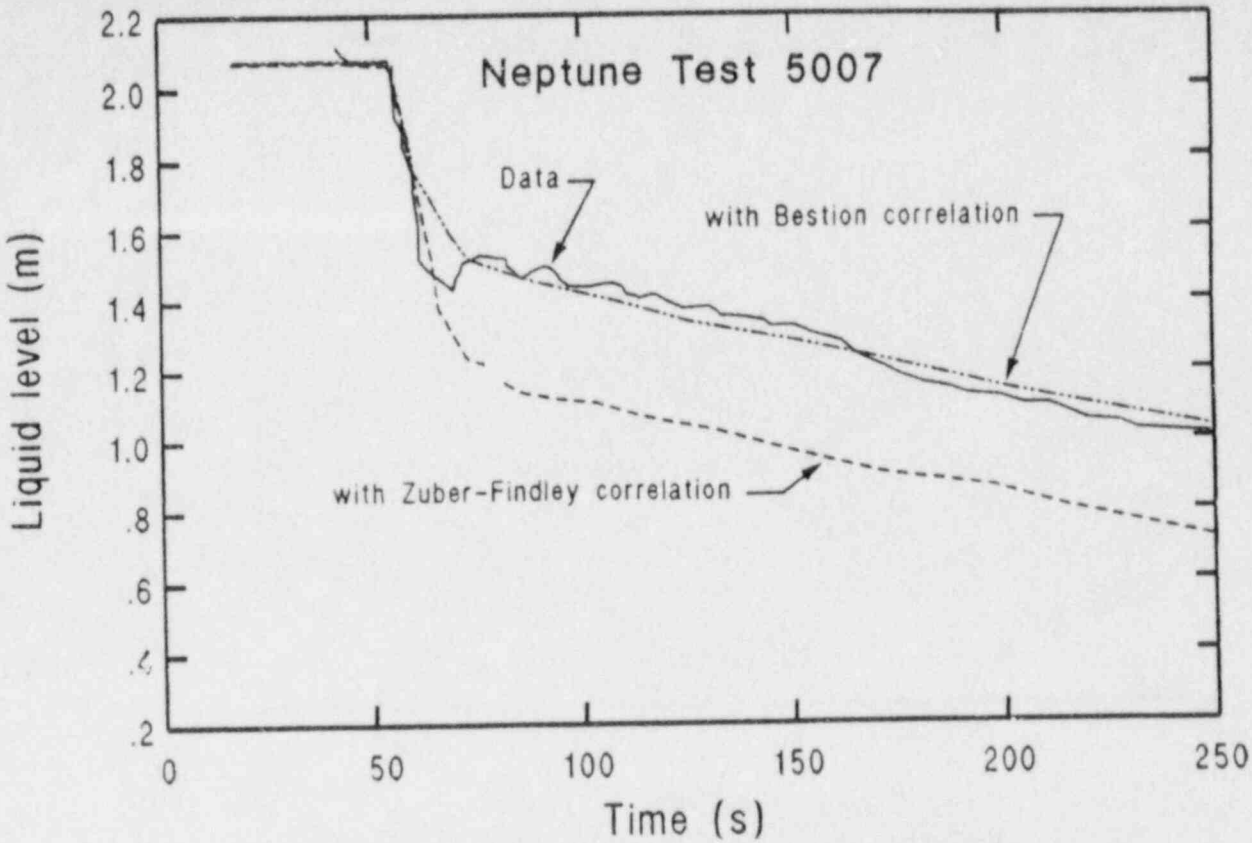

Figure 1. Comparison of measured and computed collapsed liquid levels.

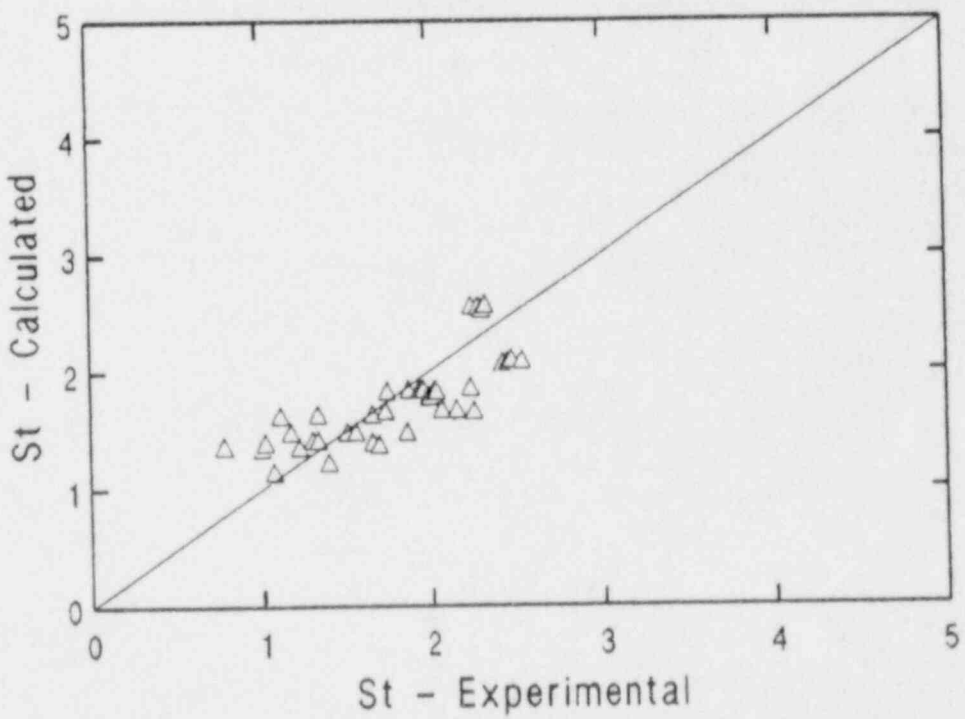

Figure 2. Comparison of measured and computed Stanton numbers.

JRC ISPRA RESULTS FROM ASSESSMENT OF RELAP5/MOD2 ON THE BASIS OF LOBI TEST DATA

H. Städtke, W. Kolar
Commission of the European Communities
Joint Research Centre, Ispra Establishment
I-21020 Ispra, Italy

ABSTRACT

In the framework of the LOBI project, various RELAP5 code versions have been used extensively for test design calculations, pre-test predictions and post-test analysis.

Important results from assessment calculations and code sensitivity studies performed in 1986/87 with RELAP5/MOD2 are presented in this paper. The assessment cases include Small Break LOCA and Special Transients Experiments. From the comparison of measured and predicted parameters, conclusions are drawn on the prediction capabilities of RELAP5/MOD2. Specific problems observed with regard to the automatic time-step control, flow regime selection, interphase heat transfer and break mass flow calculations are analysed.

The significance of these deficiencies are described and recommendations are given for the improvement of the RELAP5 code.

1. INTRODUCTION

The LOBI project represents an important part of the Light Water Reactor (LWR) research programme of the Commission of the European Communities carried out at the Joint Research Centre (JRC) in Ispra, Italy. A status report of the LOBI-MOD2 experimental and analytical programme is given in a separate paper / 1 /.

In the framework of the LOBI project, various RELAP5 code versions have been used extensively for test design calculations, pre-test predictions and post-test analyses. The results obtained can be considered as a substantial contribution to the multi-national effort for the assessment of the RELAP5 code.

The use of RELAP5 within the LOBI project started in 1983 after the conversion of RELAP5/MOD1 / 2 / from CDC to an IBM compatible form had been completed. The IBM version of the code was distributed to different institutions in Europe and the US including the NEA computer library in Paris.

Severe deficiencies observed with RELAP5/MOD1 in a number of LOBI test calculations were the starting point for various model improvements which were implemented into the code in 1984/85 leading to the Ispra version of RELAP5/MOD1 denoted RELAP5/MOD1-EUR / 3 /. This code shows significant improvements compared with the original code version with regard to reliability of predicted data, agreement with measured values and code run times. The RELAP5/MOD1-EUR code has been the main analytical tool within the LOBI project over the last few years.

In 1985/86 the RELAP5/MOD2 code / 4 / was converted from CDC to an IBM compatible form at the JRC-Ispra. In the framework of the US-NRC ICAP activities the IBM version has been distributed to several institutions outside the JRC Ispra, including the Idaho National Engineering Laboratory. Recently the updates up to cycle 36.05 have been implemented into the IBM code version. For a number of selected LOBI experiments, post-test calculations and code sensitivity studies have been performed with the RELAP5/MOD2 code. The results of these activities are summarized in this paper.

2. RELAP5 CODE VERSIONS USED

The calculated data shown in this paper were obtained with two different RELAP5 code versions:

IBM Version of RELAP5/MOD2 Cycle 36.04 (identifier RELAP5/MOD2)

The conversion of the code to an IBM compatible form was performed at the JRC Ispra in 1985/86. The correct implementation was checked by a large number of calculations using the original CDC and the IBM version of the code. This included the test cases received with the transmittal tape as well as detailed LOBI test calculations. The nearly identical results obtained indicate that the IBM version can be considered as a full equivalent to the original CDC code version.

IBM Version of RELAP5/MOD1-EUR (identifier RELAP5/MOD1-EUR)

The code is an improved version of the RELAP5/MOD1 code / 3 /. The code includes a number of model changes which were implemented in 1985/86 in order to overcome severe problems encountered with the original RELAP5/-MOD1 version. The main improvements in RELAP5/MOD1-EUR concern changes to the following models and processes:

- the non-equilibrium evaporation and condensation model
- the calculation of junction properties from adjacent volume data for low flow velocities and near stagnation conditions
- the finite difference form of the momentum flux terms in the momentum equations
- the choking model for upstream two-phase flow conditions
- the interphase drag calculation and the implementation of interphase drag models
- the prediction of state properties for liquid and vapour

Compared with the original code version, RELAP5/MOD1-EUR shows a considerable improvement with regard to the reliability of the predictions the agreement with measured data for a large number of LOBI experiments, and reduction of code run times. In all applications the code has been proven to be very robust, e.g. no code failures occurred due to numerical instabilities as were frequently observed with RELAP5/MOD1 and with RELAP5/MOD2. In the present study the RELAP5/MOD1-EUR is used as a Benchmark code to help in the analysis of discrepancies in the RELAP5/MOD2 predictions.

3. LOBI Experiments Selected for Assessment of RELAP5/MOD2 at the JRC-Ispra

Although the JRC-Ispra improved version of RELAP5/MOD1 (RELAP5/MOD1-EUR) has been the main analytical tool in supporting the LOBI experimental programme, post-test calculations and analyses were performed with RELAP5/MOD2 for selected LOBI experiments as a contribution to the international assessment programme for this code. The following LOBI experiments have been selected for the RELAP5/MOD2 assessment studies:

LOBI-MOD2 test A1-04R: Double-ended (2 x 100 %) large break LOCA test, break position in the cold leg pipe, accumulator injection only into intact loop cold leg.

LOBI-MOD2 test A2-81: 1 % small break LOCA test, break position in the cold leg pipe, emergency core cooling provided by HPIS connected only to intact loop cold leg.

LOBI-MOD2 test A1-83: 10 % small break LOCA test, break location in the cold leg pipe, emergency core cooling comprises HPIS injection into the hot leg pipe and combined accumulator injection into hot and cold leg pipes.

LOBI-MOD2 test A2-90: Simulation of a loss of normal onsite and offsite power with additional failure to SCRAM.

LOBI-MOD2-test BT-00: Simulation of a loss of main feedwater transient

For some of these experiments results of post-test calculations using RELAP5/MOD1-EUR and RELAP5/MOD2 have been presented already at the 14th Water Reactor Safety Information Meeting in Gaithersburg 1986 / 5 / and at the Topical Meeting for Anticipated and Abnormal Transients in Nuclear Power Plant in Atlanta 1987 / 6 /. In some cases, especially for the tests A2-90 and A1-83 relatively large differences between measured and predicted data were obtained for RELAP5/MOD2. In order to analyse these discrepancies, a large number of sensitivity studies have been performed with respect to numerical convergency, nodalization influences and model changes. The results of these studies are presented in the following.

The LOBI test facility and the basic RELAP5 nodalization scheme as used in all the predictions are shown in Figs. 1 and 2.

4. Results of RELAP5/MOD2 Code Assessment on the Basis of LOBI Test Data

4.1 General Remarks

Some of the severe problems encountered with the RELAP5/MOD1 code are solved in RELAP5/MOD2. For example the large numerical fluctuations in many of the predicted flow parameters as were typical for RELAP5/MOD1 are considerably reduced. Furthermore, the frequent time step reductions as result from mass error checks in RELAP5/MOD1 are largely reduced which led to a significant speed-up of the predictions, especially for slow transients. Two main reasons have contributed to the generally improved performance of RELAP5/MOD2: (1) an additional step in the numerical procedure, where at the end of a time step the final state variables are calculated from non-expanded (conservative) forms of the mass and energy balance equations and (2) changes to the interphase drag calculation including the handling of flow regime transitions and the implementation of the interphase drag models into the code.

The improvements in RELAP5/MOD2 are not, as often presumed, a result of the treatment of complete thermal non-equilibrium and the addition of a second energy equation. This is clearly demonstrated by the JRC-Ispra improved version of RELAP5/MOD1 which has kept most of the basic

features of RELAP5/MOD1 like the restriction to partial thermal non-equilibrium conditions (one phase assumed to be saturated) and the use of only one (mixture) energy equation. The generally good agreement of RELAP5/MOD1-EUR predictions with measured data for many different experiments and the considerable reduction of the CPU-times was achieved by introducing several changes to the code in order to reduce the large number of discontinuities and inconsistancies as found in the original code version.

Although several deficiencies of RELAP5/MOD1 have been resolved in RELAP5/MOD2, some problems still remain or have been newly created by other substantial changes to the code. The increased degree of freedom introduced by the assumption of complete thermal non-equilibrium demands additional constitutive models and correlations for which no, or only a very limited, data base exists. Examples are the interphase heat transfer correlations for vapour and liquid, the partitioning of wall heat transfer between the vapour and liquid phase and the distinction between latent and sensible part in the heat transfer rate from the wall to the individual phases. An attempt to describe these very complex heat transfer conditions in RELAP5/MOD2 seems to make the code predictions more sensitive to time-step selection and control as will be shown later. Another concern is related to the change in the implementation of the interphase drag models in RELAP5/MOD2 which, as will be demonstrated, can result in a large influence of the nodalization on the predicted results.

4.2 Time-Step Control and Numerical Convergency

In all the RELAP5 code versions a semi-implicit numerical method is applied to solve the governing field equations, where only those terms are treated implicitly which contribute to the pressure wave propagation or which are known to have small time constants. The heat transfer from the wall to the fluid is handled completely explicitly, which means that the heat flux between structure and fluid is based exclusively on previous time-step values. An additional constraint introduced is that all implicit terms are taken linearly in the new time values. This approach reduces the numerical problem to be solved to a system of linear equations for the new pressure values for each individual volume and the adjacent connecting volumes. This linear system of equations can be solved very efficiently by a sparse matrix solution technique without iteration steps.

For the time-step control the code user has the choice between a number of different options. In the generally recommended (and most stringent) option the time-step selection is based on two major criteria: (1) the material Courant limit evaluated on the basis of average volume phase velocities and (2) an estimation of the mass error evaluated from the difference between the mixture density calculated from the mixture mass conservation equation and the mixture density as determined by the state equations.

The use of expanded forms of the mass and energy conservation equations in RELAP5/MOD1 together with a large number of discontinuities in the constitutive relations resulted in many cases in a drastic reduction of the time-step size below the material Courant limit. As a consequence excessive CPU-times were observed especially for slow transients with low flow velocities. This has been largely improved in RELAP5/MOD2 by the introduction of a second (correction) step in the numerical procedure where the non-expanded, conservative forms of the mass and energy equations are used to calculate the final volume state parameters.

Although no systematic time-step convergency studies have been performed with RELAP5/MOD2, it might be concluded from many code applications that stable and accurate results can be obtained. However, the complete explicit treatment of the wall heat transfer together with a time step control procedure based only on hydraulic criteria may result in severe stability problems when the wall heat transfer and the flow phenomena are strongly coupled, e.g. for natural circulation conditions. This will be explained in the following by the post-test calculations and sensitivity studies performed for LOBI test A2-90 / 7 /, a simulated loss of power transient without SCRAM (ATWS case).

In a base calculation using the recommended option for an automatic time step control a far too fast a pressurization was predicted starting at 20 s into the transient after two-phase conditions occurred in the core, upper plenum and hot leg pipes. The maximum primary system pressure was largely overpredicted by about 25 bar (Fig. 3). In addition unrealistic discontinuities and fluctuations were calculated for many parameters including pressure (Fig. 3) and phase velocities at the core outlet (Fig. 5) and in the hot leg pipe of the triple loop (Fig. 7). The average time-step size as calculated by the code was within the range between 0.1 s and 0.2 s.

In a second calculation the time-step size was reduced by about one order of magnitude to 0.01 s. In this case all the numerical oscillations as observed in the base case calculation disappeared (Fig. 6 and 8) and the overprediction of the primary system pressure was drastical-

ly reduced (Fig. 4). A third calculation with a further reduction of the time-step size to 0.001 s did not show any remarkable difference to the second calculation which means that numerical convergency had been reached with a time-step size of 0.01 s.

The large sensitivity of the predicted results for LOBI test A2-90 with respect to time-step size leads to the following conclusions:

(1) RELAP5/MOD2 assessment studies without the check of time-step convergency may lead to wrong conclusions with regard to the prediction capabilities of the code.

(2) The existing criteria for the automatic time-step control in RELAP5/MOD2 are not sufficient. There exists a strong need for an additional time-step constraint with respect to the energy conservation and/or convergency of the wall heat transfer.

(3) To avoid extremely small time step sizes in case of strong coupling between wall heat transfer and fluid flow, the wall heat transfer should be treated at least in a semi-implicit manner, e.g. by using advanced time values for the fluid temperatures in the driving force for the wall heat flux. This could be implemented without large changes to the code since new time level values for the fluid temperatures are available and already used for the interphase heat transfer processes.

4.3 Flow Regime Maps

In RELAP5/MOD2 the basic structure of the flow regime maps as used already in RELAP5/MOD1 has been retained where the various two-phase flow regimes are identified on the basis of void fraction and mass flux. However, two additional flow regimes have been added which did not exist in the MOD1 version: a slug flow regime for intermediate void fraction between the bubbly and annular-mist flow regimes and the possibility of stratified conditions in vertically orientated volumes. For the definition of the different flow regimes new (dynamic) criteria have been introduced which are mainly based on the work of Taitel and Dukler / 8 / and Ishii / 9 /.

Stratified conditions in a vertical volume are assumed to exist if the following two criteria are fulfilled: (1) the mass flow density has to be below a critical value based on the conditions that the rise velocity of small vapour bubbles exceeds that of a Taylor bubble and (2) the difference in void fraction of the volume above and below has

to be larger than 0.5. If stratified conditions are identified in a volume the interphase heat transfer coefficients are drastically reduced which leads to strong deviations of both phases from the thermal equilibrium (saturation) conditions.

The way in which vertical stratification model is implemented has some consequences for dead-end volumes and for configurations where the volume orientation changes. For the cases of dead-end volumes the second criteria for vertical stratification is reduced to conditions where the void fraction in the volume below is less than 0.5. The same criteria as for dead-end volumes is applied for cases where the volume above is horizontal orientated. This means that stratified conditions may occur if the void fraction in the volume below is less than 0.5, regardless of the condition in the (horizontal) volume connected to the upper side of the volume. As a consequence, the thermodynamic conditions in a volume can largely be influenced by the orientation of a volume to which it is connected, even if the adjacent volume is relatively small. This can result in an unjustified strong influence of the nodalization on the predicted transient as will be shown for LOBI-MOD2 test A2-90.

In the RELAP5 base input deck for the LOBI test facility the relief line on top of the pressurizer was modelled by a single volume, having a slight inclination of 11 degrees (Fig. 9) which is treated by the code as a horizontal volume. For this configuration vertical stratified conditions are calculated for the top of the pressurizer over a long period of the transient leading to an excessive degree of superheating for the vapour (Fig. 11) and, as a consequence, to an overprediction of the primary system pressure (Fig. 12). Changing the nodalization of the relief line into two volumes with a vertical part at the pressurizer outlet (Fig. 9) considerably shortens the period for stratified conditions and the reduced degree of vapour superheating (Fig. 11) results in a more realistic prediction of the primary system pressure (Fig. 12).

The vertical stratification model as described above is a typical example of a 'home-made' model or correlation for which no data base or reference exists. Under certain conditions, these models might improve the calculated results, however, before implementing in the code they should be assessed against measured data from separate effects experiments.

A further problem with regard to the flow regime selection has been identified for transition from bubbly to slug flow. The dispersed bubbly flow regime is generally assumed to exist for low void fractions in horizontal and vertical flow channels. Characteristic for bubbly

flow is a large interfacial area per fluid volume which leads to a strong thermal and mechanical coupling between the two phases. With the increase of void fraction, the structure of the two-phase flow tends to change to the slug flow regime which is accompanied by a considerable reduction of the interfacial area. Therefore, compared with bubbly flow conditions, larger deviations from the thermal and mechanical equilibrium are expected for the slug flow conditions.

As a criterion for the transition from bubbly to slug flow Ishii et al. / 9 / suggested a constant void fraction of $\alpha_{tr} = 0.25$. This is used in RELAP5/MOD2 as a maximum value for the void fraction for which bubbly flow conditions can exist. In addition a correlation of Taitel and Dukler / 8 / is applied which can shift the transition void fraction to very low values, especially for tubes with small diameter. The transition criterion of Taitel and Dukler is based on experimental data obtained for air-water adiabatic flows in small tubes. It is doubtful whether this correlation can be applied also for boiling two-phase flow conditions and for rod bundles. For example, for a typical core geometry with a hydraulic diameter of about 0.01 m transition to slug flow is predicted to occur already at $\alpha \leq 0.01$. This means that the bubbly regime is largely suppressed even for nucleate or subcooled boiling conditions. The resulting consequences for the interphase heat transfer rates will be discussed in the next paragraph.

4.4 Interphase Heat Transfer

The basic assumption of a partial equilibrium between the two phases in RELAP5/MOD1 has largely simplified the modelling of interface and wall heat transfer processes. The description of heat and mass transfer phenomena at the interface can be reduced to a correlation for the evaporation/condensation rate determined by the difference between the static vapour quality and a corresponding equilibrium value as a driving force. The use of only one energy equation for the whole two-phase mixture allows the direct application of all the existing boiling and condensation heat transfer correlations which were developed in the past from a large experimental data base on the assumption of thermal equilibrium conditions in the two-phase mixture. The partitioning of the wall heat transfer between the liquid and vapour phases is done implicitly by the constraint that the least massive phase is assumed to be saturated. The fact that this restriction is adequate for many transients has been shown by the good agreement between measured and predicted data using the RELAP5/MOD1-EUR code for a large number of LOBI experiments.

The assumption of a complete thermal non-equilibrium in RELAP5/MOD2 and, as a consequence, the need for two separate energy equations has largely extended the heat transfer processes to be described. This includes the heat transfer from the interface into the liquid and vapour phase, the partitioning of the total heat transfer from the wall into the fraction of liquid and vapour respectively, and the distinction between the part of the wall heat flux which results in an increase of internal energy of the individual phases (sensible heat) and that part which contributes directly to a phase change (latent heat). For most of these processes no experimentally verified correlations exist and, therefore, 'home-made' correlations are used which largely rely on engineering judgement. Often, the final coding of the correlation used differs considerably from those documented in the code manual. An example is given in the following for modelling of the interphase heat transfer to the liquid phase.

For subcooled conditions $T_f < T_{sat}$ the heat transfer from the interface to the liquid phase is calculated using a semi-empirical correlation derived from subcooled flow boiling experiments by Unal / 10 /. However, compared with this reference the correlation used in RELAP5/MOD2 has been significantly modified which leads to a reduction of the interphase heat transfer coefficient by up to one order of magnitude as shown in Fig. 10. This reduction of the interphase heat transfer coefficient together with the suppression of the bubbly flow regime as explained in paragraph 4.3 result in an unrealistic large degree of subcooling for the liquid phase during subcooled boiling conditions for LOBI-MOD2 test A2-90 (Fig. 13). Using the original Unal's correlation for the interphase heat transfer and a minimum void fraction of $\alpha_{tr} = 0.10$ for the transition from bubbly to slug flow reduces the degree of subcooling by about 50 % (Fig. 13) and yields an improved prediction for the primary system pressure (Fig. 14).

From the evaluation above it might be concluded that the relatively large number of additional correlations and new assumptions introduced in RELAP5/MOD2 demand a systematic verification of the complete interface and wall heat transfer processes on the basis of separate effects test data.

4.5 Implementation of Interphase Drag Model

As for most hydraulic codes, a staggered mesh is used in RELAP5 as a basis for the evaluation of the finite difference equations representing the conservation of mass, momentum and energy. In this approach, the scalar or state parameters are defined at the cell (volume) centres

and the vector or flow quantities are related to the cell boundaries (junctions). It seems to be natural that the interphase drag as a vector parameter is defined as a junction quantity, as is done in all the RELAP5 code versions. However, the way in which the interphase drag model is implemented differs considerably between the code versions.

In RELAP5/MOD1 a rather complex averaging procedure is applied as explained in the the following. In a first step average void fraction and density values are calculated for all junctions from the two adjacent volumes using the volume sizes as weighting factors. In a second step the interphase drag coefficients are calculated on the basis of junction quantities using the flow regime map as defined for the upstream (donor) volume. In a third step volume related interphase drag coefficients are calculated as the arithmetic mean over all inlet and outlet junctions connected to this volume. In a fourth step the final interphase drag coefficients are calculated for all junctions as an average of the corresponding values from the upstream and downstream volumes using again the volume sizes as weighting factors. This procedure for the interphase drag calculations has two major disadvantages: (1) the use of the upstream flow regime results in a discontinuous change of the interphase drag value in case of a flow reversal and (2) due to the subsequent averaging processes the junction with the largest interphase drag value dominates all other junctions connected to this volume. As a consequence, local phase separation cannot be calculated.

In the RELAP5/MOD1-EUR code the implementation of the interphase drag calculation has been largely simplified. The first step, where average junction values for void fraction and density are calculated, is identical with the original code version. In the second step the values for the interphase drag coefficients for all junctions are calculated based on junction quantities and using the flow regimes identified in both, the upstream and downstream volumes. In a third step the final interphase drag coefficients are calculated as an average of the two values as determinated in step 2 using the volume sizes as weighting factors. The new procedure used in RELAP5/MOD1-EUR avoids discontinuous changes of the interphase drag coefficient and provides a more realistic prediction of local phase separation phenomena especially in the case of branch components with multiple junction connections.

Compared with RELAP5/MOD1 a completely different approach has been chosen for the implementation of the interphase drag calculation in RELAP5/MOD2. In a first step interphase drag coefficients are calculated for all volumes on the basis of exclusively volume related quantities. The final interphase drag coefficients for all junctions are

calculated in a second step as the average of the corresponding values for the upstream and downstream volumes using the volume sizes as weighting factors. This procedure avoids discontinuities in the interphase drag calculation similar to RELAP5/MOD1-EUR. However, the use of volume average velocities rather than junction velocities for the calculation of the interphase drag coefficient can result in completely unrealistic slip velocities, if the junction flow cross section is considerably smaller compared with the cross section in the adjacent volumes. This is demonstrated in the following in the RELAP5/MOD2 predictions for LOBI-MOD2 test A1-83.

For the LOBI-MOD2 10 % small break LOCA test A1-83, the standard nodalization scheme is used where the break is modelled as a motor valve connected to the pump side of the broken loop cold leg. With the RELAP5/MOD1-EUR code, a generally good agreement between measured and predicted quantities was achieved for all relevant parameters including primary system pressure (Fig. 15) and primary system mass inventory (Fig. 16). This suggests also that the break mass flow (Fig. 17) is accurately predicted.

Completely different results were obtained with RELAP5/MOD2 for the same LOBI experiment. Although using identical code input data as for RELAP5/MOD1-EUR, extremely large deviations from the measured data were predicted with RELAP5/MOD2, as can be seen for the primary system pressure (Fig. 15) and mass inventory (Fig. 16). This behaviour is in contrast to other LOBI test calculations performed with RELAP5/MOD2 which generally show a reasonable agreement with the experiment.

The reason for the large deviations shown in the RELAP5/MOD2 results for LOBI test A1-83 is obviously caused by a considerable underprediction of the break flow as can be concluded from the comparison of measured and predicted data for the primary system mass inventory (Fig. 16). After the occurrence of stratified flow conditions upstream of the break at about 50 s into the transient, excessive large differences in the phase velocities were calculated (Fig. 18) which led to the large drop in the break mass flow (Fig. 17). This behaviour is a direct consequence of the way in which the interphase drag model is implemented into the code. For critical flow conditions, as exist in the break for long periods of the LOCA, the interphase drag coefficient for the break junction is calculated in RELAP5/MOD2 exclusively on the basis of the flow regime and the volume average flow velocities taken from the upstream volume. With the transition to stratified flow in the main pipe, the interphase drag coefficient is strongly reduced which leads to a considerable de-coupling of the two momentum equations and, as a consequence, to the prediction of extremely large slip velocities in the break area.

The large sensitivity of the break mass flow calculation in RELAP5/MOD2 with respect to the flow regime upstream of the break can be significantly reduced if homogeneous conditions are specified for the break in the code input data. With this flow option more realistic values for the break mass flow were calculated as can be concluded from the predicted and measured primary side mass inventory (Figs. 20 and 21), which resulted in a generally improved agreement of the predicted data with the experiment, as shown for the primary side pressure (Fig. 19).

The procedure applied in RELAP5/MOD2 for the calculation of the interphase drag coefficients can also result in a strong sensitivity of the predicted data with respect to the nodalization chosen by the code user. This is demonstrated in Figs. 23 to 26 where the results of two calculations are shown which differ only in the nodalization of the break.

In the base case calculation the break junction (motor valve) was connected to the pump side of the broken loop cold leg. The results obtained show strong deviations from the measured data as already discussed. Changing the connection of the break component to the pressure vessel side of the cold leg pipe, completely different results were calculated as shown for example for the primary system pressure (Fig. 23), for the primary mass inventory (Fig. 24) and for the break mass flow and phase velocities (Figs. 25 and 26).

The strong sensitivity of the RELAP5/MOD2 predictions with respect to the break nodalization can be explained by the differences of the flow conditions between the pump side and the vessel side of the cold leg pipe. The considerably larger vapour velocities in the pipe between the break and the vessel result in a delay for the occurrence of stratified flow conditions and in generally larger values for interphase drag coefficient for the break junction. As a consequence more realistic phase velocities were predicted for the break which resulted in a generally better agreement of the prediction with the experiment.

5. Conclusions and Recommendations

For selected LOBI experiments assessment calculations have been performed using RELAP5/MOD2. The predicted results show in general a good, or at least a reasonable agreement with measured key parameters. However, for experiments simulating intermediate break LOCA and Special Transients with pressurization of the primary system, relatively large discrepancies have been observed in the RELAP5 predictions with respect to the experiment.

In order to investigate the deficiencies obtained in the predictions for specific LOBI experiments, a number of code sensitivity calculations were performed with respect to time-step convergency, influence of nodalization, and model changes. The results of these studies can be summarized as follows:

- The completely explicit treatment of the wall heat transfer together with the relatively complex modelling of the coupled interphase and wall heat transfer processes can result in numerical istabilities, especially for transients having a strong coupling between wall heat transfer and fluid flow.
- The existing time-step control in RELAP5/MOD2 is not sufficient to guarantee time-step convergence for all transient conditions.
- The way in which the vertical stratification model is implemented in RELAP5/MOD2 may result in an unjustified influence of the nodalization on the predicted system behaviour.
- The procedure chosen in RELAP5 for the implementation of the interphase drag model can result in completely unrealistic flow conditions in the break and in a large sensitivity of the predicted results with respect to small changes in the break nodalization.
- For a number of correlations, a completely different form is used in the code compared with the original equation or with the information given in the manual. At least in some cases, the modified version leads to a worse agreement with the experiment as would be the case using the original correlation.

It is felt that the problem areas identified for RELAP5/MOD2 could be solved within the existing code structure and numerical solution technique. The necessary improvements would concern the following items:

- Extension of the time-step control with regard to energy conservation and/or convergency for wall heat transfer.
- Introduction of a partially implicit treatment for the wall heat transfer process using new (advanced) time values for the fluid temperature as already done for the interphase heat transfer.
- Use of junction phase velocities rather than average volume flow velocities for the calculation of interphase drag coefficients.
- Well-defined criteria for the occurrence of stratified conditions in vertically orientated volumes.

In addition, it is strongly recommended to provide a more detailed documentation of the code, especially for the large number of correlations used and their implementation in the numerical structure. This

documentation could serve as a basis for all future improvement to the RELAP5 code which might become necessary as a result of the ongoing assessment of the code.

References

/ 1 / L. Piplies, C. Addabbo
LOBI-MOD2 Small Break LOCA and Special Transients Programme - Status and Future Plans
15th Water Reactor Safety Information Meeting, Gaithersburg, October 26-29, 1987

/ 2 / V. Ransom, et al.
RELAP5/MOD1 Code Manual, Vol I and II
Idaho National Engineering Laboratory, NUREG/CR-1826 EGG-2070

/ 3 / H. Städtke, W. Kolar
Prediction Capabilities of RELAP5/MOD1-EUR, an Improved Version of the LWR Safety Code RELAP5/MOD1
European Nuclear Conference ENC 86, Geneva, June 1-6, 1986, Transactions Volume 3, 535-542

/ 4 / V. Ransom, et al.
RELAP5/MOD2 Code Manual, Vol I and II
Idaho National Engineering Laboratory, NUREG-4312, AGG-2396

/ 5 / W. Kolar, H. Städtke, B. Worth
JRC-Ispra Experience with the IBM version of RELAP5/MOD2
14th Water Reactor Safety Information Meeting, Gaithersburg, October 1986

/ 6 / B. Worth, H. Städtke
Post-Test Analyses of LOBI-MOD2 Special Transients Tests
Topical Meeting on Anticipated and Abnormal Transients in Nuclear Power Plants, Atlanta, Georgia, April 12-15, 1987

/ 7 / J. Sanders, E. Ohlmer
Experimental Data Report on LOBI-MOD2 Test A2-90
Commission of the European Communities, Joint Research Centre Ispra
Communication No. 4031, LEC 85-35, October 1985

/ 8 / Y. Taitel, D. Bornea, A. Dukler
Modelling Flow Pattern Transition for Steady Upward Gas-Liquid Flow in Vertical Tubes
AiCHE Journal, Vol. 26, pp. 345 - 354, 1980

/ 9 / M. Ishii, K. Mishima
Study of Two-Fluid Model and Interfacial Area
NUREG/CR-1873, ANL-80-111, 1980

/10 / H. Unal
Maximum Bubble Diameter, Maximum Bubble-Growth Time and Bubble-Growth Rate during the Subcooled Flow Boiling at Water up to 17.7 MN/m^2
Inter. Journal of Heat and Mass Transfer, Vol. 19, pp. 643 - 649, 1976

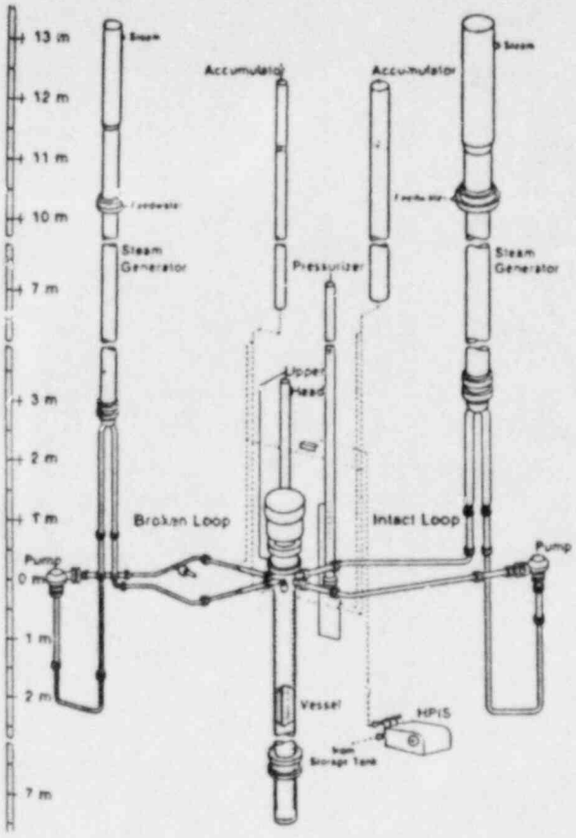

FIG. 1: LOBI-MOD2 TEST FACILITY

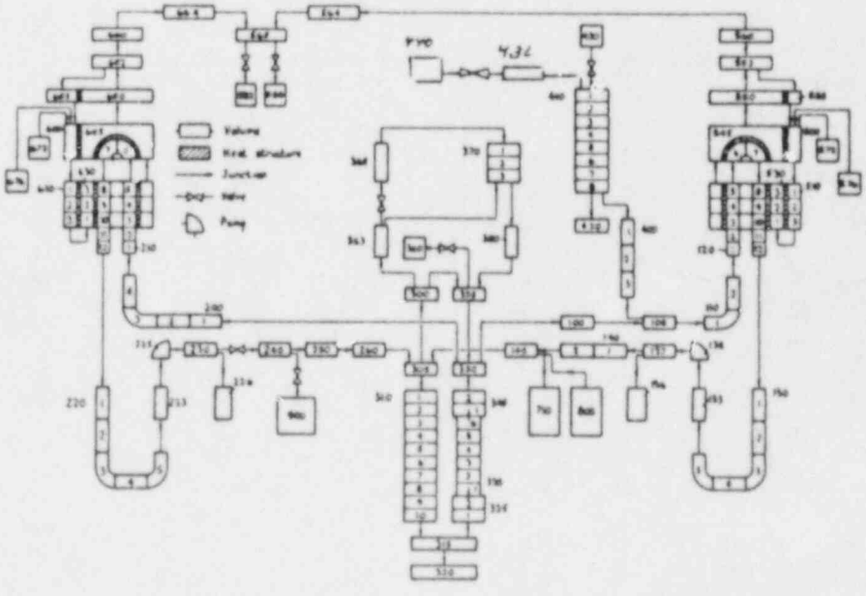

FIG. 2: STANDARD NODALIZATION FOR LOBI FACILITY

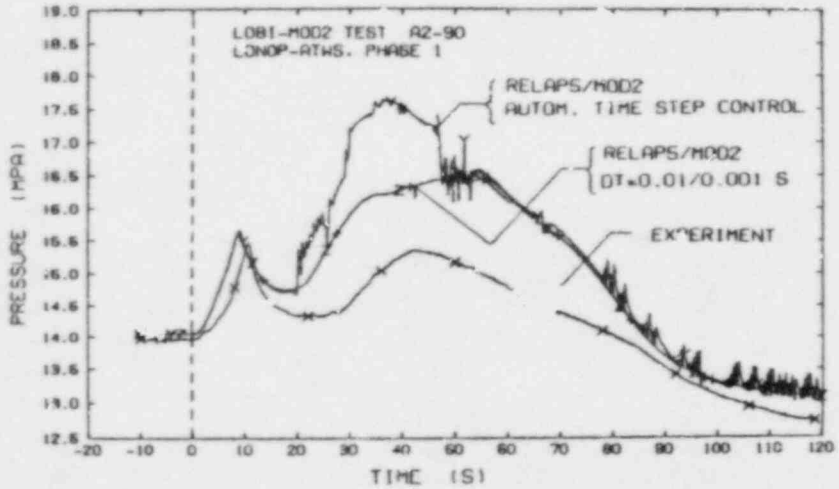

FIG. 3: PRESSURE IN UPPER PLENUM
RELAPS/MOD2: INFLUENCE OF TIME STEP SIZE

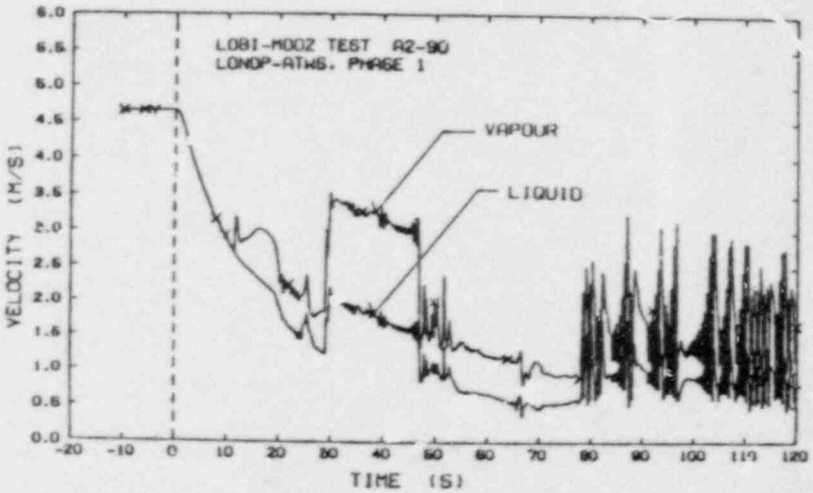

FIG. 5: CALCULATED PHASE VELOCITIES AT CORE OUTLET
RELAPS/MOD2: AUTOMATIC TIME STEP SELECTION

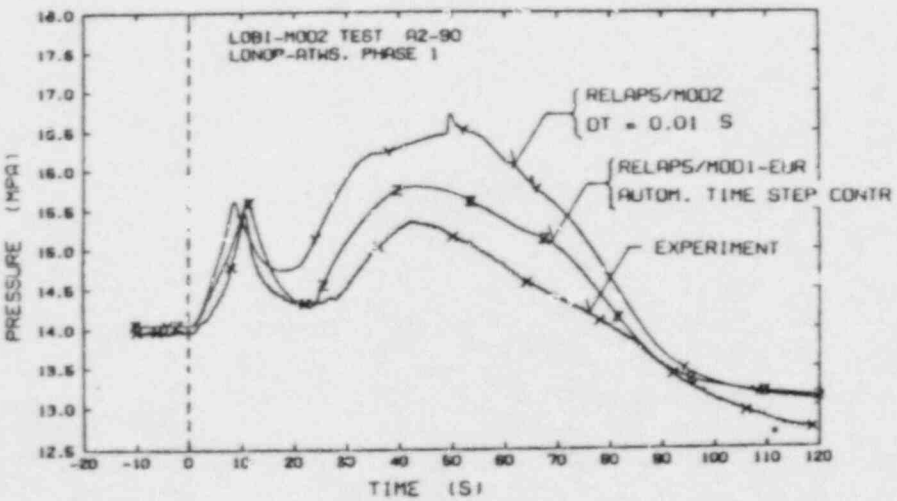

FIG. 4: PRESSURE IN UPPER PLENUM
COMPARISON RELAPS/MOD2 AND RELAPS/MOD1-EUR

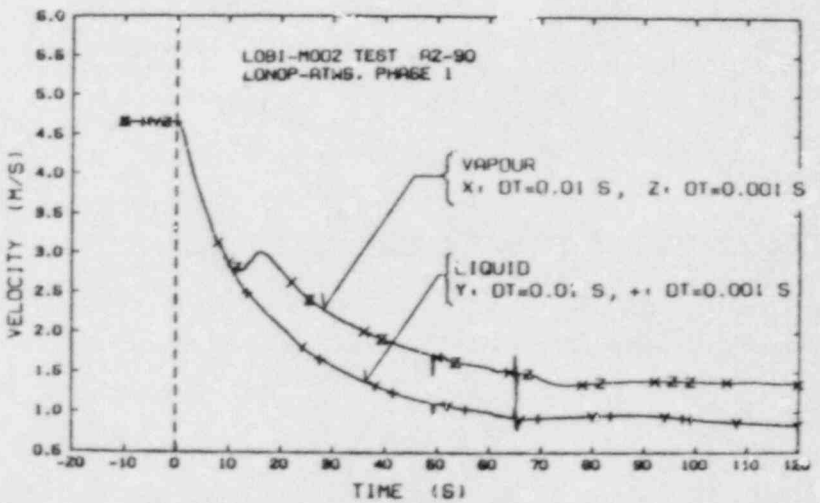

FIG. 6: CALCULATED PHASE VELOCITIES AT CORE OUTLET
RELAPS/MOD2: REDUCED MAXIMUM TIME STEP SIZE

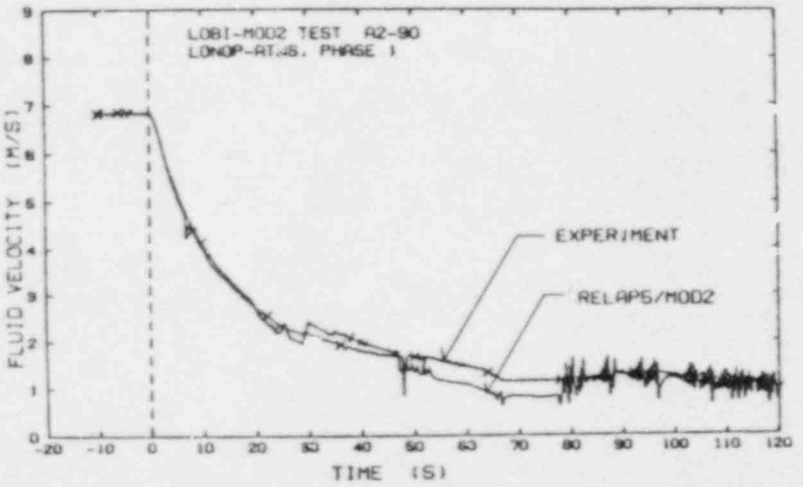

FIG. 7: LIQUID VELOCITY IN TRIPLE LOOP HOT LEG
RELAP5/MOD2, AUTOMATIC TIME STEP CONTROL

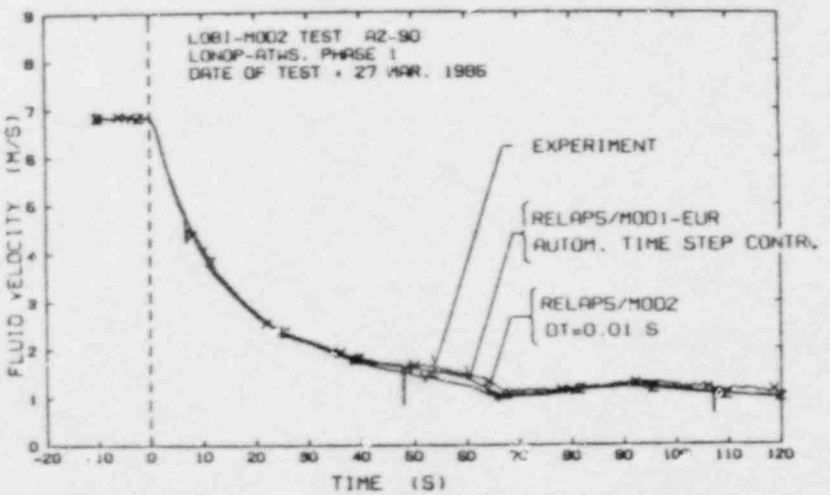

FIG. 8: LIQUID VELOCITY INTRIPLE LOOP HOT LEG
COMPARISON OF RELAP5/MOD2 AND RELAP5/MOD1-EUR

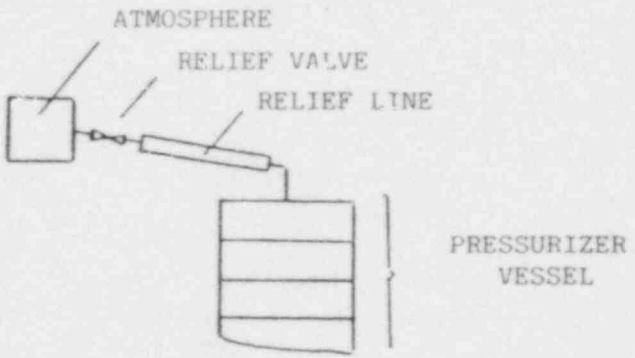

NEARLY HORIZONTAL CONFIGURATION

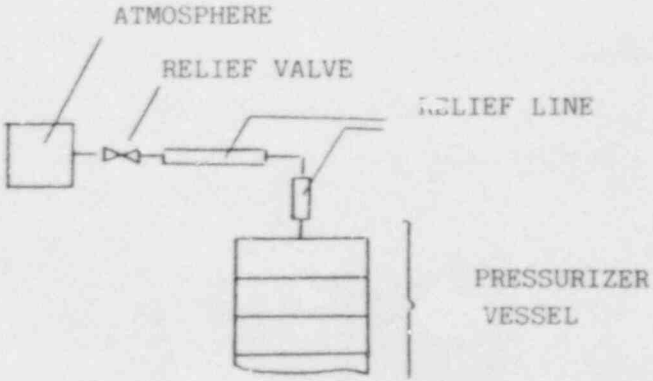

VERTICAL CONNECTION

FIG. 9: NODALIZATION FOR PRESSURIZER RELIEF LINE

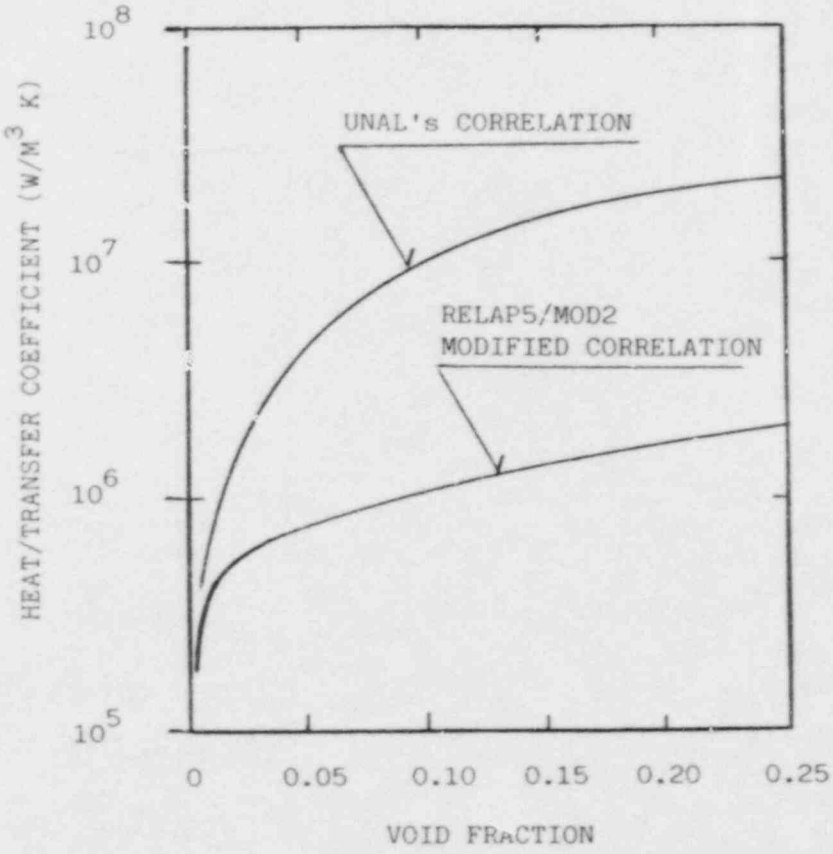

FIG. 10: INTERPHASE HEAT TRANSFER COEFFICIENT FOR LIQUID PHASE, P = 14.78 MPa VG = 2.5 M/S, VF = 2.0 M/S

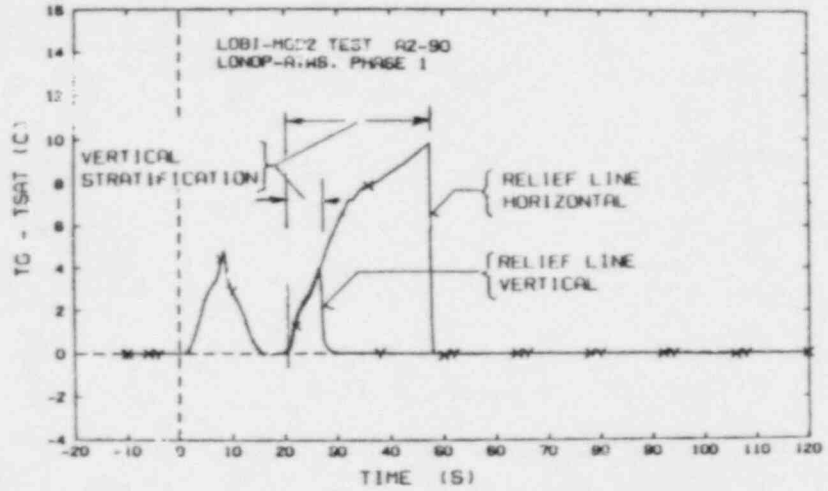

FIG. 11. DEGREE OF VAPOUR SUPERHEATING AT TOP OF PRESSURIZER
RELAP5/MOD2. INFLUENCE OF NODALIZATION FOR PRESSURIZER RELIEF LINE

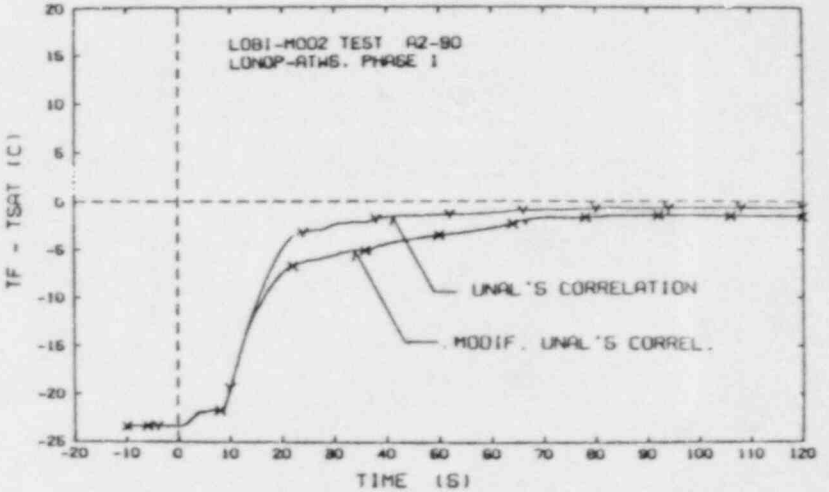

FIG. 13. DEGREE OF LIQUID SUBCOOLING AT TOP OF CORE REGION
RELAP5/MOD2. INFLUENCE OF LIQUID INTERPHASE HEAT HEAT TRANSFER COEFFICIENT

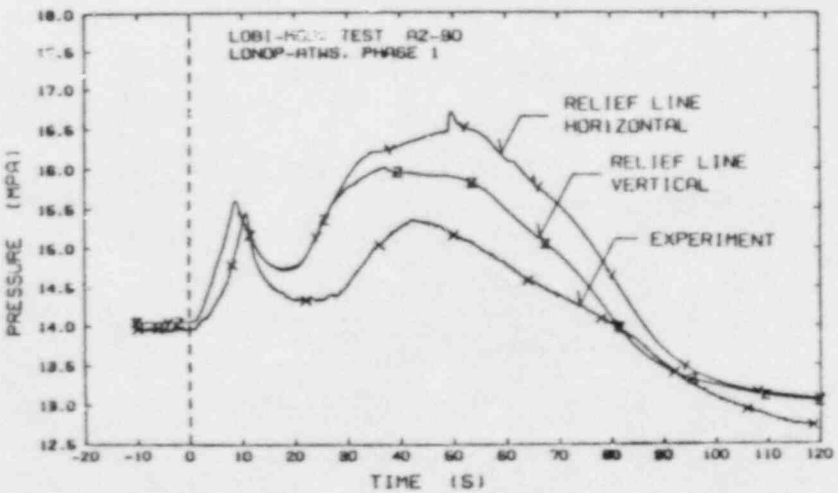

FIG. 12. PRESSURE IN UPPER PLENUM
RELAP5/MOD2. INFLUENCE OF NODALIZATION FOR PRESSURIZER RELIEF LINE

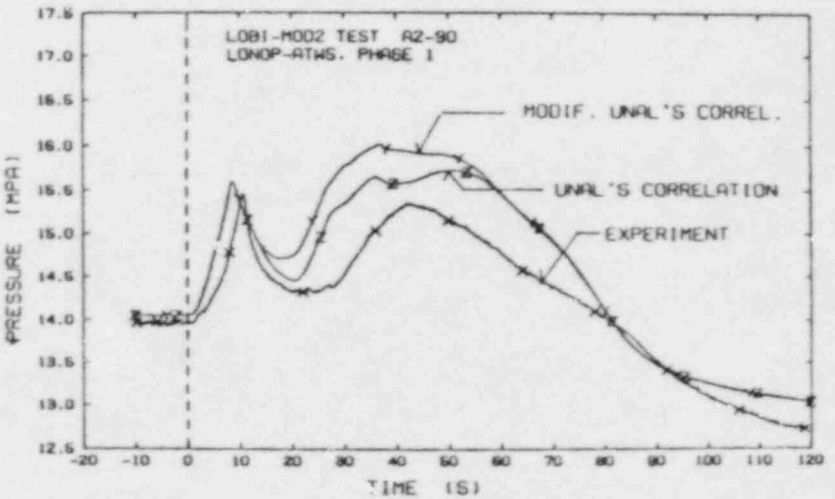

FIG. 14. PRESSURE IN UPPER PLENUM
RELAP5/MOD2. INFLUENCE OF CORRELATION FOR INTERPHASE HEAT TRANSFER

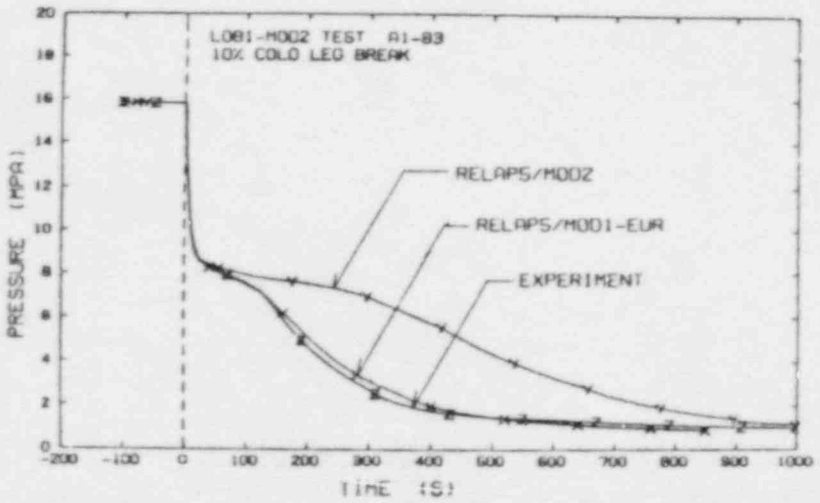

FIG. 15: PRIMARY SYSTEM PRESSURE
COMPARISON OF RELAP5/MOD2 AND RELP5/MOD1-EUR
STANDARD NODALIZATION

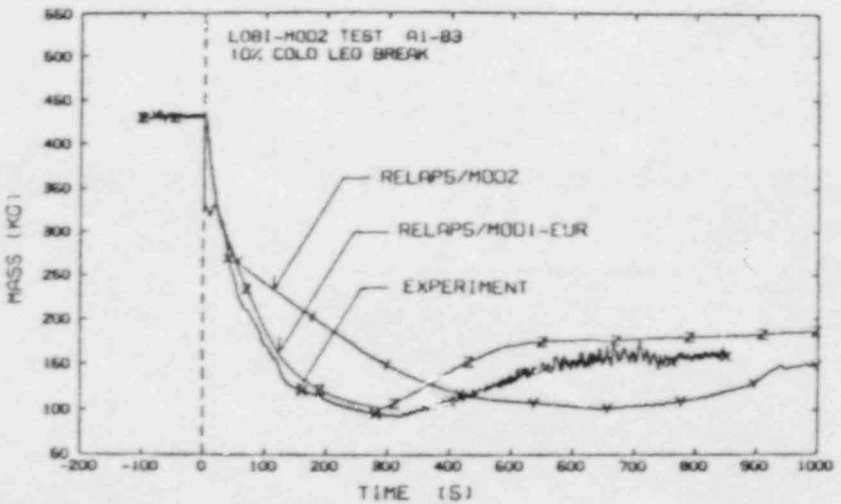

FIG. 16: PRIMARY SYSTEM MASS INVENTORY
COMPARISON OF RELAP5/MOD2 AND RELAP5/MOD1-EUR
STANDARD NODALIZATION

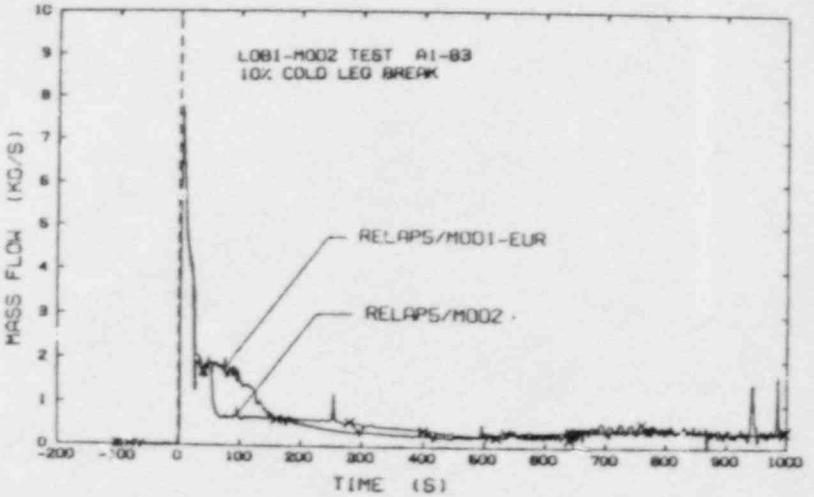

FIG. 17: BREAK MASS FLOW
COMPARISON OF RELAP5/MOD2 AND RELAP5/MOD1-EUR
STANDARD NODALIZATION

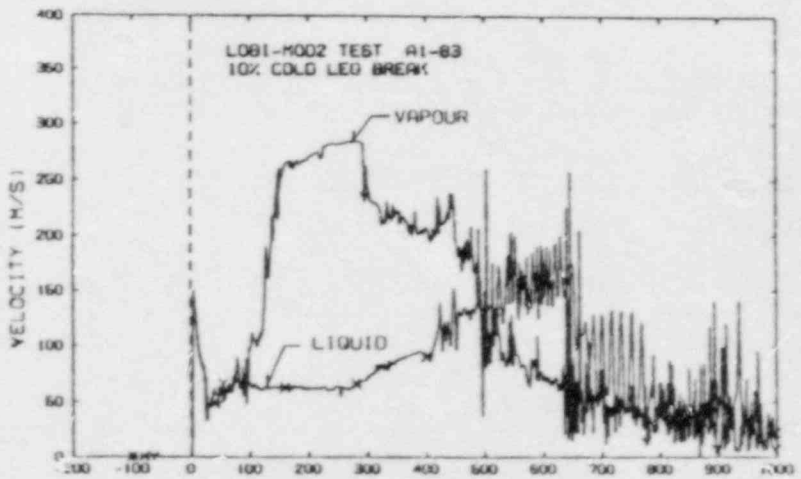

FIG. 18: PHASE VELOCITIES IN BREAK AREA
CODE: RELAP5/MOD2
STANDARD NODALIZATION

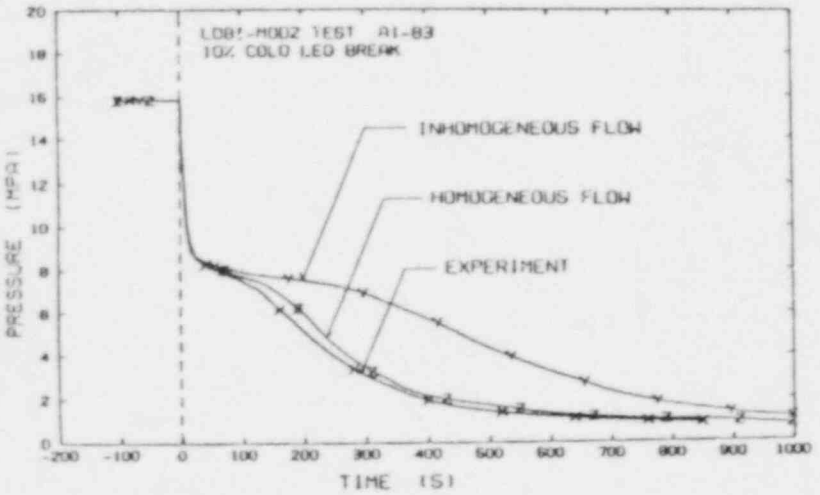

FIG. 19: PRIMARY SYSTEM PRESSURE
RELAP5/MOD2: INFLUENCE OF BREAK FLOW OPTION
STANDARD NODALIZATION

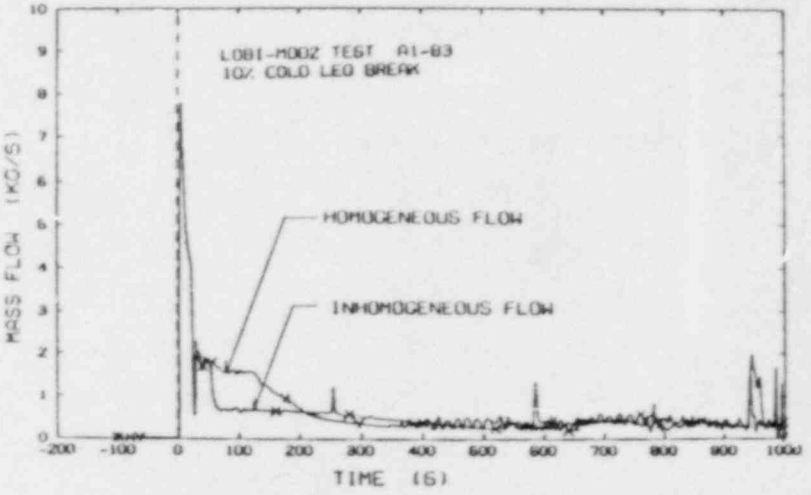

FIG. 21: BREAK MASS FLOW
RELAP5/MOD2: INFLUENCE OF BREAK FLOW OPTION
STANDARD NODALIZATION

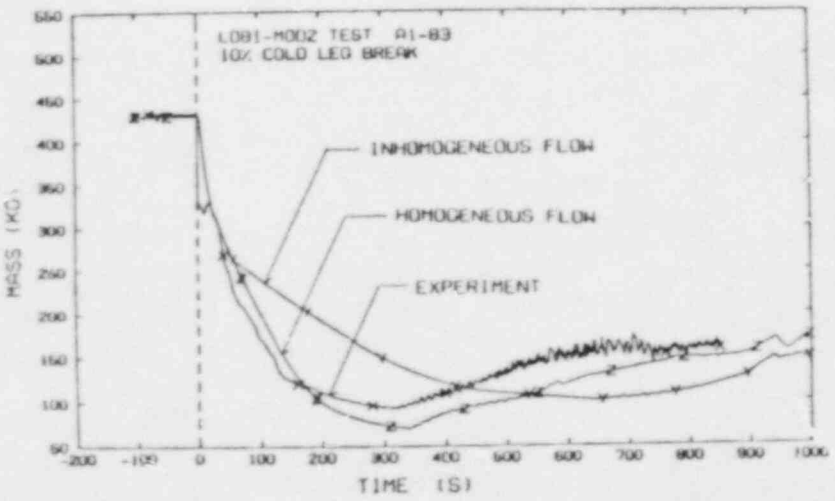

FIG. 20: PRIMARY SYSTEM MASS INVENTORY
RELAP5/MOD2: INFLUENCE OF FLOW OPTION FOR THE BREAK
STANDARD NODALIZATION

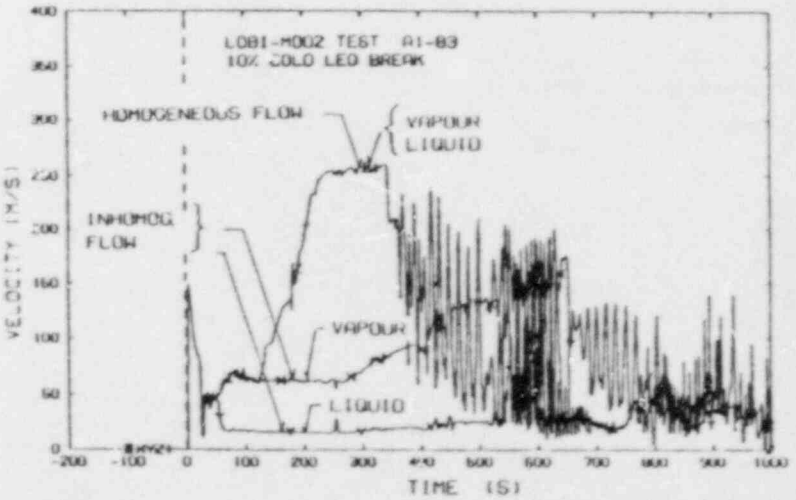

FIG. 22: PHASE VELOCITIES IN BREAK AREA
RELAP5/MOD2: INFLUENCE OF BREAK FLOW OPTION
STANDARD NODALIZATION

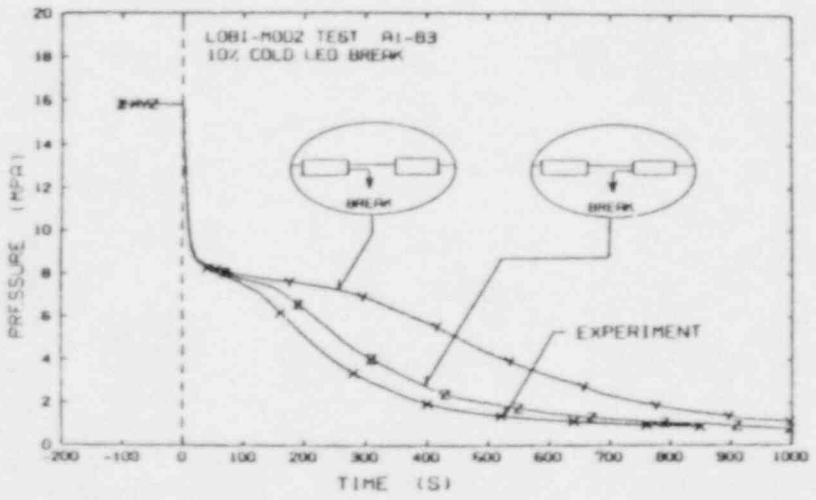

FIG. 23: PRESSURE IN PRIMARY SYSTEM
RELAP5/MOD2: EFFECT OF BREAK NODALIZATION
INHOMOGENEOUS FLOW OPTION FOR BREAK

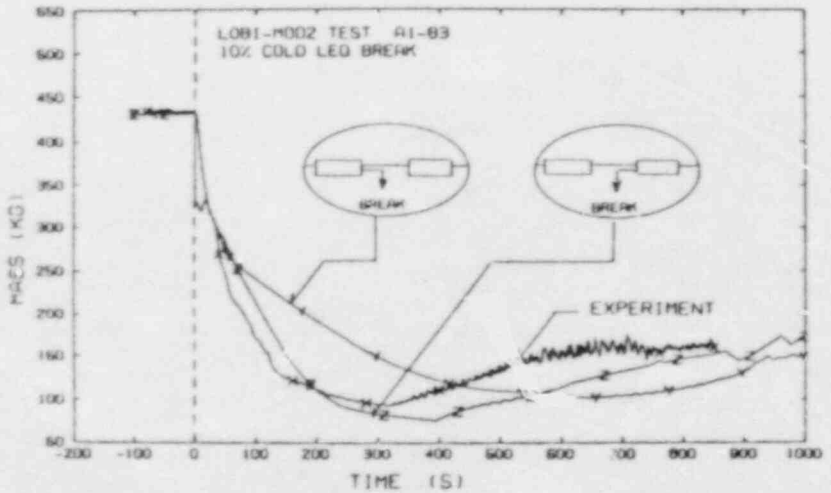

FIG. 24: PRIMARY SYSTEM MASS INVENTORY
RELAP5/MOD2: EFFECT OF BREAK NODALIZATION
INHOMOGENEOUS FLOW OPTION FOR BREAK

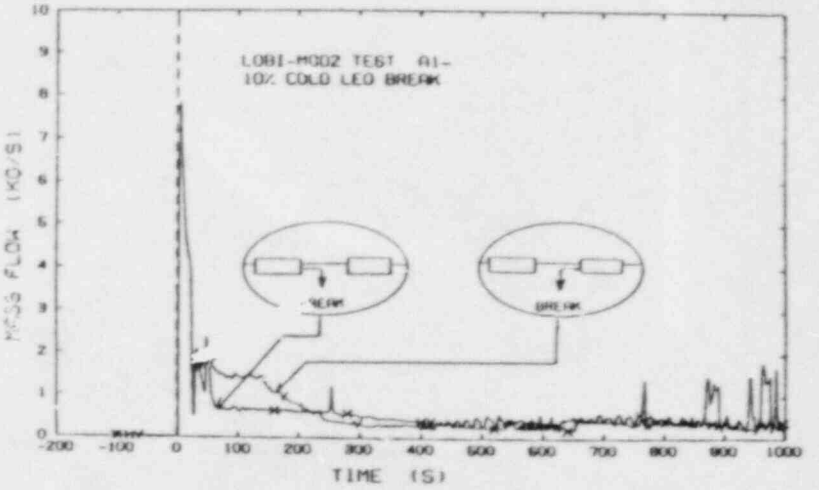

FIG. 25: BREAK MASS FLOW
RELAP5/MOD2: EFFECT OF BREAK NODALIZATION
INHOMOGENEOUS FLOW OPTION FOR BREAK

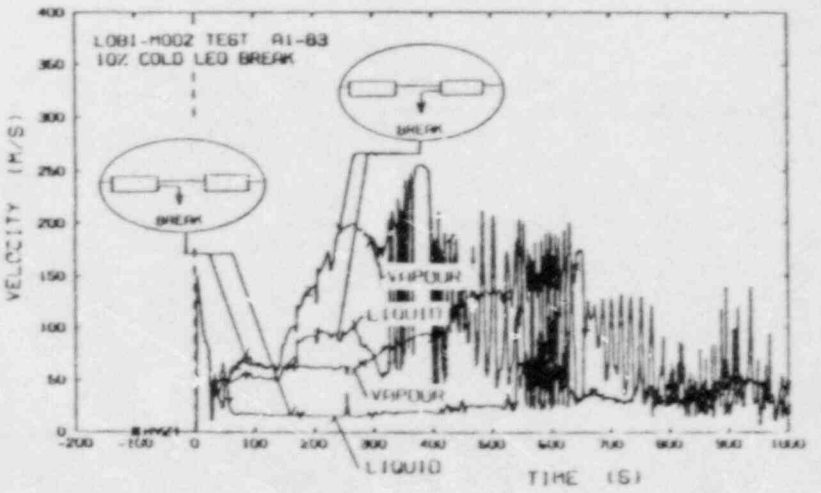

FIG. 26: PHASE VELOCITIES IN BREAK PIPE
RELAP5/MOD2: EFFECT OF BREAK NODALIZATION
INHOMOGENEOUS FLOW OPTION FOR BREAK

OVERVIEW OF CODE MAINTENANCE ACTIVITIES: TRAC-PF1/MOD1*

by

R. P. Jenks and J. W. Spore

Nuclear Technology and Engineering Division
Los Alamos National Laboratory
Los Alamos, New Mexico 87545

ABSTRACT

To support the objectives of the International Code Assessment and Applications (ICAP) program, Los Alamos provided several user support and code maintenance activities for TRAC-PF1/MOD1. Code deficiencies identified through this process were removed by developing new models or improved models for the next version of the TRAC code. Los Alamos has responded to the needs of the ICAP program by providing quality state-of-the-art software in support of ICAP and USNRC safety-analysis objectives.

I. INTRODUCTION

The TRAC-PF1/MOD1 code was frozen with the release of code changes EC14.3 in September 1987, and changes to the MOD1 code after that date were not allowed. Under the current restrictions code changes that are required to resolve TRAC user concerns will be made only to the MOD2 code.

During FY 1987 Los Alamos supported the objectives of the International Code Assessment and Applications (ICAP) program by providing several activities related to code maintenance for TRAC-PF1:

- resolution of user concerns,
- code configuration control,
- transmittal of code & updates,
- documentation & code-related news, and
- quality assurance.

---

* This work was funded by the US Nuclear Regulatory Commission, Office of Nuclear Regulatory Research, Division of Accident Evaluation.

Resolution of user concerns is accomplished through a central contact at the laboratory. At present two persons, Victor Martinez and Rick Jenks, share this responsibility. Code users call the central contact and their concerns are addressed immediately or catalogued for later review and resolution.

Code configuration control follows a logical process, beginning with the modification of the software and a tracking of the changes made, both of which are done by the librarian utility HISTORIAN. The resulting corrections are tested with a matrix of test problems and released to users. The process has recently been improved and includes additional test problems.

Code updates are transmitted by several methods. New users receive the code and the latest code changes on magnetic tape with limited implementation instructions. Other users receive the latest officially released updates on IBM floppy diskettes. Users may also obtain updates by downloading them from a specific Los Alamos VAX computer by means of a modem and their own telecommunications software.

Documentation and newsletters are distributed to users on a regular basis. New users receive the code documentation in the form of a code manual and a user's guide. The documentation is kept current with "change pages" attached to quarterly issues of *TRAC News*, the TRAC-PF1/MOD1 newsletter. General information, code problems, code changes, code assessment summaries and bibliographies of TRAC-related publications are included in each newsletter.

Q/A procedures, which have been implemented at Los Alamos during previous years of code development, have been improved. Now a formal peer-review process is in place, and code programming and documentation guidelines have been written to specify procedures that will further enhance the quality of TRAC software.

In the following five sections, activities related to code maintenance will be presented in more detail.

II. RESOLUTION OF USER CONCERNS

User support is essential to the ICAP program. It not only facilitates the application of the code, but also provides the USNRC will valuable information on code deficiencies. Resolution of code deficiencies produces an improved tool for reactor safety analysis.

Table I shows the key elements of the user-concern resolution process. User concerns are received through a central contact at the Laboratory.* Victor Martinez and Rick Jenks currently share this responsibility. Code users call the central contact, and their concerns are addressed immediately, if possible, or catalogued for later review and resolution.

---

* The "central contact" telephone number is 843-667-2021 (FTS) or 505-667-2021 (commercial).

User concerns are received in several formats: letters, telefaxes, phone calls, encounters at Los Alamos, and meetings, and indirectly through reports and papers. All concerns are directed to the central contact person for resolution. If the concern is simple enough that it can be resolved immediately, it is. Most concerns are relatively straightforward and can be resolved immediately, meaning in from two minutes to two hours. Examples of these "simple concerns" are requests for documentation, requests for simple modeling advice, requests for location of information in the Code Manual or User's Guide, requests for definition of a code variable, and other requests of this nature.

TABLE I
KEY ELEMENTS OF USER-CONCERN RESOLUTION

- Receive concern from user by means of central contact
- Respond immediately or catalog for "problem tracking"
- Electronic or written solicitation from development section for problem resolution
- Track progress: solicitation process plus "code Problem Review" meetings
- Development section works to resolve problem
- Inform users of problem-resolution status
- Inform users of final resolution

Concerns that are not simple to resolve, or that take more than two hours, are catalogued in our "problem-tracking" system. Under this system, we use one of our VAX computers to maintain and access a data base of resolved and unresolved user concerns. Table II indicates the current procedure employed in the problem-tracking system.

Several VAX utilities and a FORTRAN program are employed to make the problem-tracking process complete. The FORTRAN program, TSHOOTER, was developed to allow Los Alamos code developers easy access to information not only about current trouble forms, but also previous trouble forms that were catalogued and resolved. Figure 1 shows the main menu of TSHOOTER as it would appear to the user, indicating the various options that are available.*

The Code Development Section endeavors to resolve user concerns as quickly as possible. Our VAX MAIL utility allows for rapid electronic transfer of information among various people involved in the resolution process. As indicated in Table II (step 8), all information pertaining to the resolution of the problem is available in the trouble form data base, which is kept current as part of the procedures. Periodically, Code-Problem Review meetings are held to review outstanding user concerns and to suggest possible resolution strategies.

---

* Los Alamos plans to implement TSHOOTER into the VAX UPDATES utility when the improved version, UPDATES2, becomes available. Other features envisioned for UPDATES2 are improved "user friendliness," access to REVTRAC (a program that accesses information from the TRAC-PF1/MOD1 Assessment Report Data Base), and KERMIT (for improved data integrity during shipment of error-correction files).

TABLE II
PROCEDURE FOR CATALOGUING TROUBLE FORMS

1. Create trouble form (tform) using either a section from temp.fyxx or starting new with changes to copy of blank form. Call new file YYMMDDx.dat, where YY designates year, MM the month, DD the day and x is a lower-case letter (a–z) indicating the order of logging for a particular day. Example: 861102a.dat is the first tform catalogued on November 11, 1986.
2. Make entry to [cus.problems]curprobs showing tform number, user, and brief problem description. Open section of [cus.letters.xxxxx]xxxxxnews.tex to document the new problem, where xxxxx represents the pertinent *TRAC News* reporting period. Example: jan87news.tex is the TeX file for the January 1987 issue of *TRAC News*.
3. Send tform to Principal Investigator for Code Development using VAX MAIL utility.
4. Append tform to the end of latest temporary tform data base (temp.fyxx, where xx is latest fiscal year, 87, 88, 89, etc).
5. Update data base files oldprobs.base, oldprobs.fy85, oldprobs.fy86, etc. (input for TSHOOTER) by typing MAKEBASE to run cusutil:bmakebase.com, a DCL command file that uses the VAX batch processing mode.
6. Verify that new tform is in data base correctly, by running TSHOOTER. Check that you can access new tform.
7. Send out new listing of oldprobs.base to support staff periodically using BPRTROUB.
8. Update temp.fyxx files with feedback from developers, any resolution activities or other pertinent information. If significant efforts are undertaken and sufficient changes are made to a tform, report that change in the "old, unresolved" category of the next newsletter.
9. When tform is "closed," move segment from curprobs file to pertinent closeout file resolved.xxxxx, where xxxxx represents the pertinent tracnews reporting period. Example: resolved.jan87 contains all tforms resolved in the quarter preceding the January 1987 issue of *TRAC NEWS*. Also move entry from open to closed section in pertinent [cus.letters.xxxxx]xxxxxnews.tex.

FIGURE 1
TSHOOTER MAIN MENU

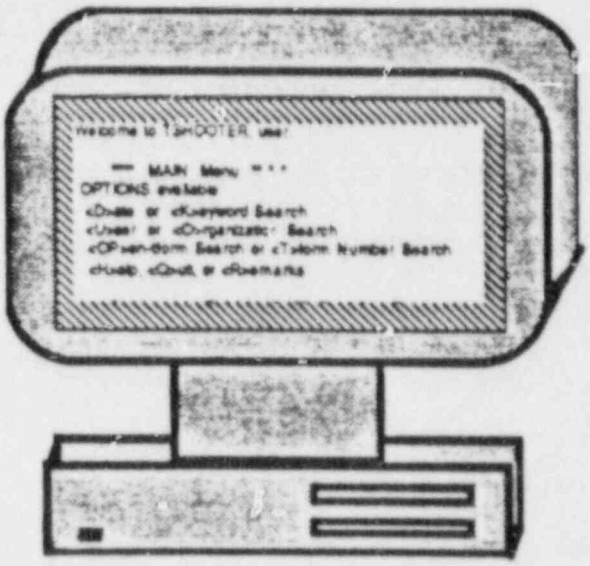

Users are kept informed of the status of problem resolution by direct communication (phone or letter) and through the quarterly *TRAC News* newsletter. When a user concern is resolved, all users are informed through the newsletter.

Table III gives statistics for the disposition of TRAC user requests from October 1985* through August 1987.

These requests range from very simple to very complex. As indicated in the table, most of the requests were relatively simple. Of the 1800 requests received, approximately 1471 were resolved immediately during this period. Over 300 could not be resolved immediately and were catalogued in the "problem tracking" system for later resolution. Most of these concerns have been addressed and have resulted in improved documentation or actual code updates to fix a code error or implement a user convenience. As of September 11, 1987, 29 of the catalogued concerns remained unresolved. The distribution of the 29 unresolved concerns is given by type with 14 code errors, 7 model deficiencies, 4 I/O problems, 4 documentation concerns, and no implementation concerns.

TABLE III
TRAC USER REQUESTS: OCTOBER 1985 THROUGH AUGUST 1987

*** ~1800 TOTAL ***

•	1471	resolved immediately	
•	329	catalogued	
•	29	unresolved (9/11/87):	
	--> 14	code errors	++++++++++++++
	--> 7	model deficiencies	+++++++
	--> 4	I/O problems	++++
	--> 4	documentation	++++
	--> 0	implementation	

During FY 1987, approximately 800 user requests were received and 110 user concerns were catalogued. Figures 2 and 3 depict the distribution of the FY 1987 catalogued concerns by problem category and by origin. The largest percentage of user concerns fell into the "code error" category (47.2%), followed by concerns about the code documentation (18.5%) and model deficiencies (13.9%). A large percentage of the concerns originated from Los Alamos and UK programs (33.3% and 20.6%, respectively) and from other domestic users, as well (18.6%).

* October 1985 is when the most recent TRAC User Support program started under ICAP, and the current system, using "central contact" persons and computerized tracking of user concerns, began.

FIGURE 2
USER CONCERNS CATALOGUED IN FY87 BY CATEGORY

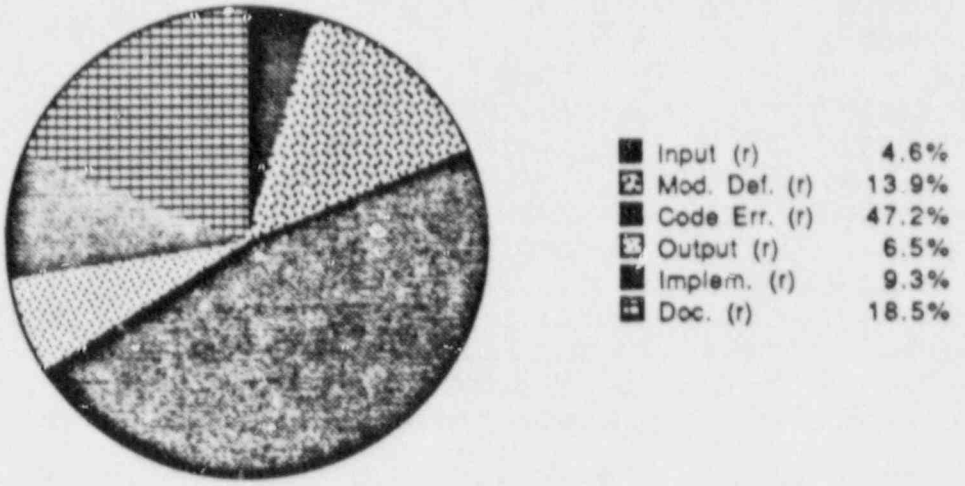

FIGURE 3
USER CONCERNS CATALOGUED IN FY87 BY ORIGIN

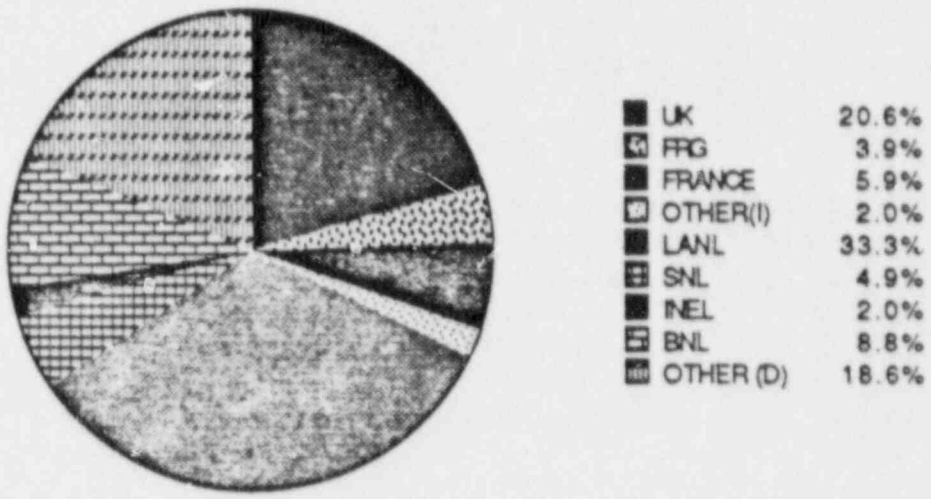

During FY 1987, 122 separate update idents were released as changes to the TRAC-PF1/MOD1 code. Of these 122 updates, 22 were user-convenience updates, ranging from adding more comment cards to TRAC to improving the readability of the TRAC run-time messages. Eleven of these update idents were associated with

improving the portability of TRAC to other computer operating systems. The balance of the update idents fell into the categories of error corrections or implementation of new models or user-convenience features (*i.e.*, multiple-source capability, new separator model, etc.). Appendix A gives a complete list of updates issued during FY87.

A sampling of recent user concerns is presented in Table IV. As code deficiencies are identified during the ICAP code assessment and application activities, new models or improved models are suggested for development in the next version of TRAC (*i.e.*, MOD2). Improvements currently targeted* for the MOD2 code are listed in the table.

TABLE IV
SAMPLING OF RECENT USER CONCERNS

Code-Error Concerns:	TFORM
CORE-rod dryout	870210b
Errors in ident STEST	861101a
Critical flow implementation error	861202a
FRIC in valves	870210c
Stratified flow	870210d
3D cell velocities	870210f
HTCOR "typos"	870210h
Boron reactivity	870828a

Model Improvement Concerns (targeted for the MOD2 code):

- multi-source VESSEL capability (in MOD1, also)
- PWR self-initialization capability (in MOD1, also)
- steam separator model (in MOD1, also)
- CCFL modeling
- fast 3D-2STEP numerics
- vectorized VESSEL coding & inversion of VESSEL data base
- generalized heat structures (RODS & SLABS)
- improved core-void / core heat-transfer modeling
- conserving momentum-flux solution
- consistent wall shear between 1D and 3D
- improved wall shear model that fixes laminar flow errors, includes surface roughness effect in turbulent regime, and improves accuracy of two-phase model
- elimination of Gauss-Seidel and development of the capacitance method for solving the VESSEL matrix equations
- replacement of subcooled boiling model with the TRAC-BWR subcooled boiling model

* This list is part of the proposed "MOD2 Development Plan" that was to have been formulated in conjunction with ICAP members at the October 1987 ICAP Specialists Meeting held October 21 and 22 in Bethesda, Maryland. A draft of the complete MOD2 code development plan will be sent to the NRC for review by December 31, 1987. It is anticipated that the final plan will be approved before February 1988.

TABLE IV
SAMPLING OF RECENT USER CONCERNS (cont)

- Model Improvement Concerns (continued):
  - ➡ general-orientation VESSEL-modeling capability
  - ➡ improved core reflood model
  - ➡ improved downcomer penetration predictive capability
  - ➡ improved upper-plenum entrainment / de-entrainment
  - ➡ improved modeling of condensation (cold and hot legs)
  - ➡ axially varying initial fuel-gap modeling capability
  - ➡ improved critical flow model
  - ➡ built-in pump energy model
  - ➡ elimination of non-standard FORTRAN and removal of calls to GETBIT
  - ➡ elimination of break-flow time-step sensitivity
  - ➡ improved accumulator modeling capabilities
  - ➡ improved fine-mesh interpolator
  - ➡ interfacial shear and heat-transfer improvements

- I/O Concerns:

VESSEL ROD output	870409a
Component order user specified	870504a

- Documentation Concerns:

UPi modeling	861007a
Direct inversion option	861203a
Azimuthal noding dependency	861218a
Pump modeling	870120a
Critical flow noding dependency	870319f
CORE heat-transfer output	870618a

- Implementation Concerns:

HISTORIAN v. UPDATE	870123a
CCFL test problem differences	870428a

III. CODE CONFIGURATION CONTROL

A configuration control process is followed in implementing code modifications into a new version of TRAC-PF1. The process ensures that several people can be changing TRAC at the same time without conflicting with each other and unintentionally introducing errors into the coding.

A flow chart of the configuration control process is given in Appendix B. The process has undergone change as deficiencies are encountered, always with the objective of ensuring the quality of the software.

IV. TRANSMITTAL OF CODE & UPDATES

New users are sent the TRAC-PF1 code on a magnetic tape with complete documentation. The transmittal package includes:

- Magnetic tape with TRAC-PF1 and supporting software (TRAP, EXCON, GRED, etc.);
- the TRAC Code Manual;[1]
- the TRAC User's Guide;[2]
- implementation instructions and examples; and
- back issues of the quarterly TRAC newsletter.[3]

As changes are made to the code, updates are created, and each update is tested with a fast-running subset of our full test-problem matrix. Appendix C contains a description of the full TRAC-PF1 test-problem matrix. Once a sufficient number of updates has been accumulated, and the code has been fully tested with the full test matrix to minimize the possibility of errors, an official update release is generated. These updates are at present distributed to code users on IBM floppy diskettes. To ensure rapid mailing, the distribution is limited, with only central contacts at each organization receiving diskettes. These central contacts distribute copies to appropriate technical people at their sites.

In addition to diskette transmittal, the "VAX UPDATES" telecommunications utility on our VAX dial-up telephone line permits users who wish to obtain code changes much more quickly to access the latest official update releases. Procedures for accessing these dial-up lines have been published in previous issues of *TRAC News*. Additional instructions can be obtained by contacting the TRAC central contacts at Los Alamos.

V. DOCUMENTATION AND CODE-RELATED NEWS

A new version of the TRAC-PF1/MOD1 code was released in the spring of 1987. This version included error corrections and added user conveniences for the MOD1 version of TRAC-PF1. It also included a self-initialization capability, a multiple-source capability, and a new steam/water separator model. Following the release of the MOD1 version of TRAC, work was initiated to provide a complete set of supporting documentation. This complete set includes:

- the TRAC User's Manual,
- the TRAC User's Guide,
- the TRAC Assessment Report,[4] and
- the models and correlations document.

The first three documents have already been released. The TRAC User's Manual and the TRAC User's Guide are distributed in convenient 3-ring binders designed so

that they can be kept current, as new models or new guidelines are developed, with "change pages." The change pages are provided routinely as attachments to the quarterly *TRAC News* newsletter.

The new models and correlations document identifies each model and correlation in the TRAC-PF1/MOD1 code. In addition, it describes how each of these has been implemented into TRAC (*i.e.*, what assumptions and approximations were used), identifies the basis or data base for the model or correlation, and attempts to address the scaling of the individual model or correlation.

In addition to the four documents described above, a quarterly newsletter is issued to code users providing information about TRAC-related activities. The following sections are contained in *TRAC News:*

- Information
- User Concerns
- Code Updates
- Assessment Summaries
- TRAC Bibliography
- Attachments: "change pages"

As with the diskette transmittal of code updates, the newsletter distribution is limited, with only central contacts at each organization receiving documentation. This limited distribution ensures the timeliness of the news distributed to code users.

VI. QUALITY ASSURANCE

The major objectives of the TRAC quality-control procedures (QCPs) are to have a code that has physically sound models and corrections, is as error-free as possible, maintains traceability, and imposes standard programming practices. These objectives are accomplished by peer review, documentation, and good communication between code developers and code users.

A. Background

TRAC software quality was controlled in the past as part of code development and code configuration control. Code development procedures called for documentation of new models and other code changes in the TRAC Manual and/or TRAC User's Guide. TRAC configuration control procedures called for peer review of code changes by a central reviewing authority, most often the code-development section manager.

The new QCPs expand the old peer-review process into a formalized and heavily documented procedure. Documentation requirements have been imposed that require the basis for a new model or code change as well as documentation of

supporting sensitivity calculations. Audit notebooks kept in our code-development archives, a central repository for information related to the quality assurance of our code, are used for this purpose.

A major portion of the previous TRAC configuration control procedure emphasized traceability. Through the use of the HISTORIAN software-librarian program and update request forms, code changes could be traced to specific code versions and developers. The new configuration-control procedures that are part of the TRAC QCPs continue to emphasize traceability. At the same time, they formalize both the peer review of code updates and the external documentation requirements.

The QCPs have been documented in detail[5] and are divided into four general areas:

- documentation and peer review procedures,
- configuration control procedures,
- update guidelines, and
- FORTRAN programming guidelines.

These areas form the basis of the TRAC QCPs.

B. Documentation and Peer Review Procedures

Documentation and peer-review procedures specify the documentation and peer review that must be performed for all code modifications, from simple one-line error corrections to major new model implementations. Computer code documentation exists in two general categories:

- **internal** documentation and
- **external** documentation.

The internal code documentation includes the FORTRAN source and comment cards. The FORTRAN source and comment cards prove very useful not only to other code developers, but to experienced code users as well.

The external code documentation includes update request forms, update comment cards, code manuals, and model audit notebooks. This information is available to all code users and provides information useful to the implementation and application of code changes.

C. Configuration Control Procedures

The new configuration control procedures dictate the steps followed to implement code modifications into new TRAC versions. These steps have been developed to minimize the potential for introducing errors into the TRAC code. These procedures also ensure that several people changing TRAC can work on the same code version

at the same time without causing coding conflicts. The new configuration control procedures minimize the amount of development time that would otherwise have been lost to fixing overlapping corrections and other, more serious, conflicts in coding.

D. Update Guidelines

Update guidelines have been developed that require extensive documentation of code changes within the HISTORIAN update files. Most code developers and many code auditors find the documentation of HISTORIAN updates to be more convenient than descriptions published in the Code Manual or User's Guide. They find that having full documentation of the code change together with the change itself improves the understanding of what was done to the coding.

The guidelines serve two main functions:

1. They establish a rigorous set of standards for comprehensive internal documentation of all updates. The same documentation appears on the update request form.

2. They attempt to ensure that only HISTORIAN commands that are compatible with the CDC UPDATE utility are used.

Many external users can see the documentation within the code updates before they are published in the quarterly newsletter or the code manuals, because all updates are available on our dial-up VAX computer.

E. FORTRAN Programming Guidelines

The new FORTRAN programming guidelines ensure that readable, maintainable, transportable, and efficient FORTRAN coding is developed. These guidelines outline the minimum documentation required within the FORTRAN source for TRAC, as well as general programming practices that must be followed in preparing changes or additions to the code. The guidelines specifically address the following areas:

- Vectorization
- EXTRACT code and Dump / Restart
- Source documentation and format
- Portability
- COMMON blocks
- Input changes
- Suggested MOD2 changes

VII. CONCLUSIONS

New user conveniences, correction of errors, and the development of new models have produced significant improvements in TRAC's user friendliness and accuracy. Improvements to documentation will help all code users by identifying when and where the code should be used and what accuracy can currently be expected. Although the TRAC-PF1/MOD1 version has been frozen, we are incorporating improvements and enhancements into the MOD2 code as we receive feedback from TRAC users.

TRAC code maintenance activities have helped ICAP member countries, Los Alamos National Laboratory, and the USNRC. The code maintenance efforts have provided resolution of user concerns, an improved configuration control process, dissemination of the code, code changes and code-related documentation to users, and an expanded quality-assurance program. These efforts will ensure a good-quality, powerful software tool for thermal-hydraulic safety analyses.

VIII. REFERENCES

1. Safety Code Analysis Group, "TRAC-PF1/MOD1: An Advanced Best-Estimate Computer Program for Pressurized Water Reactor Thermal-Hydraulic Analysis," Los Alamos National Laboratory report LA-10157-MS (NUREG/CR-3858) (July 1986).

2. B. E. Boyack, H. Stumpf, and J. F. Lime, "TRAC User's Guide," Los Alamos National Laboratory report LA-10590-MS (NUREG/CR-4442) (November 1985).

3. R. P. Jenks, *TRAC News*, Los Alamos National Laboratory newsletters, 8 quarterly issues, LALP-85-38, LALP-86-4, LALP-87-5, Vols. 1–3, Nos. 1–4 (October 1985 to July 1987).

4. M. S. Sahota and F. L. Addessio, "TRAC-PF1/MOD1 Developmental Assessment," Los Alamos National Laboratory report LA-10445-MS (NUREG/CR-4078) (August 1985).

5. J. W. Spore, P. T. Giguere, C. P. Booker and R. P. Jenks, "Quality-Control Procedures For TRAC Development and Maintenance," Los Alamos National Laboratory internal document (June 1987).

APPENDIX A

CODE UPDATES DISTRIBUTED DURING FY87

UPDATE IDENT	DATE RECEIVED	CODE VERSION	DESCRIPTION[a] OF CHANGE
lcttx	7/22/86	12.9	Fixes error in the core test
fxvdv1	7/23/86	12.9	Restores IVDV=0 option to BREAK
vm0722	7/-/86	12.9	Fixed a fatal error caused by CFT1.14
issflg1	7/-/86	12.9	Corrects logic error with ISSFLG
ranfcn	7/-/86	12.9	Removes dummy argument from ran # fun
sgagain1	7/-/86	12.9	Changes con. gain to -0.03
movcss	7/-/86	12.9	Moves css update to PREP3D
upfilm	7/17/86	12.9	Fixes error in Forsland-Rohsenow, fixes gravity orientation error, replaces Dittus-Boelter with Sieder-Tate for single-phase vapor, corrects error in exponent on Prandtl # for DB adds the hlfilm routine and modifies the hvfilm and htcor routines
updcln	8/01/86	12.9	Eliminated five undefined variables
nffix	8/06/86	12.9	Eliminated NFF=2 option
misc1	8/07/86	12.9	Miscellaneous clean up
jmahcr1	8/11/86	12.9	Input checking on user-input CB table
ssnoc1	8/11/86	12.9	Closes out controllee after successful steady state run
holltrc	8/11/86	12.9	Changes css messages to hollerith
ccfix1	8/11/86	12.9	Fixes two variables to real
table1	8/13/86	12.9	Changes output to TTY to be more readable
fxerr1	8/13/86	12.9	Fixes error in noistdy1 update
updsnd	8/13/86	12.9	Improves superheated steam choking
fxinvan	8/18/86	12.9	Fixes INVAN option
wpkmes	8/22/86	13.0	Improves messages from TF3DI
imprgs	9/03/86	13.0	Cleans up coding in INPUT, RCNTL, RDREST, and RECNTL.
cavgcr	9/03/86	13.0	Fixes CELLAV and problem with VM0722
edcore	9/05/86	13.0	Adds comment cards to routine CORE1.
upgam	9/05/86	13.0	Fixes a restart problem with CORE.
nffix1	9/05/86	13.0	Re-instates NFF=2

[a] Nomenclature:

CB—Control block
DB—Dittus-Boelter
TSC—Time-step control
VV—Vent valve
DI—Direct inversion matrix solution
UC—User convenience

UPDATE IDENT	DATE RECEIVED	CODE VERSION	DESCRIPTION OF CHANGE
edithv	9/08/86	13.0	Adds comments to HVFILM to define cfl upda list
ccflx2	9/08/86	13.0	Fixes undefined variable in ccfl update
vmerfxd	9/09/86	13.0	Fixes vessel mass error TSC
fxhtloss	9/09/86	13.0	Fixes logic error for editing of STGEN heat losses.
cpdlcm2	9/11/86	13.0	Fixes pointer problem with 7600 version
upchfi	9/15/86	13.0	Fixes TCHF iterative solution
updsnd2	9/15/86	13.0	Fixes SQRT of negative number problem in updsnd update
fxlenc	9/16/86	13.0	Fixes 7600 memory management error
tkgrf	9/18/86	13.0	Adds liquid and vapor densities to plenum graphics, etc
upicflg	9/18/86	13.0	Fixes problem with initialization of icflg
ndckrjc	9/22/86	13.0	Warns user if nodes.lt.1 in stgen
ptofcr1	9/22/86	13.0	Changes the initial steady-state power-to-flow ratio to be based on the absolute value of the core flow
bitsrj	9/23/86	13.0	Places return statements in BITS routine for 7600 version of TRAC
sym01	9/23/86	13.0	Removes sysdoc from comdeck XVOL
sym02	9/23/86	13.0	Expands description of system routine
sym03	9/23/86	13.0	Inserts doc of system routines after copyright section in TRAC
kapl1	12/04/86	13.1	Pads calls to READI & READR to make code more compatible with CYBER205
kapl2	12/17/86	13.1	Implements 205 necessary changes
kapl3	1/06/86	13.1	Implements 205 necessary changes
fxupdrn	1/06/86	13.1	Eliminates if-then logic
tsrjtrn	9/23/86	13.2	Fixes a problem with repeating conduction solution on failed time step advancement
wrnlodt	9/25/86	13.2	Warns user if memory is preset to zero.
dtyperj	9/25/86	13.2	Two variable names were changed in REVSSL.
tvrunaw1	9/25/86	13.2	Fix gamma to eliminate tv run away
fxreit	9/25/86	13.2	Correct reiteration logic
fxreitp	9/25/86	13.2	Extends fix to plenum
tlnadjp	9/25/86	13.2	Extends fix to plenum
vlvfric1	9/25/86	13.2	Corrects problem in tform 860905c Fixes reverse-flow friction for valve
msctcr	9/25/86	13.2	Corrects problem in tform 860721a: fixes MSCT for STGENs
ctest1	10/06/86	13.2	Fixes courant limit test
ptofin1	10/06/86	13.2	Initializes rpcf to 0.0
fixwfv	10/07/86	13.2	Corrects problem in tform 850911e: fixes discontinuity discovered by Dean Dobranich
nlista	10/15/86	13.2	Reorders namelist variables

UPDATE IDENT	DATE RECEIVED	CODE VERSION	DESCRIPTION OF CHANGE
waformat	10/15/86	13.2	Changes output format in warry and wiarr
souclim1	10/15/86	13.2	Changes values saved for Courant-limit location at vessel source-connection locations
upfmom2	10/15/86	13.2	Adds PI to calculate critical velocity for horizontal stratified flow
upfmom4	10/15/86	13.2	Makes the horizontal gravity head flow regime model consistent.
vmerfxf	10/24/86	13.2	Deleted unnecessary lines
jetupd01	12/14/86	13.2	Implements changes necessary for INEL NPA
twgirj	12/10/86	13.2	Properly defines twgi for graphics
vmextr1	1/26/87	13.2	Corrects error in DUMP/RESTART, adds reverse fric edit to output file, adds capability to input fine mesh data, deletes unused pointers, and other code cleanup
inlab1	12/2?/86	13.3	Adds the capability to print out labeled input decks
triinv	12 23/86	13.3	Improves trislv tri-dia solver
sscvt1	12/23/86	13.3	Corrects error in SS convergence test
fcn3iv1	12/23/86	13.3	Adds new control-block capability
logo1	12/23/86	13.3	Sends a logo cover page to output
upmwrx1	1/08/87	13.3	Corrects comments in MWRX routine
ukchok1	12/17/86	13.3	Fixes error in choked velocity calc.
chkfix	1/09/87	13.3	Fixes problem identified by 860905a
vsoucr1	1/14/87	13.3	Fixes warning for multiple sources
ctest1cr	1/14/87	13.3	Fixes Courant-limit check
vmerfxg	1/27/87	13.3	Correct logic error in vessel mass error controller for multiple vessels
initcr1	2/05/87	13.3	Fixes restart problem with ipowr
upfmom1	2/09/87	13.3	Fixes horizontal stratified flow prob
sepd	2/13/87	13.3	Implements new separator model
vmextr2	2/13/87	13.3	Deletes CTAIN & freezes order of flt, vlt, and pointers
vlvfix1	2/19/87	13.3	Fixes problem in tform 870210c
vmextr4	3/01/87	13.3	Corrects errors in M-routines
fxpack	2/24/87	14.0	Replaces aminr with amin in packit
cpulim1	2/24/87	14.0	Fixes steady state runs such that a time zero dump is written only after a normal termination
cbedit1	2/24/87	14.0	Enhances control block input edit
lab1cr	2/24/87	14.0	Makes rcntl consistent with inlab
upfmom3	10/15/86	14.0	Makes the horizontal gravity head flow regime model consistent
tlnadj1	9/25/86	14.0	Adjusts tln for nonlinear saturation line

UPDATE IDENT	DATE RECEIVED	CODE VERSION	DESCRIPTION OF CHANGE
rphfx1	2/24/87	14.0	Fixes an error in RDCRDS introduced by the KAPL2 update in the FOR77 if def
upfmom6	3/02/87	14.0	Bypasses horizontal stratified for pressurizers, accumulators, etc
vmsfix1	3/04/87	14.0	Improves time step control based on vessel mass error
formfix	3/04/87	14.0	Corrects a format statement for short edit titles
ftdvsrj	3/03/87	14.0	Adds input checks for ftd (fraction of theoretical fuel density) to VESS
ftdcrrj	3/03/87	14.0	Adds input checks for ftd to core
gravrj	3/04/87	14.0	Adds input checks for grav to 1d comp
vmextr6	3/06/87	14.0	Makes dump compatible with EXTRACT
fixtln	3/05/87	14.0	Fixes TLNADJP for when air is present
fixsnl1	3/10/87	14.0	Limits cpl and kl used by HTCOR so that negative properties do not occur. Also cjg is limited so that zero is not used in the pool-entrainment correlation
fixwfv1	3/10/87	14.0	Fixes revfix1 and revfix2
sv1cr	3/10/87	14.0	Corrects update initcr1 for a tee inside of a steam generator component
vmextr8	3/23/87	14.0	Corrects error in shift operation
xmsct1	3/13/87	14.0	Removes msct variable used in tee
vmextr9	3/26/87	14.1	Fixes extract errors in STGEN & vsllev
przvol	3/25/87	14.1	Fixes a problem with initial prizer volume after a restart from a CSS
rphfx2	3/18/87	14.1	Fixes 2 IFDEF statements for 205 version
wlabcr	4/13/87	14.1	Fixes problem with inlab=3
progcr1	4/13/87	14.1	Fixes errors in fillx & recntl
upstgn	4/21/87	14.1	Fixes a problem with heat loss calc
upfrch	4/21/87	14.1	Removes extra arguments in HTCOR
ftdfx1rj	4/27/87	14.1	Checks on ftd only if a core is there
grfchkt	4/21/87	14.1	Adds check on size of graphics dump
inlab1cr	4/30/87	14.1	Inserts a readr call that the vent valve model needs.
cbpidcr	5/08/87	14.2	Fixes problem with steady state cont.
vmextr10	6/01/87	14.2	Fixes a restart problem with core com
css4no1	6/01/87	14.2	Fixes a storage problem with css
inlab1er	5/01/87	14.2	Corrects inlab option edit for pump
ptofgn1	5/01/87	14.2	Fixes an error in power-to-flow ratio
msizver	6/01/87	14.2	Corrects a memory-size error in rvssl
css4bpc1	6/01/87	14.2	Prevents adjustment on secondary-side break pressure when controller is max
slug1	7/01/87	14.2	Changes the bubble-to-slug flow trans value to be 0.30 everywhere
restcr1	6/01/87	14.3	Fixes restart for css

APPENDIX B

CODE CONFIGURATION CONTROL FLOWCHART

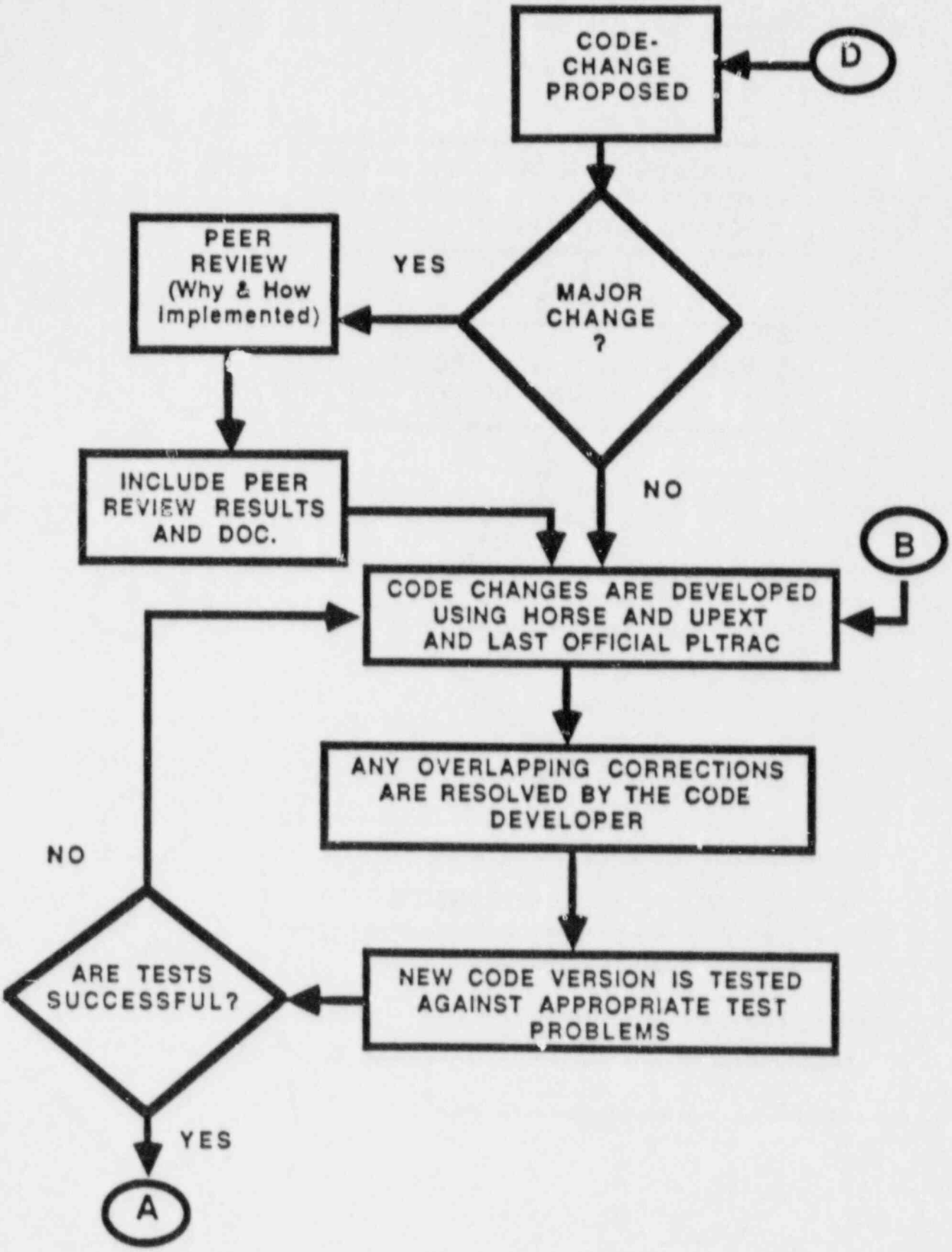
CODE-
CHANGE
PROPOSED
D
MAJOR
CHANGE
?
YES
PEER
REVIEW
(Why & How
Implemented)
INCLUDE PEER
REVIEW RESULTS
AND DOC.
NO
B
CODE CHANGES ARE DEVELOPED
USING HORSE AND UPEXT
AND LAST OFFICIAL PLTRAC
ANY OVERLAPPING CORRECTIONS
ARE RESOLVED BY THE CODE
DEVELOPER
NEW CODE VERSION IS TESTED
AGAINST APPROPRIATE TEST
PROBLEMS
ARE TESTS
SUCCESSFUL?
NO
YES
A

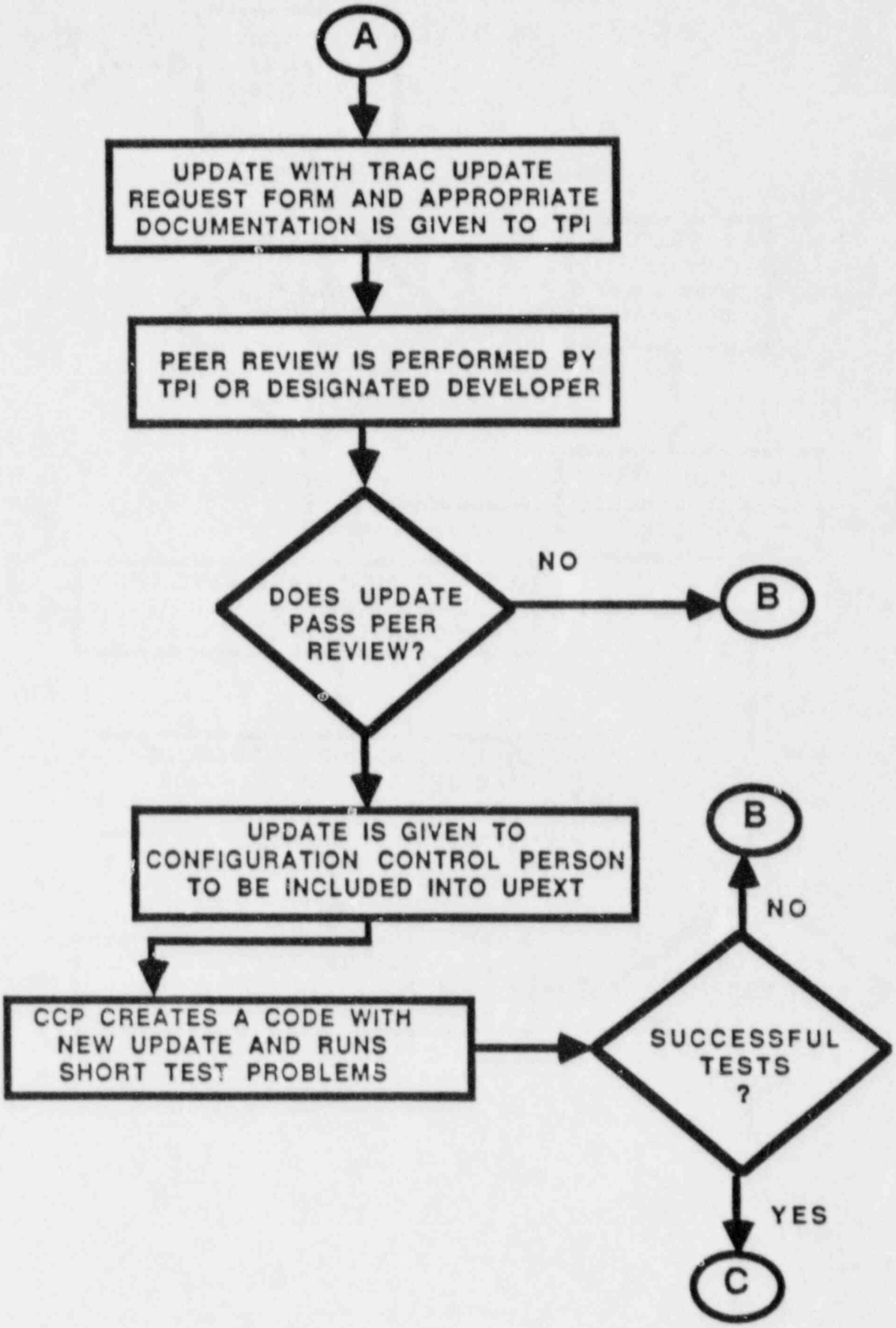
A
UPDATE WITH TRAC UPDATE REQUEST FORM AND APPROPRIATE DOCUMENTATION IS GIVEN TO TPI
PEER REVIEW IS PERFORMED BY TPI OR DESIGNATED DEVELOPER
DOES UPDATE PASS PEER REVIEW?
NO
B
UPDATE IS GIVEN TO CONFIGURATION CONTROL PERSON TO BE INCLUDED INTO UPEXT
CCP CREATES A CODE WITH NEW UPDATE AND RUNS SHORT TEST PROBLEMS
SUCCESSFUL TESTS ?
B
NO
YES
C

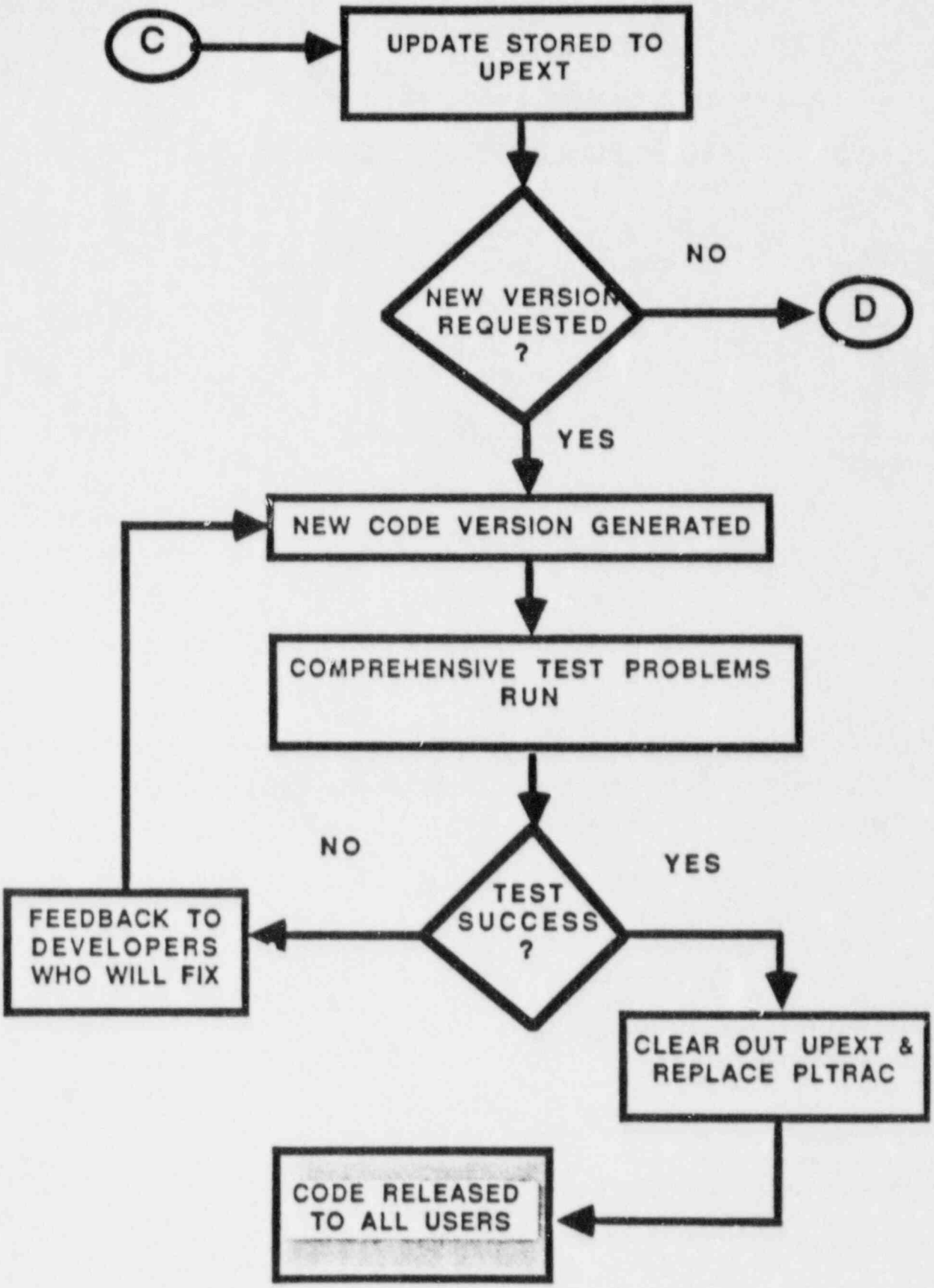
C
UPDATE STORED TO UPEXT
NEW VERSION REQUESTED ?
NO
D
YES
NEW CODE VERSION GENERATED
COMPREHENSIVE TEST PROBLEMS RUN
NO
TEST SUCCESS ?
YES
FEEDBACK TO DEVELOPERS WHO WILL FIX
CLEAR OUT UPEXT & REPLACE PLTRAC
CODE RELEASED TO ALL USERS

APPENDIX C

TRAC-PF1 TEST PROBLEM MATRIX (Short Set)

FEATURE TESTED	LOCA	POWER1	TFCORE1	CCFL	CCFL1
Restart					
Trips	X		X		X
Signal Variables	X	X	X	X	X
Control Blocks					
Pipe	X	X	X	X	X
Pump	X				
Plenum					
Tee	X				X
Accumulator	X				
Steam Generator	X				X
Prizer	X				
1-D Core		X	X		
Vessel	X			X	X
Separator					
Valve	X			X	X
Fill	X	X	X	X	X
Break	X	X	X	X	X
CCFL				X	X
Multiple Source	X				X
Self-Initialization	X				
Point Kinetics		X			
Power Decay					
Noncondensable					
Condensation					
Choked Flow					
Post-CHF			X		
Moving Mesh			X		
Boron					
Metal-Water Reaction					
Wall Friction	X				
1-D Additive Losses	X				
3-D Additive Losses	X				
Generalized Heat Structures (MOD2 only)					
User input material properties					X
Multivessel components					

TRAC-PF1 TEST PROBLEM MATRIX (Long Set)

FEATURE TESTED	LOCA1	AKIM	CCTF	CHEN	L2-6IN	PLENUM
Restart	X					
Trips	X		X		X	
Signal Variables	X	X	X		X	
Control Blocks					X	
Pipe	X	X	X	X	X	X
Pump	X				X	
Plenum						X
Tee	X	X			X	X
Accumulator	X					
Steam Generator	X					
Prizer	X				X	
1-D Core						
Vessel	X		X	X	X	
Separator						
Valve	X				X	
Fill	X	X	X	X	X	X
Break	X	X	X	X	X	X
CCFL						
Multiple Source	X					
Self-Initialization	X					
Point Kinetics Power Decay					X	
Noncondensable Condens.		X				
Choked Flow	X					
Post-CHF			X	X		
Moving Mesh			X			
Boron					X	
Metal-Water Reaction						
Wall Friction	X				X	X
1-D Additive Losses	X				X	
3-D Additive Losses	X				X	
Generalized Heat Structures (MOD2 only)						
User input material properties			X			
Multivessel components						

DESCRIPTION OF SHORT-SET TEST PROBLEMS

LOCA is a coarsely noded full-size PWR model. The input deck is set up to run a self-initialization run.
POWER1 is a TRAC simulation of the a Zion reactor test in which the reactor went from hot no-power to hot full-power. The Zion FSAR indicates that the Keff went from 1.154 to 1.1386 during this change in operating conditions. The TRAC reactor kinetics model yield a similar change in Keff.
TFCORE1 is a simulation of a hot bundle which has a small amount of water entering the top of the bundle.
CCFL is a simulation of Bankoff's perforated plate flooding experiment with saturated steam and water.
CCFL1 is a test of the capability to turn the CCFL model on in multiple locations.

DESCRIPTION OF LONG-SET TEST PROBLEM INPUT DECKS

LOCA1 is the same as LOCA in Table I; however, the tend is longer.
LOCA1R is a transient restart from the restart dump generated by LOCA1.
AKIM is a simulation of Akimoto's condensation experiment.
CCTF is a coarsely noded simulation of the CCTF test Run 14.
CHEN is a simulation of the Lehigh post-CHF heat-transfer experiment #138.
L2-6IN0 is a steady-state calculation for the LOFT test facility.
PLENUM is a test problem for the PLENUM component.

APPENDIX D

"CENTRAL CONTACTS" FOR DISTRIBUTION OF NEWSLETTERS AND CODE UPDATES

CONTACT	ORGANIZATION
ICAP:	
S. Aksan	EIR
J. de Carlos	CSN
J. Fell	UKAEE
E. Hicken	GRS, Munich
H. Holmstrom	Technical Research Center of Finland
S. Lee	KAERI
M. Reocreux	CEA
O. Sandervaag	Studsvik Energiteknik
G. Saponaro	ENEA
K. Sato	AERI
P. Schally	GRS, Cologne (2D/3D)
H. Stadtke	CEC
E. Stubbe	TRACTEBEL
F. Winkler	KWU
DOMESTIC:	
L. Buxton	SNL
R. Copeland	Advanced Nuclear Fuels (prev. Exxon)
R. Duffey	EPRI
L. Koffman	SRL
U. Rohatgi	BNL
G. Wilson	INEL
D. Bessette	USNRC

UK EXPERIENCE WITH RELAP5/Mod2

by

K H Ardron and P C Hall

Central Electricity Generating Board
Generation Development and Construction Division
Barnwood, Gloucester, UK

Tel: 011-44-452-652529

ABSTRACT

1. RELAP5/Mod2 is being used in the UK for analysis of small LOCA and pressurised transients in the Sizewell 'B' PWR.

2. To support this application and gain familiarity with the code, the CEGB and UKAEA have analysed a number of integral and separate effects tests with RELAP5/Mod2. Several reports on this work have been sent to USNRC under a UK/USNRC bilateral agreement.

3. This paper presents a review of UK experience with RELAP5/Mod2 since the code was received in the UK in February 1985. Calculations are described of small LOCA and pressurised transient experiments in the LOFT and LOBI test facilities, and boil-down tests in the UKAEA THETIS facility. Code calculations are also compared with data on pull-through/entrainment effects in two-phase flow in an off-take branch connected to a horizontal pipe containing stratified flow.

4. The code has generally been found to perform well in the calculations attempted so far, and appears to represent a considerable improvement over earlier versions of RELAP5 in respect of stability, running speed, mass conservation errors, and accuracy. The modelling difficulties identified in the UK studies have been:-

   - defects in the horizontal stratification entrainment model, used to calculate discharge from a side branch connected to a horizontal pipe in which there is stratified flow.

   - deficiencies in critical flow calculation when there is separated flow in the volume upstream of the break.

   Some calculations with modified code versions containing improved models are described to illustrate the deficiencies.

1. INTRODUCTION

RELAP5/Mod2/Cycle 36.00 was received by the UK from the USNRC in February 1985. This code version and subsequent updates, are maintained on a CRAY computer at UKAEA Harwell Laboratories, by UKAEA Winfrith staff. An IBM version of RELAP5/Mod2/Cycle 36.04 created by JRC ISPRA is also available on CEGB IBM computers.

RELAP5/Mod2 is being used by CEGB for analysis of some small break loss-of-coolant accidents and pressurised faults in the Sizewell 'B' PWR. These calculations form part of an independent assessment of safety analyses prepared by the vendor organisations.

In order to validate RELAP5/Mod2 for this application, calculations have been carried out of a number of integral and separate effects experiments. Several modelling defects have been identified in the course of this work and in some cases corrections have been implemented in UK code versions.

The present paper discusses the calculations carried out to date, and summarises the main findings. All the reported calculations have been, or are planned to be, sent to USNRC under the UK/USNRC bilateral agreement on the advanced codes RELAP5/Mod2 and TRAC-PF1/Mod1.

2. CALCULATIONS OF SEPARATE EFFECTS TESTS

2.1 THETIS Boil-down Experiments

To test the ability of RELAP5/Mod2 to calculate conditions in an uncovered core, the code was used by CEGB to simulate boil-down tests in the UKAEA THETIS rod bundle test facility. Details of the calculations are described in ref. [1].

THETIS consists of a vertical assembly of 57 electrical heater rods with a 3.6m heated length, enclosed in a 131mm dia. circular shroud tube.

In the boil-down tests, equilibrium conditions were established at a test section power of 100kW with a fixed make-up flow. The make-up flow was then isolated, and the bundle allowed to boil down at a controlled pressure. The two-phase mixture level trajectory and heat transfer in the dried out region were measured using numerous internal rod thermocouples. Extensive data on vertical differential pressures within the rod bundle were also obtained.

Figure 1 shows the test facility and the RELAP5 noding diagram. Figure 2 shows the dry-out level trajectory calculated for the boil-down tests at 4.0, 2.0, 1.0 and 0.2 MPa. Generally the code gave excellent agreement with test data at a pressure above 2.0 MPa. However, at pressures below 1.0 MPa the boil-down rate was considerably over-predicted. The errors were traced to defects in the interphase drag models in RELAP5/Mod2, which can produce large errors in void fraction at low system pressures (see below).

RELAP5/Mod2 gave very good predictions of the heat-up rate of exposed rod above the two-phase mixture level.

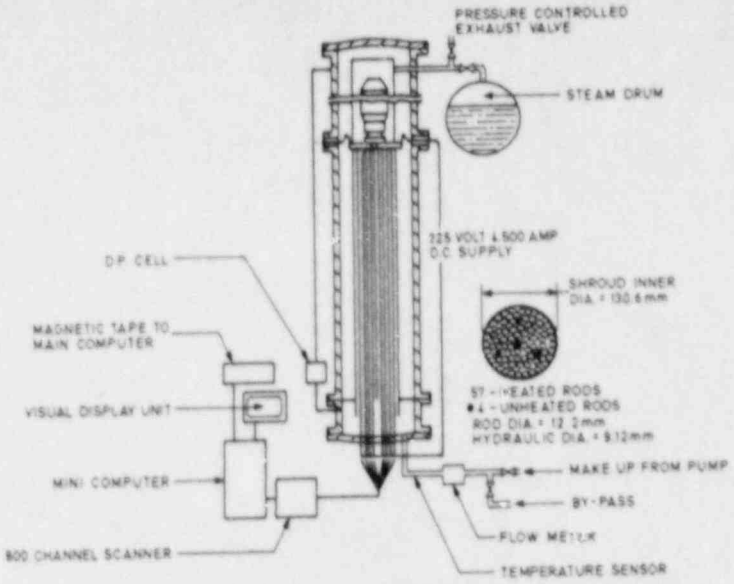

FIG.1A THETIS EXPERIMENTAL FACILITY

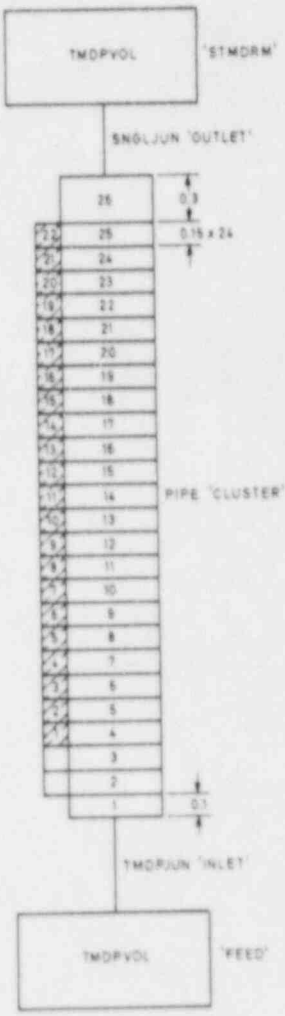

FIG.1B NODING DIAGRAM

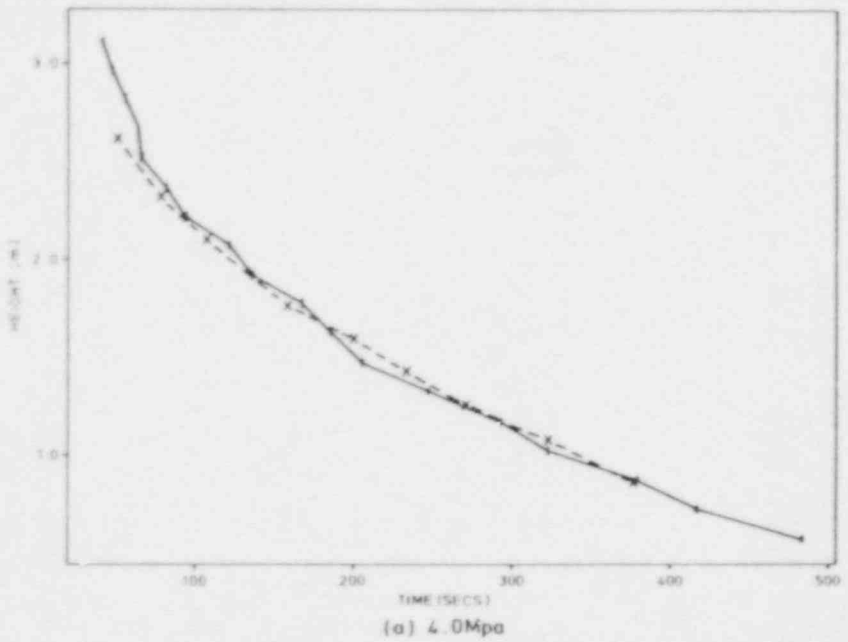

(a) 4.0Mpa

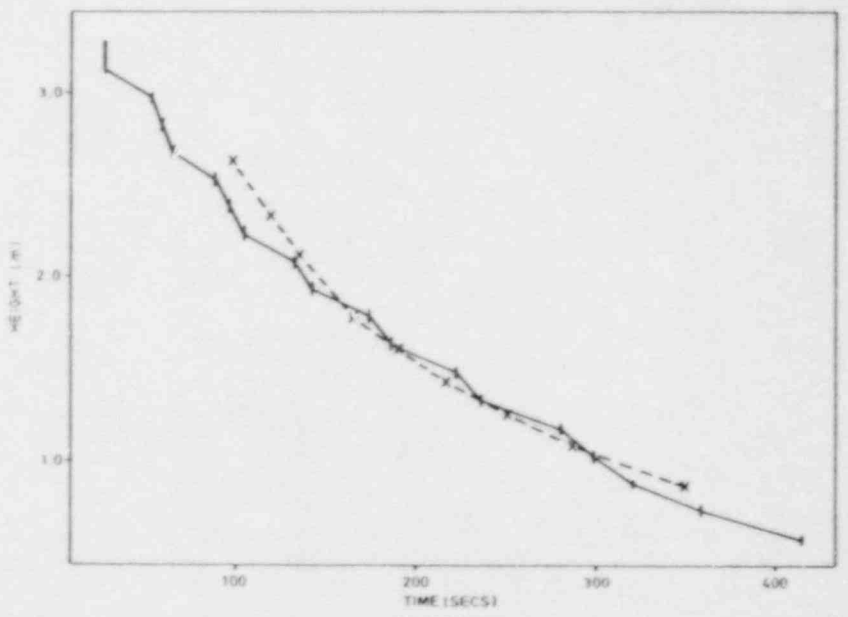

(b) 2.0Mpa

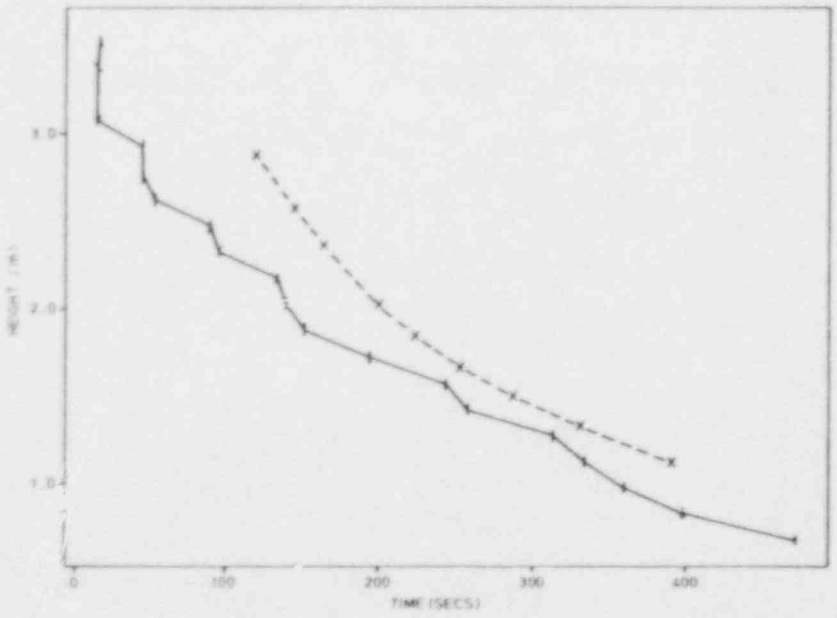

(c) 1.0 Mpa

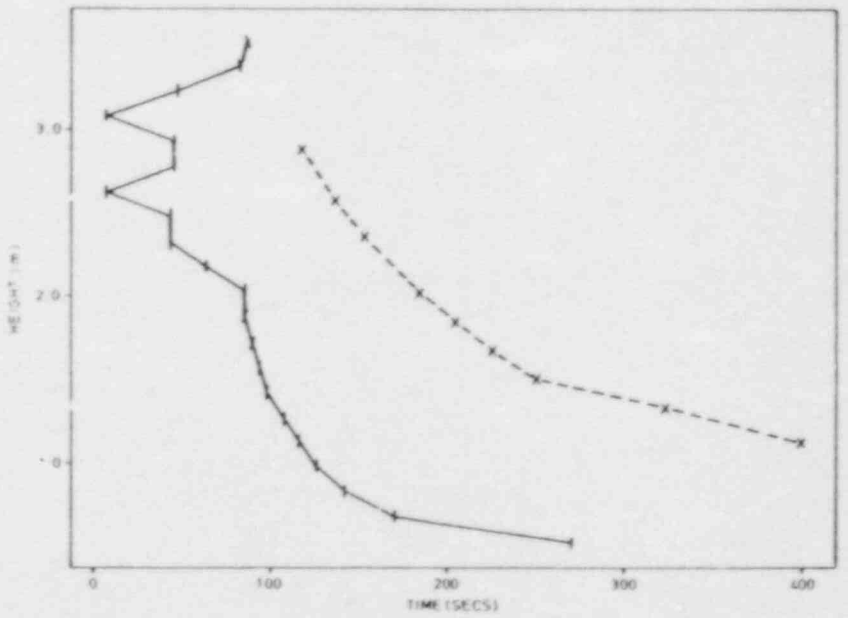

(d) 0.2 Mpa

KEY: RELAP 5/MOD 2 — EXPERIMENT

FIG. 2 DRY-OUT LEVEL HISTORIES IN BOILDOWN

2.2 Assessment of Interphase Drag Models in RELAP5/Mod2

An assessment was carried out by CEGB of the performance of the interphase drag models in RELAP5/Mod2 in vertical flow. This work is reported in ref. [2]. The method used was to extract the relationships for interphase and wall friction from the source code of RELAP5/Mod2/Cycle 36.00, and to recode them into a simple driver program. The driver program was then used to calculate void fraction in steady vertical upflow and downflow for different combinations of steam and water flow-rates, for a range of pressures and pipe sizes. Calculated void fractions were compared with test data, and with predictions of void fraction correlations.

Void fraction errors for upflow were found to increase with decreasing liquid flow-rate, increasing gas flow-rate, increasing pipe size and decreasing pressure. Figure 3 shows results for different pressures and pipe sizes obtained for natural separation conditions (zero liquid flow-rate). Code error is expressed as the percentage difference between the two-phase mixture density calculated with the RELAP5 models, and that calculated using the Wilson void fraction correlation. The latter has been extensively validated for steam-water mixtures in pipes and pin bundles, under natural separation conditions and is considered a reliable standard for comparison for the conditions of Figure 3. Also shown for comparison is the two-phase mixture density calculated using the EPRI and Zuber-Findlay drift flux correlations.

Comparisons show a systematic underprediction of density for small hydraulic diameters. However at pressures of interest in modelling small break LOCAs and pressurised transients in PWRs (>4 MPa) errors are broadly similar to errors normally expected in applying standard correlations for void fraction. At pressures below 1.0 MPa, very large density errors were observed.

2.3 Assessment of RELAP5/Mod2 Critical Flow Model

A UKAEA study [3] of the RELAP5/Mod2 critical flow treatment using a test model relevant to a small break LOCA experiment in the LOBI test facility revealed defects for conditions where the break junction was connected to a horizontal volume containing stratified flow. In the test problem the critical mass flux is calculated in an orifice of area 7.07×10^{-6} m^2 connected to an upstream volume containing horizontal stratified steam water flow at a pressure of 3.16 MPa. The steam flow to the volume is controlled using a time dependent junction. The liquid flow is not fixed but is supplied by a time dependent junction. Figure 4 shows results for the case where the liquid supply is saturated. Also shown are predictions of the isentropic homogeneous equilibrium model (HEM). The HEM calculation was based on the pressure and stagnation quality in the upstream volume (equal to the quality supplied from the time dependent junctions). It can be seen that for the usual modelling choice of allowing for slip, the RELAP5/Mod2 predicted flow rate is well below the HEM flow-rate which is considered unphysical. If the break is modelled as a homogeneous (no-slip) junction results close to the HEM are

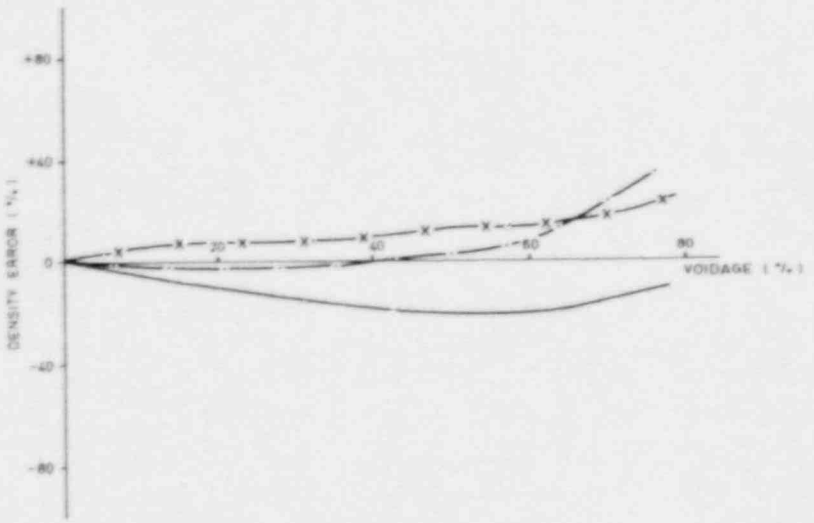

(a) p = 10MPa D = 0.01m

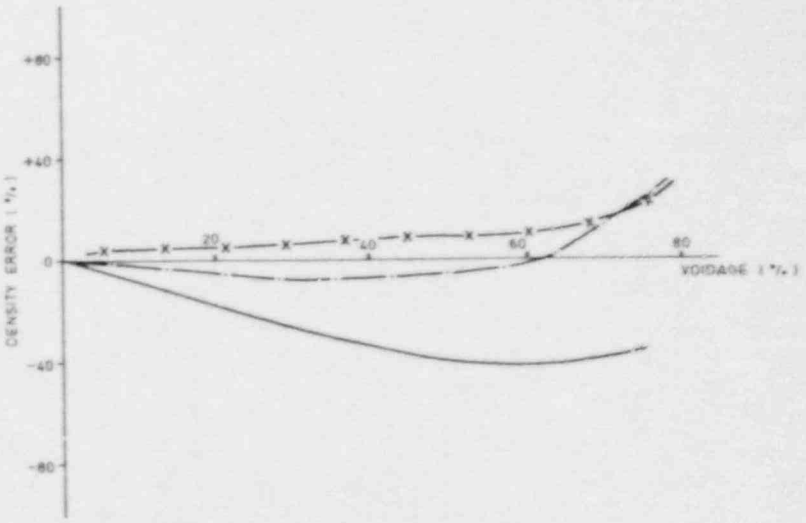

(b) p = 4.0MPa D = 0.01m

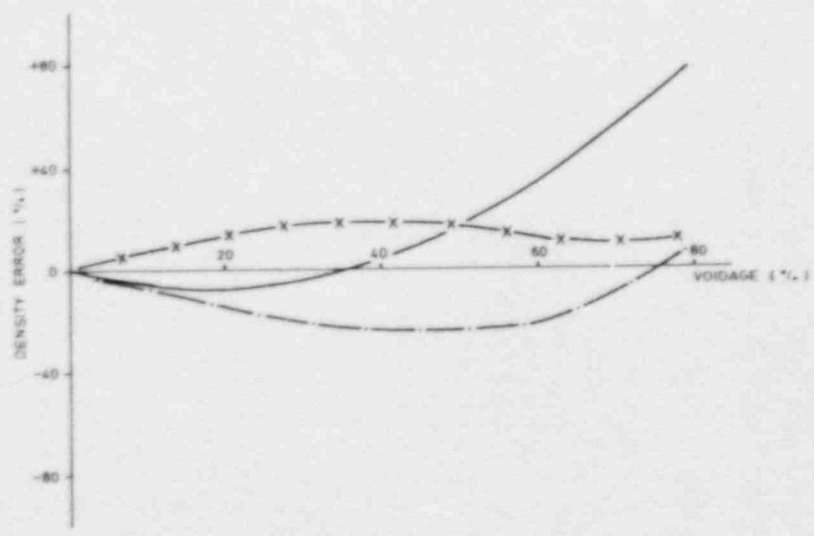

(c) p = 10MPa D = 1.0m

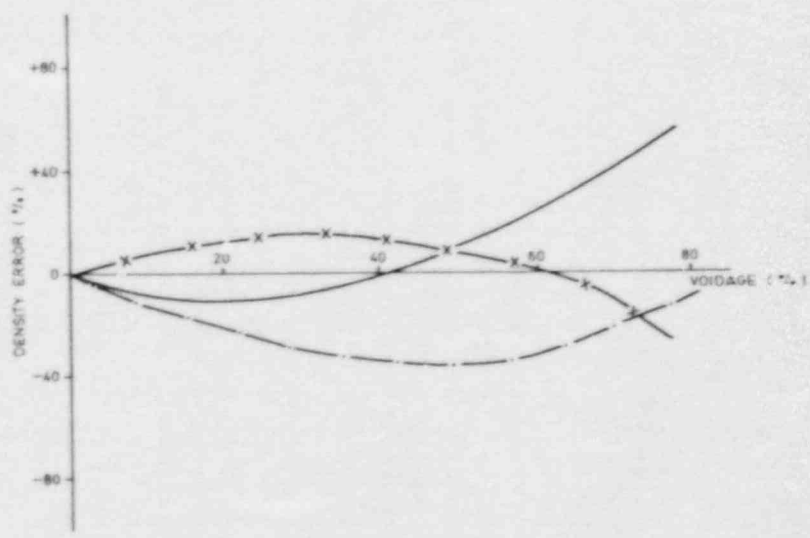

(d) p = 4.0MPa D = 1.0m

KEY ——— RELAP 5 / MOD 2 —X— EPRI —·—·— ZUBER-FINDLAY

FIG. 3 DENSITY ERRORS CALCULATED IN UP-FLOW (ZERO LIQUID FLOW-RATE)

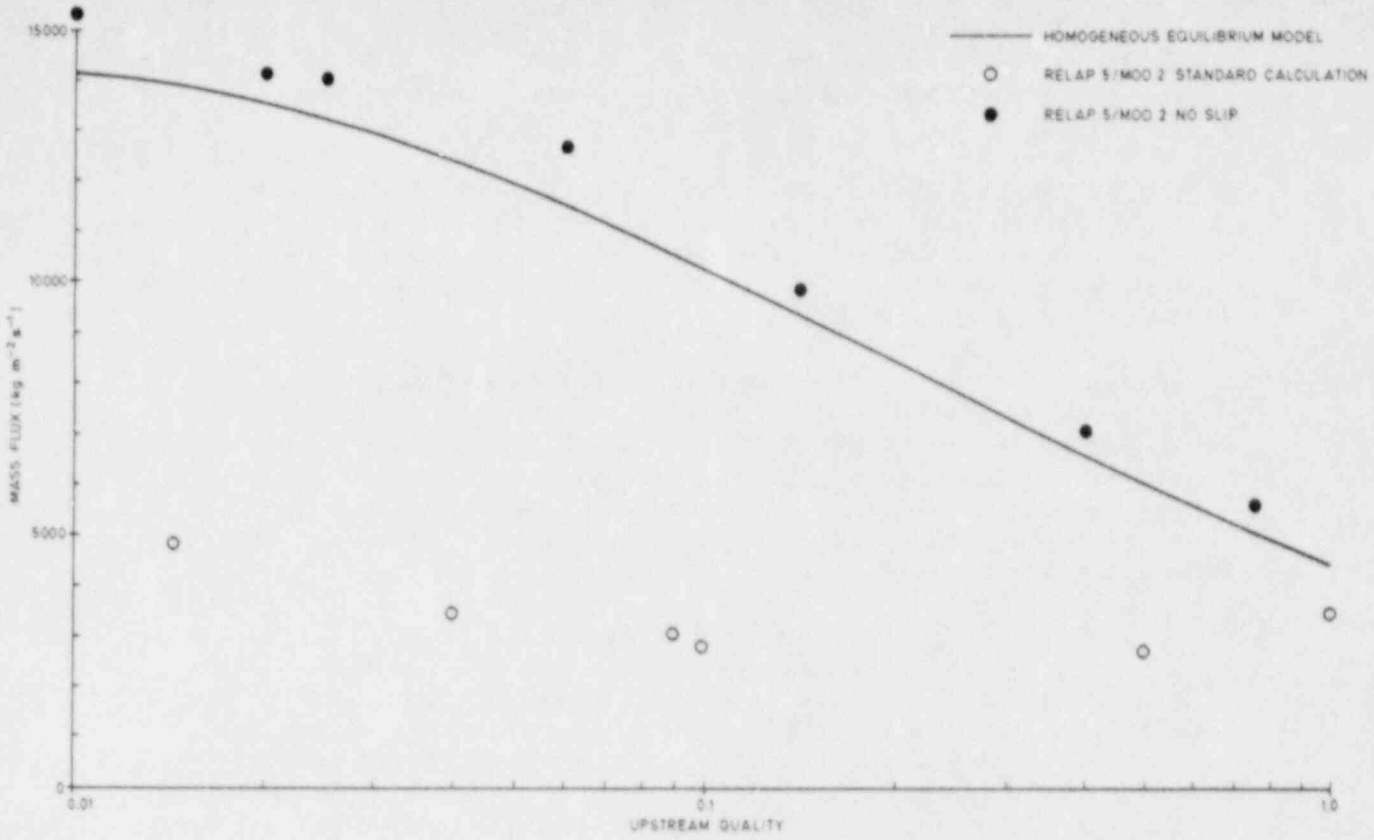

FIG. 4 RELAP 5 / MOD 2 CALCULATED CRITICAL FLOW-RATES FOR STRATIFIED UPSTREAM CONDITIONS

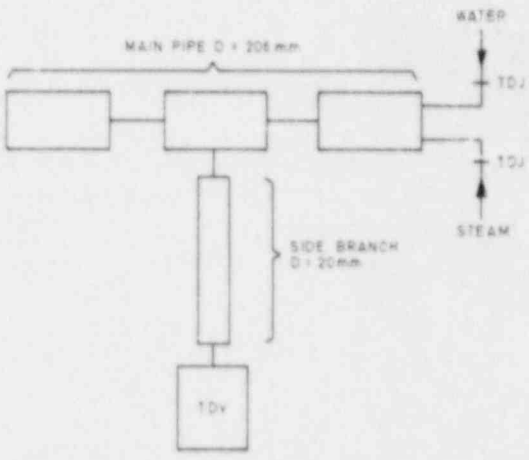

FIG. 5 TEST PROBLEM TO ASSESS RELAP 5 / MOD 2 STRATIFIED FLOW ENTRAINMENT MODEL

obtained. The anomalous result in the case with slip is believed due to inconsistent approximations in the RELAP5/Mod2 critical flow model.

The UKAEA study also considered the case where subcooled water and steam entered the break junction. It was felt that for this case the present RELAP5/Mod2 procedure, which assumes thermal-equilibrium conditions upstream of the choking point, is likely to over-predict the flow-rate.

2.4 Assessment of Horizontal Stratification Entrainment (HSE) Model

The HSE model in RELAP5/Mod2 is designed to calculate flow in an off-take pipe connected to a larger diameter horizontal pipe in which there is a stratified two-phase flow. The model is useful in small break LOCA analysis when the pipe break is located in the reactor hot or cold leg.

To test the model the code was applied to a test problem shown in Figure 5. In this problem steam and water are fed into a 206mm dia. horizontal pipe via time dependent junctions. A 20mm dia. off-take branch discharging into a time dependent volume at a fixed pressure is connected to the main pipe at mid-length.

The calculated quality of the fluid entering the off-take branch is plotted against the calculated liquid depth in the main pipe in the steady state condition, in Figure 6 (broken curves). Calculations shown are for an upward, downward and horizontal side off-take at system pressures of 0.7 and 7.0 MPa. Results are plotted in a non-dimensional form which allows comparison with test data for different pipe sizes and fluid properties.

Air-water and steam-water test results from a number of experimental facilities [4-7] are included on Figure 6 for comparison. It is seen that there is a tendency of the HSE model in RELAP5/Mod2 to significantly under-predict discharge quality, particularly for the case of the upward oriented off-take. Also shown in Figure 6 (solid curves) are predictions of a modified code version developed by CEGB and UKAEA, containing improved correlations for off-take branch quality. The modified code version is seen to give considerably improved agreement with the test data.

Further details of these calculations, and a description of the code modification, are given in ref. [8].

3. CALCULATIONS OF INTEGRAL TESTS

3.1 OECD LOFT test LP-SB-03

LOFT test LP-SB-03 simulated a 0.4% cold leg break LOCA in a PWR with failure of the high head safety injection (HHSI) systems. Cooldown was achieved by feed-and-bleed of the secondary system, which was initiated after core uncovering.

This test was calculated by CEGB using RELAP5/Mod2 Cycle 36.01. Details are given in ref. [9]. The calculation employed a model of the LOFT facility consisting of 131 nodes, 134 junctions and 123 heat structures, which had been developed from an earlier RELAP5/Mod1 model of the LOFT facility.

Excellent agreement with data was obtained in this calculation, with the timing of the draining of the legs and uncovering of the core being predicted with good accuracy. Typical results are shown in Figure 7. The main error was an over-prediction of the accumulator injection flow at the end of the experiment. This is believed to have been due to an over-prediction of the system depressurisation rate caused by an over-prediction of the rate of steam condensation on the subcooled injection flow. An error is also seen in the heat-up rate of the exposed fuel (see Fig.7d), which was under-predicted by RELAP5/Mod2. The enhanced cooling in the calculation was due to prediction of drainback of condensate from the hot-legs into the core. This drainback may also have occurred in the test but is likely to have influenced only the cooling of the peripheral rods in the core. Radial sub-division of the core would have been needed to capture this effect in the calculation.

The calculation was executed at a CPU time-to-real time ratio of 3.5 on a CRAY-1S computer. Considerable improvements were found in comparison with previous CEGB calculation of the same test with RELAP5/Mod1, in respect of mass error, execution speed and stability.

3.2 OECD LOFT Test LP-SB-01

LOFT test LP-SB-01 simulated a 1.0% hot leg break LOCA in a PWR with HHSI systems available. The reactor coolant pumps were tripped early in the test.

This test was analysed by CEGB using RELAP5/Mod2/Cycle 36.02 [10]. The LOFT model employed consisted of 120 nodes, 126 junctions and 125 heat structures.

In the early part of the test there was an extended period in which the fluid quality in the break line was less than 0.005. To obtain a satisfactory calculation of break flow during this period, it was found necessary to apply a two-phase discharge coefficient (CD2) of 1.18 which is over 40% higher than the value of 0.81 used in previous LOFT test simulations. The enhanced break flow during this period is believed due to the presence of thermal disequilibrium effects, which are characteristic of low quality critical steam-water flow in nozzles of small diameter. These effects cannot be modelled accurately by the simplified critical flow model in RELAP5/Mod2.

Typical results of the calculation using the modified value of CD2 are shown in Figure 8. Agreement is considered reasonable. The underprediction of hot leg density after 1000s is apparently due to small errors in the calculated two-phase mixture level in the reactor vessel. The test shows systematic differences between the

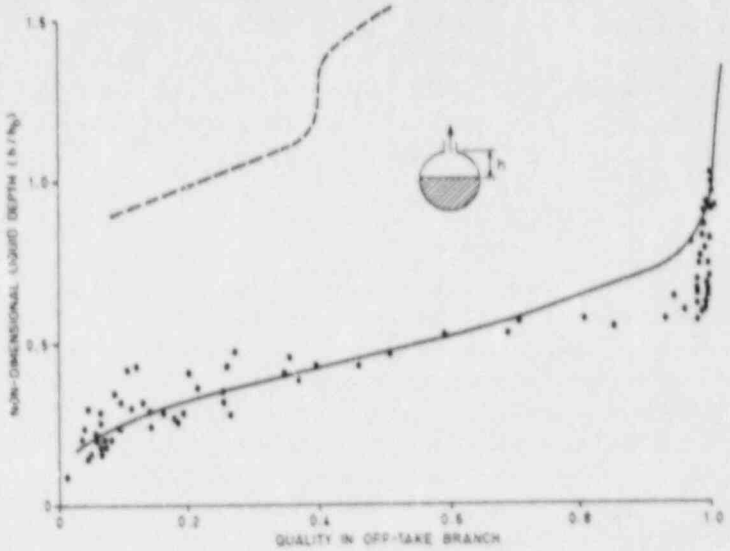

(a) UPWARD OFF-TAKE

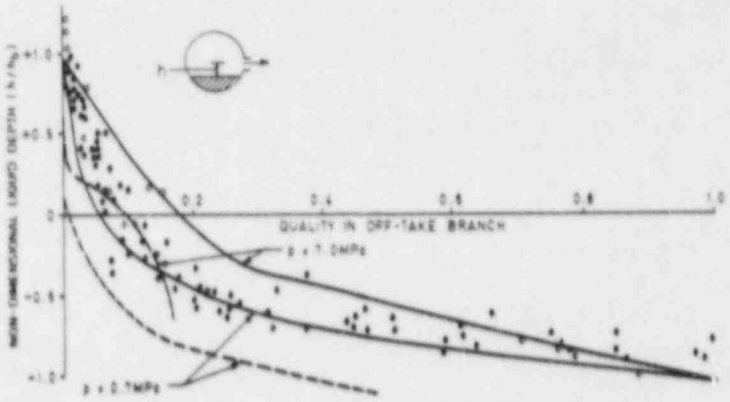

(b) SIDEWAYS OFF-TAKE

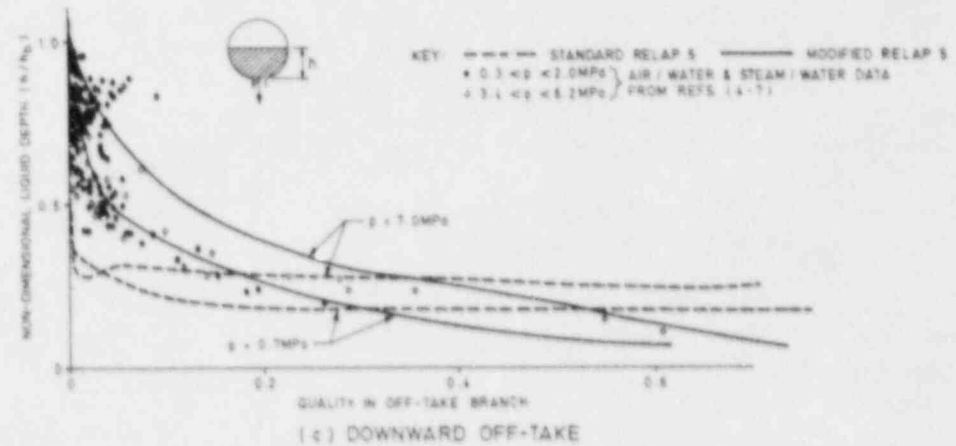

(c) DOWNWARD OFF-TAKE

FIG 6 DISCHARGE FLOW QUALITY v LIQUID DEPTH

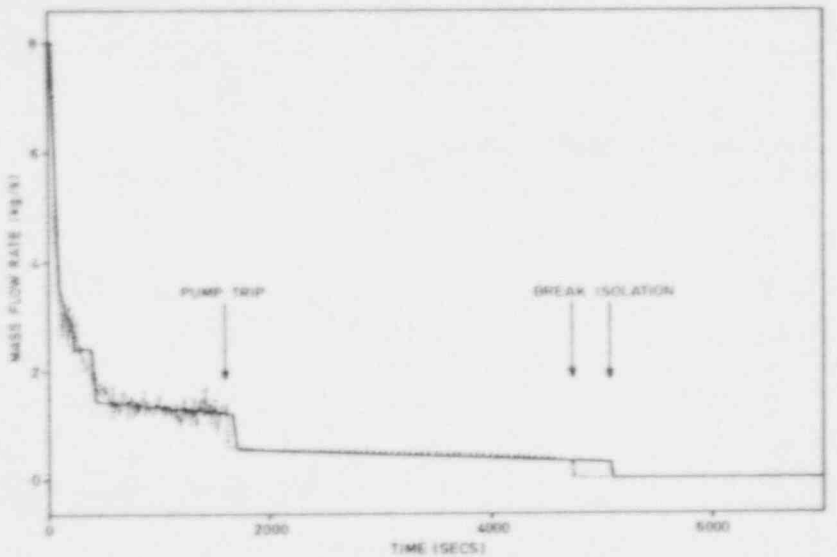

(a) BREAK DISCHARGE FLOW - RATE

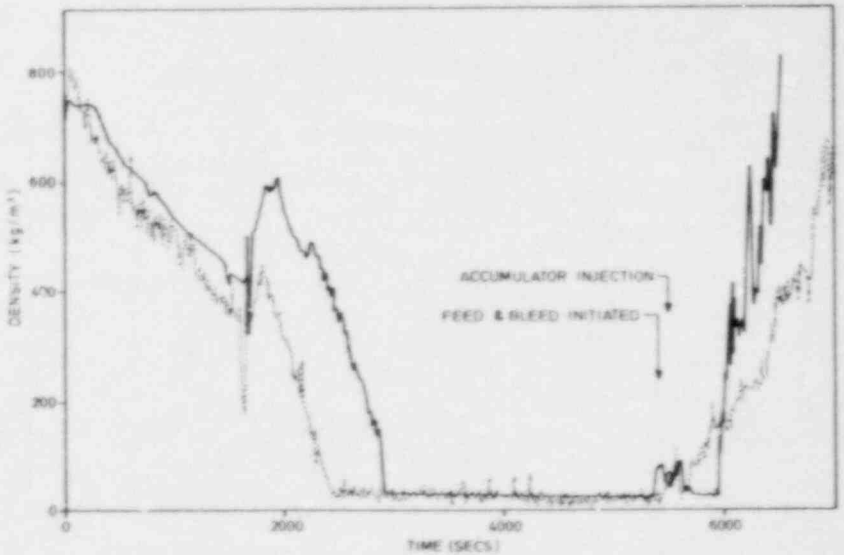

(b) HOT LEG DENSITY

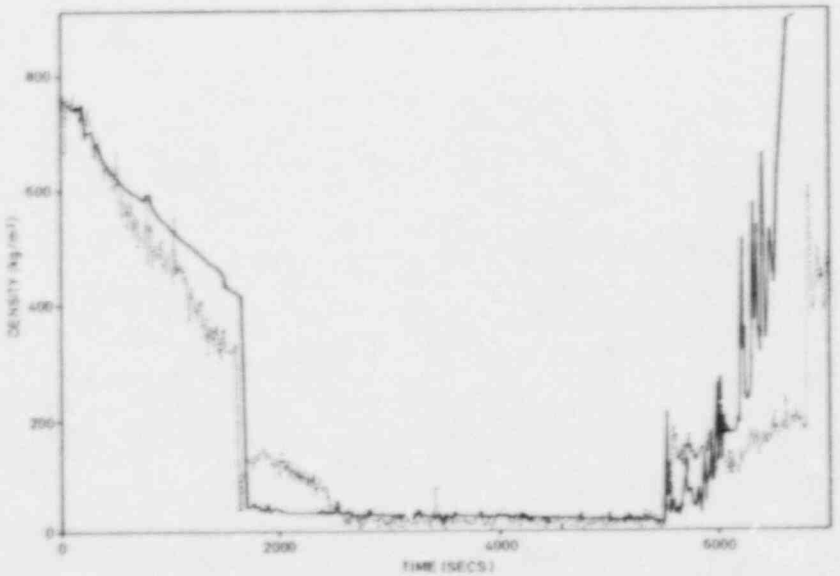

(c) COLD LEG DENSITY

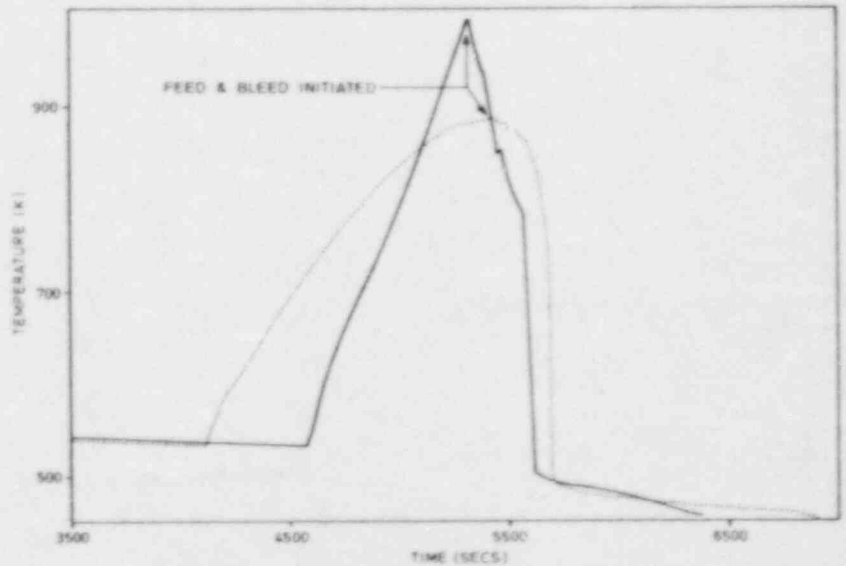

(d) FUEL CLAD TEMPERATURE, 98cm LEVEL

KEY: ——— RELAP 5 ····· TEST DATA

FIG.7 RELAP 5/MOD 2 CYCLE 36.01 CALCULATIONS OF LOFT TEST LP-SB-03

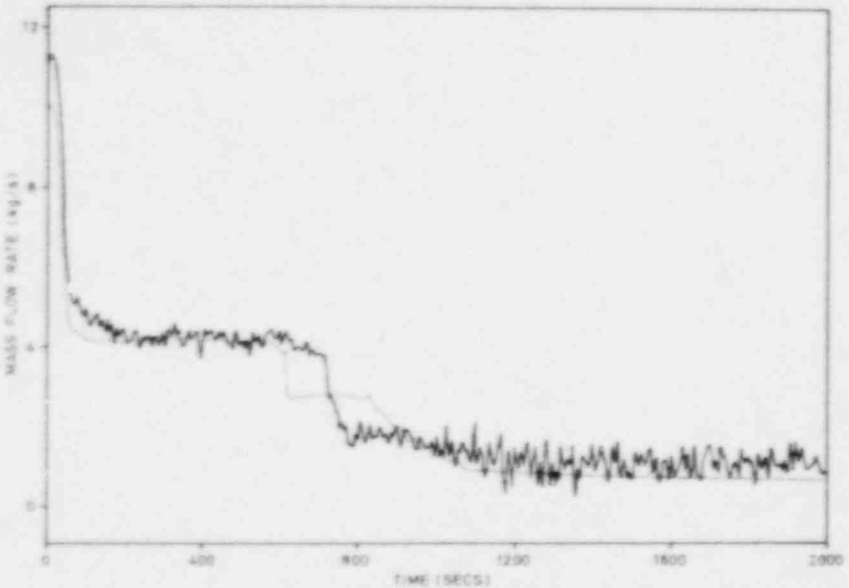

(a) BREAK DISCHARGE FLOW - RATE

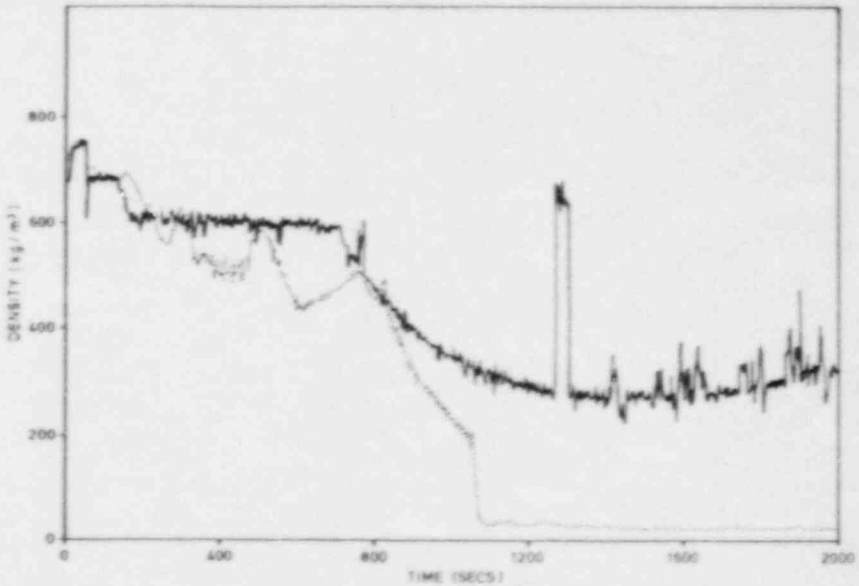

(b) HOT LEG DENSITY

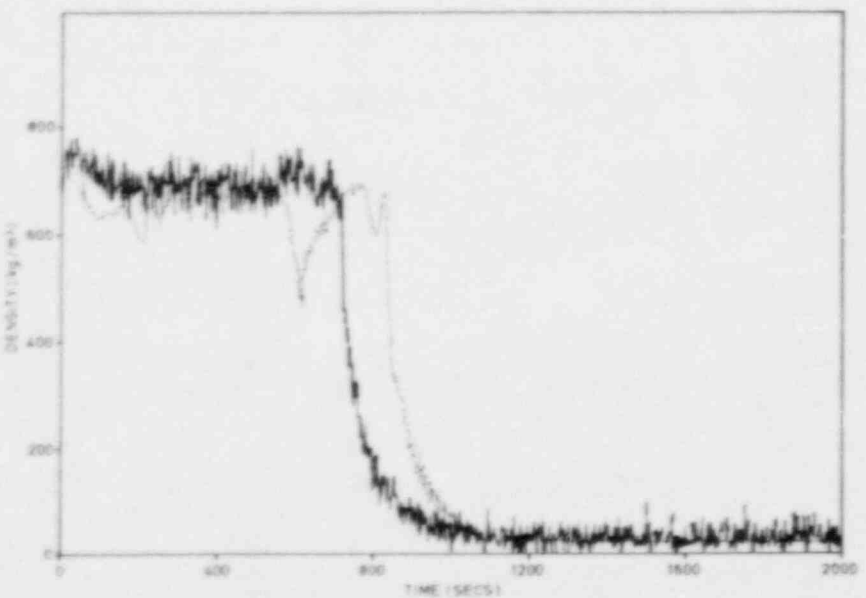

(c) BREAK - LINE DENSITY

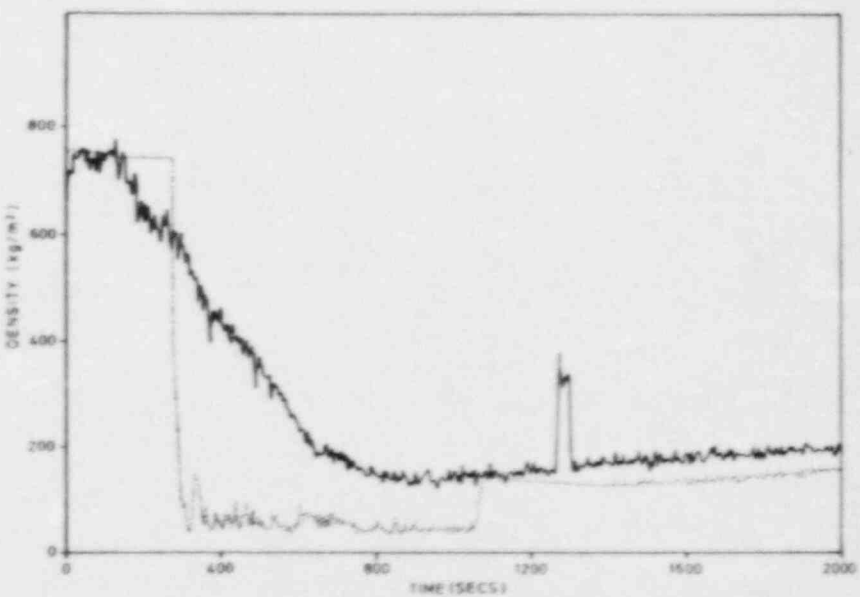

(d) COLD LEG DENSITY

KEY —— TEST DATA ····· RELAP 5

FIG. 8 RELAP 5/MOD 2 CYCLE 36.02 CALCULATIONS OF LOFT TEST LP-SB-01

fluid density in the hot leg (28cm dia.) and the break-line (2.9cm dia.) which is connected to the side of the hot leg. These density differences, which arise because of the presence of stratified flow in the hot leg, are seen to be modelled correctly by the RELAP5/Mod2 horizontal stratification entrainment (HSE) model. RELAP5/Mod1 was unable to describe this effect because it had no HSE model [11].

The calculation was executed at a CPU-to-real time ratio of 1.16 on a CRAY-IS computer. Again considerable improvements were seen over a previous CEGB calculation with RELAP5/Mod1 [11], in respect of execution speed and mass conservation errors.

3.3 OECD LOFT Test LP-SB-02

LOFT test LP-SB-02 was a counterpart test to LP-SB-01 (see above) but with reactor coolant pump trip delayed until late in the test.

The test was calculated by CEGB using RELAP5/Mod2/Cycle 36.04 [12]. The system model was the same as that used for the LP-SB-01 calculation.

Simulation of this test with the standard code version presented considerable difficulties. In particular the code failed to calculate the observed systematic differences between the hot-leg and break line densities. In consequence the mass inventory was under-predicted, leading to large errors in the loop densities late in the test. In addition, the forced circulation mass flow-rate in the loop decayed much more rapidly in the experiment than in the calculation. Also the onset of stratified flow in the hot leg was predicted to occur much too late.

An improvement in the calculated mass inventory was obtained when a UK modified code version was employed, containing the improved horizontal stratification entrainment model described in section 2.4. The new model assumes that separation effects occur in the slug flow regime as well as the stratified flow regime whereas the model in the standard code version assumes that separation effects occur only when there is stratified flow in the hot leg.

Some results of the calculations are shown in Figure 9. It is seen that the modified code version gives a reasonable prediction of break flow, and the fluid density in the hot leg and break line. However the loop flow-rate is considerably over-predicted after 1000s. (see Figure 9d). This error is believed to be due to over-prediction of inter-phase drag forces in the hot leg, associated with the failure to model the stratification of the flow in the hot leg which was observed early in the test. The reason that the code failed to describe the transition to stratified flow is not fully understood, and further data on flow regime transitions in hot leg geometries are desirable to help resolve this problem.

The calculation was executed at a CPU to real time ratio of 2.76 on a CRAY-XMP computer.

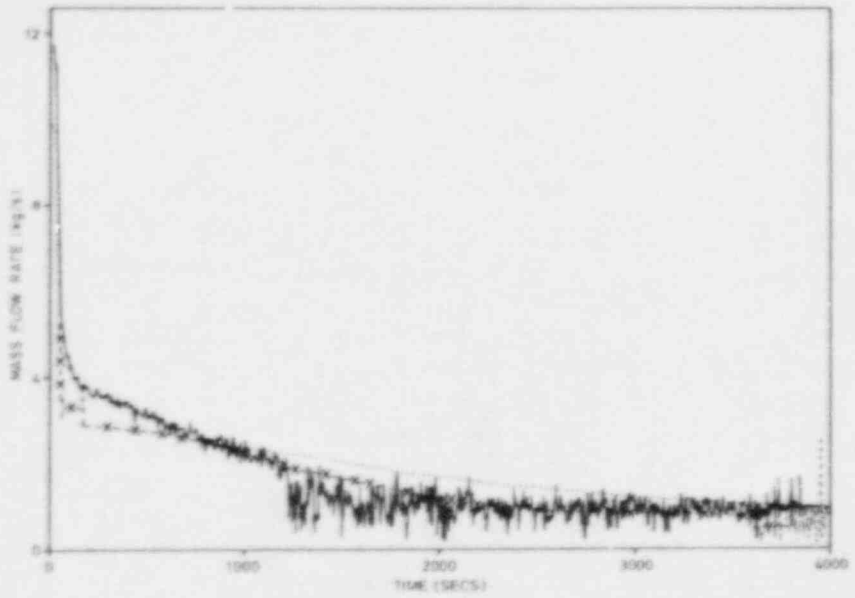

(a) BREAK DISCHARGE FLOW - RATE

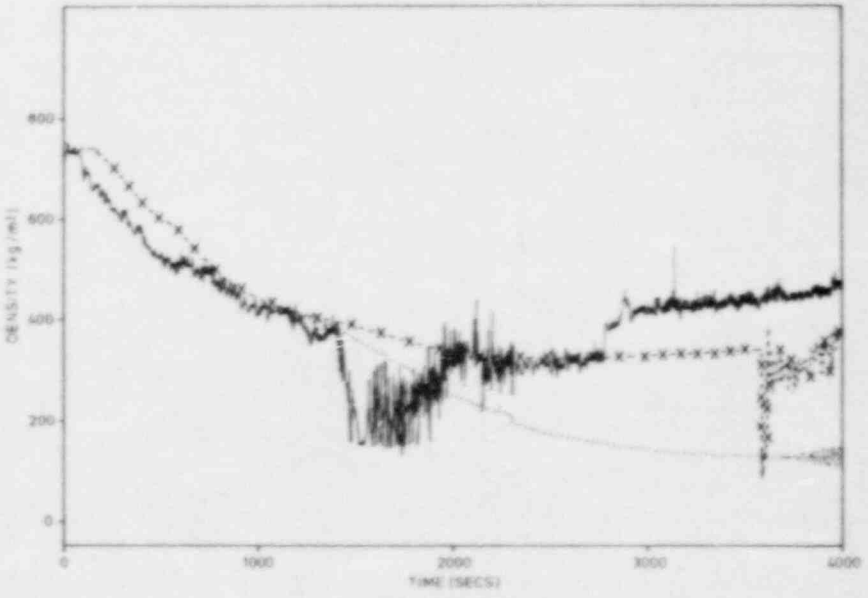

(b) HOT LEG DENSITY

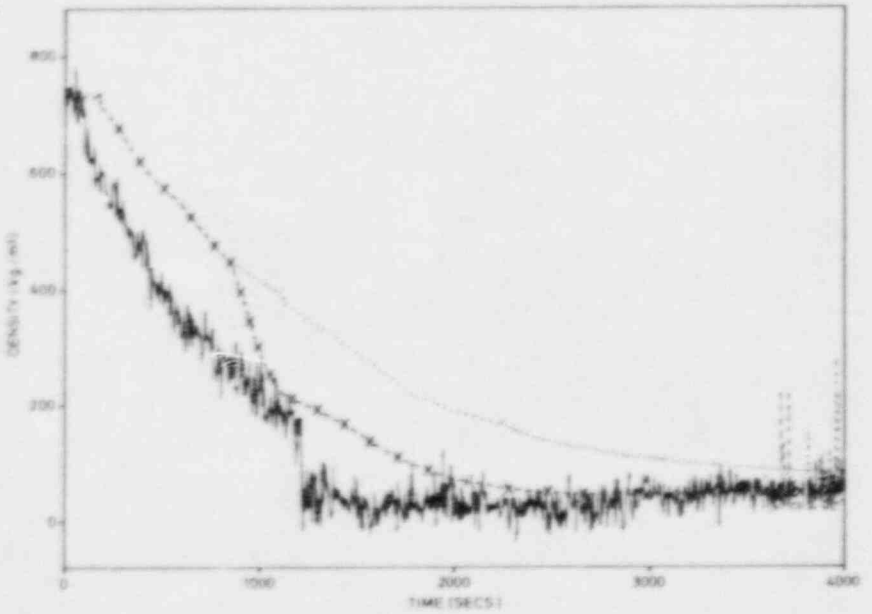

(c) BREAK - LINE DENSITY

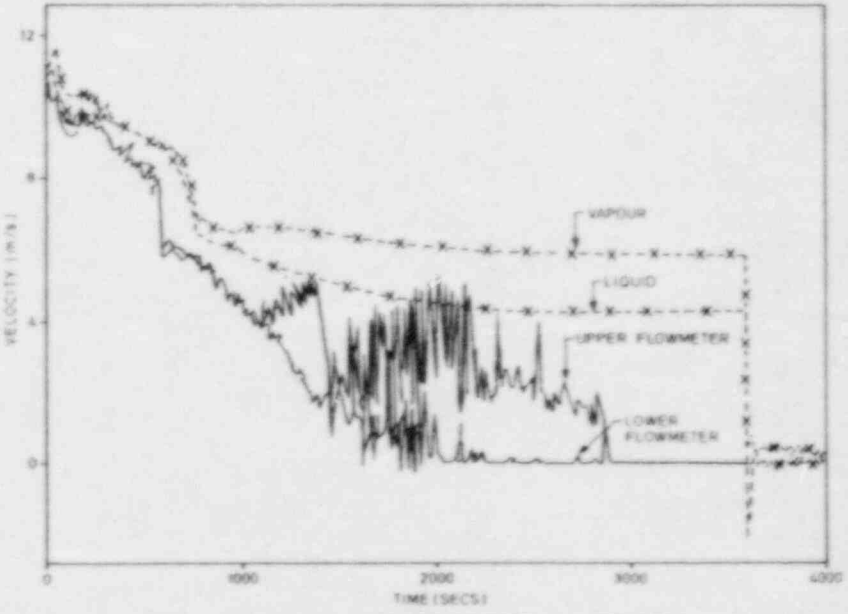

(d) GAS & LIQUID VELOCITIES IN HOT LEG

KEY ——— TEST DATA ····· STANDARD CODE X– –X– –X MODIFIED CODE

FIG 9 RELAP 5/MOD 2 CYCLE 36 04 CALCULATIONS OF LOFT TEST LP-SB-02

3.4 OECD LOFT Test LP-FW-01

LOFT test LP-FW-01 simulated a loss-of-feedwater fault in a PWR. Recovery was by primary system bleed-and-feed, where coolant was injected by the HHSI system and discharged via a pressuriser pressure relief valve.

The test was simulated by CEGB using RELAP5/Mod2/Cycle 36.04 [13]. The input model was based on that previously used for the calculations of LOFT small break LOCA tests. The model consisted of 115 volumes, 122 junctions and 123 heat structures. The relief valve area was adjusted so that good agreement was obtained with the rate of decrease of primary pressure during the period of the transient when single phase steam was discharged from the valve.

Calculations were carried out with the standard code version, as well as the UK modified code version containing improved models for the effect of flow stratification on the flow in the hot-leg surge line connection (see section 2.4). Figure 10 shows results obtained with the standard code version only.

The calculation is considered satisfactory, with most parameters predicted with acceptable accuracy. The main code error was an over-prediction of the two-phase discharge flow in the open pressuriser relief valve after 1500s, which led to an underprediction of system inventory of 20% by 6000s. The error is believed to be most likely due to minor errors in modelling inter-phase drag forces in the reactor pressure vessel, which caused the quality of fluid entering the hot leg to be underpredicted.

Calculations with the modified code version gave a somewhat improved agreement with the primary pressure and pressuriser level; however the mass inventory errors were not significantly improved.

The calculation was executed at a CPU to real time ratio of 0.75 on a CRAY-XMP computer.

3.5 LOBI Test BL-02

LOBI test BL-02 simulated a 3% cold leg break LOCA in a PWR, with HHSI systems available and manual depressurisation of the secondary system. Primary circulating pumps were tripped early in the test.

The test was calculated by CEGB using RELAP5/Mod2/Cycle 36.04 [14]. The RELAP5 input model for the LOBI facility utilised 165 nodes, 173 junctions and 150 heat structures. For the post-test calculation the break discharge coefficients for sub-cooled and saturated two-phase conditions were set to 0.85 to give a good match to the measured break flow.

Results of the post-test calculation are shown in Figure 11. The calculation is considered satisfactory. Brief dry-outs of the heater rod extensions in the upper plenum were observed at 213s and 485s due to liquid level depression in the vessel. The second

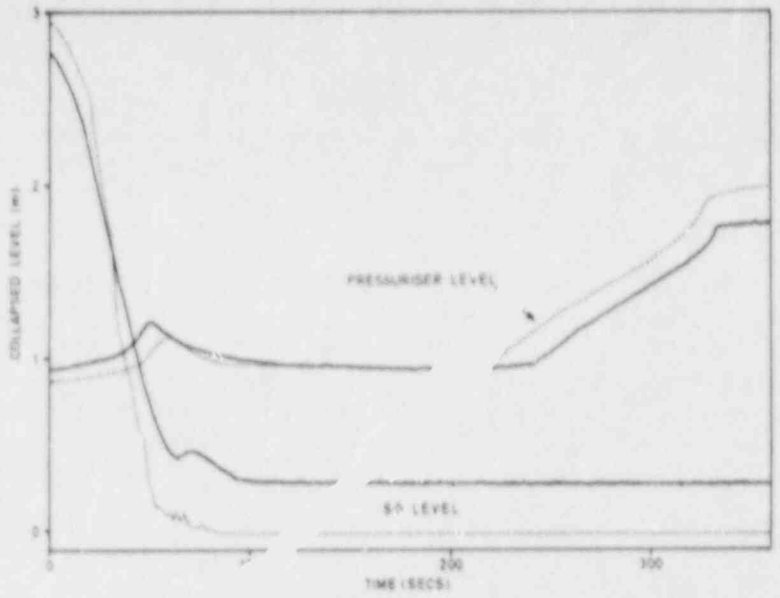

(a) COLLAPSED LIQUID LEVELS IN PRESSURISER & STEAM GENERATOR

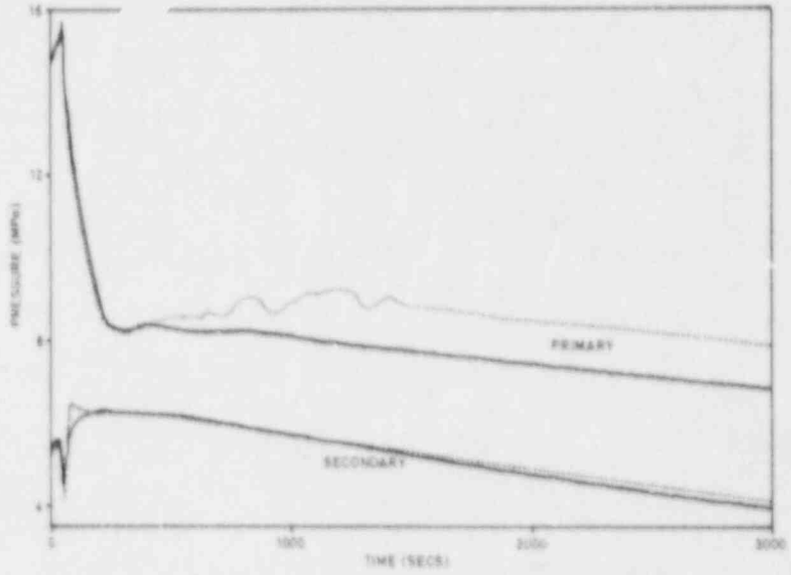

(b) PRIMARY & SECONDARY PRESSURE HISTORIES

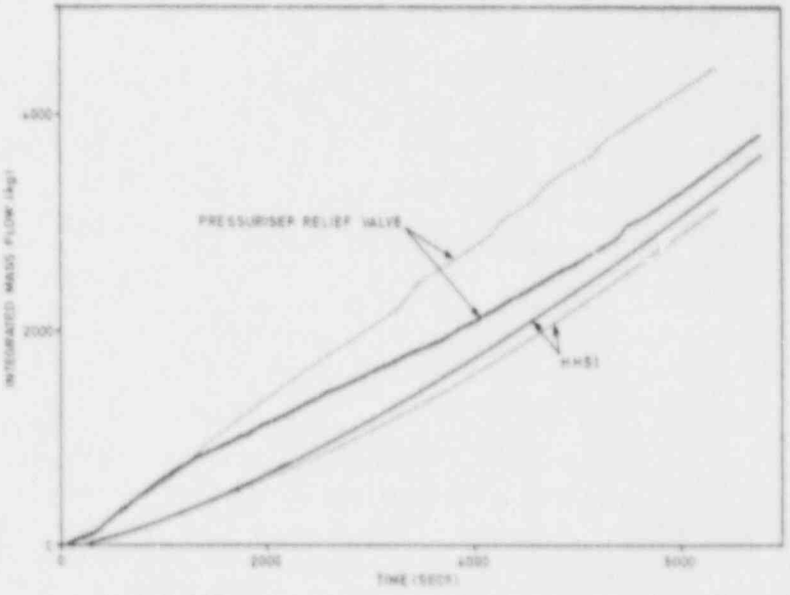

(c) INTEGRATED MASS FLOW IN PRESSURISER RELIEF VALVE & HHSI

KEY ——— TEST DATA ····· RELAP 5 CALCULATION

FIG. 10 RELAP 5/MOD 2 CYCLE 36.04 CALCULATIONS OF LOFT TEST LP-FW-01

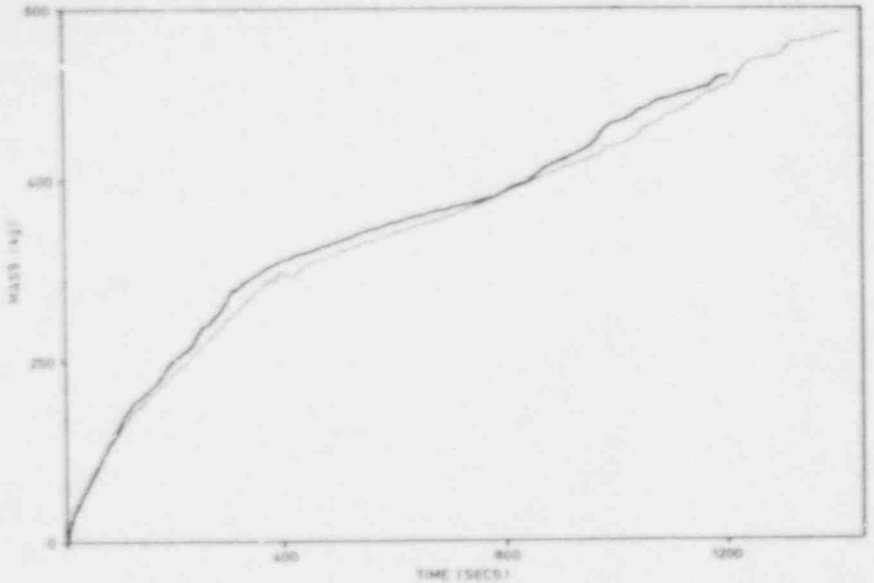

(a) BREAK DISCHARGE FLOW-RATE

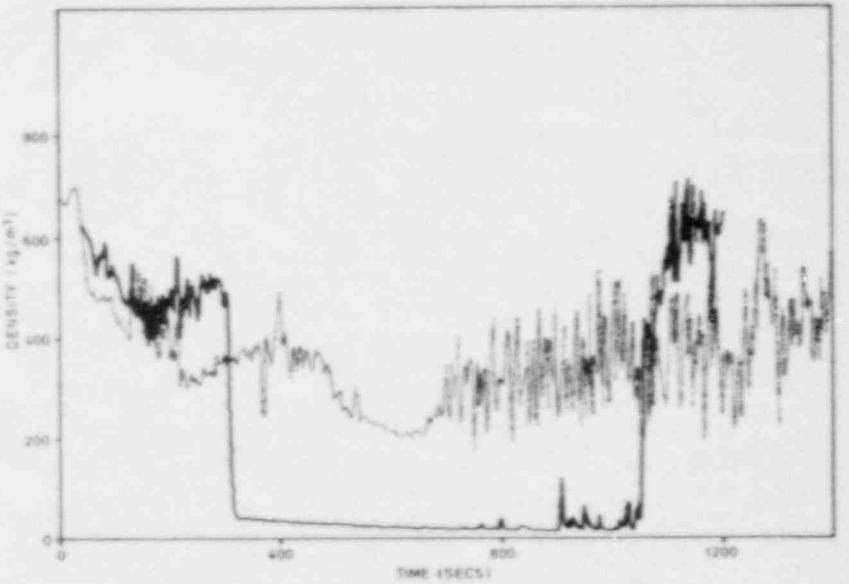

(b) INTACT LOOP HOT LEG DENSITY

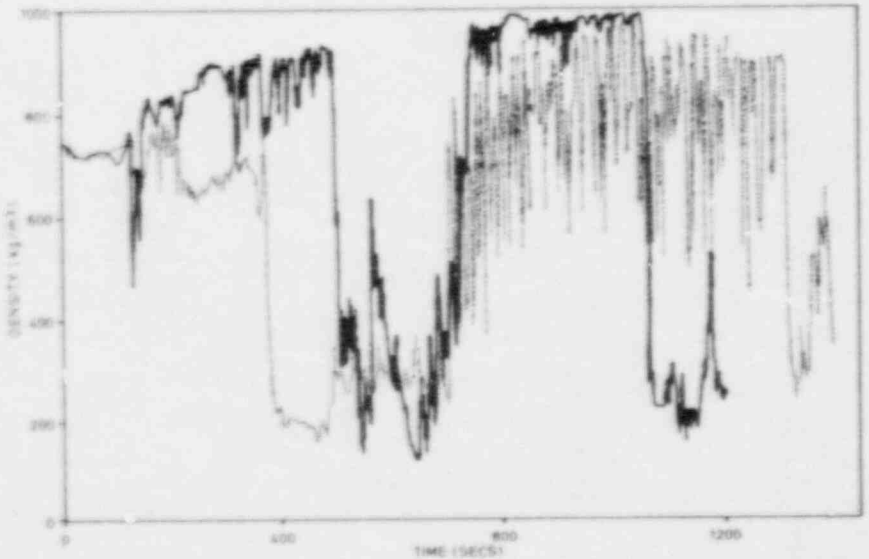

(c) INTACT LOOP COLD LEG DENSITY

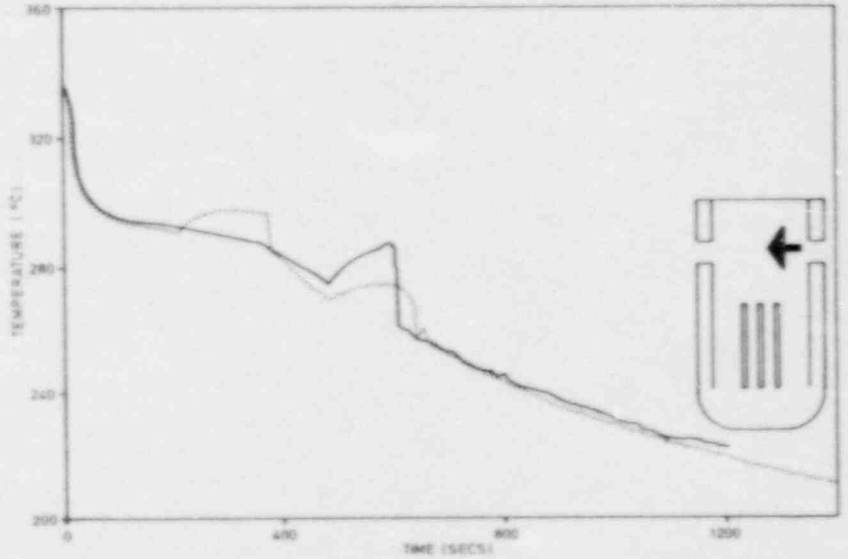

(d) CLAD TEMPERATURES ON ROD EXTENSIONS (OUTLET NOZZLE ELEVATION)

KEY: ——— RELAP 5 CALCULATION ——— TEST DATA

FIG. 11 RELAP 5/MOD 2 CYCLE 36.04 CALCULATIONS OF LOBI TEST BL-02

dry-out was successfully predicted by the code, indicating reasonable modelling of the liquid level trajectory in the reactor pressure vessel. RELAP5/Mod2 did not accurately describe liquid hold-up in the hot legs in the period 320-1050s when liquid flow was restricted by counter-current flooding due to the flow of steam condensing in the depressurising steam generators. It is noted however that in LOBI the pipe-work connecting the hot leg to the steam generator forms a sharp elbow whereas in a PWR a swept bend is used. This may have caused the flooding limit to be more restrictive in the LOBI test than in the equivalent PWR transient.

The calculation was executed at a CPU to real time ratio of approximately 2 on a CRAY-XMP computer.

4. FUTURE WORK

The assessment of the RELAP5/Mod2 code in the UK is ongoing. Calculations are also in progress within UKAEA and CEGB of the following tests:

LOBI Test	A2-81	:	Small Cold Leg Break
LOBI Test	BL-21	:	Steam Generator Tube Rupture
LOBI Test	ST-02	:	Loss-of-Feedwater
LOFT Test	L3-5	:	Small Cold Leg Break
LOFT Test	L3-6	:	Small Cold Leg Break
Semiscale Test	S-LH-1	:	Small Cold Leg Break
Semiscale Test	S-LH-2	:	Small Cold Leg Break
Semiscale Test	S-FS-1	:	Steam-line Break
MB-2 Phase I Test	3	:	Steam-Line Break

5. DISCUSSION AND CONCLUSIONS

RELAP5/Mod2/Cy 36 is being used in the UK for analysis of some small LOCAs and pressurised transients in the Sizewell 'B' PWR. To support this application, the code is being assessed against a range of separate effects and integral experiments in a joint programme involving CEGB and UKAEA.

In calculations performed so far the code has been found to perform generally satisfactorily, and is felt to represent a major improvement over RELAP5/Mod1 in terms of execution speed, stability, mass error and accuracy.

The following areas have been highlighted where model improvements may be desirable to enhance the capabilities of the code for modelling small LOCAs and pressurised faults in PWRs:

(i) critical flow modelling. It has been found that the code can produce unphysical results for cases where there are large interphase relative velocities in the volume upstream of the break.

(2) horizontal stratification entrainment model. The present RELAP5/Mod2 model has been found to systematically under-predict the fluid quality in the off-take branch, when compared with test data. Improved correlations have been incorporated in a special UK code version; it would be desirable to include similar modifications in future released versions of RELAP5.

(3) Interphase drag models. The interphase drag relationships in RELAP5/Mod2 have been found to give systematic errors in void fraction in vertical components. The errors are probably of an acceptable magnitude for high pressure conditions. However for pressures below 1.0 MPa the code is unlikely to give acceptable predictions of two-phase mixture density in vertical components.

(4) flow regime transitions. In the simulation of a LOFT experiment, the code failed to describe the transition to stratified flow in the hot leg under forced circulation conditions. Further experimental data on flow regime transitions in hot leg geometries are desirable to help explain the origin of this problem.

6. REFERENCES

[1] Croxford M G and Hall P C, "Analysis of the THETIS Boildown Experiments Using RELAP5/Mod2", CEGB Report GD/PE-N/576, March 1987

[2] Ardron K H and Clare A J, "Assessment of Interphase Drag Correlations in RELAP5/Mod1 and TRAC-PF1/Mod1", Unpublished CEGB Report, April 1987.

[3] Bryce W M, "Some Comments on the Critical Flow Model in RELAP5/Mod2", Unpublished UKAEA Internal Paper, October 1986.

[4] Smoglie C, "Two Phase Flow Through Small Branches in a Horizontal Pipe with Stratified Flow", KfK Report 3861, December 1984.

[5] Maciaszek T and Menponteil A, "Experimental Study on Phase Separation in a Tee Junction for Steam-Water Stratified Inlet Flow", Paper C2 Presented at European Two-Phase Flow Group Meeting, Munich, 10-13 June 1986.

[6] Schrock V E, Revankar S T, Mannheiner R, and Wang C H, "Small Break Critical Discharge - the Roles of Vapour and Liquid Entrainment in a Stratified Two-Phase Region Upstream of the Break", USNRC Report NUREG/CR-4761, December 1986.

[7] Anderson J L and Benedetti R L, "Critical Flow Through Small Pipe Breaks", EPRI Report EPRI NP-4532, May 1986.

[8] Ardron K H and Bryce W M, "Assessment of Horizontal Stratification Entrainment Model in RELAP5/Mod2", Unpublished CEGB Report, August 1987.

[9] Brown G and Harwood C, "RELAP5/Mod2 Calculation of OECD LOFT Test LP-SB-03", Unpublished CEGB Report, April 1986.

[10] Hall P C and Brown G, "RELAP5/Mod2 Calculation of OECD LOFT Test LP-SB-01", Unpublished CEGB Report, November 1986.

[11] Clare A J, "RELAP5/Mod1 Calculations of the OECD LOFT LP-SB-01 and LP-SB-02 Small Hot Leg Break Experiments", Unpublished CEGB Report, July 1985.

[12] Hall P C, "RELAP5/Mod2 Calculation of OECD LOFT Test LP-SB-02", Unpublished CEGB Report, August 1987.

[13] Croxford M G and Harwood C, "RELAP5/Mod2 Calculation of OECD LOFT Test LP-FW-01", Unpublished CEGB Report, May 1987.

[14] Scriven A H, "Analysis of LOBI Test BL02 (3% Cold Leg Break) with the RELAP5 Code", Unpublished CEGB Report, May 1987.

7. ACKNOWLEDGEMENT

This paper is published by permission of the Central Electricity Generating Board.

CW37001R6KEL/KHA

APPLICATION OF RELAP5/MOD2 FOR DETERMINATION OF ACCIDENT MANAGEMENT PROCEDURES

P.M. Stoop
J.P.A. van den Bogaard
A. Woudstra
H. Koning

Netherlands Energy Research Foundation (ECN), P.O. Box 1,
NL-1755 ZG Petten, The Netherlands

ABSTRACT

This paper presents the results of a number of severe accident transient analyses, which have been performed for the two Nuclear Power Plants (NPP's) under operation in the Netherlands, using the RELAP5/MOD2 computer program. The two NPP's include a natural circulation BWR of the early General Electric design, and a PWR of the Kraftwerk Union design. The transients considered include Station Blackout, ATWS, primary Feed-and-Bleed (PWR), and IB-LOCA (BWR). All transients considered may potentially end-up in a core melt situation. The influence of operator action on the course of the transient events has been investigated, especially with respect to the possibility to depressurize the plant before core melt actually occurs. The results of the analyses serve as input for a safety evaluation of both NPP's which is presently being performed as part of the post-Chernobyl activities in the Netherlands.

1. INTRODUCTION

Following the accident at the Chernobyl Nuclear Power Plant (NPP), an additional safety evaluation of the two NPP's which are in operation in the Netherlands has been required by the Dutch regulatory body. The two NPP's are:

- Dodewaard NPP:
  A natural circulation Boiling Water Reactor (BWR) of the early General Electric (GE) design, with a net output of 58 MWe and in operation since 1969.
- Borssele NPP:
  A Pressurized Water Reactor (PWR) of the Kraftwerk Union (KWU) design, with a net output of 480 MWe, and on-line since 1973.

At present, a safety evaluation of these two NPP's is being performed. As input for this safety evaluation ECN was requested to analyze a number of severe accident type of transients using the RELAP5/MOD2/Cycle 36.04 computer program [1]. The following transients, which have in common that they all potentially end-up in a core melt situation, have been considered:

- Dodewaard BWR:
  - Station Blackout
  - Anticipated Transient Without Scram (ATWS)
  - Intermediate Break Loss-of-Coolant Accident (IB-LOCA).
- Borssele PWR:
  - Loss-of-all-feedwater followed by primary feed-and-bleed
  - Station Blackout
  - ATWS.

For each type of accident, sensitivity analyses have been performed to determine the influence of specific plant parameters including possible operator actions on the course of the event. These operators actions mainly concern possible actions to bring the NPP under safe conditions, or in case melting of the core can not be prevented, actions to depressurize the system in order to avoid a high pressure core melt condition. This latter condition is generally considered to result in a more severe type of accident and therefore should be prevented whenever possible.

2. DODEWAARD ANALYSES

2.1. Dodewaard plant description

As mentioned above, the Dodewaard NPP is a BWR of the early GE design. No jet pumps or recirculation pumps are installed, and flow through the core is controlled by natural circulation. The pressure suppression concept is illustrated in fig. 2.1., and consists of two blowdown tanks. Some of the relevant rated plant conditions have been listed in table 2.1.

The Emergency Core Cooling (ECC) system is divided into a High Pressure (HP-ECC) and a Low Pressure (LP-ECC) part. The HP-ECC system consists of an Isolation Condenser (IC), which has the capacity to remove up to 12% rated core power for a period of 6 hours. When activated automatically at high Reactor Pressure Vessel (RPV) pressure, 50% of this capacity becomes available. Utilization of the remaining 50% capacity requires additional operator action. The isolation condenser can also be activated manually, independent of the system pressure. The isolation condenser system operates by natural circulation, with steam flowing from the RPV steam dome through a condensing heat exchanger, and the condensate returning by gravity to the RPV.

A total of five Dikkers Safety/Relief (S/R) valves have been installed on top of the RPV, having a total capacity equal to 2.5 times the rated turbine steam flow rate. The lowest two setpoint valves serve as Automatic Depressurization (ADS) valves, discharging steam directly to the pressure suppression system. The remaining three S/R valves discharge steam into the drywell. The different setpoint pressures of the S/R valves have been listed in table 2.2.

A number of important setpoints with respect to the automatic activation of the ECC systems and the reactor protection system have been listed in table 2.3.

2.2. Dodewaard RELAP5/MOD2 model

Fig. 2.2. represents the nodalization scheme as used for simulation of the Dodewaard reactor system and associated systems. The model includes about 50 volumes and 50 junctions. The heat capacity of the RPV and connected piping has not been included. The numbering system as used for the various hydraulic component is given in table 2.4.

Process Parameter	Value
Thermal power	183 MW_{th}
System pressure	7.55 MPa
System temperature	564 K
Core subcooling	4.8 K
Turbine steam flow	84 kg/s
Core mass flow	1200 kg/s
Core bypass flow	156 kg/s
Downcomer water level	0.54 m

Table 2.1. Dodewaard normal operating conditions.

Valve nr.	Function	Setpoint (MPa)
1	ADS-1	8.62
2	ADS-2	8.67
3	Safety valve	8.72
4	Safety valve	8.77
5	Safety valve	8.82

Table 2.2. S/R valve data.

Signal	Setpoint
HP-ECC system	8.14 MPa
LP-ECC system	1.55 MPa
High drywell pressure	0.118 MPa
Low RPV level	- 0.075 m
Low low RPV level	- 1.0 m

Table 2.3. Dodewaard setpoint values.

Series	Description
100	Downcomer
200	RPV lower plenum
300	Core flow path
400	Core bypass
500	Chimney
600	RPV upper plenum
700	LP-ECC system and main steam line
800	HP-ECC system
900	Feedwater system

Table 2.4. RELAP5/MOD2 nodalization index.

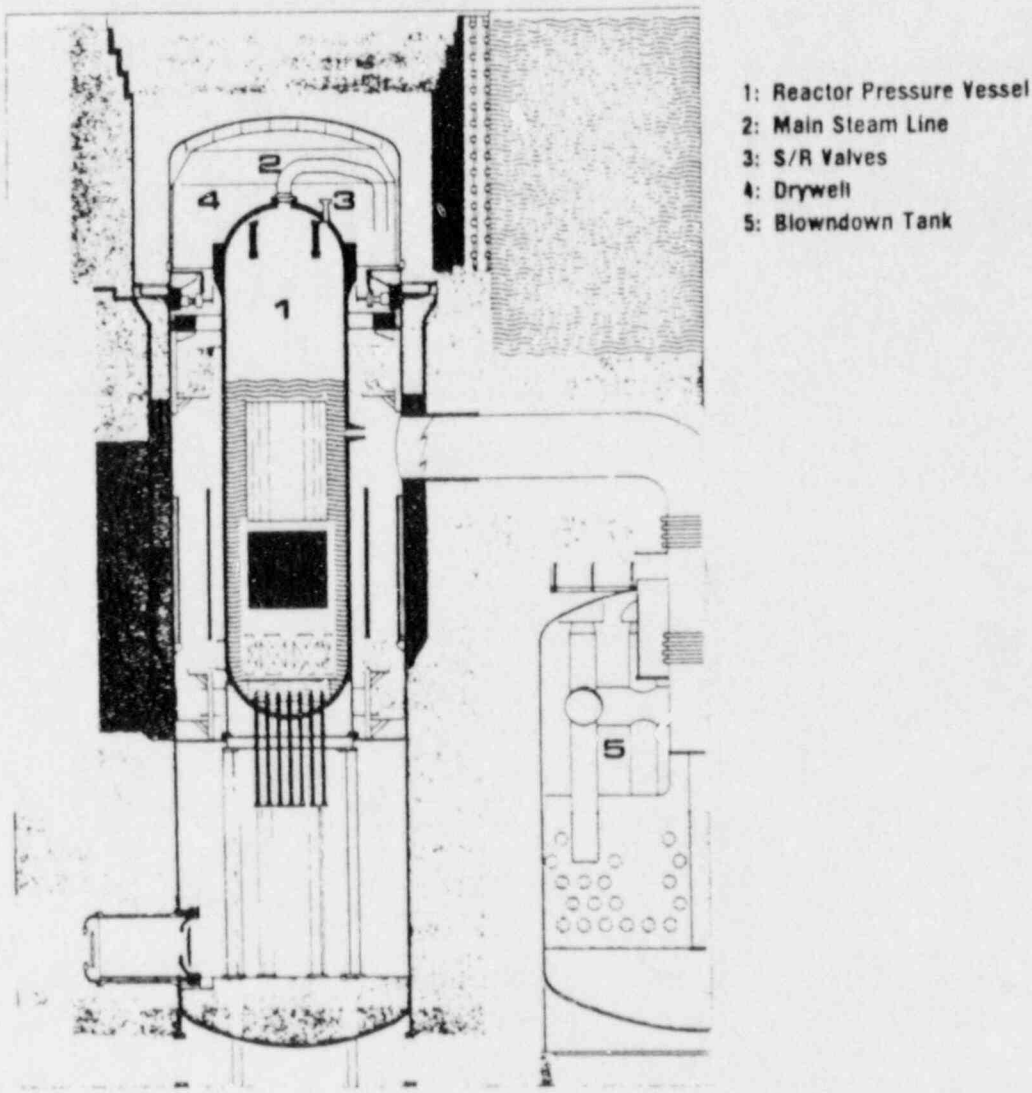

Fig. 2.1. Dodewaard pressure suppression concept.

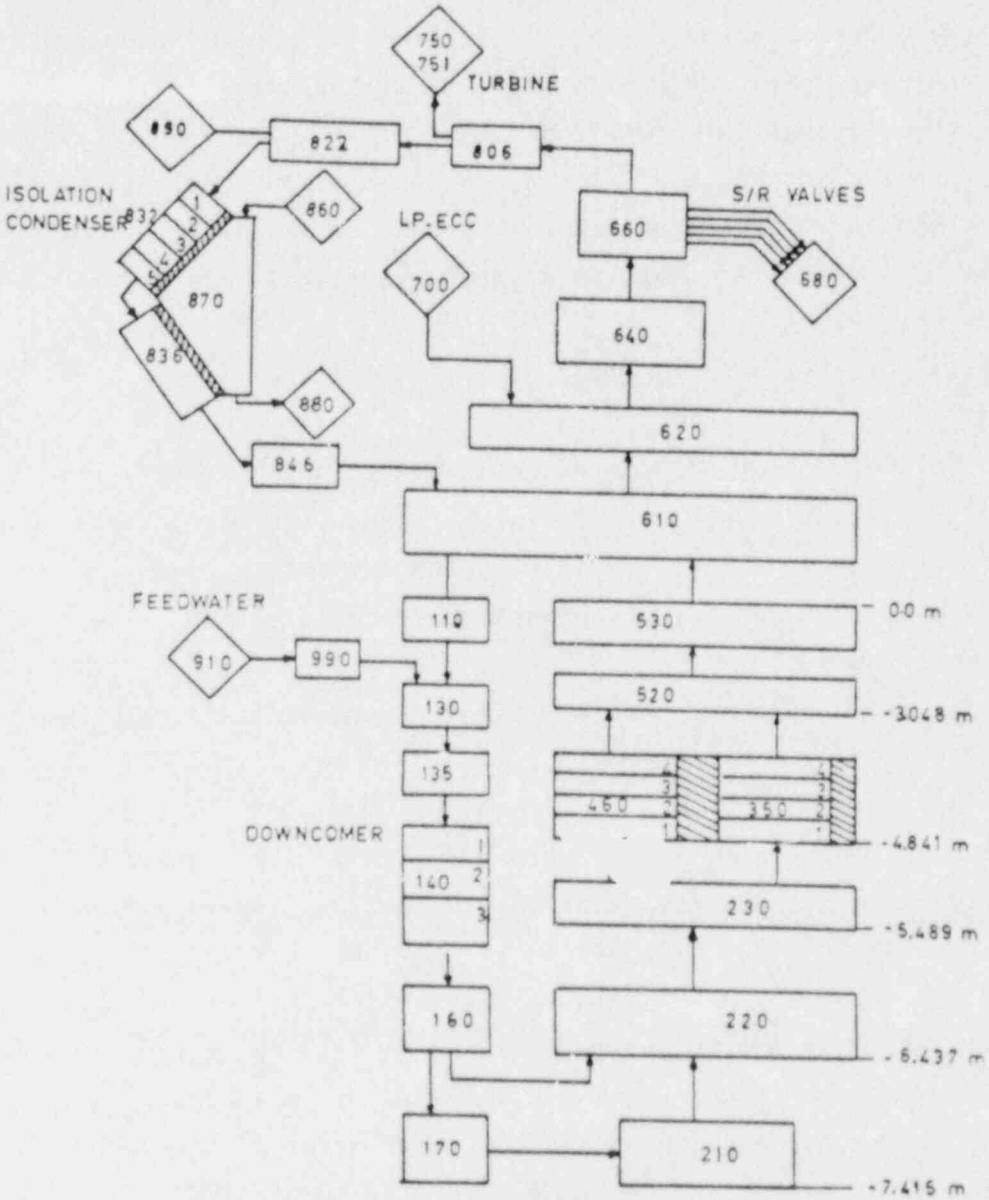

Fig. 2.2. Dodewaard RELAP5/MOD2 nodalization scheme.

2.3 Station Blackout

In the event of a station blackout transient, the turbine control valves will be closed rapidly due to turbine overspeed. Simultaneously, the steam bypass valve will open to limit the pressure increase inside the reactor system. Furthermore, the loss of the 3 KV net will result in a shut-off of the feedwater pumps and an isolation scram signal after 3 seconds. Such an isolation scram signal initiates:

- Reactor scram
- Main Steam Line (MSL) closure.

The following four station blackout situations have been analyzed:

1. 50% availability of the isolation condenser; no operator action
2. Isolation condenser unavailable; no operator action
3. Isolation condenser unavailable; opening of 1 ADS valve at RPV level = -1.0 m
4. Isolation condenser unavailable; opening of 1 ADS valve at 1/3 core level.

The resulting pressure and maximum fuel cladding temperature time histories for these four station blackout analyses are presented in resp. fig. 2.3. and 2.4. As can be observed, the availability of 50% of the isolation condenser capacity is sufficient to bring the station blackout event under control. In case of failure of the isolation condenser system, the transient will end-up in a high pressure core melt situation. Opening of one ADS valve after 20 minutes or 2.6 hours, when the RPV water level has dropped till respectively -1.0 m or 1/3 of the core height, will depressurize the system before core melt occurs. Table 2.5. summarizes the results of the four different station blackout analyses.

Event	Time (s)			
	Run 1	Run 2	Run 3	Run 4
Normal operation	< 0	< 0	↑	↑
Loss-of-feedwater	0	0	|	|
Scram and MSL closure	0	3	|	|
MSL's fully closed	5.4	13	*	*
IC system activated	6.2	13	|	|
S/R valve opening	-	24	↓	|
Water level = -1.0 m	-	1247	1247**	↓
1/3 core level	-	9430	3415	9430**
Cladding temp > 1500 K	-	12903	8635	11893
RPV pressures at 1500 K (MPa)	-	8.62	0.3	0.3

* Identical to run 2

** Opening of 1 ADS valve

Table 2.5. Dodewaard station blackout sequence of events.

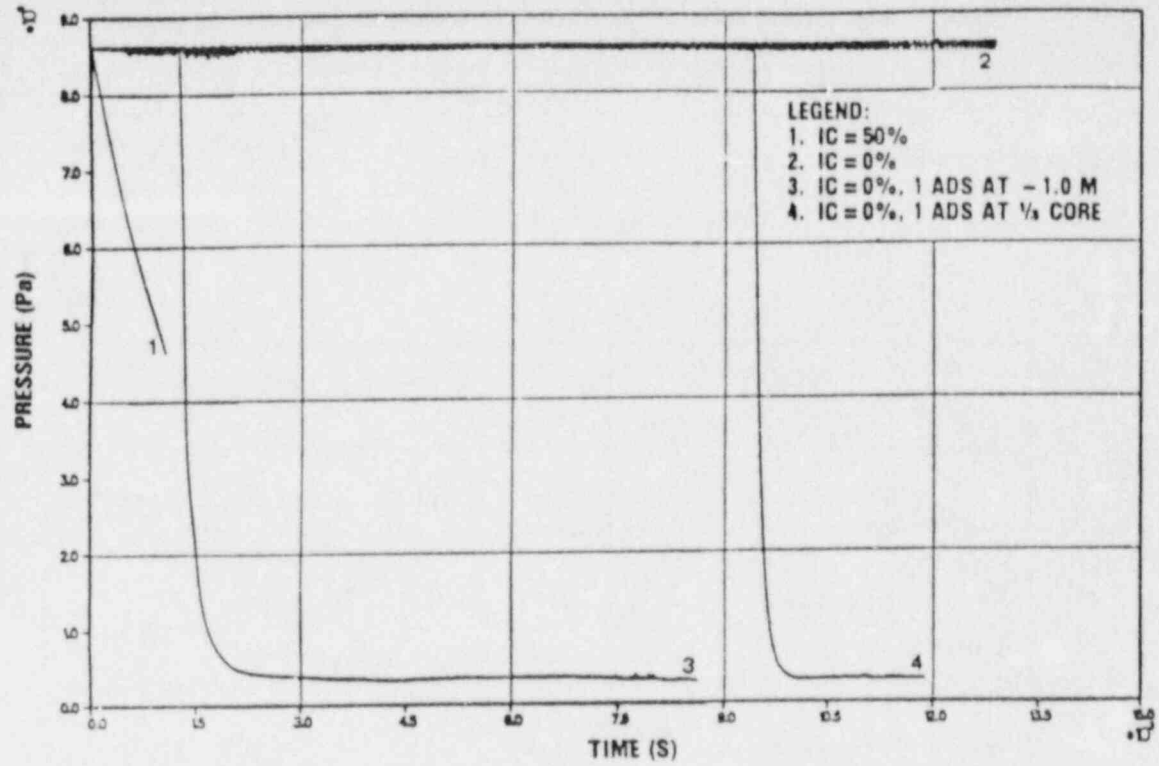

Fig. 2.3. Dodewaard station blackout RPV pressure.

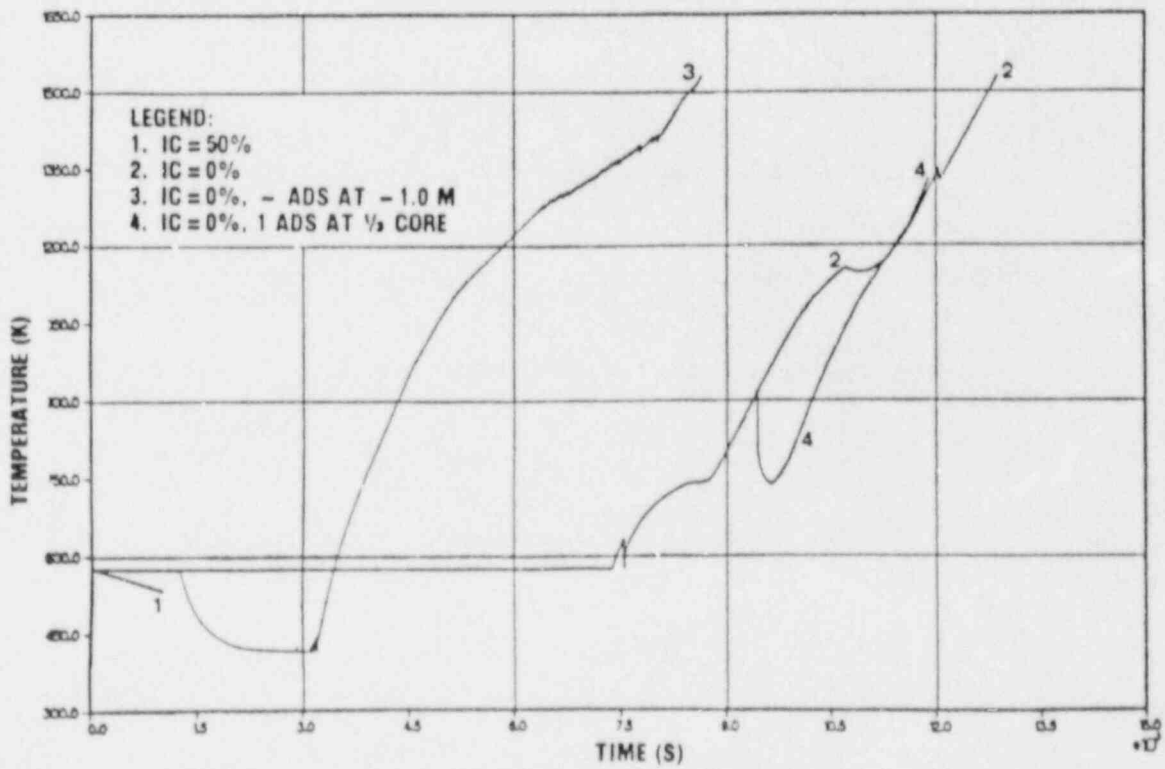

Fig. 2.4 Dodewaard station blackout maximum fuel cladding temperature.

2.4. ATWS

Two initiating events have been considered for the ATWS transient event:

1. Loss-of-all-feedwater
2. Main steam line closure

In both cases, a normal 50% availability of the isolation condenser has been assumed. Furthermore, the ADS system is considered not to be activated after a low-low RPV water level has been reached.

During an ATWS transient event, a strong coupling exists between the power produced by the reactor core and the moderator density coefficient. In both cases considered, the system pressure will be controlled by the S/R valves which are positioned on top of the RPV. Since the opening and closure behaviour of these valves directly effects the moderator density and so the reactor power, special attention has been payed to the accurate modelling of the S/R valve behaviour. Fig. 2.5. shows the resulting S/R valve model as included in the RELAP5/MOD2 input deck.

In case of the first ATWS analysis, which is initiated by a loss-of-all-feedwater event, the RPV water level will drop. A low RPV water level signal is obtained after 64 seconds, after which an isolation scram occurs. As mentioned in section 2.3., such an isolation scram includes MSL closure, while in case of an ATWS event reactor scram fails to take place. The closure of the MSL results in an increase of the RPV pressure untill the setpoint pressure of the S/R valves is reached, as shown in fig. 2.6. Prior to this, the isolation condenser has been activated. The loss-of-inventory through the S/R valves produces a negative reactivity feedback effect which leads to a strong reduction of reactor power. As can be observed from figs. 2.7.-2.9., a more or less quasi-steady state situation exists after 800 seconds, when the analysis has been terminated. The steam release through the S/R valves approaches zero, while all the energy still produced by the reactor core is being exchanged by the IC. In this steady state condition, the thermal power production of the reactor core has been reduced to 6.1% of its nominal value.

The second ATWS event analyzed is being initiated by MSL closure at time zero. As a consequence, the RPV pressure will increase towards the setpoint pressure of the S/R valves, and steam is being discharged to the blowdown tanks as well as to the drywell. In this ATWS event, an isolation scram is being initiated after a high drywell pressure signal has been obtained. Based on containment pressurization analyses, this will occur after 18 seconds. Apart from an isolation scram, a high drywell pressure signal actuates the high pressure feedwater system, ensuring sufficient feedwater supply to the RPV for a period of 1000 seconds. For computational reasons the end of feedwater supply to the RPV is assumed to occur after 500 seconds. The loss-of-inventory that follows, results in a negative moderator density coefficient and thereby in a decrease of reactor power. Figs. 2.10.-2.13. show the results of this ATWS analysis, which has been terminated after 1600 seconds. At this point in time, only a minor amount of steam is still being discharged through the lowest setpoint S/R valve. The power production of the reactor core amounts 7.4% of its nominal value.

As can be concluded from the two ATWS events analyzed, the availability of the natural circulation isolation condenser makes that these events end-up in a steady-state condition in which the energy produced by the reactor core is equal to the energy being exchanged by the isolation condenser. The sequence of events for these two ATWS cases has been summarized in table 2.6.

Event	Time (s)	
	Run 1	Run 2
Normal operation	< 0	< 0
Loss-of-feedwater	0	-
Low RPV water level	64	-
MSL closure	64	0
IC actuation	89	8.4
SRV setpoint pressure	92	12.2
High drywell pressure	100	18
End of feedwater	-	500
End of calculation	800	1600
Final steady state conditions:		
Reactor power (MW_{th})	11.2	13.5
RPV pressure (MPa)	8.61	8.61

Table 2.6. Dodewaard ATWS sequence of events.

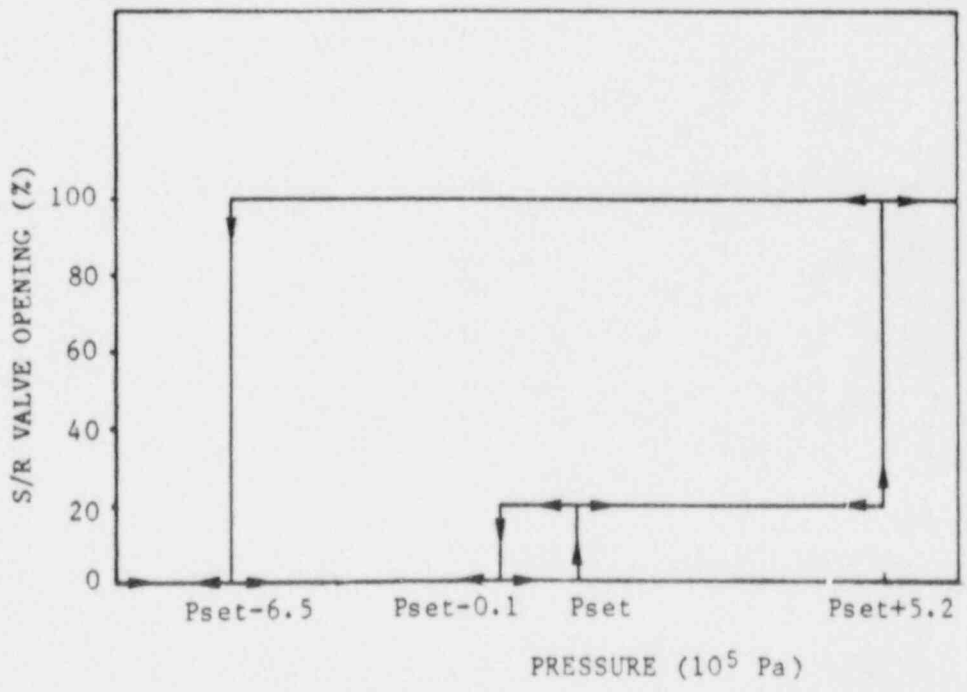

Fig. 2.5. Dodewaard safety valve opening and closing behaviour.

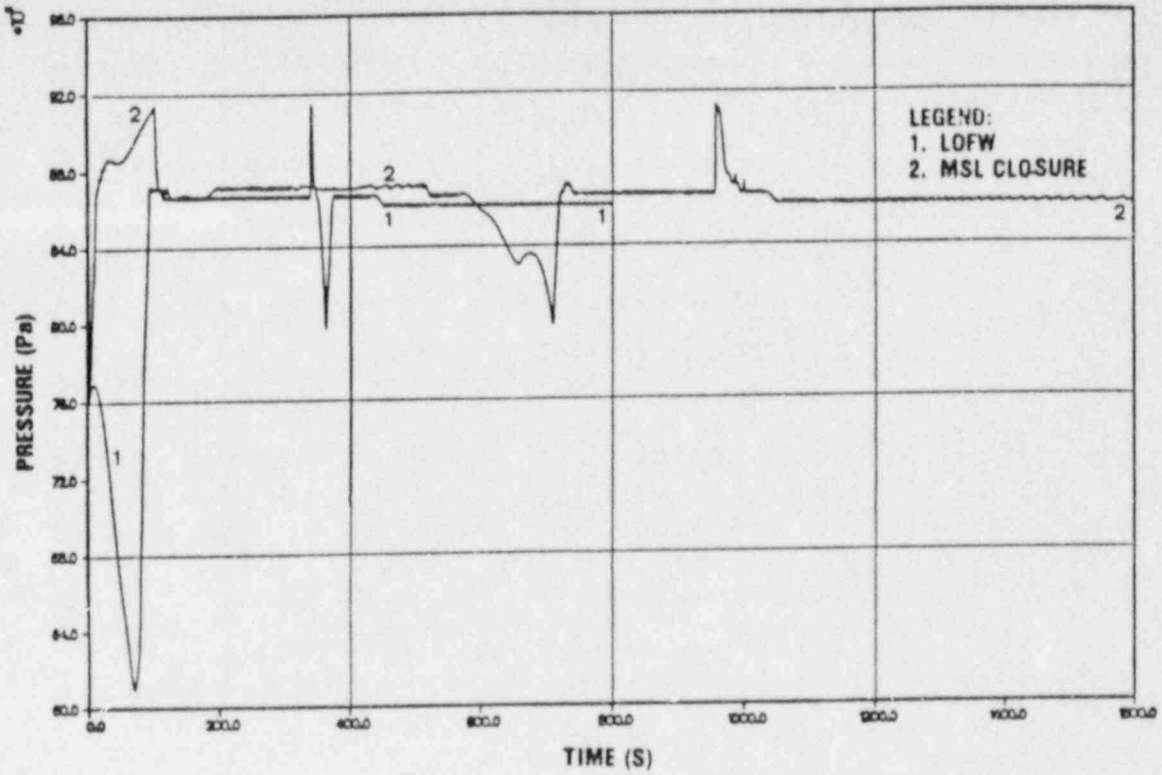

Fig. 2.6. Dodewaard ATWS RPV pressure.

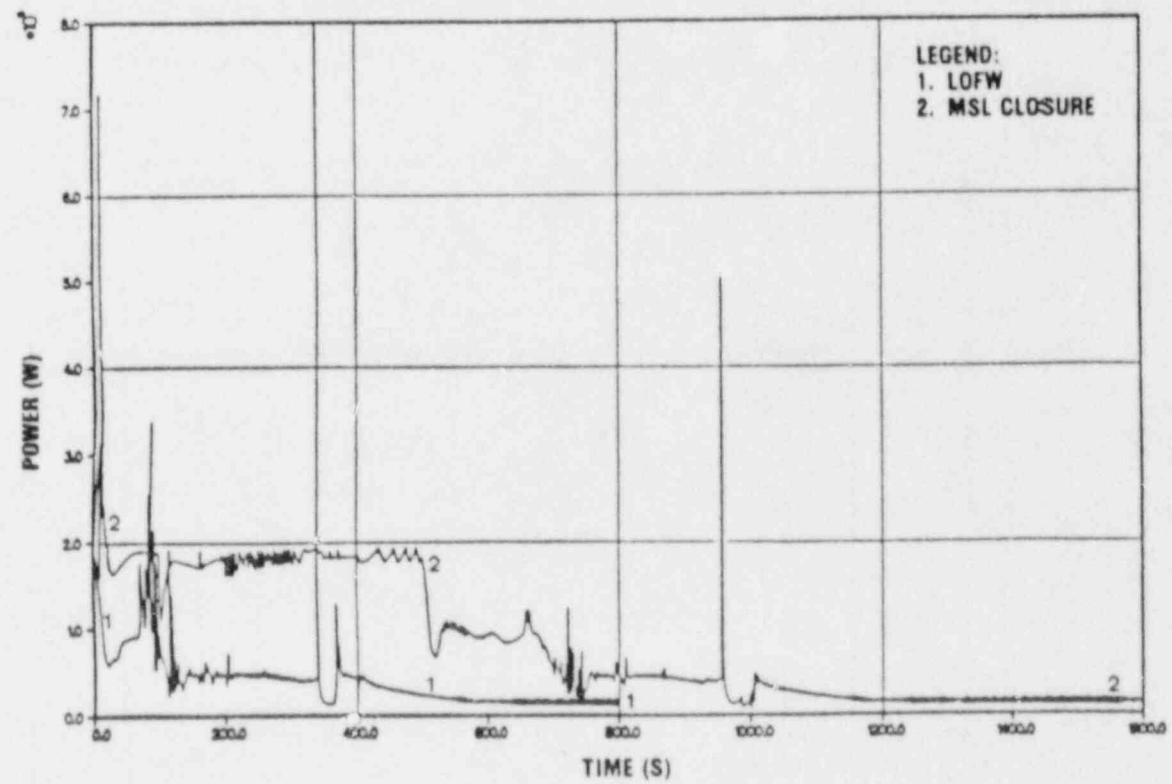

Fig. 2.7. Dodewaard ATWS reactor power.

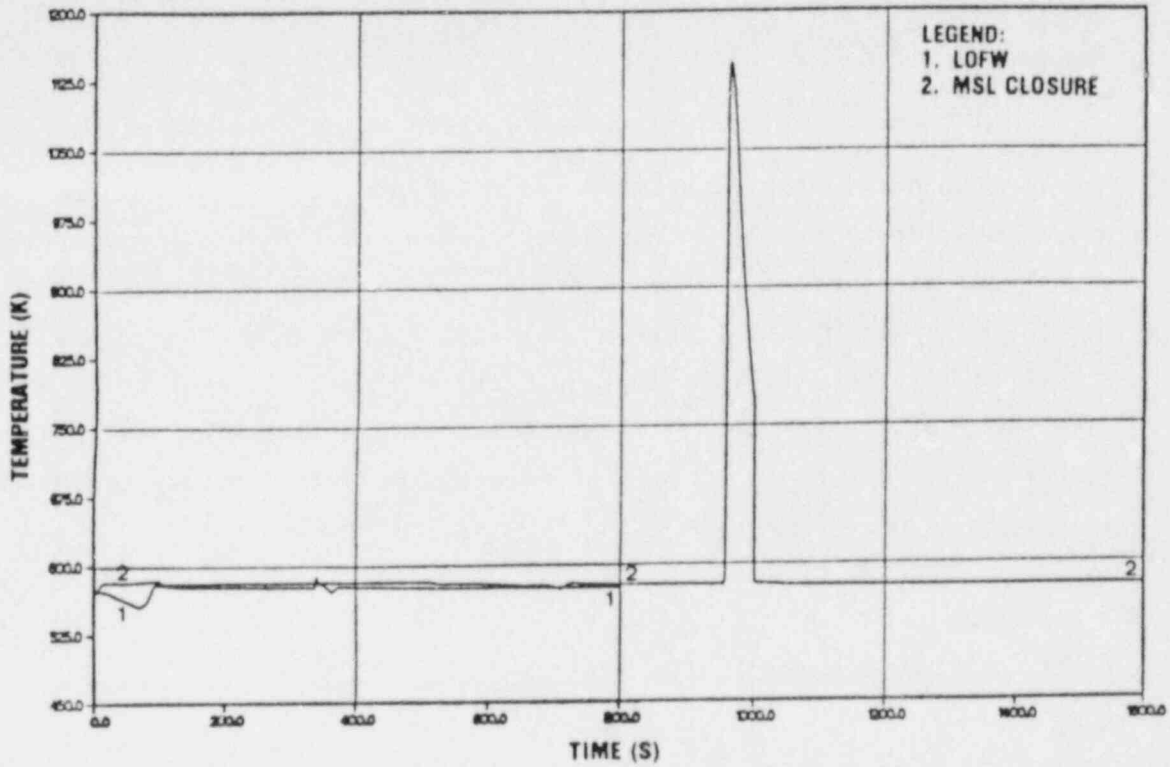

Fig. 2.8. Dodewaard ATWS maximum fuel cladding temperature.

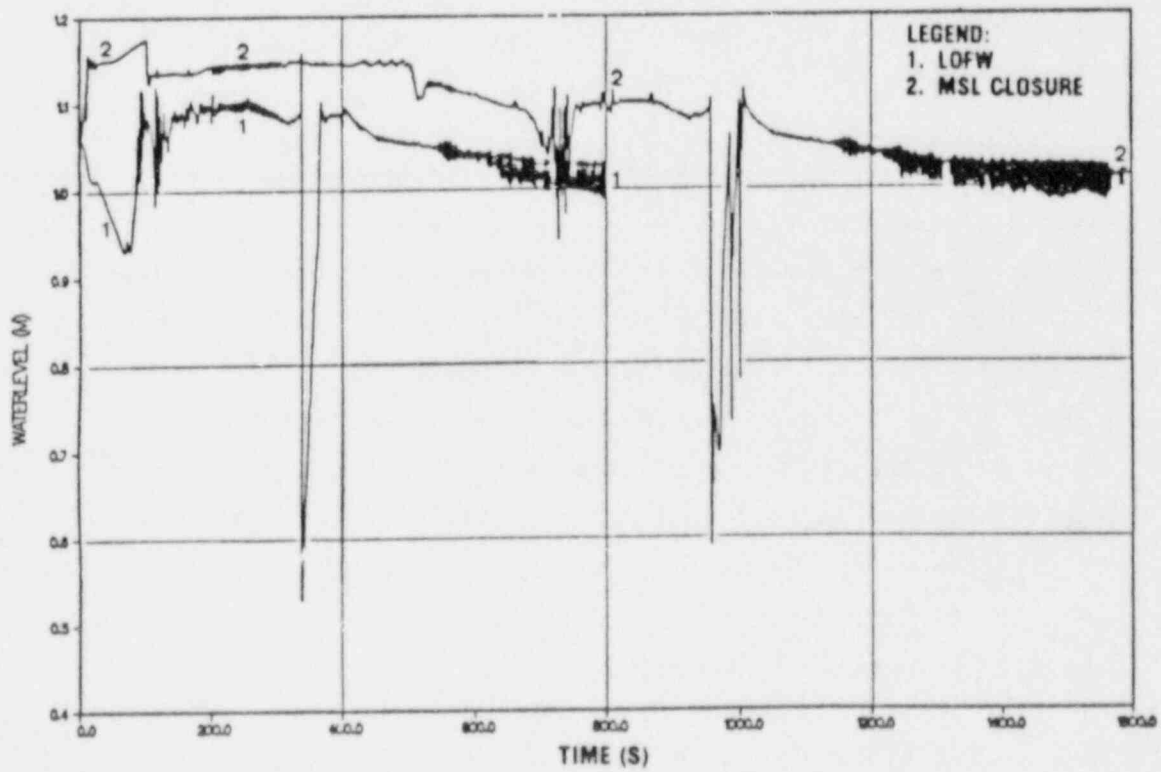

Fig. 2.9. Dodewaard ATWS core water level.

2.5 IB-LOCA

The IB-LOCA considered corresponds to a failure of one control rod drive penetration in the bottom of the Dodewaard RPV, which corresponds to an equivalent cross-sectional break area of 0.003 m^2. Within one second after the break occurs, a high drywell pressure signal is being generated resulting in an isolation scram and activation of the high pressure feedwater system. Similar to the ATWS analysis as described in section 2.4, this quaranties an undisturbed feedwater supply to the RPV for a period of 1000 seconds. the high drywell pressure signal also activates the LP-ECC system. Two IB-LOCA cases have been analyzed:

1. IB-LOCA
2. IB-LOCA and loss-of-all-feedwater

In both IB-LOCA analyses, a 50% availability of the isolation condenser has been considered. The ADS system is not assumed to be activated when the RPV water level drops below -1.0 m. The main objective of the analyses has been to determine whether core melt conditions occur before the LP-ECC system injects water into the RPV below a system pressure of 1.55 MPa. The results of the two IB-LOCA analyses are presented in figs. 2.10.-2.13.

The IB-LOCA case with availability of feedwater shows a minor increase of the system pressure following reactor scram and MSL closure. The maximum pressure however does not exceed the isolation condenser initiation pressure, reason why this system will not be activated automatically. The break mass flow rate exceeds the feedwater mass flow rate for the first 180 seconds. This, plus the fact that the injected water is relatively cold, leads to a rapid depressurization of the reactor system. Injection of cold ECC water by the LP-ECC system starts after 424 seconds. As can be observed, the core is sufficiently cooled for the complete duration of the transient and no high fuel cladding temperatures are to be expected.

The IB-LOCA event without feedwater availability results in an initial pressure increase high enough to activate the isolation condenser. The core water level drops rapidly due to the loss-of-inventory, resulting

in an empty core after 200 seconds. The fuel cladding temperature increases but does not exceed a value of 710 K before ECC water injection by the LP-ECC system starts.

Based on these analyses it can be concluded that an IB-LOCA event with a break size of 0.003 m^2 does not endanger the integrity of the fuel. The sequence of events for these analyses has been summarized in table 2.7.

Event	Time (s)	
	Run 1	Run 2*
Normal operation	< 0	< 0
IB-LOCA	0	0
Reactor scram and MSL closure	0.8	0.8
MSL's closed	10.8	10.8
IC actuation	-	16.5
LP-ECC injection	424	396
Max. cladding temp. (K)	570	710

* No feedwater

Table 2.7. Dodewaard IB-LOCA sequence of events.

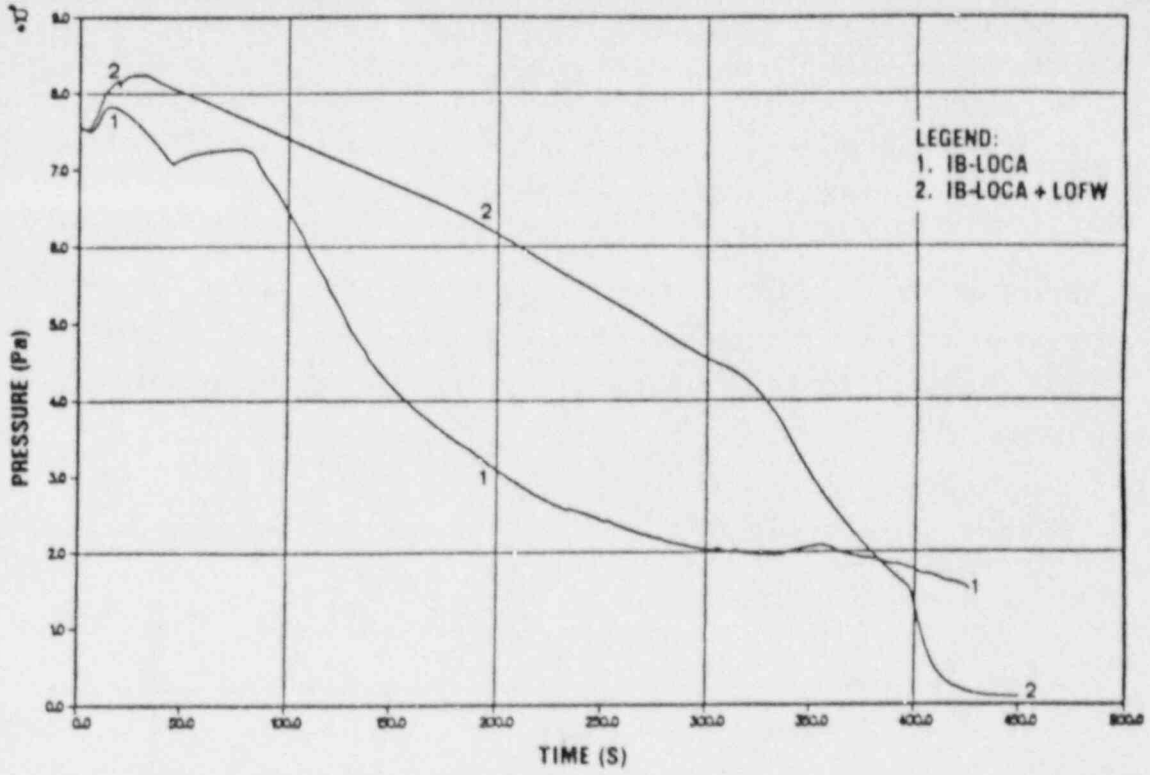

Fig. 2.10. Dodewaard IB-LOCA RPV pressure.

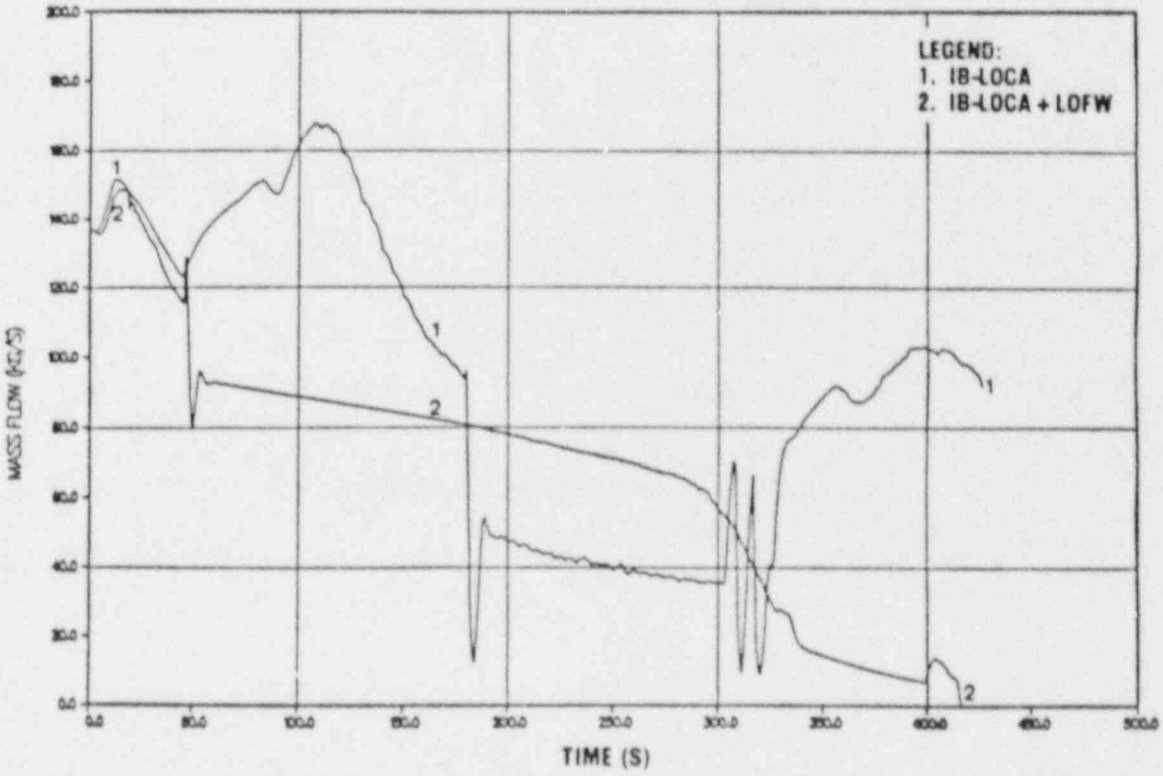

Fig. 2.11. Dodewaard IB-LOCA break mass flow.

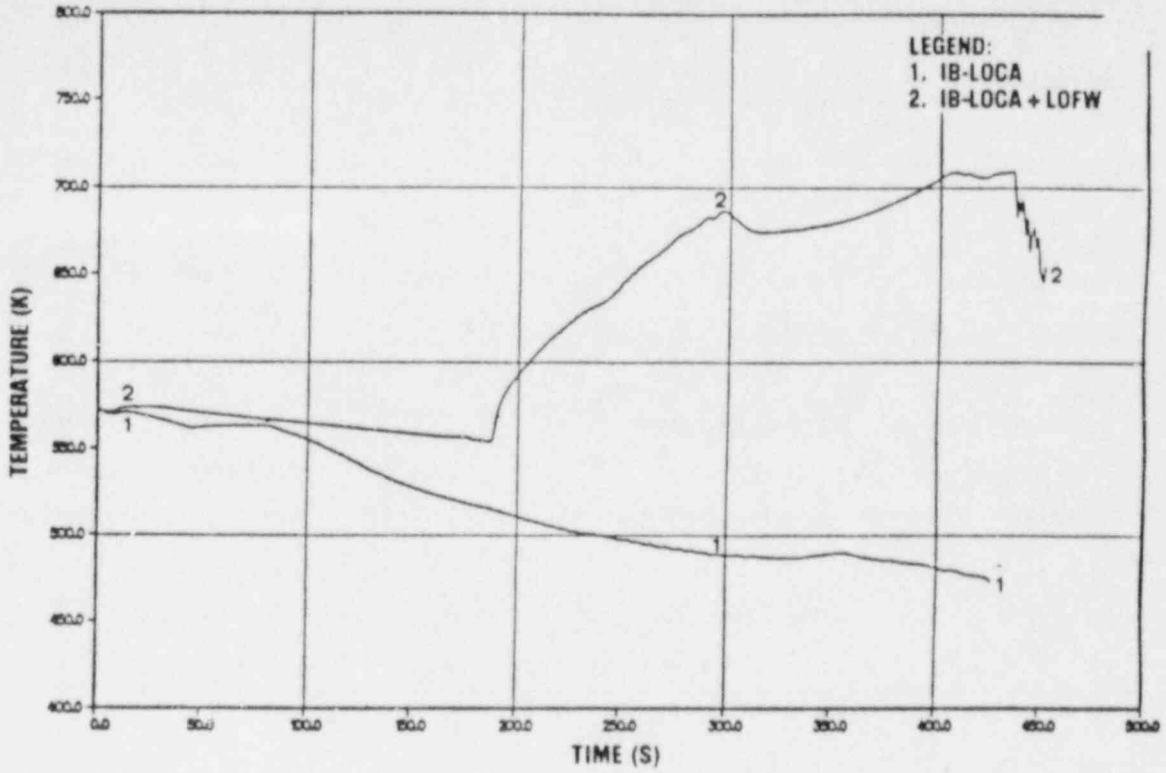

Fig. 2.12. Dodewaard IB-LOCA maximum fuel cladding temperature.

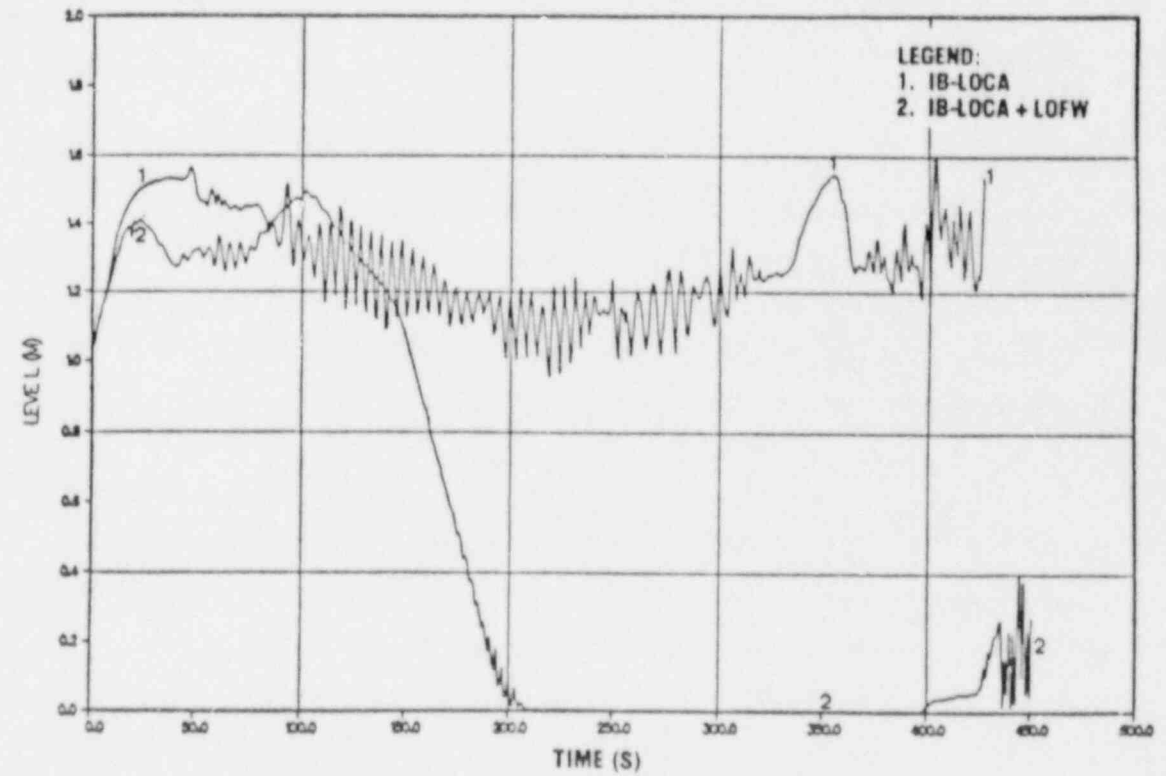

Fig. 2.13. Dodewaard IB-LOCA core water level.

3. BORSSELE TRANSIENT ANALYSES

3.1. Borssele plant description

The Borssele NPP is a two-loop PWR of the KWU design. A schematic picture of the installation is shown in fig. 3.1. A total number of six S/R valves are mounted on top of the pressurizer, which is connected to primary loop 01. The three lowest setpoint valves are the so-called Power Operated Relief Valves (PORV's), which can be opened by the operator. The S/R valve setpoints and capacity are given in table 3.1.

As indicated in fig. 3.1., ECC takes place by combined injection into the hot and cold legs of the primary loops. The ECC system consists of the following three sub-systems:

- HP-ECC system;
  Four HP-ECC pumps are installed, each with a maximum capacity of 73.6 kg/s. The HP-ECC system is a non-recirculating system, having a maximum volume of 425 m^3 of borated water available for injection.
- Accumulators;
  Four accumulators are available, each containing 21.5 m^3 of borated water.
- LP-ECC system;
  Four LP-ECC pumps are installed, each with a maximum capacity of 200 kg/s. Three modes of operation are possible, being a non-recirculation mode in which water is being taken from the ECC storage tanks, a recirculating mode in which water is being taken from the reactor building sumps, and finally a recirculation mode by taking water out of the hot legs and injection into the cold legs of the primary system (shutdown cooling).

Table 3.2. provides a list of the most important normal operating conditions of the Borssele NPP. A number of relevant setpoint values related to the Steam Generator (SG) water level and ECC system activation are given in respectively table 3.3. and 3.4.

3.2. Borssele RELAP5/MOD2 input model

Fig. 3.2. represents the nodalization scheme as used for simulation of the Borssele reactor system and associated systems. The corresponding numbering system is given in table 3.5. The model includes the reactor coolant pressure control system, the Volume Control System (VCS), the SG water level control system and the maximum steam pressure control system. Heat transfer to and from the hydraulic components is accounted for. The input model counts roughly 140 hydraulic volumes, an equal number of junctions, and about 85 heat slabs.

Valve nr.	Setpoint (MPa)	Rated capacity (kg/s)
1	16.38	16.67
2	16.38	16.67
3	16.78	33.33
4	17.17	33.33
5	17.76	33.33
6	17.76	33.33

Table 3.1. S/R valve data.

Process parameter	Value
Thermal power	1366 MW_{th}
Primary pressure	15.5 MPa
Secondary pressure	6.0 MPa
Core mass flow	9272 kg/s
Core bypass flow	733 kg/s
Steam flow per SG	369.2 kg/s
VCS mass flow	4.0 kg/s
Pressurizer water level	5.1 m
SG water level	8.1 m

Table 3.2. Borssele normal operating conditions.

Signal	SG level (m)
Normal water level	8.10
Reactor scram	3.65
Turbine trip and emergency feedwater	2.65
Emergency decay heat removal system	1.80
Zero water level measurement	0.0
Top of tube plate	- 0.35

Table 3.3. Steam Generator water level data.

System	Pressure (MPa)
HP-ECC system	10.89
Accumulator	2.5
LP-ECC system	0.8

Table 3.4. ECC injection pressures.

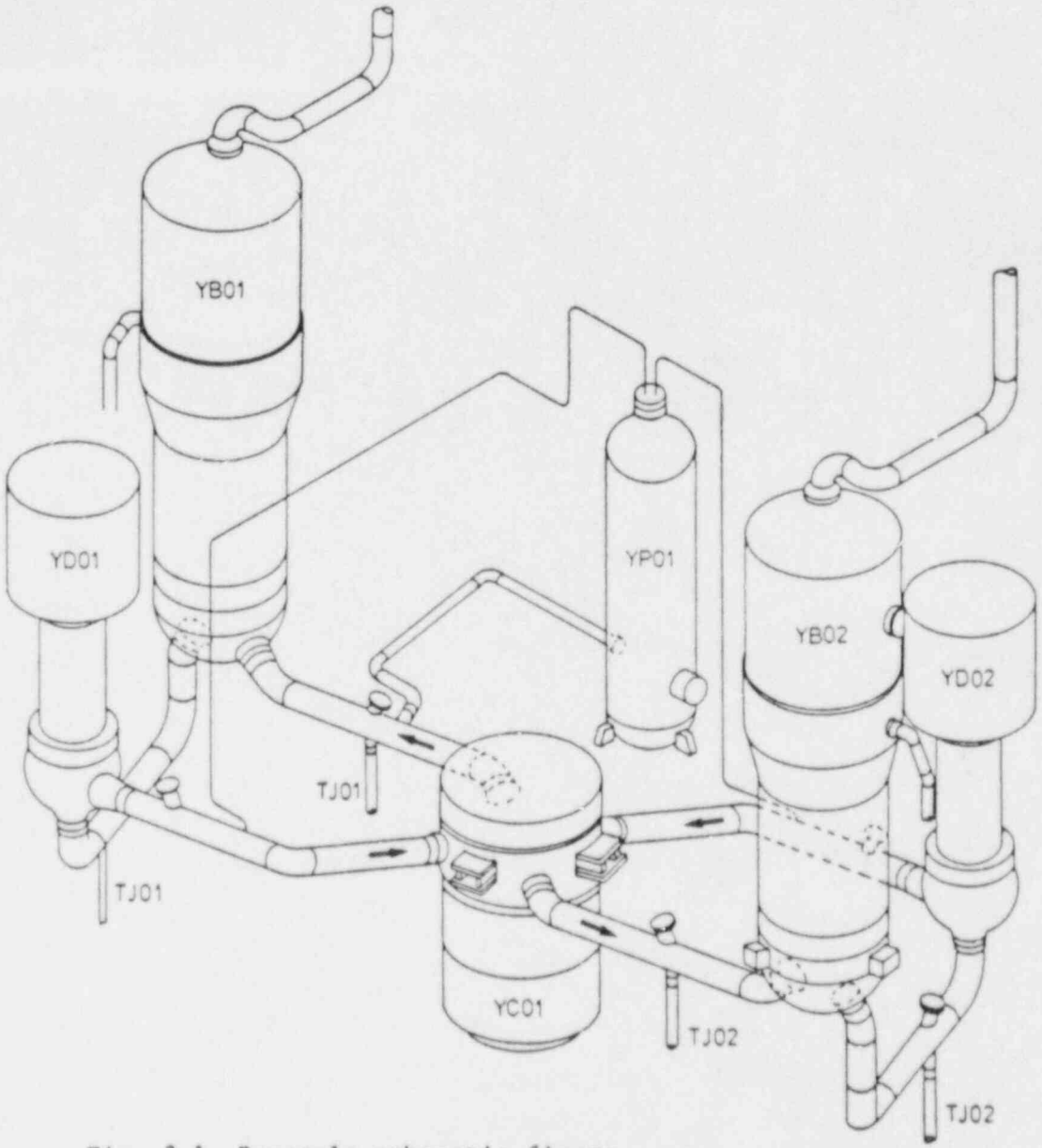

Fig. 3.1. Borssele schematic figure.

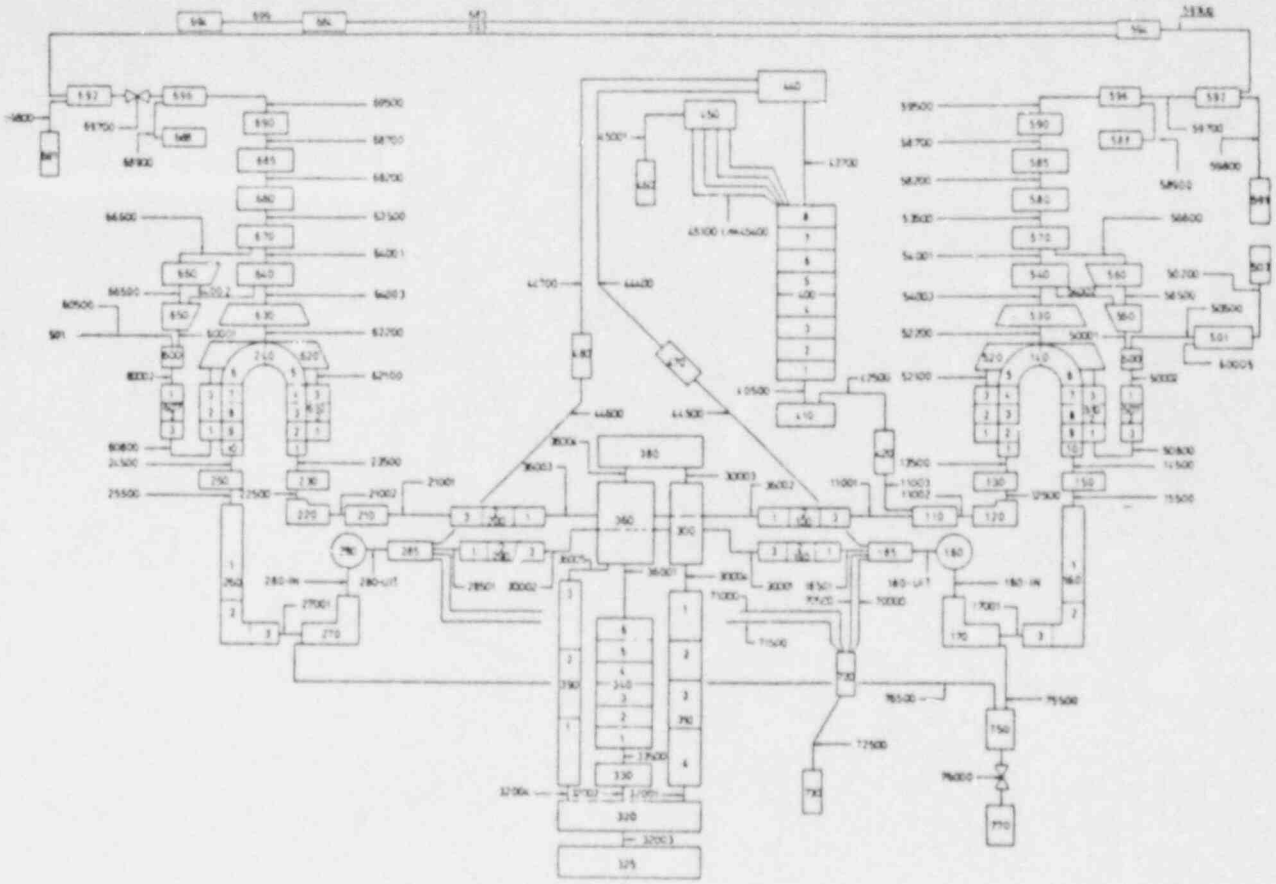

Fig. 3.2. Borssele RELAP5/MOD2 nodalization scheme.

Series	Description
100	Primary loop 01
200	Primary loop 02
300	RPV
400	Pressurizer
500	Secondary side SG 01
600	Secondary side SG 02
700	VCS
800	ECC system

Table 3.5. RELAP5/MOD2 nodalization index.

3.3. Loss-of-all-feedwater followed by primary feed-and-bleed

As initiating event a loss-of-all-feedwater event has been considered. As a consequence the steam generators will boil off causing a reactor scram and turbine trip due to a low SG water level signal. This occurs after 54 seconds. In this situation, the primary system can be depressurized by the so-called feed-and-bleed method. The feed-and-bleed procedure consists of opening of one or more PORV's on the pressurizer, shut-off of the Reactor Coolant Pumps (RCP's), and activation of the HP-ECC system. After the pressure has become less than the shut-off head of the HP-ECC pumps, cold ECC water is injected into the primary system while steam or a steam/water mixture is being discharged through the PORV's.

The main objective of the feed-and-bleed analyses has been to verify whether the limited amount of HP-ECC water is sufficient to depressurize the primary system to a pressure less than 0.8 MPa without endangering the fuel integrity. As soon as this low pressure level has been reached, the LP-ECC system is able to remove the decay heat.

Parameters which affect the course of the event are:

- The number of PORV's being opened by the operator
- The time when the operator opens the PORV's
- The number of HP-ECC pumps available.

For this reason, the following four cases have been analyzed:

1. Opening of largest PORV (33.33 kg/s) after 5 minutes
2. Opening of largest PORV (33.33 kg/s) after 15 minutes
3. Opening of largest PORV (33.33 kg/s) after 38 minutes
4. Opening of maximum PORV capacity (66.67 kg/s) after 38 minutes.

In all four cases, 50% of the HP-ECC pumps are assumed to be available. The 5 minutes period has been chosen since the SG's are boiled empty at this point in time. The 38 minute period has been selected because at this point in time the core water level has dropped till 1/3 of the core height, while the 15 minute period has been chosen arbitrarily in between.

The resulting pressure and maximum fuel cladding temperature time-histories for all four cases considered are shown in figs. 3.3. and 3.4. The corresponding sequence of events has been given in table 3.6. The most important findings are:

- All transients analyzed show a similar tendency. After opening of the PORV('s), the primary pressure decreases to a minimum value while two-phase conditions exist inside the primary system. After the primary system becomes solid, i.e. completely filled with water, the primary pressure increases to a higher level. In this situation, critical two-phase flow conditions exist inside the PORV throat. After this PORV flow changes into non-critical water discharge, a second pressure increase occurs.
- The ultimate pressure of interest is the primary pressure which remains after shut-off of the HP-ECC pumps. In all cases analyzed this pressure is higher than the LP-ECC system injection pressure. Moreover, this pressure can not be decreased any further due to the presence of zero flow conditions and hot spots inside the SG U-tubes. A similar phenomenon has been observed during the execution of a comparable experiment at the LOBI-MOD2 test facility [3]. In the Borssele analyses thermal mixing by restart of the RCP's is required to enable further primary system depressurization. Since restart of the RCP's requires half an hour preparation time, this should be considered as part of the operating procedure for this accident event.
- Restart of the RCP's has been included into the analyses for cases 1 and 3. As shown, the primary pressure in both cases decreases to a value of 0.7 MPa. Also for cases 2 and 4 a similar condition is expected to occur after thermal mixing by restart of the RCP's has been achieved.
- The HP-ECC water supply appears to be sufficient to depressurize the system.
- In most of the feed-and-bleed calculations, a temporary increase of the fuel cladding temperature occurs prior to HP-ECC system injection. The maximum fuel cladding temperature has been calculated for case 3 and equals 1500 K.

Event	Time (s)			
	Run 1	Run 2	Run 3	Run 4
Loss-of-all-feedwater	0.0	↓	↓	↓
Scram + turbine trip	54	|	|	|
Bypass valve opening	60	***	***	***
SG's empty	300*	↓	↓	↓
Opening of PRZ S/RV	-	790	790	790
15 min. after start	-	900*	-	-
Start of core boiling	410	990	1520	1520
1/3 core level	-	3030	2270*	2270**
Core empty	-	-	2930	-
HP-ECC injection	386	3265	3020	2643
Solid prim. system	2940	****	4800	4050
Non-critical PORV flow	3485	****	5700	4230
HP-ECC pumps off	3700	****	5800	5200
RCP thermal mixing	3400	****	5900	****
End of calculation	3800	4500	7430	5300
Pressure data (MPa)				
- min. 2-phase	4.6	2.7	1.8	1.1
- solid	4.8	****	4.9	2.0
- non-critical PORV	6.9	****	6.5	3.4
- final	0.7	****	0.7	****
Remaining HP-ECC water (m^3)	127	324	153	127
Max. cladding temp. (K)	620	1100	1500	917

* Opening PORV = 33.33 kg/s

** Opening PORV = 66.67 kg/s

*** Identical to Run 1

**** Not further analyzed

Table 3.6. Borssele feed-and-bleed sequence of events.

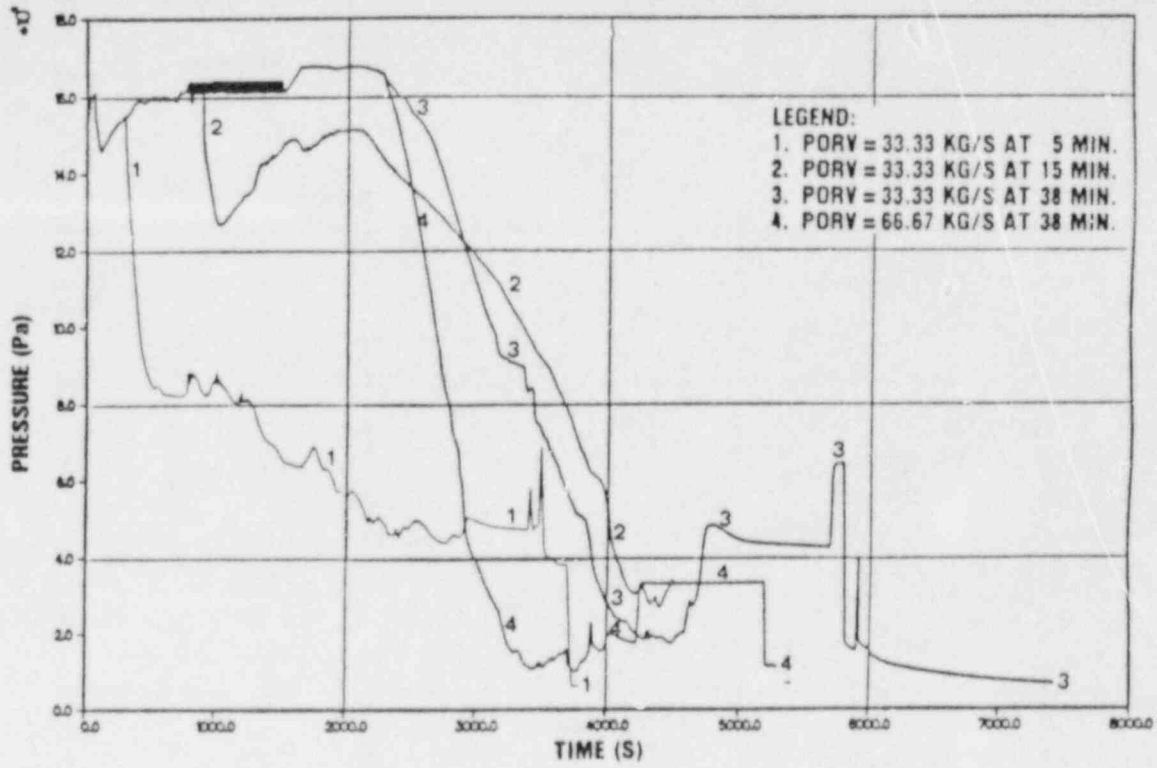

Fig. 3.3. Borssele feed-and-bleed pressurizer pressure.

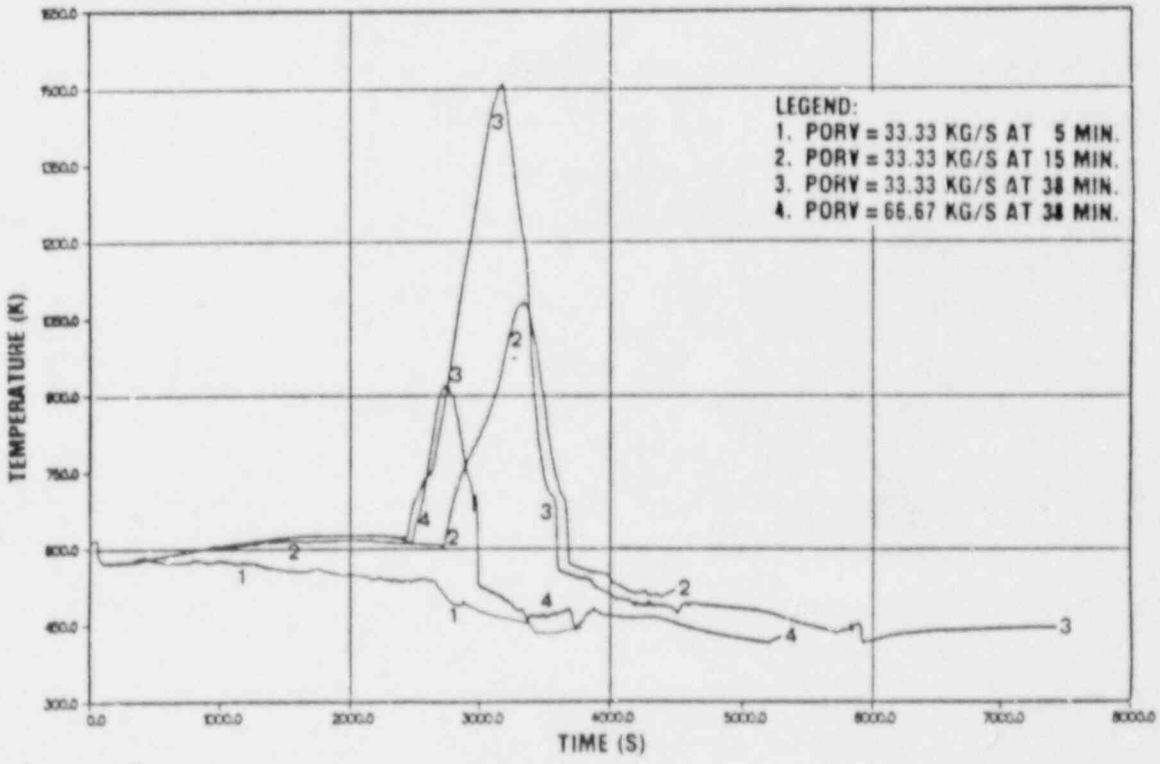

Fig. 3.4. Borssele feed-and-bleed maximum fuel cladding temperature.

3.4. Station Blackout

A station blackout accident is characterized by a complete loss-of-all on- and offside AC-power. Under these circumstances turbine trip and RCP trip occur at time zero, while the reactor scrams due to low RCP pump speed within one second. During the course of the event no VCS system or ECC systems will be available.

Without any further operator action, the station blackout event will ultimately terminate in a high pressure core melt situation, as a consequence of the continuous loss-of-inventory via the S/R valve(s). Although melting of the core can not be prevented, the primary system may be depressurized by opening of the PORV's. For this reason, the following station blackout cases have been considered:

1. TMLB'
2. Opening of minimum PORV capacity (16.67 kg/s) after 50 minutes
3. Opening of maximum PORV capacity (66.68 kg/s) after 50 minutes
4. Opening of mimimum PORV capacity (16.67 kg/s) after 108 minutes
5. Opening of maximum PORV capacity (66.68 kg/s) after 108 minutes

The 50 minute period corresponds to the moment that the SG's have been boiled empty. The 108 minute period has been chosen, since at this point in time the core water level has dropped to 1/3 of the core height.

The resulting pressure and maximum fuel cladding temperature time histories for all five station blackout events considered are presented in respectively figs. 3.5. and 3.6. The corresponding sequence of events has been given in table 3.7. As can be observed, only opening of the maximum PORV capacity is sufficient to depressurize the primary system before melting of the core occurs. This appears to be relatively independent of the time when the PORV's are being opened.

Event	Time (s)				
	Run 1	Run 2	Run 3	Run 4	Run 5
Normal operation	< 0	↑	↑	↑	↑
Station Blackout	0.0	|	|	|	|
Scram	0.7	***	***	|	|
Opening of SG S/RV	88.2	|	|	***	***
Opening of PRZ S/RV	2564	↓	↓	|	|
SG's empty	3000	3000*	3000**	|	|
Start of core boiling	4408	3187	3054	↓	↓
1/3 Core level	6500	5600	5340	6500*	6500**
Cladding temp. > 1500 K	7380	6860	6600	7728	7866
RPV pressure at 1500 K (MPa)	16.2	12.3	1.9	13.1	2.6

* Opening of min. PORV capacity

** Opening of max. PORV capacity

*** Identical to run 1

Table 3.7. Borssele station blackout sequence of events.

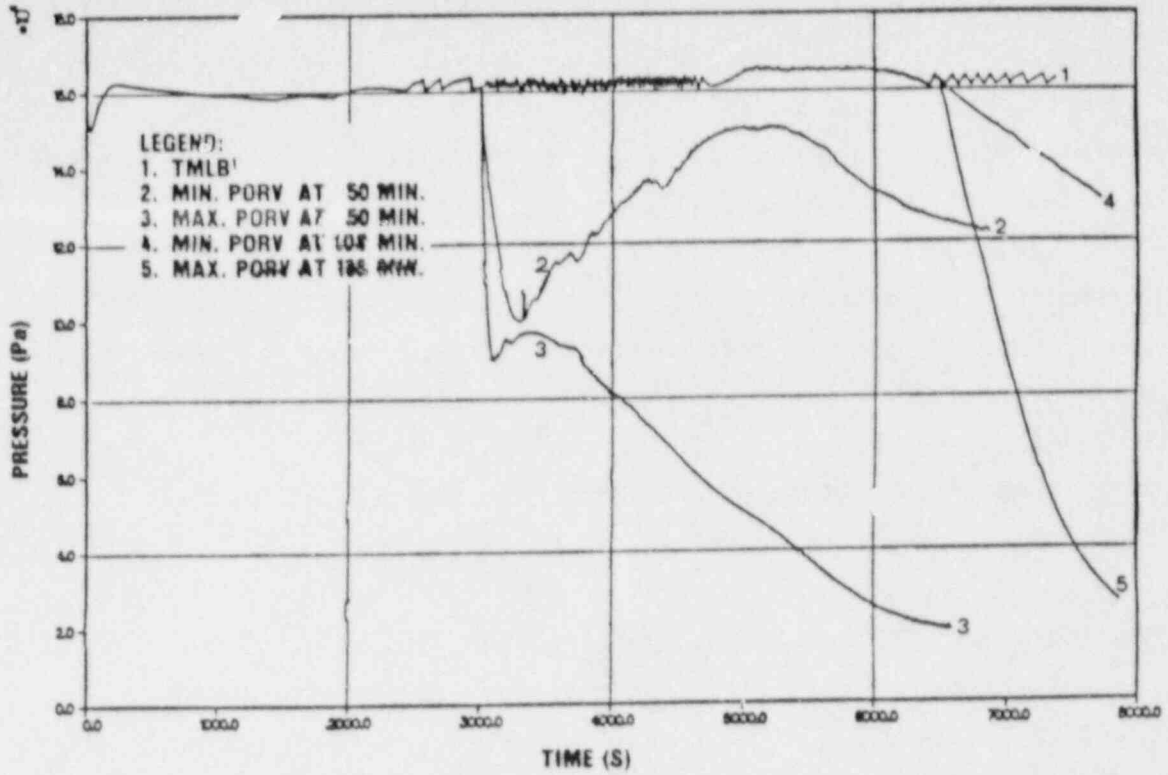

Fig. 3.5. Borssele station blackout pressurizer pressure.

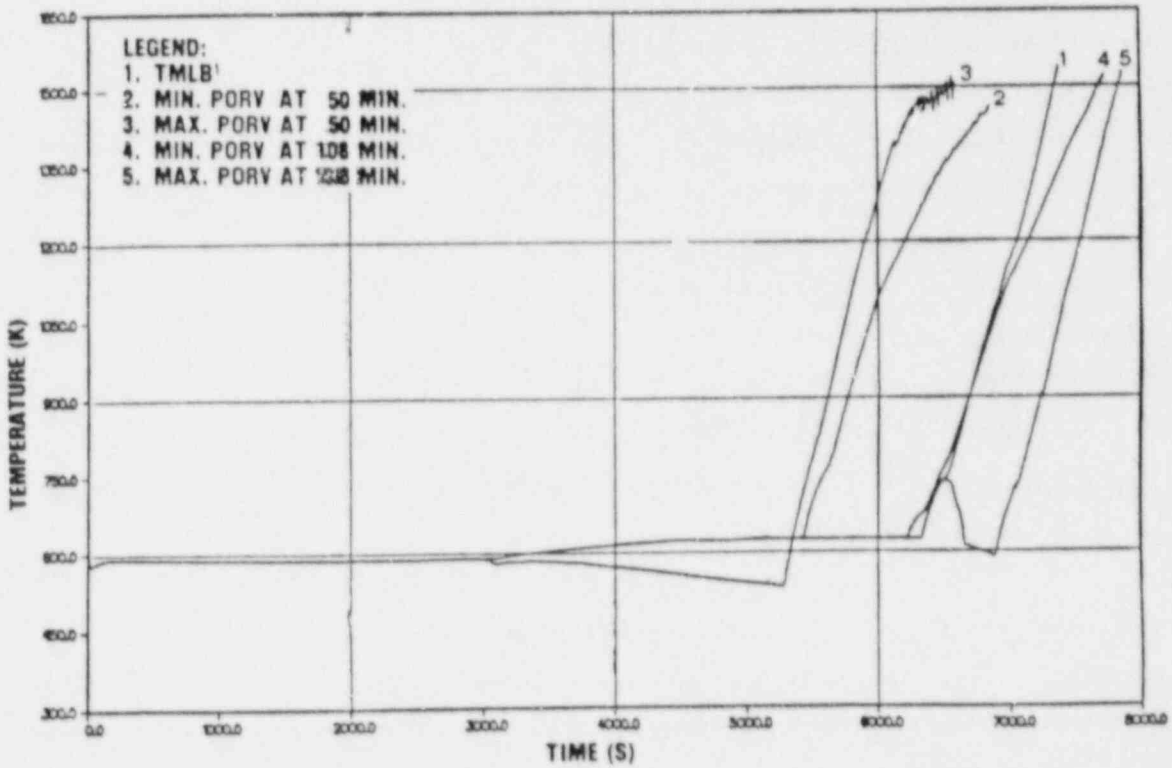

Fig. 3.6. Borssele station blackout maximum fuel cladding temperature.

3.5. ATWS

The ATWS scenario has been investigated to determine the influence of the moderator temperature coefficient on transient behaviour. Also in this case, the initiating event is thought to be a loss-of-all-feedwater event. Since the magnitude of the moderator temperature coefficient differs significantly between the begin and end of a fuel cycle, the following three cases have been analyzed:

1. Moderator temperature coefficient = $-1 \cdot 10^{-2}$ \$/°C
2. Moderator temperature coefficient = $-4 \cdot 10^{-2}$ \$/°C
3. Moderator temperature coefficient = $-8 \cdot 10^{-2}$ \$/°C

The first value corresponds to the begin-of-life value of the first core of the Borssele reactor. The second value compares to the begin-of-life value for the Borssele equilibrium core, while the final value is equal to the end-of-life value of this equilibrium core.

The initial part of the transient is identical to the feed-and-bleed analysis as presented in section 3.3. A turbine trip signal is obtained after 54 seconds due to a low SG water level while in the ATWS situation reactor scram fails to take place. Reactor power remains at a high level, thereby increasing the primary pressure and temperature, especially after 90 seconds when the SG's have been boiled empty. The increase in moderator temperature will lead to a decrease of reactor power. The greater the moderator temperature coefficient, the stronger the reduction of reactor power will be, and the milder the primary system pressure transient.

The main interest of this ATWS sensitivity analysis concerns the initial pressure increase within the primary system, which may endanger the structural integrity.

The results of the ATWS analyses are shown in figs. 3.7. and 3.8. As can be observed a strong pressure rise appears for the lowest moderator temperature coefficient considered. The initial primary system pressure increase for the two equilibrium core values of the moderator temperature coefficient is limited due to opening of the pressurizer S/R valves. No high fuel cladding temperature occurs during these short term transients.

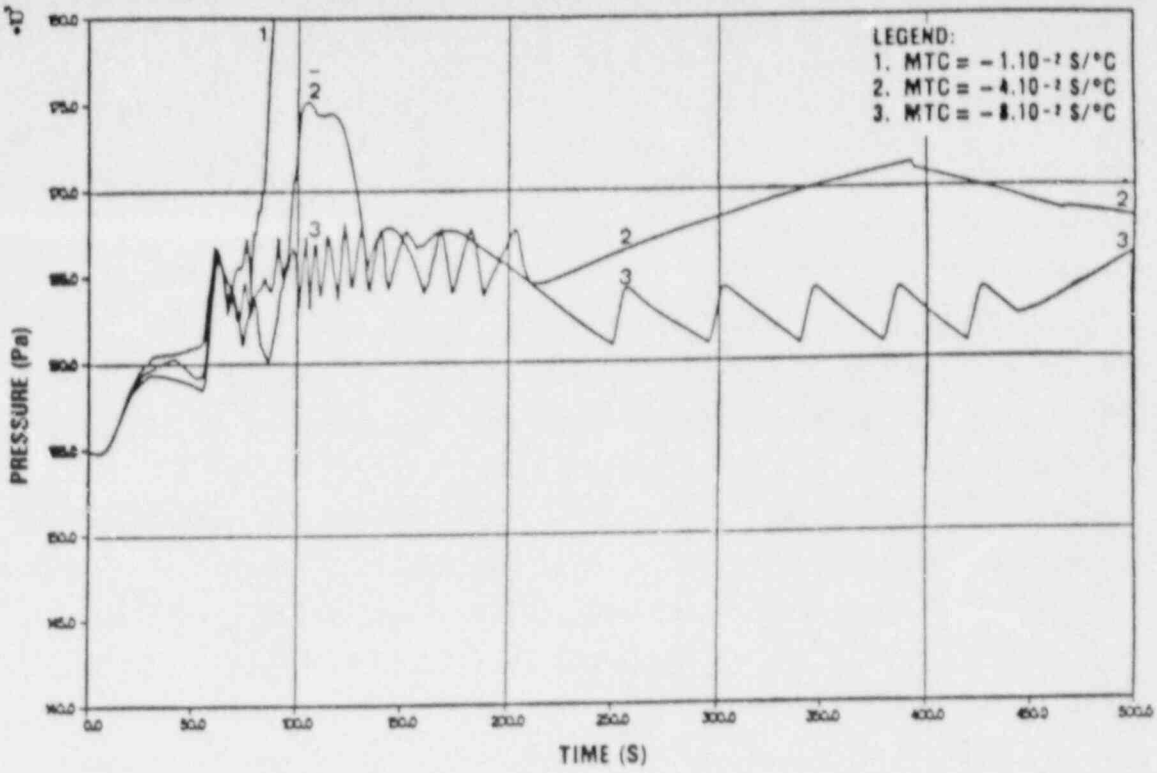

Fig. 6.1. Borssele ATWS core exit pressure.

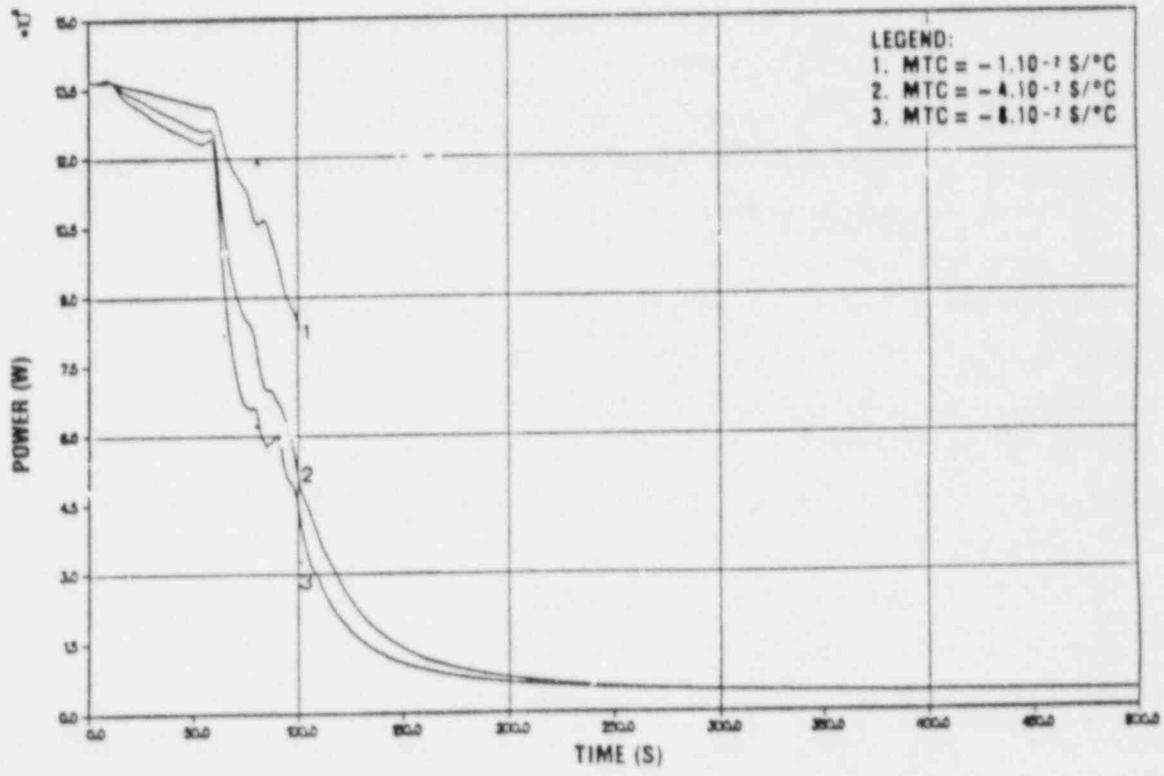

Fig. 6.2. Borssele ATWS reactor power.

4. CONCLUSIONS

Based on the RELAP5/MOD2 severe accident transient analyses for the Dodewaard BWR and the Borssele PWR, the following conclusions have been reached:

- The availability of 50% of the natural circulation isolation condenser for the Dodewaard BWR appears to be a powerfull (passive!) safety feature to limit the possible consequences of the accident events which have been considered.
- Unavailability of this isolation condenser system for a station blackout transient will result in a high pressure core melt situation. Opening of one ADS valve by the operator prior to core uncovery is sufficient to depressurize the reactor system before melting actually occurs.
- During the primary feed-and-bleed following a loss-of-all-feedwater event at the Borssele PWR, hot spots may be present inside the SG U-tubes as a consequence of a zero flow condition. These hot spots, which also have been observed during a similar experiment at the LOBI-MOD2 integral test facility, do not allow a further depressurization of the primary system. Since RCP restart requires a 30 minutes preparation period, this should be considered in the operating procedures for this type of accident.
- During a station blackout transient event, the maximum PORV capacity will be required to depressurize the primary system of the Borssele NPP before melting of the core occurs.
- The initial primary system pressure increase during an ATWS event at the Borssele PWR will not endanger the integrity of the primary system, when considering plant specific values of the moderator temperature coefficient.
- Based on the various RELAP5/MOD2 accident analyses for both NPP's and the corresponding sensitivity studies performed, much insight has been gained with respect to the course of the accident events, the phenomena which take place and the operator actions required to limit the possible consequence as much as possible.

REFERENCES

[1] Ransom, V.H. et al.,
RELAP5/MOD2 Code Manual,
NUREG/CR-4312, August 1985.

[2] Stoop, P.M., J.P.A. v.d. Bogaard, H. Koning,
Feed-and-Bleed Analysis for the Borssele Nuclear Power Plant
ECN document ECN-87-34, March 1987.

[3] Stoop, P.M., J.P.A. v.d. Bogaard, H. Koning,
Feed-and-Bleed Analysis for the Borssele Nuclear Power Plant
Presentation at the 2nd ICAP specialist meeting, AEE Winfrith,
Januari 1987.

[4] Sanders, J., E. Ohlmer,
Experimental Data Report on LOBI-MOD2 Test BT-00,
Communication No. 4038, LEC 86-38, JRC, ISPRA, April 1986.

ST-87/1487km

VALIDATION OF TRAC-PF1/MOD1 AGAINST EXPERIMENT LP-02-6 OF THE OECD-LOFT SERIES

(J.V. López; J. Blanco; J. Rivero and A. Alonso; Department of Nuclear Technology, Madrid Polytechnical University)

ABSTRACT

Experiment LP-02-6 of the LOFT-OECD series has been analysed with TRAC-PD2 and TRAC-PF1. Steady state, pretest and postest calculations with TRAC-PD2 were reported in the 14th WRSIM (1986). Modifications into the code were proposed to predict better rod temperature profile and other parameters. In this report the experiment is analysed with a frozen version of TRAC-PF1/MOD1 to serve as an ICAP exercise. The result of this work is compared with the old results from TRAC-PD2 before being modified. Although TRAC-PF1 renders results closer to experiment, still it does not reproduce correctly the rod temperature profile. No effort has been put in introducing new correlations for the minimum film boiling temperature as it was done, with positive results, for TRAC-PD2.

I.- INTRODUCTION

Experiment LP-02-6, successfully completed on October 3, 1983, is one of eight in the OECD-LOFT series. It simulates a double-ended break of a PWR main coolant inlet pipe, and was initiated from conditions representative of PWR operating conditions.

This report presents the second of the two calculations performed by the Spanish Group responsible for experiment LP-02-6. In this second calculation TRAC-PF1/MOD1 was used. The first calculation was reported at the 14th WRSIM (Ref. 1). The present study shows the main differences between this calculation and the first made with version PD2/MOD1 of TRAC, reported at length in an internal document (Ref.2).

In general, the thermohydraulic behaviour of the experiment has been simulated well in both calculations. Moreover, some improvements have been achieved with TRAC-PF1, mainly related to flow distribution.

II.- EXPERIMENT CONDUCT

A summary of the measured system conditions inmediately prior to Experiment LP-02-6 is given in Table I. Table II enumerates the

operational setpoints and Table III lists some significant events.

Experiment LP-02-6 was initiated by opening both quick-opening blowdown valves in the simulated broken loop. The reactor scrammed on low hot leg pressure at 0.1 s, and the pumps were tripped at 0.8 s. The pumps coasted down until 16.5 s, when they were disconnected from the flywheels. Flow in the core reversed almost instantaneously with experiment initiation, and fuel rod cladding temperatures started to increase at 0.9 s. The entire core heated up until 5.2 s, when positive core flow was again established due to choking of the flow in the broken cold leg. This positive core flow quenched the lower 2/3 of the core until ~ 10 s when flow in the intact cold leg decreased to below that of the broken cold leg and the core again started to heat up. A partial top-down core quench initiated at 14.8 s and lasted until 18.6 s. The lower plenum was filled by 30.7 s, the core quench was complete by 56 s, and core reflood was complete by 59 s.

Table I
Initial Conditions for Experiment LP-02-6

Parameter	Measured Value
Primary Coolant System	
Core ΔT (K)	33.1 ± 1.4
Hot leg pressure (MPa)	15.09 ± 0.08
Cold leg temperature (K)	555.9 ± 1.1
Mass flow rate (kg/s)	248.7 ± 2.6
Reactor Vessel	
Power level (MW)	46.0 ± 1.2
Maximum linear heat generation rate (kW/m)	48.8 ± 3.6
Steam Generator Secondary Side	
As per plant Operating Manual	
Pressurizer	
Liquid volume (m^3)	0.607 ± 0.02
Steam volume (m^3)	0.39 ± 0.02
Water temperature (K)	615.6 ± 5.8
Pressure (MPa)	15.3 ± 0.11
Liquid level (m)	1.04 ± 0.04

Table I
Initial Conditions for Experiment LP-02-6 (Cont.)

Parameter	Measured Value
Broken Loop	
Cold leg temperature (K)	553 ± 6
Hot leg temperature (K)	560 ± 6
Suppression Tank	
Liquid level (m)	1.34 ± 0.02
Water temperature (K)	360 ± 3
Pressure (gas space) (kPa)	160.5 ± 2.9
Emergency Core Cooling System	
Accumulator liquid level (m)	2.10 ± 0.0
Accumulator standpipe position (above inside bottom of tank)(m)	1.44 ± 0.03
Accumulator pressure (MPa)	4.11 ± 0.06
Accumulator liquid temperature(K)	302 ± 6.1
High-pressure injection flow rate (l/s)	1.04 ± 0.04
High-pressure injection liquid temperature (K)	305 ± 7
Low-pressure injection flow rate (l/s)	Verified
Low-pressure injection liquid temperature (K)	305 ± 7

Table II
Experiment LP-02-6 Operational Setpoints

Action	Reference	Measured Setpoint
Blowdown valves opened	Time (s)	0
Reactor scrammed (automatic)	Intact loop hot leg pressure (MPa)	14.8 ± 0.1
Primary coolant pumps tripped (manual)	Time (s)	0.8
High-pressure injection initiated (manual)	Time (s)	21.8
Low-pressure injection initiated (manual)	Time (s)	34.8

Table III
Chronology of Events for Experiment LP-02-6

Event	Measured Data Time (s)
Blowdown valves opened	0
End of subcooled blowdown	0.05 ± 0.05
Reactor scrammed	0.1 ± 0.01
Primary coolant pumps tripped	0.8 ± 0.01
Cladding temperatures initially deviated from saturation	0.9 ± 0.01
Control rods on bottom	1.7 ± 0.01
End of subcooled break flow	4.0 ± 0.5
Maximum cladding temperature reached (blowdown)	4.9 ± 0.2
Bottom-up core rewet initiated	5.2 ± 0.2
Bottom-up core rewet completed	9.1 ± 0.2
Partial core top-down quench initiated	14.8 ± 0.2
Pressurizer emptied	15.5 ± 0.5
Primary coolant pumps disconnected from flywheels	16.5 ± 0.01
Accumulator injection initiated	17.5 ± 0.5
Partial core top-down quench completed	18.6 ± 0.2
High-pressure injection initiated	21.8 ± 0.01
Lower plenum refill completed	30.7 ± 0.2
Low-pressure injection initiated	34.8 ± 0.01
Maximum cladding temperature reached (reflood)	41.0 ± 0.2
Accumulator injection completed	57 ± 5
Core quench completed	56 ± 0.2
Core reflood completed	59 ± 1

III.- LOFT LP-02-6 PLANT NODALIZATION.

LOFT nodalization -given in figs. 1 through 4- needed to simulate LP-02-6 with TRAC-PF1/MOD1 was based on that used in TRAC-PD2/-MOD1 calculation, with some modifications, mainly in the broken loop and in the vessel, as follows:

1.- The number of fluid cells in the broken loop cold leg has been reduced due to the choked flow model incorporated in TRAC-PF1/MOD1.

2.- Two bypass paths have been modeled in the vessel component to simulate the six real ones in the LOFT vessel.

3.- To study the behaviour of condensation and stratified flow models, the number of fluid cells near the injection point of the ECCS has been increased.

4.- Heat transfer between the main body of the steam generator secondary side and its downcomer has been included.

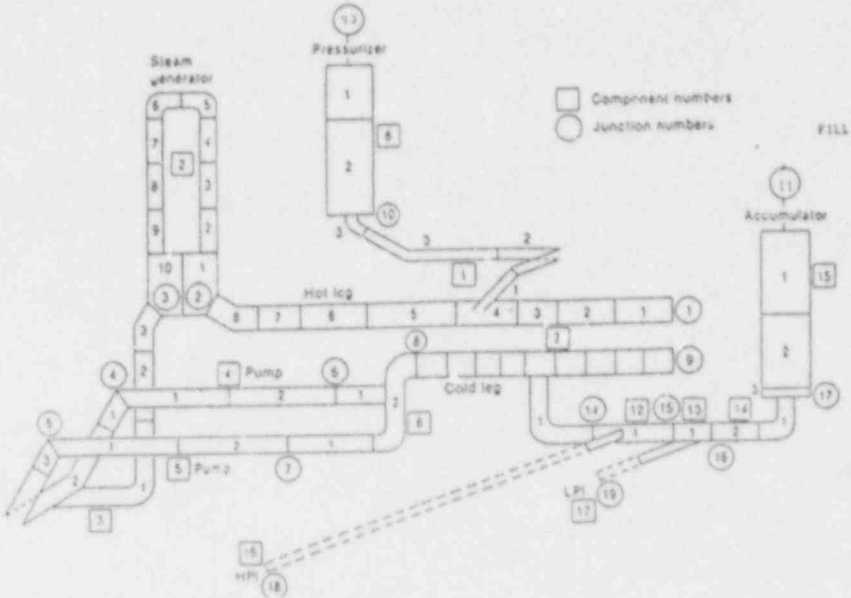

Figure 1.- Intact loop nodalization.

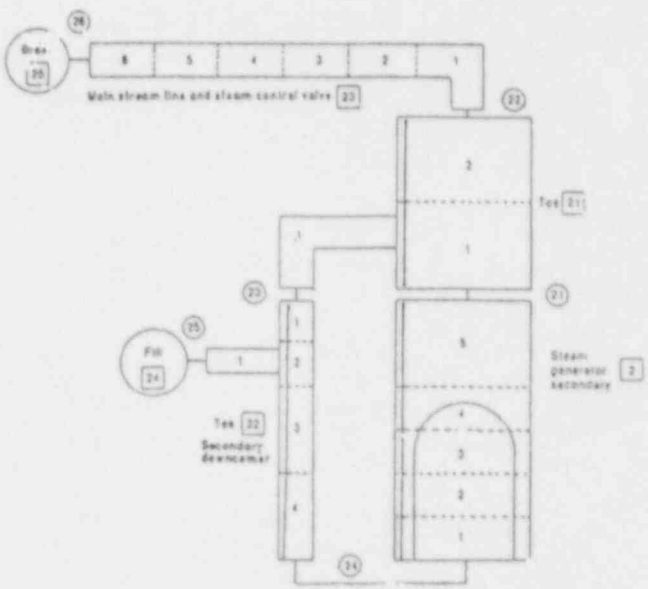

Figure 2.- Steam generator secondary side nodalization.

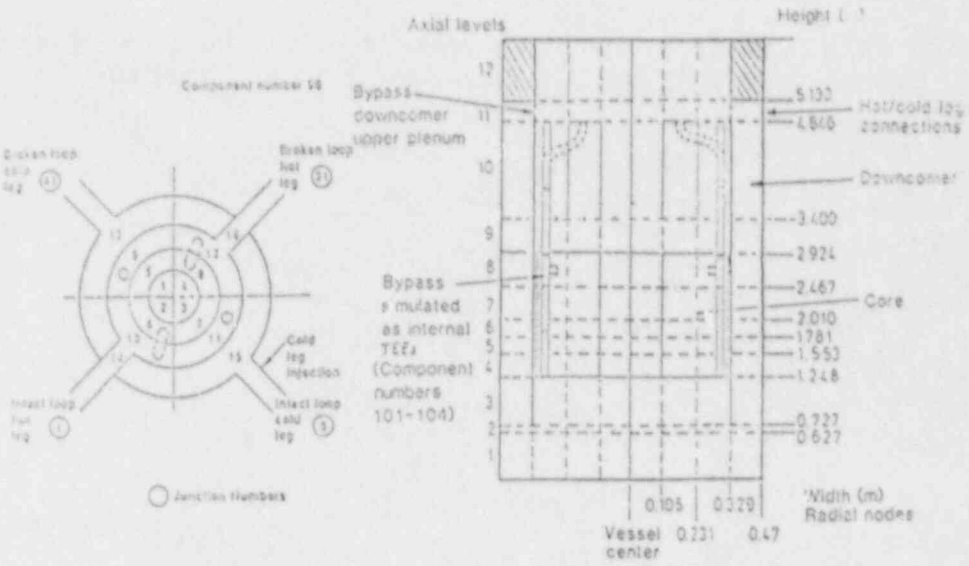

Figure 3.- Vessel nodalization.

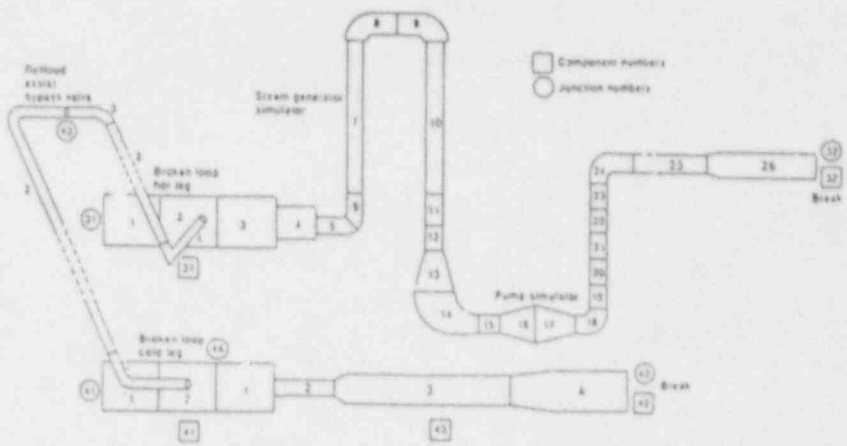

Figure 4.- Broken loop nodalization.

IV.- TRAC-PF1/MOD1 CHARACTERISTICS.

TRAC versions at present available to us are TRAC-PD2/MOD1 and TRAC-PF1/MOD1. TRAC-PD2/MOD1 was developed to analyse mainly large-break LOCAS in PWRs, and is prior to TRAC-PF1/MOD1. Besides the difference in the numerical scheme for the one-dimensional components, other major differences between both include the following,

1.- TRAC-PF1/MOD1 uses a full two-fluid, six-equation hydrodynamic model, whereas TRAC-PD2/MOD1 uses a five-equation drift-flux model for the one-dimensional components and a six-equation two-fluid model for the three-dimensional component.

2.- TRAC-PF1/MOD1 incorporates a choked flow model instead of relying on the fine noding at the break plane required by TRAC-PD2/-MOD1.

3.- In addition to the water liquid and vapor phases, TRAC-PF1-/MOD1 can model a noncondensable gas in the vapor phase and a solute in the liquid phase.

4.- TRAC-PF1/MOD1 allows to model the vessel either as a one-dimensional or as a three-dimensional component, while there is no user option when using TRAC-PD2/MOD1 and only a three-dimensional vessel is modeled.

5.- TRAC-PD2/MOD1 only includes trips to model control functions and systems. TRAC-PF1/MOD1 also includes more generalized constitutive relations that are applicable over a broader range of conditions.

6.- TRAC-PF1/MOD1 steam generator model allows to better represent the various heat structures associated with the tubes, the secondary flow shroud around the bundle and the outside shell.

V.- CALCULATION RESULTS.

Calculation of the experiment LP-02-6 with TRAC-PF1/MOD1, version 12.7, has been developed in two steps. In the first, the steady state calculation was carried out with the objective of fitting all system variables to experimental data, and the second step included the transient calculation.

For the steady state calculation with TRAC-PF1/MOD1, two important changes were done with regard to the TRAC-PD2/MOD1 execution,

1.- Several control blocks and trips were added to the input deck and, as a consequence, computer central processor unit (CPU) time during the steady state calculation got reduced. Variables related to these control blocks and trips include the following:

- Pump speed to loop mass flow rate.
- Steam generator secondary side pressure to main steam mass flow rate.

2.- Heat slabs have been added to represent heat transfer between the secondary boiler and downcomer sections, and heat losses at the external shell.

Table IV shows the results obtained after a run lasting 130 s of steady state. There are few differences in the results with regard to TRAC-PD2/MOD1 for the primary system. Secondary system variables are better calculated with TRAC-PF1/MOD1 Jue to heat structures.

Table IV
LOFT LP-02-6 Initial Conditions

PARAMETER	MEASURED VALUE	TRAC-PD2 /MOD1	TRAC-PF1 /MOD1
Reactor Vessel			
Power (MW)	46.0 ± 1.2	46.0	46.0
Intact Loop			
Mass flow rate (kg/s	248.7 ± 2.6	250.0	250.0
Hot leg pressure (MPa)	15.09 ± 0.08	15.07	15.08
Hot leg temperature (K)	589.0 ± 1.1	590.1	590.1
Cold leg temperature (K)	555.9 ± 1.1	556.8	556.6
Steam Generator			
Pressure (MPa)	5.62 ± 0.10	5.62	5.61
Feedwater mass flow rate (kg/s)	24.28	30.53	24.28
Main steam mass flow rate (kg/s)	24.28	30.53	24.29

For the transient calculation both codes provide very similar results, and the small differences are due to those new models introduced in TRAC-PF1/MOD1.

The most significant improvement is the evaluation of the mass flow rate in the broken loop cold leg (Fig. 5). The difference between both calculations is related to the choked flow model in version PF1, which avoids the use of a fine nodalization near the break plane, and becomes important during the subcooled discharge phase. While TRAC-PD2/MOD1 assumes two-phase flow since the start, TRAC-PF1-/MOD1 introduces a delay in the nucleation of the fluid occupying the broken loop cold leg, and this fact is governing the mass of coolant discharged through the break. Figure 6 shows the void fraction evolution in the broken loop cold leg for both calculations during the early seconds of the transient.

The above-mentioned improvement leads to a lower inventory in the system during the whole calculation and, as a consequence, to a lower calculated pressure, which is more realistic and closer to experimental data (Fig. 7).

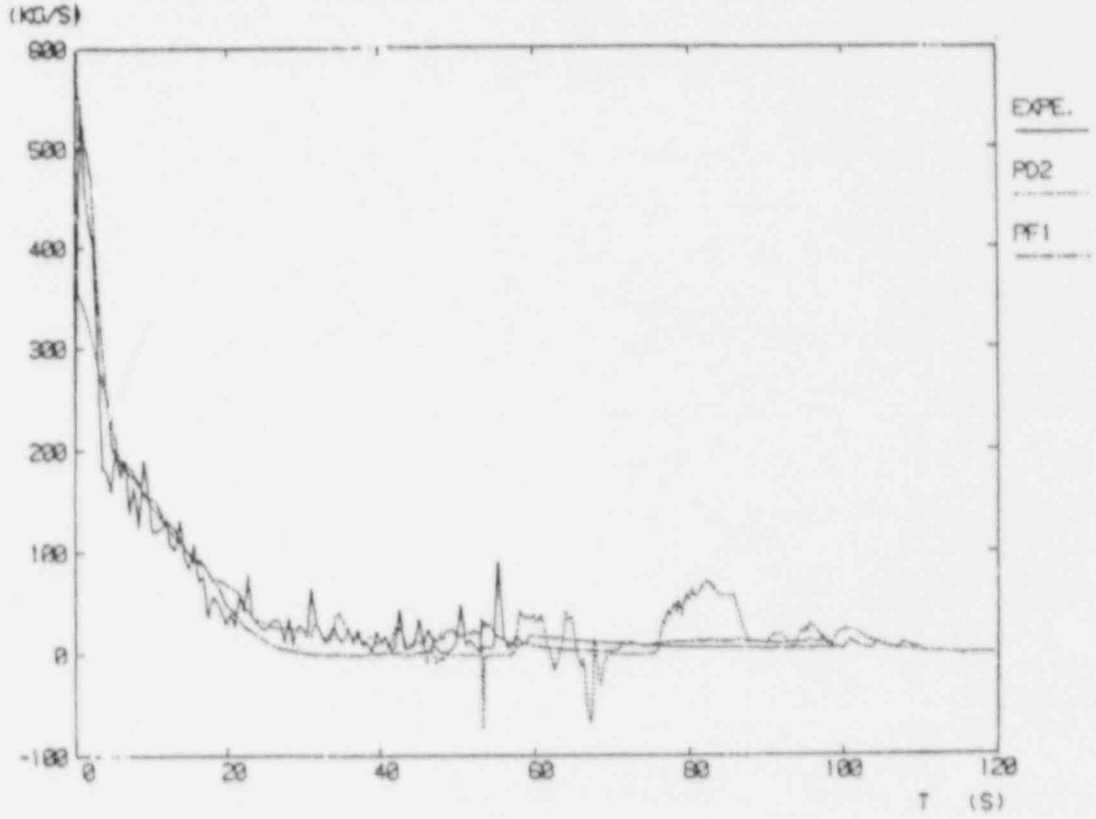

Figure 5.- Broken loop cold leg mass flow rate.

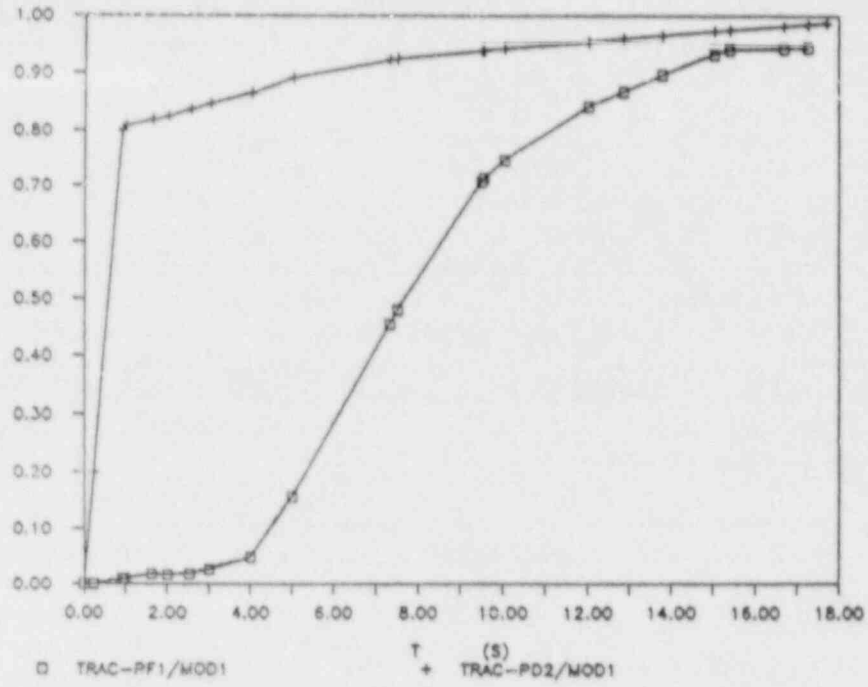

Figure 6.- Broken loop cold leg void fraction.

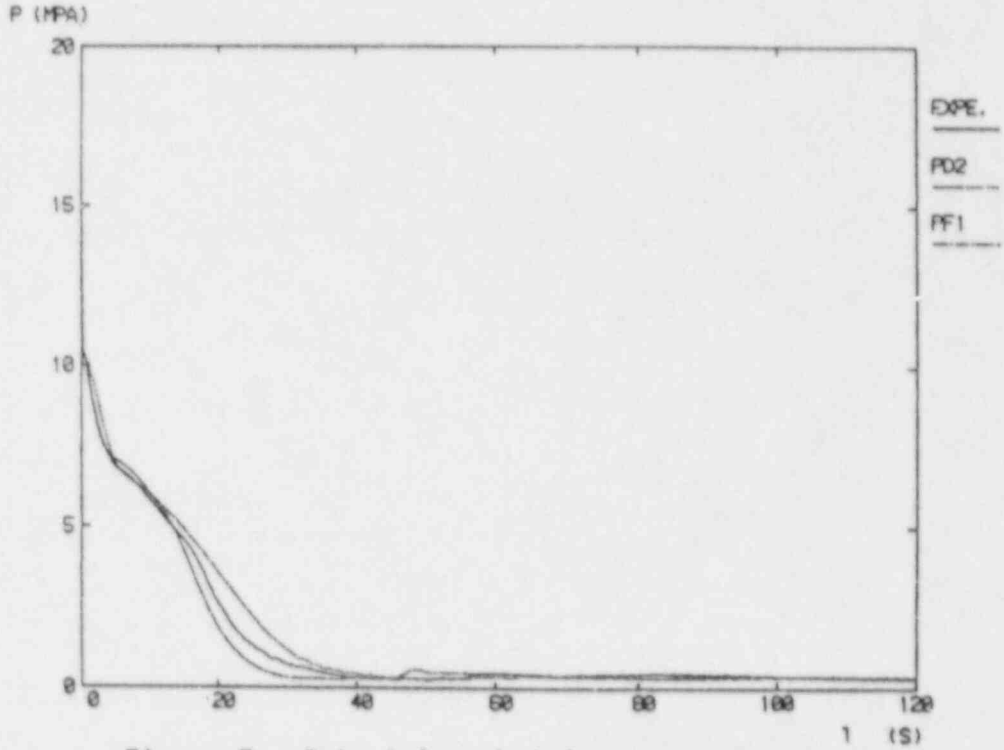

Figure 7.- Intact loop hot leg pressure.

The descent of the calculated pressure form 16 s onwards is due to the cold water discharge coming from the accumulator to the intact loop cold leg. This fact increases the condensation rate and contributes to depressurization during the discharge phase.

The succeeding evolution is right, except at 50 s, moment at which the system gets slightly pressurized again because of the nitrogen gas coming from the accumulator.

Pump speed calculation is acceptable during the initial instants of the transient (Fig. 8). The change of slope that can be observed in figure 9 when reaching 800 r.p.m. is due to flywheel disconnection. Neither code reproduces the entire calculation correctly. In our previous postest calculation with PD2 this discrepancy was observed (Ref. 1 & 2). In that case the torque and head multipliers were changed with excellent results. In this case, the original values have been kept.

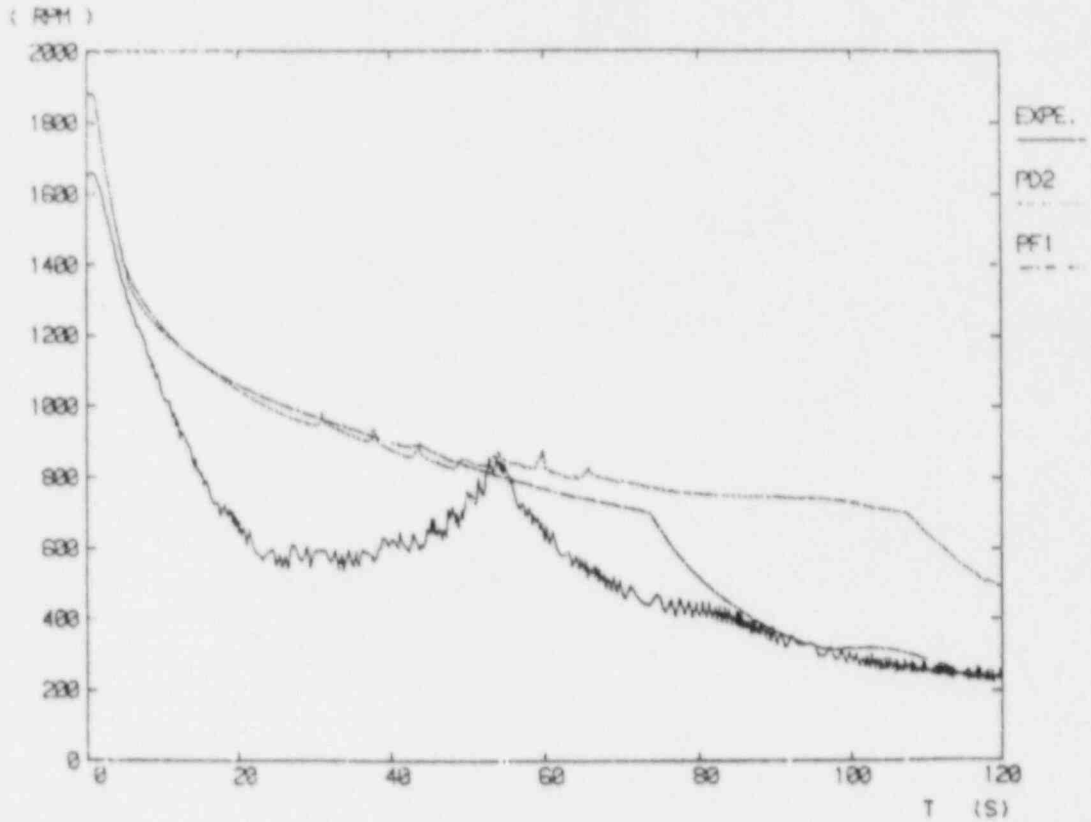

Figure 8.- Pump speed.

Mass flow rate through the core depends strongly on the coolant mass escaping through the break and on the hydraulic resistance of the flow path. Figures 9 and 10 show the evolution of core inlet and outlet mass flow rates. Both calculations behave similarly. The continuous flow of coolant from the primary system to the blowdown suppression tank reduces the liquid inventory and the core becomes uncovered. Figure 11 presents the core liquid fraction, where a first uncovery takes place around 4 s into the transient.

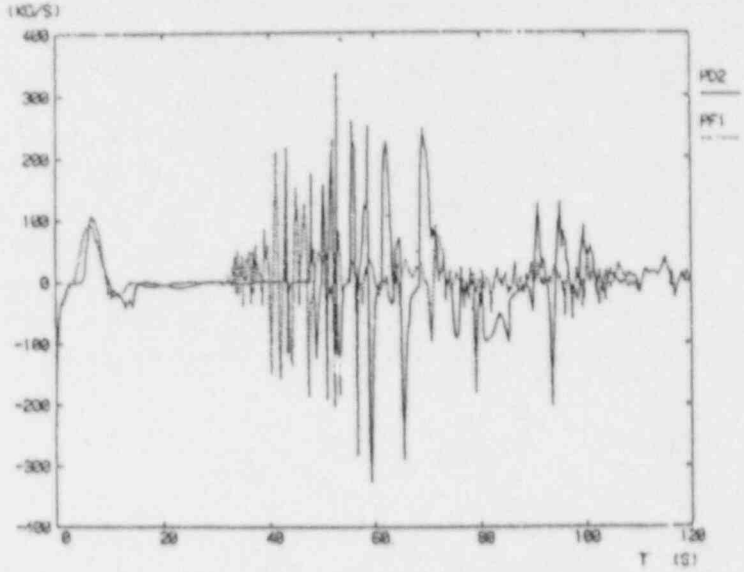

Figure 9.- Core inlet mass flow rate.

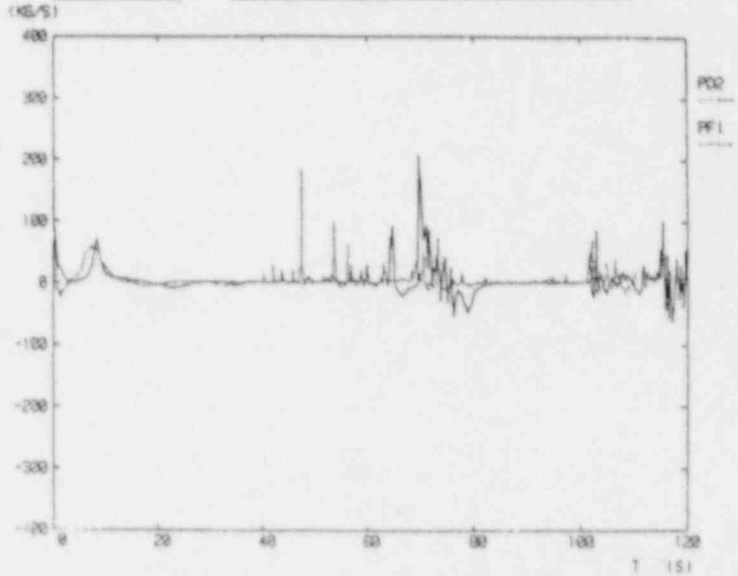

Figure 10.- Core outlet mass flow rate.

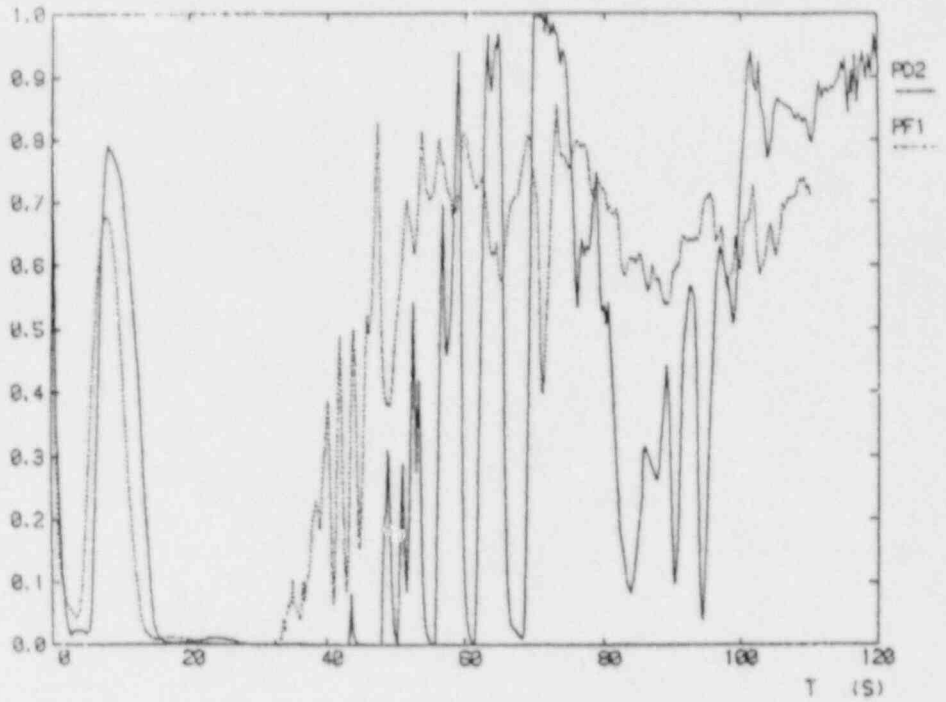

Figure 11.- Core liquid fraction.

A discrepancy between both calculations can be appreciated when considering figures 9 and 10, which is referred to the moment at which core reflood begins. It becomes earlier in the TRAC-PF1/MOD1 calculation, because of the simulation of bypass flow paths existing in the vessel.

LOFT vessel was primarly designed to contain electrical resistances instead of nuclear fuel rods. Later, the vessel was adapted to house nuclear fuel. This process led to the insertion of internals to reproduce thermohydraulic conditions of a commercial plant.

Vessel internals do not fix perfectly one to each other, so coolant flow finds ways of reaching the upper plenum without entering the core. There are six core bypass paths (Fig. 12), as explained in the work by W.C. Jones (Ref. 6), which can be gathered into two groups:

- downcomer/upper plenum bypass (paths 4 and 5)

- lower plenum/upper plenum bypass (paths 1, 2, 3 and 6)

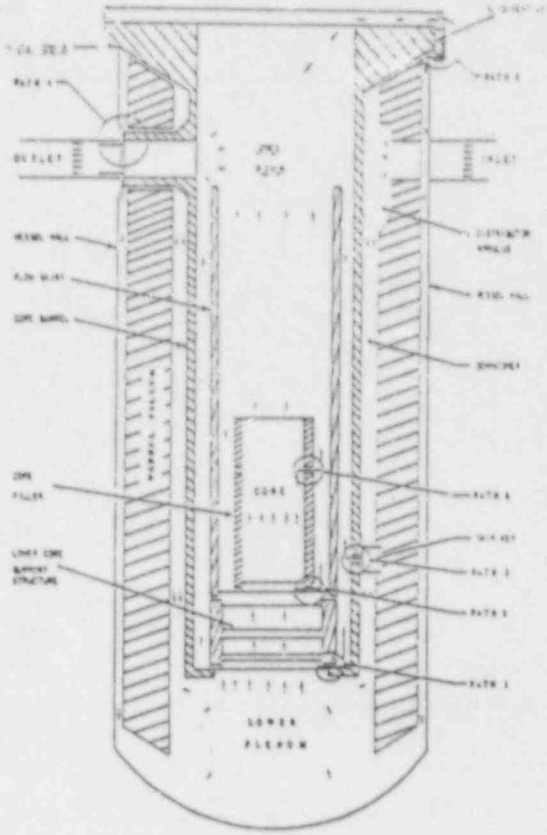

Figure 12.- Bypass paths in LOFT vessel.

It is important to simulate bypasses, because it helps in diminishing the pressure difference between upper and lower plena, so that the lower plenum refill and the core reflood can be reproduced with more realism.

During the period of time when the core is essentially uncovered, the steam escaping the core through the broken loop cold leg inhibits the entrance of cold water coming from the ECCS. This effect is smoothed due to the downcomer/upper plenum bypass, as pressure difference between downcomer and core is diminished.

Bypass paths are also important when considering the steam binding effect. Their simulation with TRAC-PF1/MOD1 leads to a higher depressurization rate and facilitates the entrance of liquid into the core.

Figure 13 shows the hottest cladding temperature at the midplane (0.647m), which corresponds to the hottest spot.

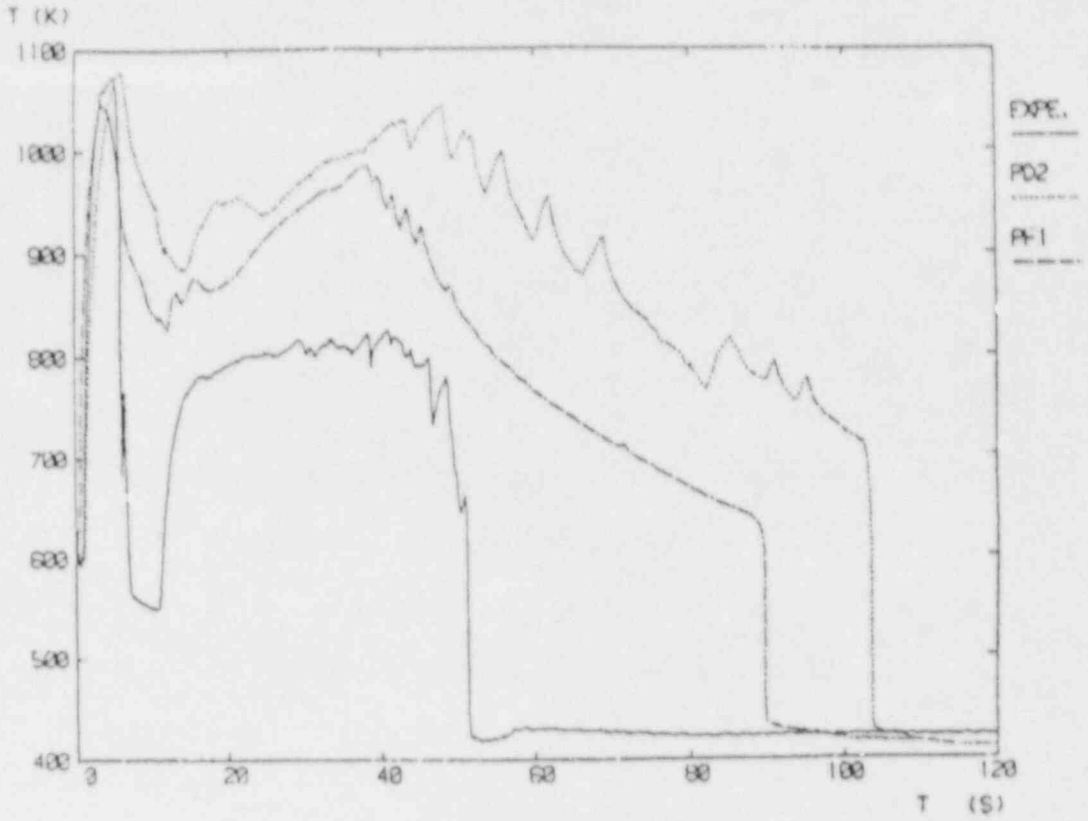

Figure 13.- Hottest cladding temperature (0.647 m).

Two-phase flow conditions in the core are reached almost instantaneously when the transient begins. That means cooling degradation of fuel rods. Departure from nucleate boiling is reached few instants into the transient. Both codes covered well the simulation of this phase, although DNB is forwarded in TRAC-PF1/MOD1 due to the higher mass evacuated through the break, which brings to a rapid reduction of the system inventory.

The first experimental temperature peak is near 1070 K. Both codes reproduced correctly this value, being TRAC-PF1/MOD1 calculation advanced because of the previously mentioned fact.

Experimental data show an early cladding quench at all axial levels. Neither code simulated this phenomenon with the required precision. TRAC-PF1/MOD1 calculation provides a minimum of 810 K, while TRAC-PD2/MOD1 does not fall below 890 K. There is still discussion about the reliability of cladding temperature data. It is possible that the heat transfer package incorporated in both codes is not suitable for high-pressure low-quality situations. Also, there is

the suspicion that external thermocouples affect quenching temperatures, so that the behaviour would not be the same without them. Finally, the most accepted theory is that, for simulating the bottom-up quench, a fine calculation of flows entering and escaping the core is needed, which is a thing that neither TRAC-PF1/MOD1 nor TRAC-PD2/-MOD1 do.

The first cladding temperature peak is not very important from the viewpoint of damage, because the pressure difference between the gap and the system is not high. The second peak is more important due to that pressure difference and to possible structural deterioration of the zicalloy. TRAC-PF1/MOD1 calculation for this second cladding temperature peak is the best of the two and the final quench is attained earlier, as a consequence of vessel bypasses simulation.

In our previous work with PD2 (Ref. 2 & 7) we discussed the effect of the minimum film boiling temperature and proposed Sakurai's correlation for low pressures, obtaining a much better prediction of clad temperature evolution and time to bottom-up quench. In this case such modifications have not been introduced into TRAC-PF1 due to the frozen nature of our calculations.

V.- CONCLUSIONS.

The TRAC-PF1/MOD1 thermohydraulic simulation for experiment LP-02-6 is quite accurate. Results are very similar to those obtained with TRAC-PD2/MOD1, apart from few differences related to new models incorporated and nodalization changes.

TRAC-PF1/MOD1 calculation improves the broken loop cold leg mass flow rate. Neither code simulated well the bottom-up quench and pumps behaviour. The reason for the former is not clear yet. With respect to pumps speed, it is needed a revision of inertia equation coefficients or of torque and head curves.

Cladding temperatures estimated by TRAC-PF1/MOD1 are lightly better than those by TRAC-PD2/MOD1, mainly in relation with the final rewetting, although both show a delay with respect to data because of the defficiency in the early quench simulation.

VI.- REFERENCES.

1.- A. Alonso et. al. Validation of TRAC-PD2 Against Experiment LP-02-6 of the OECD-LOFT Series, in Proceedings of the US NRC 14th WRSIM, NUREG/CP-0082, October 1986.

2.- Blanco, J., et al., Final Report. Analysis of Experiment LP-02-6 with TRAC-PD2/MOD1, Project OECD-LOFT-ESPAÑA, October 1987.

3.- Reeder, D.L., LOFT System and Test Description (5.5-ft Nuclear Core 1 Loses), EG&G Idaho Inc., July 1978.

4.- Adams, J.P., et al, Quick-Look Report on OECD LOFT Experiment LP-02-6, OECD LOFT-T-3404, October 1983.

5.- Los Alamos National Laboratory, TRAC-PF1/MOD1 An Advanced Best-Estimate Computer Program for Pressurized Water Reactor Thermal-Hydraulic Analysis, (Draft), May 1984.

6.- Jones, W.C., Internal Reactor Vessel Core Bypass Flows, (Internal LOFT Memo). November 1981.

7.- Rivero, J., et. al. Prediction of the Bottom-up Quench in Experiment LP-02-6 with TRAC-PD2, PIACR-S-02/87, March 1987.

STATUS OF THE RELAP5 USER GUIDELINES[a]

J. L. Jacobson and R. G. Hanson
Idaho National Engineering Laboratory
EG&G Idaho, Inc.

ABSTRACT

This paper presents an overview of a RELAP5 User Guidelines document which is currently being developed under the sponsorship of the U.S. Nuclear Regulatory Commission (USNRC) at the Idaho National Engineering Laboratory (INEL). The RELAP5 User Guidelines will provide insight for proper code use for specific applications and specific guidance relative to nodalization of nuclear power plants and experimental facilities based on a standard nodalization philosophy.

1. INTRODUCTION

The International Code Assessment and Applications Program (ICAP) has been organized by the USNRC to coordinate the domestic and international code assessment efforts. Based on these assessment efforts and specific studies to further understand nodalization effects, a User Guidelines is being produced which will assist the code user in consistent use of the RELAP5 code for applications to experimental facilities and full scale nuclear power plants. The code user will be provided with information relative to plant modeling, input deck organization and data requirements, the execution of the code from steady state through transient calculations, and the interpretation of the code output. The User Guidelines document will also provide quick reference on code input requirements.

This paper presents a summary of the User Guideline that will be published in the Spring of 1988. Section 2 presents a discussion of the regulatory significance of consistent use of a quantified computer code in the evaluation of transient response to accident sequences. Section 3 presents an overview of the contents of the User Guidelines. Section 4 provides a summary and a status discussion for the User Guidelines development effort. Section 5 is a list of references that represent an overview of the documents to be cited in the User Guidelines.

2. MOTIVATION FOR A CODE USER GUIDELINES

The USNRC is currently revising the licensing requirements for nuclear power plants to provide an optional best estimate calculational approach for licensing submittals. In support of these changes the USNRC is involved in an effort to characterize and quantify the best estimate use of thermal-hydraulic computer codes for accident evaluation. The on-going research is endeavoring to determine the scalability, applicability, and calculational uncertainty of the codes. The ICAP code assessment work

---

a. Work supported by the U.S. Nuclear Regulatory Commission, Office of Nuclear Regulatory Research under DOE Contract No. DE-AC07-76ID01570.

directly supports this code quantification effort through assessment studies and nodalization studies. The code assessment also directly supports the development and maintenance of User Guidelines. The use of assessment and application calculations for the quantification of code capability and applicability require that the code is used in a consistent and appropriate manner relative to nodalization and code options and application. Ultimately, the use of the code for best estimate licensing purposes or safety evaluations will require that the code be used consistently with guidelines that have been determined to be essential relative to Code Scalability, Applicability, and Uncertainty (CSAU) considerations. An important part of these guidelines is the specification of a standardized nodalization philosophy which, when used in the assessments, will insure they fully support the CSAU methodology.

3. USER GUIDELINES OVERVIEW

The User Guidelines is intended to be a comprehensive source of guidance to the code user over the range of applicable code applications. The User Guidelines is outlined below and this section will present a general discussion of selected sections from the outline.

1. RELAP5 CODE OVERVIEW
   - 1.1 Code description
   - 1.2 Code applications
   - 1.3 Code limitations
   - 1.4 Code use
     - 1.4.1 Input preparation
     - 1.4.2 Steady state calculation
     - 1.4.3 Transient calculation
     - 1.4.4 Output
   - 1.5 Computer requirements
   - 1.6 Execution procedures
   - 1.7 Support programs
     - 1.7.1 PYGI
     - 1.7.2 GANJA
2. DATA REQUIREMENTS
   - 2.1 Hydrodynamic geometry
   - 2.2 Heat structure parameters
   - 2.3 Core and neutronics data
   - 2.4 Control systems and trip information
   - 2.5 Initial and boundary conditions
   - 2.6 Data sources
   - 2.7 Data documents
3. GUIDELINES
   - 3.1 Input preparation
     - 3.1.1 General modeling discussion
     - 3.1.2 Facility nodalization
       - 3.1.2.1 Westinghouse standard plant model
       - 3.1.2.2 Combustion engineering standard plant model
       - 3.1.2.3 Babcock and Wilcox standard plant model
       - 3.1.2.4 Nodalization recommendations for test facilities

3.1.3 Calculation controls and trips
3.1.3.1 Miscellaneous input
3.1.3.2 Trip input
3.1.4 Hydrodynamic input
3.1.4.1 Hydrodynamic components
3.1.4.2 Single volume
3.1.4.3 Time dependent volume
3.1.4.4 Single junction
3.1.4.5 Time dependent junction
3.1.4.6 Pipe and annulus
3.1.4.7 Branch, separator, jet mixer, and turbine
3.1.4.8 Accumulator
3.1.4.9 Valve
3.1.4.10 Pump
3.1.5 Heat structures and tables
3.1.5.1 Heat structure input
3.1.5.2 General table
3.1.5.3 Thermal conductivity table
3.1.5.4 Volume heat capacity table
3.1.6 Reactor core modeling
3.1.7 Neutronics
3.1.8 Control systems and trips
3.1.9 Internal plotting package
3.1.10 Specific guidelines
3.1.10.1 Breakflow
3.1.10.2 Flow restrictions
3.1.10.3 Time-step size
3.1.10.4 Boron
3.1.10.5 Pressurizer spray and heaters
3.1.10.6 Pipe wall heat loss
3.1.10.7 Leakage paths
3.1.10.8 Noncondensibles
3.1.10.9 Pressure drops
3.1.11 Deck assembly
3.1.12 Alteration of existing deck
3.2 Steady state calculation
3.3 Transient calculation
3.3.1 General transient calculation discussion
3.3.2 Renodalization
3.3.3 Restart
3.4 Interpreting output
3.4.1 General output discussion
3.4.2 Integral plotting package
3.4.3 Minor and extended edits

As shown in the outline, the User Guidelines is divided into three major sections: an overview of the RELAP5 code; a discussion of data requirements for the development of a facility model; and code use guidelines.

3.1 RELAP5 Code Overview

This section of the document will present a description of the RELAP5 code, its limitations and range of application. A general discussion will address the use of the code, execution procedures, and supporting programs for deck and output data conditioning.

The RELAP5 computer code has been developed for best estimate transient simulation of PWRs and associated systems. The code is based on non-homogeneous and non-equilibrium models for the one dimensional two-phase flow system that is solved by a fast, partially-implicit numerical scheme to permit economical evaluation of system transients.

3.2 Data Requirements

This section presents the data required to construct an input deck for a facility and perform a transient calculation. The types of data needed for the development of a facility (or power plant) input deck include a detailed description of the hydrodynamic geometry, geometry that will control the transfer of energy from structures to fluids, and core related data (electrical heating information or neutronics information characterizing a nuclear core). In addition, required control systems (and trip information), steady state initial conditions, and transient dependent boundary conditions are discussed. As an example the thermal-hydraulic geometrical data required to model sections of a Pressurized Water Reactor (PWR) reactor vessel is presented below.

3.2.1 Reactor Vessel (Inlet Nozzles, Downcomer, Lower Plenum)

1. Inlet nozzles

Inside diameter at nozzle inlet	m, ft
Inside diameter at nozzle inlet	m, ft
Distance from nozzle inlet to nozzle outlet	m, ft
Forward flow energy loss coefficient	
Reverse flow energy loss coefficient	
Inside surface roughness	m, ft

2. Downcomer

Flow area as a function of elevation, relative to inlet nozzle centerline	m^2, ft^2
Full power inlet temperature	K, ^oF
Full power inlet pressure	Pa, psia
Elevation of top of downcomer, relative to inlet nozzle centerline	m, ft
Forward flow energy loss coefficient	
Reverse flow energy loss coefficient	
Surface roughness	m, ft
Hydraulic diameter as a function of elevation, relative to the inlet nozzle centerline	m, ft

3. Lower Plenum (below flow distributer)

Flow area as a function of elevation, relative to inlet nozzle centerline	m^2, ft^2
Total volume including structural material	m^3, ft^3
Metal-to-water volume ratio	
Forward flow energy loss coefficient	
Reverse flow energy loss coefficient	
Surface roughness	m, ft
Fractional composition of structural components (e.g., SS-306 26.4%, etc.)	
Hydraulic diameter as a function of elevation, relative to inlet nozzle centerline	m, ft

4. Lower plenum flow distributor

Flow area	m^2, ft^2
Forward flow energy loss coefficient	
Reversed flow energy loss coefficient	
Material composition	
Axial elevation at center and at edge	m, ft
Thickness	m, ft

5. Lower plenum between distributor and lower core plate

Flow area	m^2, ft^2
Hydraulic diameter	m, ft
Forward flow energy loss coefficient	
Reverse flow energy loss coefficient	
Surface roughness	m, ft
Material composition	
Total volume including structural material	m^3, ft^3
Metal-to-water volume ratio	

Within this section in the User Guidelines a discussion of sources for the required data will be presented. Also, and of primary importance, the necessity of good documentation of the data, deck construction, assumptions, and review process will be expanded upon.

3.3 Guidelines

This section of the User Guidelines will provide detailed guidance relative to model and code input preparation, steady state calculations, transient calculations, and the interpretation of output. In this section the discussion will be very specific relative to the development of input decks and the interface with the RELAP5 code required to perform calculations.

Relative to input preparation and the development of a facility model the User Guidelines will contain guidance with respect to nodalization. The primary source of input for nodalization guidance stems from a standard nodalization philosophy. The standard nodalization philosophy emphasizes

the need to model systems of different scales and types following similar criteria. The motivation for standardized use of the code is that in so doing the results of the specific code application can be linked to a code uncertainty statement that is based on a set of standard applications of the code. The standard nodalization philosophy will be specific for transient types (LBLOCA, SBLOCA, etc.) and will be subject to change if future code assessment studies suggest that a change is required. A complete discussion of the standard nodalization philosophy will be presented in the User Guidelines for large and small break LOCA type transients.

This section of the User Guidelines will specify the actual card-image input required to develop an input model of a facility including the requirements for hydrodynamic components, heat structures, core neutronics and control systems and trip logic. Specific guidance will be offered for code modeling of phenomena and/or components for which code assessment studies have been performed or where experience exists in the user community. These areas of specific guidance will include:

1. Break flow,
2. Flow restrictions,
3. Time-step size,
4. Boron control modeling,
5. Pressurizer spray and heaters,
6. Pipe wall heat loss,
7. Leakage path modeling,
8. Noncondensible, and
9. Pressure drops.

The mechanics of performing steady state and transient calculations will be discussed along with guidance relative to input deck manipulations and restarting. Finally, the User Guidelines will outline available output possibilities and present necessary information to obtain desired output.

4. SUMMARY/STATUS OF THE RELAP5 USER GUIDELINES

The INEL is currently developing the RELAP5 User Guidelines within the ICAP program. Code assessment studies and user interaction with the code development effort have been a major source of input to the User Guidelines. Another major source of input has been the CSAU program which has had considerable input relative to standard nodalization philosophy.

The User Guidelines is scheduled for release as a draft report for review in March 1988. The User Guidelines will be a living document. Thus, as additional user guidelines are provided through code assessment studies, user experiences, CSAU methodology and other future studies the User Guidelines will be updated. The RELAP User Guidelines will also be updated when new frozen versions of the code are released.

5. REFERENCES

The following reference list contains documents that have provided input or that have been identified as potential sources of information for the User Guidelines. This list is being provided in order to present an overview of the sources that will contribute information to the User Guidelines; thus, it is not all inclusive.

P. D. Bayless and R. Chambers, Analysis of a Station Blackout Transient at the Seabrook Nuclear Power Plant, EGG-NTP-6700, September 1984.

P. D. Bayless, C. A. Dobbe, and R. Chambers, Feedwater Transient and Small Break Loss of Coolant Accident Analysis for the Bellefonte Nuclear Plant, NUREG/CR-4741, EGG-2471, March 1987.

J. M. Boone, letter to R. G. Hanson, "RELAP5 User Guideline Input", OS-228.00, May 7, 1987.

B. E. Boyack, H. Stumpf, and J. F. Lime, TRAC User's Guide, NUREG/CR-4442, LA-10590-M, November 1985.

B. L. Charboneau, ICAP RELAP5 Newsletter, NUREG/BR-0103, EGG-RTH-7195 (2-86), Volume 2, Number 2, April 1986.

B. L. Charboneau, ICAP RELAP5 Newsletter, NUREG/BR-0103, EGG-RTH-7195 (3-86), Volume 2, Number 3, July 1986.

B. L. Charboneau, International Thermal-Hydraulic Code Assessment and Applications Program RELAP5 Newsletter, NUREG/BR-0103, Volume 1, Number 1, July 1985.

B. L. Charboneau, and E. C. Johnsen, International Thermal-Hydraulic Code Assessment and Applications Program RELAP5 Newsletter, NUREG/BR-0103, Volume 2, Number 1, January 1986.

M. G. Croxford, P. C. Hall, Analysis of the Thetis Boildown Experiments Using RELAP5/MOD2, United Kingdom, GD/PE-N/576 (REV), March 1987.

C. B. Davis, letter to T. R. Charlton, "Consistent RELAP5 Models", CBD-07-80, December 16, 1980.

J. Eriksson, Assessment of RELAP5/MOD2, Cycle 36.04 Against FIX-II Guillotine Break Experiment No. 5061, Sweden, Studsvik/NP-86/109, May 1987.

S. Guntay, RELAP5/MOD2 Assessment: OECD-LOFT Small Break Experiment LP-SB-3, Switzerland, December 1985.

D. G. Hall and E. C. Johnsen, RELAP5/MOD1 Quick Reference Manual, EGG-CDD-6027, October 1982.

P. C. Hall and G. Brown, RELAP5/MOD2 Calculations of OECD LOFT Test LP-SB-01, United Kingdom, GD/PE-N/544 (REV), November 1986.

R. G. Hanson, TRAC-BD1/MOD1 User's Guideline, NUREG/CR-4429, EGG-2423, November 1985.

C. Harwood and G. Brown, RELAP5/MOD2 Calculation of OECD LOFT Test LP-SB-03, United Kingdom, GD/PE-N/535 (REV), April 1986.

J. L. Jacobson, ICAP RELAP5 Newsletter, NUREG/BR-0103, EGG-RTH-7195 (3-86), Volume 2, Number 3, July 1986.

J. L. Jacobson, ICAP RELAP5 Newsletter, NUREG/BR-0103, EGG-RTH-7195 (1-87), Volume 3, Number 1, January 1987.

J. L. Jacobson, ICAP RELAP5 Newsletter, NUREG/BR-0103, EGG-RTH-7195 (4-87), Volume 3, Number 2, April 1987.

J. L. Jacobson, ICAP RELAP5 Newsletter, NUREG/BR-0103, EGG-RTH-7195 (7-87), Volume 3, Number 3, July 1987.

L. N. Kmetyk, RELAP5 Assessment: Conclusions and User Guidelines, NUREG/CR-3936, SAND84-1122, October 1984.

J. F. Kunze, letter to R. G. Hanson, "RELAP5/MOD2 Experience", April 8, 1987.

M. M. Megahed, RELAP5/MOD2 Assessment Simulation of Semiscale MOD-2C Test S-NH-3, NUREG/CR-4799, EGG-2519, October 1987.

P. Moeyaert and E. Stubbe, Assessment Study of RELAP5/MOD2 Cycle 36.04 Based on Spray Start-Up Test for DOEL-4, Belgium, October 1986.

C. K. Nithianandan, N. H. Shah and R. J. Schomaker, RELAP5/MOD2 Assessment of Babcock & Wilcox, October 1985.

V. H. Ransom, et. al., RELAP5/MOD2 Code Manual, NUREG/CR-4312, EGG-2396, August 1985.

O. Sandervag, letter to N. Lauben, "RELAP5/MOD2 Code Errors Encountered During Reflood Calculations", OS/AH, June 25, 1987.

R. R. Schultz, "RELAP5 Application Workshop", RELAP5 Application Workshop, Idaho Falls, Idaho, July 25-August 5, 1986.

E. J. Stubbe, Assessment Study of RELAP5/MOD2 Cycle 36.01 Based on the DOEL-2 Steam Generator Tube Rupture Incident of June 1979, Belgium, TE.NU/EST/ml, NUREG/IA-000B, January 1986.

S. R. Wagoner, International Thermal-Hydraulic Code Assessment and Applications Program RELAP5 Newsletter, NUREG/BR-0103, Volume 1, Number 2, October 1985.

G. E. Wilson, letter to E. Stubbe, "Transmittal of the USNRC Review of a Code Assessment Study for the Author's Review", GEW-53-87, August 17, 1987.

G. E. Wilson, letter to O. Sandervag, "Transmittal of the USNRC Review of a Code Assessment Study for the Author's Review", GEW-54-87, August 17, 1987.

R. Yuann, K. Liang, and J. L. Jacobson, RELAP5/MOD2 Assessment Using Semiscale Experiments S-NH-1 and S-LH-2, NUREG/CR-5010, EGG-2520, October 1987.

MERITS AND LIMITS OF CODE ASSESSMENT BASED ON FULL SCALE PLANT DATA

BY

E. J. STUBBE TRACTEBEL BRUSSELS

FOR PRESENTATION AT THE
FIFTEENTH WATER REACTOR SAFETY
INFORMATION MEETING
OCTOBER 26-29, 1987,
GAITHERSBURG MARYLAND U. S. A.

1. INTRODUCTION

Among the questions that need be answered by the thermalhydraulic assessment program is the scalability of the physical models used in best estimate advanced computer codes (Ref. 1).

This problem needs a special attention if the basis for plant licensing in the area of LOCA and ECCS shifts from "evaluation models" to "best estimate models", as is the tendency today.

The database for the physical models in the advanced thermalhydraulic codes is largely based on small scale separate effect tests and integral scaled down facilities (Ref. 2,3).

In view of the diversity in concept and scale of the various test facilities, there is a growing interest in performing "counterpart tests" in order to verify the scalability of the constitutive equations in function of an accepted nodalisation scheme and an applied numerical solution concept for different best estimate codes (Ref. 4).

The outcome of such counterpart tests can yield some evidence of the scalability over a range of scales varying between 1/1600 and 1/48 , such that the extrapolation to full scale remains questionable.

In an attempt to close this scaling gap for specific code models, full scale separate effect tests offer a good opportunity. However such facilities are very expensive and require artificial boundary conditions which may mask some dominating phenomena induced by loop components and their mode of operation.

There remains then the question to what extend full scale plant data could be used to try to close the scaling gap of the experimental evidence?

The proposed validation matrices contain indeed very few plant transients,and this for different reasons.

This paper tries to compile the different advantages and disadvantages that full scale plants offer for code assessment, and presents a practical exercice on a DOEL-4 transient to highlight those points.

2. MAJOR ADVANTAGES

2.1. It is evident that "full scale" data from existing power plants offer a major advantage for code assessment. Any scaling method adapted for the concept of a scaled down integral test facility has to make compromises on one or more important areas.
For instance, a commonly used power to volume scaling (SEMISCALE,LOBI,LSTF,BETHSY) leads to distortions in the areas, downcomer, structural heat, friction losses with the possible result that some phenomena may be affected by scale distortion or even scaled out completely.

2.2. The empirical correlations that mostly have been conceived on the basis of small scale separate effect tests, and tested against integral scaled down facilities, may be sensitive to noding, and to the applied numerical resolution scheme. It is well known that for every type of best estimate code, a generally accepted nodalisation scheme has been worked out for every test facility to fit the experimental data. The ISP-20 results show that some phenomena (e.g. condensation) are not well reproduced by RELAP 5/MOD2, unless a special nodalisation scheme is used,which is different from the generic nodalisation scheme used for steam generators.

2.3. The most important task in the area of code assessment is to assure an acceptable simulation for the important critical parameters for design basis accidents and severe plant transients (e.g. PCT, core subcooling, DNB, etc...)

While it is practically excluded to obtain plant data to substantiate the code models and to evaluate these critical core parameters, one should however not overlook the possibility to check some fundamental models such as heat and momentum transfer in two phase conditions based on a steam generator behaviour during milder plant transients.

Example :

The well known dynamic level shrink and swell observed in the steam generator under varying conditions of feedwater flow or steam discharge are a result of heterogeneous flow processes in the steam generator riser section. A good simulation of these phenomena requires an adequate treatment of the interfacial momentum transfer under a wide range of flow regimes, and thus constitutes a good check on the validity of these code models at full scale (Ref. 5).

Extrapolation of such assessment to primary side behaviour is only possible for those codes which use an identical flow regime dependent heat and momentum transfer equation logic for the primary and secondary systems (cf. RELAP, TRAC).

2.4. With the advances of numerical techniques in data gathering, plant dedicated digital data acquisition systems can enhance considerably the quality of the data which could be used for code assessment. Most Belgian nuclear power plants are equipped with such stand-by digital data acquisition systems which are triggered by a logic signal from the plant protection systems.

3. MAJOR DISADVANTAGES

3.1. It is obvious that the "hopefully" few abnormal transients in nuclear power plants will not cover the spectrum of code assessment required to close the scaling gap of the experimental evidence. Hence any thorough code assessment matrix should be based essentially on diverse experimental facility data, while the available plant

data should fully be used to confirm the adequacy of the available code models.

3.2. The quality of the data recorded in most nuclear power plants is rather poor compared to the quality of the data in experimental facilities. The instrumentation installed in nuclear power plants is more often selected on the basis of robustness and reliability rather than on the basis of precision. Furthermore, a serious degradation of the quality occurs in the recorders installed in the control room, since the calibration of these devices is not always reliable. In fact, the operators pilot the plant more on the trends in recorded data rather than on the absolute value displayed on the recorders.
The use of a digital data acquisition hooked up at the plant data bus, enables one to avoid this quality degradation by the recorders.

3.3. The quantity of the data available in a nuclear power plants is strictly limited to the essential data required for safe and reliable operation of the plant. Although the number of sensors may be large, a large redundancy is required for safety reasons (there are typically 6 redundant water level measurements in each steam generator).
It follows that the available data give a picture of the global status of the plant, while most detailled local information, about the coolant redistribution, such as needed for code assessment, is missing.

3.4. Whereas the initial conditions of the plant may be assumed to be known with sufficient precision, the lack of data about the boundary conditions during the transient constitutes one of the major drawbacks in trying to simulate plant transients.
These boundary conditions are influenced by operator interventions which are unfortunately not always recorded with the needed precision. (e.g. valve position as a function of time).

The boundary conditions are furthermore strongly controlled by the plant control systems which, within a certain range, can override some trends and even phenomena, due to the negative feedback present in most control systems.
For instance, a steamgenerator tube rupture will lead to an increase in the water level in the faulted steam generator. The feedwater level control system will however reduce the feedwater flow in an attempt the keep the measured level at the programmed water level. Hence, a complete simulation of a transient will require the simulation of the major plant control systems in order to reproduce the plant data.

3.5. Even with the above limitations, every available information obtained during the start-up tests or periodic tests of small or large components or entire plants, could be of potential benefit for code assessment and for modelling concepts (e.g. pressuriser spray efficiency or depressurisation can give an indication of the adequacy of the code condensation models).
However it is well known that most countries are very reluctant to release such information. Indeed, the large amount of information and data (in the form of drawings, recordings, plant description) that is required for a good simulation of the tests often has to include information which either the NSSS supplier, Architect Engineer or utilies are considering as confidential or proprietary. This is the main reason why very few plant transients are included in the code assessment matrix. However since the ICAP rules specify that proprietary, confidential or privileged information can be identified and restricted from public disclosure, it is possible to reconcile the needs for non disclosure of certain information, and the need for access to vital plant data for code assessment only.Furthermore,transmission of plant data in form of coded input data, as was the case for the ISP-20 exercise, offers another possibility to avoid such problems.

4. PRACTICAL EXAMPLE : DOEL-4 LOSS OF EXTERNAL LOAD TRANSIENT

This example typically illustrates the major advantages and disadvantages of using full scale plant data for code assessment (Ref. 6).

As part of the pre-commissioning test of the DOEL-4 power plant (a 3 Loop, 1000 MWe, Westinghouse LWR, operational since November 1985) a loss of external load transient was initiated manually to verify the return to house load without turbine trip nor reactor trip. A digital data acquisition system (DAS) was used to record about 150 analog and logic signals.

4.1. RELAP-5 model description.

The transient was simulated by means of the code RELAP 5/MOD 2/CYCLE 36.05 in order to gain more insight into the basic phenomena that govern such transient.

Fig. 1 illustrates a block nodalisation for the plant, and one recognises that besides the normal components, a lot of control systems have been modelled explicitly in order to simulate the response of the plant (e.g. feedwater level control, pressuriser pressure control, steam-dump control etc...).

By limiting the scope of simulation to the components as shown in fig. 1, it is essential to impose furthermore suitable boundary conditions on the RELAP-5 model for those parameters which are derived from non-simulated components.
E.g without simulation of the turbine - generator set, the primary coolant pump speed must be imposed as an external boundary condition, as recorded in the plant.
Table 1 summarises the list of imposed boundary conditions.

Besides modeling the control systems conform to the as-built plant drawings, it is of utmost importance to model plant component behaviour in terms of inertia and response time to fast actuation signals (e.g. steam dump valve, feedwater

regulation, pumps) in order to respect the delays introduced by these components.

4.2. Analysis and discussion of the numerical results.

The numerical simulation was performed over a period of 600 s, including a stabilisation period of 13 s prior to the initiation of the transient. This period of 600 s covers the most important phenomena which govern a successfull transition from full power to house load. At 600 s, feeding of the steam generator switched over from bottom feed to top feed. This feature was not retained in the RELAP-5 model simulation. The most representative results are illustrated in figures 2 to 5 which compare the calculated data (solid lines) to the DAS recorded data (dash-dot lines) for some essential parameters, such as primary pressure (Fig. 2), cold leg temperature (Fig. 3), main steam collector pressure (Fig. 4) and steamgenerator water level (Fig. 5).

An overall acceptable agreement is observed between calculated and measured data, which allows one to assert that the RELAP-5 MOD-2 code is capable to handle such transients and that the nodalisation is adequate to illustrate the predictive capability of the code.

However, some discrepancies are evident during the first 150 seconds, which need further investigation.

Between 0-13 s : Due to slight differences between the available steady state input deck for the plant, and the plant initial conditions, some fluctuations are observed in the numerical data which are believed to be of no importance for the remainder of the transient.

Between 13 and 30 s : An overshoot of about 2.5 bar (Fig. 2) in the primary pressure should be linked to an excessive rise in the cold leg temperature (Fig. 3). This is caused by the absence of structural heat absorption in the steam generator metal structures, when the pressure (and also the temperature)

suddenly increases upon closure of the turbine admission valves. Due to core memory limitations, structural heat was not modelled. A good representation of the initial pressure overshoot is essential to justify the absence of reactor trip on high pressure, or even to verify the actuation of the pressuriser relief-valves.

For the same period, the calculated steam generator water level drop (Fig.5) is much smaller than the recorded level fall. The location of the upper level tap (just above the upper deck plate) makes it very sensitive to acoustic pressure pulses which are generated in the main steam lines upon sudden closure of the turbine admission valves and reflected in the upper dome. Closer examination of the recorded data shows clearly sharp water level spikes which are just in opposite phase with the recorded pressure spikes. The crude nodalisation of the steamlines and the steam generator dome does not alow one to reproduce these acoustic phenomena. Discounting this effect, there still remains a level discrepancy of about 3.5 % which should be attributed to the separator modeling deficiencies.

Fig. 5 also manifests an excessive level swell following the opening of the steamdump valves. This anomaly may be traced back to too strong a coupling between the water and vapour phase in the riser in the low void regimes, which causes excessive water entrainment into the separator region where the delta-P level measurement is located. The deficiency of RELAP-5 to simulate the level swell phenomena correctly is attributed to the interfacial shear model. This anomaly feeds back, via the steam generator water level control system, to a reduction in the feedwater flow, which is reflected immediately by too high a cold leg temperature, as visible in Fig. 3 between 20 and 100 s. The design of the preheater section manifests a very tight thermal coupling between the feedwater flow rate and the cold leg temperature.

CONCLUSIONS

- From experience with simulation of the DOEL-2 steam generator tube rupture (ISP-20), and the DOEL-4 islanding test, one recognises the possibility to check the analytical simulation concept of best estimate codes against full scale plant data. However, such data should not be used to improve the existing physical models as the initial and boundary conditions are not known with sufficient precision.

- In view of the potential benefits for code assessment, a larger effort should be done to search for interesting plant data (e.g. pre-commissioning tests) which could be useful for verifying the code scalability even for a limited number of phenomena.The growing use of high quality data acquisition systems in nuclear power plants could increase considerably the quality of full scale plant data.

- More effort should be done to find ways to communicate essential plant data for code assessment with complete assurances that sensitive information about plant behaviour, components and systems shall not be distributed to third parties.

- For code assessment purposes, available plant data can constitute a highly desirable complementary data base, but should never be a substitute for experimental test data.

REFERENCES

1. Code scaling, applicability and uncertainty evaluation methodology.
Novak Zuber, USNRC
Presented at the CSNI PWG-2 , Paris June 1987.

2. CSNI code validation matrix of thermal-hydraulic codes for LWR LOCA and transients.
CSNI report 132. March 1987.

3. International Code assessment and application program.
NUREG-1270.

4. Elaboration of a guideline for Counter part Testing of Integral Loop Systems.
Prof. KARWAT 1987
Study contract for the JRC of the European Communities.

5. Assessment study of RELAP5 - MOD 2 CYCLE 36.01 : Based on the DOEL-2 steam generator tube rupture incident of June 1979.
NUREG/IA-0008 October 1986.

6. DOEL-4 Loss of external load transient - Simulation and analysis.
E. STUBBE et al, ANS Topical meeting "Anticipated and abnormal transients in nuclear power plants" ATLANTA, April 12-15, 1987.

TABLE 1 - LIST OF SIMULATED CONTROL SYSTEMS AND IMPOSED BOUNDARY CONDITIONS

Label (Fig. 1)	Control system imposed B.C.	Simulated	Description/Impact
RT	Plant reference temperature	NO	DAS data used since turbine component was not simulated. No impact on calculation since Tref drops to constant value
PP	Pressuriser pressure control (Heaters, spray valves)	YES	Heater power controlled by pressuriser pressure and water level. Spray valves controlled by pressuriser pressure
PL	Pressuriser water level	NO	DAS data input for charging and letdown. Weak feedback.
RP	Reactor coolant pump speed	NO	DAS data used since turbine-generator not simulated. Impacts only the first 20 sec. of the transient.
CR	Control rod position	NO	DAS insertion rate used.
FT	Feedwater temperature	NO	DAS data used since the balance of plant was not simulated.
FW	Steam generator feedwater flow	YES	Feedwater flow rate controlled by calculated water level, steam and feedwater flows (very strong feedback). No FW pumps.
SD	Steam dump control system	YES	Bypass steamflow controlled by difference between reference temperature and calculated average loop temperature.
TU	Turbine admission valve control	NO	Preprogrammed position from best estimate calculation. No feedback on calculated data.

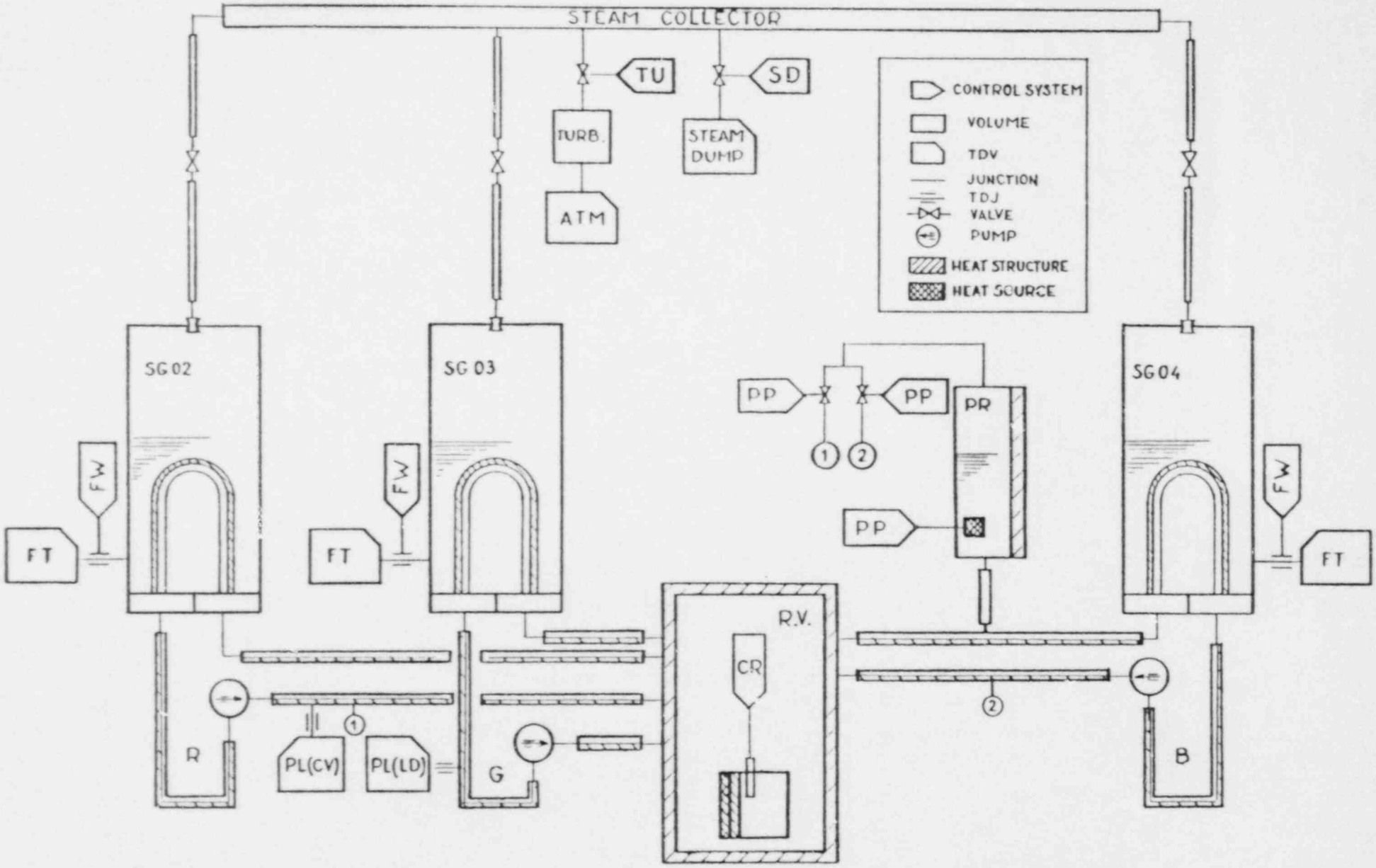

FIG. 1 : BLOCK NODALISATION FOR DOEL 4 LOSS OF LOAD TRANSIENT

DOEL+ LOSS OF EXTERNAL LOAD TRANSIENT (23/11/85)

RELAP 5 SIMULATION (06/03/87)

FIG 2 PRESSURISER PRESSURE

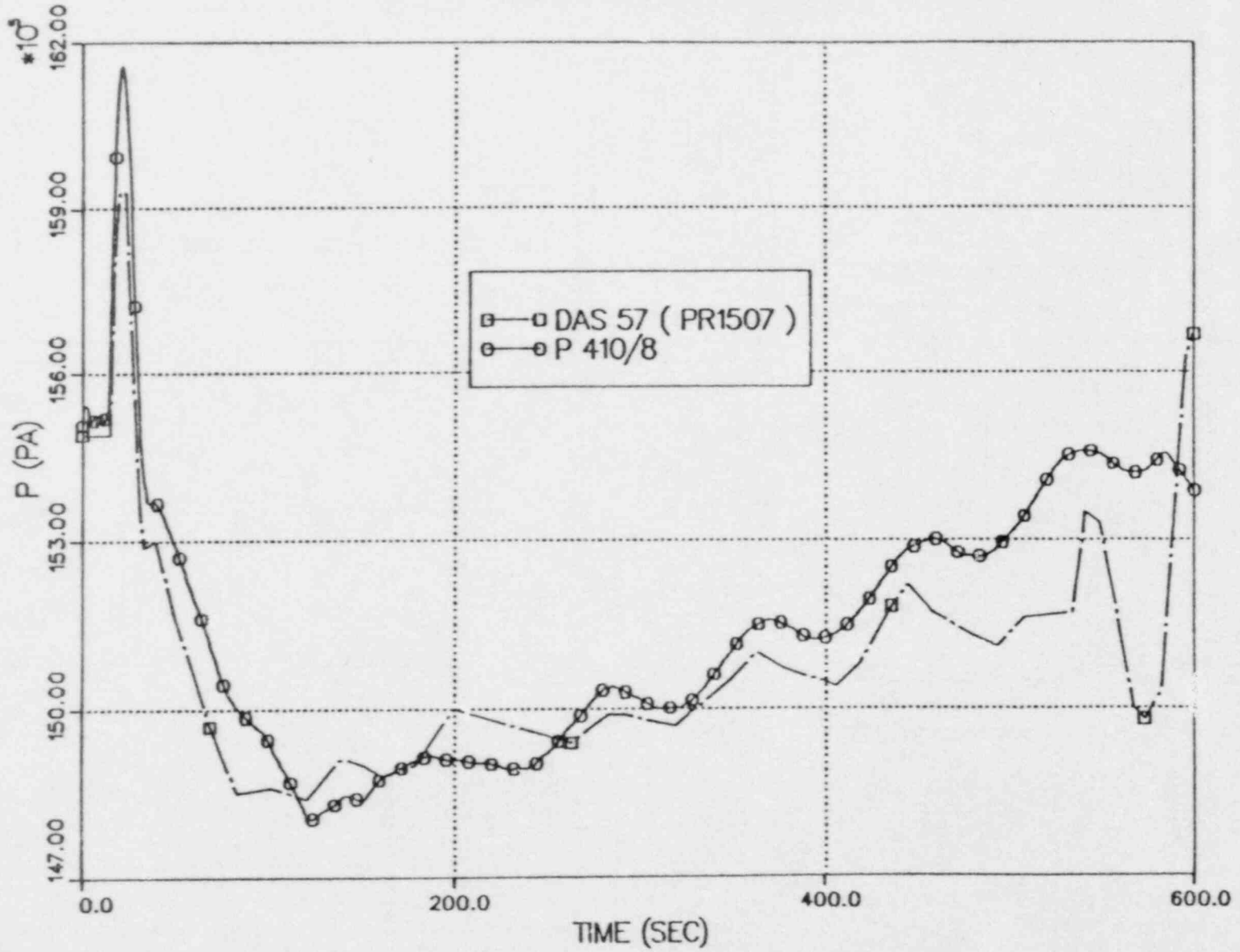

DOEL4 LOSS OF EXTERNAL LOAD TRANSIENT (23/11/85)

RELAP 5 SIMULATION (06/03/87)

FIG 3 COLD LEG TEMPERATURE

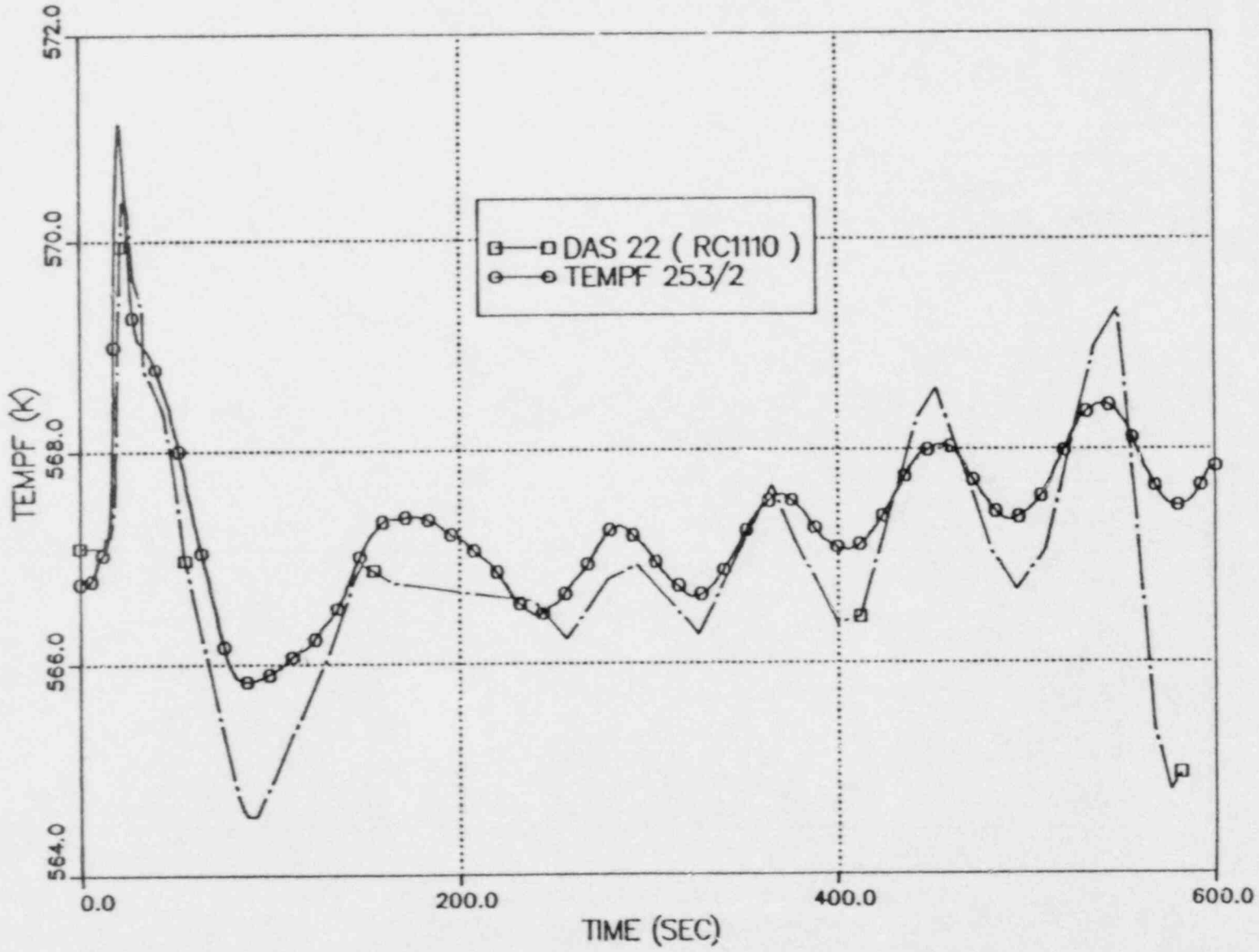

DOEL4 LOSS OF EXTERNAL LOAD TRANSIENT (23/11/85)

RELAP 5 SIMULATION (06/03/87)

FIG 4 STEAM COLLECTOR PRESSURE

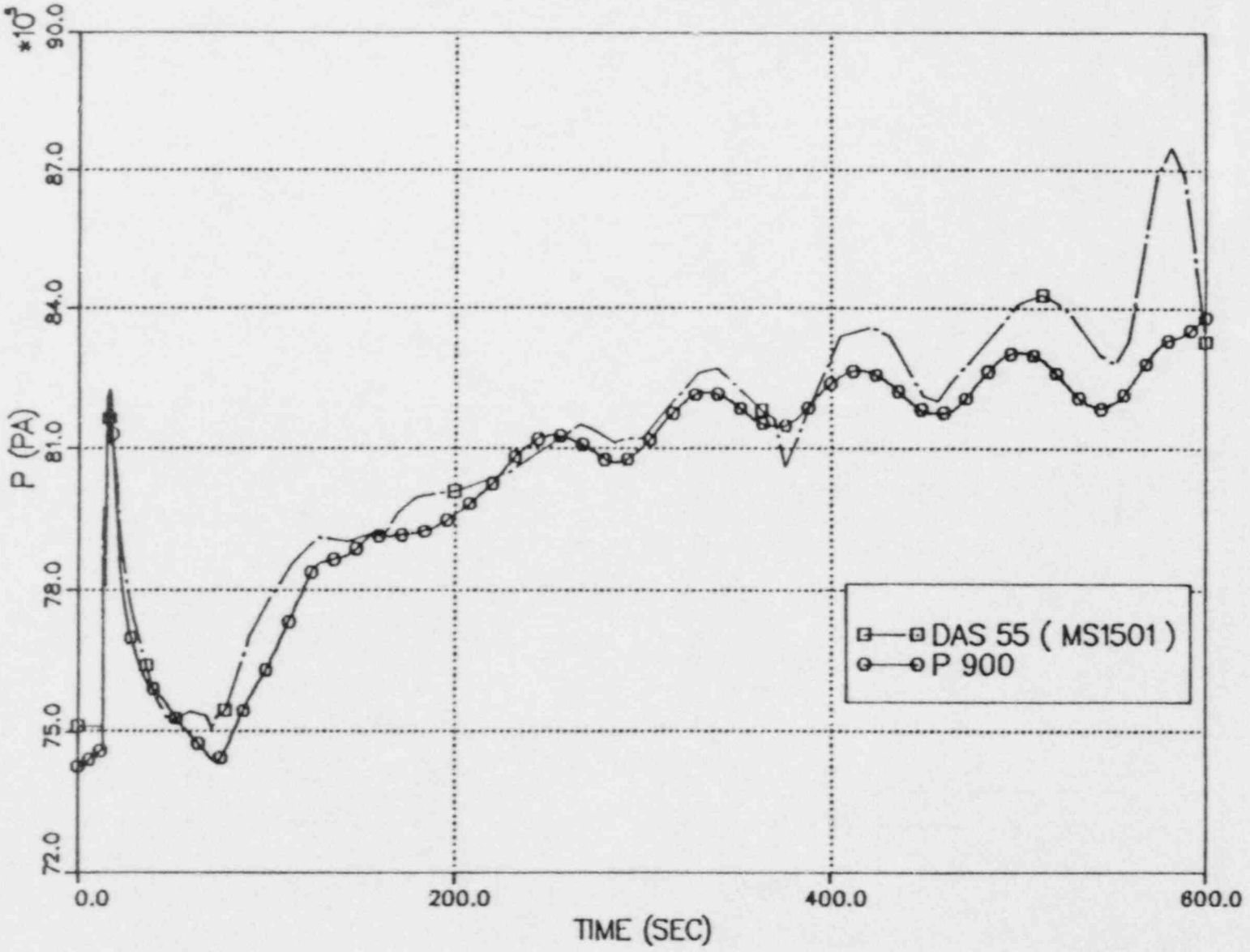

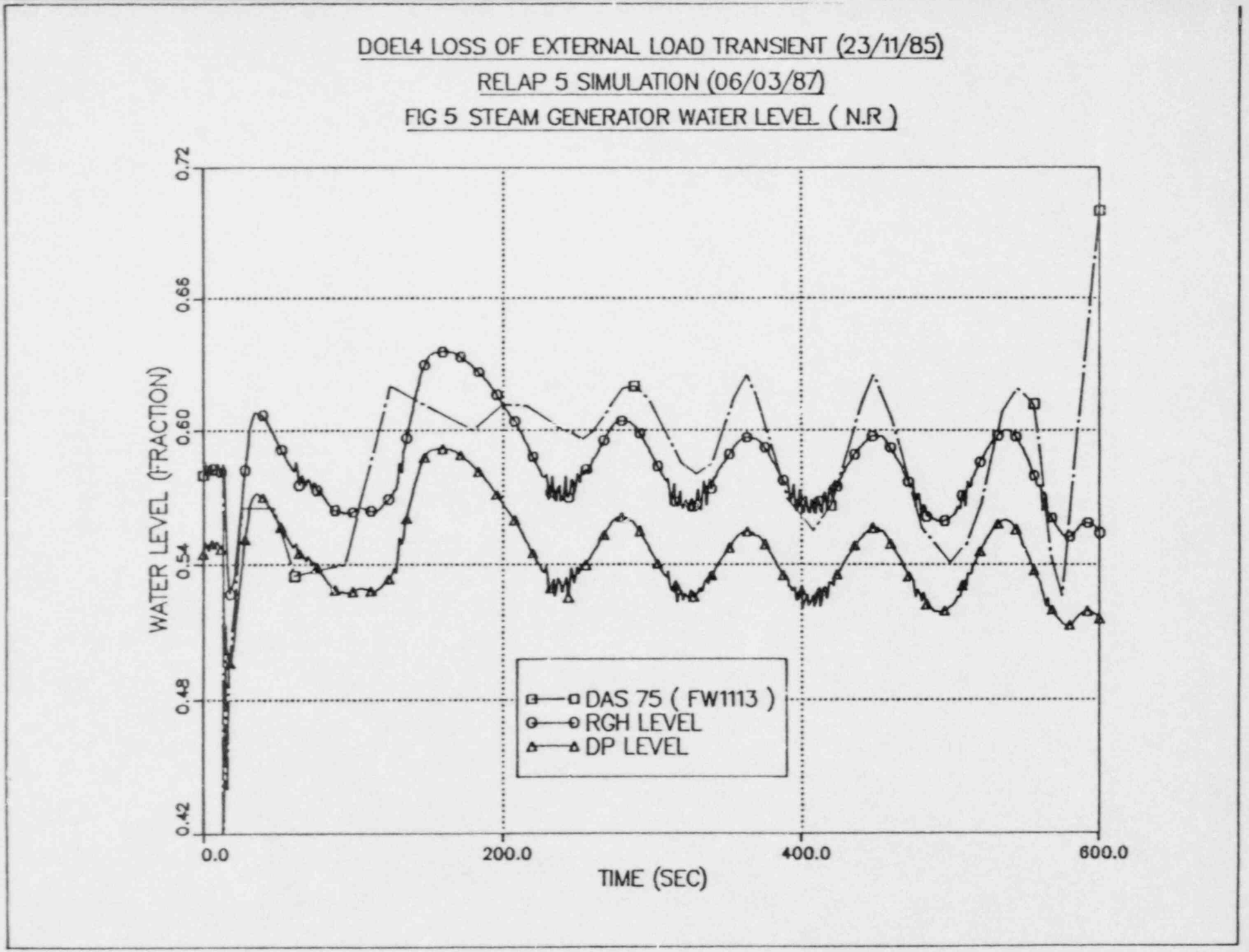
DOEL4 LOSS OF EXTERNAL LOAD TRANSIENT (23/11/85)
RELAP 5 SIMULATION (06/03/87)
FIG 5 STEAM GENERATOR WATER LEVEL (N.R)
WATER LEVEL (FRACTION)
0.72
0.66
0.60
0.54
0.48
0.42
0.0
200.0
400.0
600.0
TIME (SEC)
DAS 75 (FW1113)
RGH LEVEL
DP LEVEL

UK Experience with TRAC/PF1-MOD1 in Modelling Small Break LOCA Integral Tests

C G Richards
United Kingdom Atomic Energy Authority, Winfrith

Abstract

The TRAC-PF1/MOD1 code has been assessed in the UK against LOFT tests LP-SB-1, LP-SB-2 and LP-SB-3, and LOBI tests A2-81 (ISP18), BL-02 and BL-12. The paper summarises the main conclusions from the TRAC analysis of each test. The adequacy of TRAC for modelling these tests is then considered in terms of completeness (does TRAC contain models of the main processes?), accuracy, "quality" (eg speed, robustness), and useability.

One model omission, namely the representation of branching flow, and a number of areas requiring improvement or further assessment, are identified. This list of areas needing attention includes some aspects of TRAC which make life difficult for the code user even though it is possible to obtain reasonable results with the existing code version.

1 INTRODUCTION

As part of the UK assessment of the TRAC code for LOCA applications, TRAC-PF1/MOD1, Ref 1, has been used to simulate six small break LOCA tests in integral facilities. These are LOFT tests LP-SB-1, LP-SB-2 and LP-SB-3, and LOBI tests A2-81 (ISP18), BL-02, and BL-12. The three sets of LOBI predictions all include blind calculations, where the calculations were completed before any results from the tests were available. In the absence of a systematic approach to assessing prediction accuracy, it is arguable that blind calculations provide the best indicator of the effectiveness of codes and code users in predicting thermal-hydraulic transients. In simulating LOFT tests SB-1 and SB-2, and in post-test calculations of ISP18 attention has been focussed on identifying the areas of the TRAC code which need development to obtain significant improvement in these particular transients.

Although the tests listed above do not involve a great deal of overlap they represent only a small sample of possible transient scenarios: there are no calculations of PORV LOCA, SGTR, pump suction break, vessel break, RHRS failure, pump seal failure, intermediate breaks. Future integral test simulations should examine some of this wider spectrum of possibilities.

In assessing the code the following factors have been considered:

(a) Completeness - do the basic models allow representation of all the important phenomena?

(b) Accuracy - qualitative and quantitative.

(c) Quality - robustness, speed, clarity of coding and/or documentation etc.

(d) Useability - input/output, flexibility, documentation etc.

Modelling integral tests provides valuable information in all these areas, and provides one of the principal inputs into guiding future code development work. This paper summarises the results of the studies of the six integral tests and comments on the experience gained under the above four headings. Integral test analysis is part of a wider assessment of TRAC consisting of numerical tests, comparison of correlations with data, separate effects test modelling and plant calculations. This paper is limited as far as possible to conclusions derived from integral test analysis.

2 LOFT TESTS

A TRAC LOFT deck originally from LANL, used for large break LOCA studies, was modified to simulate the small break LOFT tests. Modifications included modelling the vessel with 1D components to take full advantage of the SETS numerical scheme. As far as possible the same deck was used for all three tests. TRAC Version 12.7 with minor error corrections was used for all three sets of calculations.

2.1 LP-SB-1

This test simulates a 1% hot leg break with pump trip at the time of scram, and 'minimum safeguards' HPIS. In the experiment a minimum primary circuit mass is reached at which the break flow is equal to the HPIS flow, after which as the primary pressure declines, the system begins to refill slowly. At this minimum mass the mixture level remains close to the level of the vessel nozzles, so that the core is well covered with two-phase coolant throughout the test.

Two principal post-test calculations, Ref 2, were carried out with TRAC. The first of these was essentially a standard TRAC calculation. The experiment shows a marked effect of the liquid level in the hot leg on the break discharge, which is not modelled in the standard version of TRAC. In order to investigate the effect of correcting this deficiency, a second calculation was carried out in which the offtake was modelled using a correlation of break line quality as a function of level in the hot leg based on Ref 3. Fig 1 shows the break line density. Agreement for the base case is poor. The application of the EPRI correlation for offtake quality, however, results in only a modest improvement. This is because the hot leg level predicted by TRAC during the 500-1000 second time period, after natural circulation and while the steam generator tubes are draining, falls below that at which vapour pull-through should first occur. This reduces the break flow and delays the full break uncovery. In the experiment the level does not fall below that at which pull-through is initiated until the steam generator tubes have drained. A number of variant calculations carried out suggest that the problem stems from TRAC's determination of the hot leg level, rather than with the break flow or offtake quality models, but the root cause has not been resolved. The hot leg level error needed to produce a significant effect is small, however, ($\lesssim$ 2 cms).

The compensating error of underprediction by the TRAC critical flow model of the subcooled break flow, even using a critical flow multiplier of 1.0 means that the main system parameters of primary pressure and primary mass, Fig 2, are quite well-predicted even for the base case. Thus even though the long

term hot leg density, Fig 3, is greatly improved by the offtake quality model the impact of this addition on the calculation of global parameters is relatively slight.

2.2 LP-SB-2

This test was run as a counterpart to LP-SB-1, to examine the effects of delaying the pump trip. In SB-2 the pumps tended to homogenise the primary coolant, resulting in an initially lower mass loss than in SB-1. While the pumps were still operating stratification occurred in the hot legs, resulting in uncovery of the break line offtake, and curtailing the mass loss from the primary system. Even after the pumps were tripped there was no uncovery of the core in the experiment.

Two principal post-test calculations (Ref 4) were carried out. The first of these was essentially a standard calculation of SB-2. Unlike SB-1, the break line density is continually over-predicted by TRAC, Fig 4. This is because the break line density is always less than the hot leg density in the test. Thus the break flow is overpredicted by TRAC and the system mass loss is significantly overpredicted, Fig 5, to the extent that when the pumps are tripped the mixture level in the vessel declines to the top of the core. (In the experiment a mixture level remains in the hot leg throughout the test). Nevertheless many system parameters were reasonably well-predicted. Fig 6 shows the primary pressure. The most interesting feature of SB-2 was the flow regime behaviour in the hot and the cold legs. The gamma densitometers indicate that significant phase separation began in the hot leg quite early in the experiment (ever before the pumps degrade at around 600 secs) and that fully stratified flow occurred at 1200 secs, ie while the pumps were still running. Thus the break line uncovered without the hot legs emptying. TRAC, although predicting the transition to stratified flow, did not simulate the consequent effect on break line density because of the lack of an offtake model. On the other hand the cold leg remained homogeneous until 1100 secs.

The second calculation of SB-2 was carried out with the break line quality input as function of hot leg liquid level. (The standard correlations used for SB-1 did not give sufficient agreement in SB-2 and an experiment-specific correlation was developed). This improved the break flow, hot leg density, primary pressure, Fig 6, and system mass, Fig 5, predictions significantly. Two problems remain, however. Firstly during the pumped circulation phase, conditions in the hot and cold legs are predicted to be very similar. Thus the cold leg is predicted to stratify at about 1100 secs, the same time as the hot leg stratifies, whereas experimentally the cold leg does not stratify until about 1400 secs. Fig 7 shows the calculated fluid distribution in the system at 1160 secs. Secondly the experimental velocity measurements in the hot leg indicate that liquid flow ceases after the hot legs have stratified, so that only steam would be circulating in the steam generator. This decoupling of the phases in the hot leg is not predicted by TRAC.

2.3 LP-SB-3

SB-3 was a 0.5% cold leg break without high pressure injection. In this test the pumps were run during the first 2000 secs of the transient, then tripped. A boildown phase ensued, leading to core heat-up which was terminated by depressurising the secondary side and bringing on the accumulator. Following the core heat up the break was closed.

A single standard TRAC calculation, Ref 5, has been carried out. Analysis to date indicates qualitatively good agreement with the data, though the time of core uncovery is rather late, and the rate of heat up too fast. Fig 8 shows the peak clad temperature excursion. The delay in heat up is mainly due to under-prediction by TRAC of the discharge rate, even using the multiplier of 1.0 (used for all the LOFT and LOBI tests). The over-prediction of the heat-up rate has been observed and investigated by other workers (Refs 6, 7), and is thought to be due to 3D effects - liquid returning to the vessel from the hot legs filters down the sides of the core and is boiled off below the mixture level interface, enhancing cooling of the whole core. In a 1D calculation this liquid would be dispersed into the top cell of the core where it would cool the top of the core preferentially, but would not slow the temperature rise of the centre of the core. Although the subsequent depressurisation phase can be reasonably well-predicted by adjusting the steam bypass valve flow area, some problems remain in simulating the accumulator flow.

3 LOBI TESTS

The TRAC model of LOBI was developed at AEEW from basic engineering information for participation in ISP18, and has subsequently been used with only minimal modifications for blind predictions of other LOBI tests. The model uses only the 1D components of TRAC.

3.1 A2-81 (ISP18)

Test A2-81 was a 1% cold leg break with minimum HPIS and a controlled secondary side cooldown of 100°C/hour. The test was used to mount a double-blind International Standard Problem. Ref 8, reports AEEW pre- and post-test TRAC calculations of the test. The transient was a relatively mild one, being characterised by a slow emptying of the primary system for about 2400 secs, followed by a gradual refill when the pressure had declined sufficiently for the ECCS to exceed the break flow. The bypass between upper plenum and downcomer was of sufficient size that the loop seals did not clear, and the mixture level in the vessel remained at the level of the nozzles, so there was no clad temperature excursion.

The TRAC pre-test predictions of this test were carried out using a modified version 12.0. There was significant over-prediction of mass loss from the primary circuit, Fig 9, leading to clearing of the broken loop seal. It should be noted that high accuracy was not expected, however, since a series of pre-test sensitivity studies had indicated (Ref 9) that the results were subject to significant uncertainties. Post-test calculations used version 12.2 of TRAC (with modifications). Parameter studies confirmed sensitivity to condensation on stratified flow, critical flow from stratified thermal non-equilibrium conditions, as well as bypass flow size. The test results could be fitted satisfactorily by varying these (Fig 9). The over-prediction by the standard code of condensation on stratified flow is thought to be the main reason why in the first 1000 secs the break flow is over-predicted. The problem with the later break flow is due to the under-prediction of break flow by the critical flow model itself when supplied with stratified upstream conditions of subcooled liquid and saturated steam. It was also clear that heat exchange with structures, and heat losses, play an important role, which creates particular difficulties in TRAC. The effect of adding an offtake model was found to be less significant than for the LOFT tests.

3.2 BL-02

This test was a 3% cold leg break with minimum ECCS. Because of the larger break size, some depression of the mixture level in the vessel occurs prior to loop seal clearance, as well as afterwards. Both loop seals clear. There is no core uncovery. The primary pressure falls to the accumulator set point at about 650 secs and the accumulator refills the primary circuit to the level of the break.

A pre-test calculation was done with TRAC version 12.5, Ref 10. Agreement with the test results is generally reasonable, being closer to the data than was achieved for ISP18, but the 'shape' of the vessel mixture level depression is wrong - TRAC predicts a level depression to the top of the core after loop seal clearance, and misses the level depression before loop seal clearance. Fig 10 shows the differential pressure between the top of the core and the hot leg nozzles. In addition it is predicted that only the broken loop seal clears. These last two discrepancies are related to the absence of hold up in the steam generators in the calculation. The code fails to calculate counter-current flow limitation in the broken and intact loop hot leg to steam generator tube flow path. The test also suggests that the code over-predicts the void fraction both in the vessel downcomer and in the core, confirming observations elsewhere, eg Ref 11, on the performance of the TRAC interphase friction model.

3.3 BL-12

The most recent test we have calculated with TRAC-PF1/MOD1, using version 13.0, is BL-12, a 1% cold leg break with no HPIS and no steam dump recovery. This potentially severe test gave rise to a prolonged boildown with core uncovery at 2000 secs. As the boildown progressed the core heated up so that after about 700 secs the maximum clad temperature had reached 650°C. Although the pressure had fallen to the accumulator set point (4.1 MPa) before this time, injected accumulator water was insufficient to turn around the clad temperatures, and so the heater power was tripped to avoid damage to the heater bundle.

The pre-test calculation gives a qualitatively reasonable prediction of the result. Over-prediction of the break flow leads to the core beginning to uncover about 250 secs early. As with LOFT SB-3 the heat-up rate is somewhat over-predicted, Fig 11, though the reasons may be different. The main discrepancy, however, is that the accumulator flow is much higher in the TRAC calculation than is measured, and it succeeds in turning round the clad temperature rapidly, just before the 650°C point is reached. Further analysis of this test is planned. Possible problem areas seem to be condensation/mixing of accumulator water and perhaps core interphase friction.

4 CODE ADEQUACY

In the previous sections the basic results of six integral test analyses have been summarised. It is notable that the pre- and post-test calculations provide different sorts of information about the adequacy of codes. The pre-test calculations give an indication of the sort of accuracy achievable in practice with one-off predictions of transients with a code and model which has not been tuned to a particular facility. The actual accuracy, of course, is dependent on the balance of dominant phenomena, and is rig and

transient dependent. The post-test calculations allow a detailed diagnosis of the causes of discrepancies, and provide pointers to code improvements which will reduce these discrepancies, or occasionally suggest that the data should be re-evaluated.

The remarks concerning code adequacy set out in the Sections below are based mainly on the experience gathered from the above tests, but have inevitably been reinforced or supplemented by information derived from other sources. The code assessment conclusions will be considered under the four headings set out in the introduction.

All the analyses reported indicate some deficiencies in modelling accuracy and/or lack of ability to model governing phenomena. None of the deficiencies was so serious as to invalidate the use of the code for studying the above transients. In many cases the deficiencies have only a minor effect on the overall interpretation of the calculation result.

(a) Completeness

In contrast to previous generations of codes, only one major omission in the basic constitutive models is apparent from the analyses carried out, namely a model to represent branching flow. Currently in TRAC the quality of flow entering the side pipe of a TEE is unaffected by the flow regime in the main pipe, or by the orientations of the offtake pipe and the main pipe. This is most clearly shown by the LOFT SB-1 and SB-2 simulations, where the break line was a 1½ inch pipe leaving the side of an 11 inch horizontal hot leg pipe. The effect is most acute when the main pipe flow is stratified. Internally, in the 1D components, TRAC lacks a means of differentiating the void fraction donored across a cell edge from the average cell void fraction. This distinction would probably be a pre-requisite for a physically-based offtake model. The introduction of junction void fraction as a separate entity from the cell void fraction would be beneficial for the development of other models which may be of more importance in transients other than those analysed so far. It is possible, for instance, that the failure to calculate the cessation of liquid flow in the primary loop in LOFT during test SB-2 is due to the way in which elbows are treated in TRAC. With stratified flow at the inlet to an upward elbow the liquid content of the outlet flow ought to be determined by an appropriate entrainment correlation, rather than the average cell void fraction. A stratification model appropriate to vertically oriented pipes, and plenums, could also be developed more easily if a distinction between cell edge and cell centre void fraction was made. Experimental data to assist in defining appropriate correlations to be used in an offtake model appropriate to large pipes and main pipe flows which are not fully stratified (ie relatively high mass flux) will be obtained using the pipeline facility at Harwell, UK.

Other code deficiencies could be classed as defects in existing constitutive models, although some developments to overcome these defects, such as improvement of flow regime determination, might arguably be categorised better as new models. These are discussed in the next Section.

(b) Accuracy

Improving integral test prediction accuracy is one possible element of increasing confidence in plant calculations. Qualitative predictions already appear reasonable for many variables much of time; quantitative accuracy requirements in integral tests are, however, difficult to define. Model deficiencies, even when known and understood, have two practical effects which need to be considered if they are to be tolerated. Firstly, they make the process of assessing the likely outcome of a transient more involved and more difficult. Secondly, they widen the uncertainty band associated with it. For the purpose of providing one-off calculations that preserve all the major features of small LOCA of the type considered above, TRAC cannot yet be judged adequate on the basis of its current performance. Whether it matters that qualitative errors occur is a question which can only be resolved by observing the effects of similar model uncertainties on plant calculations.

The models which have been found, or are strongly suspected, to be the cause of the main discrepancies, are the following:

(i) Interphase Friction

The LOBI rig is well-equipped with differental pressure tappings within the vessel. Using the option INVAN=1 for interphase friction in the core, the core void fraction is significantly over-predicted while in the bubbly/slug regime; using INVAN=0 results in under-prediction. Test BL-02 also suggests that interphase friction in the downcomer annulus is over-predicted, though there are other possible explanations for the predicted voidage. Over-prediction of core interphase friction may also have a role to play in the too rapid heat up of the SB-3 core and BL-12 core simulator.

In test BL-02, counter-current flow limiation is not predicted by TRAC in the hot leg to steam generator tube flow path, whereas it appears to occur in the experiment. Assessment of the suitability of the current interphase friction package for predicting possible liquid hold up in steam generator tubes in a small break LOCA should be carried out in a more proto-typical geometry. Other work on separate effects tests, Ref 12, has already indicated significant errors in CCFL prediction in less-complicated geometry.

(ii) Condensation

Condensation of steam flowing from the upper plenum to the top of the downcomer via bypass paths was a significant contributor to error in the pre-test calculations of ISP18. Fig 12 shows the sensitivity of ISP18 calculation to condensation heat transfer. While the magnitude of the effect of noding on the overall condensation rate has not been evaluated in depth, it seems likely that the interphase condensation rate predicted by the simple model in TRAC was somewhat too high. Indications from test BL-12 and possibly SB-3 are also that condensation on the

injected accumulator flow has a greater positive feedback on the flow-rate than is observed in the experiments, though further work is needed to confirm this. Whether it is possible to improve predictions by improving the correlation used for heat transfer coefficient and surface area, or whether current noding is simply too coarse, allowing too much mixing by numerical diffusion has not yet been investigated. This is almost certainly an area which deserves further attention.

(iii) Critical Flow

Several aspects of the critical flow model warrant comment on the basis of the above analyses. For all tests a multiplier of 1.0 was used for both subcooled and two-phase flow. In the very low quality two-phase region TRAC generally under-predicts the observed break flow rate. For LOBI the effective error appears to be less than 10%, but is up to 20% for the LOFT tests. Separate effects data suggest that the variation of the TRAC critical flow with quality at very low qualities is not large enough. This is known to be a difficult regime to model accurately.

A less justifiable problem with the TRAC critical flow model is highlighted by the ISP18 calculations. The current model does not operate in a physically reasonable way under conditions where the supplying volume is in thermal disequilibrium, as occurred in test A2-81. In fact the TRAC model can predict decreasing flow with increasing subcooling under these conditions. In the ISP18 study this led to under-prediction of the break flow in intermediate stages of the transient, producing too rapid a refilling of the system.

It should be noted that the TRAC critical flow model contains considerable noding dependency not described in the documentation.

Further assessment of the model against separate effects data is required, almost certainly accompanied by improvement of the existing model to observe the difficulties associated with non-equilibrium conditions.

(iv) Flow Regime Map

Current flow regime maps are based on local conditions, and derive mainly from data relating to small pipes. Within TRAC the flow regime map is used in determining interphase friction and interphase mass transfer. In the final TRAC simulation of test SB-2 the time when the hot leg fully stratifies is fairly well-predicted. In obtaining this agreement, however, the Taitel-Dukler expression for critical gas velocity for the transition to stratified flow was corrected to agree with the published Taitel-Dukler formula. Without this correction the time of stratification would have been predicted significantly later. TRAC recognises a transition region between homogeneous and stratified flow, preceding the time of complete stratification,

but it is clear from the LOFT data that a significant density gradient exists within the hot leg from an earlier time than suggested by the TRAC interpolation region. The effect of this intermediate flow regime on void fraction of branching flows needs to be taken into account as indicated in (a) above.

The second point emerging from SB-2 is that some account of inlet conditions will have to be taken in predicting flow regime in the relatively short pipe runs in plants. The hot and cold leg flow regimes are predicted to be the same by TRAC in SB-2 whereas in practice they were quite different.

Although the flow regime map in TRAC may be biased towards small pipe data, the implementation of the stratified flow transition appears to be about right for the SB-2 hot leg. A review of the flow map against large pipe data would be helpful, but should not be carried out in isolation from the effect of inlet conditions.

(v) Pumps

Several difficulties concerned with the pump model arose in the integral analyses. Two are discussed below under the heading code useability. The third concerns difficulties in modelling the pump's characteristics. While the LOFT facility is complicated by having two pumps in parallel, it is clear that even for LOFT, where separate effects tests of the pumps have been undertaken, there is considerable uncertainty regarding the correct two-phase characteristics to use. Because the current pump model is non-mechanistic it is utterly reliant on the supply of data from test conditions corresponding closely to those in the transient of interest. If critical plant transients involving pumps operating under two-phase conditions are to be calculated, then a more mechanistic (and therefore extrapolatable) model would be highly desirable.

(c) Quality

Table 1 gives the running speed obtained with TRAC in the integral test analyses. The running speed of TRAC can be quite variable during the calculation of a complete LOCA transient. In 1D, the normal steady state running speed is high; the code will manage quite happily with 0.5-1.0 sec time steps. Large parts of many transients will also run satisfactorily with a time step of 0.5 secs. The overall CPU time is determined mainly by the length of periods during which TRAC runs much more slowly, with timesteps around or below 0.1 secs. No single reason for slow running has been determined. Some observations are:

- Slow running is usually associated with oscillatory behaviour somewhere in the circuit.

- Oscillations can occur due to model discontinuities or to physically-based instabilities. Condensation and the presence of levels close to a junction are both conducive to this problem.

- Small cells can exacerbate convergence difficulties in spite of the fact that the numerical scheme can violate the Courant limit.

Outright code failures (usually appearing as the code trying to reduce the time step below a specified minimum) are now relatively rare. It will be seen from the table that if the causes of intermittent slow running could be eliminated from TRAC, a run time ratio of ~ 0.7 should be achievable for a 200 cell 1D problem (time step 0.5 secs)on a CRAY-XMP. In individual cases substantial improvements have arisen from relatively minor code changes, eg ISP18 (improved implementation of condensation model). In general, however, this is a neglected area of work - most examples of slow running have not been investigated. The likely benefits of a consistent attack on this problem are demonstrated by the development of the Ispra version of RELAP5/MOD1 - RELAP5/MOD1/EUR (Ref 13). Primary directions in work to improve TRAC would be to improve the smoothness of the constitutive packages (taking into account their implementation) and probably to try to increase the degree of implicitness in some of the interphase terms.

No problems with mass conservation have been observed in TRAC calculations.

The current running speed is sufficient to allow one-off calculations to be carried out satisfactorily; the cost of a calculation is only a small contribution to the overall cost of analysing a transient. The running speed is still slow enough to make extensive sensitivity studies difficult.

There are other reasons in addition to sheer speed, that make it desirable to have predictions which are 'smoother' than those produced by many of the current codes, including TRAC. Rapid fluctuations which occur in some calculated quantities such as flow rates and densities make it difficult to relate the course of a transient directly to individual constitutive models. If these fluctutions are non-physical they can dramatically distort the predicted system response because many phenomena are highly non-linear in nature. Furthermore the constitutive relationships are often based on steady state experiments, and may not be appropriate to rapidly fluctuating conditions.

It is difficult to comment objectively on the quality of the coding. As is noted in the next Section, considerable reference to the coding had to be made in the course of working with TRAC. In many ways the TRAC coding is well structured - its modular component and function orientated structure and clearly suggestive naming conventions for example. The code does suffer from some very long subroutines, the use of bit-packing (eg in the water packing logic) and from being written in FORTRAN IV rather than FORTRAN77. Comments are rather sparse and the legacy of having been written for a machine with a small fast memory is still apparent.

(d) Useability

Input/output arrangements in TRAC were found to be broadly satisfactory when supplemented by local graphics utilities and the LANL EXTRACT program to simplify restarts involving component change. The local graphics utilities consist of interactive programs, Refs 14, 15, 16, to produce line graphs and system mimics from TRAC ouput, and a graphical input checker which displays the geometry of the input data.

Modelling Flexibility

A number of limitations in the modelling capability of current versions of TRAC give rise to the need for difficult and perhaps unacceptable compromises in modelling integral systems. These are:

(i) Heat Structure Modelling

The modelling of heat exchange between the fluid and structures is particularly important in small integral test rigs, where the surface area to volume ratio of the coolant is relatively large. The current version of TRAC has only a primitive heat structure modelling capability. The UK has recently implemented the LANL PF1/MOD2 heat structure coding for 1D components, and this provides a much more satisfactory level of detail.

(ii) PLENUM Component

The PLENUM component is a useful addition to TRAC, allowing multiple connections in areas such as the downcomer annulus or the upper plenum. It is not entirely satisfactory in its present form because the geometry is incompletely specified in the input data. Quantities such as plenum height, and area of cross-section in horizontal and vertical direction, are used within the code, but are derived in a rather arbitrary way from the input plenum volume and junction lengths. In addition the PLENUM cannot contain heat structures.

(iii) PUMP Component

There are two minor defects in the PUMP component. Firstly the PUMP is a PIPE-type component and does not allow pump seal injection within the component. Secondly a no slip condition is forced at the rotor, even when the rotor is stationary. Thus counter-current flow through the pump is impossible. These difficulties may be alleviated by replacing the PUMP by a TEE part way through a transient, but that is not regarded as a satisfactory permanent solution.

Documentation

The current documentation consists of the User Manual and User Guidelines. While extensive, this documentation does not contain sufficient information on the way in which constitutive models are implemented in the code to allow the user to predict the effects of noding changes on other interactions between the models and the numerics. In order to answer questions such as: what is the effect on the flow stratification criterion of lumping together three pipes, in parallel, or what velocity will be used to determine interphase condensation heat transfer within a cell, it is necessary to inspect the relevant FORTRAN coding.

Sensitivity Studies

Because the uncertainties in some constitutive models across the range of applications for TRAC are large, sensitivity studies are likely to be

required to establish confidence in the deductions from calculations. These sensitivity studies cannot at present be carried out through input data. This increases the difficulty of carrying out sensitivity analysis, and makes it more error prone. Ideally parameters within models which are uncertain, or a compromise, are best identified by the code developers at the development stage of a model. By bringing such parameters out as data, while providing best general default values, frozen code calculations and sensitivity studies may be carried out with equal integrity.

5 SUMMARY

Pre-test and post-test calculations using TRAC-PF1/MOD1 of six integral small break tests have been described. This experience has provided information as part of a wider assessment of TRAC consisting of correlation assessment, separate effects test modelling and studies relevant to large break LOCA. The main points arising from the integral studies are set out below.

(a) Completeness

In contrast to previous generations of codes only one major omission in the basic constitutive models is apparent from the analyses carried out, namely a model to represent branching flow. Currently in TRAC the quality of flow entering the side pipe of a TEE is unaffected by the flow regime in the main pipe or by the orientations of the offtake pipe and the main pipe.

(b) Accuracy

Although deficiencies are noted in all the calculated transients, these are not in general sufficiently large to give rise to misleading conclusions. It is clear, however, that a number of models could benefit from further development if all the experimental trends are to be qualitatively captured. Quantitative predictions are already reasonable for many variables much of the time; quantitative accuracy requirements in integral tests are, however, difficult to define. Models requiring improvement include interphase condensation heat transfer, interphase friction and critical flow.

(c) Quality

Running speed is sufficient to allow one-off calculations to be carried out satisfactorily (ie the cost of a calculation is only a small contribution to the overall cost of analysing a transient). The running speed is still slow enough to make extensive sensitivity studies difficult. Furthermore, the running speed is very variable through the course of some transients. The most recent versions of the code seem to show improved reliability over earlier versions and complete failures are now rare. However, rapid fluctuations still occur in some calculated quantities such as flow rates and densities, and these can make it difficult to relate the course of a transient directly to individual constitutive models.

(d) Useability

Input/output arrangements in the code were found to be broadly satisfactory when supplemented by local graphics utilities, and the LANL EXTRACT program to simplify restarts. A number of limitations in the modelling capability of current versions of TRAC give rise to the need for difficult and perhaps unacceptable compromises in modelling integral systems. The main ones are the primitive heat structure modelling capabilities and the incomplete specification of the PLENUM component geometry.

Because the uncertainties in some constitutive models across the range of applications for TRAC are large, sensitivity studies are likely to be required to establish confidence in the deductions from calculations. These sensitivity studies cannot at present be carried out through input data. This increases the difficulty of carrying out sensitivity analysis and makes it more error-prone.

Current documentation, while extensive, does not contain sufficient information of the way in which the constitutive models are implemented in the code to allow the user to predict the effects of noding changes or other interactions between the models and the numerics.

6 CONCLUSIONS

Recent versions of TRAC show reasonable predictive capability for major trends. Greater accuracy would be desirable if confidence is to be placed in the details rather than the gross features of predictions.

The limitations of the current documentation, which force the user to make reference to the coding, and sensitivity of results to modelling techniques mean that there is a long learning curve in applying TRAC to complex problems with confidence. This is not a criticism unique to TRAC.

One model ommission and a number of areas requiring improvement or at least further assessment have been identified, as follows:

Branching flow models
Flow regime maps
Interphase friction
Critical flow
Condensation
Pumps
Plenum
Heat structures
Numerics-speed/smoothness
Documentation
Dials

Despite these criticisms the TRAC code is already a powerful tool for analysing a wide class of water reactor transients. It is becoming steadily more refined, and we would hope that it will continue to develop towards a more mature product, ie a code capable of giving acceptably accurate predictions for a wide class of transients without the user needing a deep

understanding of the inner workings of the code. Some sensitivity studies, however, are likely to be necessary for some time to come if there is a need to quantify margins of uncertainty.

ACKNOWLEDGEMENT

The work described in this paper includes substantial contributions from Miss E Allen and Mr A P Neill of AEE Winfrith who carried out the TRAC analyis of LOFT tests LP-SB-1 and LP-SB-3, and from Mr F Pelayo of Consejo de Seguridad Nuclear, Madrid who carried out the analysis of LOFT test LP-SB-2.

REFERENCES

1 Liles, D et al. TRAC-PF1/MOD1. An Advanced Best Estimate Computer Program for Pressurised Water Reactor Thermal-Hydraulic Analysis. NUREG-CR/3858, July 1986.

2 Allen, E J. TRAC-PF1/MOD1. Post-Test Calculations of the OECD LOFT Experiment LP-SB-1. AEEW - R 2254. To be published.

3 Anderson, J L and Benedetti, R L. Critical Flow Through Small Pipe Breaks. EPRI NP-4532, Project 2299-2, Final Report, May 1986.

4 Pelayo, F. TRAC-PF1/MOD1 Post-Test Calculations of the OECD LOFT Experiment LP-SB-2. AEEW - R 2202. To be published.

5 Neill, A P and Allen, E J. TRAC-PF1/MOD1 Post-Test Calculations of OECD Loft Experiment LP-SB-3. AEEW - R 2275. To be published.

6 Harwood, C and Brown, G D. RELAP5/MOD2 Calculations of OECD LOFT Test LP-SB-3. CEGB Report GD/PE-N/535, 1986.

7 Alemberti, A. Experiment Analysis and Summary Repot on OECD LOFT Nuclear Experiment LP-SB-3 (Draft).

8 Richards, C G. Blind and Post-Test Calculations of ISP18 with TRAC-PF1/MOD1. AEEW - R 2013.

9 Richards, C G. TRAC-PF1/MOD1 Simulation of a Small Break LOCA in LOBI. Specialist Meeting on Small Break LOCA Analysis in LWR's, Pisa, Italy, 23-27 June 1985.

10 Richards, C G. Pre-Test Calculations of LOBI Test BL-02 Using TRAC-PF1/MOD1. AEEW - M 2416. To be published.

11 Dawson, J T. TRAC-PF1/MOD1 Calculations of a Simulated Core Boildown Experiment. Specialist Meeting on Small Break LOCA Analysis in LWR's, Pisa, Italy, 23-27 June 1985.

12 Richards, C G. TRAC-PF1/MOD1 Simulation of CISE Pressuriser Flooding Experiments. AEEW - M 2470. To be published.

13 Kolar, W, Staedtke, H, Worth, B. JRC Ispra Experience with the IBM Version of RELAP5/MOD2. Proceedings of the NRC Fourteenth Water Reactor Safety Information Meeting, Washington, October 1986.

14 O'Mahoney, R. PLUS86. A Plotting Utility System for Thermal-Hydraulics Interface Files Using Ghost 80. AEEW - M 2009. To be published.

15 Makings, S, Richards, C G, Martin, A P. User's Guide to SMART - System Mimic for Analysis of Reactor Transients. AEEW - M 2114, September 1985.

16 Masterman, R, Wilmot, G. TRIPPSM - TRAC Input Plotting Package Including a Smart Picture Editor. Part I: Users Guide. AEEW - M 2459. To be published.

TABLE I

TRAC Run-Time Statistics in Small Breaks (1D)

Transient	CPU/Real Time	Cells	Average Time Step
LP-SB-1	2.8#	142	0.08 secs
LP-SB-2	2.3 (XMP)	142	0.10
LP-SB-3	1.2 (XMP)	171	0.22
LOBI ISP18	2.9* (1S)	192	0.16
LOBI BL-02	3.0 (1S)	196	0.16
LOBI BL-12	1.6 XMP)	203	0.20

substantial improvement can be obtained by renoding the bypass
* final post-test calculation

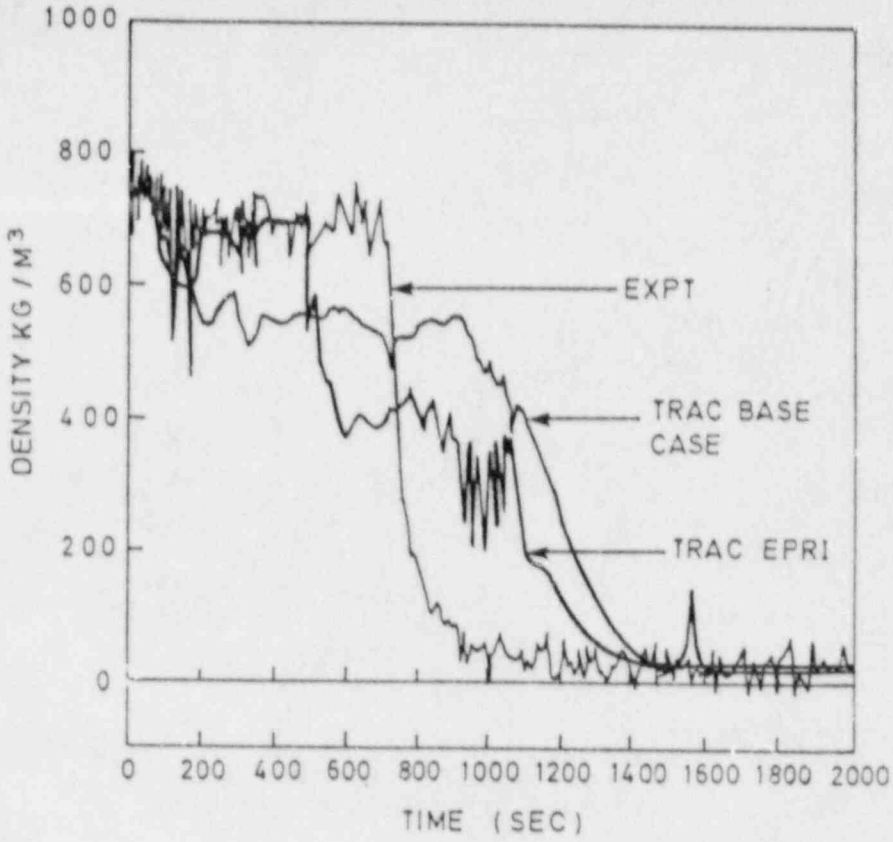

Figure 1. Break line density LP-SB-1

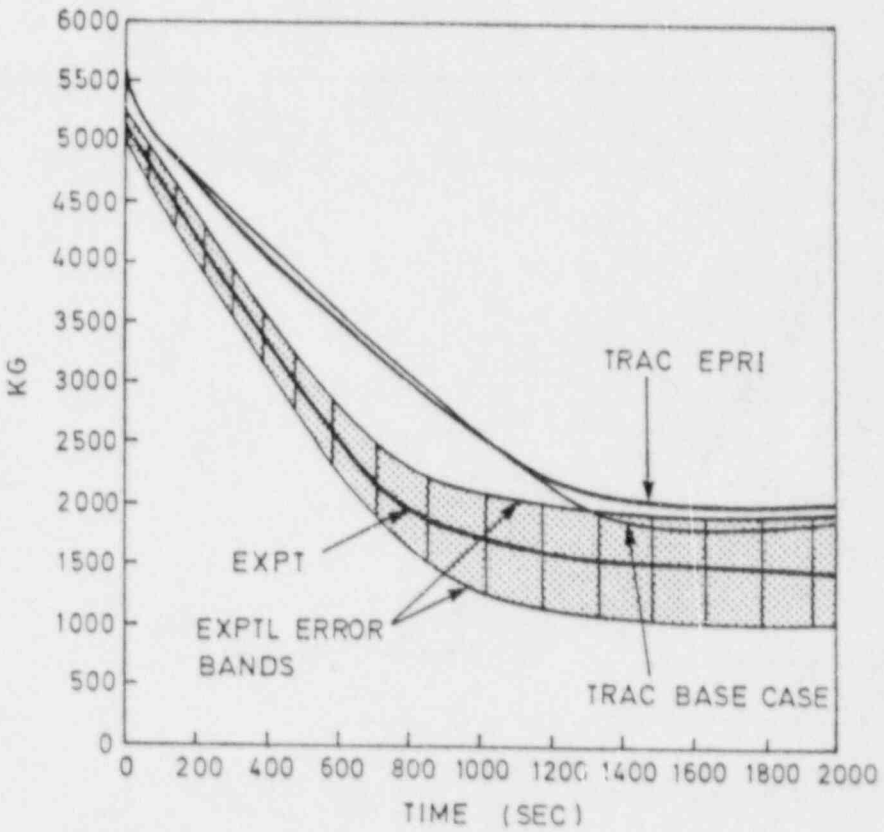

Figure 2. Primary system mass inventory LP-SB-1

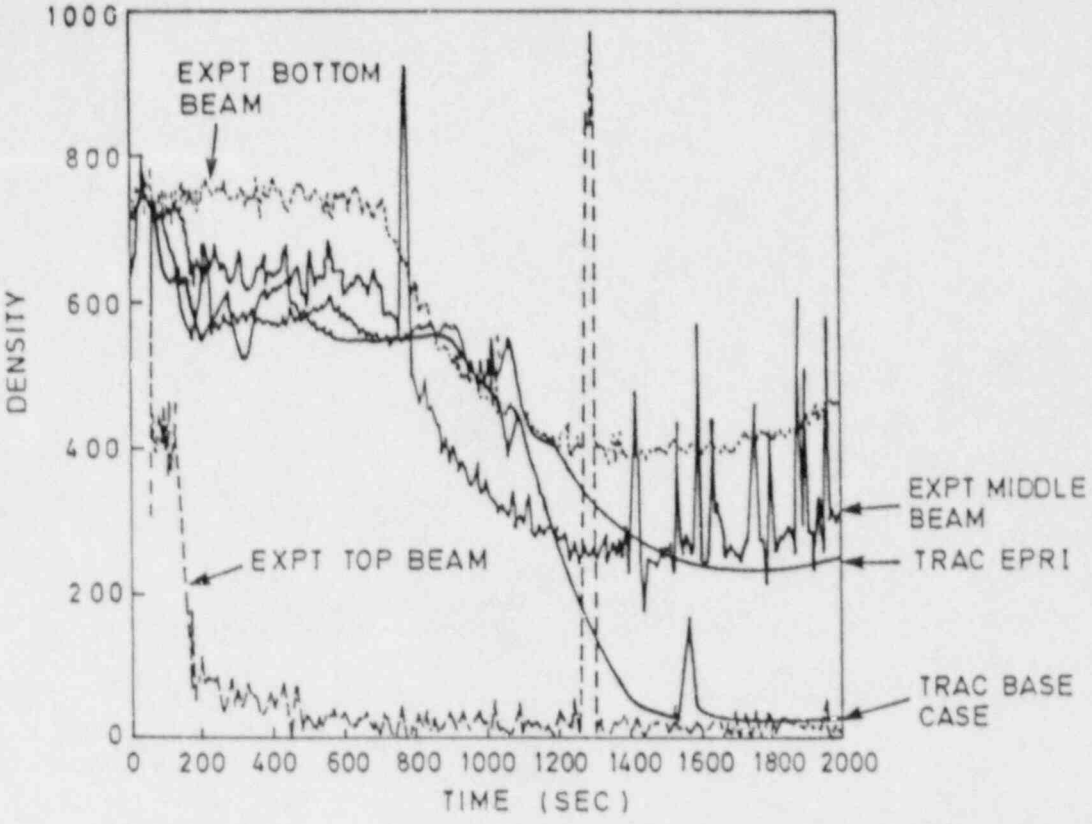

Figure 3. Hot leg density LP-SB-1

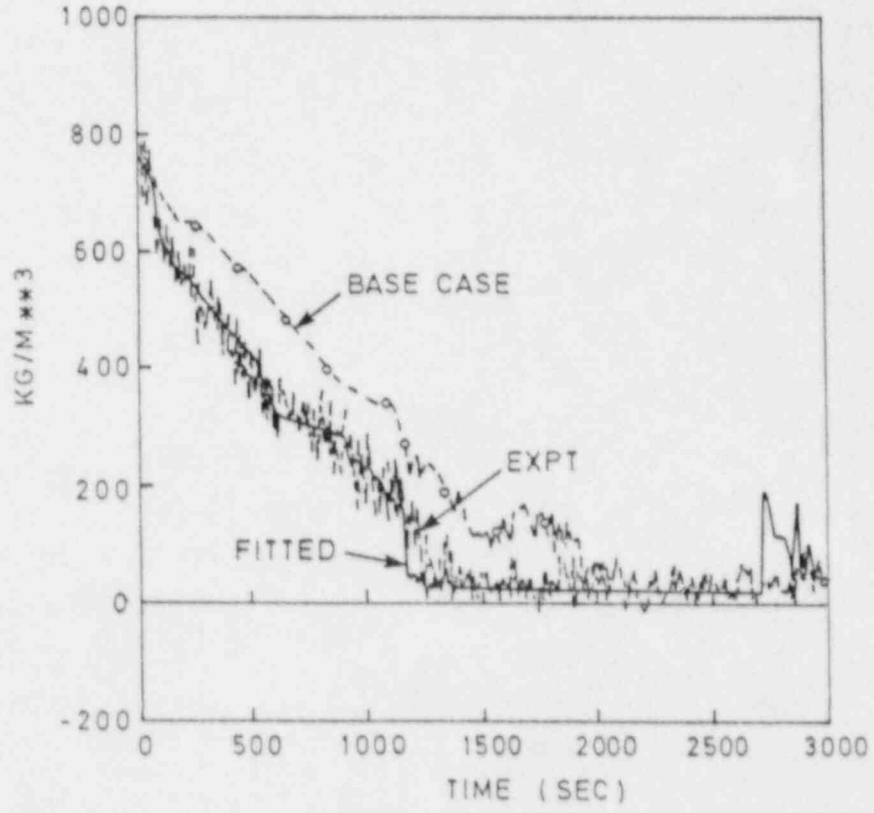

Figure 4. Density in the break line LP-SB-2

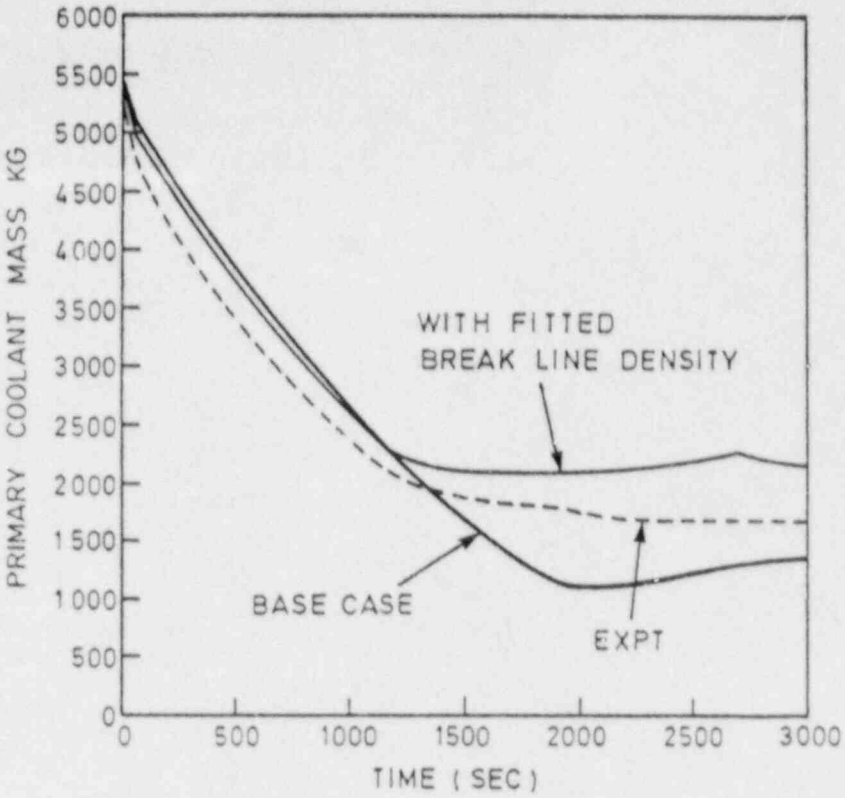

Figure 5. Transient mass inventory LP-SB-2

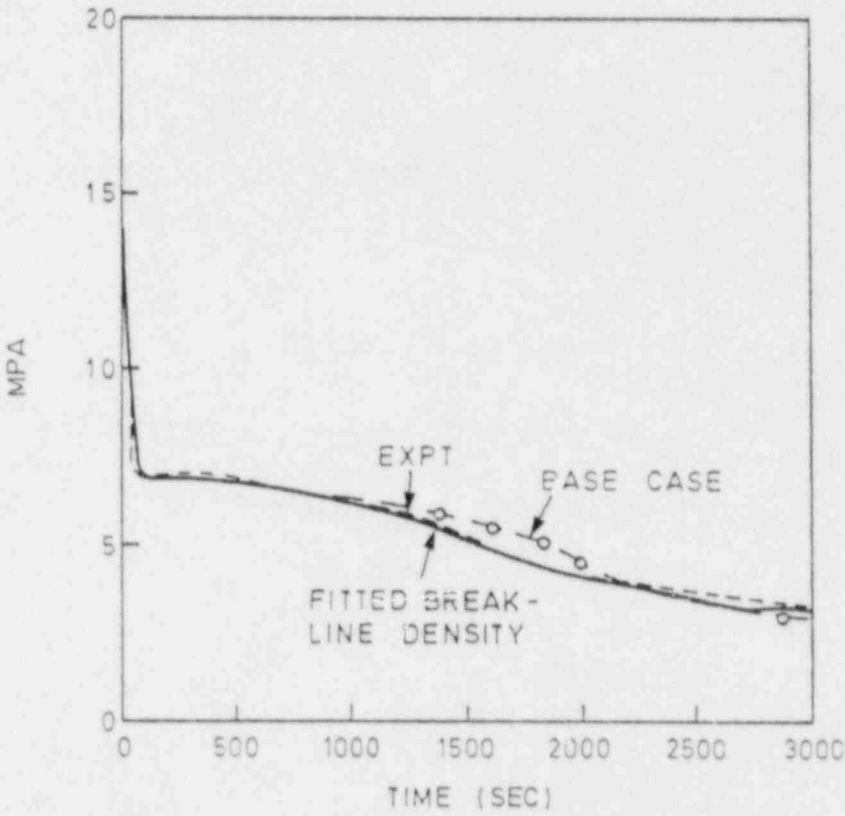

Figure 6. Intact loop hot leg pressure LP-SB-2

S.M.A.R.T. SYSTEM MIMIC FOR ANALYSIS OF REACTOR TRANSIENTS

TITLE OF FRAME:- LOFT SB-2 (RUN 8) CORRELATED BREAK LINE QUALITY

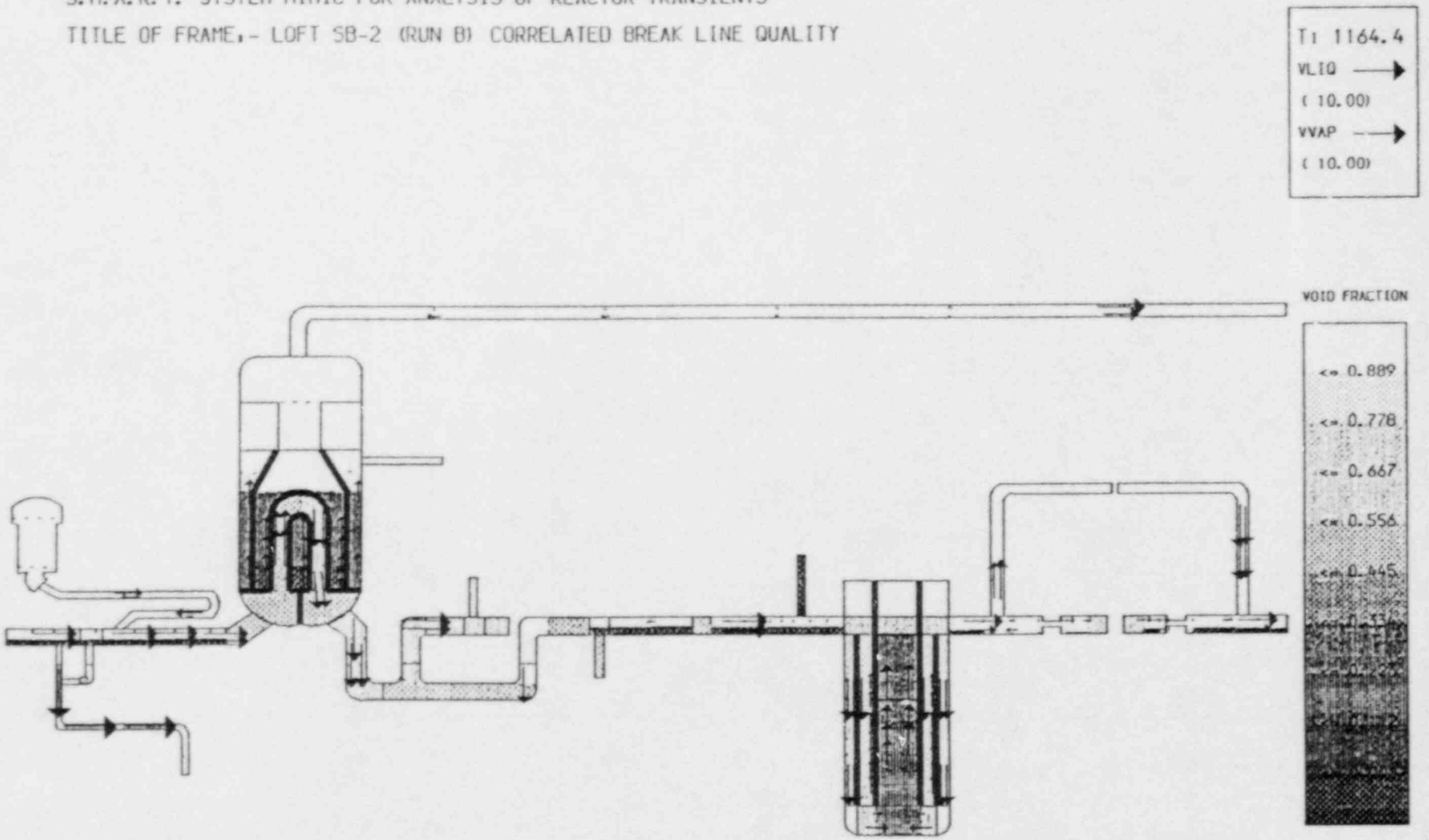

FIGURE 7

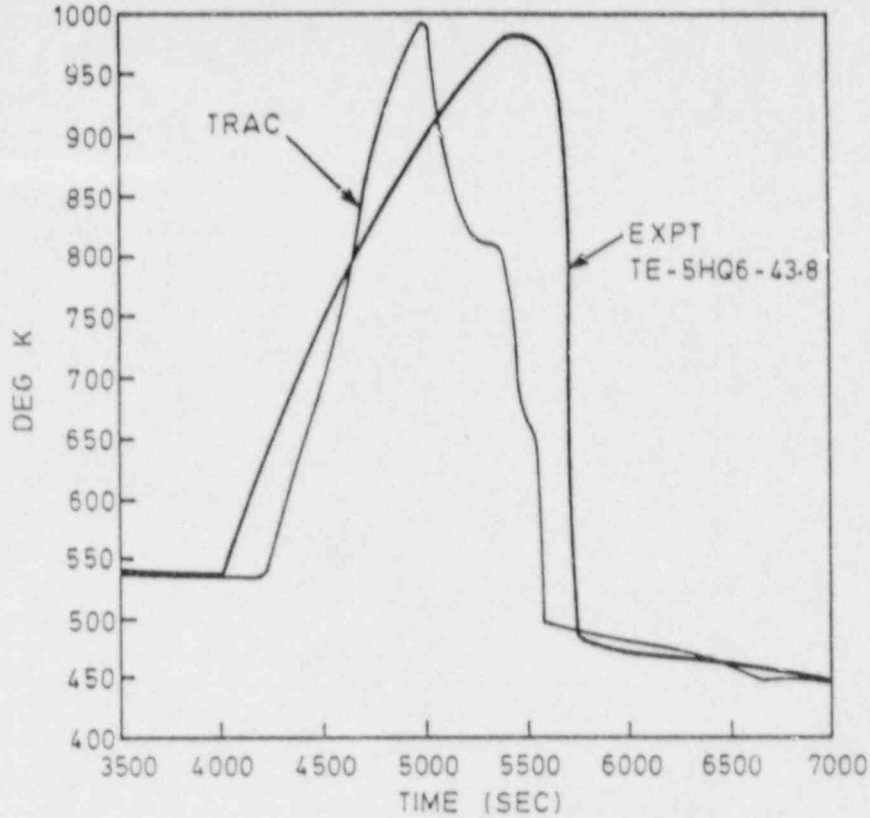

Figure 8. Max cladding temperature LP-SB-3

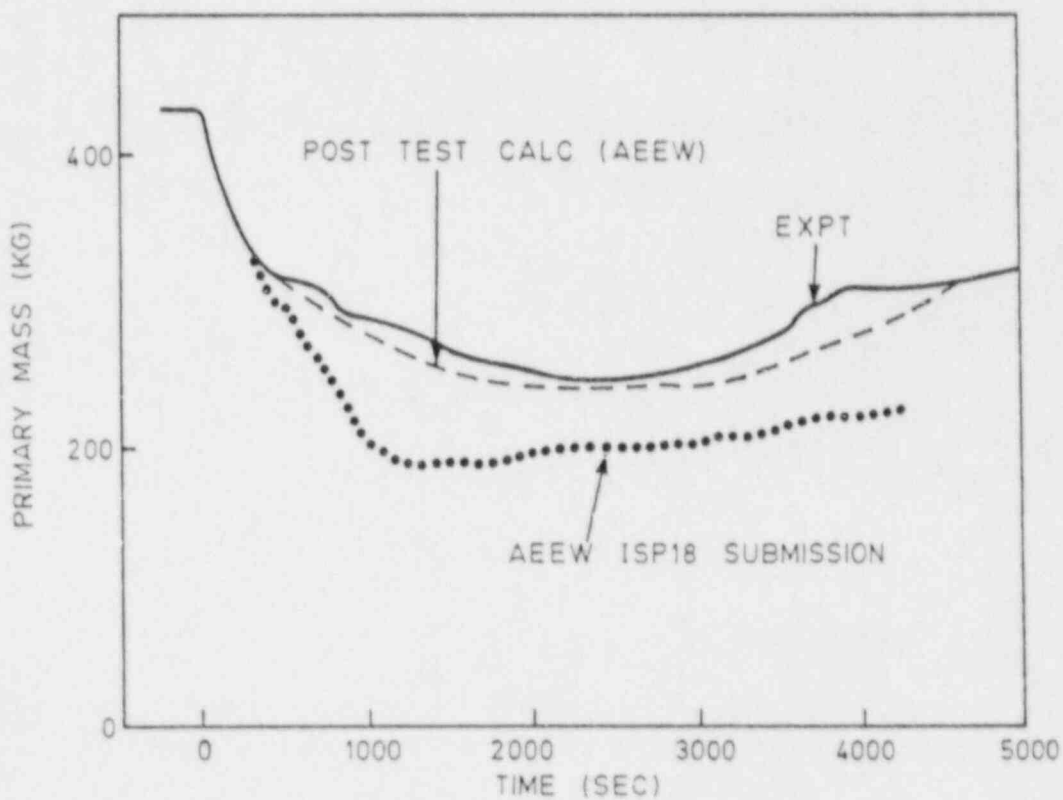

Figure 9. LOBI A2-81 (ISP18) primary mass

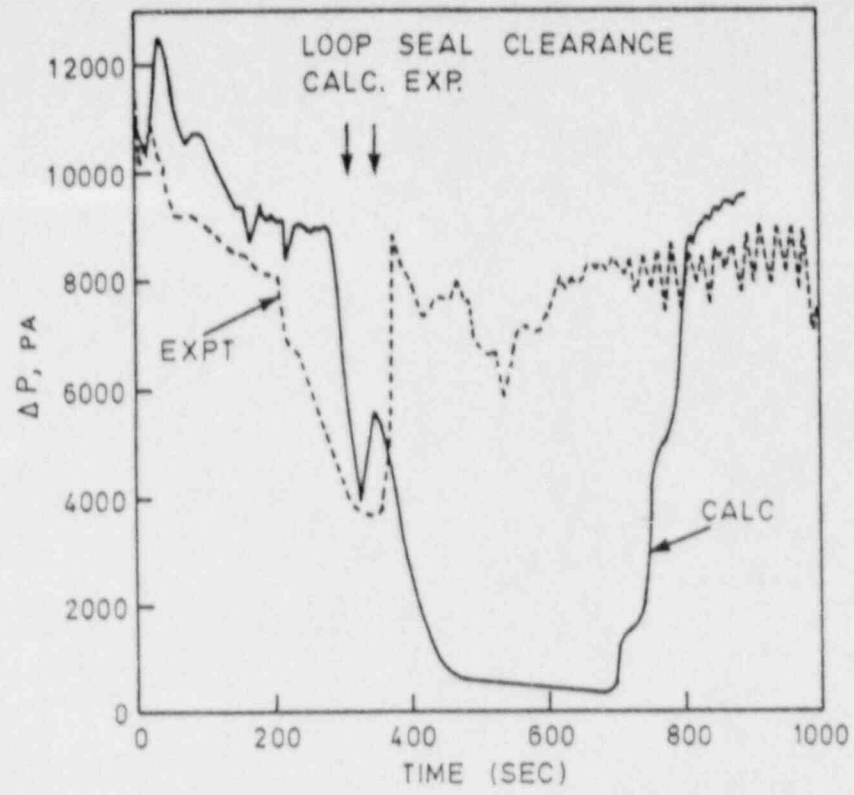

Figure 10. Pressure difference : Top of heated length to nozzle BL-02

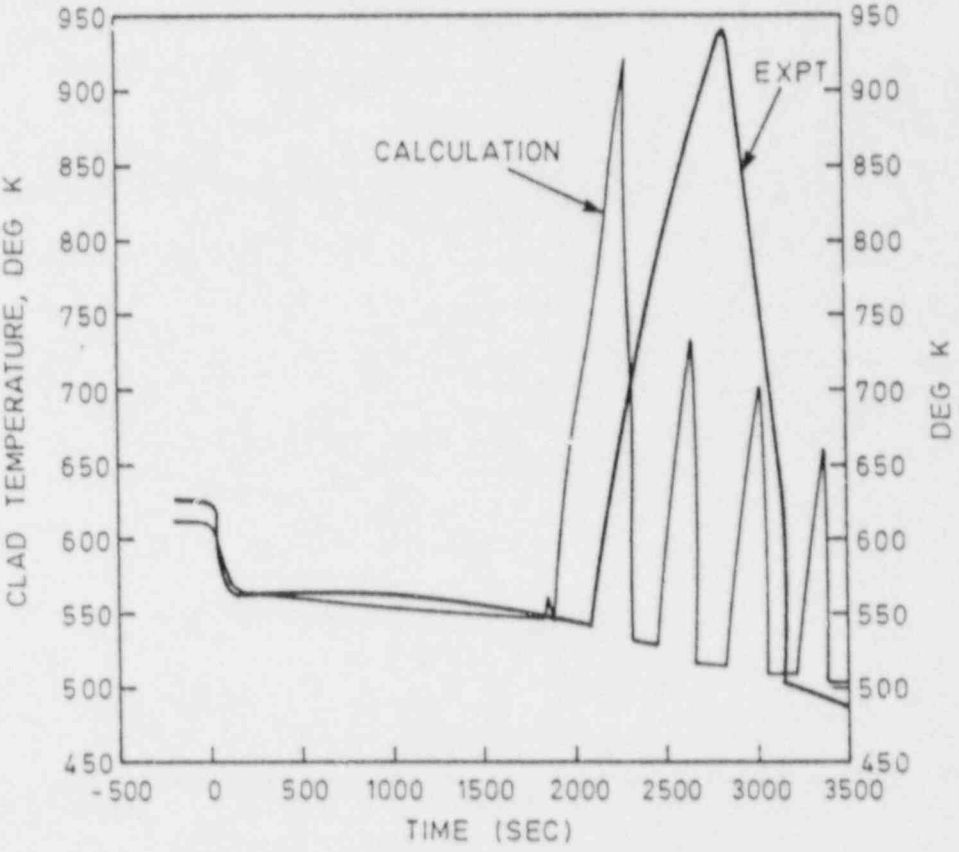

Figure 11. LOBI test BL-12 pre-test calculation

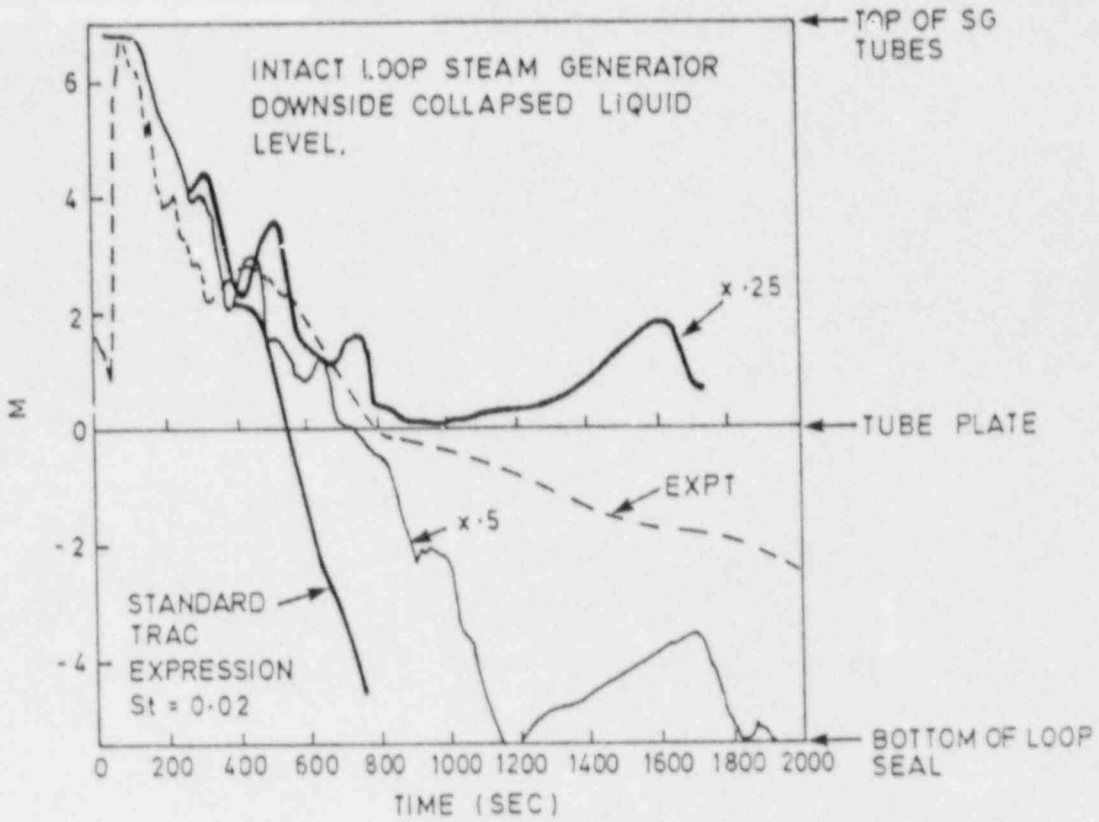

Figure.12. Effect of reducing interphase condensation rate by 0·5 and 0·25

EXPERIENCE WITH USE OF RELAP-5/MOD 2 AND TRAC-PF1/MOD 1 IN THE FEDERAL REPUBLIC OF GERMANY

BY

F. J. WINKLER

SIEMENS (KWU)

ERLANGEN, FRG

K. WOLFERT

GESELLSCHAFT FÜR REAKTORSICHERHEIT

GARCHING, FRG

Abstract

FRG's participation in ICAP with SIEMENS (KWU) and GRS as executing agents of the BMFT is primarily to establish internationally assessed and approved computer codes for accident analysis of LWR's. In SIEMENS (KWU) RELAP 5/MOD 2 is used as the main thermohydraulic code for LOCA-analysis over the entire transient range. Therefore more emphasis is placed on the updated FRG-ICAP matrix on assessing RELAP 5/MOD 2 for large break LOCA-analysis. In KWU and GRS TRAC-PF1 is used mainly for multidimensional PWR-benchmark studies and research in particular for UPTF pre- and post test analysis. The updated FRG-ICAP matrix includes 42 specified assessment studies with 8 yet to be defined. In the paper the types of analysis performed in the FRG at KWU and GRS using RELAP-5/MOD 2 and TRAC-PF1 are explained. Examples of results from RELAP-5 and TRAC-PF1 calculation are also presented and significant findings discussed.

I. Introduction

Federal Republic of Germany's participation in ICAP - with SIEMENS (KWU) and GRS as executing agents of the BMFT - is primarily to establish internationally assessed and approved computer codes for accident analysis of LWR's.

For this reason the advanced thermohydraulic computer codes

RELAP-5/MOD 2
TRAC-PF1
TRAC-BF

have been selected for the performance of

- licensing analysis
- best estimate studies of postulated accident conditions
- benchmark calculations
- thermohydraulic research.

RELAP-5/MOD2 is used at SIEMENS (KWU) as the main thermohydraulic licensing code for

- PWR-LOCA analysis of large breaks and small leaks over the entire transient range from

  blowdown through
  refill to
  reflood and for

- PWR-special transient NON-LOCA accident analysis.

In addition to RELAP-5 GRS developed the ATHLET-CODE which is used at GRS for LOCA, accident and transient analysis of PWR's and BWR's.

TRAC-PF1/MOD 1 is applied at both SIEMENS (KWU) and GRS mainly for

- PWR-LOCA analysis where multidimensional effects are important
- PWR-LOCA benchmark calculations
- Best estimate calculations to establish initial and boundary conditions for 2D/3D experiments
- Pre- and post Test analysis of UPTF experiments.

Furthermore TRAC-PF1 is applied at SIEMENS (KWU) for

- Best estimate PWR-LOCA studies
- Thermohydraulic research
- Calculation of single and two phase wave propagation in piping systems.

TRAC-BF is planned to be used at SIEMENS (KWU) for BWR-LOCA benchmark analysis.

For this reason the **FRG contribution to ICAP** includes the participation in the assessment of

RELAP-5/MOD 2
TRAC-PF1
TRAC-BF

for LOCA and NON-LOCA transient analysis.

Based on the application of RELAP-5/MOD 2 as main thermohydraulic licensing code for LOCA-analysis the objectives of the FRG contribution to ICAP have been modified to place more emphasis on assessing RELAP-5/MOD 2 for large break LOCA-analysis over the entire transient range. In particular experimental results from the test facilities PKL, UPTF, CCTF and SCTF will be employed for the large break RELAP-5 assessment.

Experimental results from PKL, SCTF, Karlstein component test facility with emphasis on UPTF will be used for TRAC-PF1 assessment.

Both codes and TRAC-BF will utilize PWR and BWR plant data for transient analysis assessment.

In addition to the ICAP contribution comparable assessment studies with the GRS code ATHLET are planned in the FRG.

II. Updated FRG-ICAP Matrix

The updated FRG-ICAP assessment matrix is shown in Fig.1. The matrix includes 42 specified assessment studies with 8 yet to be defined. 13 assessment studies are performed or in preparation. In the updated matrix the UPTF test facility has been given particular emphasis due to its unique full scale feature and realistic simulation of hydrodynamic multidimensional effects.

The multidimensional effects and full size feature of UPTF is useful for assessing the effects of scale and geometry of both RELAP-5 and the multidimensional TRAC-PF1.

With regard to the emphasis given to RELAP-5 as a main licensing tool 5 UPTF RELAP-5/MOD 2 assessment studies have been included.

III. Experience with RELAP-5/MOD 2

In the frame of the extended application of RELAP-5/MOD 2 at SIEMENS (KWU) the following types of analysis were performed covering the field from PWR-licensing calculations to ICAP-studies:

- PWR large break and small leak LOCA-analysis

- Studies related to the noding of the core for realistic simulation of GPWR-type flooding behaviour

- Post test calculation of 1300 MW GPWR-commissioning test

- Post Test calculations of PKL-I and PKL-II small leak and large break experiments

- Post Test calculation of experiments related to pressure wave propagation in piping systems

In particular the following examples of results of RELAP-5/MOD 2 calculations will be presented and the significant findings discussed.

- 1300 MW GPWR NODALIZATION STUDY with particular interest to the noding of the core.

- Post test calculation of the PKL-II B 5 experiment simulating a 2A cold leg break with cold leg ECC injection.

1300 MW GPWR Nodalization Study

A RELAP-5/MOD 2 nodalization study for a 1300 MW GPWR was performed by Dr. Curca-Tivig (KWU) to achieve realistic simulation of GPWR-type LOCA flooding behaviour. In this study 3 parallel channel simulation of the core was investigated. As shown in Fig. 2 the 3 intact loops of the primary system are simulated by one loop whereas the broken loop is represented by another single loop. The core noding exists of 3 channels one simulating the break through region with 29 fuel assemblies, one main channel for the flooding region with 163 fuel assemblies and one hot channel simulating 1 fuel assembly attached to the latter as shown in Fig. 3.

The calculated pressure transients in the primary system and the secondary side of the steam generator are depicted in Fig. 4 indicating also the onset of the simultaneous ECC-injection into the hot- and cold legs at 26 bar. The immediate break through into the core of the ECC water injected via the hot legs can be identified clearly on the response of the collapsed water level in the break through channel as can be seen in Fig. 5. The collapsed water level behaviour in the flooding region represented by the main channel is shown in Fig. 6. The corresponding steam qualities in the 3 channels simulating the core are depicted for various levels in Fig. 7, Fig. 8 and Fig. 9. The resulting cladding temperatures at the midplane of the active core for the average and hot rods in the 3 core channels are shown in Fig. 10.

The results of this noding study indicate that a realistic core behaviour description for large break LOCAs can be achieved by 3 channel simulation of the core using RELAP-5/ MOD 2.

PKL II B 5 Experiment Post Test Calculation

The post test calculation of the cold leg large break with cold leg ECC injection PKL-II B 5 experiment was performed by Mr. Dang-Viet (KWU). A schematic view of the PKL-II test facility is shown in Fig. 11. The nodalization scheme applied to in the study with complete 3 LOOP simulation of the facility is shown in Fig. 12. The comparison between experimental and calculated collapsed water levels in the downcomes (Fig. 13, Fig. 14) and in the core region (Fig. 15, Fig. 16) are in good agreement. The measured temperatures on the primary side of the steam generator in Fig. 17 indicate clearly superheated steam in the U tubes. On the contrary the results of the RELAP-5/ MOD 2 post test calculation show oscillatory decrease down to saturation temperatures (Fig. 18) indicating higher water entrainment into the steam generators. The water entrainment causing additional steam production in the steam generators leads to steam binding effects. The influence of the steam binding on the flooding of the electrically heated rod bundle can be seen in the delayed cladding temperature response of the calculated temperatures in Fig. 19.

Main Findings of RELAP-5/MOD 2 Calculation

GPWR-Nodalization Study:

- For 3 channel simulation of the core RELAP-5/MOD 2 predicated major trends of the thermohydraulic in core region correctly and in agreement with experimental results.

- Water entrainment in the core region seems to be too high causing too early quenching of the rods in the upper core region compared to relevant experiments.

PKL-II B 5 Post test calculation:

- RELAP-5/MOD 2 predicted the major trends of the thermohydraulic in particular collapsed water levels in the downcomers and in the core region correctly and in good agreement with the experiment.

- Too high water entrainment into steam generators was calculated causing steam binding and delayed core quench compared with the experimental results.

IV. Experience with TRAC-PF1

The following types of analysis mainly related to LOCA research were performed in the FRG at GRS and Siemens (KWU) using TRAC-PF1.

- 3 dimensional GPWR large break LOCA-analysis used for specification of UPTF-experiments.

- Calculations to establish realistic initial and boundary conditions for UPTF-experiments.

- Pre- and post test calculations for UPTF-experiments.

- Post test calculations of single and two phase pressure wave propagation in piping systems resulting from rapid valve opening and closing.

In particular results of the TRAC-PF1 post test calculation of the UPTF experiment No. 12 will be presented and the significant findings discussed.

Post Test TRAC-PF1 Calculation of UPTF Test No. 12

The post test TRAC-PF1 calculation of the UPTF Separate Effect Test No. 12 was performed by Dr. Gläser at GRS. The aim of the UPTF Test No. 12 was the investigation of flow behaviour at the tie plate for hot leg ECC injection and steam upflow in the core as illustrated in Fig. 21. The radial vessel noding including the injection configuration and the position of the broken LOOP is depicted below.

In the experiments immediate continous break through at the tie plate adjacent to the injection ports was observed. The total mass flow rate across tie plate was calculated much smaller than measured, see Fig. 20. The calculated tie plate water mass flow rate in water downflow area indicates oscillatory behaviour not observed in the experiment (Fig. 22). The comparison of the steam mass flow rates in Fig. 23 shows good agreement between calculational and experimental results. The tie plate mass balance in the analysis shows a much smaller total water downflow than measured in the experiment (Fig. 24).

Part of the reason can be seen as a consequence of the water accumulation in the hot leg which can be concluded from the high broken hot leg mass flow rate towards the steam generator calculated by TRAC-PF 1.

Main Findings of TRAC-PF1 Post Test Calculation of UPTF Test No. 12

- Water mass flow rate downwards through the tie plate calculated much smaller than measured in the experiment.

- No continous break through calculated as observed in experiment.

- Too high mass flow rate in broken hot leg calculated by TRAC-PF1 compared to experiment.

V. Conclusions

It is foreseen, that the proposed FRG-ICAP contribution will be useful for the range of licensing accident conditions and in particular for the large break LOCA code assessment. Based on the experience obtained using RELAP-5/MOD 2 and TRAC-PF1 the following remarks and recommendations related to the application and further improvement of the codes can be made.

- In a broad variety of application RELAP-5/MOD 2 and TRAC-PF1/MOD 1 predicted major trends of the transients correctly
- The following special areas in the codes need further improvement
  - . Counter current flow at tie plate and downcomer
  - . Core void distribution and core heat transfer
  - . Condensation in upper plenum, downcomer and ECC-injection port
  - . Flow regimes in bundles, pipes and anulus.
- More emphasis has to be directed in the codes to consistence among flow regimes, interfacial drag, evaporation/condensation and interfacial- and wall heat transfer.

In our opinion the encouraging outcome of the studies in connection with new experimental results should be of an important impact on improving the thermohydraulic models of the codes and represents an essential contribution in establishing internationally assessed and approved computer codes for accident analysis of LWR's.

Fig. 1

CODE	NUMBER OF STUDIES	IDENTIFICATION OF TEST FACILITY AND EXPERIMENT	ASSESSMENT STUDIES		
			PERFORMED OR IN PREPARATION	DEFINED	TOTAL
-	2	GENERAL CONTRIBUTIONS NUREG/IA-002, NUREG/IA-003	2	-	2
RELAP 5/MOD 2	14	PKL-I AND PKL-II			
		LARGE BREAK	2 1	1	6
		SMALL LEAK	1 1		
		UPTF			
		INTEGRAL TEST		2	
		SEPARATE EFFECT TEST		3	5
		PWR			
		COMMISSIONING-TEST	1	2	3
TRAC-PF1/MOD 1		PKL-II			
		LARGE BREAK		1	1
		UPTF			
		INTEGRAL TEST		2	
		SEPARATE EFFECT TEST		6	10
		KARLSTEIN CALBR. TEST	2		
		PWR			
		LARGE BREAK	3		3
TRAC-BF	7	BWR			
		COMMISSIONING TEST		7	7
RELAP-5 OR TRAC-PF1	13	PWR			
		COMMISSIONING TEST		5	5
		EXPERIMENT OPEN			8
	50	STATUS OF ASSESSMENT	13	31	50

FRG - ICAP MATRIX (STATUS Oct. 1987)

Fig. 2

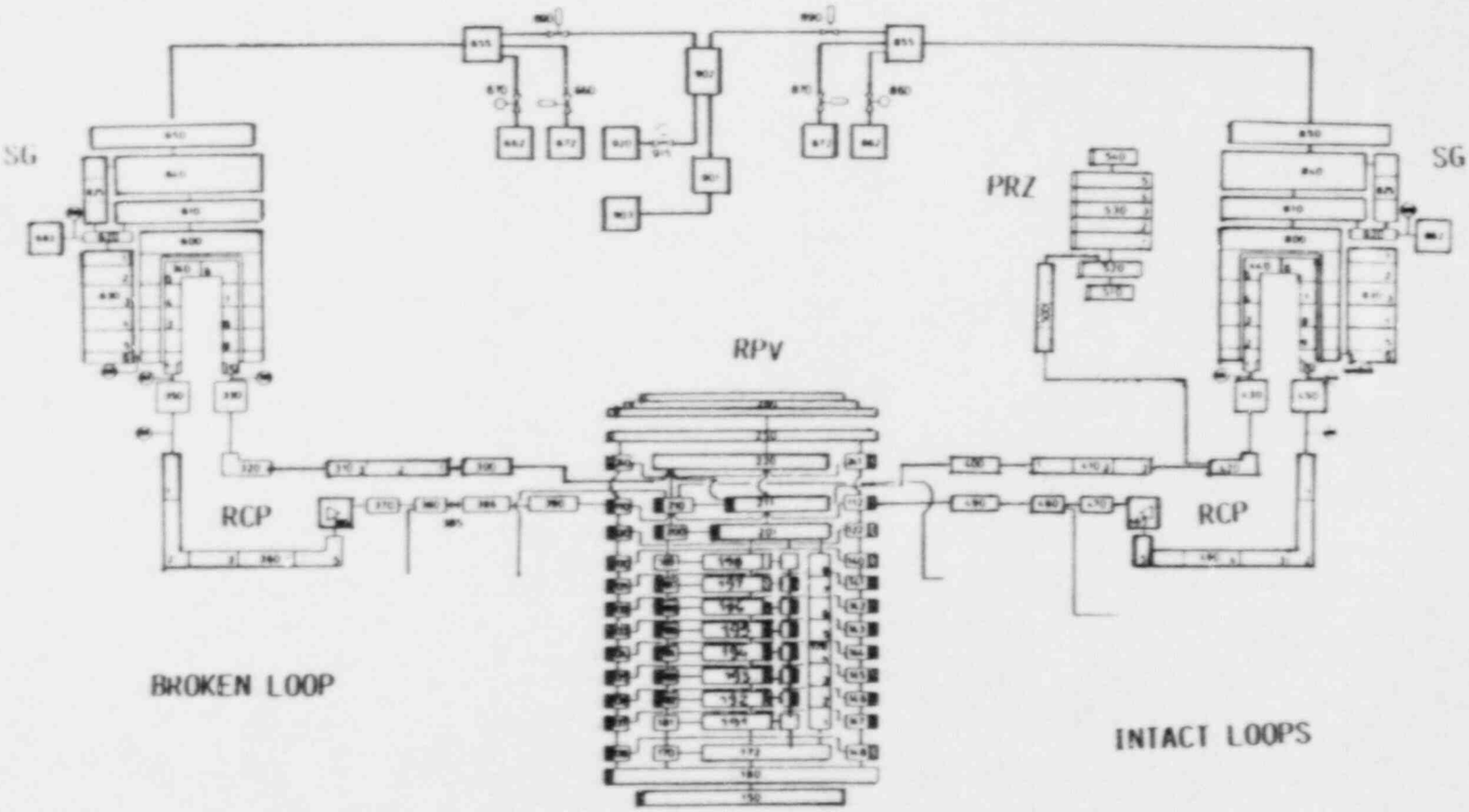

1300 MW GPWR: NODALIZATION STUDY 2A - COLD LEG BREAK RELAP5/MOD2 LOCA ANALYSIS

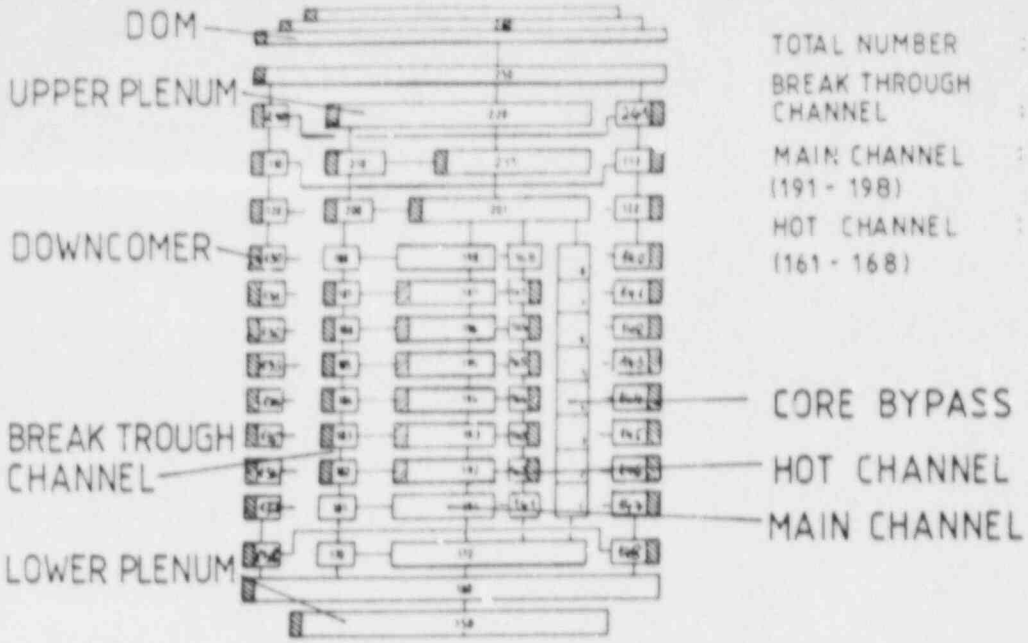

1300 MW GPWR : NODALIZATION STUDY
REACTOR VESSEL NODALIZATION

Fig. 3

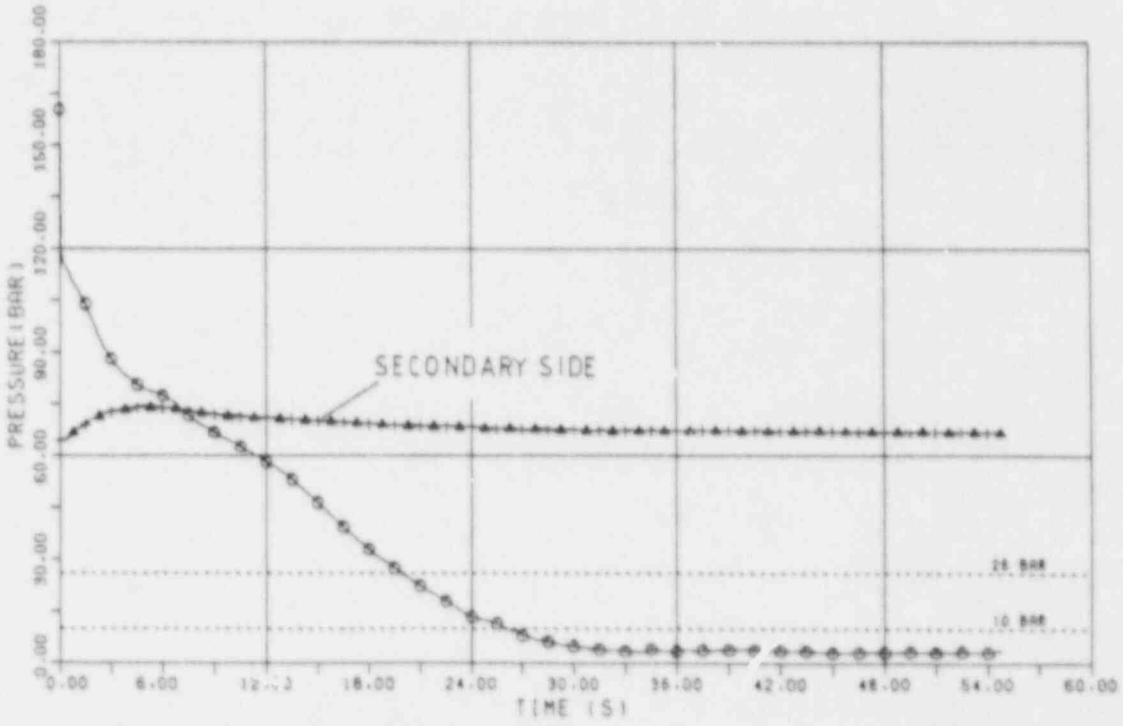

1300 MW GPWR : LB-LOCA NODALIZATION STUDY
SYSTEM PRESSURE

Fig. 4

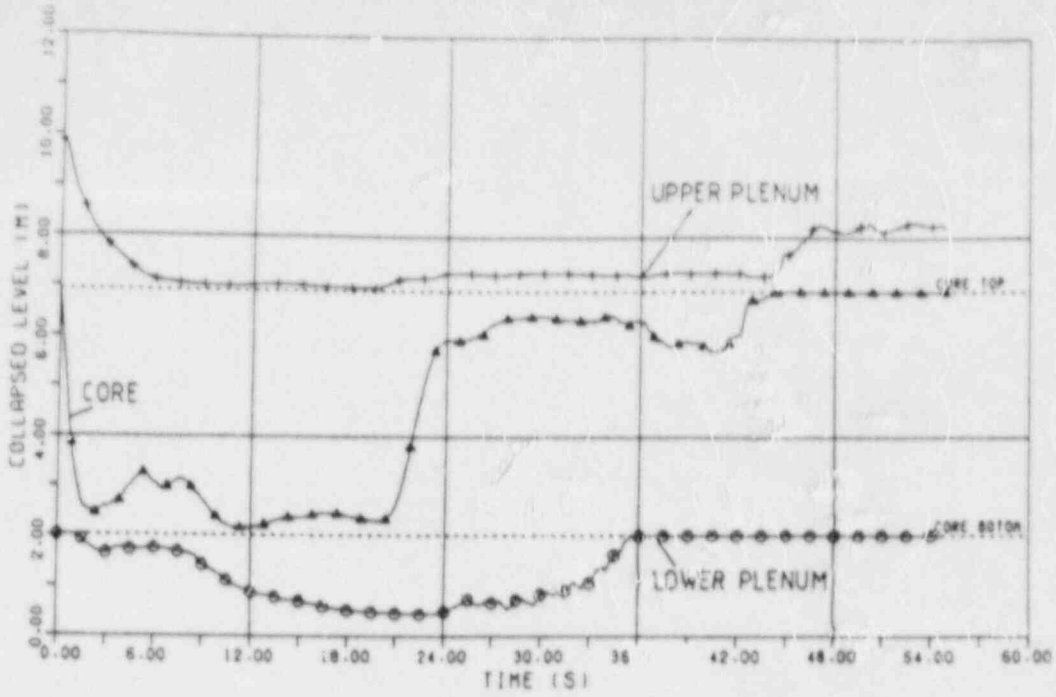

1300 MW GPWR : NODALIZATION STUDY
COLLAPSED WATER LEVEL IN BREAK-THROUGH CHANNEL

Fig. 5

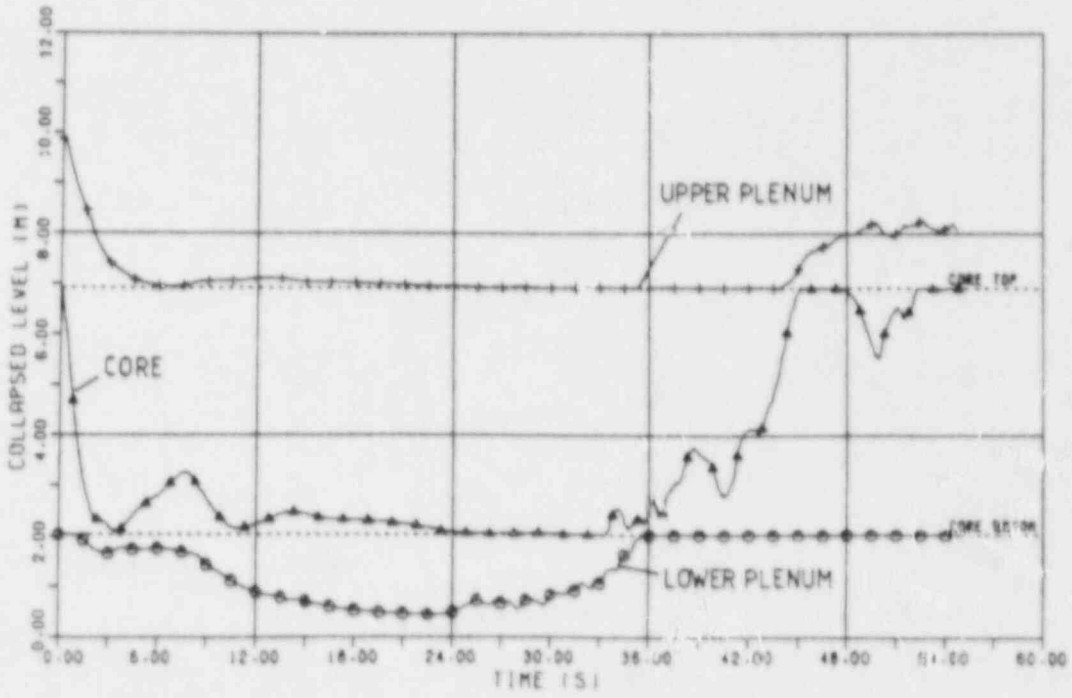

1300 MW GPWR : NODALIZATION STUDY
COLLAPSED WATER LEVEL IN MAIN CHANNEL

Fig.6

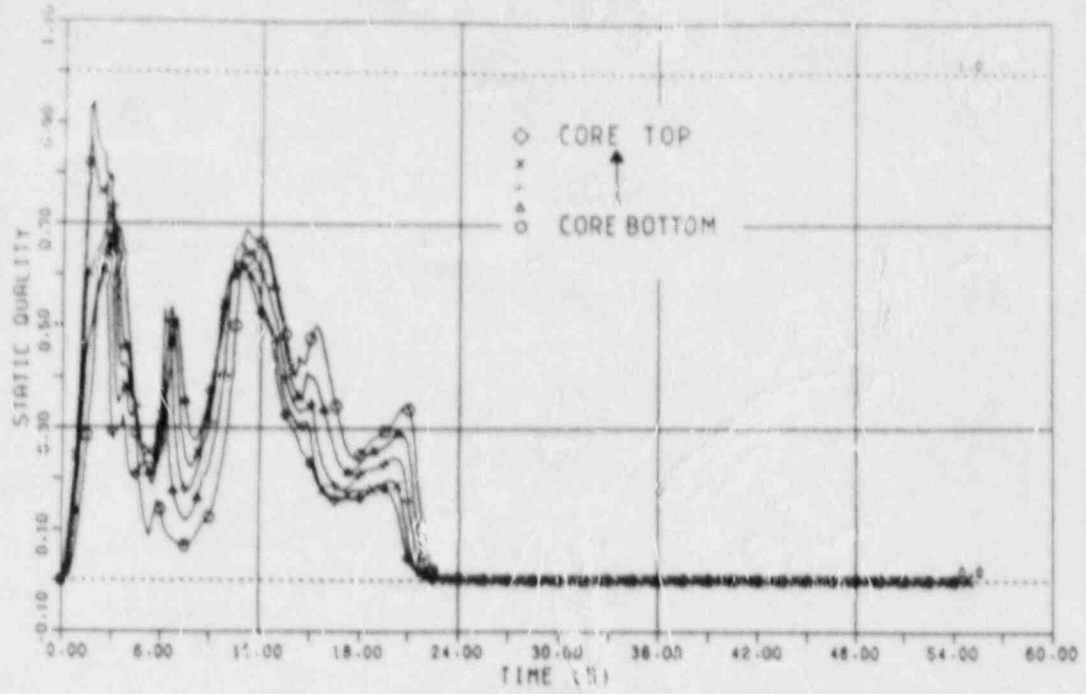

1300 MW GPWR: NODALIZATION STUDY
STEAM QUALITY IN BREAK THROUGH CHANNEL

Fig. 7

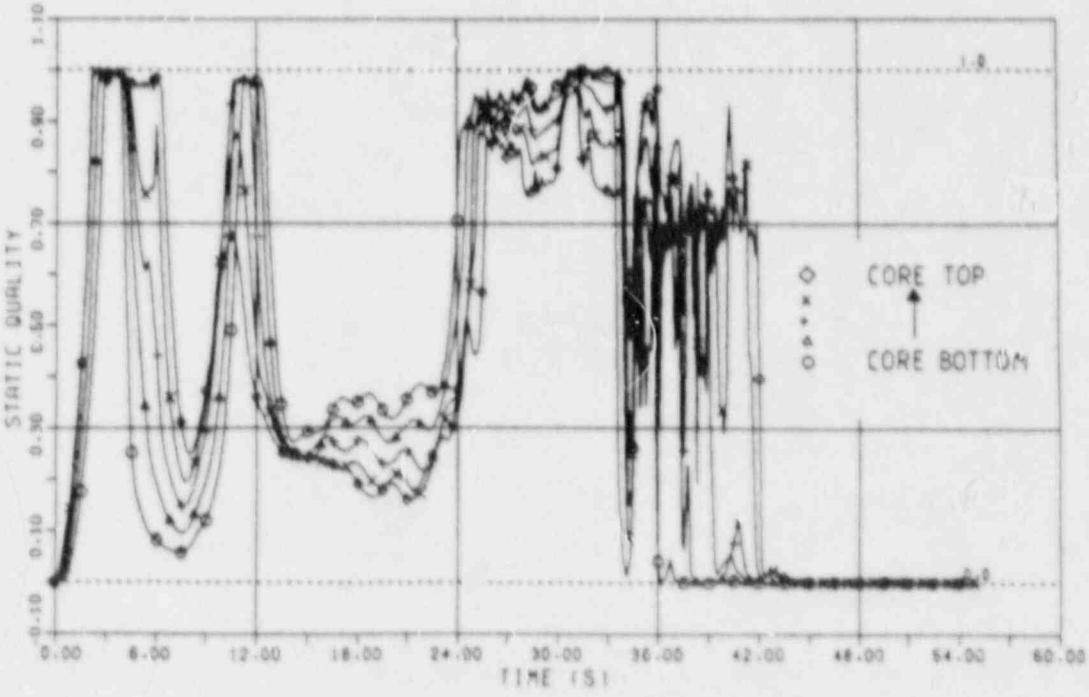

1300 MW GPWR : NODALIZATION STUDY
STEAM QUALITY IN MAIN CHANNEL

Fig. 8

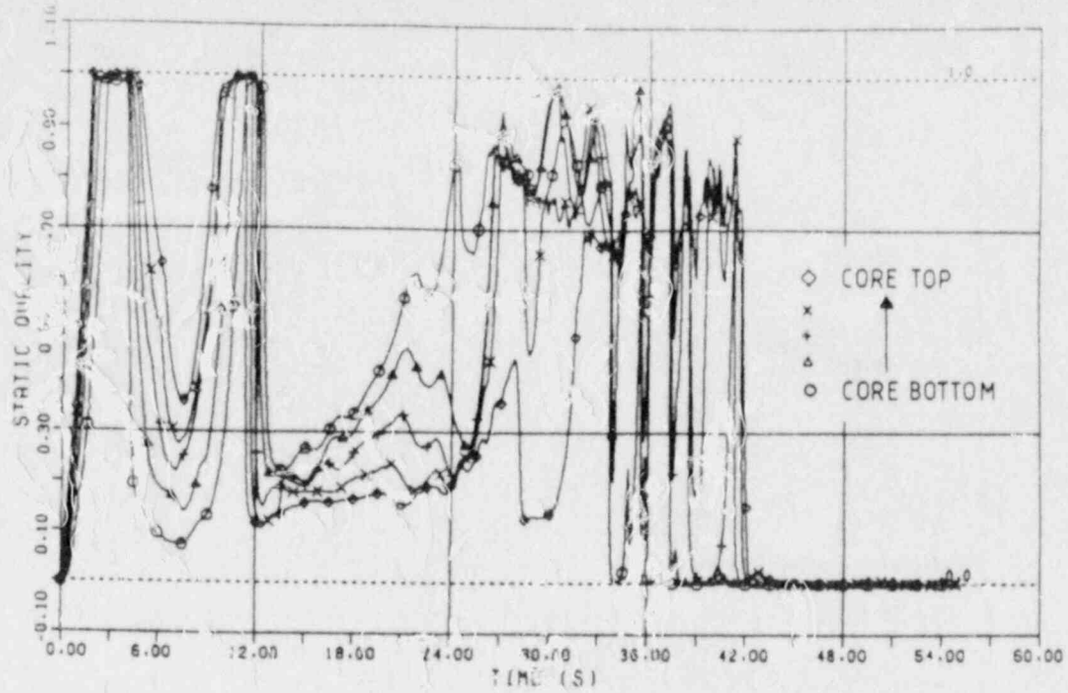

1300 MW GPWR NODALIZATION STUDY
STEAM QUALITY IN HOT CHANNEL

Fig. 9

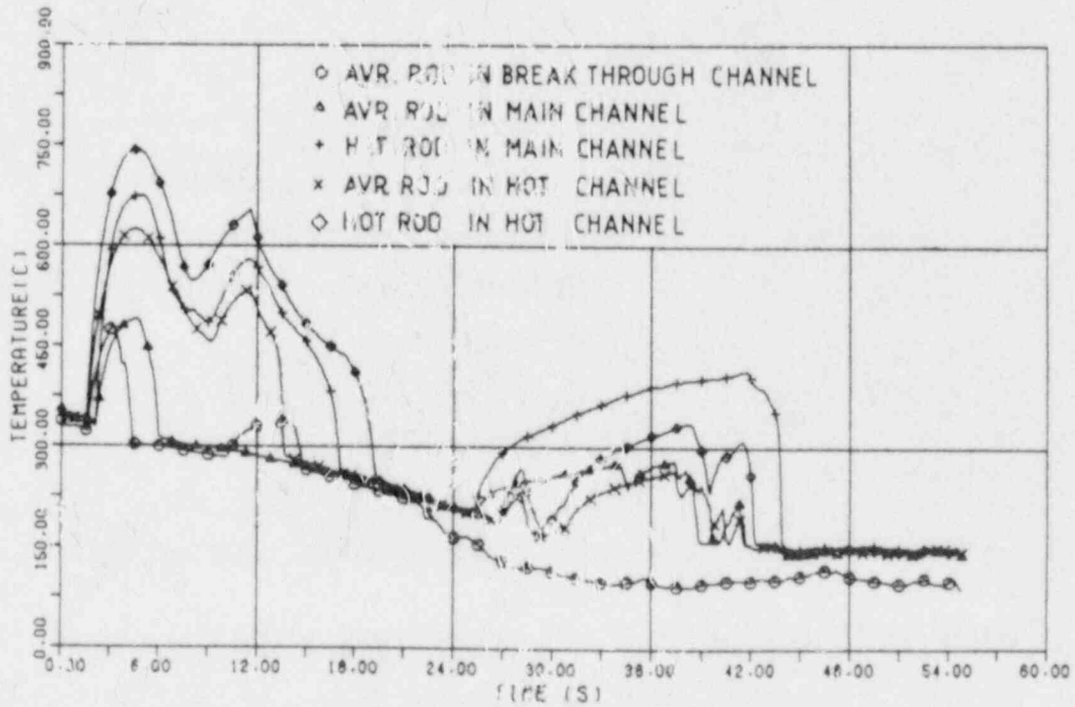

1300 MW GPWR : NODALIZATION STUDY
CLADDING TEMPERATURE IN THE FOURTH AXIAL ZONE OF THE ACTIVE CORE

Fig. 10

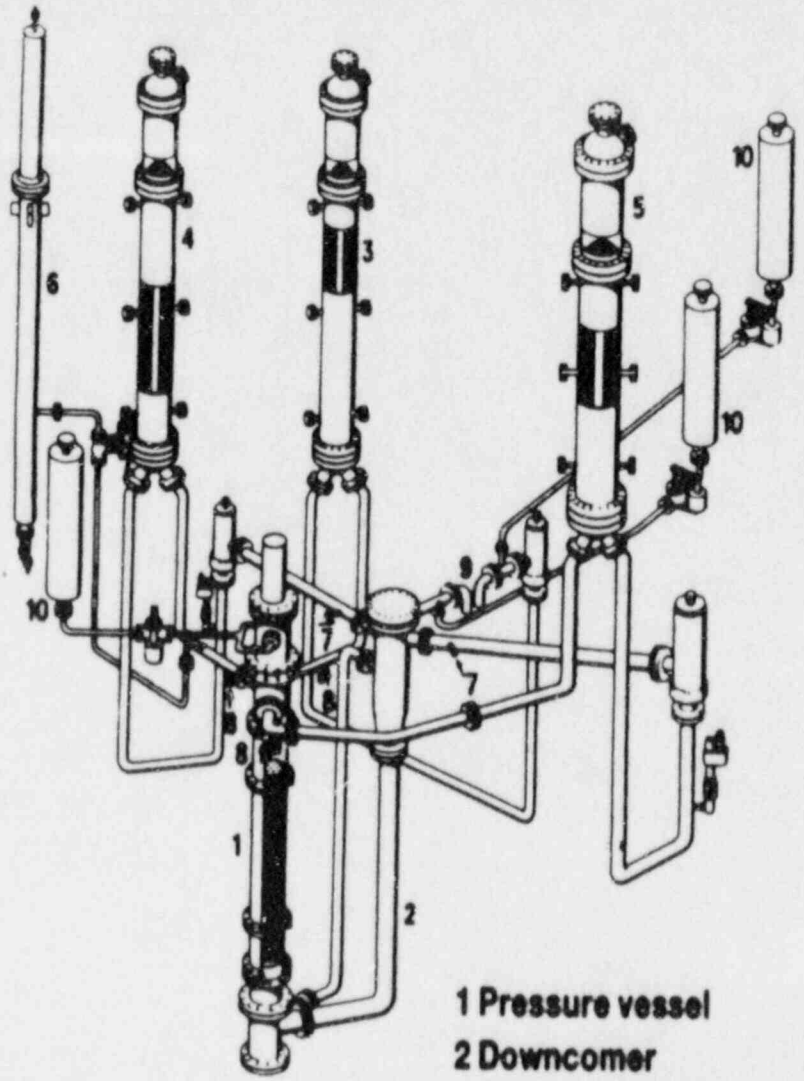

1 Pressure vessel
2 Downcomer
3 Steam generator 1 (broken loop)
4 Steam generator 2 (intact loop)
5 Steam generator 3 (double loop)
6 Pressurizer
7 Cold leg ECC injection
8 Hot leg ECC injection
9 Cold leg break
10 Conditioning-water storage tank

PKL II Test Facility

Reactor: 1300 MWe Standard

Elevation scaling:	1:1
Volume and power scaling:	1:145

Fig. 11

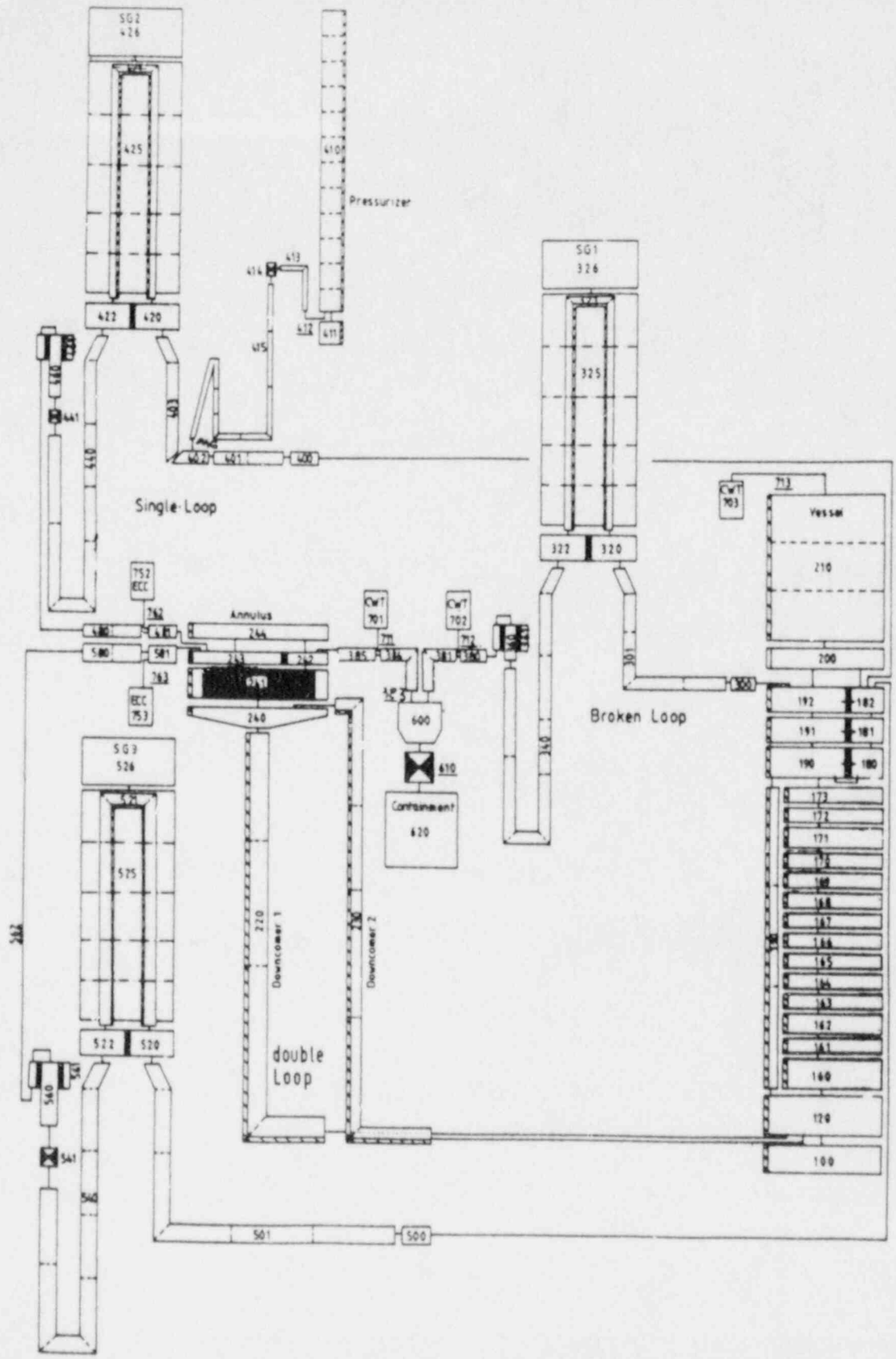

PKL-II B 5, RELAP5/MOD2 NODALIZATION SCHEME (2A-COLD LEG BREAK, COLD LEG ECC-INJECTION)

Fig. 12

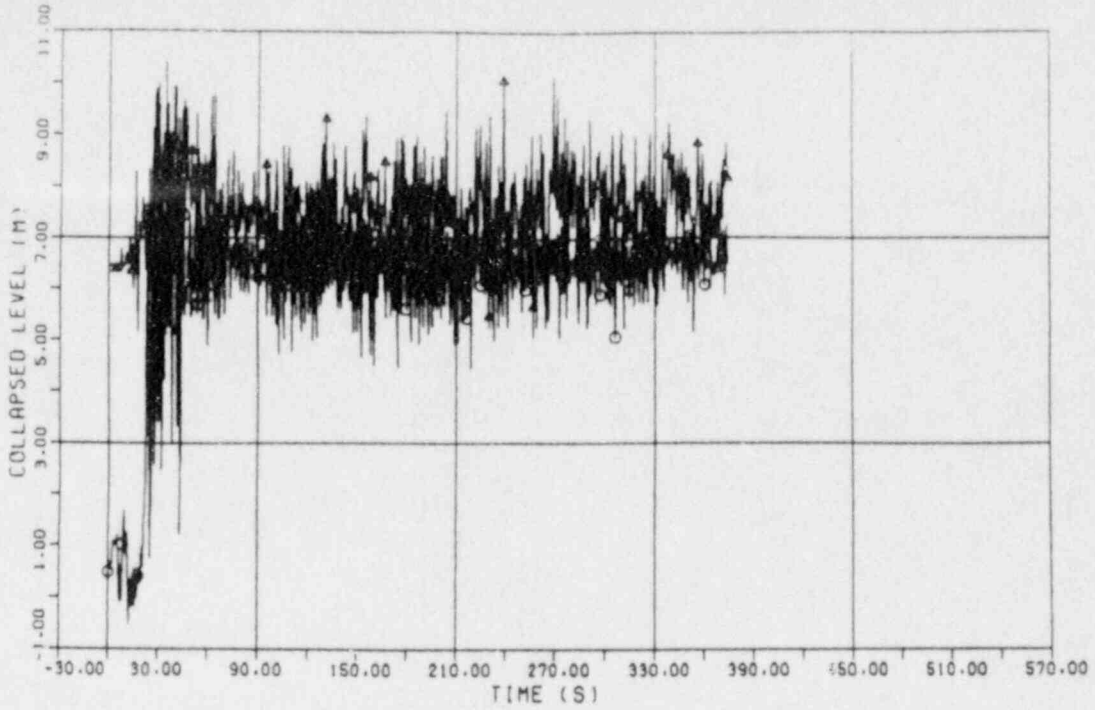

PKL-II B 5, EXPERIMENT
COLLAPSED WATER LEVEL IN DOWNCOMER

Fig. 13

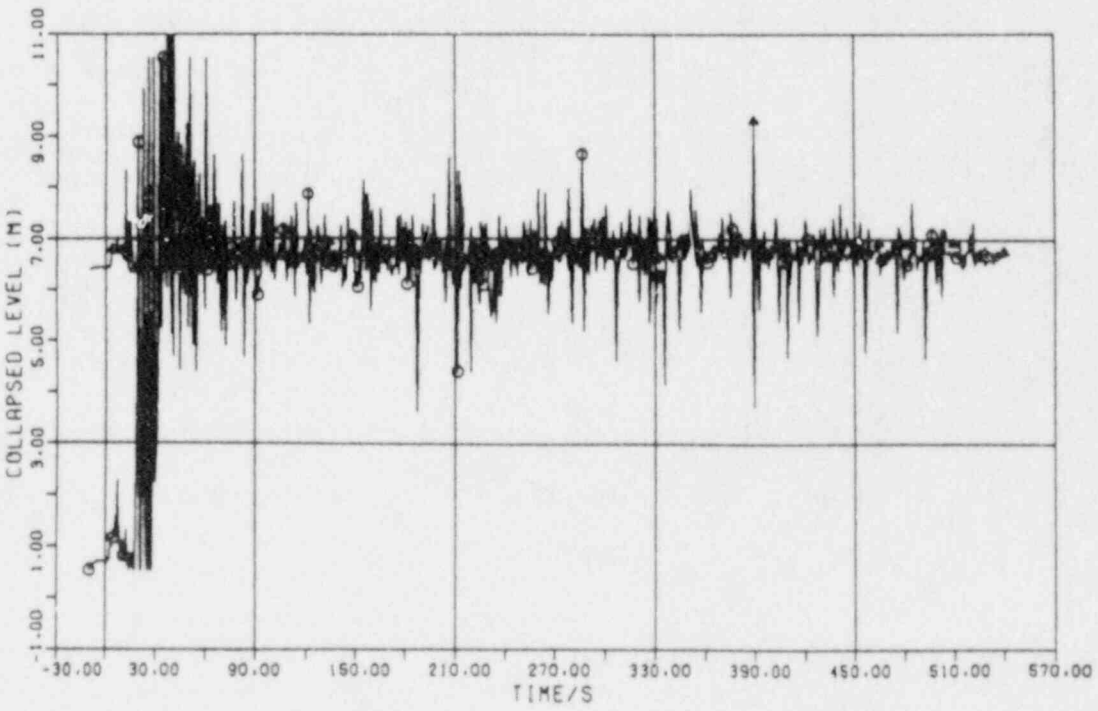

PKL-II B5, RELAP5/MOD2 CALCULATION
COLLAPSED WATER LEVEL IN DOWNCOMER

Fig. 14

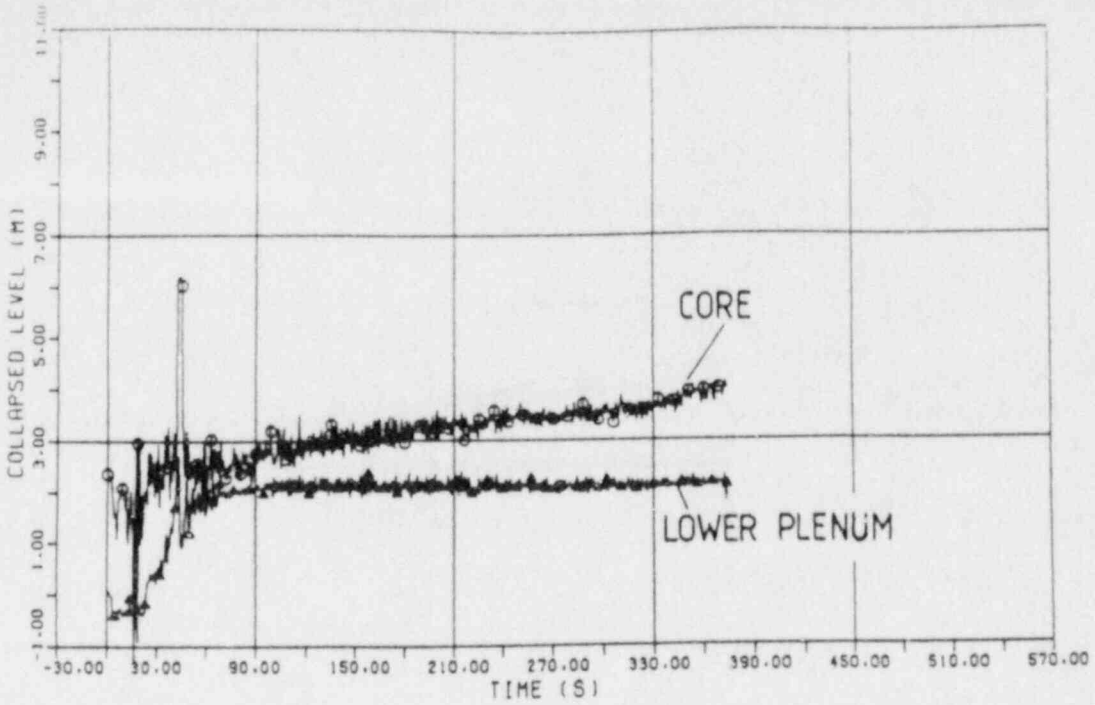

PKL-IIB5, EXPERIMENT
COLLAPSED WATER LEVEL IN TEST VESSEL

Fig. 15

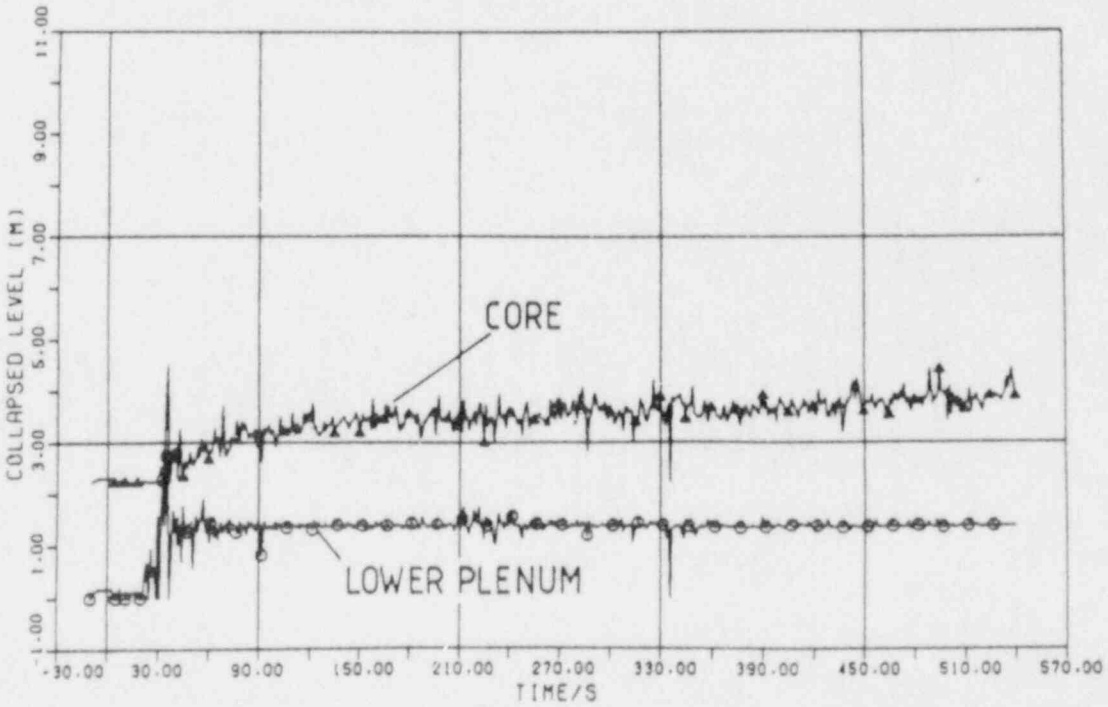

PKL-IIB5, RELAP5/MOD2 CALCULATION
COLLAPSED WATER LEVEL IN TEST VESSEL

Fig. 16

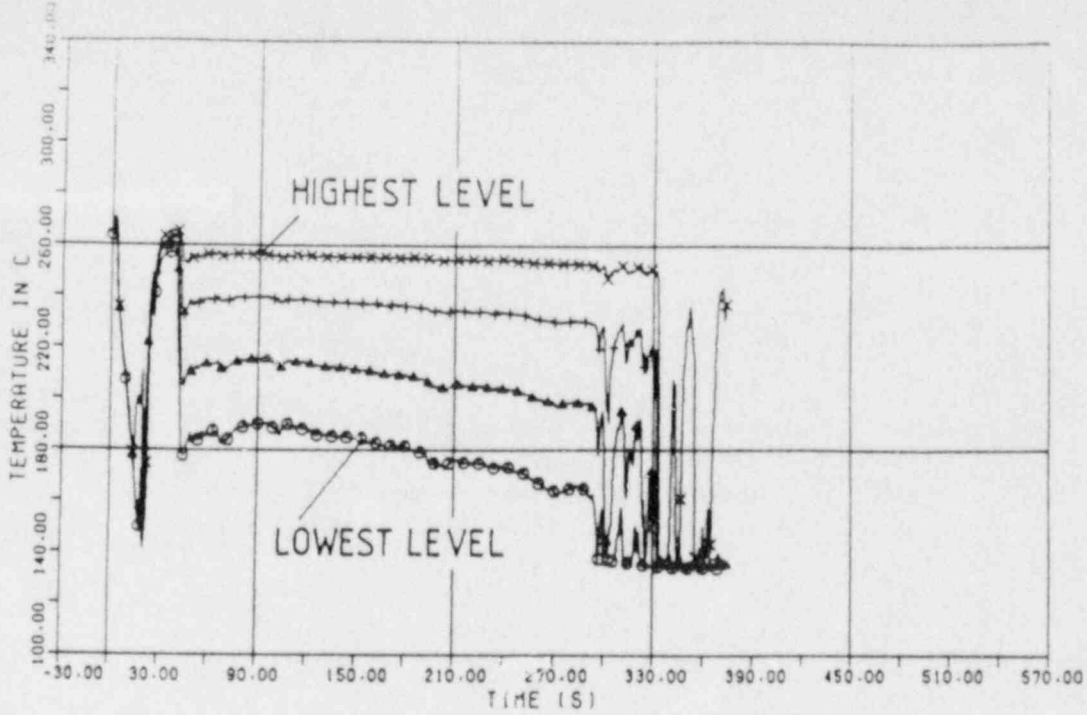

PKL-II B5, EXPERIMENT
STEAM GENERATOR PRIMARY TEMPERATURES
AT VARIOUS LEVELS

Fig. 17

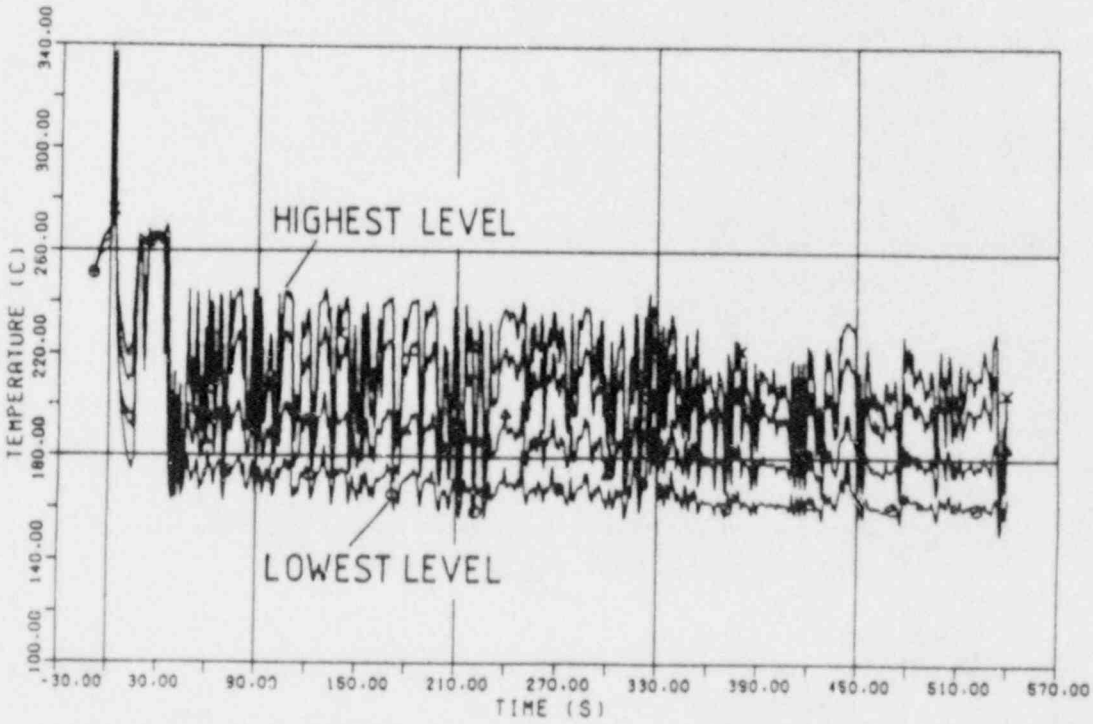

PKL-II B5, RELAP5/MOD2 CALCULATION
STEAM GENERATOR PRIMARY TEMPERATURES
AT VARIOUS LEVELS

Fig. 18

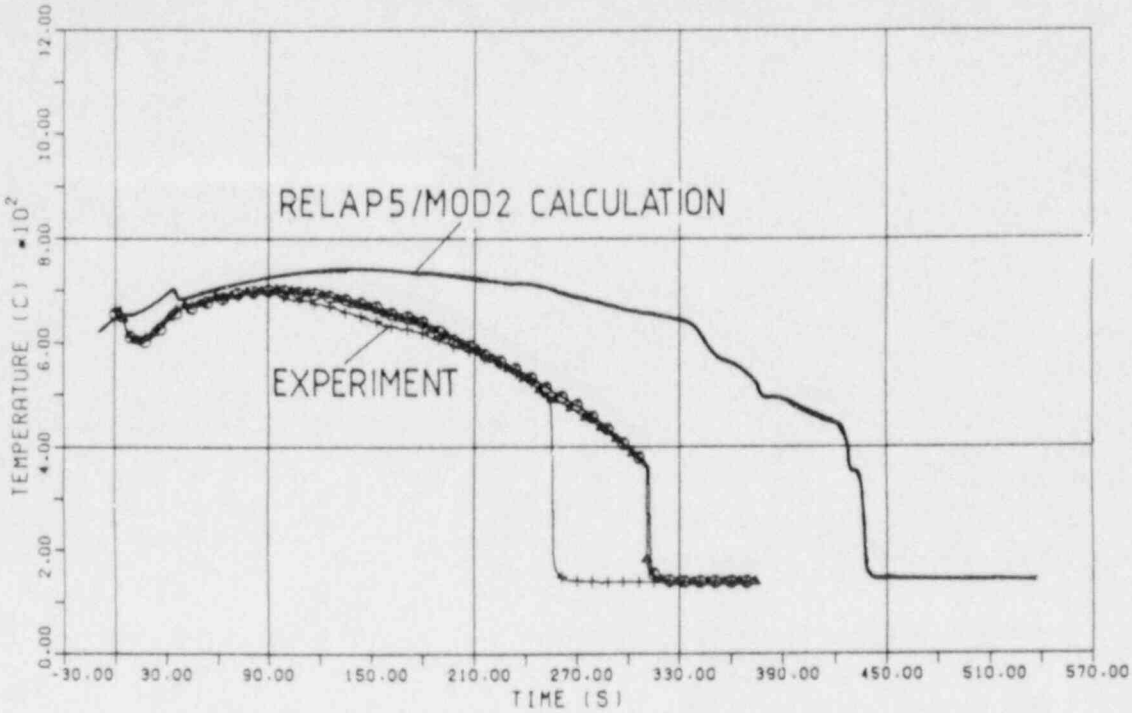

PKL-IIB5
MAX. CLADDING TEMPERATURES IN HIGH POWER ZONE AT VARIOUS RODS

Fig. 19

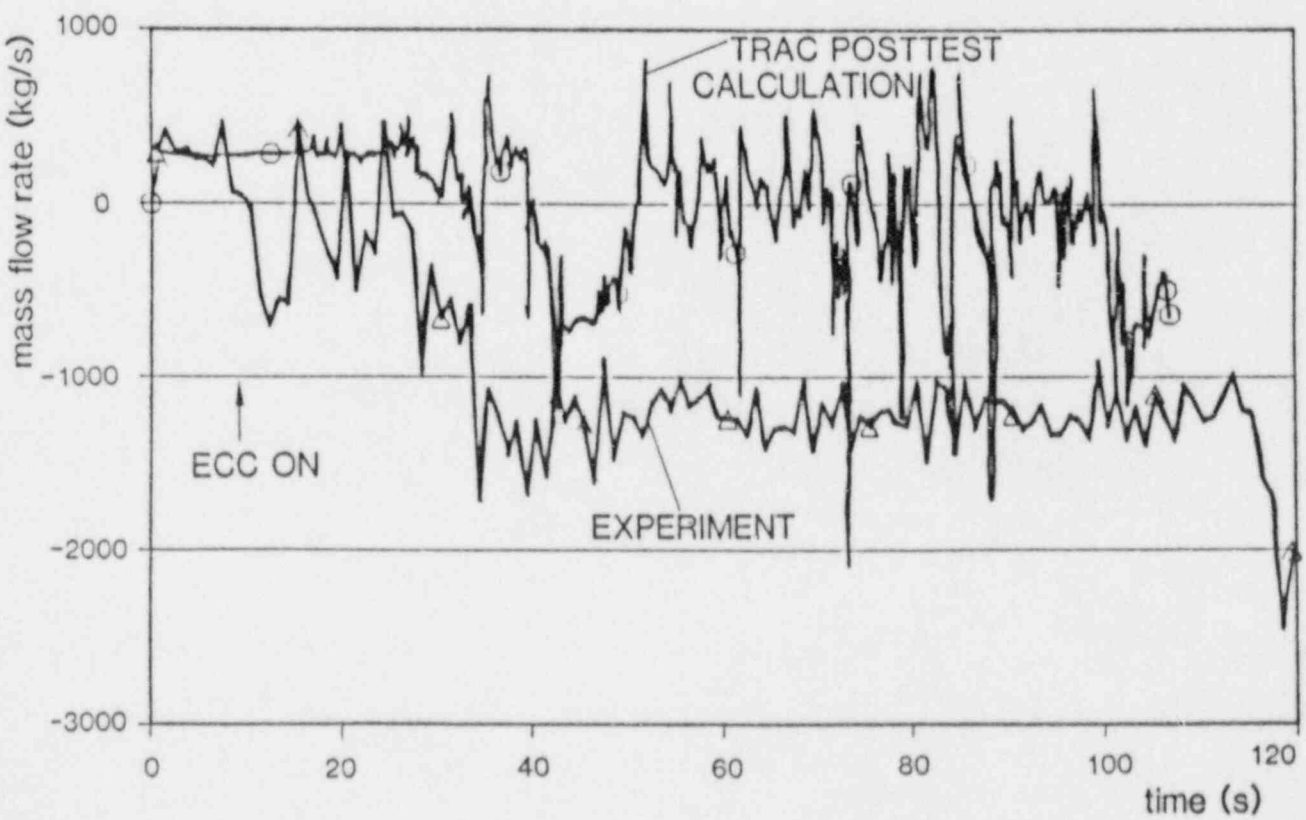

UPTF TEST NO.12: TOTAL TIE PLATE MASS FLOW RATE

Fig. 20

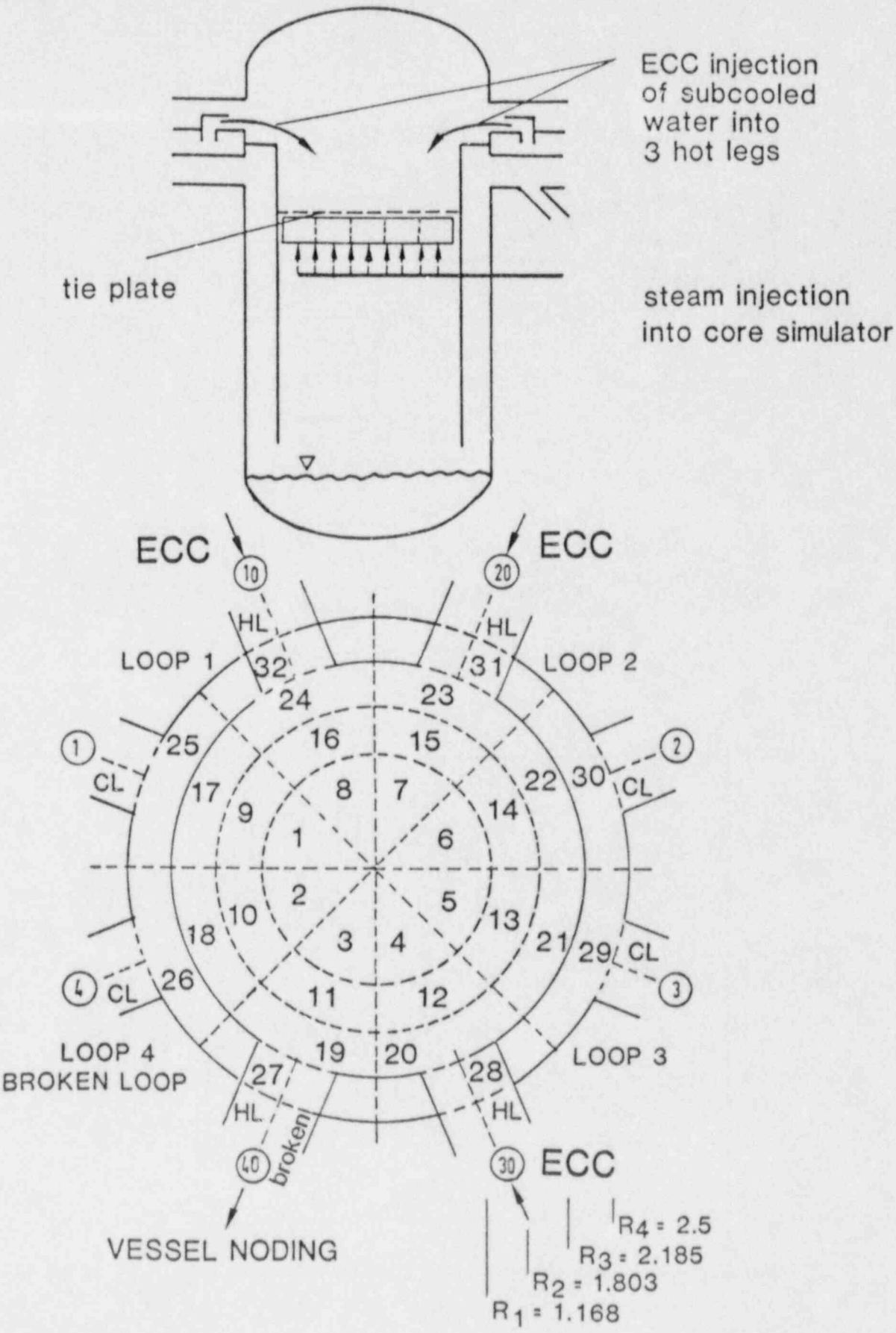

UPTF-TEST NO.12

Fig. 21

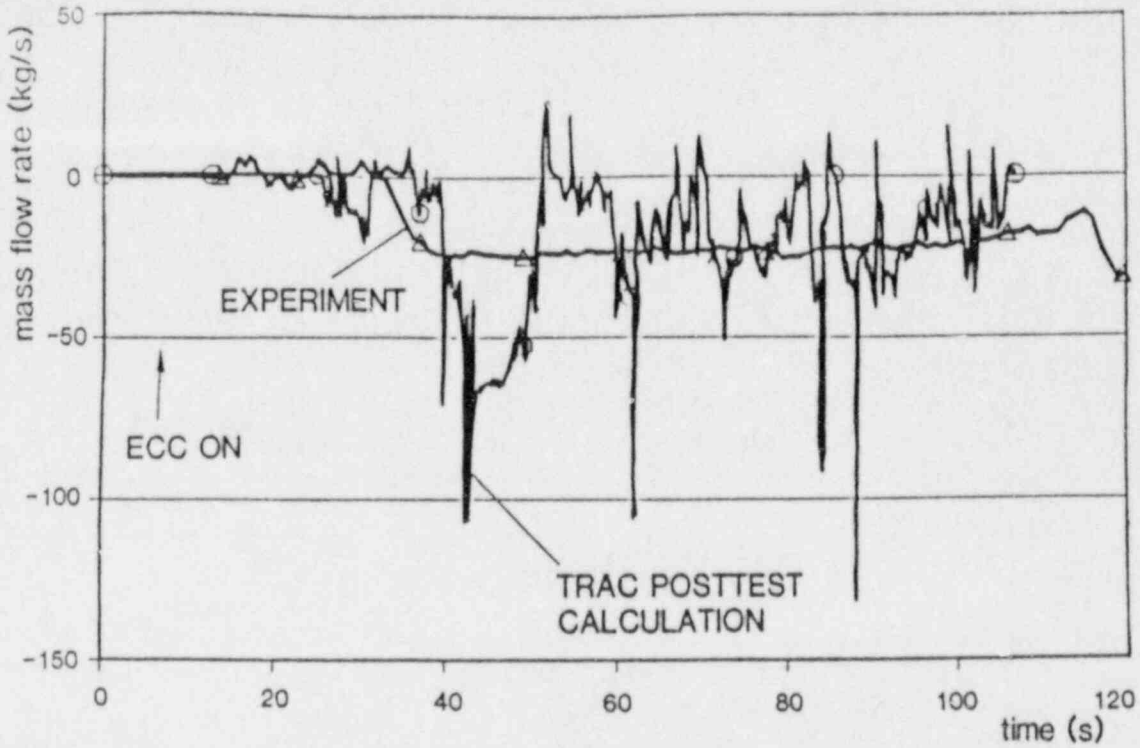

UPTF TEST NO.12: TIE PLATE WATER MASS FLOW RATE IN WATER DOWNFLOW AREA (1 FUEL ASSEMBLY)

Fig. 22

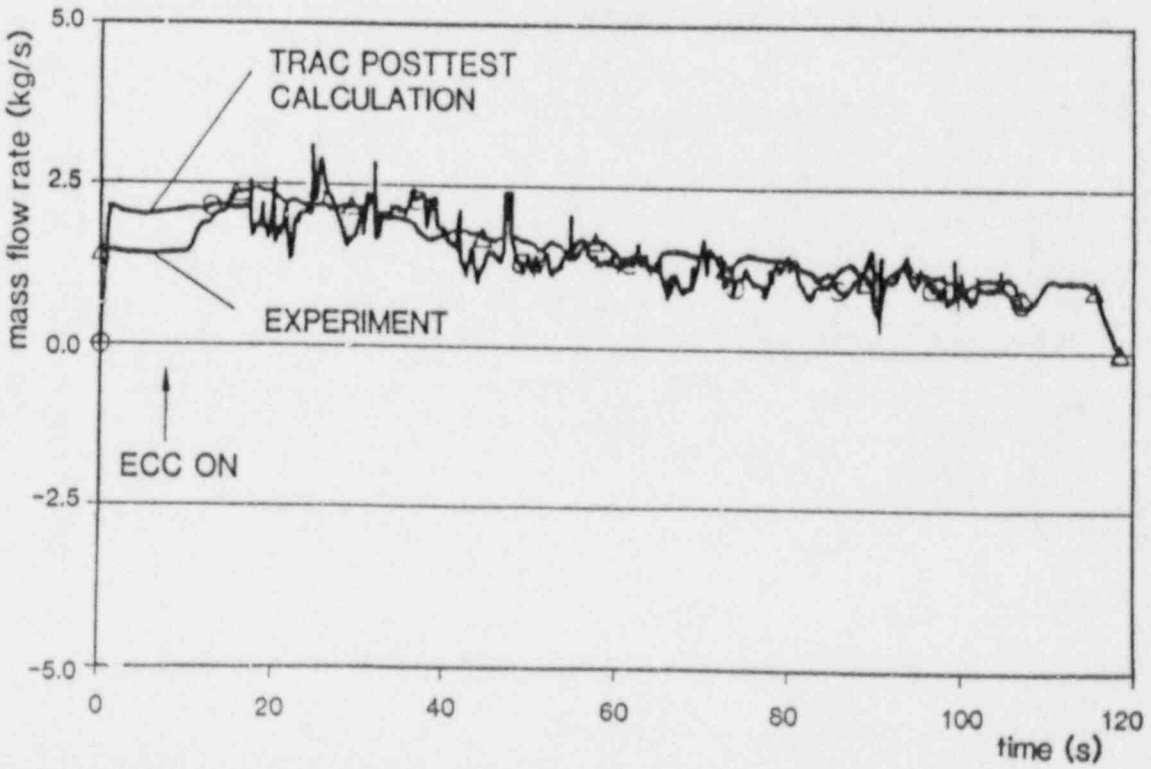

UPTF TEST NO.12: TIE PLATE STEAM MASS FLOW RATE IN STEAM UPFLOW AREA (1 FUEL ASSEMBLY)

Fig. 23

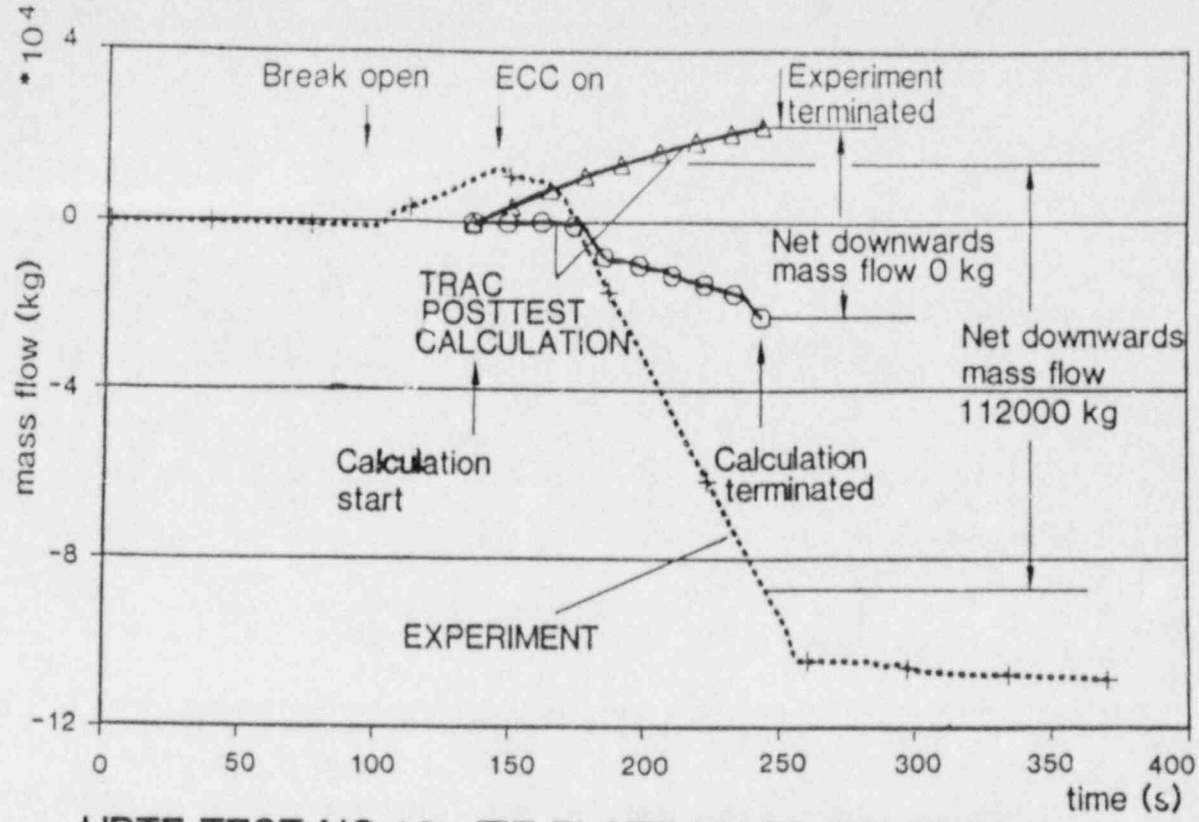

UPTF TEST NO.12: TIE PLATE MASS BALANCE

Fig. 24

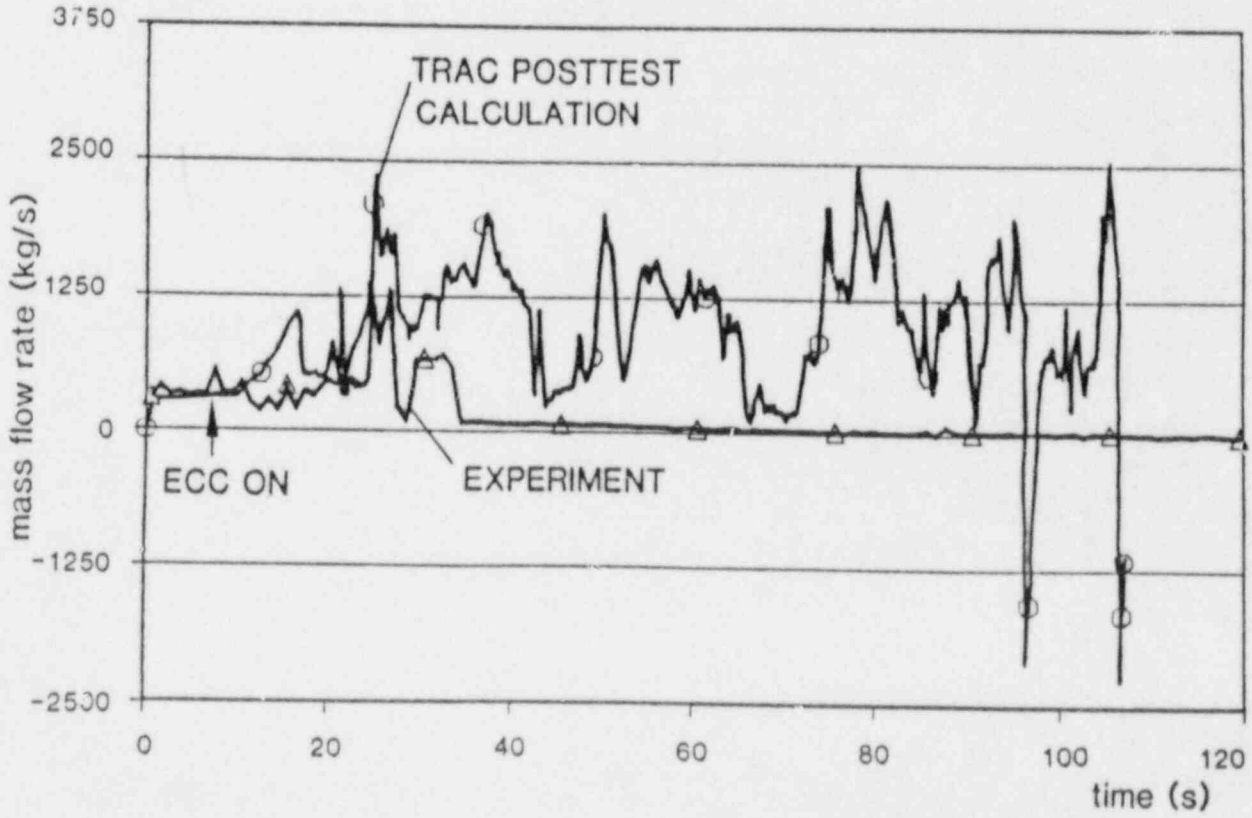

UPTF TEST NO.12: BROKEN HOT LEG MASS FLOW RATE

Fig. 25

PHENOMENA IDENTIFICATION AND RANKING TABLES (PIRT) FOR LBLOCA*

R. A. Shaw, R. A. Dimenna, T. K. Larson, G. E. Wilson
Idaho National Engineering Laboratory, EG&G Idaho, Inc.

ABSTRACT

The U. S. Nuclear Regulatory Commission is sponsoring a program to provide validated reactor safety computer codes with quantified uncertainties. The intent is to quantify the accuracy of the codes for use in best estimate licensing applications. One of the tasks required to complete this program involves the identification and ranking of thermal-hydraulic phenomena that occur during particular accidents. This paper provides detailed tables of phenomena and importance ranks for a PWR LBLOCA.

The phenomena were identified and ranked according to perceived impact on peak cladding temperature. Two approaches were used to complete this task. First, a panel of experts identified the physical processes considered to be most important during LBLOCA. A second team of experienced analysts then, in parallel, assembled complete tables of all plausible LBLOCA phenomena, regardless of perceived importance. Each phenomenon was then ranked in importance against every other phenomenon associated with a given component. The results were placed in matrix format and solved for the principal eigenvector. The results as determined by each method are presented in this report.

1. INTRODUCTION

The rules governing operation of emergency core cooling (ECC) on light water reactors in the United States were based conservatively on the understanding of ECC performance in 1974. Similar conservatisms were built into rules concerning computer calculations of ECC performance during loss-of-cooling accidents (LOCA's). Since 1974 much research has been performed and the understanding of LOCA's has increased greatly. Calculations of LOCA's can now be performed with considerably less uncertainty than in 1974; consequently, new rules have been proposed that will allow the use of best-estimate (BE) codes for more realistic simulations of plant behavior.[1]

Although the economic benefits of the proposed rule change could be large, there are also substantial safety implications. For that reason, the new rule will require the licensees to quantify the uncertainty in any BE LOCA calculation to a high level of probability.[2] That requirement is consistent with the Nuclear Regulatory Commission's (NRC) desire to have validated computer codes with quantified uncertainties.

---

* Work supported by the U.S. Nuclear Regulatory Commission, Office of Nuclear Regulatory Research under DOE Contract No. DE-AC07-76ID01570.

One of the tasks the NRC has undertaken in support of the trend toward best-estimate codes is the uncertainty quantification of the TRAC-PF1[3] code for a large-break LOCA. The intent is to display the feasibility and a methodology for the determination of code uncertainty. The large LOCA was chosen because it has usually been calculated to be the most severe and limiting LOCA when Appendix K calculation methods are used.[2] The performance of this task will require a thorough knowledge of the thermal-hydraulic processes present during a large-break LOCA and the models used in the code. The former of these subtasks is the subject of this report.

There were several objectives of this work. It was desired to identify and rank the importance of key plant components with regard to impact on peak cladding temperature (PCT) during a large-break LOCA. Secondly, it was desired to identify and rank the importance of all thermal-hydraulic phenomena present in a particular component during each phase of the transient, again with respect to PCT. Two semi-independent methods were used to accomplish these objectives, each of which are discussed in detail in the following sections.

The first method consisted of assembling a panel of persons each of whom had extensive experience in reactor safety analysis. This experts panel included a wide cross-section of the nuclear community, with representatives from regulation, industry, and research. The decision method in this case was basically one of consensus agreement. The level of focus was at the system level and addressed only the phenomena considered to be of high importance during the LOCA.

The second method, which was performed by another group of experienced analysts at the Idaho National Engineering Laboratory, consisted of a literature review and an importance analysis using an analytic hierarchy method in which all importance rankings were made in a binary (pairwise) manner. This method consisted of the following steps:

a. Identification of all plausible thermal-hydraulic phenomena regardless of perceived importance,

b. Initial phenomena ranking at the component level,

c. Ranking of the components,

d. Processing of the data in b and c above to determine the phenomena ranking at the systems level (i.e. ranking comparable to that of the experts).

The second section of this paper provides background information on the proposed rule change and the role of the subject work. Sections 3 and 4 discuss both identification and ranking methods and presents the results of each analysis. The final section summarizes the results and conclusions.

2. BACKGROUND

Title 10 of the Code of Federal Regulations, Section 50.46,[4] provides the regulations that specify how ECC systems (ECCS) are to be designed for nuclear power plants in the United States. One section of that document

requires that calculations of ECCS behavior be performed to show that the ECCS meet certain criteria in the event of a LOCA; specifically, it places limits on PCT, cladding oxidation, hydrogen generation, and core geometry. It also requires that these calculations be performed by using the methods outlined in Appendix K to Part 50, "ECCS Evaluation Models."[2]

These regulations were published in 1974, with a limited knowledge of LOCA phenomena, ECCS performance, and calculational abilities; however, nearly one billion dollars has been spent on ECCS research since 1974. The results include greatly improved understanding of the LOCA and ECCS performance and reduced uncertainty in calculating ECCS performance.[1] Furthermore, this research has shown that Appendix K methods are highly conservative and that actual temperatures during a large-break LOCA would be much lower than those calculated using Appendix K methods. Basically, the research done since 1974 has provided sufficient knowledge to allow realistic, i.e., best-estimate, calculations of ECCS performance with quantifiable uncertainty, thus obviating the excessive conservatism now restricting the operation of some reactors.[2]

The NRC staff has been considering a revision to the ECCS rule since 1978, but no formal action was adopted until 1983 when an interim method (SECY-83-472) of evaluating ECCS performance was adopted until an official rule change could be put in place. Licensees seeking to operate under the interim, or final, rules will be required to perform best-estimate LOCA calculations in which the models have been compared to applicable experimental data. Furthermore, an estimate of the uncertainty in the calculation must be provided at a high probability level. SECY-83-472 and the proposed final rule do, however, grant the licensees permission to continue operating under the Appendix K rules.

Current NRC research is directed toward addressing the scalability, applicability, and uncertainty analyses of the NRC-sponsored best-estimate thermal-hydraulic codes such as TRAC and RELAP5. The work described in this report was performed in conjunction with the uncertainty analysis of TRAC-PF1/MOD1 for large-break LOCA; however, it is sufficiently general as to be applicable to any large-break LOCA analysis.

The ability to demonstrate a code is applicable to a transient, and then determine its uncertainty requires a thorough understanding of the thermal-hydraulic behavior in the plant. Thus, the first step is to identify the thermal-hydraulic phenomena present during the transient of interest. Next, the relative importance upon the key safety criteria of all phenomena that are to be simulated by the best-estimate computer codes must be estimated. This knowledge will help the code developer identify and prioritze the models used in his code that require improvement or replacement.

The transient of interest in this report is a large cold leg break; the safety criterion upon which all the importance rankings are made was the peak cladding temperature.

3. RESULTS OF THE EXPERTS PANEL

The experts panel assembled included representatives from regulation, industry, and research. Each member has extensive experience in LOCA analysis. Dr. Novak Zuber of the NRC served as panel chairman. All decisions were made on the basis of consensus.

Basically, the experts panel performed two functions; they identified and ranked the phenomena considered to be of highest importance during each phase of a large-break LOCA, e.g. blowdown, refill, and reflood. The results are presented in Table 1. There are two items of note regarding this and all other tables of importance in this report. One, all rankings were developed on the basis of perceived impact on PCT. It was well understood that many of the phenomena were coupled, but the ranks represent the subjective estimate of the individual effect of each on PCT. Second, all rankings in this report will be cast on a scale of 1-9, with 7-9 being high importance.

Table 1 shows that the fuel rod stored energy has an important effect on PCT during blowdown; later, in reflood, decay heat and oxidation become more important. There are important phenomena taking place in the core in all three phases of the transient. Entrainment is important in the upper plenum and hot leg during reflood because it removes mass from the core and also contributes to the steam binding potential, which is also listed as highly-important. The phenomena associated with the cold leg and downcomer, are important during the latter stages of the transient, for example, condensation due to ECC injection and 3-D flow in the downcomer during ECC bypass. The importance of critical flow through the break is high during blowdown, but obviously diminishes as the break flow decreases with time and eventually unchokes.

Observation of Table 1 shows that the experts, by performing their analysis at an overview or system level, indirectly ranked the component importances as well. Table 2 shows the relative importances of the plant components for each phase of the transient. Note that although particular components are important during blowdown and refill, there are important thermal-hydraulic phenomena occurring in most of the components during reflood.

4. INEL RANKING OF PHENOMENA USING AHP

Although it can be stated with reasonable certainty that the experts panel addressed the large-break LOCA phenomena of highest importance, a validation of the panel's conclusions was most desirable. For this reason and the desire to have a comprehensive ranking of more than just the most important phenomena, the second stage of the task was started. This second stage was performed at INEL by non-panel member engineers experienced in LOCA analysis. It consisted of completing the tables of phenomena, including those considered to be of medium and low importance with regard to PCT, performing an importance analysis, comparing the results with the experts panel results, and resolving any differences. Each of these subtasks will be discussed in the following paragraphs.

TABLE 1. EXPERTS PANEL RANKINGS OF PWR LARGE-BREAK LOCA PHENOMENA OF HIGH IMPORTANCE

Components	Phenomena	Rank During		
		Blowdown	Refill	Reflood
Fuel rod	Stored energy	9		
	Decay heat			8
	Oxidation			8
	Gap conductance			8
Core	Post-CHF heat transfer	7	8	
	Rewet/top quench	8	7	
	Reflood heat transfer			9
	3-D flow			9
	Void generation/ distribution			9
Upper plenum	Entrainment/deentrainment			9
Hot leg	Entrainment/deentrainment			9
Pressurizer	Early quench	7		
Steam generator	Steam binding			9
	2-phase performance	9		
Pump	2-phase pressure drop due to form loss			8
Cold leg/accum	Condensation		9	
	Noncondensible gases			9
Downcomer	Entrainment/deentrainment		8	
	Condensation		9	
	Hot wall			7
	Multi-dimensional flow		9	
Lower plenum	Sweepout		7	
	Hot wall			7
Break	Critical flow	9	7	
Loops	2-phase pressure drop	7		
	Flow split		7	
	Oscillations		7	9

TABLE 2. PLANT COMPONENTS AND RELATIVE IMPORTANCES FOR PWR LARGE-BREAK LOCA AS DETERMINED BY THE EXPERTS PANEL.

Component	Relative Importance		
	BLOWDOWN	REFILL	REFLOOD
Fuel rod	9	1	8
Core	8	8	9
Upper plenum	1	1	9
Hot Leg	1	1	9
Pressurizer	7	1	1
Steam generator	1	1	9
Pumps	9	5	8
Cold leg/accumulators	1	9	9
Downcomer	1	9	7
Lower plenum	1	7	7
Break	9	7	1
Loops	7	7	9

4.1 Phenomena Identification

As mentioned above, this part of the work was performed at INEL by non-panel members knowledgable in LOCA analyses, both experiments and codes. The INEL team reviewed the work of the experts and agreed that the plant had been properly partitioned into components. INEL also agreed with the experts panel on the selection of the highly important phenomena.

Completion of the tables of phenomena was accomplished following an extensive review of large-break LOCA literature. The literature covered most of the domestic experiments and many code calculations. Eventually tables representing each of the three major phases of the LOCA (blowdown, refill, and reflood) were completed. The intent in completing these tables was to include any thermal-hydraulic phenomena thought to occur in a given component regardless of its perceived importance. Figures 1, 2, and 3 present the completed tables of phenomena for blowdown, refill, and reflood, respectively; the format is representative of the hierarchical analysis method described in the next section.

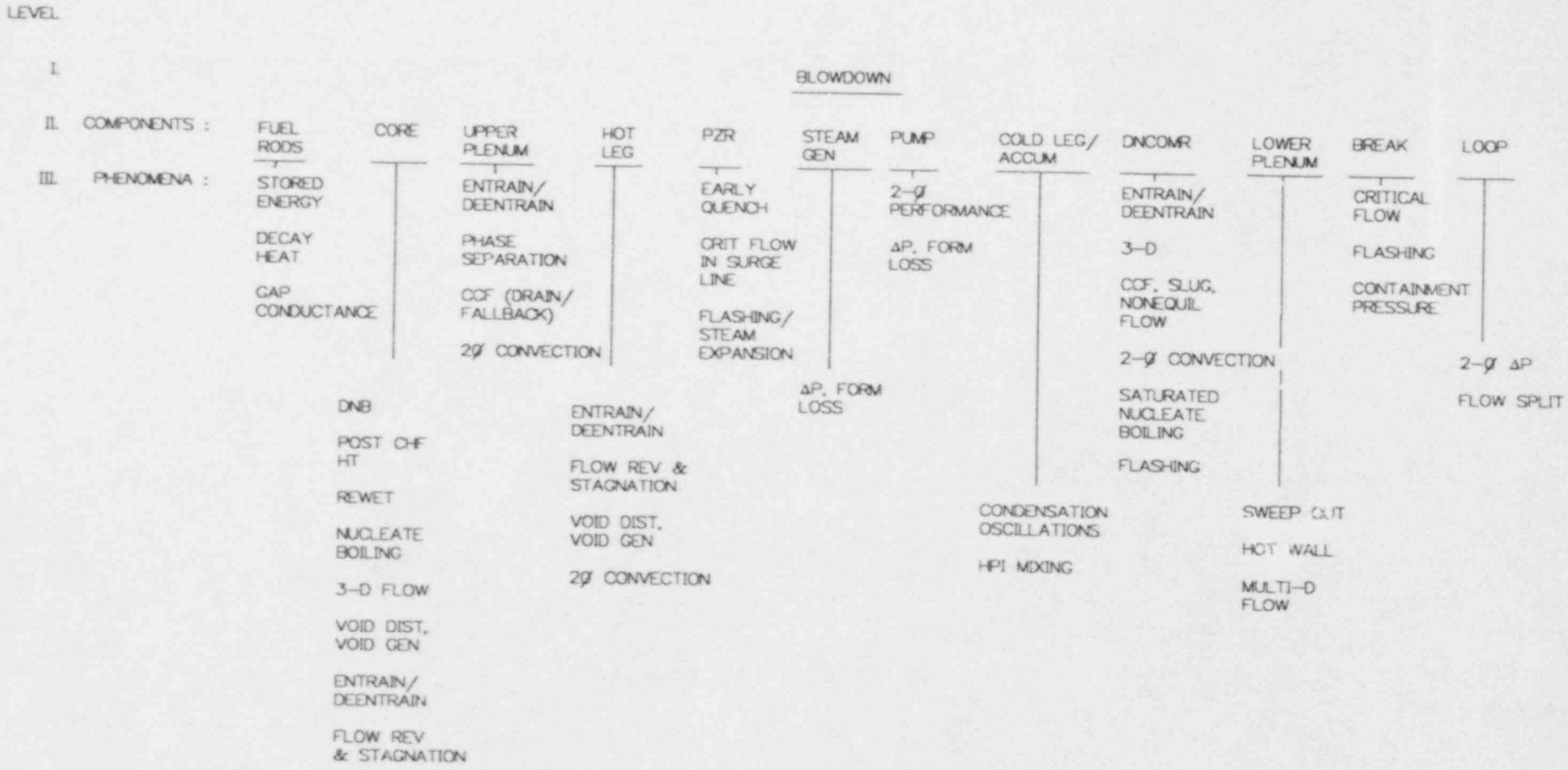

Figure 1. Component and phenomena hierarchy during LBLOCA blowdown.

NSL00715

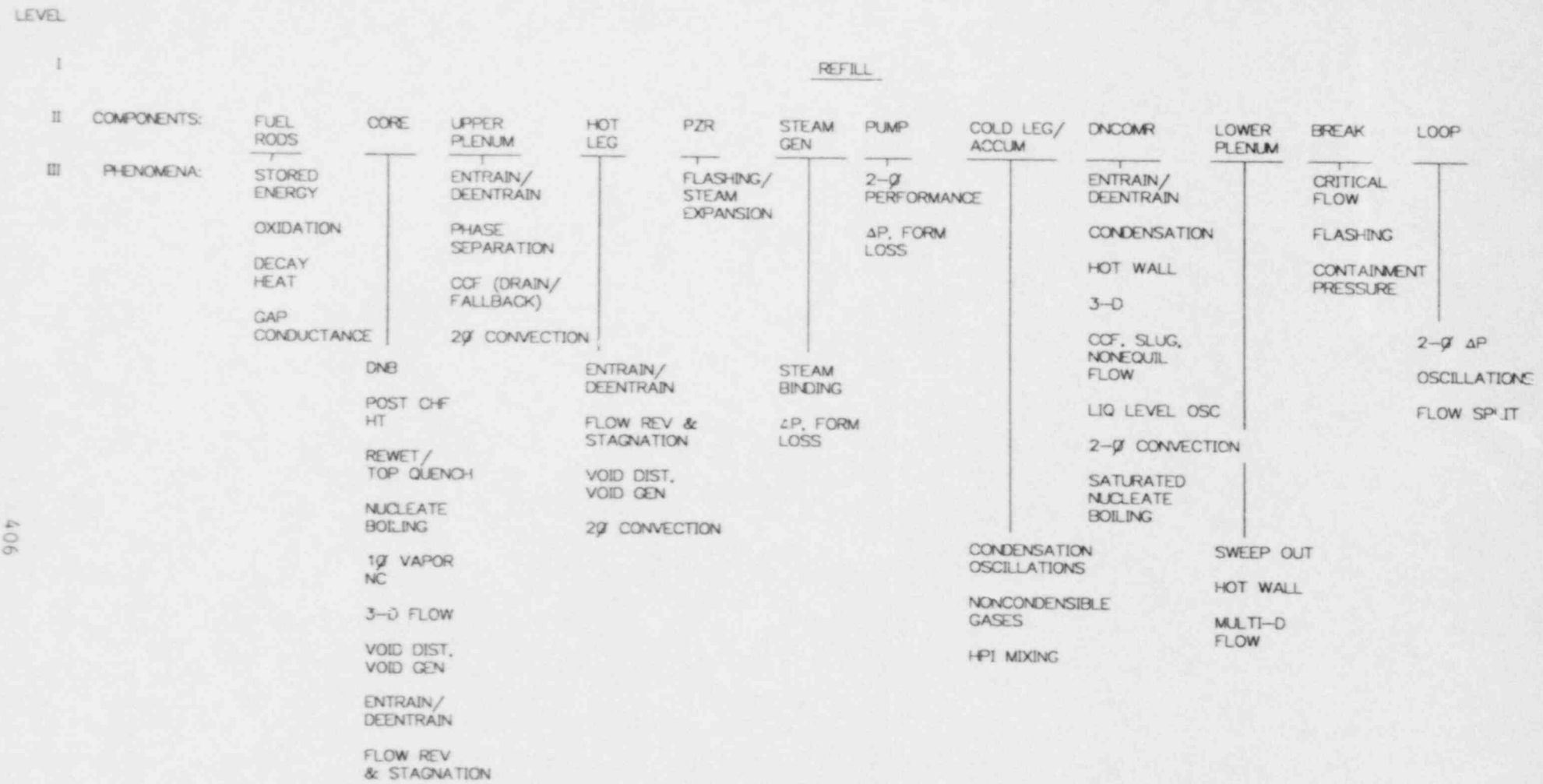

Figure 2. Component and phenomena hierarchy during LBLOCA refill.

NSL00716

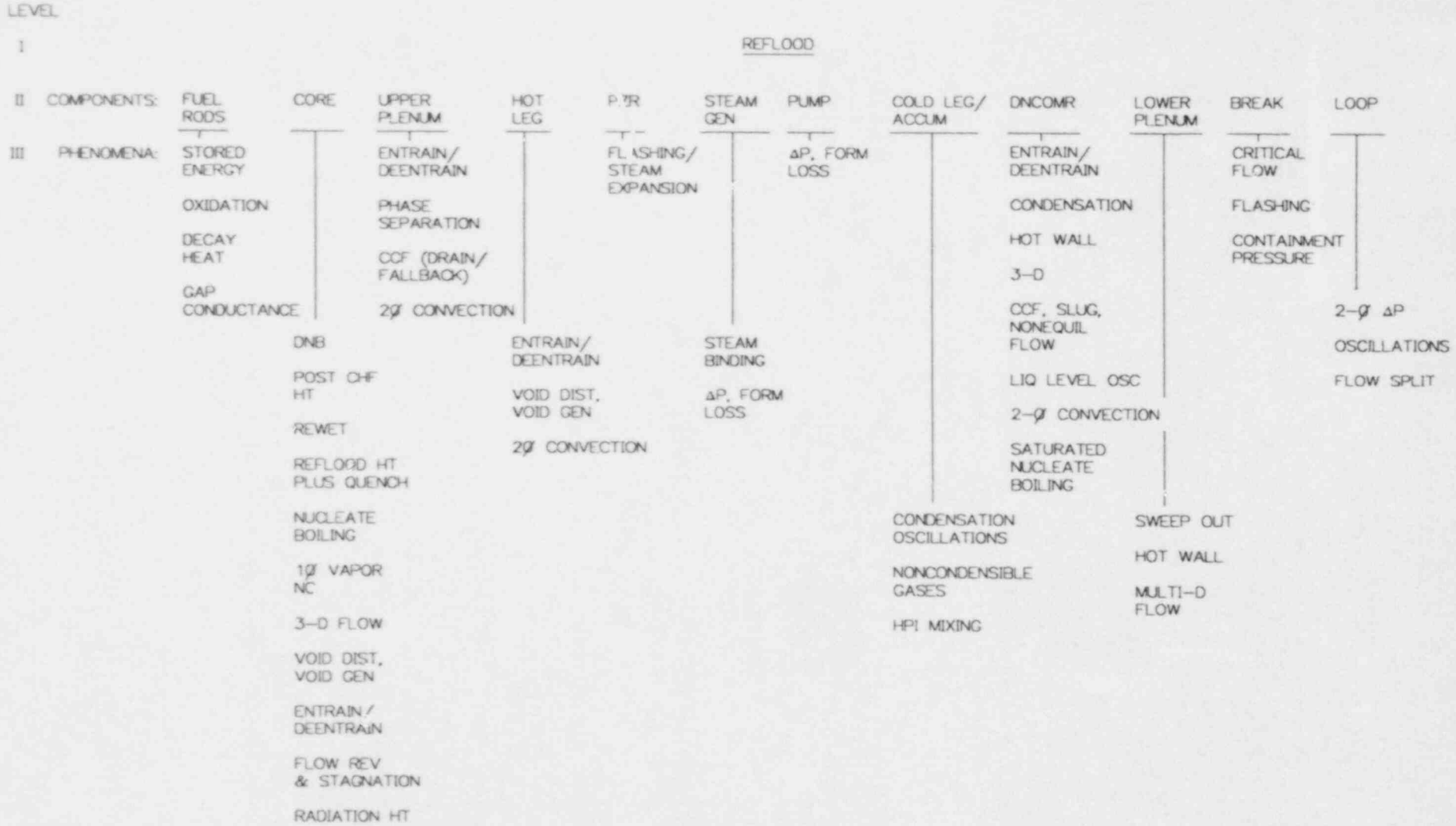

Figure 3. Component and phenomena hierarchy during LBLOCA reflood.

NSL00717

4.2 Importance Analysis

Once the lists of phenomena were prepared, the importance analysis was conducted. The method chosen is called the analytic hierarchy process (AHP). Basically AHP is a method of breaking down a complex, unstructured situation into its component parts; arranging these parts into a hierarchic order; assigning numerical values to subjective judgements on the relative importance of each part; and synthesizing the judgements to determine which variables have the highest importance.[5] By using AHP in the subject application, judgements on the relative importance of LOCA phenomena have to be made on a binary, or pair-wise, basis. Another feature of AHP is that it provides a measure of consistency for the subjective decisions made; too great a departure from perfect consistency indicates a degree of randomness and the need to reconsider some of the judgements. And finally, AHP is easy to understand and use and can be run on basic office computers (i.e., personal computers).

Use of AHP for the current problem required that each phenomenon in a given component be compared to every other phenomenon occurring in the same component and each comparison assigned a rank of 1 to 9. A rank of 9 meant that the first phenomenon was very much more important than the second phenomenon with regard to PCT. For example, referring to Figure 1, if stored energy were ranked a 9 versus decay heat, it would mean that stored energy was considered very much more important than decay heat with regard to PCT during blowdown. A range was also placed on each ranking; this was done to account for the uncertainties the analysts associated with the subjective decision-making process. Ranking justifications and references, where possible, were recorded to provide a permanent record of the rationale used in assigning the ranks.

After performing the initial importance ranking on a pairwise basis for all the phenomena, the hierarchy was input into the AHP program. The AHP then produced the rankings on a system-level basis for comparison with the experts' rankings. The results were then cast into the familiar 1-9 format and are presented in Table 3. Note that a dash indicates that that phenomenon was not included in the analysis of that particular phase of the LOCA (i.e., the phenomenon did not occur or was completely insignificant).

One of the factors that consensus decision-making cannot assure is the consistency of the input. A certain degree of consistency in establishing ranks or priorities is necessary to get valid results. Perfect consistency is not necessary for valid results; however, the judgements could have such low consistency that they appear to be random. The AHP provides a measure of consistency for each set of input. Called a consistency ratio, it should not exceed 10 percent.[5] If the value is more than 10 percent, the judgements may be somewhat random, or inconsistent, and should be revised. The AHP input used in these calculations resulted in consistency ratios of 3.3%, 4.7%, and 3.6% for the blowdown, refill, and reflood hierarchies respectively. It can thus be assumed that adequate consistency exists in the binary ranks.

TABLE 3. SUMMARY OF EXPERTS RANKINGS AND AHP CALCULATED RESULTS

	BLOWDOWN		REFILL		REFLOOD	
	Exp Rank	Base (AHP)	Exp Rank	Base (AHP)	Exp Rank	Base (AHP)
Fuel rod						
stored energy	9	9		2		2
oxidation		-		1	8	7
decay heat		2		1	8	8
gas conductance		3		1	8	6
Core						
DNB		6		2		2
post-CHF	7	5	8	8		4
rewet	8	8	7	6		1
reflood heat transfer		-		-	9	9
nucleate boiling		4		2		2
1-phase vapor nat circ		-		6		4
3-D flow		1		3	9	7
void generation/dist		4		6	9	7
entrainment/deentrainment		2		3		6
flow reversal/stagnation		3		1		1
radiation heat transfer						3
Upper plenum						
entrainment/deentrainment		1		1	9	9
phase separation		2		1		2
CCF drain/fallback		1		2		6
2-phase convection		2		1		5
Hot leg						
entrainment/deentrainment		1		1	9	9
flow reversal		2		1		-
void distribution		1		1		4
2-phase convection		2		2		3
Pressurizer						
early quench	7	7		-		-
critical flow in s.l.		7		-		-
flashing		7		2		2
Steam generator						
steam binding		-		2	9	9
delta-p, form losses		2		2		2
Pump						
2-phase performance	9	9	5	5		
delta-p, form losses		3		3	8	8

TABLE 3. (CONT'D)

	BLOWDOWN		REFILL		REFLOOD	
	Exp Rank	Base (AHP)	Exp Rank	Base (AHP)	Exp Rank	Base (AHP)
Cold leg/accum						
condensation		2	9	9		5
noncondensible gases		-		1	9	9
HPI mixing		-		3		2
Downcomer						
entrainment/deentrainment		2	8	8		2
condensation		-	9	9		2
countercurrent, slug, noneq		1		8		2
hot wall		-	5	4	7	3
2-phase convection		2		3		2
saturated nucleate boiling		1		2		2
3-D effects		2	9	7		2
flashing		1		-		-
liquid level oscillations		-		3		7
Lower plenum						
sweep out		2	7	6		5
hot wall		1		7	7	6
multi-dimensional effects		1		2		7
Break						
critical flow	9	9	7	7		1
flashing		3		2		1
containment pressure		2		4		2
Loop						
2-phase delta-p	7	7		7		6
oscillations		-	7	7	9	9
flow split		7	7	7		2

4.3 Comparison of Results

Both the experts' rankings and the AHP results are included in Table 3. It can be seen that good agreement exists between the two methods. (Note that direct comparisons can be made only against the phenomena ranked by the experts panel.) In over 50% of the cases, the two approaches produced identical ranks. Approximately 80% of the cases were within ± 1; over 95% were within ± 2.

There were a few cases in which the INEL results placed a phenomena in the high-importance category (7-9) after the experts had not, for example, critical flow in the surge line (7) and pressurizer flashing (7) during

blowdown, and countercurrent flow in the downcomer (8) and hot wall effects in the lower plenum (7) during refill. These variations in ranking were resolved as follows.

The INEL analysts and certain members of the experts panel reexamined the potential pressurizer influence on PCT during blowdown. Both experimental[6] and calculational[7] results tended to show pressurizer behavior may be of medium importance (4, 5, 6 rank); thus, it is not likely to be of high important (7, 8, 9 rank) during blowdown. The INEL ranking of selected phenomena in the downcomer and lower plenum during refill tended to be of the same order of importance as the ranking of other phenomena in the components for which there was good agreement between the two methods of ranking. Thus, the INEL results tended to confirm the experts ranking of these two components during refill.

Only one phenomenon produced a significant difference of opinion (>3) between the experts panel and the INEL team. The experts ranked hot wall effects in the downcomer during reflood as a 7, whereas the INEL results using AHP produced a rank of 3. Review of the pairwise rankings that led AHP to produce the lower importance shows that the INEL group believed that most of the energy in the downcomer structure would be removed during the refill phase of the transient and that this phenomena was subject to scale considerations. It was judged that the safer course of action will be to consider the downcomer as highly important during both refill and reflood.

4.4 Sensitivity Studies

It was understood that the importance ranking process was a subjective exercise and, thus, any particular ranking would be open to debate. In an effort to address the sensitivities of the results to realistic variations in individual rankings, a range was applied to the rankings involving the high importance phenomena as determined by the experts panel. A separate AHP run was then performed with the rank of each highly-important phenomenon set to its upper limit, and a second with the rank set to its lower limit. To illustrate, consider the stored energy in the fuel rod during blowdown. The experts ranked it as highly-important; therefore, it was desired to examine the sensitivity of its ranks. In this case, that meant that only the stored energy-vs-decay heat rank and the stored energy-vs-gap conductance rank had to be exercised over their range. (Note that oxidation was not considered during blowdown.) Similar studies were performed for each of the phenomena ranked highly important by the experts panel.

The results of the sensitivity calculations showed that the effects of realistic changes in individual rankings of highly-important phenomena in a certain component were limited to that component. For example, when fuel rod stored energy during blowdown was studied, changes in overall importance ranking was noticed only within the fuel rod component; no changes occurred in phenomena importances in any other component. In addition, the changes that did occur were in general of low significance (<3 units from the baseline calculations). These facts are considered confirmation of the validity of the baseline results.

5. CONCLUSIONS

Based upon two separate assessments, the most important thermal-hydraulic phenomena during the blowdown phase of a large-break LOCA are stored energy in the fuel rod, flow resistance through the pumps, and break critical flow. During the refill phase, condensation in the cold leg and downcomer and 3-D effects in the downcomer are the most important phenomena. Upper plenum and hot leg entrainment, the related steam binding and the effects of noncondensible gases that may enter the system when the accumulators empty are the phenomena of highest importance during reflood. It may thus be concluded that these are the areas upon which the code applicability and uncertainty efforts must be concentrated.

The AHP proved to be a good method to rank the importance of thermal-hydraulic phenomena occurring during a large-break LOCA. The method was simple and inexpensive to use on ordinary office personal computers.

The documentation of individual rankings[8] provides a detailed reference of all reasons for the AHP input and the subsequent uniformity in system level rankings by two methods.

Good agreement was obtained between the results of the experts panel and the AHP analysis, both qualitatively and quantitatively. In over 95% of the comparisons of highly-important phenomena, the difference between the two methods was two or less.

Sensitivity calculations were performed to identify the effects of realistic variations in individual rankings. The principal conclusion drawn from these studies was that the uncertainty associated with an individual ranking was not sufficient to significantly shift the baseline results. This supports the validity of rankings of the high importance phenomena and components.

6. REFERENCES

1. Compendium of ECCS Research for Realistic LOCA Analysis, Draft Report for Comments, NUREG-1230, April, 1987.

2. W. Beckner and J. Reyes, Jr., "Revision of the ECCS Rule", Nuclear Safety, 28, No. 1, January-March, 1987.

3. D. Liles, et. al., TRAC-PF1/MOD1: An Advanced Best-Estimate Computer Code for Pressurized Water Reactor Thermal-Hydraulic Analysis, NUREG/CR-3858, LA-10157-MS, 1985.

4. Code of Federal Regulations, Title 10: Energy, Chap. 1: Nuclear Regulatory Commission, Part 50: Acceptance Criteria for Emergency Core Cooling Systems (ECCSs) in Light Water Reactors.

5. T. Saaty, "Decision-Making for Leaders", Belmont, California, Lifetime Learning Publications, Wadsworth Inc., 1982.

6. C. Davis, Experimental Parameters Sensitivity Study, CAAP-TR-043, February, 1979.

7. G. Johnsen, et. al., A Comparison of Best-Estimate and Evaluation Model Calculations: The BE-EM Study, PG-R-76-009, EG&G Idaho, Inc., December 1976.

8. R. A. Shaw, et. al., Development of a Process Identification and Ranking Table (PIRT) for Thermal-Hydraulic Phenomena During a PWR Large-Break LOCA, to be published December, 1987.

TRAC-PF1/MOD1 UNCERTAINTY QUANTIFICATION FOR LBLOCA BLOWDOWN PCT[a]

K. R. Katsma, R. A. Dimenna, and G. E. Wilson
Idaho National Engineering Laboratory
EG&G Idaho, Inc.
P.O. Box 1625
Idaho Falls, ID 83415

ABSTRACT

Over the past few years, an effort has been made to define and quantify the uncertainty in NRC supported computer programs designed to predict the response of nuclear power plants to hypothetical accident scenarios. This paper describes a method to assess the many mathematical models, correlations, and empiricisms used in the codes, and to determine the uncertainty in their predictive capability due to scale effects, lack of data base, variability in the input or thermo-physical data, plant conditions, etc. The Code Scaling, Applicability, and Uncertainty evaluation methodology is a structured process to analyze the combination of these models and correlations and their numerical representation of interrelated thermo-hydraulic processes that take place during a transient event. It provides criteria to determine their ability to accurately represent the significant phenomena that occur during the transient, and to quantify the uncertainty in the final calculated results. The initial application of the methodology to a large break loss-of-coolant accident is described.

1. INTRODUCTION

In 1974, a set of licensing criteria for nuclear power plants (NPPs) was established by NRC (10CFR50[1]) that required calculations be performed to show that the ECCS would maintain fuel cladding temperatures below a specified limit in the event of a break in a reactor coolant pipe or an inadvertent valve opening. The purpose of the criteria was to prevent cladding oxidation and hydrogen generation. A large amount of conservatism was included, as the understanding of ECCS performance was limited. To account for potential uncertainty, a calculational procedure, Appendix K[1], was defined. Each step of this procedure included conservative assumptions to ensure that calculated cladding temperatures provided a large safety margin.

During the past thirteen years, significant progress has been made in the understanding of ECCS performance during loss-of-coolant scenarios. Computer codes advanced from homogenous equilibrium assumptions to nonhomogenous calculations with separate mass, momentum, and energy equations for vapor and liquid phases. Separate effects experiments have

---

a. Work supported by the U.S. Nuclear Regulatory Commission, Office of Nuclear Regulatory Research under DOE Contract No. DE-AC07-76ID01570.

been conducted to develop and assess models in the codes and study particular phenomena. Integral test facilities have been developed to assess the codes over temperature and pressure ranges typical of those expected during a LOCA transient. Experimental facilities and the improved codes have demonstrated that calculations based on the Appendix K procedure are highly conservative.

The increased understanding of large break LOCA (LBLOCA) and ECCS phenomena lead the NRC to propose a rule change[2] that would allow for best estimate calculations to be used in place of the current Appendix K conservatisms. However, the use of best estimate codes will require that the uncertainty in the calculation be quantified. This uncertainty must then be included with any calculated results used to meet licensing requirements.

The NRC has proposed a Code Scaling, Applicability, and Uncertainty (CSAU) evaluation methodology[3] with several purposes in mind. The one addressed here, is to quantify the uncertainty in thermal-hydraulic codes when applied to nuclear reactor safety analysis. The process is designed to evaluate a) the applicability of the code to simulate various nuclear reactor transients by evaluating and ranking significant phenomena during the transient, b) the ability of the code to represent those phenomena, and c) the uncertainty in the code simulation as measured by comparison to separate and integral effects experiments.

A Technical Program Group (TPG) was formed to develop, implement, and demonstrate the CSAU methodology. The initial application of this methodology has been initiated at the Idaho National Engineering Laboratory (INEL) to quantify the uncertainty in the peak clad temperature for a LBLOCA using the TRAC-PF1/MOD1[4] code.

This paper describes the current work to identify sources of calculational uncertainty in the application of TRAC to the blowdown phase of a LBLOCA transient. It includes the steps taken to minimize uncertainties where possible, and to quantify those that remain. Uncertainty quantification for the refill and reflood time domains will proceed at the completion of the blowdown phase.

2. THE CSAU METHODOLOGY

The NRC has initiated a study to quantify the uncertainty in the peak cladding temperature as computed by the TRAC-PF1/MOD1 code for a large break loss of coolant accident using the CSAU methodology. The methodology is outlined by the flow diagram shown in Figure 1. It represents a structured procedure to identify and quantify the uncertainty in code calculations from four general sources.

The four general sources of calculational uncertainty identified in applications of large thermal-hydraulic codes to reactor accident transients are:

1. Uncertainty from code input. This includes such input specifications as plant operating parameters, initial conditions, and user supplied boundary conditions needed to completely specify the accident transient.

2. Uncertainty from code and experiment assessment. This includes the assessment of code calculational ability through separate effects and integral effects experiment comparisons. Measurement uncertainties and other errors associated with carefully performed experiments would be considered in this category. Though they are not code uncertainties per se, they affect the determination of code calculational capability.

3. Uncertainties from code deficiencies. Code deficiencies are considered those calculational aspects of the code that are not adequately supported by experimental data, that represent only estimated reactor system response, or that are not available to represent a given phenomenon. In these cases, the uncertainty of the code in representing the phenomena is estimated and carried as a penalty on the final calculated result.

4. Uncertainty from differences in scale. Code assessments against experimental data are susceptible to uncertainties because of differences in scale between the experimental facility and the full scale nuclear reactor plant. These scale differences can be manifested as differences in observed phenomena in the experimental facility or as differences in the code calculated response, correctly or incorrectly, as it is applied to different facilities. These effects are quantified and applied to the uncertainty of the final calculated result.

The various steps in the CSAU process as applied to the LBLOCA transient are discussed next.

2.1 Scenario Specification

The determination of code applicability and uncertainty is transient dependent, for the models and correlations exercised in performing the calculation change to represent the local phenomena. Therefore, the selection and application of a computer code to a specified reactor transient requires an evaluation of the transient based on the phenomena that are expected to occur. The transient scenario identifies those processes which have to be addressed and which at a later step will be used to determine the important phenomena and aid in the evaluation of the code models. The CSAU methodology focuses on those processes considered to be important to a specific scenario.

Scoping studies for a LBLOCA have shown that the large double ended cold leg guillotine (DECLG) break is the limiting transient with respect to peak cladding temperature. Such a transient is conveniently analyzed in three time domains, the blowdown phase, or rapid decompression and expulsion of fluid from the vessel, the refill phase when the emergency coolant is injected into the system, and the reflood phase when the core is again

filled with water and the rods quenched. A particular scenario for a large break may indicate that critical flow at the break, rapid pressure changes, transient heat transfer and critical heat flux, degradation of the pumps due to two phase flow, reactivity feedback due to voiding in the core, and initial stored energy in the fuel rods must be modeled for the blowdown phase. Extending the scenario to the ECC injection and refill phase, additional code capabilities will be required for condensation due to ECC mixing, countercurrent flow, and vapor generation. The reflood portion of a large break scenario will require modeling of the complex reflood heat transfer of hot fuel rods, vapor void fraction in the core, entrainment and deentrainment of liquid drops from two phase mixture flow, quench front tracking, and other phenomena.

Specification of the LBLOCA requires a good description of the initial plant conditions. This includes plant power, operating history, plant geometry and components, etc. The scenario description then includes the important phenomena and events that must be considered from initiation of the transient event through the various phases. In addition to the phenomena described above, events such as valve opening and closing, control rod movement, and ECC injection are important.

2.2 Select NPP and Frozen Code

The scenario definition depends on both the type of transient to be analyzed and the particular plant in which it occurs. The present application of the CSAU evaluation methodology will address a four loop Westinghouse (W) pressurized water reactor with 17 x 17 fuel rod assemblies. The plant model will be evaluated from the beginning of the transient (i.e., steady state operation) through core recovery when the fuel rods are quenched.

The CSAU methodology emphasizes the use of "frozen" code version. This ensures that changes to the code after an evaluation has been completed don't impact the conclusions. Calculations, data comparisons, assessments, etc., run with previous versions of the code should not be a part of the uncertainty determination unless it can be clearly demonstrated that any code changes did not affect the calculation of the system variables.

The TRAC code has been selected to perform a LBLOCA analysis. During the past several years, several versions of the code have been released. The current released version is TRAC-PF1/MOD1, Version 14.3, released September 3, 1987. The NRC has specified Version 14.3 should be frozen for this study.

2.3 Code Documentation and QA

The capability of a computer code to model and calculate postulated NPP accident scenarios is provided by the field equations and the closure relations. Adequate documentation of the code must be provided to assess whether the code can be applied to a postulated scenario for a specific NPP. The current documentation for TRAC consists of the code theory manual[4] and users guide.[5] These two documents provide details of the models in the code, information on the numerical solution methods and the

use of the code, and the complete input specifications. Also, there have been assessment reports published[6,7,8,9] for each version of TRAC released.

The CSAU methodology also specifies the need for a code quality assurance (QA) document. This document addresses important questions relating to the ability of the code to perform the required analysis, such as:

1. Are the closure equations adequate to model the phenomena and processes important to the identified scenario?

2. Do the closure relations have the capability to scale up processes from test facility to full scale?

3. What relations have been modified from their source to provide better assessment based on experiments?

4. Is there an effect of tuning on full scale scenarios for which the code may generate non-conservative results?

The objectives of the QA document are to provide detailed information on the closure equations and criteria for their use, describe how they are coded, and provide the technical rationale for using them in the range of interest defined for the scenario.

The Los Alamos National Laboratory is currently preparing a QA document for Version 14.3 of TRAC-PF1. The document will include:

1. Field equations: 1-D and 3-D steam/water equations, noncondensible gas, liquid solute, selection criteria based on flow regimes, and implications of finite differencing.

2. Flow regime map, references, constants if different from references, assumptions, variations in application (interfacial heat transfer, wall heat transfer, interfacial mass transfer, interfacial drag, wall drag), basis for flow regime, assessment, and scaling considerations.

3. Constitutive relations for energy field equations including interfacial heat transfer (condensation, boiling and flashing), wall-to-fluid heat transfer including the correlations, logic, transitions, and the general energy source term.

4. Constitutive relations for mass transfer (condensation and evaporation).

5. Constitutive relations for momentum transport, including interfacial drag and wall drag.

6. Flow process models such as pumps, breaks, fills, steam water separators and others.

7. Heat structure models, including fuel rod conduction, pipe and vessel structure heat conduction, and reactor core power.

The discussion of each model will include the:

- Basis for the model (references, range of data, statement of accuracy)
- Assumptions made in implementing the model
- Constants (original and modifications)
- Model as coded (flow regime dependencies)
- Weighting, averaging, magnitude limits, etc.
- Variations in the application of a correlation, special cases
- Assessments of significantly modified or unpublished correlations
- Effects of applying the correlation outside its data base
- Scaling considerations

2.4 Process Screening and Ranking

The next step in the CSAU methodology is to address the physical processes and those components where the processes occur, and to rank the importance of the processes and components for each phase of the transient. This ensures that the analysis will focus on those aspects of the transient and calculation that are most significant in determining the final results, and that the emphasis of the code analysis will be on those models that have the greatest impact on the conclusions.

Development of a Process Identification and Ranking Table (PIRT) is described as a cost effective and traceable means of ranking the transient phenomena. The details of this process are discussed in a related paper.[10] The PIRT procedure ranks each process or component against every other process or component in a pairwise fashion, and assigns a relative importance of 1 to 9 to the phenomena in each comparison. The pairwise ranks are then assimilated to give an overall ranking based on a preselected hierarchy. The process is specifically designed to allow engineering judgement in the determination of relative importance of phenomena, and provides a measure of the consistency of that judgement in the final results. The result of the process is that the most significant phenomena in the transient have a high rank (9), and the less significant phenomena have lower ranks (down to 1). These ranks are then used to focus the rest of the analysis.

This process has been applied to a LBLOCA scenario and the ranking tables for the important components given in References 3 and 10. For the peak cladding temperature during blowdown, the following components and phenomena are the major contributors:

Component	Phenomena
fuel rod	stored energy
break	critical flow
pump	two-phase degradation

These components and phenomena will receive the primary attention in quantifying the calculation of PCT for the TRAC-PF1 code. Components and processes with lower ranks are examined later, for they are expected to have a less significant effect on the calculational uncertainty.

2.5 Applicability

During the previous steps the transient scenario has been analyzed, important phenomena and the affected components identified and ranked (PIRT) and the code manual and QA reviewed. For the TRAC-PF1/MOD1 uncertainty analysis for a LBLOCA (blowdown phase), the following steps have been completed to determine the applicability:

1. From the scenario, the important processes were identified and ranked. The important contributors to the blowdown PCT have been identified as the fuel rod stored energy, break critical flow, and pump degradation. Each of these phenomena are modeled in the code, and the uncertainty of each will be addressed in the a later section.

2. INEL personnel have met with LANL to review the early QA documentation and no deficiencies with respect to blowdown PCT have been identified. Only the uncertainties in the model coefficients and physical properties have to be quantified. Additional uncertainties in other models will have to be addressed for the refill-reflood phases.

The conclusion from the steps taken to date confirm that the TRAC code is applicable to the present analysis.

2.6 Nodalization of Plant

The ultimate use of the best estimate codes is the application to the safety analysis of full scale NPPs. Plant models are usually large, and often several cases must be run. Therefore, the plant licensing models are normally nodalized with just enough detail to capture the important phenomena. Part of the CSAU methodology is the recognition that the models used for code assessment must use the same noding philosophy as those used for licensing calculations. Otherwise, the determination of code applicability and uncertainty is considerably more complicated.

As shown in the CSAU methodology diagram, the selection of the plant model is an iterative process. This is extremely important, as many of the code closure equations and flow process models were developed with assessment against small scale experiments (SET). The assessment models were typically finely nodalized to determine the ability of the code to simulate real phenomena and to aid the analyst in understanding the test results. For integral test assessment, the nodalization was probably more closely related to that characteristic of an NPP licensing model. Since both SET and IET experiments have been used extensively to assess the codes, it is necessary to relate these nodings to that of an NPP. Nodalization sensitivity studies included as part of the assessment process serve to determine the minimum required nodalization to represent particular phenomena. By then using the same or similar noding for SET, IET, and NPP calculations, potential scaling problems and/or compensating errors may be identified. If potential problem areas are demonstrated, the problems must be resolved during this iterative process or they will have to be resolved in the uncertainty analysis in a later step.

Figures 2 and 3 show a nodalization used to represent the W four-loop model used in the present application. The following procedure was used to define the model.

1. A review of assessment reports of both SET and IET applicable to LBLOCA was made.

2. Based on the initial review, a first model was developed.

3. This model was then reviewed with a group of experienced code applications personnel. Each component was examined based on the PIRT to ensure that the nodalization was sufficient to capture the important phenomena.

4. The final nodalization was compared with integral test assessments thought to be most applicable to the present LBLOCA model. This data base was the LOFT LBLOCA series.

Table I shows a comparison of the noding used in TRAC calculations for the large break series of LOFT experiments, and the noding used for the NPP. The loop modeling is very similar and should adequately describe the phenomena in the loops. The vessel noding is also similar, with added detail in the upper regions of the NPP to capture the geometric detail.

Nodalization can be a sensitive area of the calculation. By performing the process as detailed in the CSAU method, added confidence can be obtained that the plant model will simulate the phenomena for the prescribed scenario.

2.7 Code and Experimental Accuracy

One method of defining code accuracy is to compare code predictions against experimental data. This has been done extensively for the TRAC code through the developmental and independent assessment programs.

Figure 4 illustrates the differences in the peak cladding temperatures (for various rods and elevations) as predicted by a TRAC-PF1/MOD1 model versus experimental values for LOFT test LP-02-6.[11] The arithmetic mean for these points is 2.6K, with a standard deviation of 66K. These results further illustrate the applicability of TRAC to a LBLOCA transient. Additional scatter diagrams have been prepared by Brookhaven National Laboratory (BNL) for the reflood time domain. Other parameters may also be plotted as scatter diagrams to help define uncertainty between code and experiment.

2.8 Scaling and Effect

To some degree, scaling has been addressed in the iterative process described above when defining the plant nodalization. However, it should be stressed that important phenomena must be identified and scaled; otherwise, scale distortion may alter or eliminate one or more of the significant processes.

The primary integral effects test facilities have been scaled by a power-to-volume ratio (P/V) criterion. With P/V scaling, a facility that maintains full elevation of its components with respect to the prototype plant preserves time scales, fluid mass and energy distributions, and velocities. Of primary importance is that the volumetric heat generation and heat removal rates will be the same as the prototype plant, and the rate dependent phenomena will be simulated.

The peak cladding temperature, the principal calculated parameter for the blowdown phase of the LBLOCA, depends not only on the thermal-hydraulic scaling, but also on the fuel rod scaling itself. From a geometrical point of view, the fuel (or heater) rods in the blowdown experiment facilities appear to be full scale. They are generally full diameter and frequently are full length. An energy balance on the fuel rod cladding indicates a few key parameters, perhaps the most significant of which is the local linear heat generation rate (LHGR) governing the time dependent cladding temperature response. Figure 5 shows measured PCT vs. local LHGR. Several integral facilities are included on the plot, including LOFT with 5.5 ft rods, and Semiscale and LOBI with 12 ft rods. The relative consistency of PCT vs. LHGR indicates little effect related solely to the size of the experimental facility. Instead, local parameters appear to be of greater significance, and these parameters are essentially full scale. They are the local LHGR, time to DNB, and the power profile used to drive the experiments. The time to DNB is a function of the power-to-volume ratio used to scale the facility, and the three IET facilities shown in Figure 4 used a consistent P/V. The power parameters and fuel rod material properties all affect the cladding temperature through the initial and transient stored energy, whereas the DNB time and fluid conditions affect the energy removal rate. With the possible exception of heater rod material properties, these factors are generally good approximations to full scale and imply that measured PCT values are good full scale approximations.

2.9 Perform NPP Calculations

In order to quantify the uncertainty for the blowdown PCT, three models have been identified by the CSAU methodology for special evaluation:

1. Stored energy in the fuel rods.

2. Discharge of fluid at the break.

3. Degradation of the pump for two phase flow.

In order to address these contributors, a matrix of calculations is shown in Table 2. The stored energy is primarily determined by the gap conductance (H_g), the fuel conductivity (K_f), and the rod peaking factor (P_f). Another determinent in the heat removal from the clad is the convective heat transfer coefficient (H_c), although to a lesser degree, since even a poor heat transfer coefficient can be expected to remove the clad heat and effect a turnaround. The effects of clad conductivity (K_c) and fuel and clad heat capacity (Cp_f, Cp_c) have been determined by analytical analysis to be very small, and are not included in the uncertainty calculations. Variations in these parameters have been determined from reviews of the thermo-physical parameters in MATPRO and are expected to cover $\pm$95% of the range in data based on a uniform probability distribution.

Variations in the break discharge coefficient have been based on Marviken data, as this is the largest scale data available. Twelve Marviken tests were simulated with TRAC, and the discharge coefficient defined by

$$C_d = \frac{\text{Measured flow rate}}{\text{Predicted flow rate}}$$

From these tests, a nominal C_d was calculated and correlated with L/D for the discharge pipe. This procedure defined a correlation for the nominal value of the discharge coefficient for both subcooled and saturated blowdown, as well as a correlation for standard deviation. From these correlations, the nominal and uncertainty values for the discharge coefficients were defined.

The pump was also evaluated for its effect on the uncertainty in the calculation. The uncertainty in the current TRAC model is due to inadequate accounting for flow rate and pressure dependent ρ_g, ρ_l, and lack of data on specific speed and size effects. A new set of homologous curves was developed based on W 1/3-scale pump data. A mean value of the degradation function and an estimated standard deviation were developed. The model is based on correct specific speed pump data and has an uncertainty band to account for flow rate and pressure effects. In the pump review, data from the Combustion 1/5-scale model and the Creare 1/20-scale model were investigated. Conclusions were that there is some size effect (scaling consideration), and that the small sizes degrade more than the large pump model. Table 2 shows that a wide range of degradation is applied to the pump model (conservative approach).

Table 2 specifies five calculations to obtain the blowdown PCT with uncertainties for the pump, break and stored energy. In order to do this with a minimum of calculations, a special code update was made to be used in conjunction with the TRAC supplemental rods so that the fuel rod parameters can be varied with each rod. Thus, for five full scale runs (nominal, two break flow variations and two pump variations), the sensitivity of the peak cladding temperatures should be obtained. For the matrix shown, 90 temperatures dependent on parameter variations are specified.

The major uncertainties due to the models have been identified and provided for in the calculations. Other factors would be input parameters such as the initial power level, time of life of the fuel rods, etc. However, these are considered uncertainties due to state, and though they may affect the PCT, they are not considered uncertainties with the code itself. If it is deemed necessary, additional calculations can be made to vary several initial conditions.

2.10 Effect of Reactor Input Parameters and State

From the NPP calculations a large number of PCT's are obtained and can be compared. At this point, all that can be determined is the fuel rod for each case that gave the maximum PCT. The importance of the calculations is determined in the next step, in which the variations are accumulated and the uncertainty quantified.

2.11 Combine Biases and Uncertainties

The determination of the uncertainty in the calculation of PCT for LBLOCA has been a question of study for at least eight years. In 1979, EPRI published a statistical analysis of the PCT calculation for the RELAP4/MOD3 code.[12] This was followed by two Sandia reports on the uncertainty in the calculations of RELAP4/MOD6.[13,14] More recent studies at defining the uncertainties were reported at the past two Water Reactor Safety Meetings[15,16,17] which looked at various methods that might be applied to uncertainty quantification. Additional references that address accuracy quantification are given in references 18, 19, and 20.

One of the purposes of the CSAU methodology is to address the proposed rule change related to the licensing procedure. This change would allow best estimate calculations for PCT, with a statement of the "uncertainty" in the calculation.

A first approach may be defined as an "engineering approach". Since the code calculations are very time consuming and costly, a non-probablistic effort which attempts to bound the expected value of PCT is desirable. One approach is to do a sensitivity study by varying the parameters on a one-by-one basis, then adding the results, either algebraically or by root mean squares, to determine an upper bound PCT*. This approach can lead to a statement such as:

"It is believed that PCT < PCT* under all reasonable circumstances".

However, it must be stated that there is no statistical significance to this statement. No statement can be applied that indicates a level of confidence or other statistical measure. However, if only positive contributors are used, this approach should give a conservative result, and could be as large a conservatism as used for present licensing criteria, though this is not expected.

A first statistical approach might be the "linear error propagation"[21,22] or "derivative" method. This method assumes that the variations about the mean are not large (Taylor series approximations) and that the derivatives required can be obtained. This method may work well for submodels where the derivatives can be obtained analytically. However, for the TRAC code, the derivatives would have to be obtained numerically, and the procedure may not be as easy to apply. If the PCT is relatively smooth for the wide range of the variables that are being used in the blowdown PCT calculations, suitable results may be obtained.

The probablistic procedure that has been applied to the nuclear thermal-hydraulic codes to date has been the response surface methodology. In this procedure, the concept is to replace the long running computer code by a simple algebraic equation. However, a certain number of full plant calculations are required to determine the algebraic function. If there are a large number of parameters with uncertainty, then a large number of plant calculations are required.

In the CSAU methodology, engineering judgement is used extensively in defining key processes, key variables, significant events, etc. With these defined, many of the variables may be considered not significant, and the number of parameters that must be considered reduced. If this set is small enough, a statistical approach such as response surface becomes more realistic. From the process screening and ranking, for the LBLOCA blowdown PCT, six major contributors have been identified. If, for each of these contributors, a probability density function (pdf) can be defined, a probabilistic approach may be used. A uniform pdf, which implies "zero knowledge", can be used if a more definable pdf such as a normal distribution cannot be defined. With the probabilistic study, the statement of uncertainty can be expanded from an "engineering" statement to a "statistical" statement, such as

$$\Pr \{PCT < PCT^*\} = \alpha$$

The uncertainty may then be stated as "the probability that the calculated PCT is within α of the PCT*" has been determined with a certainty of some percent, based on the range of the input uncertainties.

In the present application, it is planned to investigate all three combinations, addition, linear error propagation, and response surface for the blowdown PCT. A large number of experiments and previous response surface calculations indicate the feasibility. However, extending some of the procedures to the refill-reflood phases has not been tested. Many more parameters and phenomena would have to be evaluated, and the procedures may be to difficult to apply.

2.12 Total Uncertainty

The total uncertainty is obtained by adding the uncertainties due to:

1. Code and experiment, as stated in Section 2.7.

2. Scaling as discussed in Section 2.8.

3. Code deficiencies as discussed in the applicability section 2.5.

4. Reactor plant parameters and state from Section 2.9, 2.10.

The total uncertainty is specified by

$$\Delta PCT = \Delta PCT(1) + \Delta PCT(2) + \Delta PCT(3) + \Delta PCT(4)$$

This ΔPCT is then a measure of the uncertainty of the code calculation for PCT. We note that three of these pieces of uncertainty are engineering based. The fourth term may be "engineering based" or "statistically based". However, the result is considered an error band for the calculation, and not a probabilistically based statement of confidence.

3. STATUS OF APPLICATION OF THE CSAU METHODOLOGY

The CSAU methodology is now being applied to the TRAC-PC1/MOD1 code at INEL. Some of the analysis has been completed, such as the definition of the plant model, process identification and values of input parameters, etc. The QA document is being prepared at LANL.

The Cray XMP computer system using a UNI-COS based operating system has been installed at the INEL in September. Version 14.3 and the special version of 14.3 for the uncertainty study are being implemented on this system. The steady state and transient input decks have been prepared by running on Version 14.0 at Kirtland AFB on a Cray system under CTSS. It is planned that the calculations will be initiated in October.

4. ACKNOWLEDGEMENTS

The CSAU evaluation methodology has been established by the NRC and its consultants and contractors. In preparing for the application of this procedure, the NRC, consultants to the NRC, and the national laboratories are all contributing to the process. A significant amount of the effort has been due to the Technical Program Group (TPG) of the NRC. Personnel form the national laboratories at Los Alamos and Brookhaven, as well as Idaho have been significant contributors. The input and support of the various groups will significantly aid in the application of this methodology to the TRAC code and a LBLOCA analysis.

5. REFERENCES

1. Code of Federal Regulations, Title 10: Energy, Chap. 1: Nuclear Regulatory Commission, Part 50: Acceptance Criteria for Emergency Core Cooling Systems (ECCSs) in Light Water Reactors.

2. Beckner, W. and Reyes, J., Jr., "Revision of the ECCS Rule," Nuclear Safety, 28, No. 1, January-March, 1987.

3. Compendium of ECCS Research of Realistic LOCA Analysis, Draft Report, NUREG-1230, April 1987.

4. TRAC-PF1/MOD1: An Advanced Best-Estimate Computer Program for Pressurized Water Reactor Thermal-Hydraulic Analysis, NUREG/CR-3858, July 1986.

5. B. E. Boyack, et. al., TRAC User's Guide, NUREG/CR-4442, November 1985.

6. T. D. Knight, et. al., TRAC-PD2 Developmental Assessment, NUREG/CR-3208, January 1985.

7. T. D. Knight, et. al., TRAC-PD2 Independent Assessment, NUREG/CR-3866, June 1984.

8. B. E. Boyack, et. al., TRAC-PF1 Developmental Assessment, NUREG/CR-3280, February 1983.

9. M. S. Sahota, F. L. Addessio, TRAC-PF1/MOD1 Developmental Assessment, NUREG/CR-4278, August 1985.

10. R. A. Shaw, et. al., Development of a Process Identification and Ranking Table (PIRT) for Thermal-Hydraulic Phenomena During a PWR Large Break LOCA, to be published, December 1987.

11. T. D. Knight, TRAC Analysis of LOFT LP-02-6, LA-UR-85-3723, October 1985.

12. J. A. Marshall, et. al., Application of Statistical Evaluation Methodology to the RELAP Code, EPRI NP-1053, April 1979.

13. G. P. Steck, et. al., Uncertainty Analysis for a PWR Loss-of-Coolant Accident: 1. Blowdown Phase Employing the RELAP4/MOD6 Computer Code, NUREG/CR-0940, January 1980.

14. M. Berman, I. J. Hall, Uncertainty Analysis for a PWR Loss-of-Coolant Accident: 11. Alternative Core Damage Estimators, NUREG/CR-1364, May 1980.

15. G. E. Wilson, et. al., "Development and Application of Methods to Characterize Code Uncertainty", Thirteenth Water Reactor Safety Information Meeting, October 1985.

16. L. N. Kmetyk, et. al., "Methodology for Code Accuracy Quantification", Thirteenth Water Reactor Safety Information Meeting, October 1985.

17. F. Odar, R. G. Hanson, "Code Uncertainty Quantification", Fourteenth Water Reactor Safety Information Meeting, October 1986.

18. M. Majumdar, et. al., Review of the Methodology for Statistical Evaluation of Reactor Safety Analysis, EPRI 309, September 1975.

19. R. L. Iman, J. C. Helton, A Comparison of Uncertainty and Sensitivity Analysis Techniques for Computer Models, NUREG/CR-3904, March 1985.

20. L. N. Kmetyk, et. al., Independent Code Assessment: Sandia-Proposed Accuracy Quantification Methodology, NUREG/CR-3969, August 1986.

21. M. E. Cunningham, et. al., Application of Linear Propagation of Errors to Fuel Rod Temperature and Stored Energy Calculations, NUREG/CR-1753, October 1986.

22. Y. Beers, Introduction to the Theory of Error, Addison-Wesley Publishing Company, Inc., 1953.

TABLE I. COMPARISON OF NODING FOR LOFT LARGE BREAK ANALYSIS AND THE SELECTED NODING FOR THE NUCLEAR POWER PLANT

Component	L2-2	L2-3	L2-5	LP-02-6	NPP
Hot leg	8	8	8	8	5
Pressurizer	3	3	3	3	5
Surge line	3	3	3	3	3
SG primary	10	10	10	10	10
SG secondary	7	7	7	7	7
Pump suction	3	3	3	3	5
Pump	2	2	2	2	2
Cold leg	5	5	5	5	4
Accumulator and ECC	8	8	8	8	12
Vessel	192	192	192	192	180
Lower plenum (axial)	3	3	3	3	3
Core (axial)	5	5	5	5	5
Upper plenum (axial)	4	4	4	4	7
θxrxZ	4x4x12	4x4x12	4x4x12	4x4x12	4x3x15
Reference	PF1 Assessment	PD2 Assessment	PD2 Assessment	LA-UR-85-3723	TPG Minutes

TABLE 2. INITIAL CALCULATIONS TO BE MADE TO DETERMINE PCT

	Gap Variation	Fuel Conductivity	Convective HT Coeff.	Rod Peaking Factor	Combination
CASE 1 Nominal Case	None	None	None	None	None
CASE 2 Increased Break Flow +1σ	±46% ±80%	+5,10% -10%	±25% ±50%	-5.6% +2.8% +5.6%	Hg -46% K_f -10% Hg -46%, H_{conv} -25% Hg -80%, H_{conv} +50% Hg +80%, H_{conv} -50%
CASE 3 Increased Break Flow +2σ	↓	↓	↓	↓	↓
CASE 4 Increased Pump Degradation +1.3σ	↓	↓	↓	↓	↓
CASE 5 Increased Pump Degradation +3.6σ	↓	↓	↓	↓	↓

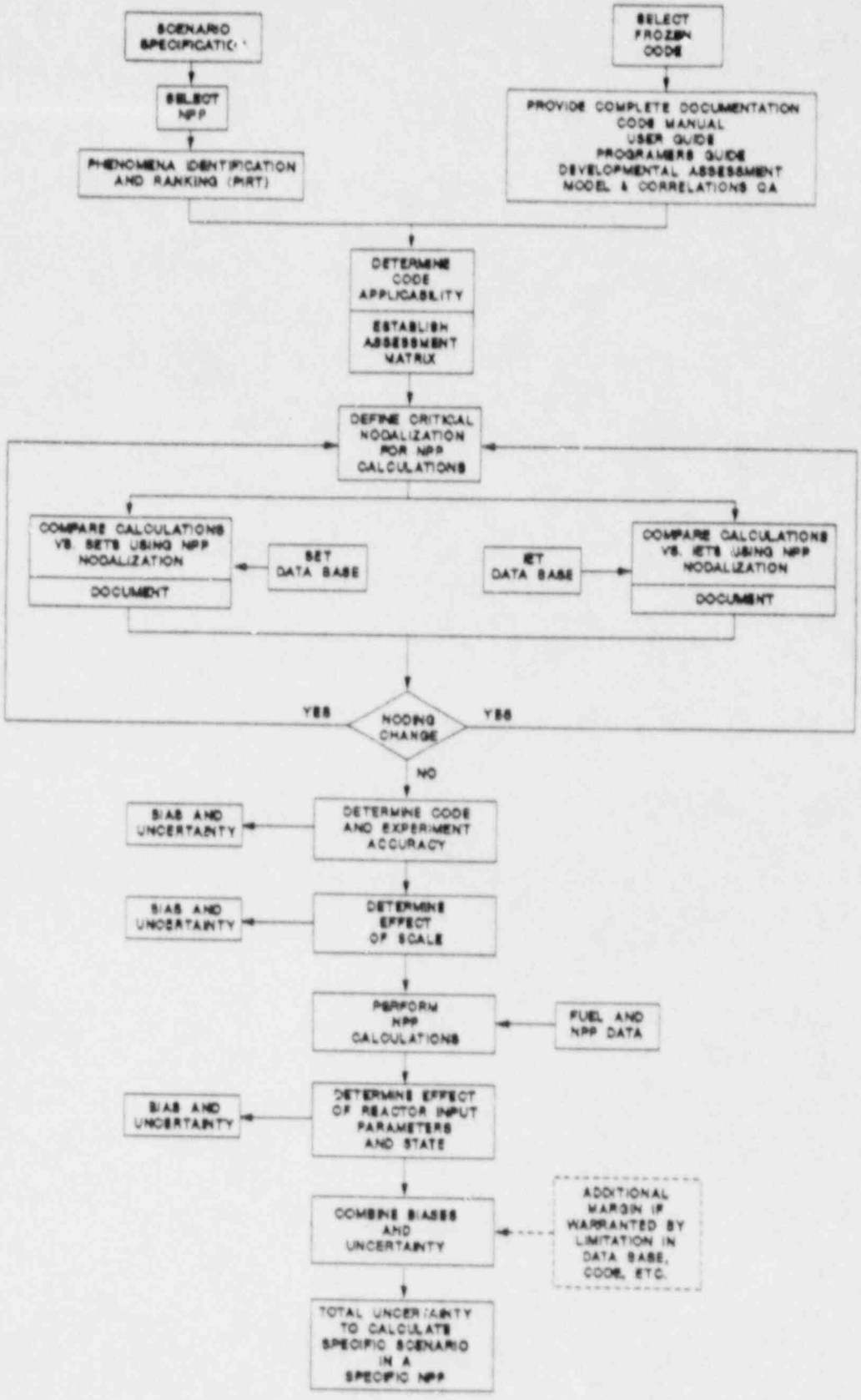

NSL00755

Figure 1. Code scaling, applicability and Uncertainty (CSAU) Methodology

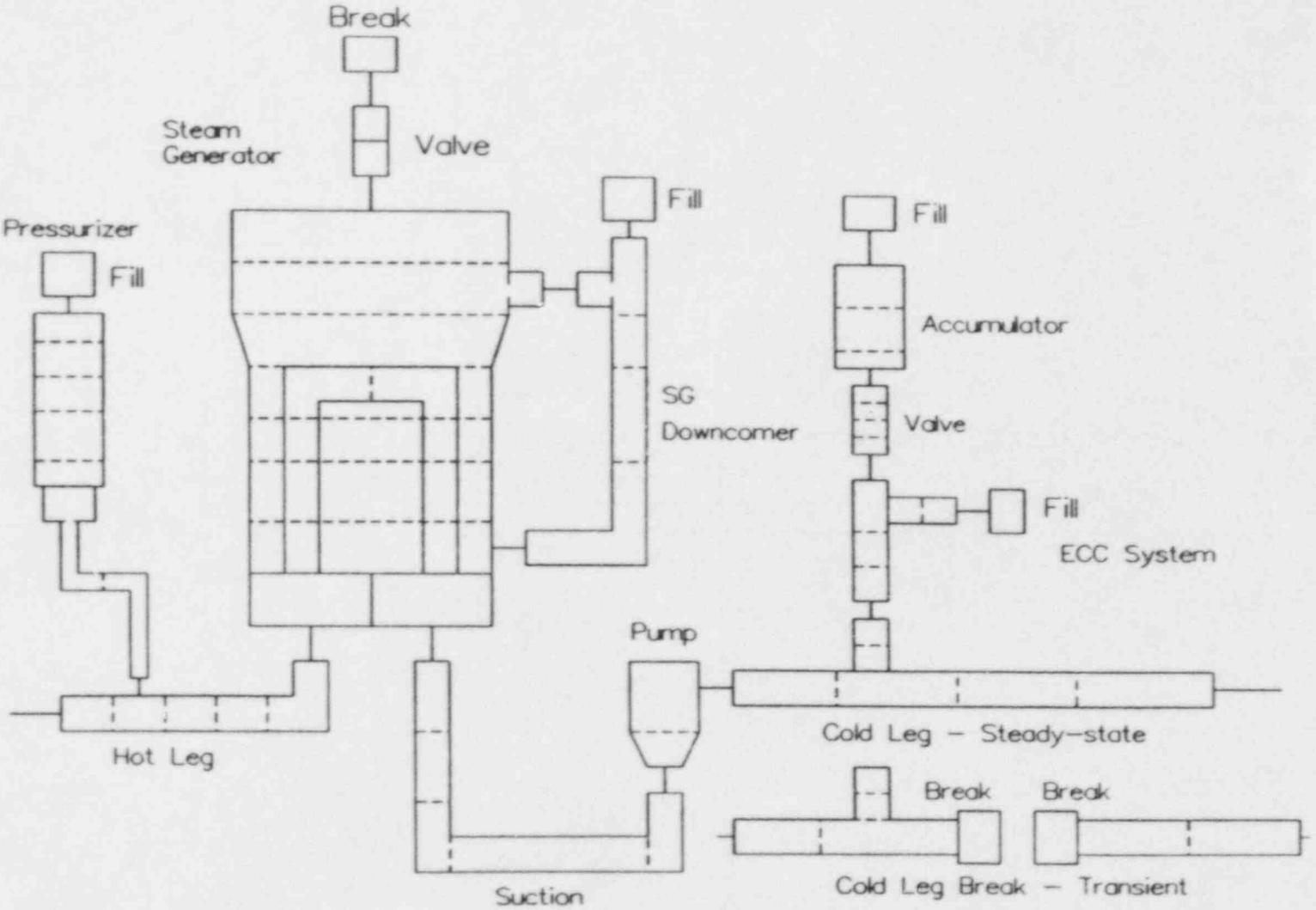

Figure 2. Loop noding.

NSL00689

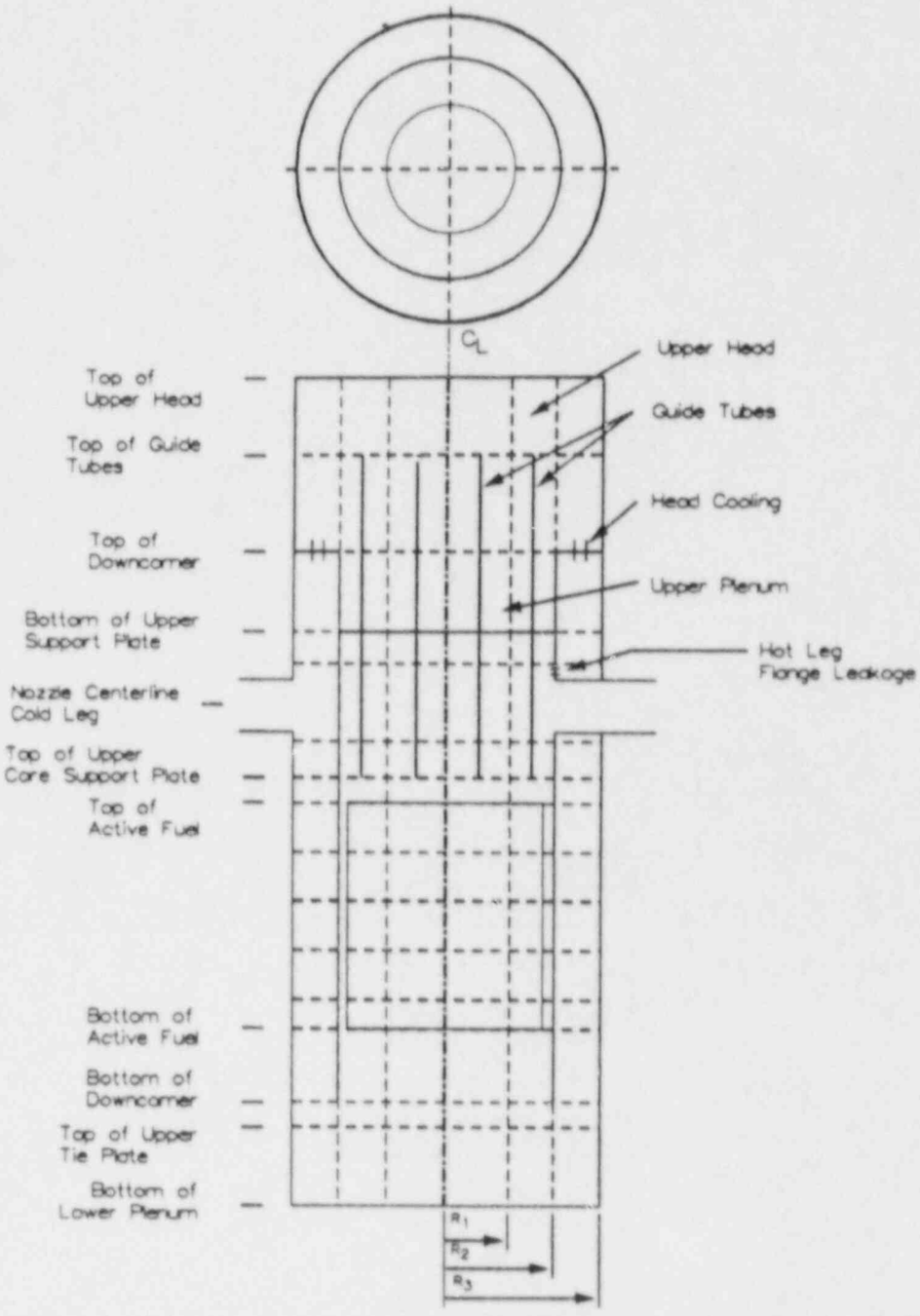

Figure 3. Vessel axial noding.

NSL 00692

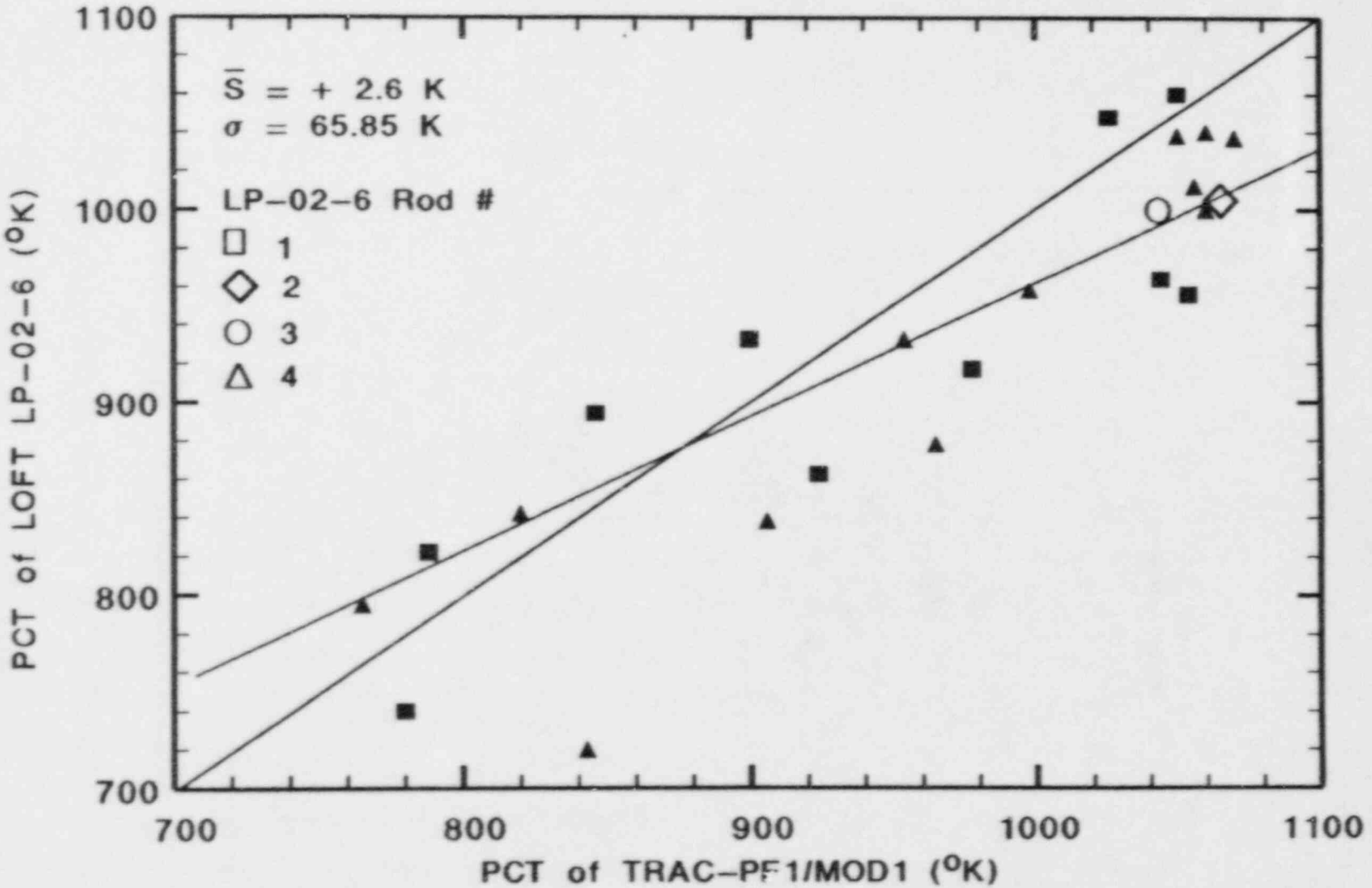

Figure 4. Experimental PCT vs. calculated PCT for LOFT LP–02–6 and TRAC–PF1/MOD1.

NSL00732

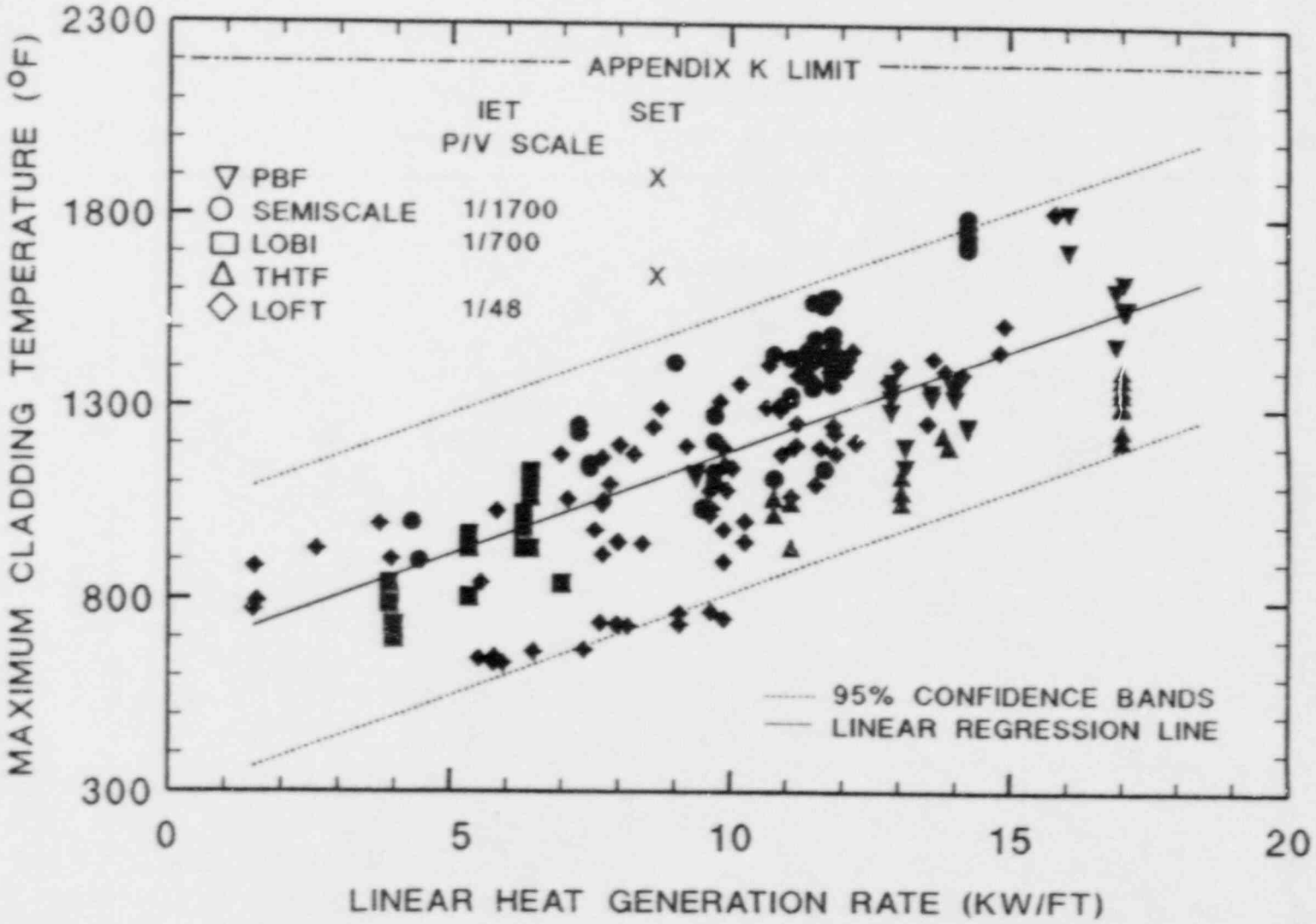

Figure 5. Maximum cladding temperature vs. linear heat generation rate.

NSL00735

THERMAL STRATIFICATION TESTS IN HORIZONTAL FEEDWATER PIPELINES

L. Wolf*; U. Schygulla; M. Geiss*; E. Hansjosten
Kernforschungszentrum Karlsruhe GmbH, Project HDR,
Postfach 3640, 7500 Karlsruhe 1, FRG
*Battelle-Institut e.V., Am Römerhof 35,
D-6000 Frankfurt/Main, FRG

ABSTRACT

In recent years a particular form of crack formation has occured in a number of BWRs und PWRs at the internal surfaces of horizontal feedwater piping upstream of the reactor pressure vessels or steam generators, respectively. To obtain more detailed and consistent sets of experimental data for fluid and inside/outside pipe wall surface temperatures to assess the effects for load combinations resulting from thermal shock, stratification and striping phenomena, an experimental test program, abbreviated TEMR, T33, has been performed at the large-scale HDR-facility under close to realistic conditions. This paper summarizes some of the major experimental findings from out of 25 experiments representing typical BWR and PWR conditions. Informations are also provided about the mixing layer height, thermal characteristics and the heat transfer coefficient. A first assessment of the comparison between blind pre-test predictions using simple engineering models and sophisticated, multi-dimensional codes and experimental data is provided.

1. INTRODUCTION

In recent years a particular form of crack formation has occured in a number of PWRs and BWRs on the internal surfaces of horizontal feedwater piping upstream of the steam generators and reactor pressure vessels, respectively. The cracks were concentrated on the lower piping halves and their orientation was circumferential.

Under low power conditions and hot standby or during startup and shutdown processes the feedwater mass flow is reduced to a few percent of the rate at full power. Under such conditions stratified flow develops and leads to the formation of a rather thin, separating mixing layer between the cold and hot fluid regions: its height depends primarily on the mass flow, the exit conditions and the density ratio. This phenomenon of temperature stratification was confirmed by numerous in service measurements in both PWR- and BWR-plants /1-4/ and in laboratory test models /5-6/.

Whereas in-plant measurements are primarily hampered by lack of instrumentation in the fluid and at the inside pipe surface, the scaled down laboratory experiments mostly resorted to simulating fluids under atmospheric conditions in transparent facilities leaving the question about proper extrapolation towards prototypical conditions.

The measurements revealed that slight changes in the flow rate cause the separating layer to be raised or lowered inside the horizontal pipe section. The stratified flow changes back to the so-called slug flow at approximately 6 % of full load flow when the layer height reaches 9/10th of the pipe diameter.

Thermal stratification causes an azimuthally varying temperature distribution in the pipe and results in a stress distribution which resembles that of a bimetallic strip. In the hot upper region of the pipe compressive stresses develop as a results of constrained expansion. Since the pipe is flexible, the thermal moment gives rise to a bending stress which is superimposed on the membrane stress. These low-cycle axial and tangential stresses due to stratification depend on

- the interface level
- the mixing zone height

These thermal stresses vary both in magnitude and sign as the hot/cold interface is raised or decreased by altering the feedwater flow rate to maintain the steam generator inventory.

The separating mixing layer between cold and hot fluid regimes is characterized by a wavy-type interace subjecting the pipe inside surface in its vicinity to fluctuating thermal loads. The frequency of the fluctuation depends on a variety of flow parameters. The high-cycle thermal fluctuations cause the portion of the pipe circumference in the mixing zone be subjected alternately to cold and hot water. Typical frequencies were found to be in the range of 0.1 to 10 Hz. Thus, the pipe surface in this zone is locally loaded between low- and high cycle thermal fatigue. Due to the finite value of the heat transfer coefficient at the inside pipe surface, the peak pipe inside surface temperature variation is always less than the peak fluid temperature variation. Under typical conditions and the range of frequencies cited above, the peak pipe inside surface temperature variations range between 25 % and 50 % of the imposed fluid temperature fluctuations. The actual magnitude of the high-cycle alternating thermal stress at the inside pipe surface depends on the:

- peak-to-peak fluid temperature difference
- heat transfer coefficient
- physical pipe properties

Analysis have shown that these high-cycle stresses primarily affect the pipe inside surface and attenuate rather fast towards the outside pipe surface.

Combining all of the thermal stress components cited above can easily account for the type of crack formations experienced in BWR and PWR feedwater lines. Analytical results suggest that thermal fatigue usage factor can approach unity in rather short periods of operation.

The technical solution of this problem necessitates a reduction of the potential for stratification and of the temperature differences. Remedial actions comprised of changes in the construction of the feedwater spargers

both for BWRs and PWRs together with accompanying changes in the operational guidelines have been developed and implemented in the German plants /7/.

In order to examine the major stratification phenomena listed above for both BWRs and PWRs upon temperature and stress distributions, under close to realistic conditions, the HDR-test series TEMR, T33, was performed during the second half of 1986. The major objectives of this test series were:

1. Examination of the hydraulic and thermal behavior of stratified layers in horizontal pipe sections
2. Measurement of azimuthal pipe inside and outside wall temperatures
3. Determination of mixing zone heights for different cold layer heights, their respective amplitudes and frequencies of the temperature fluctuations
4. Determination of thermal shock and thermal stratification phenomena during the initial cooldown period and at steady-state-conditions
5. Measurement of the developing flow pattern in the cold and hot fluid regions, respectively by fluid velocity measurements using temperature correlation technique.
6. Determination of stresses from strain gage measurements around the pipe circumference
7. Examination of global pipe deformations due to stratification effects
8. Measurement of detailled strain distribution field in the elbow with imposed, highly asymmetric internal temperature distribution

2. EXPERIMENTAL FACILITY AND INSTRUMENTATION

Fig. 1 shows the isometry of the complete piping system and components constituting the experimental test section for the TEMR-test series. This pipe system consists of many pipe sections of different geometries (diameter, wall thickness, etc.) assembled to form the total system. This system is fixed at its one end at the concrete structures of the containment walls and welded to the S-nozzle at the RPV on its other end. The most important pipe section of interest for the TEMR-experiments is the horizontal section between the S-nozzle and the first elbow where the stratefication into the horizontal pipe initiates from the cold fluid which ascends from the cold water inlet shown in Fig. 1.

Further details of the horizontal pipe section are provided in Fig. 2. The inside diameter of the pipe is 397 mm, its lengths close to 6 m. Along its length, several measurement sections have been inserted as shown schematically in Fig. 2.

The pressure vessel nozzle is protected by a thermal sleeve as shown in Fig. 3. As the insert A and Fig. 3 shows, the thermal sleeve is not welded to the pipe but is pressed tightly against it by virtue of a plastic belt.

In order to enable a continuous, uninterrupted facility operation and measurements for both BWR (with sparger) and PWR (without sparger), an orifice manipulator was developed and installed at the inlet of the thermal sleeve as shown in Fig. 2. Details of the orifice manipulator are depicted in Fig. 4, which shows how the oblong, details of which are shown in Fig. 5, slides hydraulicly driven in front of the thermal sleeve.

Fig. 5 indicates that for the BWR-typical experiments the slit-type orifice is used as shown in the upper part of the figure, whereas for the simulation of the builtup and decay of hot water pocket at pipe or component discontinuities, the orifice with the narrow slit at its bottom is used. The open flow cross-sections of the individual slits and their respective arrangements have been scaled to simulate the rows of holes in a typical BWR feedwater sparger.

For PWR-typical TEMR-experiments, the complete oblong in front of the thermal sleeve is withdrawn such as to provide the whole free flow cross-section of the horizontal pipe into the pressure vessel.

The selection of the sensor types and their applications rests upon the excellent experience, accuracy and reliability obtained from the foregoing HDR thermal mixing experiments /8, 9/.

The most important data taken during the TEMR-experiments are the fluid and pipe surface temperatures, the fluid velocities in the lower and upper portions of the stratification pipe and the strains at the inside and outside pipe surfaces.

For the measurement of temperatures, thermocouples with hot junction and a magnesium insulated stainless steel jacketed cable have been used. The diameter of the hot junction has been swagged down to 0.5 mm. A typical arrangement of a pair of thermocouples welded at the pipe inside surface by virtue of a small foil with thickness of 75 µm is shown in Fig. 6. The L-shaped sensor measures the fluid temperature 10 mm away from the pipe surface.

The thermocouples used for measuring the temperature fluctuations needed to determine the fluid velocity by correlation technique /10/ have a hot junction diameter of only 0.25 mm with a response time of 11 ms. In order to obtain two velocity components, always one triplet of thermocouples is applied as shown in Fig. 7 which also depicts the thermocouple rates to accurately position the sensors into the pipe axis. This rake is also used to mount seven L-shaped fluid thermocouples in order to follow the interface between cold and hot flow regions.

For the application of strain gages at the pipe in- and outside surfaces, two different types have have been developed:

inside: Platin/Wolfram alloy wire with a steel jacket wire
outside: Nickel/Chrome alloy wire with a Teflon jacket wire

The gages are of half-bridge type with a dummy strain gage for the temperature compensation of the thermal coefficient of resistance. All strain gages are attached at the surfaces by spot welding. At all important strain gage positions additional wall thermocouples are applied as close as possible to the strain gages.

Large efforts have been put into the application of consistent triplets of thermocouples in the fluid and at the inside/outside pipe wall surfaces, respectively in different axial planes and around the pipe circumference Fig. 8 gives a schematic overview of the axial, radial and azimuthal thermocouple positions in the primary measurement pipe section I (compare Fig. 2). The thermocouple rake carries at its top and bottom two thermocouple triplet arrangements for determining the velocity components by the method of temperature fluctuation correlation and a series of axially distributed fluid thermocouples for obtaining center-line temperatures. The triplets of thermocouples in the fluid and at the pipe surfaces together with their azimuthal positions are depicted in the radial cross-section. One angular segment has been especially densely instrumented in order to get optimal resolution of hydraulic and thermal characteristics of the mixing layer. One triplet is positioned every 2.5^{o} from 90 to 105^{o} over this segment. The associated circumferential distribution of pairs of axial and azimuthal strain gages is shown in Fig. 9 together with the additional thermocouples. As shown in Fig. 9, three and six strain gage pairs are mounted at the inside and outside pipe surfaces, respectively.

Additional informations about the TEMR-test facility and its associated measurement plan are given in the respective design report /11/.

3. TEST MATRIX

In order to comply with all of the major issues of the test objectives for both BWR and PWR conditions a test matrix had been designed /11/ consisting of a total of 25 experiments as shown in Table I which can be grouped into the following categories:

A. Experiments T33.1 through T33.13: BWR conditions
B. Experiments T33.14 through T33.19+25: PWR condition

The remaining five experiments (T33.20-24) were devoted towards the examination of the builtup and decay of hot water pockets. The range of system pressure examined was between 1 to 40 bar with the cold water inlet temperature always kept at $30^{o}C$ and the initial hot fluid temperature ranging between $100^{o}C$ and $250^{o}C$ according to the system pressure. This spectrum of experimental conditions together with the range of cold fluid volumetric flow between 0.0008 and 0.013 m^3/s was anticipated to result in cold fluid heights between 0.1 and close to 0.4 m. Further details about the test matrix are provided in /11/.

4. EXPERIMENTAL RESULTS AND DISCUSSIONS

4.1 Introduction

In the following, experimental data for the BWR-Test, T33.9, and the PWR-Test T33.19 (compare Table I) will be shown. Both experiments are characterized by about the same height of the cold fluid layer in the region of densely applied instrumentation. The initial conditions for the two experiments were as follows:

T33.9: P = 40 bar; T_h = 250°C; T_c = 30°C; V = 0.00078 m^3/s
T33.19: P = 20 bar; T_h = 212°C; T_c = 30°C; V = 0.0013 m^3/s.

Comparisons with some results of blind pre-test predictions are presented for T33.7 and T33.9.

4.2 Fluid and Pipe Surface Temperature Histories

4.2.1 BWR-Test T33.9

Fig. 10 shows the transient fluid temperatures at angular positions between 90° and 105°. The time zero has been set to coincide with the time of the arrival of the cold water at the first thermocouple at the bottom of the feedwater pipe just downstream from the elbow. First, a precursory cooldown due to conduction starts because of thermal shock at positions below 105°. Then, starting at 60 sec a rather instantaneous thermal shock affects the position at 105° when the cold liquid layer reaches this height which is accompanyied by large amplitude temperature fluctuations. The slope of the cooldown shock decreases starting at 120 sec. For positions higher than 105° cooldown thermal shocks are delayed and gradients milder. The position of 90° obviously remains under hot fluid conditions throughout the whole transient. The cooldown results in a temperature drop of more than 210°C within 4 min at position 105°C. Besides the transient cooldown there is a remarkable change of thermal fluctuations noticeable from position to position, with higher amplitudes at position 95° than at 100°, 105° or 90° respectively. This is indicative of the mixing zone which may exist in the segment between 95° and 100°. Temperature fluctuations of about 30°C prevail and last over the whole time span.

Fig. 11 shows the responses of the associated inside surface thermocouples at the same angular positions as the fluid thermocouples discussed above. As compared to Fig. 10 temporal gradients are smaller and fluctuations are substantially damped by boundary layer and conductive effects. A careful comparison of the traces for the sensors at 90° and 95° reveals that the surface temperatures are by about 20°C lower than the respective fluid temperatures. This surprising effect is the result of substantial heat conduction effects in the azimuthal direction towards the cold bottom of the pipe.

Fig. 12 depicts the responses of the associated outside surface thermocouples at the same angular positions as the inside surface. Again, temperatures at 90° and 95° are quite lower than those at the inside. This leads to the following important conclusions for the conditions shown in these graphs:

(a) Extrapolation from thermal fluid response in transparent model facilities towards real plants is not necessarily straight forward, because of the complicated coupling between convective and conductive transport phenomena and their interdependencies.

(b) Indications are that in the vicinity of the mixing layer, no simple, unique correspondence exists between outside thermocouple readings and actual fluid and inside pipe surface responses both with respect to transient behavior as well as associated thermal loads; this may pose a problem for interpreting on-line surveillance data relying only on outside thermocouples.

From the data as depicted in Fig. 11, the bandwidth of the temperature fluctuations around final steady-state conditions are plotted over the region of interest in Fig. 13. The following conclusions can be drawn from this figure:

(1) The region of fluctuating temperatures is extremely narrow (~3 mm).
(2) Waves are smeared out and can be barely identified.
(3) Comparison of the deduced mixing layer height B with pre-test estimates based on classical instability theory shows that the theory overpredicts the measured value by a substantial margin (nearly factor 2); The wave amplitudes are overpredicted by the same factor.
(4) The deduced wave frequency is about 1.7 Hz versus the pre-test prediction of 2.6 Hz.

All pre-test estimates referenced above and partly listed in Fig. 13 have been taken from /12/.

4.2.2 PWR-Test T33.19

The same series of figures as shown for the BWR-experiment are shown for this PWR-test in Figs. 14 through 17. The following observations hold in comparison with Figs. 10 through 13:

(a) Temperature fluctuations in the fluid and at the inside surface are much larger for this PWR-tests than for T33.9. Initially, fluid temperature fluctuations are larger than 90°C.
(b) The energy exchange processes encompass a much broader liquid depth with hot lumps penetrating below 105° and cold lumps reaching easily 90° and beyond, i.e. the mixing zone is very much expanded versus the confined band observed previously for T33.9.
(c) The same surface temperature behavior (lower than fluid) can be observed for the PWR-test as noticed before for the BWR-test.
(d) Although the pipe inside surface temperature fluctuations are substantially larger than for the previously discussed BWR-test T33.9, no thermal fluctuations are noticeable at the pipe outside surface as Fig. 16 clearly shows.
(e) The region of fluctuating temperatures is much broader for this PWR-test (~13 mm).
(f) Waves can be clearly identified.
(g) Comparison of the deduced mixing layer height B with pre-test estimates based on classical instability theory shows substantial underprediction by the latter, wave amplitudes are overpredicted by a factor of 7.
(h) The deduced wave frequency is 0.7 Hz versus the pre-test estimate of 0.5 Hz, whereas the deduced wave length of 0.57 m compares favorably with the pre-test estimate of 0.55 m.

All pre-test estimates referenced above and partly listed in Fig. 17 have been taken from /12/.

In summary, a first assessment of the thermal fluctuations in the fluid and at the pipe inside surface observed for all BWR and PWR-typical experiments as listed in Table I indicates that the inside surface temperature fluctuations range between 10 and 40 % of the fluctuations measured in the fluid.

4.3 Heat Transfer Coefficient at Bottom of Cold Fluid

For the evaluation of the heat transfer coefficient at the bottom of the horizontal stratification pipe, a special set of consistent fluid/pipe inside and outside surface thermocouples has been applied. This triplet was mounted into a glow-plug type as described in /13/, assuring the exact positioning of the thermocouples to fit as close as possible the pipe surfaces. In order to deduce the heat transfer coefficient, the same procedure as applied to the TEMB-series for the assessment of the heat transfer at the bottom of the cold leg has been applied to the TEMR-experiments. It is fully described in /14/.

Fig. 18 compares the calculated Nusselt-numbers according to the Dittus-Boelter correlation versus the Nu-numbers derived from the TEMR-experiments and some TEMB-experiments which deem applicable to the stratification phenomenon under consideration. As can be seen from Fig. 18, the computed Nu-numbers using the Dittus-Boelter correlation underpredicts the majority of the data by a substantial margin except for rather low Nu-numbers. The same observations hold for comparisons with correlations by Hansen, Prandtl, and VDI.

However, when the predicted values are multiplied by the ratio Pr_{cold}/Pr_{hot}, the agreement between predicted and experimentally derived Nu-numbers improves markedly as shown in Fig. 19 over the whole spectrum considered. Deviations fall within an acceptable bandwidth of ± 20 %.

4.4 Cold Water Layer Heights

Fig. 20 summarizes the measured cold fluid layer heights for the BWR- and PWR-typical experiments as functions of the Froude-number, which has been determined by using the measured velocity and the hydraulic diameter of the cold fluid region. Test numbers appearing more than once represent experiments where different mass flows have been used consecutively during two or even more experimental phases. It is apparent from Fig. 20 that the Froude-number dependence of the cold layer heights is distinctively different for the BWR and PWR-TEMR experiments. This reflects the different hydraulic behaviors of both types of experiments, i.e. the presence of the sparger for the BWR versus the non-existence of any additional resistance in case of the PWR-experiments. Naturally, the gradient of the straight line in Fig. 20 depends on the constructive details of the flow openings. On the other hand, the straight line representing the PWR typical experiments should also the cold layer heights derived from the earlier HDR-TEMB thermal mixing tests with injections through HPI-nozzles far away from the RPV. This will be validated in the near future.

4.5 Axial Strains

Fig. 21 shows the azimuthal distribution of the measured axial strain obtained by the strain gages at the pipe outside surface as depicted in Fig. 9 for T33.9. At the same time, Fig. 21 compares the experimental result with a blind pre-test prediction using an analytical prediction method originally developed in /15/ and modified by /16/. The analytical model allows to determine the steady-state, two-dimensional temperature field and all structural quantities by analytical means for the stratification pipe including a beam model for the rest of the pipe system depicted in Fig. 1. The comparison in Fig. 21 shows satisfactory agreement considering the pre-test character of the calculation assuming a step-like fluid temperature jump at the interface between cold and hot fluid region which as Fig. 13 shows is a rather good approximation. Fig. 21 shows a systematic tendency of the analytical model to overpredict the tensile stresses in the cold fluid region as well as the compressive stresses in the hot region.

Possible reasons for the existing deviations could be the fluid temperature approximation, the assumption of a constant heat transfer coefficient and simplifications in the beam model not accounting for the additional flexibility of the elbow (compare Fig. 1). Additional results and comparisons for other BWR-TEMR experiments are contained in /16/.

Fig. 22 shows the azimuthal distribution of the measured axial strain obtained by the strain gages at the pipe outside surface as depicted in Fig. 9 for the PWR-experiment T33.19. No computations are available yet for any of the PWR-type of expriments for comparison.

5. ANALYTICAL AND COMPUTATIONAL RESULTS AND DISCUSSIONS

5.1 Fluid Temperatures

Contrary to the previous HDR-TEMB thermal mixing experiments /8, 9/, the TEMR test series was accompanied by only a few analytical and computational predictions for the fluid temperatures. Rather, design and planning relied foremost upon the simple engineering-type of estimates as discussed in chapter 4.2.1 and 4.2.2 and shown in Figs. 13 and 17.

Figs. 23 and 24 show the only results of the applications of advanced, finite difference codes for the fluid region available thus far.

Fig. 23 compares the azimuthal distribution of the fluid temperature close to the wall with a blind pre-test computation with the transient, 3-D computer code SOLA-PTS using 2704 nodes for the horizontal pipe section. This computation was performed by Battelle-Frankfurt. Nonuniform noding was used for the vertical (smallest node size: 10 mm) and horizontal directions, whereas an uniform mesh was employed in the axial flow direction. No attempt was undertaken to simulate the elbow. Rather the inflow condition at the elbow and was approximated. As shown in Fig. 23, the SOLA-prediction meets the hot and cold region temperatures very well but misses the position of the transition zone as well as the gradient. Reasons for the deviations are that the actual, mass flow during experiment was 25 % less than that applied for the pre-test prediction. In addition, the chosen mesh is not fine and appropriate yet for the steep azimuthal gradient observed for T33.9.

Fig. 24 shows the same comparison but for the post-test prediction with COMMIX 1B for test T33.7. This computation was performed by KfK/INR. The model for this computation discretized the complete elbow with an additional piece of the straight vertical pipe (compare Fig. 1). Measured data were used as input where appropriate. The comparison in Fig. 24 shows that the hot fluid temperature is somewhat underpredicted whereas the cold fluid temperature is overpredicted. Again as for the SOLA-calculation the temperature gradient is too flat, possibly because of still too coarse noding and/or overemphasis in calculated mixing and numerical diffusion.

Additional, future post-test computations with SOLA-PTS and COMMIX-1B may show improved agreements and pinpoint present defiencies.

5.2 Pipe Temperatures

Besides of the application of conventional finite-difference and finite element codes for solving the heat conduction problem in the pipe wall by both KWU-Offenbach and KWU-Erlangen, the Battelle-Institut at Frankfurt used a multigrid, adaptive FEM-code to demonstrate its usefulness and capabilities for cases with strong discontinuities such as the temperature distribution for T33.9 within an extremely narrow transition zone. The code AUTOFEM 2D can solve the steady-state, two dimensional heat conduction problem with temperature-dependent material properties and locally variable boundary conditions for arbitrary domains including extreme singularities. The code runs on an APOLLO workstation in a completely interactive mode including pre- and post-processors. A description of AUTOFEM 2D is given in /17/.

As indicated in Fig. 25 an extreme discontinuity between hot (250°C) and cold (30°C) fluid regions is assumed. Also shown in Fig. 25 is the initial triangulation in finite element zones. The input is minimal for this initial step. The rest is done automatically by the code. In a second and/or consecutive steps the AUTOFEM 2D refines locally the mesh as shown in Fig. 26 (total of 390 nodes) in accordance with the needs to simulate the steep gradients with a given accuracy. The refinement is only performed by the code where needed in order to minimize computation time and storage. Fig. 27 depicts the calculated isotherms in the vicinity of the transition zone. This one of many possible graphical representations using the graphics capabilities of the workstation.

Finally, for the TEMR experiment T33.9, Fig. 28 compares the azimuthal temperature distributions at the pipe inside surface as measured and predicted by AUTOFEM 2D and the analytical method already introduced in chapt. 4.5. Both calculational methods compare very well with the data especially considering their blind pre-test characters. Further improvements for the AUTOFEM 2D results seem feasible for post-test computations. Its calculational results have been validated both on behalf of the TEMR-data as well as by the predictions of the analytical method /16/.

Acknowledgements

This work has been fully supported by the German Federal Ministry of Research and Technology (BMFT) within the framework of the Project HDR at KfK, Karlsruhe, FRG. The excellent cooperation by the various institutions is greatly appreciated. The enormous efforts undertaken by the HDR- and PHDR-staff is highly regarded.

REFERENCES

/1/ PWR Pipe Crack Study Group: Investigation and Evaluation of Cracking Incidents in Piping in Pressurized Water Reactors, NUREG-0691, Sept. 1980.

/2/ Bamford, W.H. et al.: Fatigue Crack Growth in Pressurized Water Reactor Feedwater Lines, ASME Pressure Vessel and Piping Conference, USA, June 1981, 81-PVP-2.

/3/ Kußmaul, K. et al.: Safety Analysis of Circumferentially Cracked Feedwater Piping of Light Water Reactors, Third Intl. Seminar on Assuring Structural Integrity of Steel Reactor Pressure Boundary Components, Monterey, USA, Aug. 29-30, 1983, pp. 251-284.

/4/ Miksch, M. et al.: Loading Conditions in Horizontal Feedwater Pipes of LWRs Influenced by Thermal Shock and Thermal Stratification Effects, Nucl. Eng. Des. 84 (1985), 179-187.

/5/ Simon, U. et al.: Evaluations of Stratified Flows (in German), VGB Kraftwerkstechnik 62 (1982), 641-645.

/6/ Hu, M.H. et al.: Flow Model Test for the Investigation of Feedwater Line Cracking for PWR Steam Generators, ASME Pressure Vessel and Piping Conf., Denver, USA, June 1981, 81-PVP-4.

/7/ Miksch, M.; Schücktanz, G.: Constructive Measures for Minimization of Thermal Stresses for Thermal Stratification and their Effects Upon Fatigue (in German), Annual Meeting KTG, Mannheim 1982.

/8/ Wolf, L. et al: Results of Thermal Mixing Tests of the HDR-Facility and Comparisons with Best-Estimate and Simple Codes, Nucl. Eng. Des. 99 (1987), 287-304.

/9/ Wolf, L. et al.: Application of Engineering and Multi-Dimensional, Finite Difference Codes to HDR Thermal Mixing Experiments TEMB, Proc. 14th Water Reactor Safety Information Meeting, Gaithersburg, MD, USA, Oct. 27-31, 1986, NUREG/CP 0082 Vol. 5, pp. 395-444, also to appear in Nucl. Eng. Des.

/10/ Jansen, K.; Bader, H.-J.: Supplemental Data Report for HDR-TEMB Experiments T32; Measured Cold Leg Velocities and Heat Transfer Coefficients (in German), PHDR-Working Report No. 3.476/85, 1986.

/11/ Schygulla, U.; Wolf, L.: Design Report: Thermal Stratification Experiments in a Horizontal Piping Section, HDR-Test Group TEMR T33, PHDR-Working Report No. 3.495/86, Nov. 1986.

/12/ Schnellhammer, W.: HDR-TEMR Stratification Tests, Comparison of Pre-Test Estimates with Data for Fluid Layer Heights, Mixing Zones, Wave Lengths and Frequencies, (in German), KWU-Report ST 131/87/0076, Offenbach (April 1987).

/13/ Jansen, K.; Bader, H.J.: Supplemental Report to the Data Report for TEMB (Experiments T32.15, 17, 18), (in German), PHDR Working Report 3.451/85 (1985).

/14/ Schygulla, U.; Hansjosten, E.; Bader, H.J.; Jansen, K.: Assessment of Heat Transfer and Fluid Dynamics in Cold Leg and Downcomer of HDR-TEMB Experiments, Trans. 9th Intl. Conf. SMiRT, Lausanne, Switzerland, Aug. 17-21, 1987, Vol. D, pp. 313-317.

/15/ Sammieto, G.S.; Pardo, E.: Transient Thermal Stresses and Stress Intensity Factors Induced by Thermal Stratifiction in Feedwater Lines, Trans. 8th Intl. Conf. SMiRT, Brussels, Belgium, Aug. 1985, Vol. F, pp. 339-345.

/16/ Geiß, M.: Test Group TEMR-Pre-test Predictions for Structural Loads for Test Group T33, Batteile-Report for PHDR, No. R-66.481-01.

/17/ Reinhardt, H.-J.: Geiß, M.: Applications of an Adaptive Multigrid FEM-Code to Thermal Problems in HDR-Experiments, Trans. 9th Intl. Conf. SMiRT, Lausanne, Switzerland, Aug. 17-21, 1987, Vol. B, pp. 505-509.

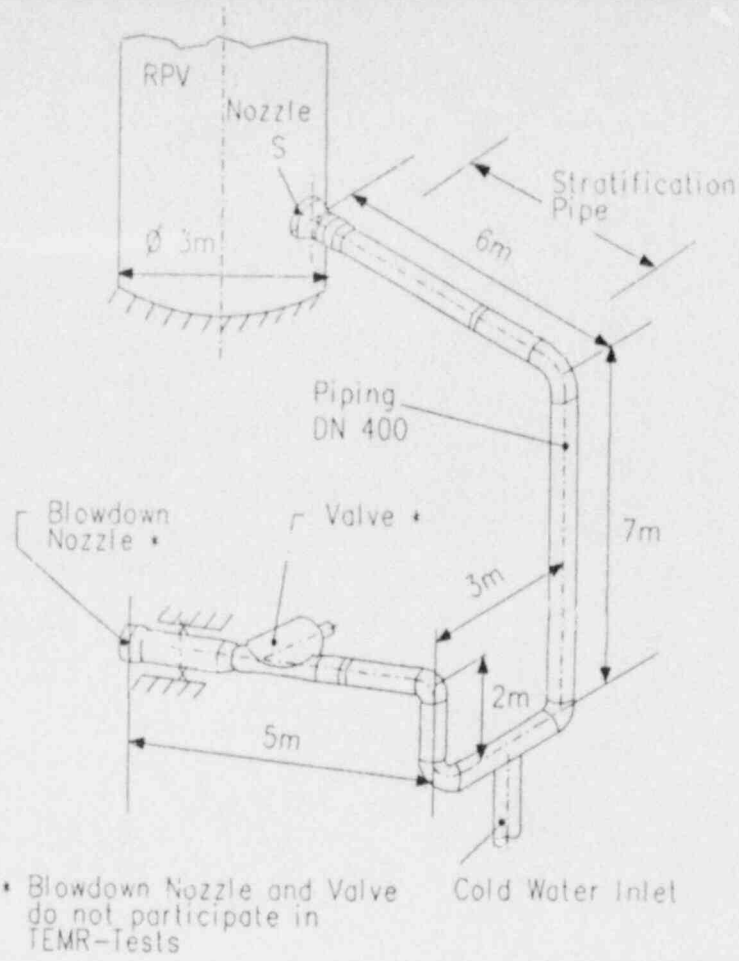

Fig. 1: Isometry of the TEMR-Piping System

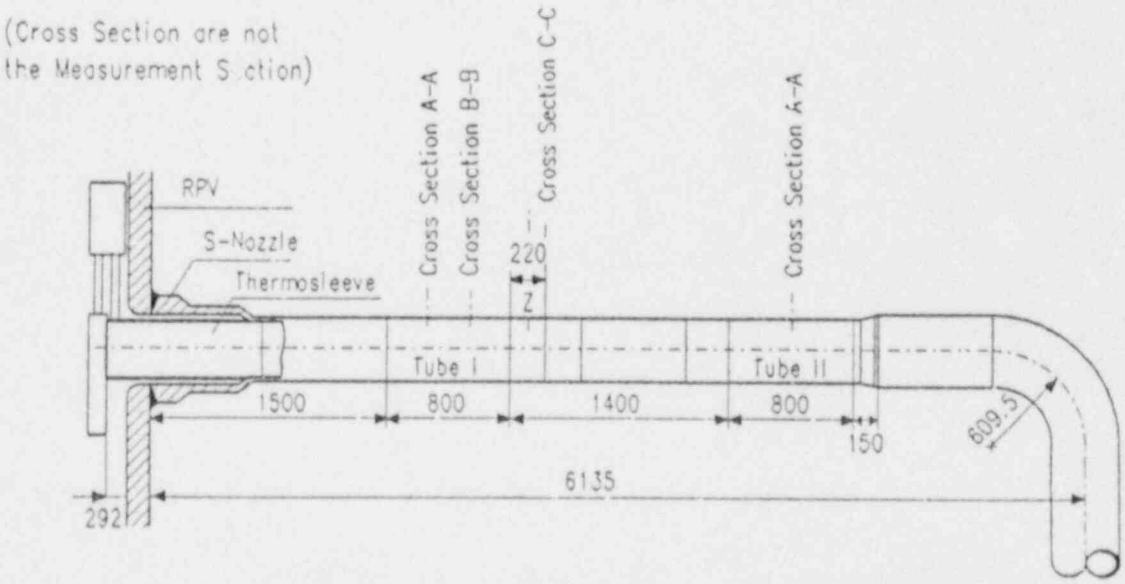

Fig. 2: Overall Arrangement of TEMR Horizontal Pipe Section With Thermal Sleeve, Orifice Manipulator and Measurement Tubes I, II

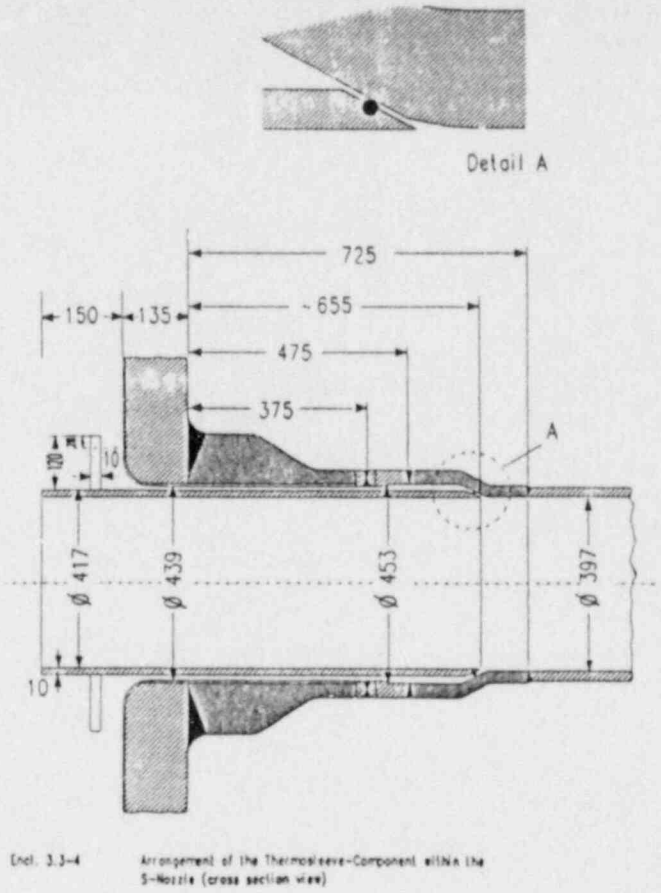

Encl. 3.3-4 Arrangement of the Thermosleeve-Component within the S-Nozzle (cross section view)

Fig. 3: Arrangement of the Thermal Sleeve Inside the S-Nozzle

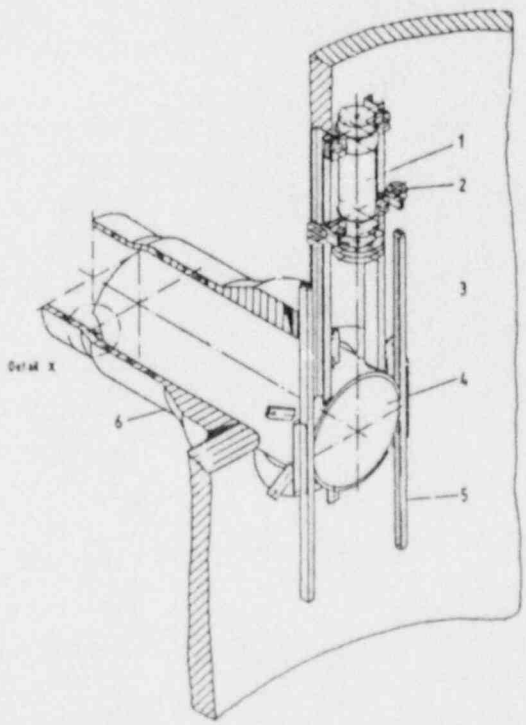

Fig. 4: Perspective View of Orifice Manipulator Inside Reactor Pressure Vessel

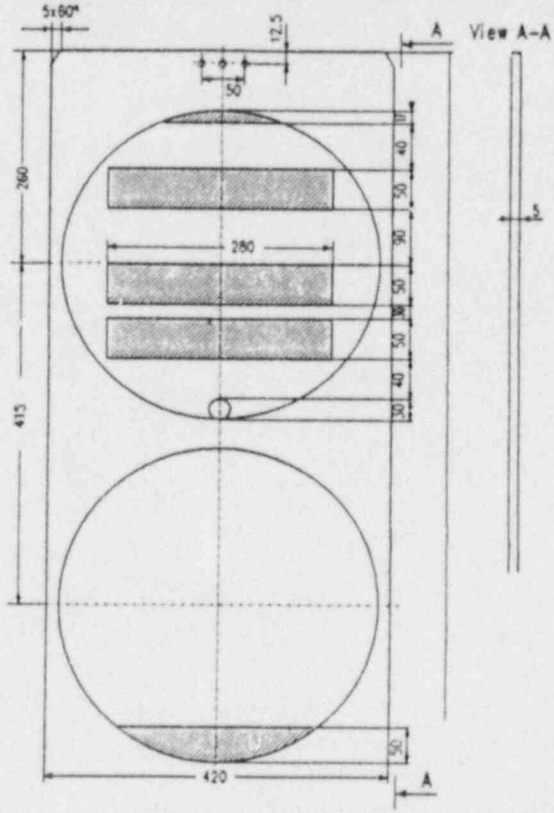

Fig. 5: Oblong With the Two Types of Orifices
Top: BWR Freedwater Sparger Simulation
Bottom: Hot Water Packet Simulation

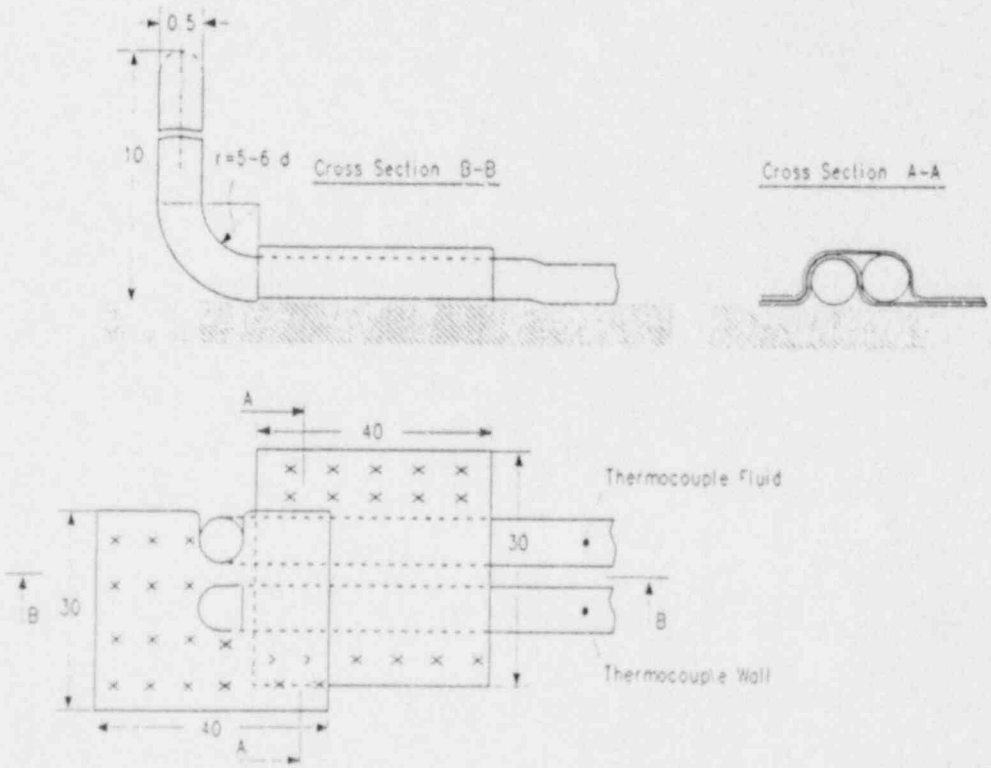

Fig. 6: Combined Fluid and Wall Thermocouple Pair

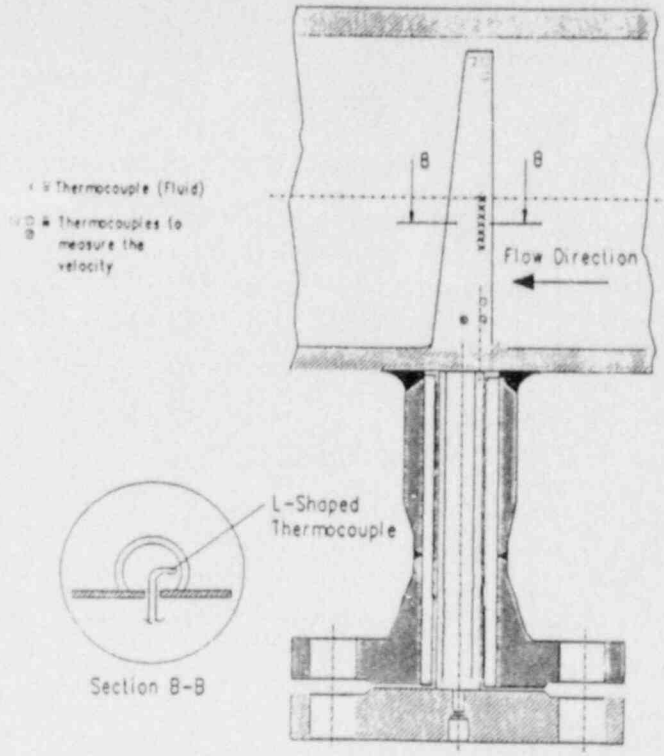

Fig. 7: Fluid Thermocouple Rake

Legende:

- Thermoelement wall
- Thermoelement fluid
- Thermoelement wall/fluid
- Velocity

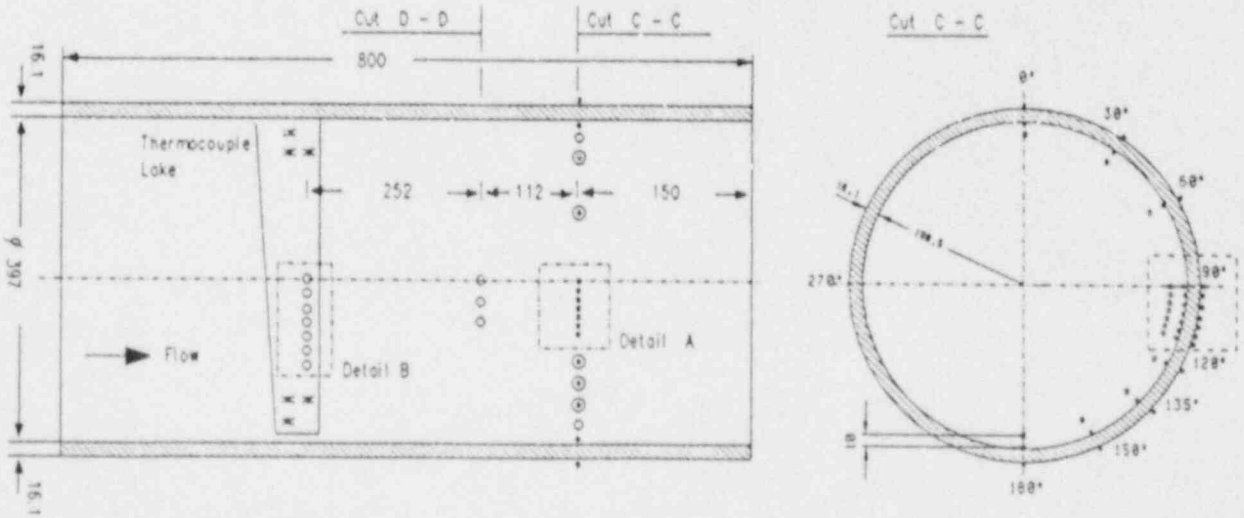

Fig. 8: Axial and Radial Cross-Sections Through TEMR-Pipe With Thermocouple Positions

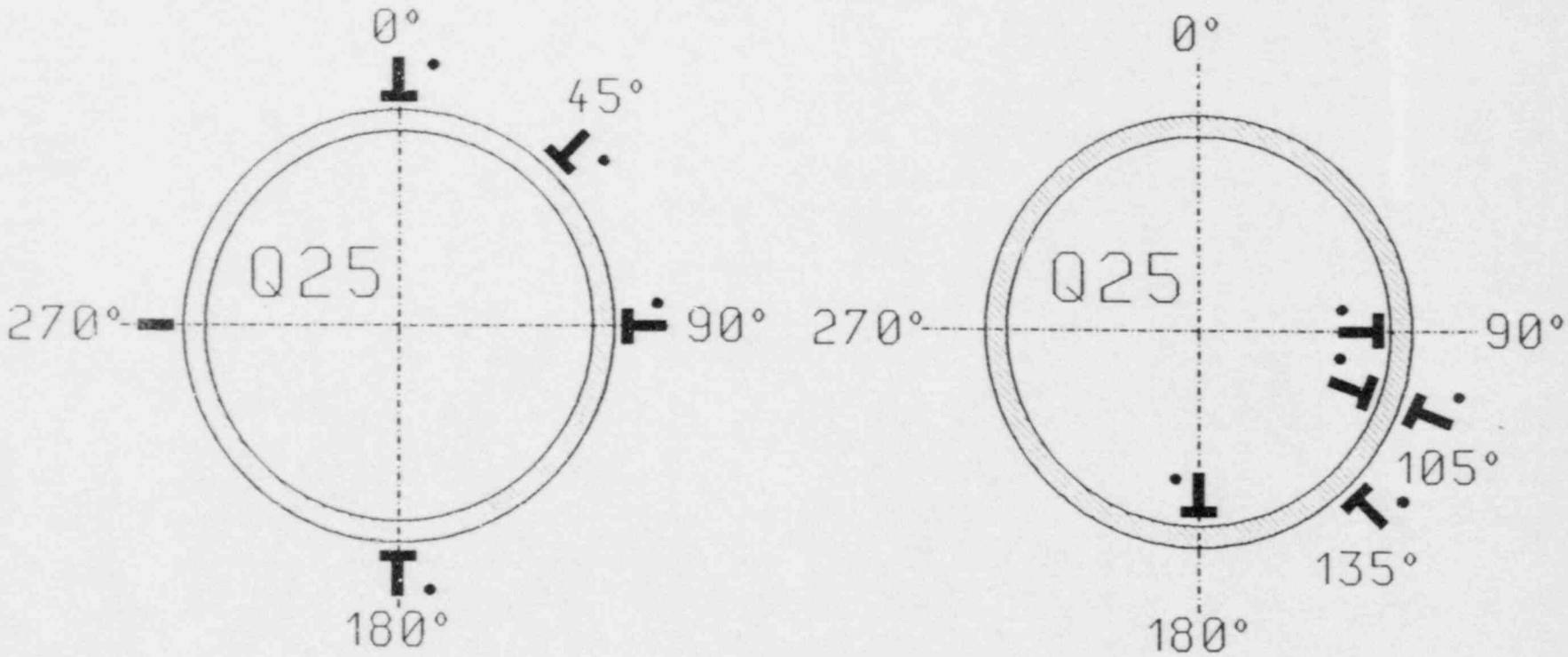

Fig. 9: Azimuthal Distribution of Axial and Circumferential Strain Gages and Thermocouples Positioned in the Same Axial Plane

Experiment	Pressure	Temperature		Density		Volume Flow	Height of Cold Fluid	Orifice		w/o Orifice
		Hot	Cold							
		T_H	T_K			V		1	2	
Nr.	bar	°C	°C	$\frac{kg}{m^3}$	$\frac{kg}{m^3}$	$\frac{m^3}{s}$	m			
T33.1	2.0	106.5	18.5	953.3	998.6	0.00097		×		
T33.2	7.3	158.3	23.0	907.6	995.2	0.00117		×		
T33.3	24.2	210.3	29.0	852.9	997.1	0.0015		×		
T33.4	44.0	252.0	25.7	796.7	998.8	0.0015		×		
T33.5	1.9	105.2	22.0	954.3	997.9	0.0029		×		
T33.6	7.2	160.6	30.0	906.7	996.0	0.0012		×		
T33.7	26.0	211.5	38.7	851.4	993.8	0.0050		×		
T33.8	21.1	211.0	134.0	851.8	920.1	0.0046		×		
T33.9	44.4	249.7	41.0	799.7	993.7	0.0056		×		
T33.10	24.0	211.4	32.0	851.4	996.1	0.0037		×		
						0.0060				
						0.0037				
T33.11	1.9	104.9	33.2	947.2	994.7	0.0089		×		
T33.12	5.6	158.9	53.8	908.3	986.5	0.0132		×		
T33.13	1.9	104.7	40.0	954.6	992.4	0.0130		×		
T33.14	6.5	157.0	27.0	910.1	996.9	0.0010				×
T33.15	6.4	157.8	31.1	909.4	995.1	0.0068				×
T33.16	6.5	156.5	45.0	910.6	990.4	0.0105				×
T33.17	22.1	212.0	25.9	850.6	997.5	0.0006				×
T33.18	22.9	214.0	35.6	848.3	995.0	0.0068				×
T33.19	22.4	214.0	54.5	848.3	987.0	0.0129				×
T33.25	44.0	252.2	35.1	796.4	995.8	0.0009				×
						0.0075				
						0.0131				
T33.20	7.4	161.4	34.5	906.0	994.5	0.0068			×	
T33.21	8.0	153.3	56.0	913.7	985.4	0.0130			×	
T33.22	22.6	212.5	23.7	850.1	998.3	0.0016			×	
T33.23	22.3	210.9	40.6	851.3	993.0	0.0068			×	
T33.24	23.1	215.0	65.0	847.1	975.9	0.0132			×	

Table I: Complete Test Matrix of the HDR-TEMR Stratification Experiments

BWR:
T33.9

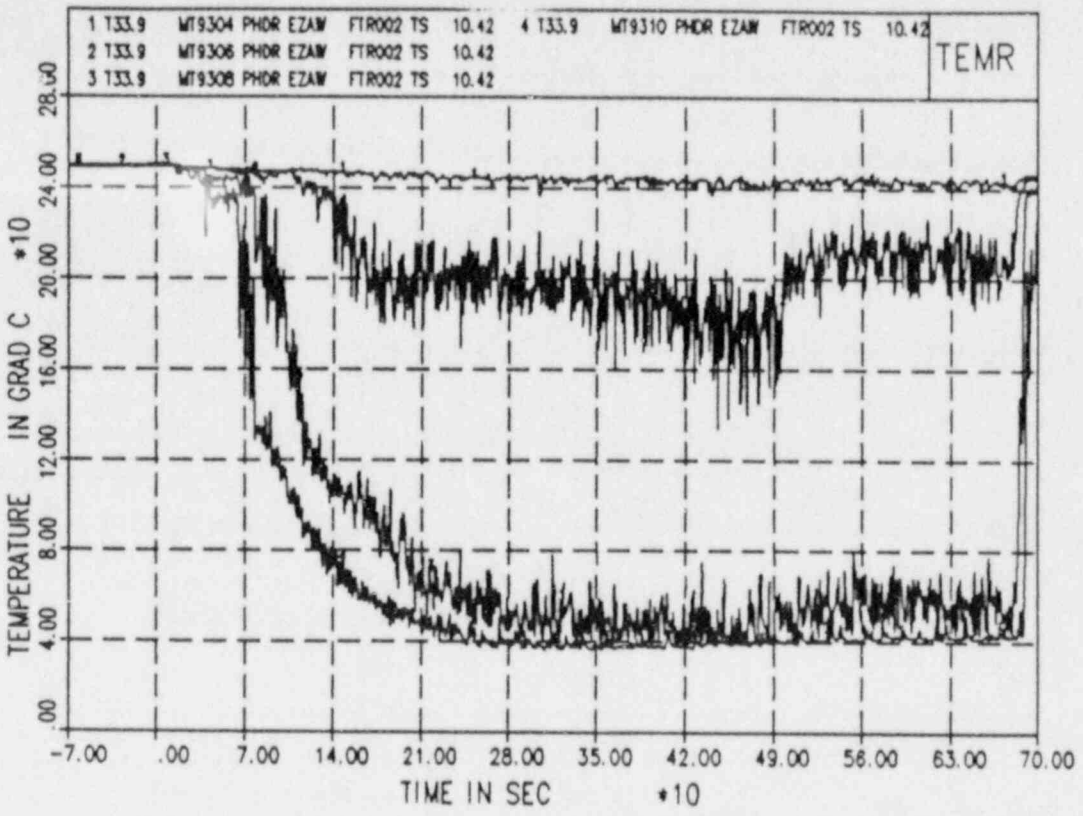

Fig. 10: T33.9 (BWR) - Fluid Temperatures Close to the Wall Between 90° and 150°

BWR:
T33.9

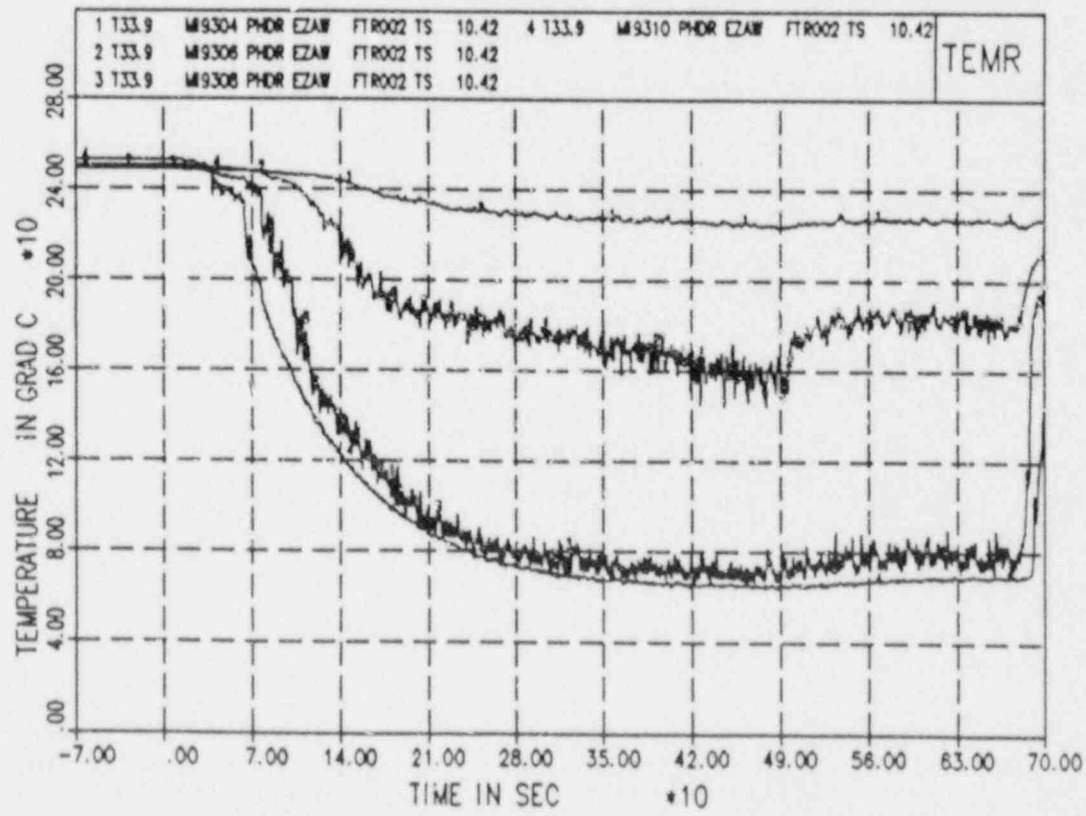

Fig. 11: T33.9 (BWR) - Pipe Inside Surface Temperatures Between 90° and 150°

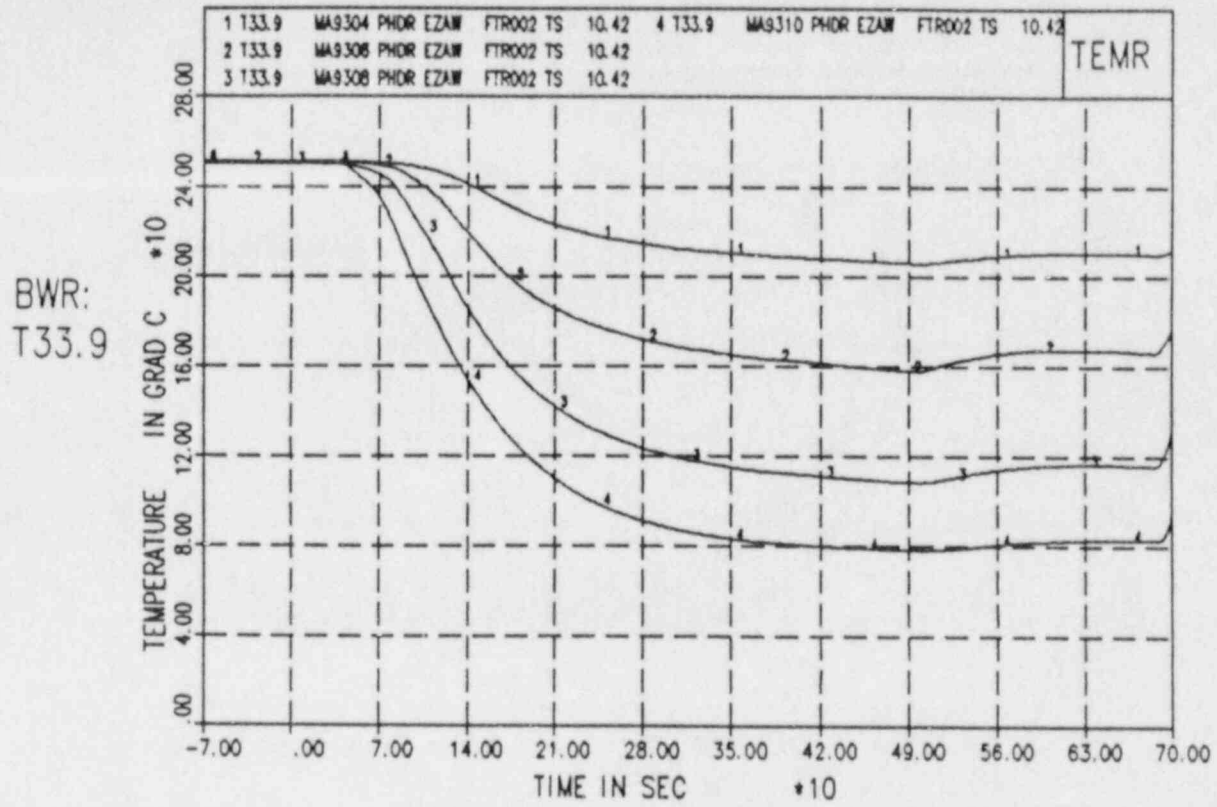

Fig. 12: T33.9 (BWR) - Pipe Outside Surface Temperatures Between 90° and 150°

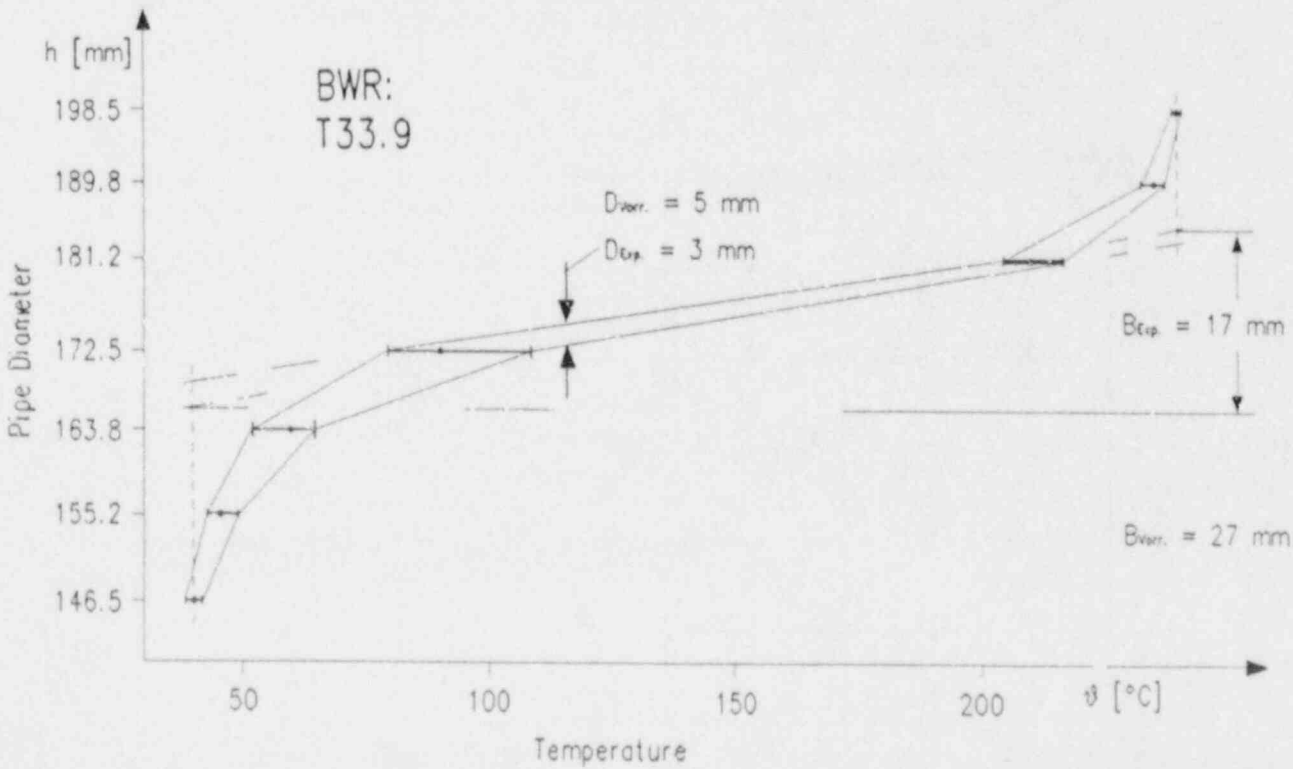

Fig. 13: T33.9 (BWR) - Evaluated Cold Water Height and Transition Mixing Layer Characteristics from Temperature Fluctuations

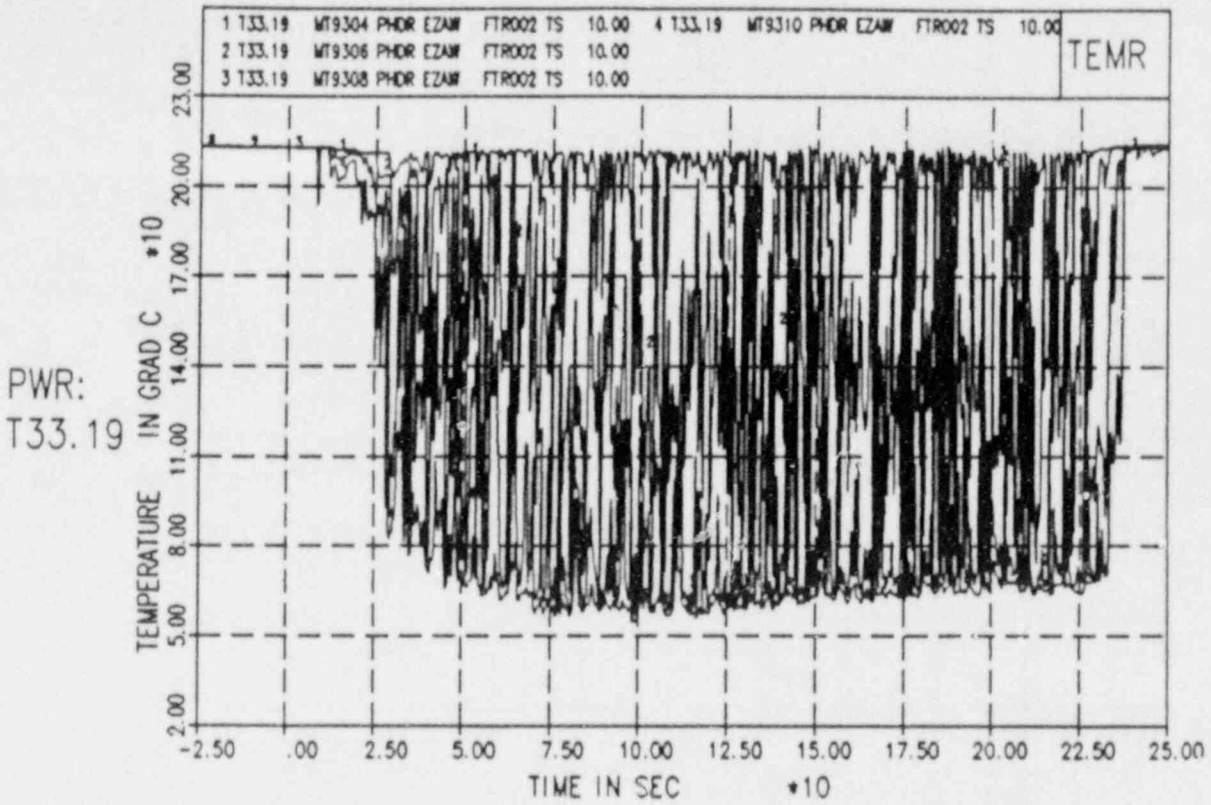

Fig. 14: T33.19 (PWR) - Fluid Temperatures Close to the Wall Between 90° and 150°

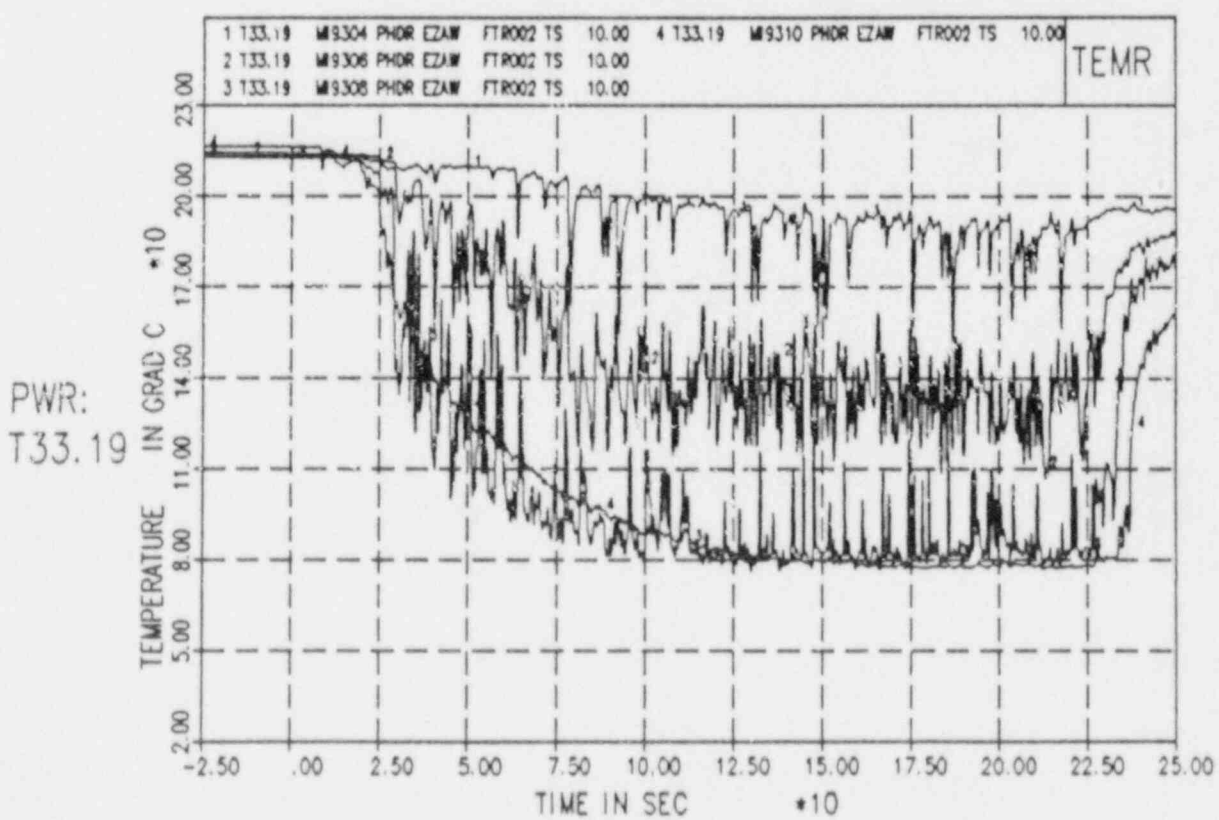

Fig. 15: T33.19 (PWR) - Pipe Inside Surface Temperatures Between 90° and 150°

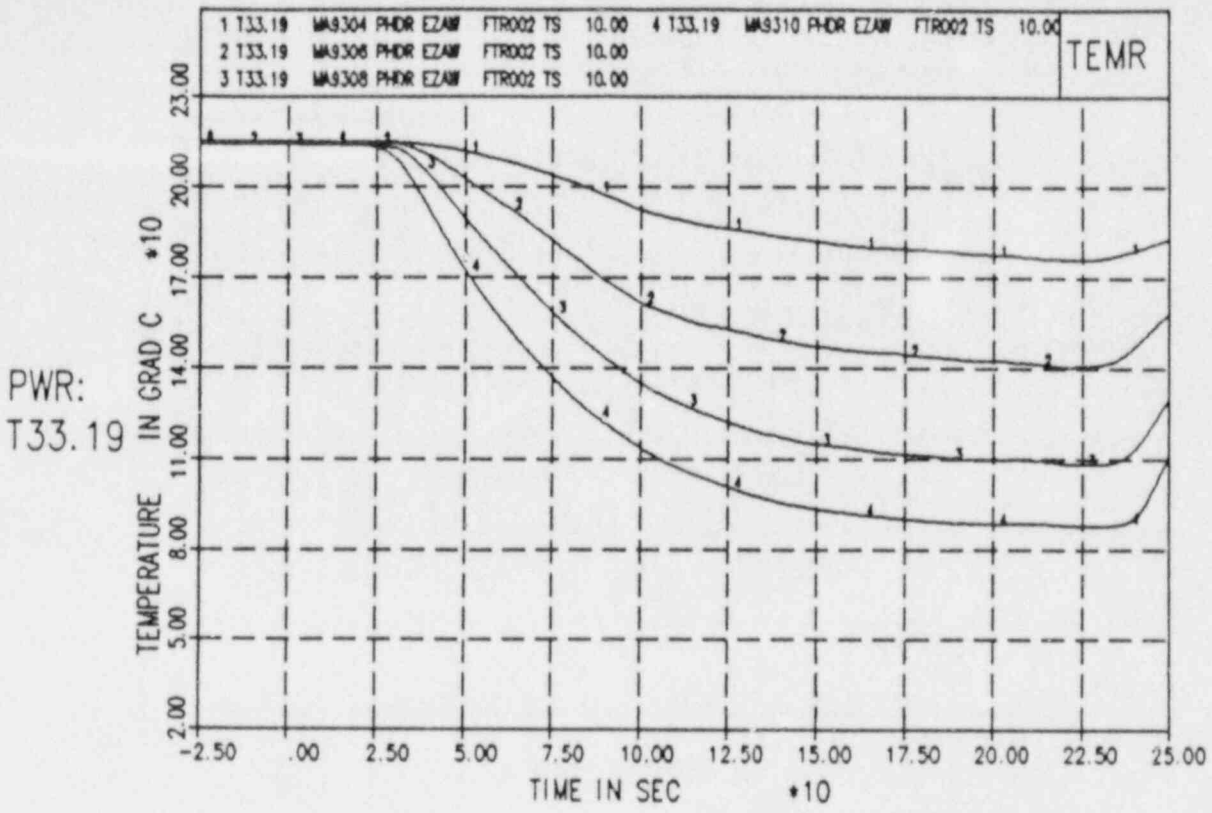

Fig. 16: T33.19 (PWR) - Pipe Outside Surface Temperatures Between 90° and 150°

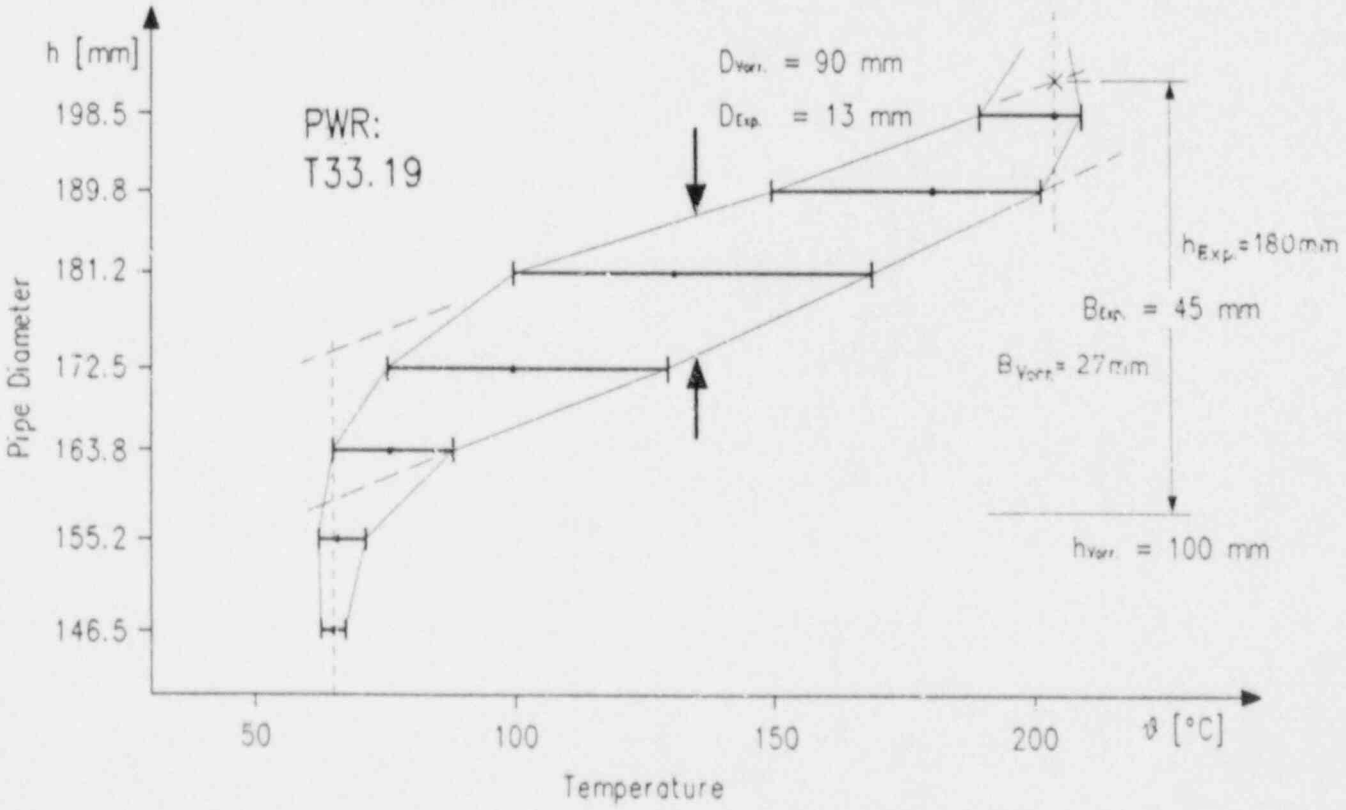

Fig. 17: T33.19 (PWR) - Evaluated Cold Water Height and Transition Mixing Layer Characteristics from Temperature Fluctuations

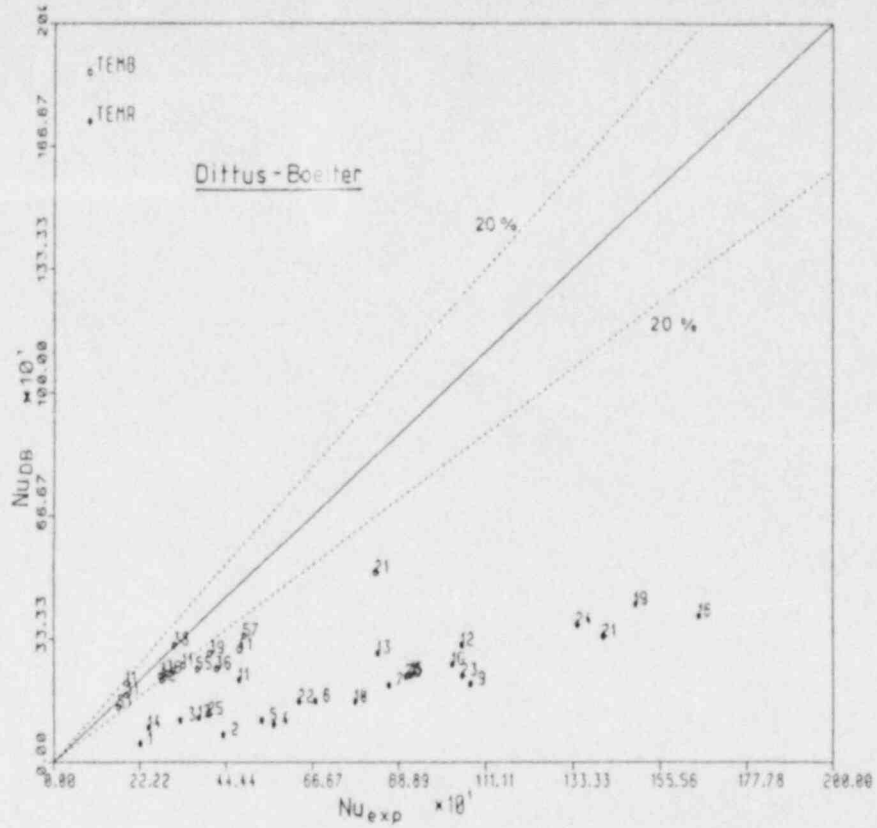

Fig. 18: Comparison of Nu - Numbers (Dittus - Boelter) Versus Experimental Nu - Numbers

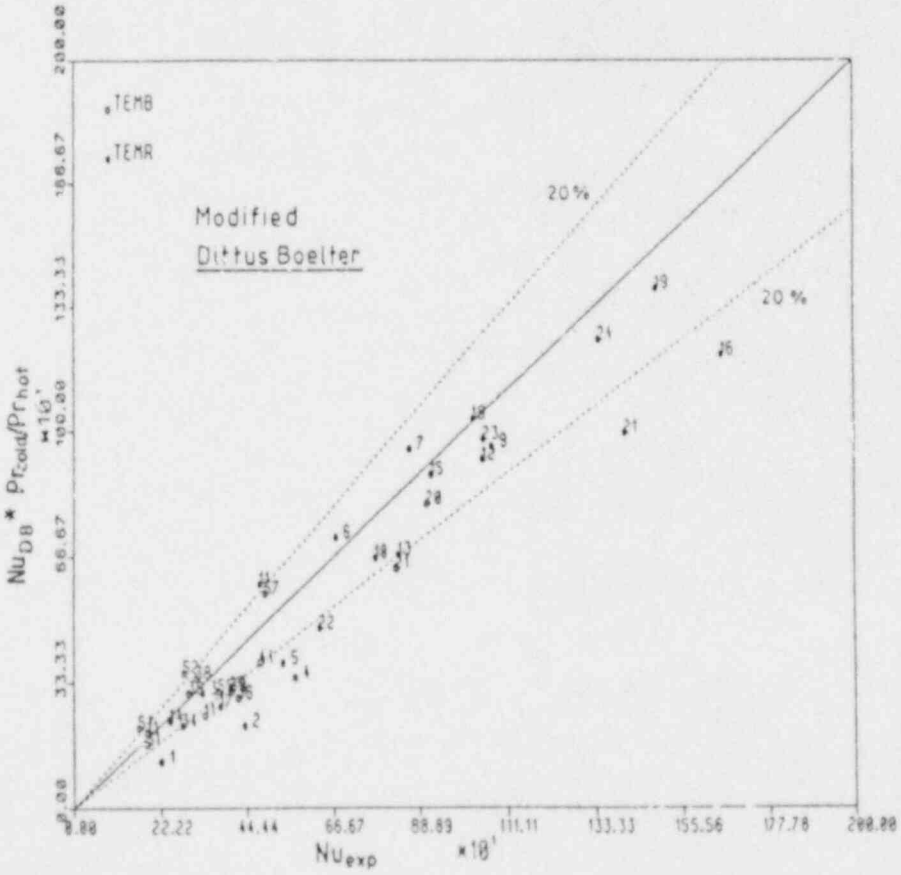

Fig. 19: Comparison of Nu - Numbers (Dittus - Boelter) Modified by Pr - Number Ratio Versus Experimental Nu - Numbers

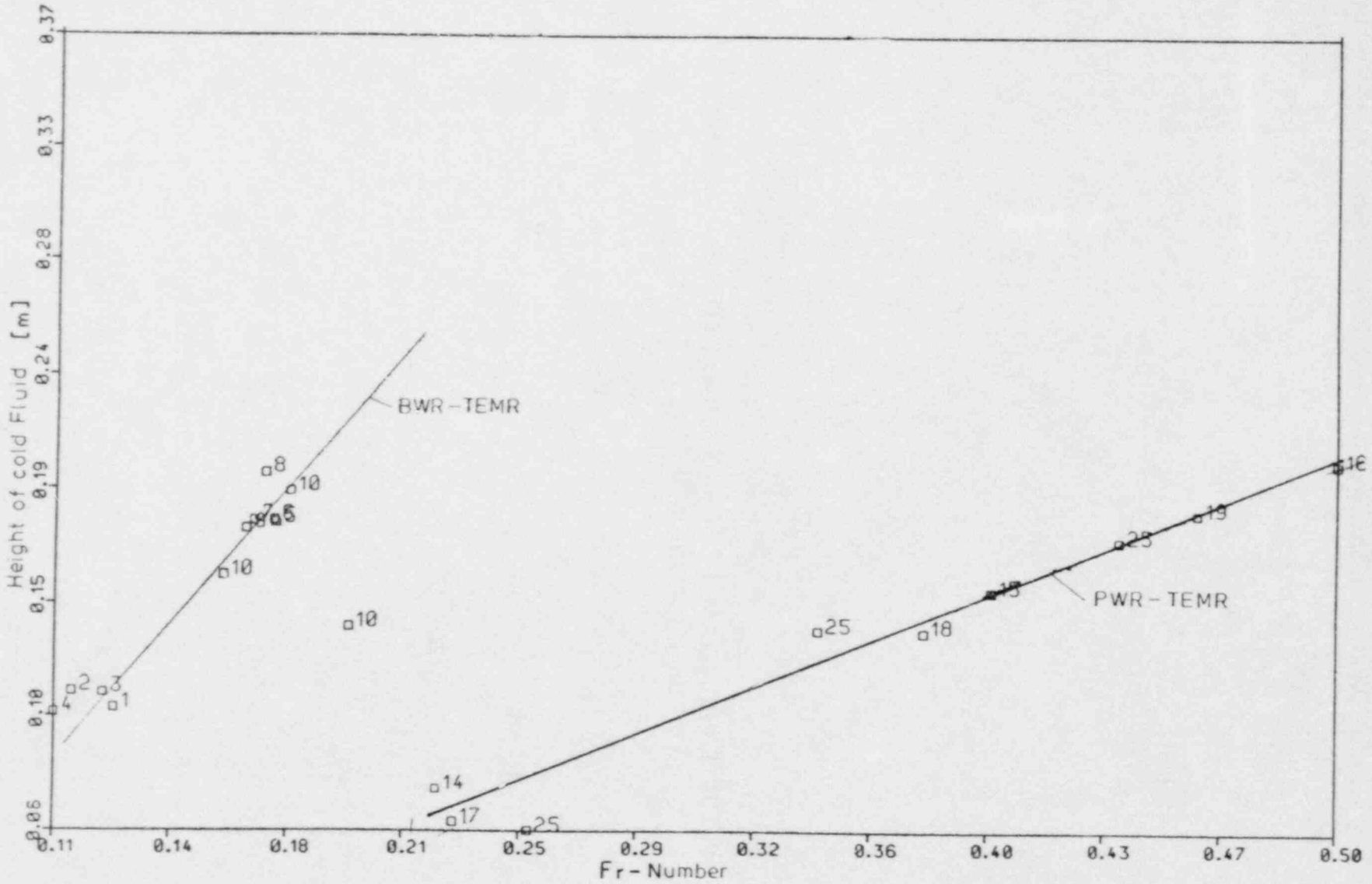

Fig. 20: Measured Cold Water Layer Heights for BWR and PWR Conditions Versus Froude - Numbers

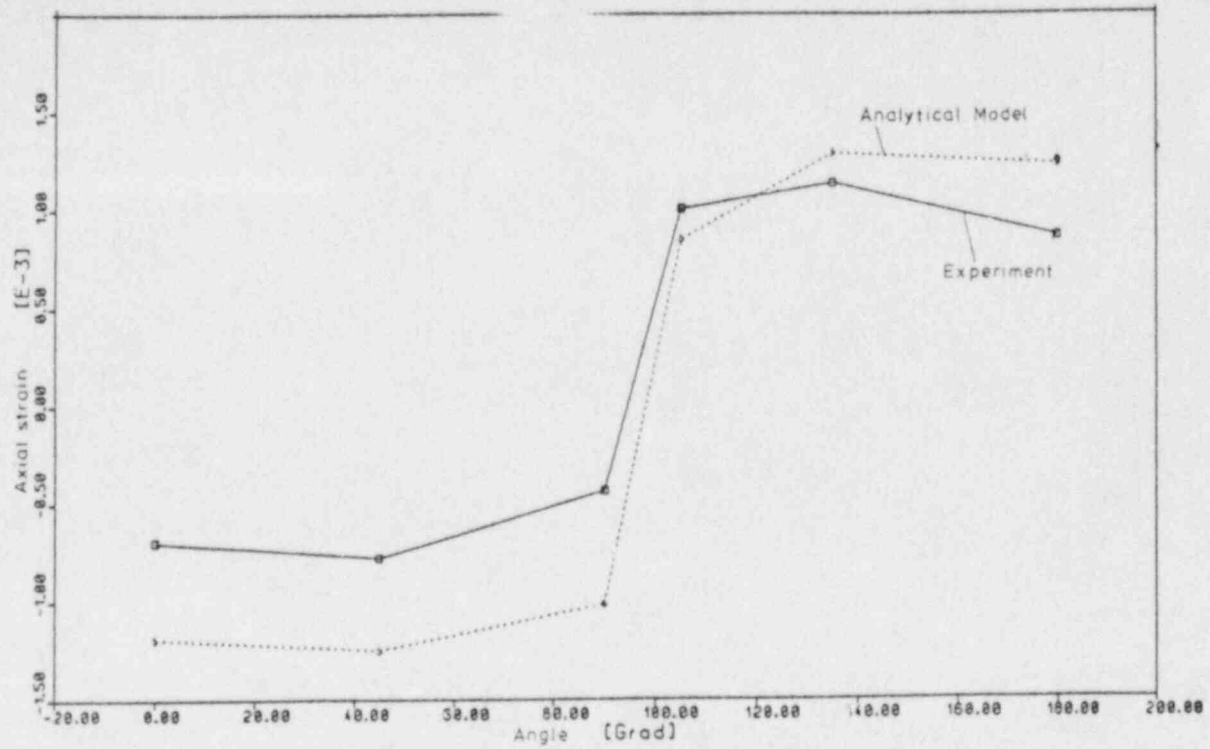

Fig. 21: T33.9 (BWR) - Measured Versus Analytically Calculated Axial Strains Around Pipe Outside Surface Circumference

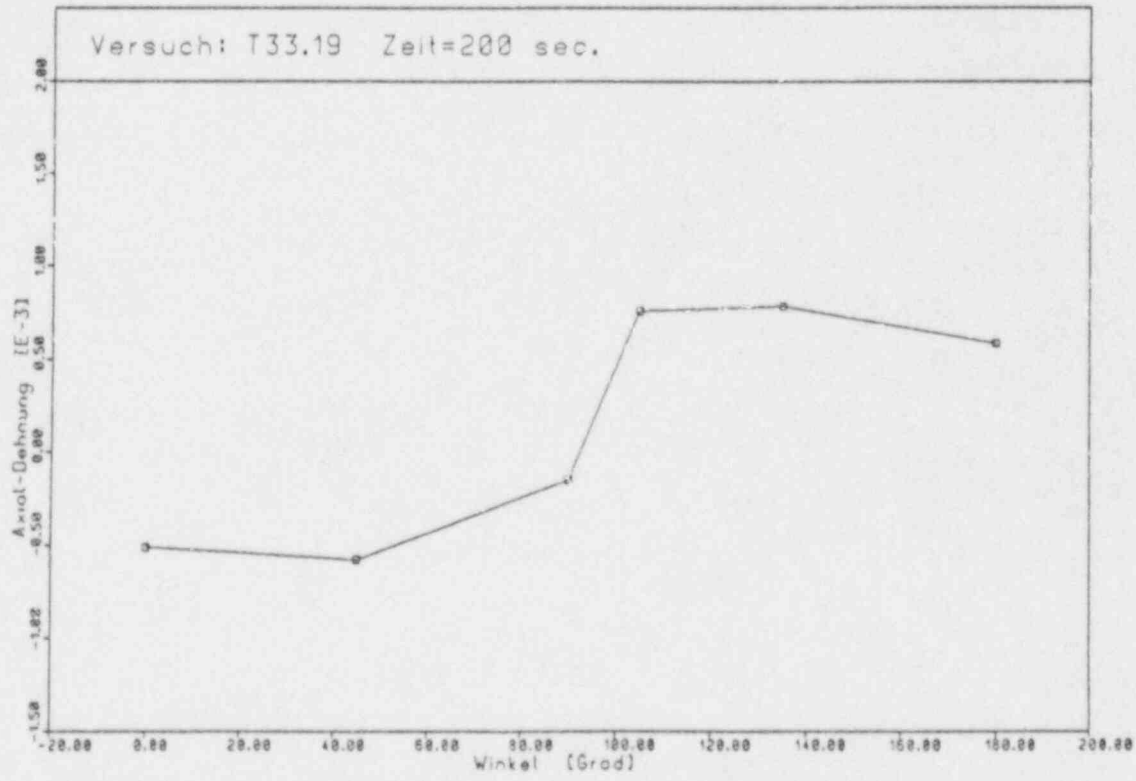

Fig. 22: T33.19 (PWR) - Measured Axial Strains Around Pipe Outside Surface Circumference

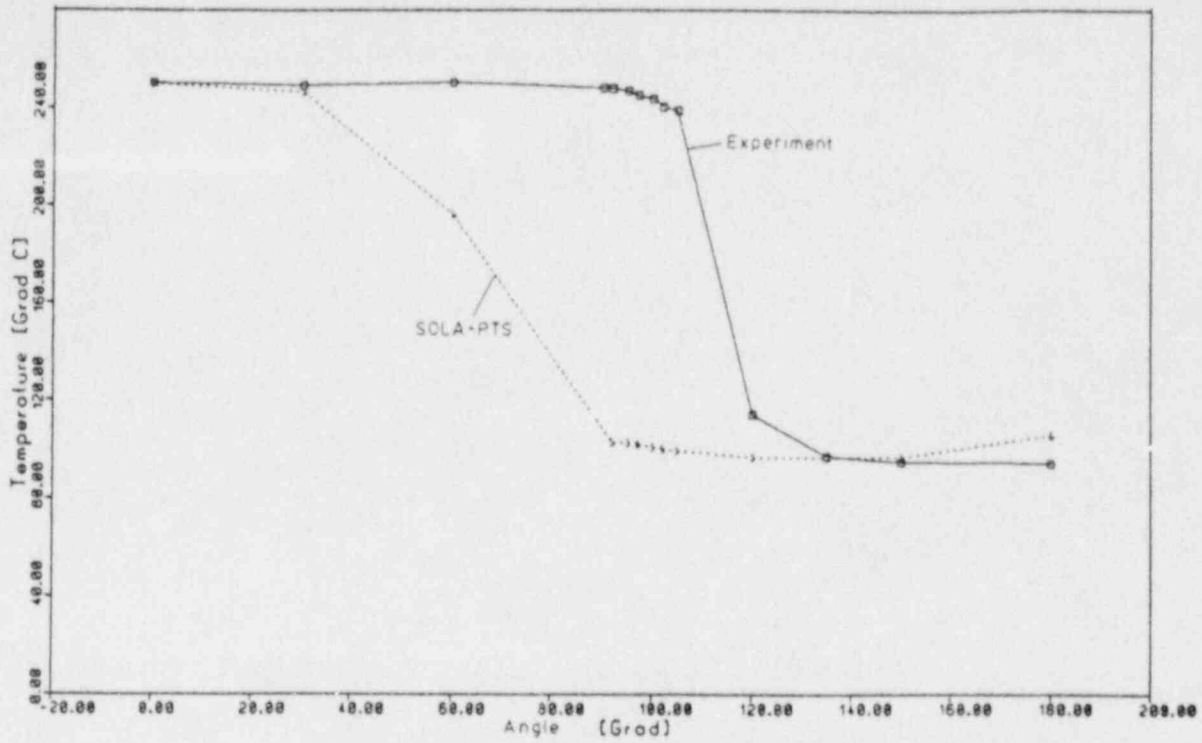

Fig. 23: T33.9 (BWR) - Comparison Between Measured and Pre - Test (SOLA-PTS) Predicted Circumferential Fluid Temperature Distributions Close to the Wall at t = 60 sec.

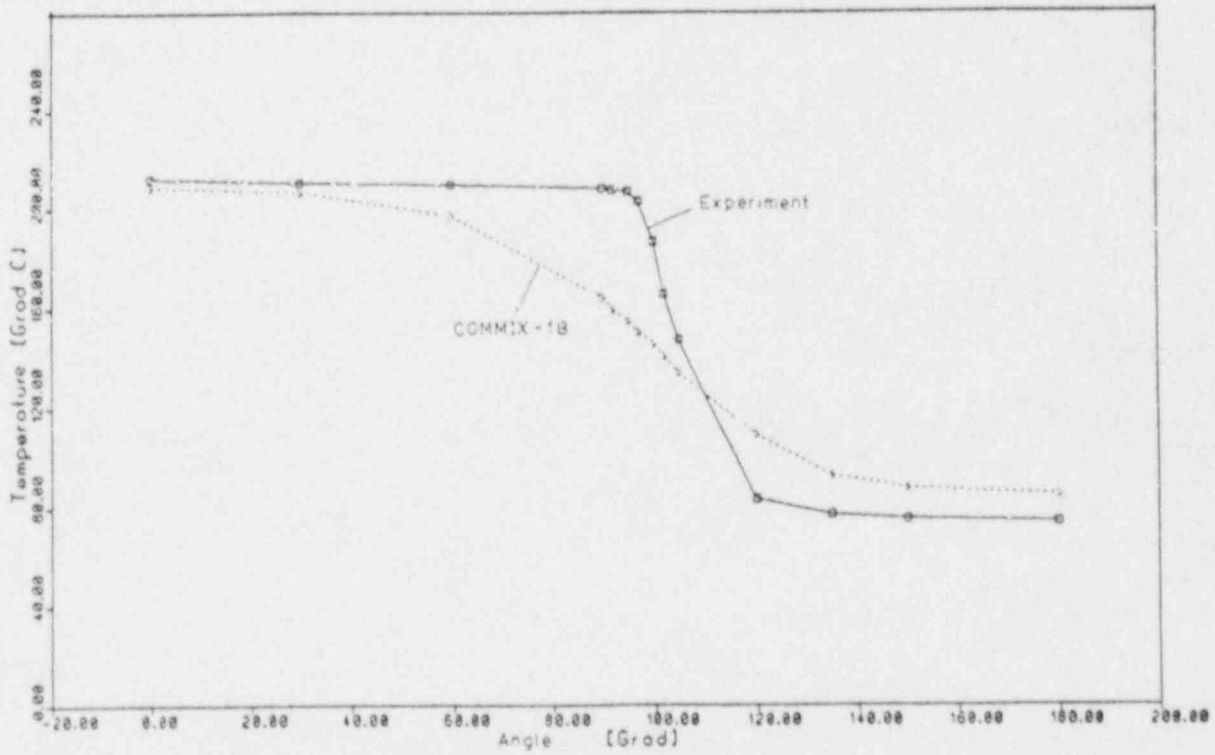

Fig. 24: T33.7 (BWR) - Comparison Between Measured and Post - Test (COMMIX-1B) Predicted Circumferential Fluid Temperature Distributions Close to the Wall at t = 60 sec.

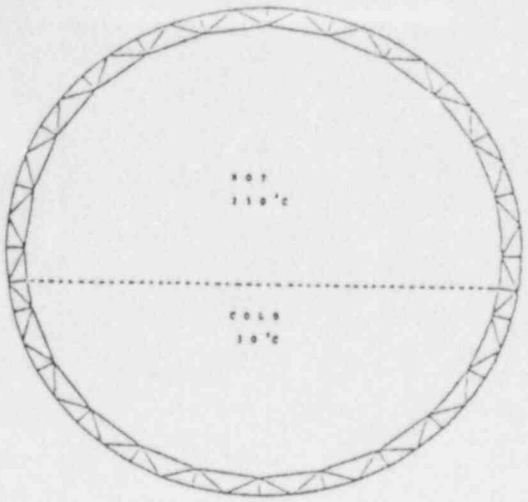

Fig. 25: Initial FEM-Net for AUTOFEM2D (74 Nodes)

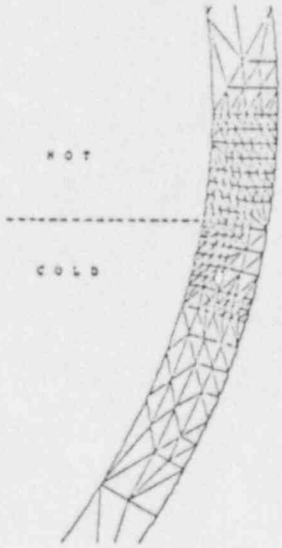

Fig. 26: Adaptive Net at Transition Zone

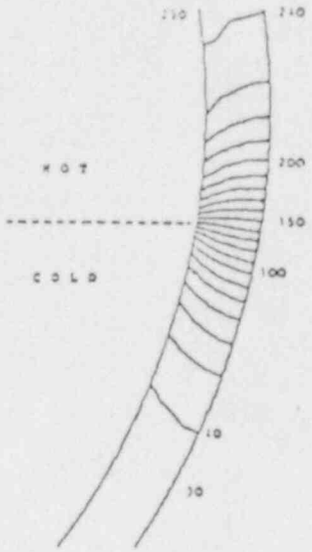

Fig. 27: T33.9 - Isotherms in the Vicinity of Transition Zone

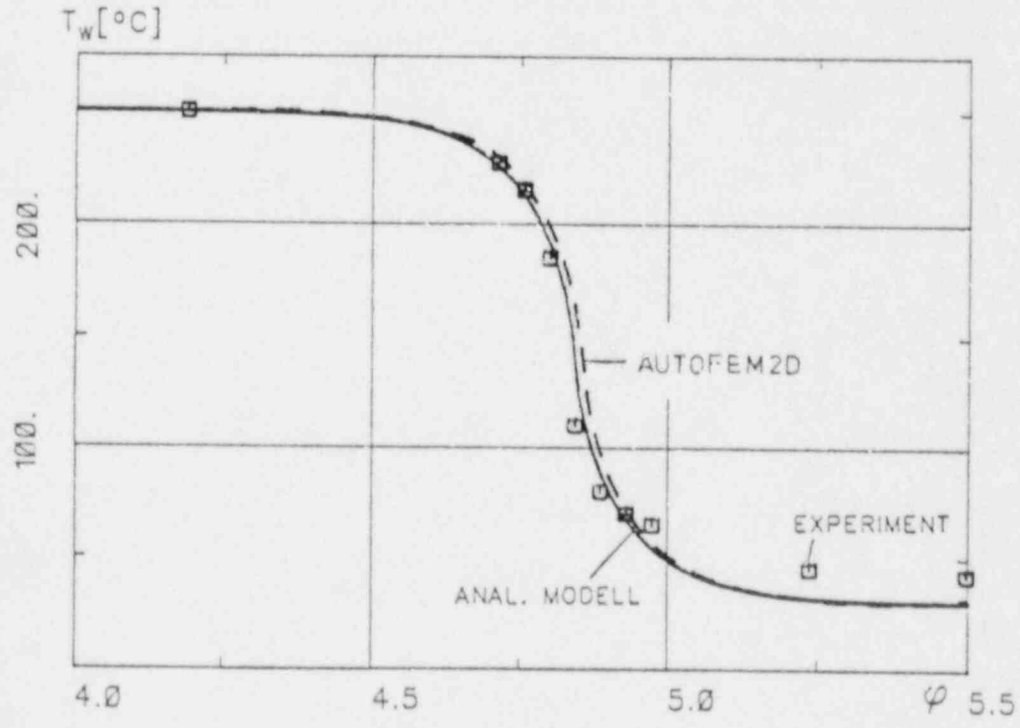

Fig. 28: T33.9 (BWR) - Comparison Between Measured and Predicted Surface Temperatures with Analytical and Adaptive FEM - Model

22.10.1987 8:12:08 USER= .HANSJOSTEN

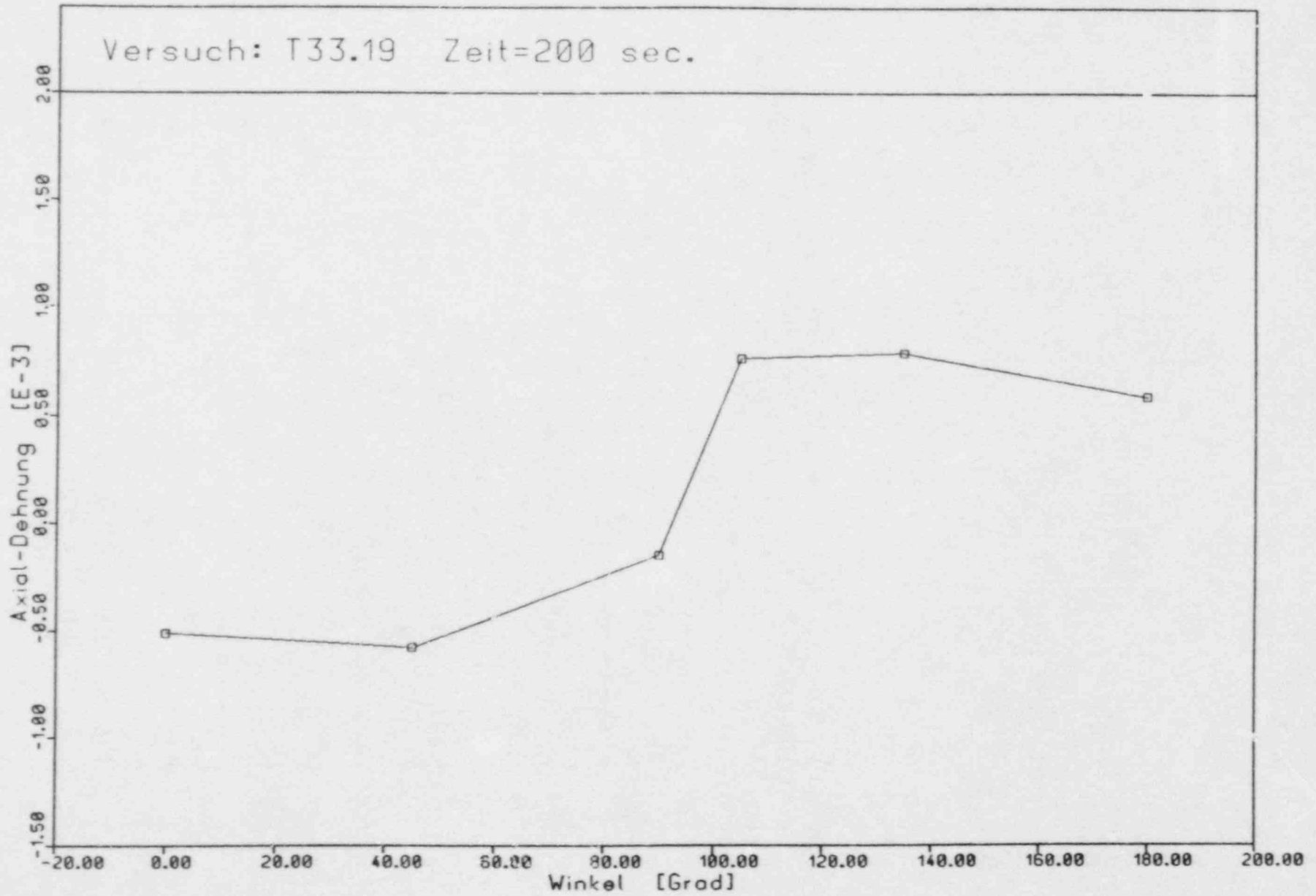

NRC FORM 335 (2 84) NRCM 1102, 3201, 3202

SEE INSTRUCTIONS ON THE REVERSE

U.S. NUCLEAR REGULATORY COMMISSION

BIBLIOGRAPHIC DATA SHEET

1. REPORT NUMBER (Assigned by TIDC add Vol. No., if any)

NUREG/CP-0091
Vol. 5

2. TITLE AND SUBTITLE

Proceedings of the Fifteenth Water Reactor Safety Information Meeting

3. LEAVE BLANK

4. DATE REPORT COMPLETED

MONTH: January | YEAR: 1988

5. AUTHOR(S)

Compiled by Allen J. Weiss, BNL

6. DATE REPORT ISSUED

MONTH: February | YEAR: 1988

7. PERFORMING ORGANIZATION NAME AND MAILING ADDRESS (Include Zip Code)

Office of Nuclear Regulatory Research
U. S. Nuclear Regulatory Commission
Washington, D. C. 20555

8. PROJECT/TASK/WORK UNIT NUMBER

9. FIN OR GRANT NUMBER

A-3283

10. SPONSORING ORGANIZATION NAME AND MAILING ADDRESS (Include Zip Code)

Same as Item 7 above

11a. TYPE OF REPORT

Proceedings of conference on safety research

b. PERIOD COVERED (Inclusive dates)

October 26-29, 1987

12. SUPPLEMENTARY NOTES

Proceedings prepared by Brookhaven National Laboratory

13. ABSTRACT (200 words or less)

This six-volume report contains 140 papers out of the 164 that were presented at the Fifteenth Water Reactor Safety Information Meeting held at the National Bureau of Standards, Gaithersburg, Maryland, during the week of October 26-29, 1987. The papers are printed in the order of their presentation in each session and describe progress and results of programs in nuclear safety research conducted in this country and abroad. Foreign participation in the meeting included twenty-two different papers presented by researchers from Belgium, Czechoslovakia, Germany, Italy, Japan, Russia, Spain, Sweden, The Netherlands and the United Kingdom. The titles of the papers and the names of the authors have been updated and may differ from those that appeared in the final program of the meeting.

14. DOCUMENT ANALYSIS - a. KEYWORDS/DESCRIPTORS

reactor safety research
nuclear safety research

b. IDENTIFIERS/OPEN-ENDED TERMS

15. AVAILABILITY STATEMENT

Unlimited

16. SECURITY CLASSIFICATION

(This page) Unclassified

(This report) Unclassified

17. NUMBER OF PAGES

18. PRICE

UNITED STATES
NUCLEAR REGULATORY COMMISSION
WASHINGTON, D.C. 20555

OFFICIAL BUSINESS
PENALTY FOR PRIVATE USE, $300

SPECIAL FOURTH-CLASS RATE
POSTAGE & FEES PAID
USNRC
PERMIT No. G-67

120555078877 1 1AN1R21R4
US NRC-OARM-ADM
DIV OF PUB SVCS
POLICY & PUB MGT BR-PDR NUREG
W-537
WASHINGTON DC 20555